

GW - 31

**REPORTS**

**YEAR(S):**

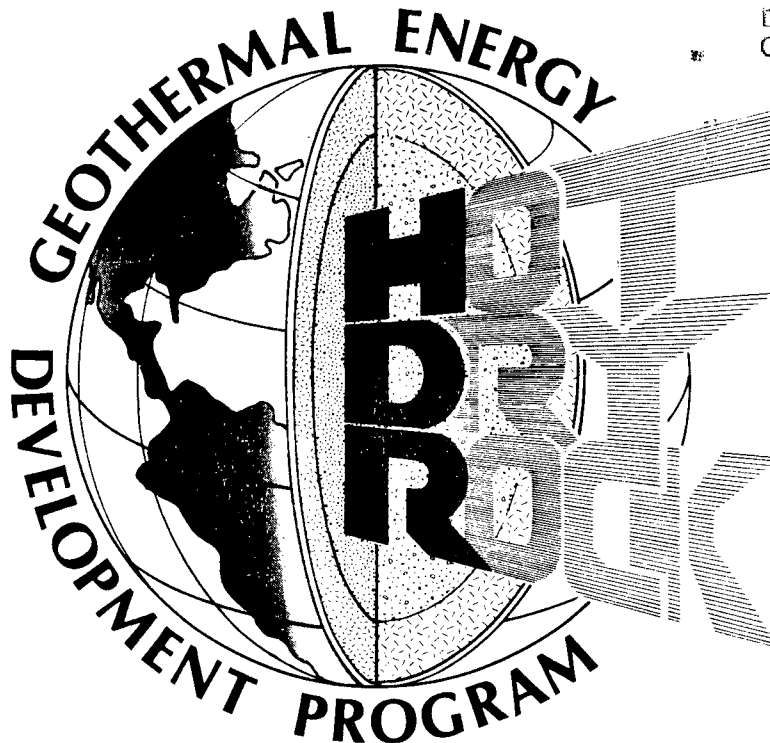
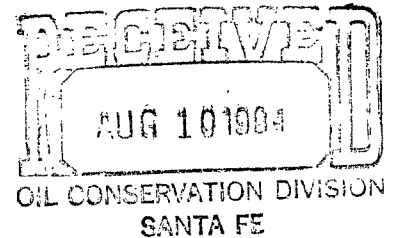
1974 - 1984

HDR-84-DP01

JUNE 1984

Work copy

**HOT DRY ROCK  
GEOHERMAL ENERGY  
DEVELOPMENT PROGRAM**

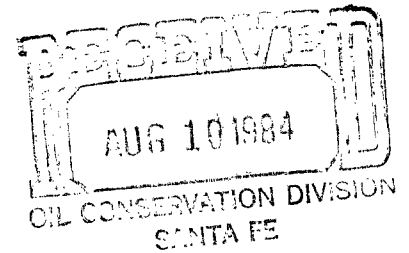


**DISCHARGE PLAN FOR  
GEOHERMAL OPERATIONS  
AT FENTON HILL  
SANDOVAL COUNTY, N. M.**

**PREPARED BY  
LOS ALAMOS NATIONAL LABORATORY**

**SUBMITTED BY  
U. S. DEPARTMENT OF ENERGY  
LOS ALAMOS AREA OFFICE**

**Hot Dry Rock Geothermal Energy  
Development Program**



**Discharge Plan  
for  
Geothermal Operations  
at  
Fenton Hill  
Sandoval County, N. M.**

**Prepared By  
the  
Los Alamos National Laboratory**

**June 1984**

**Submitted By  
U. S. Department of Energy  
Los Alamos Area Office**

## TABLE OF CONTENTS

	Page
I. INTRODUCTION	4
II. HDR PROGRAM BACKGROUND	5
III. FENTON HILL PROJECT STRUCTURE	10
IV. FENTON HILL PROJECT - ENVIRONMENTAL DESCRIPTION	14
A) Geology and Geomorphology	14
B) Climate and Surface Hydrology	16
C) Hydrology	17
D) Water Quality	19
V. FENTON HILL PROJECT - PROJECT DESCRIPTION	20
A) Location and Facilities	20
B) Geothermal System	21
C) Water Supply System	21
D) Waste Products Produced	22
VI. PRESENT DISPOSAL PRACTICES	26
A) Drilling and Workover Operations	26
B) Sanitary Sewage System	28
C) Garbage and Trash Disposal	28
VIII. PROPOSED DISCHARGE PLAN	30
A) Proposed Disposal of Solid and Liquid Waste	30
B) Contingency Plan	34
C) Monitoring and Inspection	35
D) Reporting	35
E) Transfer of Project	36
F) Conclusions	36

## LIST OF ILLUSTRATIONS

- Fig. 1. Hot Dry Rock Concept
- Fig. 2. Reservoir Drawdown Curves
- Fig. 3. HDR Program Overview Schedule
- Fig. 4. The Fenton Hill Location
- Fig. 5. Aerial View of Fenton Hill
- Fig. 6. Aerial View of 5.7 M Gal Pond
- Fig. 7. Modified 1.0 M Gal Pond

## APPENDICES

- Appendix A Fenton Hill Pond and Well Water Analysis
- Appendix B Aquifer Evaluation at Fenton Hill
- Appendix C Geology Reports
- Appendix D As Completed Well Pipe String Sections
- Appendix E As Built Drawings - 5.7 m gal reservoir
- Appendix F Site Maps of Fenton Hill

## I. INTRODUCTION

This document is prepared specifically to respond to a request from the Energy and Minerals Department, Oil Conservation Division, State of New Mexico. Director, Energy and Minerals Department, Joe D. Ramey has asked the Department of Energy, Los Alamos Area Office to furnish a Discharge Plan for Geothermal Operations, Fenton Hill.<sup>[1]</sup>

To provide a familiarity with the Fenton Hill Project and to facilitate better understanding of any discharge plan for the site a background review of the Hot Dry Rock Program and a discussion of the structure of the Fenton Hill Project prefaces the discharge discussions.

The discharge plan is organized to respond to the regulations of the New Mexico Water Quality Control Commission, dated Sept. 20, 1982.

Furnished as appendices are Water Sample analysis, Aquifer Evaluation, the detailed as built drawings for the 5.7 million gallon, lined and covered, water storage reservoir recently completed at the site; and recent reports on the Geothermal Resource studies of the Jemez Mountains and Valles Caldera.

The Los Alamos Hot Dry Rock (HDR) Program, sponsored by the U.S. Department of Energy (DOE), Division of Geothermal and Hydropower Technologies, is a research program to develop the technology necessary to economically extract the energy contained at accessible depths within the earth's crust. The Fenton Hill Project is the field site for the application and testing of this research. The site is operated in cooperation with the U.S. Department of Agriculture, National Forest Service.

---

[1] Letter of Jan. 10, 1983 Joe D. Ramey to Harold Valencia, Re: "Request for Discharge Plan for Geothermal Operations at Fenton Hill, Sandoval County, NM."

## II. HDR PROGRAM BACKGROUND

The Hot Dry Rock Geothermal Energy Program began in 1972 as a research, development and demonstration project at the Los Alamos National Laboratory ("Los Alamos"). That project is known as the Fenton Hill Project and derives its name from that of the test site, Fenton Hill, located about 35 miles (55 km) west of Los Alamos, New Mexico. This site is situated on the western rim of the Valles Caldera, a comparatively young silicic volcano which was active as recently as one hundred thousand years ago.

The Fenton Hill Project was supported entirely by the United States Government, through the U.S. Department of Energy (DOE) and its predecessor organizations, until U.S. Fiscal year (FY) 1980. Beginning in that year and continuing to the present, the Government of West Germany through the Kernforschungsanlage-Julich GmbH (KFA) and the Government of Japan through the New Energy Development Organization (NEDO) became cosponsors of the Project with the DOE.

The overall objective of the Project is to develop and demonstrate the technology required for the commercial extraction of energy from xerolithic geothermal sources, hot rock formations that contain insufficient natural geofluid for economic production and popularly called "hot-dry rock" (HDR). Work in the project has proceeded in two major phases. In the first phase, the project was focussed upon confirming experimentally the feasibility of the HDR heat-energy extraction technique proposed by Los Alamos. That technique, illustrated by Fig. 1, involves artificial introduction of water into, and closed-loop circulation through, a man-made geothermal reservoir created by hydraulic fracturing at depth of the hot, low-permeability rock between two boreholes. In addition to the deep geothermal reservoir the closed loop includes a surface system with pumps and heat dissipation equipment. This was

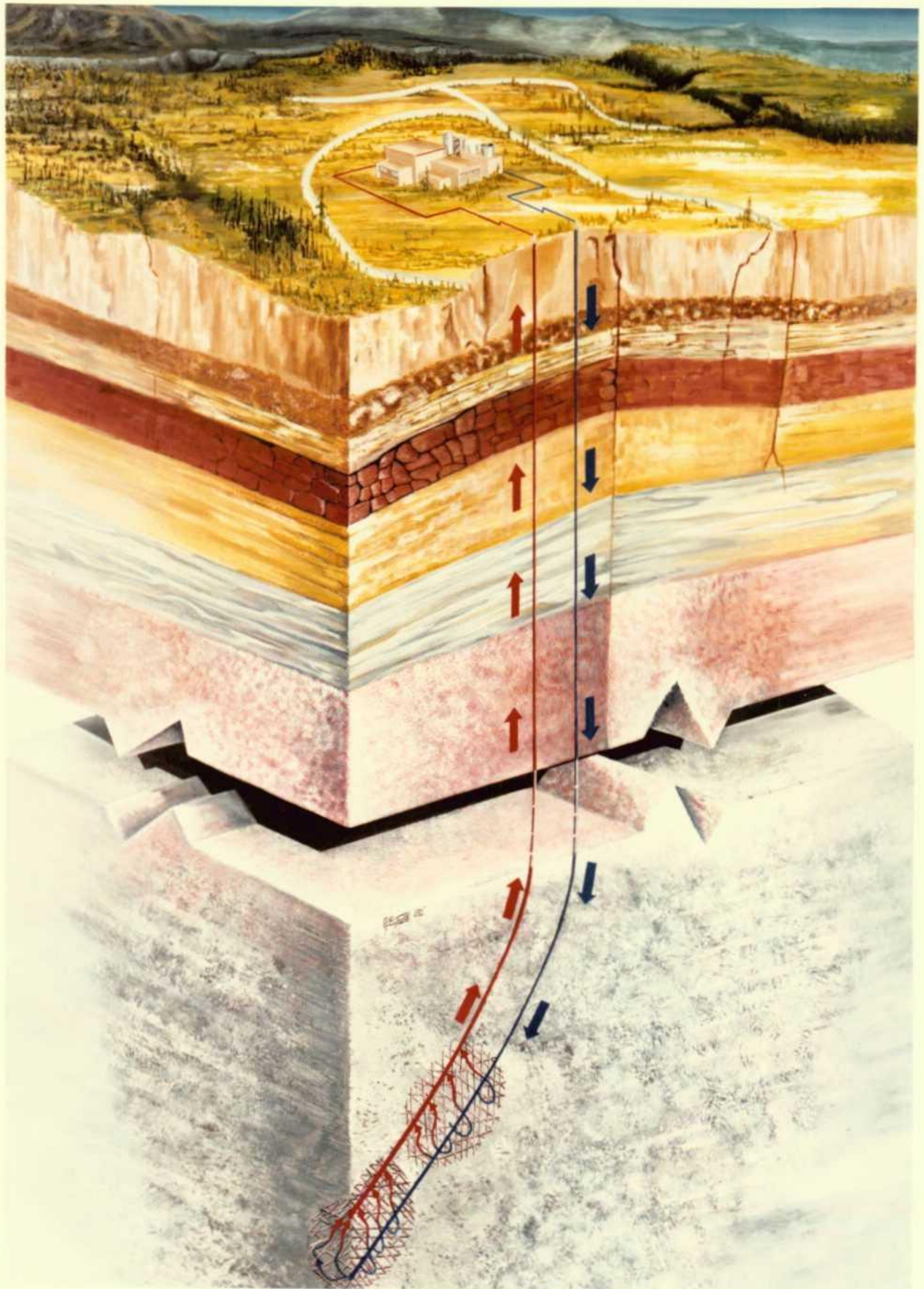


FIGURE 1. HOT DRY ROCK CONCEPT

LOS ANGELES  
CNB3 1631

successfully accomplished in the 1977-1981 period using a small "research" reservoir, created at a depth of about 9840 ft (3 km) in 180°C rock and operated for short periods of time at a nominal energy extraction rate of 5 thermal megawatts. The two lower curves in Fig. 2 show the verification of performance of the research reservoir in its initial, and subsequently enlarged, configurations. With that success, the HDR Program was expanded in 1978 to include activities other than the Fenton Hill Project. Those activities, since completed as shown in Fig. 3, consisted primarily of evaluating the United States HDR resource, together with some preliminary economic, environmental and other relevant institutional studies.

Meanwhile, the second phase of the Fenton Hill Project continues as planned. This phase is dedicated to the development of commercially usable technology for the creation, control and useful-life assessment of a reservoir more nearly representative of an industrial application. This is being accomplished with a larger "engineering" reservoir, presently under construction, at a depth of about 14 760 ft (4.5 km) in 300°C rock. In its final configuration, the engineering reservoir is expected to have a performance characteristic at least as good as the upper curve in Fig. 2 and produce a nominal 35 MW<sub>t</sub> of power.

The Fenton Hill Project serves a dual purpose: first, as the HDR energy extraction development per se, and secondly, as a field laboratory for development and testing of special materials, drilling- and fracturing-related equipment, downhole instrumentation, and reservoir interrogation techniques essential to the technology.

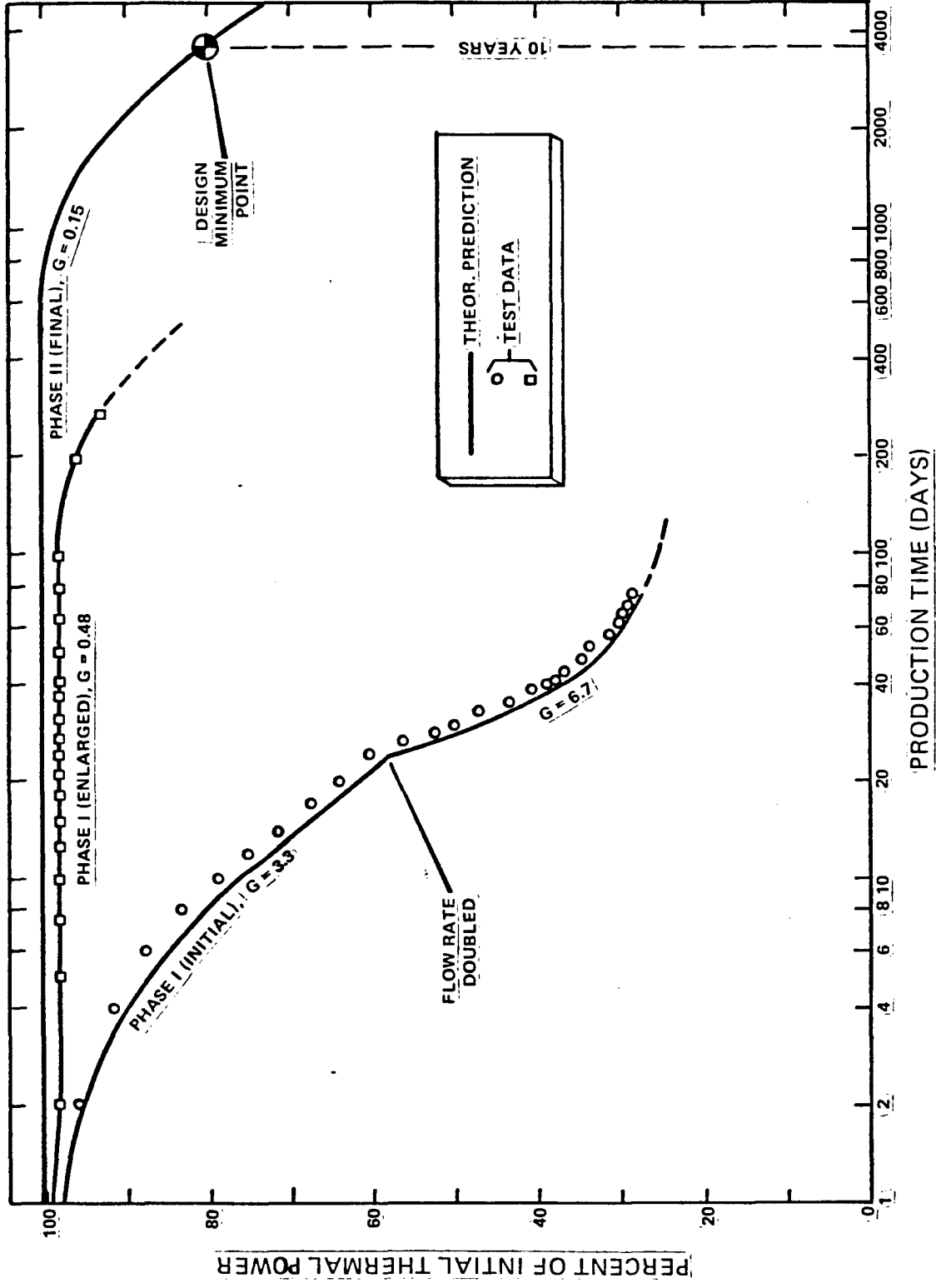


FIG. 2. RESERVOIR THERMAL DRAWDOWN PERFORMANCE CURVES UNDER CONSTANT LOADING  
 (Reservoir Loading Parameter,  $G$ , = Circ. Mass Flow/Effective Area,  $\text{kg/hr-m}^2$ )



### III. FENTON HILL PROJECT STRUCTURE

#### Research System (Phase I)

The research reservoir, accessed through wells EE-1 and GT-2, was established in its initial configuration in 1977 and enlarged to its present configuration in 1979. This reservoir was used to: (a) demonstrate initial technical feasibility; (b) provide short-term information on predictability of drawdown, time-variation of impedance, water loss rate, geofluid chemistry, and stop/start transients; (c) serve as a test bed for evaluation of reservoir enhancement techniques, such as operation under various back pressure and flowing conditions; (d) evaluation of high-risk/high-payoff reservoir-extension workover techniques and (e) conduct a small preliminary electric generation experiment.

This work was completed in mid-1981. While no further major operations are planned in the research system, the EE-1 and GT-2 wells are available for occasional use as laboratories for in situ field testing of downhole instruments and equipment, and as listening stations for emplacement of microseismic instrumentation during fracturing and other operations in the Phase II system.

#### Engineering System (Phase II)

Construction of the Phase II system was initiated in parallel with completion of the Phase I system testing, as indicated in Fig. 3. This effort consists of completing the construction and testing of the engineering reservoir, spanning the period through FY 1987, followed by a six-month period for shutdown and restoration of the test site and for final documentation of the HDR Program.

The primary objective of the Phase II effort is to demonstrate creation and control of a multiple-fracture reservoir with extended longevity by

creating a larger system (35+15 Mwt) with a projected life in excess of 10 years. A third well, EE-2, was completed in FY 1980 to a vertical depth of 14 750 ft (4.4 km) and a bottom-hole temperature of 327°C. This well will serve as the injection well for the Phase II system. A fourth well, EE-3, was completed in FY 1981 to a vertical depth of 13 120 ft (4.0 km) and a bottom-hole temperature of 286°C. Using these wells, the engineering reservoir will be constructed.

In December 1983 and during the spring and early summer of 1984 a series of hydraulic fracture experiments were carried out in wellbores EE-2 and EE-3 to establish a fracture connection between the wells. Results of these experiments have indicated that a very large underground reservoir has been established but that a very limited, if any, connection has been established between the wellbores.

The next step will be to contract for a large workover rig to possibly redrill EE-3 into the large fracture area extending from deep in EE-2 and develop a satisfactory flow connection between the two wells to establish the Phase II reservoir configuration. Due to funding restrictions this operation will start in the spring of 1985.

Design and construction of the Phase II surface system will begin in parallel with establishment of the final-configuration reservoir. Long-lead procurements will be initiated early, including high-pressure, remotely-operated valves, air-cooled heat-exchanger units, and additional circulation pumps, if required. Construction of the surface system will begin in the first quarter of FY 1986 and is scheduled to be completed in the last quarter of FY 1986. The installation will be designed such that most of it, other than air-cooled heat rejection units, is configurationally representative of an industrial pilot plant application. Upon completion of

construction, the Phase II loop will be activated for a protracted energy-extraction test. Testing of the Phase II reservoir will continue for about one year beyond this point, into the last quarter of FY 1987. After an extended period of continuous operation, it is expected that assessment of the minimum reservoir lifetime will be possible.

Careful environmental surveillance will continue throughout Phase II, particularly for possible seismic and hydrologic effects. This effort will not only ensure protection of the Fenton Hill environment, but also provide a documented case history for use in future environmental analyses, assessments, and impact statements.

#### Technical Supporting Activities

Of paramount importance to the Phase II Fenton Hill site operations is a group of ongoing scientific and engineering support activities. These include:

- Theoretical analysis, data processing, and modeling. This includes not only analysis of data on the characteristics and behavior of the existing Fenton Hill system but also predictions concerning hot dry rock geothermal systems in general.
- Laboratory studies, including rock properties measurements, chemical analyses, and simulations. Determination of physical and mechanical properties and heat transfer and fracturing behavior of reservoir rocks is essential to understand and model reservoir behavior.
- Chemical studies of rock-water interactions. Both laboratory and field experiments are needed to anticipate and solve scaling, plugging and corrosion problems.
- Physical modeling to investigate such things as thermal stress cracking and fluid flow in irregular geometries.

- Instrumentation development. Improved equipment and techniques are needed to map reservoir fracture systems and determine reservoir properties. During the Phase II effort, the key diagnostic instruments developed in Phase I will be thermally upgraded to contend with the engineering reservoir's higher temperatures and pressures. In addition, a high-temperature borehole acoustic televiewer (BAT) will be developed for joint and fracture mapping, and a biaxial extensometer (BAE) will be constructed for studying changes in intrawellbore strain patterns.
- Regular calibration and maintenance of both downhole and surface instrumentation will continue to assure accurate, reliable test data. Replacement high-temperature instrument cables will be procured, quality-tested and mounted, as necessary.
- Thermochemical tracer methods will be developed, and calibrated against positive thermal drawdown data, to provide a relatively rapid and routine method of assessing accessible reservoir size.

#### IV. FENTON HILL PROJECT - ENVIRONMENTAL DESCRIPTION

##### A. Geology and Geomorphology

The project site is a part of the southern extension of the Rocky Mountains that lies between the structural features of the San Juan Basin to the west and the Rio Grande Depression to the east. For site location see Fig. 4.

Precambrian rocks of granite and gneiss outcrop along the flanks and crest of the Nacimiento Mountains. These are overlain by Pennsylvanian and Permian limestones, sandstones, and shales. The Cenozoic volcanic rocks form the upper surface of the Jemez Plateau overlying the Permian, Pennsylvanian, and Precambrian rocks.<sup>[2]</sup>

During and after the drilling of the first two deep holes at the Fenton Hill site petrologic, geochemical, and geophysical logging investigations were performed. A detailed lithologic log was constructed from these results.

Drill hole GT-2 initially penetrated to a depth of 9613 ft (2.93 km). The upper 2395 ft (0.73 km) consisted of Cenozoic and Paleozoic rocks; 7218 ft (2.20 km) of Precambrian rocks were drilled. GT-2B, the drill hole eventually used in the Phase I system, was a kick off reaching TD of 8924 ft (2.72 km). GT-2B has a 9 5/8 inch borehole with 7 5/8 inch casing to a depth of 8661 ft (2.64 km).

Drill hole EE-1 was drilled to a TD of 10,039 ft (3.06 km). This also has an open borehole of 9 5/8 inch with 8 5/8 inch casing to 8629 ft (2.63 km) and 7 5/8 inch casing to 9613 ft (2.93 km). In both EE-1 and GT-2B a 10 3/4 inch intermediate casing extends from the surface to well into the granitic rocks.

---

[2] W.D. Purtyman, Geology of the Jemez Plateau west of Valles Caldera, LA-5124 MS, February, 1973.

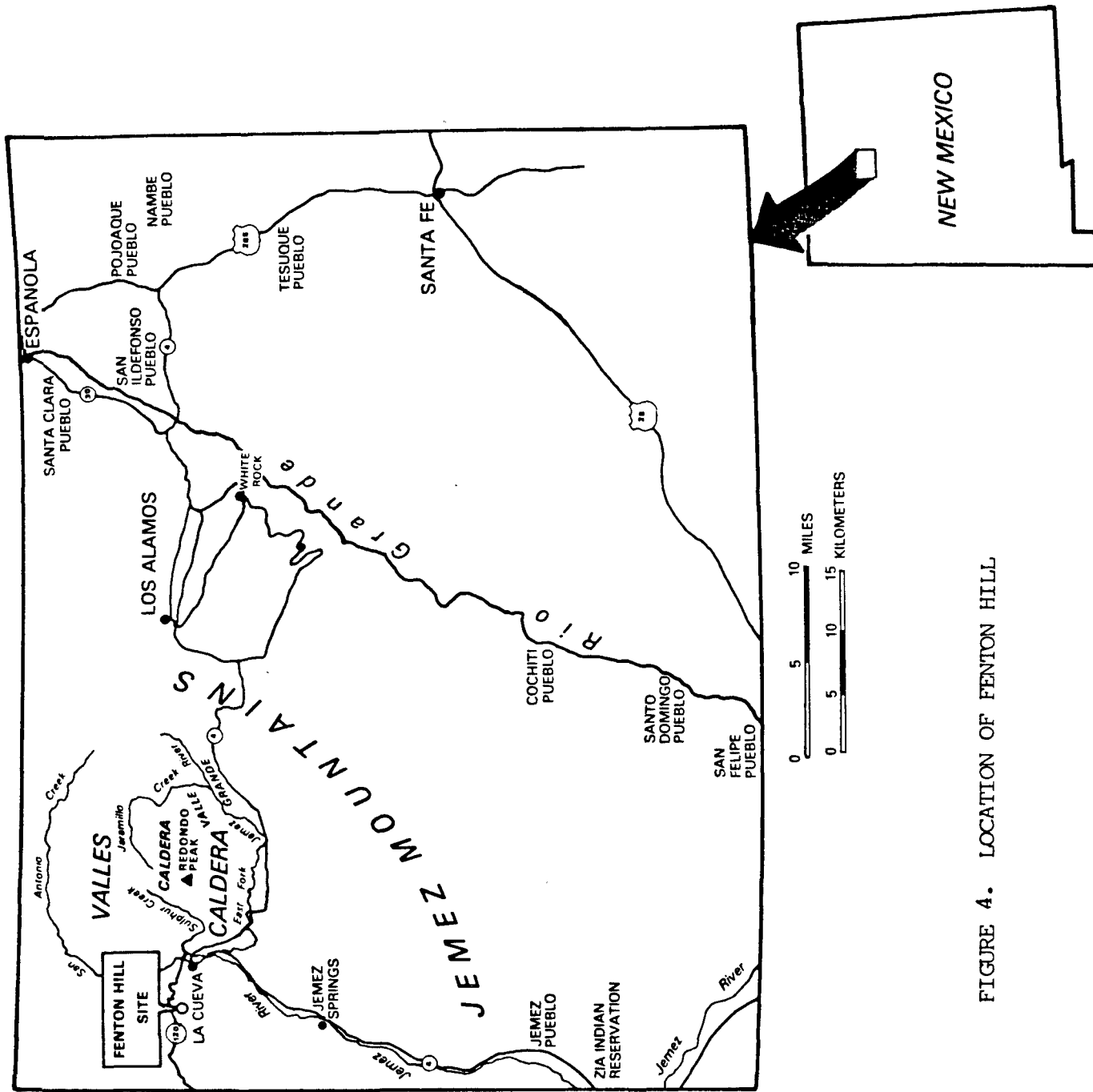


FIGURE 4. LOCATION OF FENTON HILL

Drill holes EE-2 and EE-3 were extended somewhat deeper than GT-2 and EE-1 in order to reach higher reservoir temperatures for the Phase II system. EE-2 is 8 3/4 inch open hole section to TD of 15 289 ft (4.66 km). The 9 5/8 inch casing extends to 11 581 ft (3.53 km) and the 13 5/8 inch intermediate casing has a set point at 2592 ft (0.79 km).

The EE-3 hole was drilled to a TD at 13 943 ft (4.25 km). The openhole section is also 8 3/4 inch diameter. 9 5/8 inch casing extends to 10 794 ft (3.29 km) and the 13 5/8 inch intermediate casing set point is 2559 ft (0.78 km).

Completion details for the four major wellbores at Fenton Hill are provided in Appendix D. The geology of the Jemez Plateau and a study of the geothermal system of the Jemez Mountains are part of Appendix C.

#### B. Climate and Surface Hydrology

The site is located on the Jemez Plateau, which is a part of the western arm of the Rocky Mountains that extends into northern New Mexico from southern Colorado. The surface of the plateau is formed by volcanic ash extruded during the volcanic activity that produced the Valles Caldera.

The altitudes of mountains bounding the Jemez Plateau on the east and west range from about 10 000 ft at the westernmost dome in the caldera (San Antonio Mountain) to a little over 9000 ft along the crest of the Nacimiento Mountains. The major drainage in the area is the Rio Cebolla and Jemez River, with its tributary, San Antonio Creek. The experimental site is on the plateau between the Rio Cebolla and San Antonio Creek. A high ridge along the western part of the plateau is parallel to San Antonio Creek. Otherwise the surface of the plateau slopes gently downward to the west and southwest. The altitude of the area ranges from 8000 to 9000 ft along the crest of the ridge

to about 7000 to 8000 ft where the plateau terminates in steep slopes or cliffs above the Rio de Las Vacas. The plateau surface is cut into a number of mesas by southwest-trending streams.

The average annual precipitation in the area is estimated to range from about 14 inches (36 cm) at lower elevations to about 22 inches (56 cm) in the mountains. Average annual air temperatures range from 40 to 50°F.

The high mountain slopes are forested mainly with ponderosa pine and some fir and spruce. Groves of aspen and live oak are found in the higher canyons, with some willow and poplar along the streams at the lower elevations. About 5000 acres of the forest, west of La Cueva and south of State Road 126, were burned in a forest fire in 1971.

### C. Hydrology

The upper surface of the Fenton Hill site is formed by the Bandelier Tuff which, in turn, is underlain by the Paliza Canyon Formation and Abiquiu Tuff.

The volcanic aquifer is within the Abiquiu Tuff and lower part of the Paliza Canyon Formation. The aquifer is underlain by the Abo Formation that perches the aquifer in the volcanics.

The Bandelier Tuff is a series of ashflows of moderately welded to welded rhyolite tuff. The tuff ranges from light to dark gray and consists of quartz and sanidine crystals with crystal and lithic fragments of latite and rhyolite in an ash matrix. The thickness at the site is about 50 ft (15 m).

The Paliza Canyon Formation underlies the Bandelier Tuff. The formation is composed of andesite and basalt andesite breccias that are interbedded with sand and gravels. The thickness at the site is about 310 ft (94 m). The Abiquiu Tuff underlies the Paliza Canyon and is composed of a light gray, friable tuffaceous sandstone. The sandstone is composed of quartz, chal-

cedony, and fragments of the rhyolite and quartzite in a tuffaceous matrix. The upper part of the section is interbedded with angular fragments of basalts. The lower part contains rock fragments and pebbles derived from Precambrian crystalline rocks. The thickness of the Abiquiu Tuff is about 90 feet (27 m) at the site.

The Abo Formation underlying the Abiquiu Tuff is composed of clay, shale, siltstones, fine-grained sandstones and some thin lenses of limestone. The Abo Formation is relatively impermeable.

The upper surface of the Abo Formation had been fluted and dissected by erosion before the deposition of the volcanics. These erosional channels in the Abo, which were subsequently filled with volcanic debris, comprise the aquifer that has supplied water to the site. The amount of storage in this aquifer is determined mainly by the width and spatial extent of the channels. Topographic highs of the Abo surface limits the aquifer's thickness and lateral extent, and will "disconnect" portions of the aquifer where the Abo surface is above the saturated section.

Generalized contours on the top of the Abo Formation in the area of Fenton Hill indicate the formation dips to the southwest at about 80 ft/mi. The general movement of water is toward the southwest where a series of springs and seeps discharge from the volcanics into the middle and lower reaches of Lake Fork Canyon.

The depth to the top of the aquifer at the site is about 370 ft (113 m). Water level measurements in observation wells in the immediate area of the site indicate that the water table is near flat. [3]

---

[3] N. M. Becker, W. D. Purtymun, W. C. Ballance, Aquifer Evaluation at Fenton Hill, October and Movember, 1980, LA-8964-MS, October 1981.

Further details on the hydrology of the site are provided in Appendix B.

#### D. Water Quality

Water quality data have been collected from established surface and ground water stations and from ponds and pond discharge at Fenton Hill Site located in the Jemez Mountains as part of a continuing program of environmental studies. Most of these stations were established in 1973 with water quality data having been collected since that time. There have been slight variations in the chemical quality of water from the surface and ground water locations; however, these variations are within normal seasonal fluctuations. The discharge from ponds at Fenton Hill infiltrates into alluvium of the canyon within 1310 ft (400 m) of the site. Monitoring of surface and spring discharge down gradient from the ponds failed to detect any effects resulting from release of water from the ponds. There has been an increase in total dissolved solids and calcium in water from Well FH-1 which furnishes the water supply for the site. This is probably due to the decreasing water level in the well resulting in yield from beds with a slightly different quality than found in previous yield. [4]

Appendix A of this plan provides a complete report on the water quality in the vicinity of Fenton Hill.

---

[4] Water quality in the vicinity of Fenton Hill, 1981, 1982, (Draft) Los Alamos National Laboratory.

Under this proposed  
plan will there  
be any discharges  
to the environment?  
No - Sep. 30

## V. FENTON HILL PROJECT - PROJECT DESCRIPTION

### A. Location and Facilities

The Fenton Hill Geothermal site is located in the Jemez Mountains of north central New Mexico. It is about 35 miles (55 km) west of Los Alamos and 10 miles north of Jemez Springs. The U.S. Public Land description is NE 1/4 Sec. 13, T19N, R2E, New Mexico Principal Meridian, and the coordinate location is 1,776,000 N, 374,000 E, New Mexico State Plane grid (Central Zone). The developed and fenced site, comprising 7.13 hectares (17.63 acres) lies within the west half of the Santa Fe National Forest. Because of its location well above nearby streams on top of a narrow (1/2 mile wide) ridge no site flooding danger exists and local runoff is diverted from the developed area.

Access to the site is primarily by State Road 4 and State Road 126 from the Los Alamos/Santa Fe area and State Roads 44, 4 and 126 from the Bernalillo/Albuquerque or Farmington areas. The research program continues throughout the year and access is maintained to the site at all times. Laboratory staff, contractor personnel or security people are at the site full time. The geothermal test area is not a classified area and is fenced and gated only for protective purposes and admission can be readily obtained for all official visits by checking in at the operations-shop building at the west entrance.

A general location map is shown as Fig. 4. The topographic map of the immediate area with one-foot contour interval and an enlarged site plan is provided as Appendix F.

## B. Geothermal System

In the geothermal operations at Fenton Hill there is no task or activity planned with a scheduled effluent discharge. However, there is the possibility of accidental or emergency discharge of liquid that could exceed the limits established by the Water Quality Control Commission. The Discharge Plan addresses this situation.

In FY 1985 the workover operations for redrilling and development of the deep underground energy reservoir will be carried out. In FY 1986 and FY 1987 the experimental operation of the energy extraction system is the major activity. This system consists of the deep fractured reservoir, the injection and extraction wellbores and the closed loop surface piping. Flow rates will vary from 100 to 400 gpm at pressures to 5000 psi. Fluid loss rates in the reservoir should be low. Charging and make up water will be provided from the 5.7 M gal reservoir. Failures in the closed loop section are possible and could require venting of part or all of the system. For limited venting the 1 M gal service pond would be utilized. For more capacity the 5.7 M gal reservoir would be used. In either case the vented fluid would be utilized to reactivate the system and would be stored only temporarily.

The critical components in this effluent control system are the 5.7 M gal water reservoir and the 1 M gal service pond. The large reservoir was completed in 1982 and has been filled for the fracture pumping now underway. As built drawings and specifications for this reservoir are provided as Appendix E.

### C. Water Supply System

The water supply for Fenton Hill is furnished by a well completed at a depth of about 449 ft. (137 m) into a perched aquifer. The aquifer is in the Abiquiu Tuff and is perched on clays and siltstones of the Abo Formation. The aquifer is of limited extent, being terminated to the east along the canyon cut by San Antonio Creek. The movement of water in the aquifer is to the southwest, where a part is discharged through seeps and springs along the lower reach of Lake Fork Canyon and the Rio Cebolla.

The supply well, FH-1, was completed in November 1976. Cumulative production from the well since 1976 through 1982 has been  $117.7 \times 10^6$  gal. Average monthly water levels were compiled for supply well FH-1 and wells FH-2 and FH-3. All three wells are completed in the same aquifer, the Abiquiu Tuff. Since 1976 through 1982 the water level in FH-1 has declined about 8.9 ft (2.7 m) from production to supply the site. Pumpage has exceeded recharge to the aquifer.

*where  
are  
wells  
on  
drawings*

Calcium and bicarbonate are predominate ions in water from well FH-1. There has been little, if any, change in bicarbonate from 1976 through 1982. There has been some variation in calcium concentration from 1976 through 1980; however, the variations have shown a general increase during this period.

The water supply system, in addition to the FH-1 well is made up of a pressure tank and a distribution system to furnish domestic water to the shop-office facility and several residential type trailers on the forest land near the site.

D. Waste Products Produced

The circulating fluid in the geothermal loop at Fenton Hill will contain elements and ions dissolved from the granodiorite by the water placed into the system. Because the temperature is rather high, up to 315°C (600°F), there will be changes in the solubility of the minerals. The solubilities may increase or decrease as the temperature rises. However based on our past experience we anticipate that the concentrations of the various dissolved minerals will not generally exceed the following inorganic species:

$S_iO_2$	800 ppm	
$Na^+$	1000 ppm	
$K^+$	150 ppm	
Ca	50 ppm	~ 3600 TDS
$HCO_3^-$	600 ppm	
$H_2S$	10 ppm	
$SO_4$	300 ppm	
$F^-$	5 ppm	
As	5 ppm	
Ba	30 ppm	
Cr	1 ppm	
CN	0.02 ppm	
$PB^{--}$	0.1 ppm	
$NO_3^-$ as N	0.1 ppm	
$Se^{--}$	0.02 ppm	
$Ag^+$	0.03 ppm	
$Cl^-$	1500 ppm	
? $Ca$ $Cu$	0.03 ppm	
Fe	15.00 ppm	

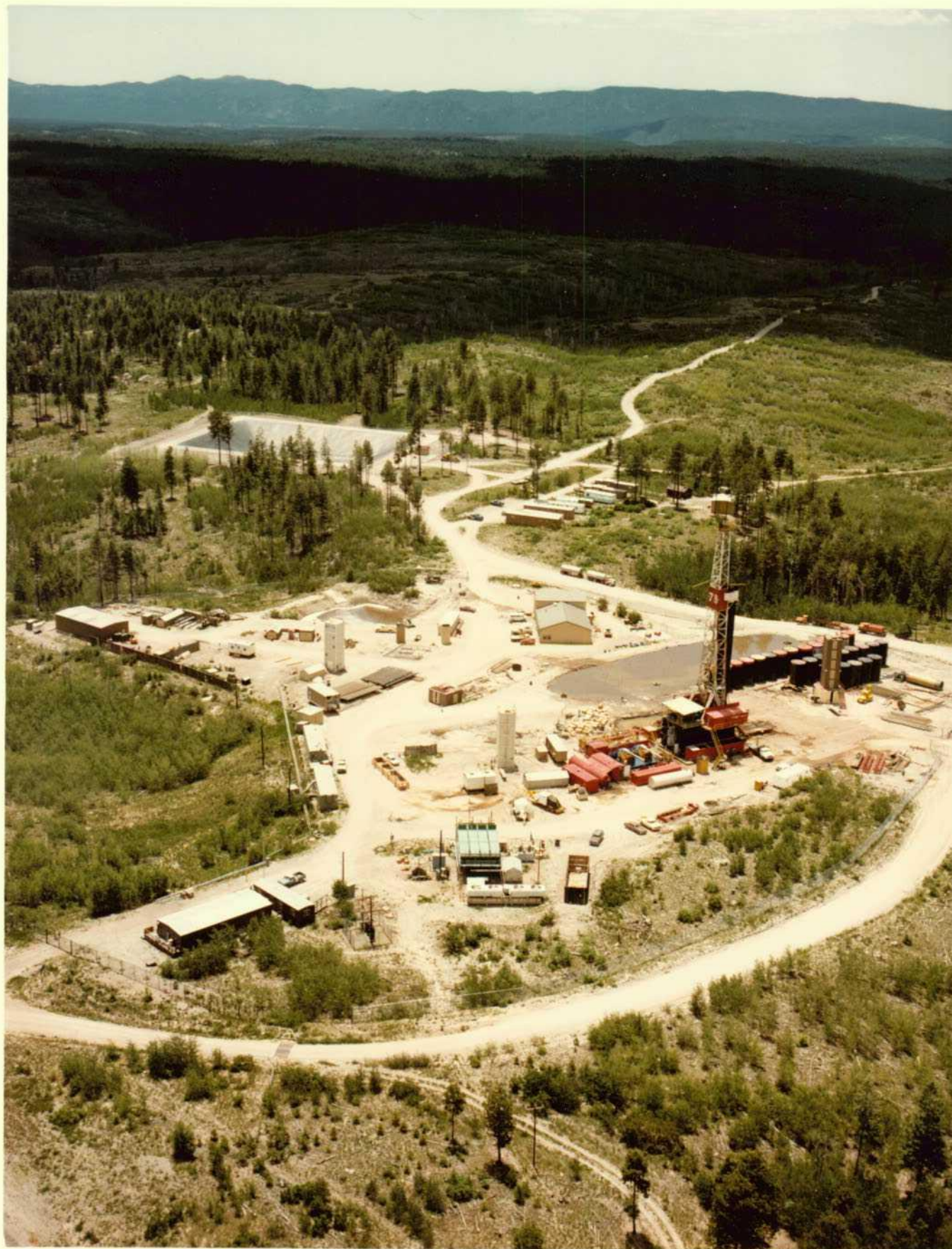


FIGURE 5.  
AERIAL VIEW OF FENTON HILL

TOP RANGE  
RNS2033074

Mn 0.75 ppm  
 Zn 0.5 ppm  
 B 30 ppm

We do not anticipate organic materials except perhaps some oil or grease from pumps and other equipment in the system.

The average concentration of these elements or ions or molecular species should be much lower than the values listed above.

The above expected maximum concentrations are based on analyses performed at Los Alamos National Laboratory. Copies of many of these analyses are in Appendix A.

Some of these ions, elements and molecular species may have come from drilling operations. Almost all of the analyses cited in the appendices were performed during 1982, a year in which drilling operations were being carried out. Since the drilling operations will be completed in FY 1985 and are not anticipated during the operation of the loop it may be that some of the estimated maximum concentrations are high. Concentrations may become higher or lower as we circulate because of changes in downhole temperatures and in flow rates.

Solid wastes consist of materials used in development of the downhole geothermal system. These include lubricating muds, cementing wastes, and chemicals used for treatment purposes. The following is a composition analyses of the material in the bottom of the service pond:

Element	<u>HSE-7 Lab</u>		<u>ESS-1 Lab</u>	
	Conc. ppm	Error ±ppm	Conc. ppm	Error Std. Dev. ppm
Ag	3.69	0.64	0.4	0.4
Al	6781	764	14500	100

*Existing?  
Where  
Located?*

*which one*

Element	<u>HSE-7 Lab</u>		<u>ESS-1 Lab</u>	
	Conc. ppm	Error ±ppm	Conc. ppm	Error Std. Dev. ppm
As	0.346	0.086	210	20
B			416	5
Ba	2003	108	16700	200
Ca	13600	360	16900	700
Cd	39.4	4	0.8	0.4
Cr	174.	81	29.3	0.4
Co			3.2	0.4
Cu	272	9.6	372	1.0
Fe	2357	448	13600	400
H <sub>2</sub> O			280000	Dried at 90°C
Hg	460	380		
K	2737	26	14100	800
Li	105	2.2	169	8
Mg	9906	91.	2720	400
Mn	434	12	600	40
Na	5175	78	19200	400
Ni			18	1
Pb	16327	26.33	340	20
Sc	0.74	0.04	Not detected	
Sr			112	4
Zn	270	19	304	12

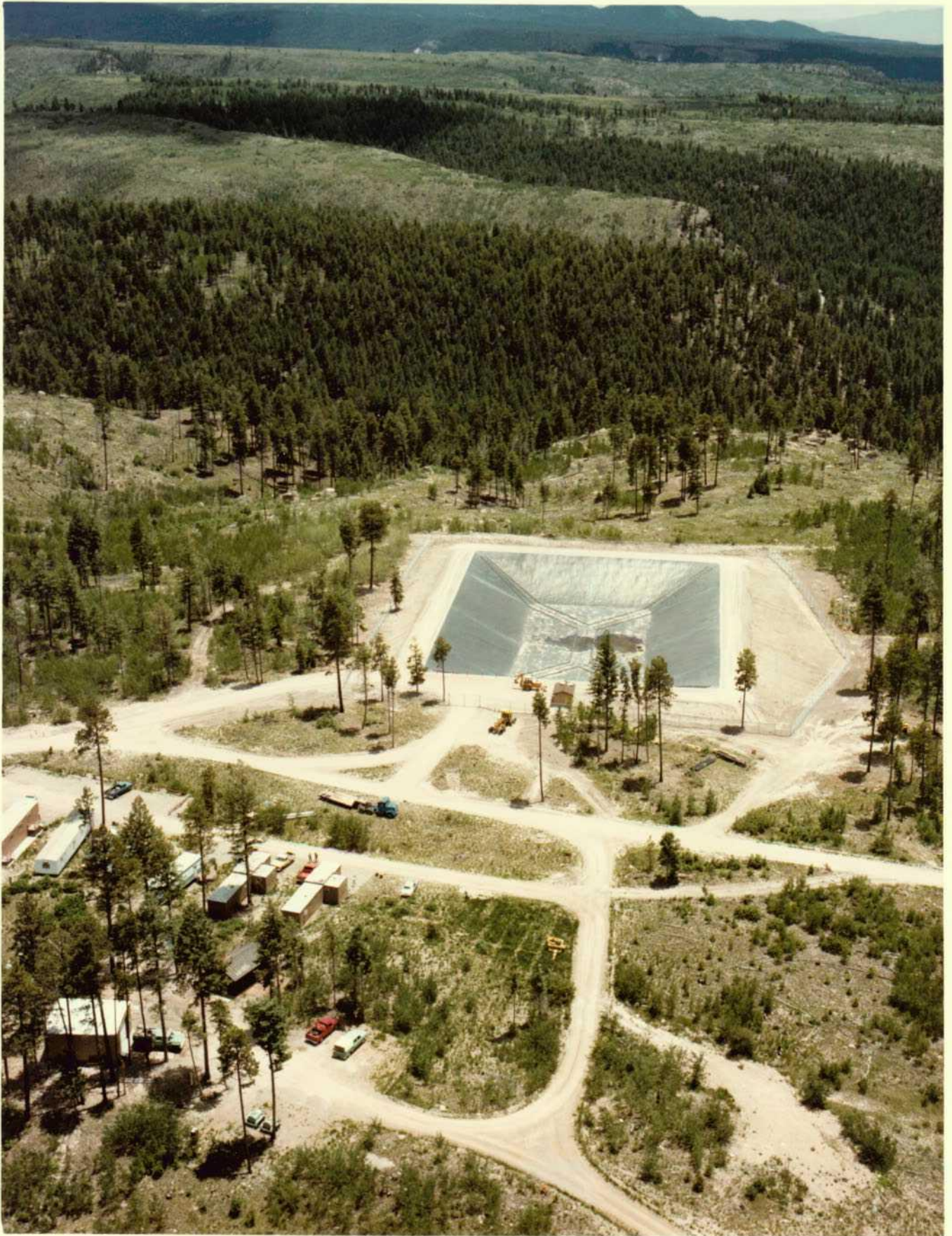


FIGURE 6.  
AERIAL VIEW OF 5.7 M GAL POND

RM 2033077

## VI. PRESENT DISPOSAL PRACTICES

### A. Drilling and Workover Operations

The service ponds at the Fenton Hill site were developed to support the drilling operations, first to establish the Phase I system above two deep holes about 10 000 ft (3 km) completed in dry Precambrian granitic rock, and finally in the Phase II system where two holes were completed to a depth of 14 000 to 15 000 ft (4.5 km) to develop a system at a higher temperature.

These drilling operations have used chemical additives (drilling mud) and cement resulting in fluids high in sodium, calcium, sulfate, and chlorides. Drilling fluids and water from the circulation loop have been stored in two ponds at the site. Periodically these ponds have been drained into the adjacent dry canyon when additional storage is needed. The water, under controlled discharge, is lost to evapotranspiration or infiltration into the alluvium and underlying tuff within 13 100 ft (4 km) of the outfall from the lower pond.

The large 5.7 M gal water storage pond was completed at the site in the fall of 1982. The pond has been constructed in accordance with the "as-built" drawings provided as Appendix E.

A heavy "Hypalon" lining is provided to prevent water seepage and a cover to reduce evaporation loss. The enclosing berm contains a reinforced concrete core as anchor for the liner and cover and provides for a maintenance roadway 14 ft (4.5 m) wide, 3 ft (1 m) above the maximum water level.

The subliner drainage system, comprised of a system of perforated drain lines in gravel filled trenches provides for easy detection of any minor breach in the liner.

GT 2  
↑

With the completion of the 5.7 M gal storage reservoir, no further storage limits are anticipated. Of the two service ponds at the site the lower pond is partially empty and unused except as an overflow from the upper EE-2/EE-3 pond. This configuration will be maintained through the present workover operations expected to last most of the summer and through the workover period in 1985.

After then?

B. Sanitary Sewage System

The sewage system at the Fenton Hill site was designed and constructed under contract to the U.S. Forest Service. The disposal system, septic tank and field, are located on Forest Service land and maintained by the Forest Service.

On the geothermal site the only connection to this system is the sanitary waste from the shop-office building. This waste is collected in a sump and pumped to the disposal line near the trailer area. By agreement with the Forest Service the DOE/Los Alamos Laboratory is responsible for the maintenance and operation of this pumping station and immediate collection lines. Disposal is the responsibility of the Forest Service.

The principal use of the sanitary sewage system is servicing the small residential trailer area on Forest Service land near the geothermal site. Seven trailer slots and two service buildings are located here. Operation is by the U.S. Forest Service with shared use of the trailer hook-ups.

C. Garbage and Trash Disposal

*only?* Garbage and trash from the geothermal site are disposed of in the landfill site serving the town of Jemez Springs. Disposal is made at the site under permit from the Santa Fe National Forest Service (Use Permit #2723). This

landfill site is about seven miles south of Jemez Springs and 17 miles from the Fenton Hill Project.

Under DOE approved contract CJC Inc., La Cueva, NM provides maintenance and some construction services to the Los Alamos Laboratory Geothermal Operations at Fenton Hill. As part of this service CJC collects the garbage and trash from Fenton Hill on a weekly basis and hauls it to the Jemez Springs landfill site. Jemez Springs officials are responsible for proper burial of the trash and maintenance of the disposal site.

## VII. PROPOSED DISCHARGE PLAN

### A. Proposed Disposal of Solid and Liquid Waste

In the geothermal operations at Fenton Hill there is no task or activity planned with a scheduled effluent discharge. However, there is the possibility of accidental or emergency discharge of liquid that could exceed the limits established by the Water Quality Control Commission.

Under the drilling and workover activities workover operations presently scheduled in FY 1985 will consist of re-drilling and pumping experiments in the open wellbore sections of the deep underground reservoir area to establish connections between the system pair of wellbores. Water for the re-drilling will be circulated from the 1 M gal EE-2/EE-3 pond. Water for the charging and makeup will be held initially in a 5.7 M gal lined reservoir on the 15 acre site. If cycling or venting of this fluid is required during or after pumping, the open 1 M gal pond adjacent to the pair of wells will be utilized for temporary holding.

In FY 1986 and FY 1987 the experimental operation of the geothermal system is the major activity. This system consists of the deep fractured reservoir,

*No venting as was done in '81*

*Where Located?*

the injection and extraction wellbores and the closed loop surface piping. Flow rates will vary from 100 to 400 gpm at pressures to 5000 psi. Fluid loss rates in the reservoir should be low. Charging and make up water will be provided from the 5.7 M gal reservoir. Failures in the closed loop section are possible and could require venting of part or all of the system. For limited venting the 1 M gal service pond would be utilized. For more capacity the 5.7 M gal reservoir would be used. In either case the vented fluid would be utilized to reactivate the system and be stored only temporarily.

The critical components in this effluent control system are the 5.7 M gal water reservoir and the 1 M gal service pond. The large reservoir was completed in 1982 and has been filled for the fracture pumping now underway. As built drawings for this reservoir are provided as Appendix F.

This 5.7 M gal reservoir has a heavy "Hypalon" lining, field assembled from many sections. Experience to date indicates a small leak rate that varies from 0 to 2 gpm depending on the water volume in the reservoir. This leakage is collected in the subliner drainage system to be picked up by a 5000 gal tank to be installed at the drain line exit. A pair of electric pumps will return the water over the berm to the reservoir. This installation is to be completed in the summer of 1984 prior to the next major workover operation.

The service pond has been used as a drilling pond for the EE-2/EE-3 pair of deep wells. It has been cleaned since the last drilling and now serves as a cycling pond for the fracture pumping. This pond presently has a clay liner but only limited capability exists to examine the integrity of the pond. During operation of the geothermal loop it may become necessary temporarily to

*details*

*Reservoir  
completed  
in 1982  
has been  
drilled  
system  
out of  
pilot  
well  
test  
etc.*

discharge the circulating water into this pond. To prevent the loss of this water and to avoid if possible mixing it with the fresh water supply in the existing five million gallon storage pond it is proposed to modify this 1 M gal service pond to serve as a retaining pond.

At present it appears that the circulating water in the geothermal loop may contain amounts of various elements such as Li, B, F, and As (see Appendix A). The plan is to circulate the water and to retain it in the loop where these elements will reach some equilibrium value. As long as the water is in the loop these elements are of little or no consequence. However, it may be necessary during operation of the geothermal loop to empty or partially empty the loop. The water from the loop must be stored temporarily until it can be reinjected into the loop. During the temporary storage it would be desirable to avoid contaminating the fresh water supply and it is necessary to make certain that the water does not enter an aquifer.

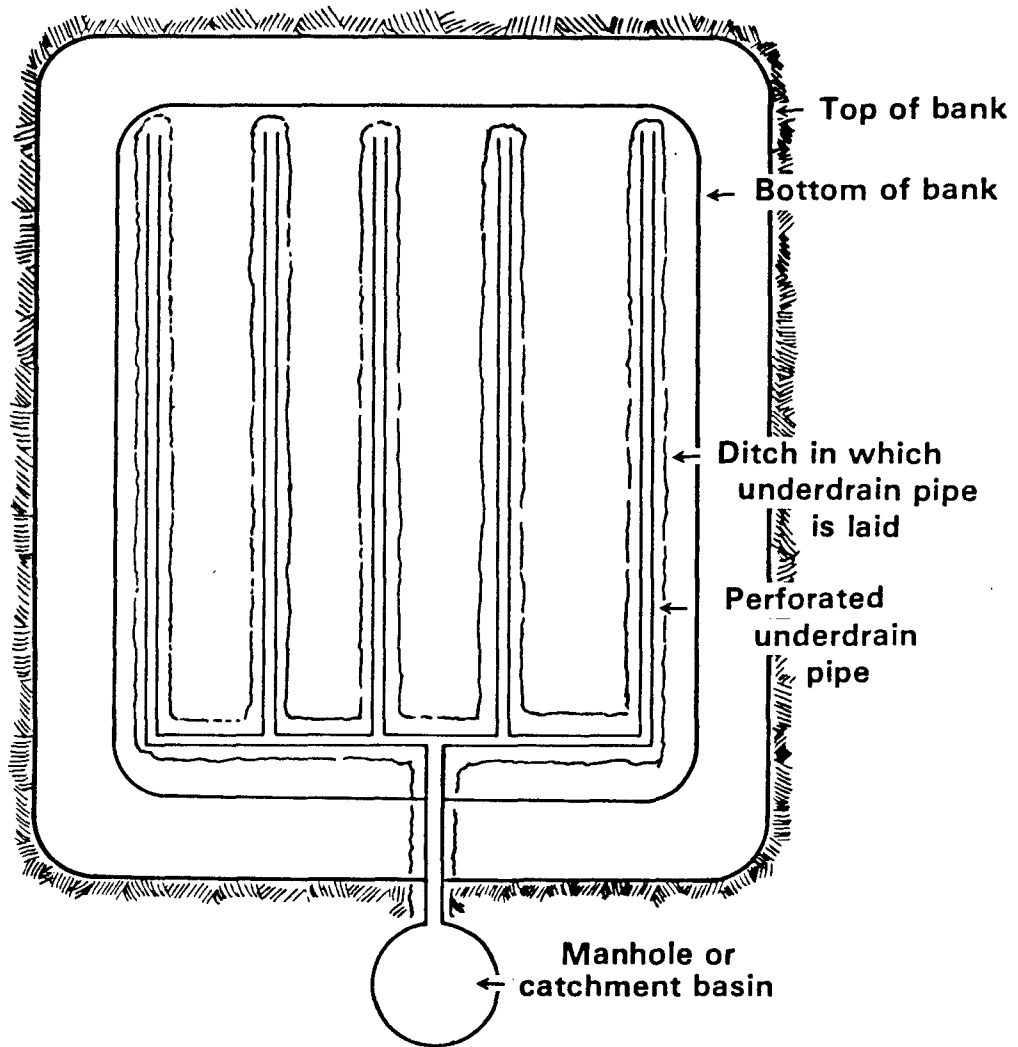
A general plan for a retaining pond is shown in Fig. 7. This pond will hold about one million gallons. The bottom of the pond will consist of a soil clay mixture designed to be impervious to the water. Beneath the impervious layer there will be a pervious layer of gravel and sand and in this pervious layer will be a collection system consisting of perforated pipe. The discharge from the collection system will be into a manhole or catchment basin. The manhole or catchment basin will be monitored to determine whether the impervious layer at the bottom of the pond is indeed impervious.

Another feature of the pond may be some pieces of casing or drill pipe placed so as to prevent destruction of the underdrainage system in case the pond needs cleaning.

To summarize; the retaining pond would ordinarily be empty. During maintenance operations the water from the loop would be temporarily stored in the

*erosion control when empty?*

### Plan



### Cross Section

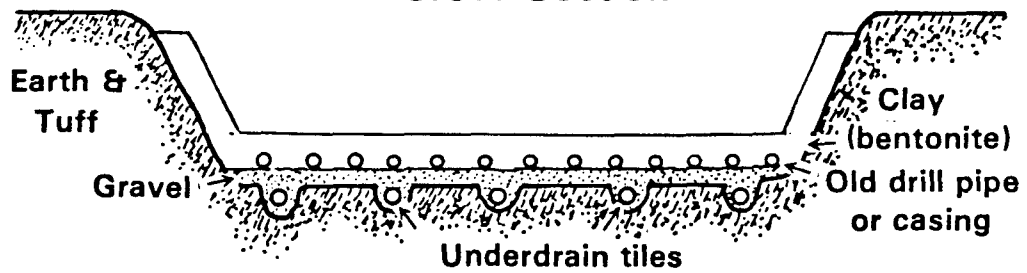


Fig. 7.  
Modified 1 M gal Pond.

pond. During the temporary storage period the pond would be monitored to detect any leakage into the surrounding soil.

Working drawings of the retaining pond will be submitted to the OCD before the pond is constructed. At present the plan is to build the pond as soon as major workover operations are completed in 1985.

If any further drilling or completion operations become necessary a supplemental water discharge plan will be submitted.

After the major workover operation, the circulating loop will be constructed. At this time the service pond will be cleaned. The mud pit from earlier drilling operations is to be backfilled and graded to fit into the local site topography. The grading will provide mounding over the pond area to divert rain water and runoff. The service pond will be relined, a drainage and leak monitoring system provided and the pond made ready to serve the loop operations for the final flow tests scheduled in FY 1986 and FY 1987.

Solid waste removal from the service pond is to be placed in the older mud pit and covered with natural backfill. This mud pit area is to be graded to prevent any possible erosion from natural runoff or from a possible breach of the service pond.

#### B. Contingency Plan

The 1 M gal service pond developed for drilling and workover operations is considered as the temporary holding facility for liquid that may be vented from the geothermal system.

If it should be necessary to vent more liquid than the capacity available in the service pond, the 5.7 M gal storage reservoir can be used. This lined and covered reservoir will normally not be full when the geothermal system is

Where is this  
GT-2

good

Is this pond same as other?  
the service pond on p 34 same as retaining pond on p. 32

fully charged and circulating and what liquid is in the reservoir will be water stored for make up of losses in the underground system. The liquid vented will be returned to the geothermal system after repairs.

A major failure or breach of the liner and berm of the 5.7 M gal reservoir could result in the loss of 5.7 M gal of water. This should produce a "sheet-like" movement down the broad relief of the topography to the south and southwest. Movement of released water would be topographically controlled. Little water should reach the road along Lake Fork Canyon due to soil and underlying tuff absorption and the relatively low topographic relief of the very large area above the Lake Fork Canyon rim.<sup>[5]</sup>

### C. Monitoring and Inspection

The critical monitoring requirement for the geothermal system is to determine on a routine basis any leakage from the 1 M gal service pond and the 5.7 M gal reservoir if it should be utilized on a contingency basis.

The larger reservoir now has a collecting system under the bottom liner collecting to an open concrete drain box where visual inspection for leaks can be made. This is to be modified to provide for recirculation of any leakage. In the 1 M gal service pond, drainage pipe will be installed under the liner and brought to a central point where monitoring can be carried out. Monitoring equipment will be a float type instrument at the pond drain with appropriate alarm to the site operations building to alert personnel of leakage and who will subsequently take samples for analysis and determine disposal or transfer as needed.

---

[5] Revision to Appendix H. Environmental Analysis of the Fenton Hill HDR Geothermal Test Site - March 1980.

In both cases visual inspection will be made of the monitoring stations on a routine weekly basis to verify soundness of the storage and any possible leakage. These inspections will be logged in the regular inspection log for the site.

#### D. Reporting

The Los Alamos National Laboratory will report through the DOE-Los Alamos Area Office on a yearly basis the following data:

Changes or modifications to the geothermal research program that would result in changes to this plan. *NO*

Any discharge of liquids exceeding the limits established by the Water

Quality Control Commission resulting from a breach of the service pond or reservoir or any other part of the geothermal system.

#### E. Transfer of Project

The present schedule calls for completion of the geothermal R&D effort at the Fenton Hill site by the Los Alamos Laboratory in FY 1987. Upon completion of this work a change in use and operation of the site is anticipated and could include the following.

- ° A transfer of the geothermal system and operation of the site to a utility or industry for further development
- ° Return of the site to the U.S. Forest Service or their designee
- ° Continued use of the site by the Los Alamos Laboratory or DOE designee.

In all cases the transfer and continued operation will be in accordance with the current Memorandum Of Understanding (MOU) between the U.S. Forest Service and the U.S. Department of Energy.

If shutdown and abandonment of the geothermal system is required it will be done in compliance with the regulations of the U.S. Department of Interior,

Bureau of Land Management and the U.S. Department of Agriculture, National Forest Service.

As applicable this Discharge Plan will be transferred with the site. The New Mexico Oil Conservation Division will be informed of the change in operations of the Fenton Hill site six months in advance in order to review continuity of the Waste Disposal Plan.

#### F. Conclusions

Of principal concern in the Discharge Plan is the liquid and solid material from the geothermal operations that may require disposal outside the system.

The 1.0 M gal service pond is to be used as the holding tank for liquids that may be vented from the system. This pond is to be modified after workover completion to provide seepage integrity and monitoring capability. Contingency storage is provided by the recently completed 5.7 M gal storage pond. This large pond has a competent leak detection and collection system that is to be modified to recirculate the water leakage. Storage of the liquid is temporary and it ultimately is returned to the geothermal system.

Solid waste will result from cleaning of the 1.0 M gal pond and will be made up of materials used in the workover operations in the development of the geothermal system. This waste will be placed in a no longer used mud pit from the early drilling operations at the site. This pit will be filled and graded to prevent leakage and erosion. OK

Intensive monitoring will be carried out during the geothermal operations to assure that no waste products, that may be detrimental to national or cultural uses of the surrounding areas are discharged without proper treatment or containment.

APPENDIX A

FENTON HILL POND AND WELL WATER ANALYSIS

Water Quality in the Vicinity of Fenton Hill, 1980,  
LA-9007-PR, Los Alamos National Laboratory

APPENDIX A

POND WATER SAMPLES - 1982 OBSERVED VALUES

Parameter	Limit	Ave.	Min.	Max.
* Arsenic (As)*	0.1 mg/1	0.88	0.012	2.5
Barium (Ba)*	1.0 mg/1	0.91	0.10	2.33
* Cadmium (Cd)*	0.01 mg/1	1.7	--	23.3
Chromium (Cr)*	0.05 mg/1	0.026	0.005	0.06
Cyanide (CN)	0.2 mg/1	0.01	0.007	0.016
Fluoride (F)*	1.6 mg/1	2.3	1.2	4.5
Lead (Pb)*	0.05 mg/1	0.04	0.002	0.08
Total Mercury (Hg)	0.002 mg/1	0.0005	0.0001	0.0017
Nitrate (NO <sub>3</sub> as N)	10.0 mg/1	0.31	0.08	0.90
Selenium (Se)	0.05 mg/1	0.03	--	0.011
Silver (Ag)	0.05 mg/1	0.008	--	0.027
Uranium (U)	5.0 mg/1	--	--	--
Benzene	5.0 mg/1	--	--	--
Radioactivity: combined Radium-226 and Radium-228	30.0 pCi/1	0.2 <sub>±</sub> .2	0.05 <sub>±</sub> 0.01	0.75 <sub>±</sub> 1.0
Polychlorinated biphenyls (PCB's)	0.001 mg/1			
Toluene	15.0 mg/1			
Carbon Tetrachloride	0.01 mg/1			
1, 2-dichloroethane (EDC)	0.02 mg/1			
1, 1-dichloroethylene (1, 1-DCE)	0.005 mg/1			
1, 1, 1, 2-tetrachloroethylene (PCE)	0.02 mg/1			
1,1, 2-trichloroethylene (TCE)	0.01 mg/1			
Chloride (Cl)*	250. mg/1	394	90	905
Copper (Cu)	1.0 mg/1	0.08	0.02	0.27
Iron (Fe)*	1.0 mg/1	5.1	1.3	13.4
Manganese (Mn)*	0.2 mg/1	0.29	0.14	0.52
* Phenols*	0.005 mg/1	81.5	0.24	343.0
Sulfate (SO <sub>4</sub> )	600. mg/1	161	71.0	211.0
Total Dissolved Solids (TDS)*	1000. mg/1	3205	2275	3670
Zinc (ZN)	10.0 mg/1	0.24	0.11	0.45
pH	between 6 & 9		8.0	8.8
Aluminum (Al)	5.0 mg/1			
* Boron (B)*	0.75 mg/1	10.3	2.3	25.0
Cobalt (Co)	0.05 mg/1			
Molybdenum (Mo)	1.0 mg/1			
Nickel (Ni)	0.2 mg/1			

\* Exceeded WQCC Standard

\* Greatly exceeded WQCC standard

#	LOCATED	COLLECT	ANALYSIS	RESULT	STD DEV	UNIT
POND01	GT-2 POND	05/17/79	BA	0.210		PPM
POND01	GT-2 POND	05/17/79	CA	15.3		PPM
POND01	GT-2 POND	05/17/79	CL	394		PPM
POND01	GT-2 POND	05/17/79	CD	0.003		PPM
POND01	GT-2 POND	05/17/79	CO3	3.6		PPM
POND01	GT-2 POND	05/17/79	COND	2100		MMHO/CM
POND01	GT-2 POND	05/17/79	CR	0.006		PPM
POND01	GT-2 POND	05/17/79	CU	0.012		PPM
POND01	GT-2 POND	05/17/79	EH	354		M VOLT
POND01	GT-2 POND	05/17/79	F	4.40		PPM
POND01	GT-2 POND	05/17/79	FE	1.06		PPM
POND01	GT-2 POND	05/17/79	HCO3	271		PPM
POND01	GT-2 POND	05/17/79	K	21.8		PPM
POND01	GT-2 POND	05/17/79	MG	4.73		PPM
POND01	GT-2 POND	05/17/79	MN	0.008		PPM
POND01	GT-2 POND	05/17/79	MO	0.050		PPM
POND01	GT-2 POND	05/17/79	NA	370		PPM
POND01	GT-2 POND	05/17/79	NI	0.005		PPM
POND01	GT-2 POND	05/17/79	PB	N.D.	<0.01	PPM
POND01	GT-2 POND	05/17/79	PH	8.34		PH
POND01	GT-2 POND	05/17/79	SI02	63.4		PPM
POND01	GT-2 POND	05/17/79	SD4	236		PPM
POND01	GT-2 POND	05/17/79	SR	0.420		PPM
POND01	GT-2 POND	05/17/79	ZN	0.002		PPM
POND02	EE-1 POND	07/17/79	BA	0.128		PPM
POND02	EE-1 POND	07/17/79	CA	60.8		PPM
POND02	EE-1 POND	07/17/79	CL	33.7		PPM
POND02	EE-1 POND	07/17/79	CD	0.003		PPM
POND02	EE-1 POND	07/17/79	CO3	49.2		PPM
POND02	EE-1 POND	07/17/79	COND	1280		MMHO/CM
POND02	EE-1 POND	07/17/79	CR	0.008		PPM
POND02	EE-1 POND	07/17/79	CU	0.006		PPM
POND02	EE-1 POND	07/17/79	EH	189		M VOLT
POND02	EE-1 POND	07/17/79	F	0.37		PPM
POND02	EE-1 POND	07/17/79	FE	0.038		PPM
POND02	EE-1 POND	07/17/79	HCO3	0		PPM
POND02	EE-1 POND	07/17/79	K	14.2		PPM
POND02	EE-1 POND	07/17/79	MG	0.05		PPM
POND02	EE-1 POND	07/17/79	MN	0.002		PPM
POND02	EE-1 POND	07/17/79	MO	0.028		PPM
POND02	EE-1 POND	07/17/79	NA	82.5		PPM
POND02	EE-1 POND	07/17/79	NI	0.001		PPM
POND02	EE-1 POND	07/17/79	PB	N.D.	<0.01	PPM
POND02	EE-1 POND	07/17/79	PH	11.45		PH
POND02	EE-1 POND	07/17/79	SI02	27.8		PPM
POND02	EE-1 POND	07/17/79	SD4	59		PPM
POND02	EE-1 POND	07/17/79	SR	0.800		PPM
POND02	EE-1 POND	07/17/79	ZN	N.D.	<0.005	PPM
POND03	EE-1 POND	10/10/79	CA	143		PPM

#	LOCATED	COLLECT	ANALYSIS RESULT	STD DEV	UNIT
POND03	EE-1 POND	10/10/79	CL	121	PPM
POND03	EE-1 POND	10/10/79	CO3	192	PPM
POND03	EE-1 POND	10/10/79	COND	6600	MMHO/CM
POND03	EE-1 POND	10/10/79	HCO3	0	PPM
POND03	EE-1 POND	10/10/79	K	25.7	PPM
POND03	EE-1 POND	10/10/79	NA	1113	PPM
POND03	EE-1 POND	10/10/79	PH	11.48	PH
POND03	EE-1 POND	10/10/79	SI02	57.5	PPM
POND03	EE-1 POND	10/10/79	SO4	2680	PPM
POND04	EE-1 POND	10/15/79	CA	112	PPM
POND04	EE-1 POND	10/15/79	CL	151	PPM
POND04	EE-1 POND	10/15/79	CO3	234	PPM
POND04	EE-1 POND	10/15/79	EH	177	M VOLT
POND04	EE-1 POND	10/15/79	FE	0.05	PPM
POND04	EE-1 POND	10/15/79	K	29.9	PPM
POND04	EE-1 POND	10/15/79	NA	1440	PPM
POND04	EE-1 POND	10/15/79	PH	9.97	PH
POND04	EE-1 POND	10/15/79	SI02	69.9	PPM
POND04	EE-1 POND	10/15/79	SO4	2751	PPM
POND05	GT-2 POND	10/15/79	CA	166	PPM
POND05	GT-2 POND	10/15/79	CL	125	PPM
POND05	GT-2 POND	10/15/79	CO3	146	PPM
POND05	GT-2 POND	10/15/79	EH	161	M VOLT
POND05	GT-2 POND	10/15/79	K	36.0	PPM
POND05	GT-2 POND	10/15/79	NA	1320	PPM
POND05	GT-2 POND	10/15/79	PH	11.02	PH
POND05	GT-2 POND	10/15/79	SI02	37.9	PPM
POND05	GT-2 POND	10/15/79	SO4	3029	PPM
POND06	EE-1 POND	10/16/79	CA	127	PPM
POND06	EE-1 POND	10/16/79	CL	207	PPM
POND06	EE-1 POND	10/16/79	CO3	296	PPM
POND06	EE-1 POND	10/16/79	EH	230	M VOLT
POND06	EE-1 POND	10/16/79	FE	0.07	PPM
POND06	EE-1 POND	10/16/79	K	29.1	PPM
POND06	EE-1 POND	10/16/79	NA	1515	PPM
POND06	EE-1 POND	10/16/79	PH	10.58	PH
POND06	EE-1 POND	10/16/79	SI02	73.5	PPM
POND06	EE-1 POND	10/16/79	SO4	3278	PPM
POND07	GT-2 POND	10/29/79	B	3.43	PPM
POND07	GT-2 POND	10/29/79	CA	95.7	PPM
POND07	GT-2 POND	10/29/79	CL	162	PPM
POND07	GT-2 POND	10/29/79	COND	3950	MMHO/CM
POND07	GT-2 POND	10/29/79	EH	420	M VOLT
POND07	GT-2 POND	10/29/79	F	2.04	PPM
POND07	GT-2 POND	10/29/79	FE	1.55	PPM
POND07	GT-2 POND	10/29/79	HCO3	151.3	PPM
POND07	GT-2 POND	10/29/79	K	26.2	PPM
POND07	GT-2 POND	10/29/79	NA	710	PPM
POND07	GT-2 POND	10/29/79	PH	7.59	PH

#	LOCATED	COLLECT	ANALYSIS RESULT	STD DEV	UNIT
POND07	GT-2 POND	10/29/79	SI02	75.0	PPM
POND07	GT-2 POND	10/29/79	SD4	1540	PPM
POND08	EE-1 POND	01/00/80	B	3.90	PPM
POND08	EE-1 POND	01/00/80	BA	0.074	PPM
POND08	EE-1 POND	01/00/80	CA	32.0	PPM
POND08	EE-1 POND	01/00/80	CD	0.006	PPM
POND08	EE-1 POND	01/00/80	CL	135	PPM
POND08	EE-1 POND	01/00/80	CD	0.003	PPM
POND08	EE-1 POND	01/00/80	COND	11000	MMHO/CM
POND08	EE-1 POND	01/00/80	CR	0.002	PPM
POND08	EE-1 POND	01/00/80	CJ	0.055	PPM
POND08	EE-1 POND	01/00/80	EH	595	M VOLT
POND08	EE-1 POND	01/00/80	F	7.08	PPM
POND08	EE-1 POND	01/00/80	FE	0.500	PPM
POND08	EE-1 POND	01/00/80	HCO3	1918	PPM
POND08	EE-1 POND	01/00/80	K	53.3	PPM
POND08	EE-1 POND	01/00/80	LI	6.0	PPM
POND08	EE-1 POND	01/00/80	MG	0.45	PPM
POND08	EE-1 POND	01/00/80	MN	0.061	PPM
POND08	EE-1 POND	01/00/80	MO	0.001	PPM
POND08	EE-1 POND	01/00/80	NA	1773	PPM
POND08	EE-1 POND	01/00/80	NI	0.010	PPM
POND08	EE-1 POND	01/00/80	PR	0.080	PPM
POND08	EE-1 POND	01/00/80	PH	7.76	PH
POND08	EE-1 POND	01/00/80	SI02	130.0	PPM
POND08	EE-1 POND	01/00/80	SD4	3775	PPM
POND08	EE-1 POND	01/00/80	SR	0.420	PPM
POND08	EE-1 POND	01/00/80	ZN	0.160	PPM
POND09	GT-2 POND	04/29/80	B	1.7	PPM
POND09	GT-2 POND	04/29/80	CA	32.0	PPM
POND09	GT-2 POND	04/29/80	CL	97.0	PPM
POND09	GT-2 POND	04/29/80	COND	1190	MMHO/CM
POND09	GT-2 POND	04/29/80	EH	13	M VOLT
POND09	GT-2 POND	04/29/80	F	1.56	PPM
POND09	GT-2 POND	04/29/80	K	11.0	PPM
POND09	GT-2 POND	04/29/80	NA	205	PPM
POND09	GT-2 POND	04/29/80	NO3	1.91	PPM
POND09	GT-2 POND	04/29/80	PH	8.55	PH
POND09	GT-2 POND	04/29/80	SI02	58.0	PPM
POND09	GT-2 POND	04/29/80	SD4	203	PPM

#	LOCATED	COLLECT	ANALYSIS	RESULT	STD DEV	UNIT
POND10	EE-1 POND	06/23/80	B	0.24		PPM
POND10	EE-1 POND	06/23/80	CA	20.0		PPM
POND10	EE-1 POND	06/23/80	CL	20.9		PPM
POND10	EE-1 POND	06/23/80	CD3	23.6		PPM
POND10	EE-1 POND	06/23/80	EH	99		M-VOLT
POND10	EE-1 POND	06/23/80	F	3.2		PPM
POND10	EE-1 POND	06/23/80	HCO3	128.4		PPM
POND10	EE-1 POND	06/23/80	K	5.5		PPM
POND10	EE-1 POND	06/23/80	MG	1.80		PPM
POND10	EE-1 POND	06/23/80	NA	72.0		PPM
POND10	EE-1 POND	06/23/80	PH	9.40		PH
POND10	EE-1 POND	06/23/80	SI02	36.0		PPM
POND10	EE-1 POND	06/23/80	SO4	29.0		PPM
POND11	GT-2 POND	06/23/80	B	1.26		PPM
POND11	GT-2 POND	06/23/80	CA	29.0		PPM
POND11	GT-2 POND	06/23/80	CL	15.0		PPM
POND11	GT-2 POND	06/23/80	F	2.6		PPM
POND11	GT-2 POND	06/23/80	K	4.3		PPM
POND11	GT-2 POND	06/23/80	MG	2.55		PPM
POND11	GT-2 POND	06/23/80	NA	186		PPM
POND11	GT-2 POND	06/23/80	SI02	73.0		PPM
POND11	GT-2 POND	06/23/80	SO4	9.3		PPM
POND12	GT-2 POND	08/04/80	B	7.8		PPM
POND12	GT-2 POND	08/04/80	CA	28		PPM
POND12	GT-2 POND	08/04/80	CL	268		PPM
POND12	GT-2 POND	08/04/80	COND	1920		MMHO/CM
POND12	GT-2 POND	08/04/80	F	11.1		PPM
POND12	GT-2 POND	08/04/80	K	30		PPM
POND12	GT-2 POND	08/04/80	LI	5.4		PPM
POND12	GT-2 POND	08/04/80	MC	1.90		PPM
POND12	GT-2 POND	08/04/80	NA	332		PPM
POND12	GT-2 POND	08/04/80	PH	8.07		PH
POND12	GT-2 POND	08/04/80	SI02	122		PPM
POND12	GT-2 POND	08/04/80	SO4	157		PPM
POND13	EE-1 POND	08/20/80	B	4.0		PPM
POND13	EE-1 POND	08/20/80	CA	16		PPM
POND13	EE-1 POND	08/20/80	CL	166		PPM
POND13	EE-1 POND	08/20/80	CD3	66		PPM
POND13	EE-1 POND	08/20/80	COND	4400		MMHO/CM
POND13	EE-1 POND	08/20/80	EH	190		M VOLT
POND13	EE-1 POND	08/20/80	F	5.3		PPM
POND13	EE-1 POND	08/20/80	HCO3	891		PPM
POND13	EE-1 POND	08/20/80	K	34		PPM
POND13	EE-1 POND	08/20/80	LI	2.4		PPM
POND13	EE-1 POND	08/20/80	MG	1.20		PPM
POND13	EE-1 POND	08/20/80	NA	965		PPM
POND13	EE-1 POND	08/20/80	PH	8.91		PH
POND13	EE-1 POND	08/20/80	SI02	118		PPM
POND13	EE-1 POND	08/20/80	SO4	1250		PPM

#	LOCATED	COLLECT	ANALYSIS	RESULT	STD DEV	UNIT
POND14	SLUDGE SAMPLE,20G/L,14 DAY LEACH	02/11/80	B	0.03		PPM
POND14	SLUDGE SAMPLE,20G/L,14 DAY LEACH	02/11/80	CA	12.8		PPM
POND14	SLUDGE SAMPLE,20G/L,14 DAY LEACH	02/11/80	CL	2.70		PPM
POND14	SLUDGE SAMPLE,20G/L,14 DAY LEACH	02/11/80	CO3	0		PPM
POND14	SLUDGE SAMPLE,20G/L,14 DAY LEACH	02/11/80	COND	195		MMHO/CM
POND14	SLUDGE SAMPLE,20G/L,14 DAY LEACH	02/11/80	EH	268		M VOLT
POND14	SLUDGE SAMPLE,20G/L,14 DAY LEACH	02/11/80	F	0.31		PPM
POND14	SLUDGE SAMPLE,20G/L,14 DAY LEACH	02/11/80	HCO3	52.1		PPM
POND14	SLUDGE SAMPLE,20G/L,14 DAY LEACH	02/11/80	K	3.10		PPM
POND14	SLUDGE SAMPLE,20G/L,14 DAY LEACH	02/11/80	MG	0.42		PPM
POND14	SLUDGE SAMPLE,20G/L,14 DAY LEACH	02/11/80	NA	22.8		PPM
POND14	SLUDGE SAMPLE,20G/L,14 DAY LEACH	02/11/80	NI	N.D.	<1	PPM
POND14	SLUDGE SAMPLE,20G/L,14 DAY LEACH	02/11/80	PH	6.90		PH
POND14	SLUDGE SAMPLE,20G/L,14 DAY LEACH	02/11/80	SI02	19.6		PPM
POND14	SLUDGE SAMPLE,20G/L,14 DAY LEACH	02/11/80	SD4	36.4		PPM
POND15	SLUDGE SAMPLE,20G/L,7 DAY LEACH	04/04/80	B	0.19		PPM
POND15	SLUDGE SAMPLE,20G/L,7 DAY LEACH	04/04/80	CA	79.0		PPM
POND15	SLUDGE SAMPLE,20G/L,7 DAY LEACH	04/04/80	CL	6.78		PPM
POND15	SLUDGE SAMPLE,20G/L,7 DAY LEACH	04/04/80	CO3	82.6		PPM
POND15	SLUDGE SAMPLE,20G/L,7 DAY LEACH	04/04/80	COND	550		MMHO/CM
POND15	SLUDGE SAMPLE,20G/L,7 DAY LEACH	04/04/80	EH	97		M VOLT
POND15	SLUDGE SAMPLE,20G/L,7 DAY LEACH	04/04/80	F	1.08		PPM
POND15	SLUDGE SAMPLE,20G/L,7 DAY LEACH	04/04/80	HCO3	4.2		PPM
POND15	SLUDGE SAMPLE,20G/L,7 DAY LEACH	04/04/80	K	3.80		PPM
POND15	SLUDGE SAMPLE,20G/L,7 DAY LEACH	04/04/80	MG	0.03		PPM
POND15	SLUDGE SAMPLE,20G/L,7 DAY LEACH	04/04/80	NA	12.5		PPM
POND15	SLUDGE SAMPLE,20G/L,7 DAY LEACH	04/04/80	PH	10.82		PH
POND15	SLUDGE SAMPLE,20G/L,7 DAY LEACH	04/04/80	SI02	18.6		PPM
POND15	SLUDGE SAMPLE,20G/L,7 DAY LEACH	04/04/80	SD4	101.8		PPM
POND16	SLUDGE SAMPLE,20G/L,16 DAY LEACH	08/19/80	B	0.03		PPM
POND16	SLUDGE SAMPLE,20G/L,16 DAY LEACH	08/19/80	CA	3.10		PPM
POND16	SLUDGE SAMPLE,20G/L,16 DAY LEACH	08/19/80	CL	13.3		PPM
POND16	SLUDGE SAMPLE,20G/L,16 DAY LEACH	08/19/80	CO3	0		PPM
POND16	SLUDGE SAMPLE,20G/L,16 DAY LEACH	08/19/80	COND	155		MMHO/CM
POND16	SLUDGE SAMPLE,20G/L,16 DAY LEACH	08/19/80	EH	387		M VOLT
POND16	SLUDGE SAMPLE,20G/L,16 DAY LEACH	08/19/80	F	0.7		PPM
POND16	SLUDGE SAMPLE,20G/L,16 DAY LEACH	08/19/80	HCO3	48		PPM
POND16	SLUDGE SAMPLE,20G/L,16 DAY LEACH	08/19/80	K	2.20		PPM
POND16	SLUDGE SAMPLE,20G/L,16 DAY LEACH	08/19/80	LI	0.04		PPM
POND16	SLUDGE SAMPLE,20G/L,16 DAY LEACH	08/19/80	MG	0.21		PPM
POND16	SLUDGE SAMPLE,20G/L,16 DAY LEACH	08/19/80	NA	25.0		PPM
POND16	SLUDGE SAMPLE,20G/L,16 DAY LEACH	08/19/80	PH	6.76		PH
POND16	SLUDGE SAMPLE,20G/L,16 DAY LEACH	08/19/80	SI02	12.0		PPM
POND16	SLUDGE SAMPLE,20G/L,16 DAY LEACH	08/19/80	SD4	27.7		PPM
POND17	GT-2 **DUMP**	12/22/80 15:15	B	6.5		PPM
POND17	GT-2 **DUMP**	12/22/80 15:15	CA	32		PPM
POND17	GT-2 **DUMP**	12/22/80 15:15	CL	188		PPM
POND17	GT-2 **DUMP**	12/22/80 15:15	CO3	0		PPM
POND17	GT-2 **DUMP**	12/22/80 15:15	COND	1920		MMHO/CM

#	LOCATED	COLLECT	ANALYSIS RESULT	STD DEV	UNIT
POND17	GT-2 **DUMP**	12/22/80 15:15	EH	-198	M VOLT
POND17	GT-2 **DUMP**	12/22/80 15:15	F	7.5	PPM
POND17	GT-2 **DUMP**	12/22/80 15:15	FE	2.96	PPM
POND17	GT-2 **DUMP**	12/22/80 15:15	HCO3	888	PPM
POND17	GT-2 **DUMP**	12/22/80 15:15	K	28	PPM
POND17	GT-2 **DUMP**	12/22/80 15:15	LI	4.2	PPM
POND17	GT-2 **DUMP**	12/22/80 15:15	MG	2.00	PPM
POND17	GT-2 **DUMP**	12/22/80 15:15	NA	404	PPM
POND17	GT-2 **DUMP**	12/22/80 15:15	FH	8.10	PH
POND17	GT-2 **DUMP**	12/22/80 15:15	SI02	170	PPM
POND17	GT-2 **DUMP**	12/22/80 15:15	SO4	339	PPM
POND18	GT-2 **DUMP**	02/17/81 12:00	B	6.3	PPM
POND18	GT-2 **DUMP**	02/17/81 12:00	CA	31	PPM
POND18	GT-2 **DUMP**	02/17/81 12:00	CL	199	PPM
POND18	GT-2 **DUMP**	02/17/81 12:00	CO3	0	PPM
POND18	GT-2 **DUMP**	02/17/81 12:00	COND	2100	MMHO/CM
POND18	GT-2 **DUMP**	02/17/81 12:00	EH	-177	M VOLT
POND18	GT-2 **DUMP**	02/17/81 12:00	F	7.0	PPM
POND18	GT-2 **DUMP**	02/17/81 12:00	FE	0.99	PPM
POND18	GT-2 **DUMP**	02/17/81 12:00	HCO3	699	PPM
POND18	GT-2 **DUMP**	02/17/81 12:00	K	28	PPM
POND18	GT-2 **DUMP**	02/17/81 12:00	LI	4.4	PPM
POND18	GT-2 **DUMP**	02/17/81 12:00	MG	2.00	PPM
POND18	GT-2 **DUMP**	02/17/81 12:00	NA	416	PPM
POND18	GT-2 **DUMP**	02/17/81 12:00	FH	8.05	PH
POND18	GT-2 **DUMP**	02/17/81 12:00	SI02	145	PPM
POND18	GT-2 **DUMP**	02/17/81 12:00	SO4	157	PPM
POND19	GT-2	05/27/81	B	9.6	PPM
POND19	GT-2	05/27/81	BR	2.3	PPM
POND19	GT-2	05/27/81	CA	3.4	PPM
POND19	GT-2	05/27/81	CL	347	PPM
POND19	GT-2	05/27/81	CO3	1450	PPM
POND19	GT-2	05/27/81	COND	15000	MMHO/CM
POND19	GT-2	05/27/81	EH	-83	M VOLT
POND19	GT-2	05/27/81	F	2.6	PPM
POND19	GT-2	05/27/81	HCO3	560	PPM
POND19	GT-2	05/27/81	K	70	PPM
POND19	GT-2	05/27/81	LI	2.6	PPM
POND19	GT-2	05/27/81	MG	0.36	PPM
POND19	GT-2	05/27/81	NA	4240	PPM
POND19	GT-2	05/27/81	NO3	91	PPM
POND19	GT-2	05/27/81	PH	10.60	PH
POND19	GT-2	05/27/81	PO4	N.D.	(0.1) PPM
POND19	GT-2	05/27/81	SI02	210	PPM
POND19	GT-2	05/27/81	SO4	5170	PPM
POND19	GT-2	05/27/81	ZN	4.3	PPM
POND20	EE-1 BEFORE DREDGING	05/27/81	B	12.0	PPM
POND20	EE-1 BEFORE DREDGING	05/27/81	BR	N.D.	(0.1) PPM
POND20	EE-1 BEFORE DREDGING	05/27/81	CA	11	PPM

* LOCATED	COLLECT	ANALYSIS RESULT	STD DEV	UNIT		
POND20	EE-1 BEFORE DREDGING	05/27/81	CL	366	PPM	
POND20	EE-1 BEFORE DREDGING	05/27/81	CO3	200	PPM	
POND20	EE-1 BEFORE DREDGING	05/27/81	COND	16000	MMHO/CM	
POND20	EE-1 BEFORE DREDGING	05/27/81	EH	-225	M VOLT	
POND20	EE-1 BEFORE DREDGING	05/27/81	F	3.4	PPM	
POND20	EE-1 BEFORE DREDGING	05/27/81	HCO3	3800	PPM	
POND20	EE-1 BEFORE DREDGING	05/27/81	K	70	PPM	
POND20	EE-1 BEFORE DREDGING	05/27/81	LI	2.5	PPM	
POND20	EE-1 BEFORE DREDGING	05/27/81	MG	1.24	PPM	
POND20	EE-1 BEFORE DREDGING	05/27/81	NA	4120	PPM	
POND20	EE-1 BEFORE DREDGING	05/27/81	NO3	35	PPM	
POND20	EE-1 BEFORE DREDGING	05/27/81	PH	8.74	PH	
POND20	EE-1 BEFORE DREDGING	05/27/81	PO4	N.D.	<0.1	PPM
POND20	EE-1 BEFORE DREDGING	05/27/81	SI02	162	PPM	
POND20	EE-1 BEFORE DREDGING	05/27/81	SO4	4980	PPM	
POND21	EE-1 EAST POND	06/15/81	B	2.5	PPM	
POND21	EE-1 EAST POND	06/15/81	BR	N.D.	<0.1	PPM
POND21	EE-1 EAST POND	06/15/81	CA	5.6	PPM	
POND21	EE-1 EAST POND	06/15/81	CL	91	PPM	
POND21	EE-1 EAST POND	06/15/81	CO3	454	PPM	
POND21	EE-1 EAST POND	06/15/81	COND	3200	MMHO/CM	
POND21	EE-1 EAST POND	06/15/81	EH	-146	M VOLT	
POND21	EE-1 EAST POND	06/15/81	F	1.0	PPM	
POND21	EE-1 EAST POND	06/15/81	HCO3	682	PPM	
POND21	EE-1 EAST POND	06/15/81	K	9.6	PPM	
POND21	EE-1 EAST POND	06/15/81	LI	0.2	PPM	
POND21	EE-1 EAST POND	06/15/81	MG	2.20	PPM	
POND21	EE-1 EAST POND	06/15/81	NA	784	PPM	
POND21	EE-1 EAST POND	06/15/81	NO3	3.6	PPM	
POND21	EE-1 EAST POND	06/15/81	PH	9.75	PH	
POND21	EE-1 EAST POND	06/15/81	PO4	N.D.	<0.1	PPM
POND21	EE-1 EAST POND	06/15/81	SI02	222	PPM	
POND21	EE-1 EAST POND	06/15/81	SO4	323	PPM	
POND22	EE-1 MIDDLE POND	06/15/81	B	2.7	PPM	
POND22	EE-1 MIDDLE POND	06/15/81	BR	0.75	0.1	PPM
POND22	EE-1 MIDDLE POND	06/15/81	CA	3.7	PPM	
POND22	EE-1 MIDDLE POND	06/15/81	CL	96	PPM	
POND22	EE-1 MIDDLE POND	06/15/81	CO3	460	PPM	
POND22	EE-1 MIDDLE POND	06/15/81	COND	3200	MMHO/CM	
POND22	EE-1 MIDDLE POND	06/15/81	EH	-133	M VOLT	
POND22	EE-1 MIDDLE POND	06/15/81	F	0.7	PPM	
POND22	EE-1 MIDDLE POND	06/15/81	HCO3	627	PPM	
POND22	EE-1 MIDDLE POND	06/15/81	K	9.0	PPM	
POND22	EE-1 MIDDLE POND	06/15/81	LI	0.2	PPM	
POND22	EE-1 MIDDLE POND	06/15/81	MG	2.20	PPM	
POND22	EE-1 MIDDLE POND	06/15/81	NA	800	PPM	
POND22	EE-1 MIDDLE POND	06/15/81	NO3	5.6	PPM	
POND22	EE-1 MIDDLE POND	06/15/81	PH	9.79	PH	
POND22	EE-1 MIDDLE POND	06/15/81	PO4	N.D.	<0.1	PPM

LOCATED	COLLECT	ANALYSIS RESULT	STD DEV	UNIT	
POND22	EE-1 MIDDLE POND	06/15/81	SI02	185	PPM
POND22	EE-1 MIDDLE POND	06/15/81	SD4	158	PPM
POND23	EE-1 WEST POND	06/15/81	B	3.2	PPM
POND23	EE-1 WEST POND	06/15/81	BR	N.D.	(0.1) PPM
POND23	EE-1 WEST POND	06/15/81	CA	3.3	PPM
POND23	EE-1 WEST POND	06/15/81	CL	178	PPM
POND23	EE-1 WEST POND	06/15/81	CO3	36	PPM
POND23	EE-1 WEST POND	06/15/81	COND	4900	MMHO/CM
POND23	EE-1 WEST POND	06/15/81	EH	-173	M VOLT
POND23	EE-1 WEST POND	06/15/81	F	1.1	PPM
POND23	EE-1 WEST POND	06/15/81	HCO3	2290	PPM
POND23	EE-1 WEST POND	06/15/81	X	18.0	PPM
POND23	EE-1 WEST POND	06/15/81	LI	0.4	PPM
POND23	EE-1 WEST POND	06/15/81	MG	6.20	PPM
POND23	EE-1 WEST POND	06/15/81	NA	1260	PPM
POND23	EE-1 WEST POND	06/15/81	NO3	7.4	PPM
POND23	EE-1 WEST POND	06/15/81	PH	8.49	PH
POND23	EE-1 WEST POND	06/15/81	PD4	8.1	0.1 PPM
POND23	EE-1 WEST POND	06/15/81	SI02	219	PPM
POND23	EE-1 WEST POND	06/15/81	SD4	114	PPM
POND24	GT-2 POND **DUMP**	07/22/81 11:00	B	8.5	PPM
POND24	GT-2 POND **DUMP**	07/22/81 11:00	CA	22	PPM
POND24	GT-2 POND **DUMP**	07/22/81 11:00	CL	179	PPM
POND24	GT-2 POND **DUMP**	07/22/81 11:00	CO3	0	PPM
POND24	GT-2 POND **DUMP**	07/22/81 11:00	COND	7900	MMHO/CM
POND24	GT-2 POND **DUMP**	07/22/81 11:00	CU	N.D.	PPM
POND24	GT-2 POND **DUMP**	07/22/81 11:00	EH	-192	M VOLT
POND24	GT-2 POND **DUMP**	07/22/81 11:00	HCO3	3280	PPM
POND24	GT-2 POND **DUMP**	07/22/81 11:00	NA	1150	PPM
POND24	GT-2 POND **DUMP**	07/22/81 11:00	PH	8.4	PH
POND24	GT-2 POND **DUMP**	07/22/81 11:00	SI02	186	PPM
POND24	GT-2 POND **DUMP**	07/22/81 11:00	SD4	669	PPM
POND25	EE-1 EAST POND	08/31/81 14:20	BR	2.7	PPM
POND25	EE-1 EAST POND	08/31/81 14:20	CA	N.D.	(1) PPM
POND25	EE-1 EAST POND	08/31/81 14:20	CL	86.9	PPM
POND25	EE-1 EAST POND	08/31/81 14:20	CO3	587	PPM
POND25	EE-1 EAST POND	08/31/81 14:20	COND	4000	MMHO/CM
POND25	EE-1 EAST POND	08/31/81 14:20	CU	0.12	PPM
POND25	EE-1 EAST POND	08/31/81 14:20	EH	-31	M VOLT
POND25	EE-1 EAST POND	08/31/81 14:20	F	N.D.	(0.1) PPM
POND25	EE-1 EAST POND	08/31/81 14:20	HCO3	1210	PPM
POND25	EE-1 EAST POND	08/31/81 14:20	NA	596	PPM
POND25	EE-1 EAST POND	08/31/81 14:20	NO3	0.03	PPM
POND25	EE-1 EAST POND	08/31/81 14:20	PH	9.98	PH
POND25	EE-1 EAST POND	08/31/81 14:20	PD4	0.84	PPM
POND25	EE-1 EAST POND	08/31/81 14:20	SI02	200	PPM
POND25	EE-1 EAST POND	08/31/81 14:20	SD4	66.7	PPM
POND26	EE-1 MIDDLE POND	08/31/81 14:20	BR	1.4	PPM
POND26	EE-1 MIDDLE POND	08/31/81 14:20	CA	1.2	PPM

#	LOCATED	COLLECT	ANALYSIS RESULT	STD DEV	UNIT
POND26	EE-1 MIDDLE POND	08/31/81 14:20	CL 72.6		PPM
POND26	EE-1 MIDDLE POND	08/31/81 14:20	CO3 931		PPM
POND26	EE-1 MIDDLE POND	08/31/81 14:20	COND 3700		MMHO/CM
POND26	EE-1 MIDDLE POND	08/31/81 14:20	CU 0.41		PPM
POND26	EE-1 MIDDLE POND	08/31/81 14:20	EH 1		M VOLT
POND26	EE-1 MIDDLE POND	08/31/81 14:20	F N.D.	0.1	PPM
POND26	EE-1 MIDDLE POND	08/31/81 14:20	HCO3 0		PPM
POND26	EE-1 MIDDLE POND	08/31/81 14:20	NA 583		PPM
POND26	EE-1 MIDDLE POND	08/31/81 14:20	NO3 1.1		PPM
POND26	EE-1 MIDDLE POND	08/31/81 14:20	PH 11.49		PH
POND26	EE-1 MIDDLE POND	08/31/81 14:20	SI02 206		PPM
POND26	EE-1 MIDDLE POND	08/31/81 14:20	SO4 233		PPM

## FENTON HILL POND SAMPLES

SELECT REPORT

10/01/82 09:00

PAGE 1

LOCATED	COLLECT	ANALYSIS RESULT	STD DEV	UNIT
POND24 GT-2 POND **DUMP**	07/22/81 11:00 CR	N.D.	<0.03	PPM
POND24 GT-2 POND **DUMP**	07/22/81 11:00 FE	0.46		PPM
POND24 GT-2 POND **DUMP**	07/22/81 11:00 NI	0.13		PPM
POND24 GT-2 POND **DUMP**	07/22/81 11:00 SI	82		PPM
POND24 GT-2 POND **DUMP**	07/22/81 11:00 SR	0.367		PPM
POND25 EE-1 EAST POND	08/31/81 14:20 CR	0.11		PPM
POND25 EE-1 EAST POND	08/31/81 14:20 FE	1.66		PPM
POND25 EE-1 EAST POND	08/31/81 14:20 NI	N.D.	<0.03	PPM
POND25 EE-1 EAST POND	08/31/81 14:20 SI	80		PPM
POND25 EE-1 EAST POND	08/31/81 14:20 SR	0.249		PPM
POND26 EE-1 MIDDLE POND	08/31/81 14:20 CR	0.66		PPM
POND26 EE-1 MIDDLE POND	08/31/81 14:20 FE	2.17		PPM
POND26 EE-1 MIDDLE POND	08/31/81 14:20 NI	0.20		PPM
POND26 EE-1 MIDDLE POND	08/31/81 14:20 SI	112		PPM
POND26 EE-1 MIDDLE POND	08/31/81 14:20 SR	0.258		PPM
POND27 EE-2 POND	01/06/82 12:22 AG	N.D.	<0.001	PPM
POND27 EE-2 POND	01/06/82 12:22 B	0.37		PPM
POND27 EE-2 POND	01/06/82 12:22 BA	0.190		PPM
POND27 EE-2 POND	01/06/82 12:22 BR	0.89		PPM
POND27 EE-2 POND	01/06/82 12:22 CA	2.2		PPM
POND27 EE-2 POND	01/06/82 12:22 CD	N.D.	<0.001	PPM
POND27 EE-2 POND	01/06/82 12:22 CL	42.3		PPM
POND27 EE-2 POND	01/06/82 12:22 CO	N.D.	<0.001	PPM
POND27 EE-2 POND	01/06/82 12:22 CO3	0		PPM
POND27 EE-2 POND	01/06/82 12:22 COND	340		MMHO/CM
POND27 EE-2 POND	01/06/82 12:22 CR	0.001		PPM
POND27 EE-2 POND	01/06/82 12:22 CU	0.021		PPM
POND27 EE-2 POND	01/06/82 12:22 F	N.D.	<0.02	PPM
POND27 EE-2 POND	01/06/82 12:22 FE	0.54		PPM
POND27 EE-2 POND	01/06/82 12:22 HCO3	137		PPM
POND27 EE-2 POND	01/06/82 12:22 K	8.4		PPM
POND27 EE-2 POND	01/06/82 12:22 LI	0.2		PPM
POND27 EE-2 POND	01/06/82 12:22 MG	0.03		PPM
POND27 EE-2 POND	01/06/82 12:22 MD	N.D.	<0.01	PPM
POND27 EE-2 POND	01/06/82 12:22 NA	75		PPM
POND27 EE-2 POND	01/06/82 12:22 NH4	1.85		PPM
POND27 EE-2 POND	01/06/82 12:22 NI	N.D.	0.001	PPM
POND27 EE-2 POND	01/06/82 12:22 NO3	N.D.	<0.02	PPM
POND27 EE-2 POND	01/06/82 12:22 PH	6.66		PH
POND27 EE-2 POND	01/06/82 12:22 PO4	N.D.	<0.02	PPM
POND27 EE-2 POND	01/06/82 12:22 SI	196		PPM
POND27 EE-2 POND	01/06/82 12:22 SI02	422		PPM
POND27 EE-2 POND	01/06/82 12:22 SO4	17.3		PPM
POND27 EE-2 POND	01/06/82 12:22 TSS	242		MG/LITER
POND28 GT-2 POND BY DAM	03/19/82 10:00 F	0.46		PPM
POND28 GT-2 POND BY DAM	03/19/82 10:00 BR	N.D.	<0.01	PPM
POND28 GT-2 POND BY DAM	03/19/82 10:00 CA	20		PPM
POND28 GT-2 POND BY DAM	03/19/82 10:00 CL	27.2		PPM
POND28 GT-2 POND BY DAM	03/19/82 10:00 CO3	0		PPM

FENTON HILL POND SAMPLES

SELECT REPORT

10/01/82 09:05

PAGE 2

NO	LOCATED	COLLECT	ANALYSIS RESULT	STD DEV	UNIT
POND28	GT-2 POND BY DAM	03/19/82 10:00	COND	630	MMHO/CM
POND28	GT-2 POND BY DAM	03/19/82 10:00	EH	269	M VOLT
POND28	GT-2 POND BY DAM	03/19/82 10:00	F	0.44	PPM
POND28	GT-2 POND BY DAM	03/19/82 10:00	HCO3	237	PPM
POND28	GT-2 POND BY DAM	03/19/82 10:00	K	3.62	PPM
POND28	GT-2 POND BY DAM	03/19/82 10:00	MG	2.20	PPM
POND28	GT-2 POND BY DAM	03/19/82 10:00	NA	130	PPM
POND28	GT-2 POND BY DAM	03/19/82 10:00	NO3	0.98	PPM
POND28	GT-2 POND BY DAM	03/19/82 10:00	PH	7.88	PH
POND28	GT-2 POND BY DAM	03/19/82 10:00	PO4	0.84	PPM
POND28	GT-2 POND BY DAM	03/19/82 10:00	SI	12	PPM
POND28	GT-2 POND BY DAM	03/19/82 10:00	SI02	25	PPM
POND28	GT-2 POND BY DAM	03/19/82 10:00	SD4	45.4	PPM
POND29	GT-2 POND BY SPRAYER DURING TREATMENT	03/24/82	B	0.27	PPM
POND29	GT-2 POND BY SPRAYER DURING TREATMENT	03/24/82	BR	N.D.	<0.01 PPM
POND29	GT-2 POND BY SPRAYER DURING TREATMENT	03/24/82	CA	22	PPM
POND29	GT-2 POND BY SPRAYER DURING TREATMENT	03/24/82	CL	18.8	PPM
POND29	GT-2 POND BY SPRAYER DURING TREATMENT	03/24/82	CO3	0	PPM
POND29	GT-2 POND BY SPRAYER DURING TREATMENT	03/24/82	COND	390	MMHO/CM
POND29	GT-2 POND BY SPRAYER DURING TREATMENT	03/24/82	EH	318	M VOLT
POND29	GT-2 POND BY SPRAYER DURING TREATMENT	03/24/82	F	0.58	PPM
POND29	GT-2 POND BY SPRAYER DURING TREATMENT	03/24/82	HCO3	131	PPM
POND29	GT-2 POND BY SPRAYER DURING TREATMENT	03/24/82	K	2.40	PPM
POND29	GT-2 POND BY SPRAYER DURING TREATMENT	03/24/82	MG	2.40	PPM
POND29	GT-2 POND BY SPRAYER DURING TREATMENT	03/24/82	NA	60	PPM
POND29	GT-2 POND BY SPRAYER DURING TREATMENT	03/24/82	NO3	N.D.	<0.02 PPM
POND29	GT-2 POND BY SPRAYER DURING TREATMENT	03/24/82	PH	7.14	PH
POND29	GT-2 POND BY SPRAYER DURING TREATMENT	03/24/82	PO4	N.D.	<0.02 PPM
POND29	GT-2 POND BY SPRAYER DURING TREATMENT	03/24/82	SI	6	PPM
POND29	GT-2 POND BY SPRAYER DURING TREATMENT	03/24/82	SI02	15	PPM
POND29	GT-2 POND BY SPRAYER DURING TREATMENT	03/24/82	SD4	38.9	PPM
POND30	GT-2 POND BY DAM DURING TREATMENT	03/24/82	B	0.36	PPM
POND30	GT-2 POND BY DAM DURING TREATMENT	03/24/82	BR	0.17	PPM
POND30	GT-2 POND BY DAM DURING TREATMENT	03/24/82	CA	18	PPM
POND30	GT-2 POND BY DAM DURING TREATMENT	03/24/82	CL	41.9	PPM
POND30	GT-2 POND BY DAM DURING TREATMENT	03/24/82	CO3	48	PPM
POND30	GT-2 POND BY DAM DURING TREATMENT	03/24/82	COND	1530	MMHO/CM
POND30	GT-2 POND BY DAM DURING TREATMENT	03/24/82	EH	-52	M VOLT
POND30	GT-2 POND BY DAM DURING TREATMENT	03/24/82	F	0.55	PPM
POND30	GT-2 POND BY DAM DURING TREATMENT	03/24/82	HCO3	511	PPM
POND30	GT-2 POND BY DAM DURING TREATMENT	03/24/82	K	6.40	PPM
POND30	GT-2 POND BY DAM DURING TREATMENT	03/24/82	MG	1.60	PPM
POND30	GT-2 POND BY DAM DURING TREATMENT	03/24/82	NA	390	PPM
POND30	GT-2 POND BY DAM DURING TREATMENT	03/24/82	NO3	N.D.	<0.02 PPM
POND30	GT-2 POND BY DAM DURING TREATMENT	03/24/82	PH	9.16	PH
POND30	GT-2 POND BY DAM DURING TREATMENT	03/24/82	PO4	N.D.	<0.02 PPM
POND30	GT-2 POND BY DAM DURING TREATMENT	03/24/82	SD4	42.0	PPM
POND30	GT-2 POND BY DAM DURING TREATMENT	03/24/82	SI	16	PPM
POND30	GT-2 POND BY DAM DURING TREATMENT	03/24/82	SI02	36	PPM

#	LOCATED	COLLECT	ANALYSIS	RESULT	STD DEV	UNIT
POND31	GT-2 POND AT INTAKE DURING TREATMENT	03/29/82	B	0.27		PPM
POND31	GT-2 POND AT INTAKE DURING TREATMENT	03/29/82	BR	N.D.	<0.01	PPM
POND31	GT-2 POND AT INTAKE DURING TREATMENT	03/29/82	CA	14		PPM
POND31	GT-2 POND AT INTAKE DURING TREATMENT	03/29/82	CL	17.2		PPM
POND31	GT-2 POND AT INTAKE DURING TREATMENT	03/29/82	CO3	0		PPM
POND31	GT-2 POND AT INTAKE DURING TREATMENT	03/29/82	COND	350		MMHO/CM
POND31	GT-2 POND AT INTAKE DURING TREATMENT	03/29/82	EH	298		M VOLT
POND31	GT-2 POND AT INTAKE DURING TREATMENT	03/29/82	F	0.32		PPM
POND31	GT-2 POND AT INTAKE DURING TREATMENT	03/29/82	HCO3	117		PPM
POND31	GT-2 POND AT INTAKE DURING TREATMENT	03/29/82	K	2.28		PPM
POND31	GT-2 POND AT INTAKE DURING TREATMENT	03/29/82	MG	1.40		PPM
POND31	GT-2 POND AT INTAKE DURING TREATMENT	03/29/82	NA	62		PPM
POND31	GT-2 POND AT INTAKE DURING TREATMENT	03/29/82	NO3	N.D.	<0.02	PPM
POND31	GT-2 POND AT INTAKE DURING TREATMENT	03/29/82	PH	7.33		PH
POND31	GT-2 POND AT INTAKE DURING TREATMENT	03/29/82	PO4	N.D.	<0.02	PPM
POND31	GT-2 POND AT INTAKE DURING TREATMENT	03/29/82	SI	4		PPM
POND31	GT-2 POND AT INTAKE DURING TREATMENT	03/29/82	SIO2	11		PPM
POND31	GT-2 POND AT INTAKE DURING TREATMENT	03/29/82	SD4	30.9		PPM
POND32	GT-2 POND AT INTAKE DURING TREATMENT	04/05/82	BR	0.92		PPM
POND32	GT-2 POND AT INTAKE DURING TREATMENT	04/05/82	CL	79.6		PPM
POND32	GT-2 POND AT INTAKE DURING TREATMENT	04/05/82	COND	3100		MMHO/CM
POND32	GT-2 POND AT INTAKE DURING TREATMENT	04/05/82	F	0.88		PPM
POND32	GT-2 POND AT INTAKE DURING TREATMENT	04/05/82	NO3	N.D.	<0.02	PPM
POND32	GT-2 POND AT INTAKE DURING TREATMENT	04/05/82	PH	9.51		PH
POND32	GT-2 POND AT INTAKE DURING TREATMENT	04/05/82	PO4	0.89		PPM
POND32	GT-2 POND AT INTAKE DURING TREATMENT	04/05/82	SD4	52.5		PPM
POND33	GT-2 POND BY DAM DURING TREATMENT	04/05/82	BR	0.94		PPM
POND33	GT-2 POND BY DAM DURING TREATMENT	04/05/82	CL	79.2		PPM
POND33	GT-2 POND BY DAM DURING TREATMENT	04/05/82	COND	3100		MMHO/CM
POND33	GT-2 POND BY DAM DURING TREATMENT	04/05/82	F	0.88		PPM
POND33	GT-2 POND BY DAM DURING TREATMENT	04/05/82	NO3	N.D.	<0.02	PPM
POND33	GT-2 POND BY DAM DURING TREATMENT	04/05/82	PH	9.51		PH
POND33	GT-2 POND BY DAM DURING TREATMENT	04/05/82	PO4	0.85		PPM
POND33	GT-2 POND BY DAM DURING TREATMENT	04/05/82	SD4	52.4		PPM
POND34	EE-1 POND	04/13/82 10:00	B	0.35		PPM
POND34	EE-1 POND	04/13/82 10:00	BR	0.18	0.05	PPM
POND34	EE-1 POND	04/13/82 10:00	CA	42		PPM
POND34	EE-1 POND	04/13/82 10:00	CL	40.3		PPM
POND34	EE-1 POND	04/13/82 10:00	CO3	0		PPM
POND34	EE-1 POND	04/13/82 10:00	COND	470		MMHO/CM
POND34	EE-1 POND	04/13/82 10:00	EH	393		M VOLT
POND34	EE-1 POND	04/13/82 10:00	F	0.28		PPM
POND34	EE-1 POND	04/13/82 10:00	HCO3	140		PPM
POND34	EE-1 POND	04/13/82 10:00	K	2		PPM
POND34	EE-1 POND	04/13/82 10:00	MG	4.58		PPM
POND34	EE-1 POND	04/13/82 10:00	NA	42		PPM
POND34	EE-1 POND	04/13/82 10:00	NO3	N.D.	0.05	PPM
POND34	EE-1 POND	04/13/82 10:00	PH	7.21		PH
POND34	EE-1 POND	04/13/82 10:00	PO4	N.D.	<0.05	PPM

## FENTON HILL POND SAMPLES

SELECT REPORT

10/01/82 09:16

PAGE 4

#	LOCATED	COLLECT	ANALYSIS	RESULT	STD DEV	UNIT
POND34	EE-1 POND	04/13/82 10:00	SI02	54		PPM
POND34	EE-1 POND	04/13/82 10:00	SD4	29.6		PPM
POND34	EE-1 POND	04/13/82 10:00	TS	429		MG/L
POND34	EE-1 POND	04/13/82 10:00	TSS	400		MG/LITER
POND35	GT-2 POND **DUMP**	04/14/82 09:45	B	2.59		PPM
POND35	GT-2 POND **DUMP**	04/14/82 09:45	BR	0.71	0.05	PPM
POND35	GT-2 POND **DUMP**	04/14/82 09:45	CA	34		PPM
POND35	GT-2 POND **DUMP**	04/14/82 09:45	CL	116		PPM
POND35	GT-2 POND **DUMP**	04/14/82 09:45	CD3	0		PPM
POND35	GT-2 POND **DUMP**	04/14/82 09:45	COND	3500		MMHO/CM
POND35	GT-2 POND **DUMP**	04/14/82 09:45	EH	9		M VOLT
POND35	GT-2 POND **DUMP**	04/14/82 09:45	F	0.92		PPM
POND35	GT-2 POND **DUMP**	04/14/82 09:45	HCO3	1548		PPM
POND35	GT-2 POND **DUMP**	04/14/82 09:45	K	12		PPM
POND35	GT-2 POND **DUMP**	04/14/82 09:45	MG	2.34		PPM
POND35	GT-2 POND **DUMP**	04/14/82 09:45	NA	900		PPM
POND35	GT-2 POND **DUMP**	04/14/82 09:45	NO3	N.D.	<0.05	PPM
POND35	GT-2 POND **DUMP**	04/14/82 09:45	PH	7.90		PH
POND35	GT-2 POND **DUMP**	04/14/82 09:45	PO4	N.D.	<0.05	PPM
POND35	GT-2 POND **DUMP**	04/14/82 09:45	SI02	80		PPM
POND35	GT-2 POND **DUMP**	04/14/82 09:45	SD4	154		PPM
POND36	GT-2 POND **DUMP**	04/14/82 14:30	B	2.57		PPM
POND36	GT-2 POND **DUMP**	04/14/82 14:30	BR	0.77	0.05	PPM
POND36	GT-2 POND **DUMP**	04/14/82 14:30	CL	123		PPM
POND36	GT-2 POND **DUMP**	04/14/82 14:30	CD3	0		PPM
POND36	GT-2 POND **DUMP**	04/14/82 14:30	COND	3500		MMHO/CM
POND36	GT-2 POND **DUMP**	04/14/82 14:30	EH	-15		M VOLT
POND36	GT-2 POND **DUMP**	04/14/82 14:30	F	0.91		PPM
POND36	GT-2 POND **DUMP**	04/14/82 14:30	HCO3	1536		PPM
POND36	GT-2 POND **DUMP**	04/14/82 14:30	NO3	N.D.	<0.05	PPM
POND36	GT-2 POND **DUMP**	04/14/82 14:30	PH	7.83		PH
POND36	GT-2 POND **DUMP**	04/14/82 14:30	PO4	N.D.	<0.05	PPM
POND36	GT-2 POND **DUMP**	04/14/82 14:30	SI02	81		PPM
POND36	GT-2 POND **DUMP**	04/14/82 14:30	SD4	163		PPM
POND37	EE-1 POND	04/15/82 10:00	B	0.34		PPM
POND37	EE-1 POND	04/15/82 10:00	BR	0.60	0.05	PPM
POND37	EE-1 POND	04/15/82 10:00	CA	44		PPM
POND37	EE-1 POND	04/15/82 10:00	CL	40.7		PPM
POND37	EE-1 POND	04/15/82 10:00	CD3	0		PPM
POND37	EE-1 POND	04/15/82 10:00	COND	450		MMHO/CM
POND37	EE-1 POND	04/15/82 10:00	EH	391		M VOLT
POND37	EE-1 POND	04/15/82 10:00	F	0.26		PPM
POND37	EE-1 POND	04/15/82 10:00	HCO3	136		PPM
POND37	EE-1 POND	04/15/82 10:00	K	2		PPM
POND37	EE-1 POND	04/15/82 10:00	MG	4.79		PPM
POND37	EE-1 POND	04/15/82 10:00	NA	34		PPM
POND37	EE-1 POND	04/15/82 10:00	NO3	N.D.	<0.05	PPM
POND37	EE-1 POND	04/15/82 10:00	PH	7.15		PH
POND37	EE-1 POND	04/15/82 10:00	PO4	N.D.	<0.05	PPM

## FENTON HILL POND SAMPLES

SELECT REPORT

10/01/82 09:22

PAGE 5

#	LOCATED	COLLECT	ANALYSIS RESULT	STD DEV	UNIT
POND37	EE-1 POND	04/15/82 10:00	SI02	59	PPM
POND37	EE-1 POND	04/15/82 10:00	SD4	24.6	PPM
POND38	RUNOFF BELOW GT-2 **DUMP**	04/16/82 14:00	B	0.03	PPM
POND38	RUNOFF BELOW GT-2 **DUMP**	04/16/82 14:00	BR	N.D.	<0.05 PPM
POND38	RUNOFF BELOW GT-2 **DUMP**	04/16/82 14:00	CA	8	PPM
POND38	RUNOFF BELOW GT-2 **DUMP**	04/16/82 14:00	CL	6.8	PPM
POND38	RUNOFF BELOW GT-2 **DUMP**	04/16/82 14:00	CD3	0	PPM
POND38	RUNOFF BELOW GT-2 **DUMP**	04/16/82 14:00	COND	83	MMHO/CM
POND38	RUNOFF BELOW GT-2 **DUMP**	04/16/82 14:00	EH	410	M VOLT
POND38	RUNOFF BELOW GT-2 **DUMP**	04/16/82 14:00	F	0.11	PPM
POND38	RUNOFF BELOW GT-2 **DUMP**	04/16/82 14:00	HCO3	21	PPM
POND38	RUNOFF BELOW GT-2 **DUMP**	04/16/82 14:00	K	2	PPM
POND38	RUNOFF BELOW GT-2 **DUMP**	04/16/82 14:00	MG	2.14	PPM
POND38	RUNOFF BELOW GT-2 **DUMP**	04/16/82 14:00	NA	2	PPM
POND38	RUNOFF BELOW GT-2 **DUMP**	04/16/82 14:00	NO3	N.D.	<0.05 PPM
POND38	RUNOFF BELOW GT-2 **DUMP**	04/16/82 14:00	PH	7.09	PH
POND38	RUNOFF BELOW GT-2 **DUMP**	04/16/82 14:00	PO4	N.D.	<0.05 PPM
POND38	RUNOFF BELOW GT-2 **DUMP**	04/16/82 14:00	SI02	11	PPM
POND38	RUNOFF BELOW GT-2 **DUMP**	04/16/82 14:00	SD4	7.8	PPM
POND39	GT-2 POND **DUMP**	04/19/82 10:00	B	0.87	PPM
POND39	GT-2 POND **DUMP**	04/19/82 10:00	BR	2.30	0.05 PPM
POND39	GT-2 POND **DUMP**	04/19/82 10:00	CA	76	PPM
POND39	GT-2 POND **DUMP**	04/19/82 10:00	CL	68.3	PPM
POND39	GT-2 POND **DUMP**	04/19/82 10:00	CD3	52	PPM
POND39	GT-2 POND **DUMP**	04/19/82 10:00	COND	1390	MMHO/CM
POND39	GT-2 POND **DUMP**	04/19/82 10:00	F	5.02	PPM
POND39	GT-2 POND **DUMP**	04/19/82 10:00	HCO3	395	PPM
POND39	GT-2 POND **DUMP**	04/19/82 10:00	K	16	PPM
POND39	GT-2 POND **DUMP**	04/19/82 10:00	MG	2.08	PPM
POND39	GT-2 POND **DUMP**	04/19/82 10:00	NA	270	PPM
POND39	GT-2 POND **DUMP**	04/19/82 10:00	NO3	0.11	0.05 PPM
POND39	GT-2 POND **DUMP**	04/19/82 10:00	PH	9.10	PH
POND39	GT-2 POND **DUMP**	04/19/82 10:00	PO4	N.D.	<0.05 PPM
POND39	GT-2 POND **DUMP**	04/19/82 10:00	SI02	155	PPM
POND39	GT-2 POND **DUMP**	04/19/82 10:00	SD4	125	PPM
POND40	GT-2 POND **DUMP**	06/02/82 14:00	B	1.37	PPM
POND40	GT-2 POND **DUMP**	06/02/82 14:00	BR	1.15	0.05 PPM
POND40	GT-2 POND **DUMP**	06/02/82 14:00	CA	32	PPM
POND40	GT-2 POND **DUMP**	06/02/82 14:00	CL	79.1	PPM
POND40	GT-2 POND **DUMP**	06/02/82 14:00	CD3	14.4	PPM
POND40	GT-2 POND **DUMP**	06/02/82 14:00	COND	1690	MMHO/CM
POND40	GT-2 POND **DUMP**	06/02/82 14:00	EH	86	M VOLT
POND40	GT-2 POND **DUMP**	06/02/82 14:00	F	4.68	PPM
POND40	GT-2 POND **DUMP**	06/02/82 14:00	FE	0.4	PPM
POND40	GT-2 POND **DUMP**	06/02/82 14:00	HCO3	621	PPM
POND40	GT-2 POND **DUMP**	06/02/82 14:00	K	14	PPM
POND40	GT-2 POND **DUMP**	06/02/82 14:00	NA	390	PPM
POND40	GT-2 POND **DUMP**	06/02/82 14:00	NH4	N.D.	<0.01 PPM
POND40	GT-2 POND **DUMP**	06/02/82 14:00	NO3	N.D.	<0.05 PPM

TON HILL POND SAMPLES

SELECT REPORT

10/01/82 09:28

PAGE 6

LOCATED	COLLECT	ANALYSIS RESULT	STD DEV	UNIT
D40 GT-2 POND **DUMP**	06/02/82 14:00 PH	9.04		PH
ID40 GT-2 POND **DUMP**	06/02/82 14:00 PO4	N.D.	<0.05	PPM
ID40 GT-2 POND **DUMP**	06/02/82 14:00 SIO2	166		PPM
ID40 GT-2 POND **DUMP**	06/02/82 14:00 SD4	173		PPM
ID41 EE-1 POND	06/22/82 10:00 S	0.23	0.05	PPM
D42 GT-2 POND **DUMP**	07/12/82 10:00 BR	9.6		PPM
ID42 GT-2 POND **DUMP**	07/12/82 10:00 CL	1190		PPM
D42 GT-2 POND **DUMP**	07/12/82 10:00 CO3	0		PPM
ID42 GT-2 POND **DUMP**	07/12/82 10:00 COND	5800		MMHO/CM
ID42 GT-2 POND **DUMP**	07/12/82 10:00 EH	31		M VOLT
D42 GT-2 POND **DUMP**	07/12/82 10:00 F	4.39		PPM
ID42 GT-2 POND **DUMP**	07/12/82 10:00 HCO3	889		PPM
ID42 GT-2 POND **DUMP**	07/12/82 10:00 NH4	4.20		PPM
ID42 GT-2 POND **DUMP**	07/12/82 10:00 PH	7.98		PH
ID42 GT-2 POND **DUMP**	07/12/82 10:00 S	1.47		PPM
ID42 GT-2 POND **DUMP**	07/12/82 10:00 SD4	107		PPM
ID43 GT-2 POND **DUMP**	07/30/82 11:00 PH	8.68		PH
ID44 GT-2 POND **DUMP**	08/02/82 09:00 B	14.8		PPM
ID44 GT-2 POND **DUMP**	08/02/82 09:00 BR	4.3		PPM
ID44 GT-2 POND **DUMP**	08/02/82 09:00 CA	24		PPM
ID44 GT-2 POND **DUMP**	08/02/82 09:00 CL	614		PPM
D44 GT-2 POND **DUMP**	08/02/82 09:00 COND	3100		MMHO/CM
ID44 GT-2 POND **DUMP**	08/02/82 09:00 EH	302		M VOLT
D44 GT-2 POND **DUMP**	08/02/82 09:00 F	2.4		PPM
ID44 GT-2 POND **DUMP**	08/02/82 09:00 FE	N.D.	<1	PPM
ID44 GT-2 POND **DUMP**	08/02/82 09:00 HCO3	597		PPM
ID44 GT-2 POND **DUMP**	08/02/82 09:00 K	95		PPM
D44 GT-2 POND **DUMP**	08/02/82 09:00 LI	7.8		PPM
D44 GT-2 POND **DUMP**	08/02/82 09:00 MG	N.D.	<1	PPM
D44 GT-2 POND **DUMP**	08/02/82 09:00 NA	570		PPM
D44 GT-2 POND **DUMP**	08/02/82 09:00 NH4	2.80		PPM
D44 GT-2 POND **DUMP**	08/02/82 09:00 NO3	0.31	0.05	PPM
D44 GT-2 POND **DUMP**	08/02/82 09:00 PH	8.59		PH
D44 GT-2 POND **DUMP**	08/02/82 09:00 PO4	N.D.	<0.05	PPM
D44 GT-2 POND **DUMP**	08/02/82 09:00 S	N.D.	<0.01	PPM
D44 GT-2 POND **DUMP**	08/02/82 09:00 SIO2	96		PPM
D44 GT-2 POND **DUMP**	08/02/82 09:00 SD4	65		PPM
D45 GT-2 POND **DUMP**	08/02/82 15:30 PH	8.59		PH
D46 GT-2 POND **DUMP**	09/01/82 15:00 B	37.0		PPM
ID46 GT-2 POND **DUMP**	09/01/82 15:00 BR	4.6		PPM
ID46 GT-2 POND **DUMP**	09/01/82 15:00 CA	28		PPM
ID46 GT-2 POND **DUMP**	09/01/82 15:00 CL	667		PPM
D46 GT-2 POND **DUMP**	09/01/82 15:00 CO3	0		PPM
ID46 GT-2 POND **DUMP**	09/01/82 15:00 COND	3500		MMHO/CM
ID46 GT-2 POND **DUMP**	09/01/82 15:00 EH	284		M VOLT
ID46 GT-2 POND **DUMP**	09/01/82 15:00 F	2.6		PPM
ID46 GT-2 POND **DUMP**	09/01/82 15:00 FE	N.D.	<1	PPM
ID46 GT-2 POND **DUMP**	09/01/82 15:00 HCO3	669		PPM
ID46 GT-2 POND **DUMP**	09/01/82 15:00 K	86		PPM

LOCATED	COLLECT	ANALYSIS RESULT	STD DEV	UNIT
POND46 GT-2 POND **DUMP**	09/01/82 15:00 LI	9.2		PPM
POND46 GT-2 POND **DUMP**	09/01/82 15:00 MG	N.D.	<1	PPM
POND46 GT-2 POND **DUMP**	09/01/82 15:00 NA	647		PPM
POND46 GT-2 POND **DUMP**	09/01/82 15:00 ND3	0.25	0.05	PPM
POND46 GT-2 POND **DUMP**	09/01/82 15:00 PH	7.44		PH
POND46 GT-2 POND **DUMP**	09/01/82 15:00 PD4	N.D.	<0.05	PPM
POND46 GT-2 POND **DUMP**	09/01/82 15:00 S	N.D.	<0.01	PPM
POND46 GT-2 POND **DUMP**	09/01/82 15:00 SI02	87		PPM
POND46 GT-2 POND **DUMP**	09/01/82 15:00 SD4	184		PPM

#	LOCATED	COLLECT	ANALYSIS METHOD	RESULT	STD DEV	UNIT
WELL09	FH DOMESTIC WATER	06/20/79	AG HGA AA	N.D.	<0.01	PPM
WELL09	FH DOMESTIC WATER	06/20/79	BA AA	0.168		PPM
WELL09	FH DOMESTIC WATER	06/20/79	BR ION C	N.D.	<0.1	PPM
WELL09	FH DOMESTIC WATER	06/20/79	CA AA	51		PPM
WELL09	FH DOMESTIC WATER	06/20/79	CD HGA AA	N.D.	<0.01	PPM
WELL09	FH DOMESTIC WATER	06/20/79	CL ION C	18.9		PPM
WELL09	FH DOMESTIC WATER	06/20/79	CO HGA AA	0.002		PPM
WELL09	FH DOMESTIC WATER	06/20/79	COND ELECT	350		MMHO/CM
WELL09	FH DOMESTIC WATER	06/20/79	CR HGA AA	N.D.	<0.01	PPM
WELL09	FH DOMESTIC WATER	06/20/79	CU HGA AA	0.024		PPM
WELL09	FH DOMESTIC WATER	06/20/79	EH ELECT	391		M VOLT
WELL09	FH DOMESTIC WATER	06/20/79	F ION C	0.12		PPM
WELL09	FH DOMESTIC WATER	06/20/79	FE AA	0.052		PPM
WELL09	FH DOMESTIC WATER	06/20/79	HCO3 TITRATE	140		PPM
WELL09	FH DOMESTIC WATER	06/20/79	K AA	4.4		PPM
WELL09	FH DOMESTIC WATER	06/20/79	MG AA	4.95		PPM
WELL09	FH DOMESTIC WATER	06/20/79	MN HGA AA	0.001		PPM
WELL09	FH DOMESTIC WATER	06/20/79	MO HGA AA	N.D.	<0.01	PPM
WELL09	FH DOMESTIC WATER	06/20/79	NA AA	12.6		PPM
WELL09	FH DOMESTIC WATER	06/20/79	NI HGA AA	N.D.	<0.01	PPM
WELL09	FH DOMESTIC WATER	06/20/79	NO3 ION C	N.D.	<0.1	PPM
WELL09	FH DOMESTIC WATER	06/20/79	PB HGA AA	N.D.	<0.01	PPM
WELL09	FH DOMESTIC WATER	06/20/79	PH ELECT	7.83		PH
WELL09	FH DOMESTIC WATER	06/20/79	SI02 COLOR	70		PPM
WELL09	FH DOMESTIC WATER	06/20/79	SO4 ION C	9.64		PPM
WELL09	FH DOMESTIC WATER	06/20/79	SR AA	0.154		PPM
WELL09	FH DOMESTIC WATER	06/20/79	ZN HGA AA	0.041		PPM
WELL10	FH DOMESTIC WATER SAMPLE	09/03/80	B COLOR	N.D.	<0.01	PPM
WELL10	FH DOMESTIC WATER SAMPLE	09/03/80	BR ION C	N.D.	<0.1	PPM
WELL10	FH DOMESTIC WATER SAMPLE	09/03/80	CA AA	35		PPM
WELL10	FH DOMESTIC WATER SAMPLE	09/03/80	CL ION C	12.6		PPM
WELL10	FH DOMESTIC WATER SAMPLE	09/03/80	COND ELECT	260		MMHO/CM
WELL10	FH DOMESTIC WATER SAMPLE	09/03/80	EH ELECT	384		M VOLT
WELL10	FH DOMESTIC WATER SAMPLE	09/03/80	F ION C	.20		PPM
WELL10	FH DOMESTIC WATER SAMPLE	09/03/80	HCO3 TITRATE	136		PPM
WELL10	FH DOMESTIC WATER SAMPLE	09/03/80	K AA	4.0		PPM
WELL10	FH DOMESTIC WATER SAMPLE	09/03/80	LI AA	.40		PPM
WELL10	FH DOMESTIC WATER SAMPLE	09/03/80	MG AA	3.60		PPM
WELL10	FH DOMESTIC WATER SAMPLE	09/03/80	NA AA	10.8		PPM
WELL10	FH DOMESTIC WATER SAMPLE	09/03/80	NO3 ION C	N.D.	<0.1	PPM
WELL10	FH DOMESTIC WATER SAMPLE	09/03/80	PH ELECT	7.77		PH
WELL10	FH DOMESTIC WATER SAMPLE	09/03/80	SI02 COLOR	71		PPM
WELL10	FH DOMESTIC WATER SAMPLE	09/03/80	SO4 ION C	6.2		PPM
WELL11	FH DOMESTIC WATER	09/16/80	B COLOR	N.D.	<0.01	PPM
WELL11	FH DOMESTIC WATER	09/16/80	BR ION C	N.D.	<0.1	PPM
WELL11	FH DOMESTIC WATER	09/16/80	CA AA	34		PPM
WELL11	FH DOMESTIC WATER	09/16/80	CL ION C	12.8		PPM
WELL11	FH DOMESTIC WATER	09/16/80	COND ELECT	270		MMHO/CM
WELL11	FH DOMESTIC WATER	09/16/80	EH ELECT	314		M VOLT

WELL13	FH DOMESTIC WATER	12/31/81	LI AA	N.D.	<0.1	PPM
WELL13	FH DOMESTIC WATER	12/31/81	MG AA	6.0		PPM
WELL13	FH DOMESTIC WATER	12/31/81	MO HGA AA	N.D.	<0.01	PPM
WELL13	FH DOMESTIC WATER	12/31/81	NA AA	14		PPM
WELL13	FH DOMESTIC WATER	12/31/81	NI HGA AA	N.D.	<0.001	PPM
WELL13	FH DOMESTIC WATER	12/31/81	NO3 ION C	0.53		PPM
WELL13	FH DOMESTIC WATER	12/31/81	PH ELECT	7.330		PH

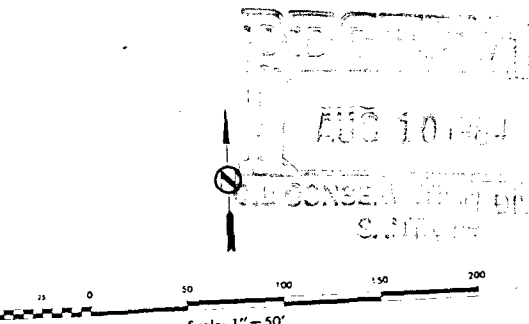
#	LOCATED	COLLECT	ANALYSIS METHOD	RESULT	STD DEV	UNIT
WELL11	FH DOMESTIC WATER	09/16/80	F ION C	0.14		PPM
WELL11	FH DOMESTIC WATER	09/16/80	HCO3 TITRATE	128		PPM
WELL11	FH DOMESTIC WATER	09/16/80	K AA	4.5		PPM
WELL11	FH DOMESTIC WATER	09/16/80	LI AA	0.02		PPM
WELL11	FH DOMESTIC WATER	09/16/80	MG AA	3.60		PPM
WELL11	FH DOMESTIC WATER	09/16/80	NA AA	11.5		PPM
WELL11	FH DOMESTIC WATER	09/16/80	NO3 ION C	N.D.	<0.1	PPM
WELL11	FH DOMESTIC WATER	09/16/80	PH ELECT	7.84		PH
WELL11	FH DOMESTIC WATER	09/16/80	SiO2 COLOR	69		PPM
WELL11	FH DOMESTIC WATER	09/16/80	SO4 ION C	6.8		PPM
WELL12	FH DOMESTIC WATER	10/14/80	B COLOR	0		PPM
WELL12	FH DOMESTIC WATER	10/14/80	BR ION C	N.D.	<0.1	PPM
WELL12	FH DOMESTIC WATER	10/14/80	CA AA	34		PPM
WELL12	FH DOMESTIC WATER	10/14/80	CL ION C	12.0		PPM
WELL12	FH DOMESTIC WATER	10/14/80	COND ELECT	250		MMHO/CM
WELL12	FH DOMESTIC WATER	10/14/80	EH ELECT	244		M VOLT
WELL12	FH DOMESTIC WATER	10/14/80	F ION C	0.15		PPM
WELL12	FH DOMESTIC WATER	10/14/80	HCO3 TITRATE	142		PPM
WELL12	FH DOMESTIC WATER	10/14/80	K AA	2.5		PPM
WELL12	FH DOMESTIC WATER	10/14/80	LI AA	N.D.	<0.01	PPM
WELL12	FH DOMESTIC WATER	10/14/80	MG AA	3.70		PPM
WELL12	FH DOMESTIC WATER	10/14/80	NA AA	10.5		PPM
WELL12	FH DOMESTIC WATER	10/14/80	NO3 ION C	N.D.	<0.1	PPM
WELL12	FH DOMESTIC WATER	10/14/80	PH ELECT	7.58		PH
WELL12	FH DOMESTIC WATER	10/14/80	SiO2 COLOR	71		PPM
WELL12	FH DOMESTIC WATER	10/14/80	SO4 ION C	6.3		PPM
WELL13	FH DOMESTIC WATER	12/31/81	AG HGA AA	N.D.	<0.001	PPM
WELL13	FH DOMESTIC WATER	12/31/81	B COLOR	0.37		PPM
WELL13	FH DOMESTIC WATER	12/31/81	BA HGA AA	0.076		PPM
WELL13	FH DOMESTIC WATER	12/31/81	BR ION C	0.27		PPM
WELL13	FH DOMESTIC WATER	12/31/81	CA AA	56		PPM
WELL13	FH DOMESTIC WATER	12/31/81	CD HGA AA	N.D.	<0.001	PPM
WELL13	FH DOMESTIC WATER	12/31/81	CL ION C	48.8		PPM
WELL13	FH DOMESTIC WATER	12/31/81	CO HGA AA	N.D.	<0.001	PPM
WELL13	FH DOMESTIC WATER	12/31/81	COND ELECT	470		MMHO/CM
WELL13	FH DOMESTIC WATER	12/31/81	CR HGA AA	0.002		PPM
WELL13	FH DOMESTIC WATER	12/31/81	CU HGA AA	0.013		PPM
WELL13	FH DOMESTIC WATER	12/31/81	F ION C	0.10		PPM
WELL13	FH DOMESTIC WATER	12/31/81	FE AA	0.040		PPM
WELL13	FH DOMESTIC WATER	12/31/81	HCO3 TITRATE	145		PPM
WELL13	FH DOMESTIC WATER	12/31/81	K AA	5.2		PPM
WELL13	FH DOMESTIC WATER	12/31/81	LI AA	N.D.	<0.1	PPM
WELL13	FH DOMESTIC WATER	12/31/81	MG AA	6.0		PPM
WELL13	FH DOMESTIC WATER	12/31/81	MO HGA AA	N.D.	<0.01	PPM
WELL13	FH DOMESTIC WATER	12/31/81	NA AA	14		PPM
WELL13	FH DOMESTIC WATER	12/31/81	NI HGA AA	N.D.	<0.001	PPM
WELL13	FH DOMESTIC WATER	12/31/81	NO3 ION C	0.53		PPM
WELL13	FH DOMESTIC WATER	12/31/81	PH ELECT	7.330		PH
WELL13	FH DOMESTIC WATER	12/31/81	PO4 ION C	N.D.	<0.1	PPM

#	LOCATED	COLLECT	ANALYSIS METHOD		RESULT	STD DEV	UNIT
WELL13	FH DOMESTIC WATER	12/31/81	SI	AA	33.3		PPM
WELL13	FH DOMESTIC WATER	12/31/81	SI02	COLOR	71		PPM
WELL13	FH DOMESTIC WATER	12/31/81	SO4	ION C	13.6		PPM

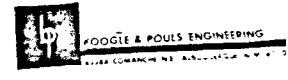




- 500 NEW MEXICO STATE PLANE  
GRID COORDINATE CENTRAL ZONE 1
- FIELD CONTROL POINT
  - BUILDING
  - IMPROVED ROAD
  - UNIMPROVED ROAD & CULVERT
  - TRAIL
  - MASONRY WALL
  - WOOD FENCE
  - WIRE FENCE
  - PIPE
  - SIGN
  - POLE
  - GRADED AREA
  - FLOW LINE
  - DITCH
  - POND
  - INDEX CONTOUR
  - INTERMEDIATE CONTOUR
  - DEPRESSION
  - SPOT ELEVATION



CONTOUR INTERVAL 1 FOOT  
DATUM IS MEAN SEA LEVEL  
COMPILED BY PHOTOGRAMMETRIC METHODS  
DATE OF PHOTOGRAPHY JUNE 27 1979  
THIS MAP COMPLIES WITH THE NATIONAL  
STANDARD MAP ACCURACY REQUIREMENTS



TOPOGRAPHIC MAP  
OF THE  
**GEOTHERMAL SITE**  
SANDOVAL COUNTY, NEW MEXICO  
FOR  
LOS ALAMOS SCIENTIFIC LABORATORIES  
AUGUST 1979

LA-9007-PR  
Progress Report

UC-11  
Issued: September 1981

## **Water Quality in the Vicinity of Fenton Hill, 1980**

W. D. Purtymun  
R. W. Ferenbaugh  
W. H. Adams

**Los Alamos** Los Alamos National Laboratory  
Los Alamos, New Mexico 87545

# WATER QUALITY IN THE VICINITY OF FENTON HILL, 1980

by

W. D. Purtymun, R. W. Ferenbaugh, and W. H. Adams

## ABSTRACT

Water quality data have been collected from established surface and ground water stations and from ponds and pond discharge at Fenton Hill Site located in the Jemez Mountains as part of a continuing program of environmental studies. Most of these stations were established in 1973 with water quality data having been collected since that time. There have been slight variations in the chemical quality of water from the surface and ground water locations; however, these variations are within normal seasonal fluctuations. Water in the ponds used for storage at the site is highly mineralized because of drilling operations or discharge from circulation tests in the fractured reservoir of the deep geothermal holes. Water from the ponds or direct discharges from the circulation tests are discharged into an adjacent dry canyon. The discharge infiltrates into alluvium of the canyon within 400 m of the ponds. Monitoring of surface and spring discharge downgradient from the ponds failed to detect any effects resulting from release of water from the ponds. Analyses of water from the supply well at the site indicated the chemical concentrations were below U.S. Environmental Protection Agency (USEPA) and State of New Mexico standards or criteria for domestic or municipal uses.

---

## I. INTRODUCTION

In 1973, a preliminary study was made of the Jemez River and Rio Guadalupe drainages to establish baseline water quality data before the start of experimental work on the hot dry rock geothermal project by the Los Alamos National Laboratory at the Fenton Hill Site (TA-57).<sup>1</sup> Geologic and hydrologic investigations were made in the area and at TA-57 from 1972 through 1974.<sup>2,3</sup> These studies provided the basis for selecting locations for water quality monitoring stations. Water quality data from the permanently established stations have been published for 1974 through 1979.<sup>4-9</sup> This report presents an interpretation and evaluation of the data for 1980.

Fenton Hill Site is located about 30 km west of Los Alamos on the western flank of the Valles Caldera (Fig. 1). Studies at the site are based on the concept of extracting heat from dry geothermal reservoirs by developing artificial hydrothermal systems. The site contains two deep holes (each 3000 m), completed in dry Precambrian granitic rock. The holes are connected by a large fracture, which was induced by hydrologic pressurization. Water is circulated under pressure through this system to recover heat from fracture areas. The system is complete, and initial tests have been conducted.

A second system is now being developed to a depth of about 4500 m to test the system at a higher temperature. The drilling operations to complete the second system, now in progress, use chemical additives (drilling mud)

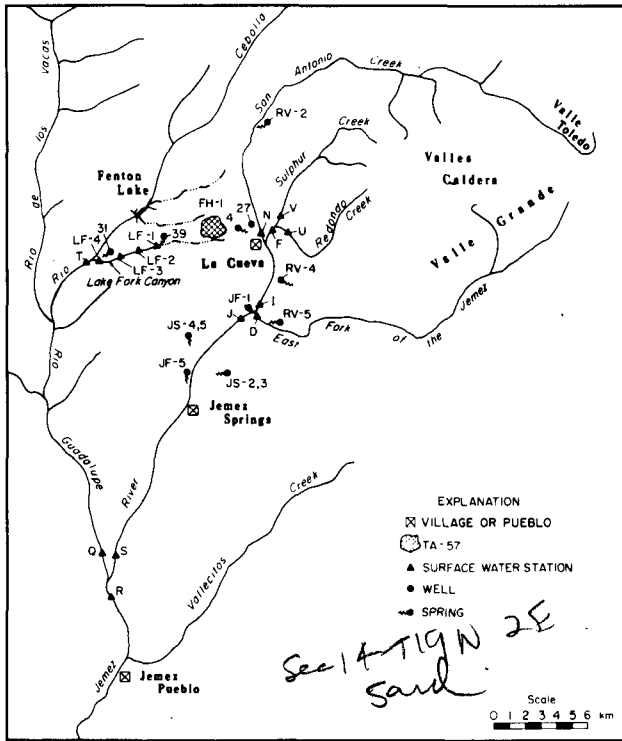


Fig. 1. Location of sampling stations.

and cement. This results in drilling fluids high in sodium, calcium, sulfate, and chlorides. Water from the circulation loop contains moderate concentrations of silica, calcium, magnesium, sodium, sulfates, and chlorides, with moderate to high amounts of fluoride. At times the water has been found to contain elevated concentrations of arsenic, boron, cadmium, and lithium in relation to those concentrations in natural waters. Drilling fluids and water from the circulation loop are stored in two ponds at the site. Periodically, these ponds are drained into the adjacent dry canyon when additional storage is needed. The water, under controlled discharge, is lost to evapotranspiration or infiltration into the alluvium and underlying tuff within 400 m of the outfall from the lower pond.

## II. SURFACE AND GROUND WATER

Water samples for analyses were collected in May and November, 1980 (Figs. 1 and 2), from the immediate drainage area of the site and in the major drainage of the Jemez River and Rio Guadalupe, downgradient from the site. Routine analyses were made for silica, calcium, magnesium, sodium, carbonate, bicarbonate, sulfate,

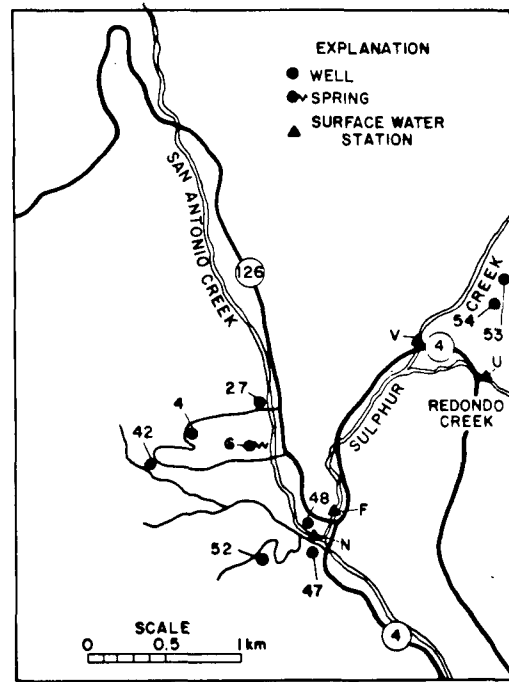


Fig. 2. Location of sampling stations at La Cueva.

chloride, fluoride, nitrate, total hardness, TDS (total dissolved solids), conductance, and pH. Samples were also analyzed for arsenic, boron, cadmium, and lithium. These trace metals are often present in water in the storage ponds at the Fenton Hill Site. All analyses were performed using methods described in a USEPA document.<sup>10</sup>

The discussion of water quality is organized around stations with common chemical properties and TDS.

### A. Surface Water

Surface water stations (nine on the Jemez River, the Rio Guadalupe, and their tributaries) are identified by capital letters in Figs. 1 and 2 and are keyed to detailed analyses presented in Appendix A. There are four general groups of surface water based on common chemical properties of predominate ions and TDS. The predominate ions are (1) sodium and chloride, (2) calcium and bicarbonate, (3) calcium and sulfate, and (4) sodium and bicarbonate.

Sodium and chloride waters are found in base flow of runoff at Locations U, R, and S (Fig. 3). Location U is on Redondo Creek, which drains the interbasin of the

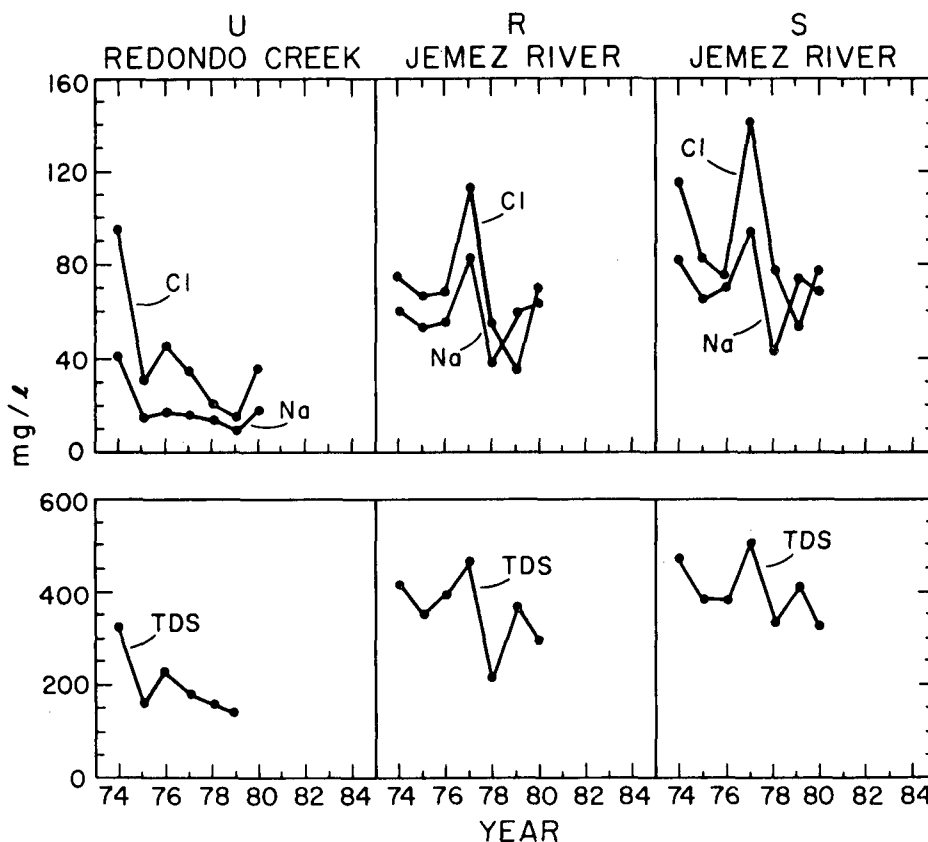


Fig. 3. Sodium, chloride, and TDS in surface water at Locations U, R, and S, 1974-1980.

Valles Caldera, the site of hydrothermal (wet geothermal) development. Locations R and S are on the lower end of the Jemez River. Location R is below the confluence of the Rio Guadalupe with the Jemez River and Location S is above the confluence (Fig. 1).

Calcium and bicarbonate waters are found at Locations N, T, and Q (Fig. 4). Location N is on San Antonio Creek, which drains the northern part of the Valles Caldera, and Location T is located on the Rio Cebolla below the Fenton Hill Site. The Rio Cebolla is a tributary to the Rio Guadalupe at Location Q (Fig. 1). Calcium and bicarbonate waters are also found in surface water in Lake Fork Canyon (Table I). Four surface water stations, LF-1, -2, -3, and -4, are located downgradient from the Fenton Hill Site (Fig. 1). These stations have been sampled and analyzed since 1978 to determine if any chemical changes have occurred as the result of the release of water from the ponds.

Calcium and sulfate waters are found in base flow at Locations V and F (Fig. 5). Location V is on Sulphur Creek and Location F is also on Sulphur Creek below

the junction with Redondo Creek (Fig. 1). The discharge of water from thermal and mineral springs in the Valles Caldera determines the chemical composition of the water at these locations.

Sodium and bicarbonate waters are found at Location J (Fig. 6). Location J is on the Jemez River below the confluence of San Antonio Creek and the East Fork of the Jemez. These two streams drain the interior of the Valles Caldera (Fig. 1).

The mineral and thermal springs along the Jemez Fault discharge into the river above Locations S and R. The springs contain excessive amounts of naturally occurring arsenic, boron, and lithium, which are responsible for the downstream quality of water in the Jemez River (Table II). Other stations contain little or no arsenic, boron, and lithium. Cadmium is low, at or near the limits of detection, at all surface water stations.

Each surface water station has a chemical characteristic reflecting the source of water in the drainage area. The chemical concentrations at each individual station may be modified by snowmelt or rainfall runoff. Thus,

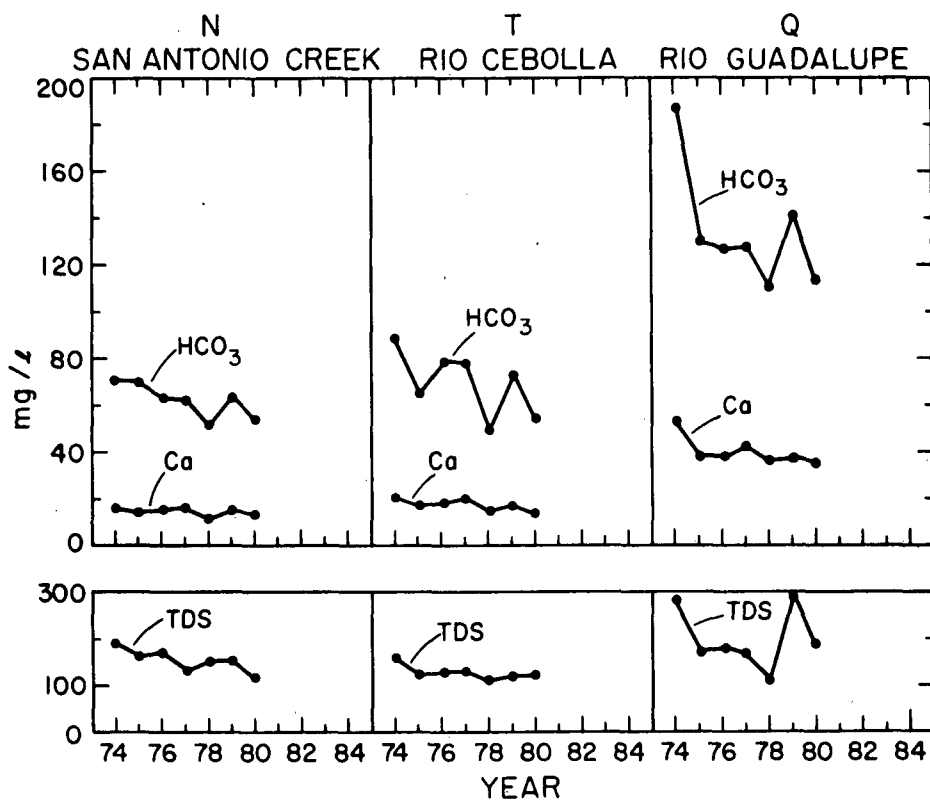


Fig. 4. Calcium, bicarbonate, and TDS in surface water at Locations N, T, and Q, 1974-1980.

TABLE I

PREDOMINATE IONS OF CALCIUM AND BICARBONATE  
IN SURFACE WATER IN LAKE FORK CANYON  
(analyses in mg/l)

Station	Year	No. of Analyses	Ca	HCO <sub>3</sub>	TDS
LF-1	1978-79	3	17 ± 1	51 ± 25	174 ± 33
(6065) <sup>a</sup>	1980	2	15 ± 1	54 ± 14	115 ± 32
LF-2	1978-79	3	18 ± 1	50 ± 14	189 ± 50
(7285) <sup>a</sup>	1980	1	23	80	134
LF-3	1978-79	3	12 ± 2	56 ± 4	143 ± 34
(8500) <sup>a</sup>	1980	2	15 ± 3	63 ± 10	120 ± 3
LF-4	1978-79	4	16 ± 1	70 ± 2	150 ± 29
(9420) <sup>a</sup>	1980	2	18 ± 3	76 ± 8	146 ± 3

<sup>a</sup>Numbers indicate meters below Lower Pond (GTP-3).

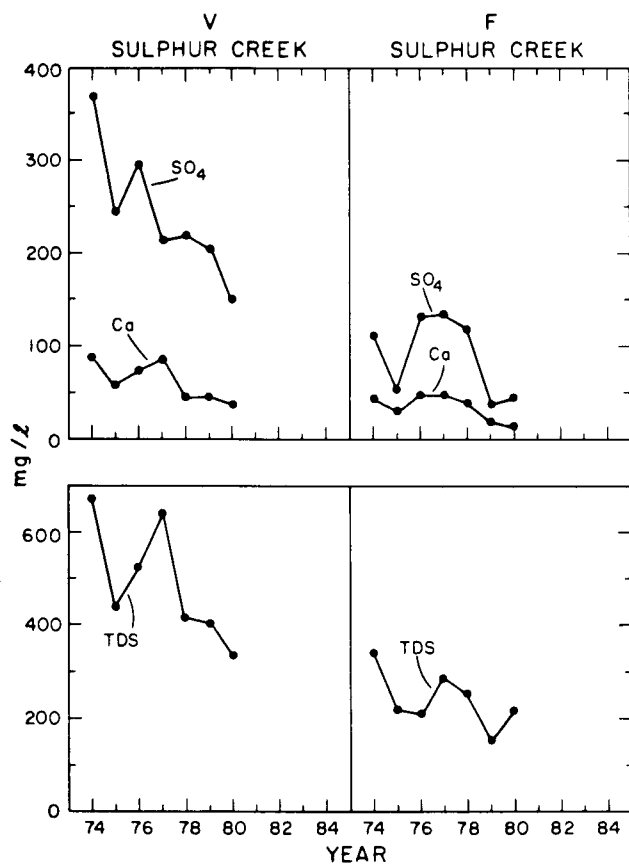


Fig. 5. Calcium, sulfate, and TDS in surface water at Locations V and F, 1974-1980.

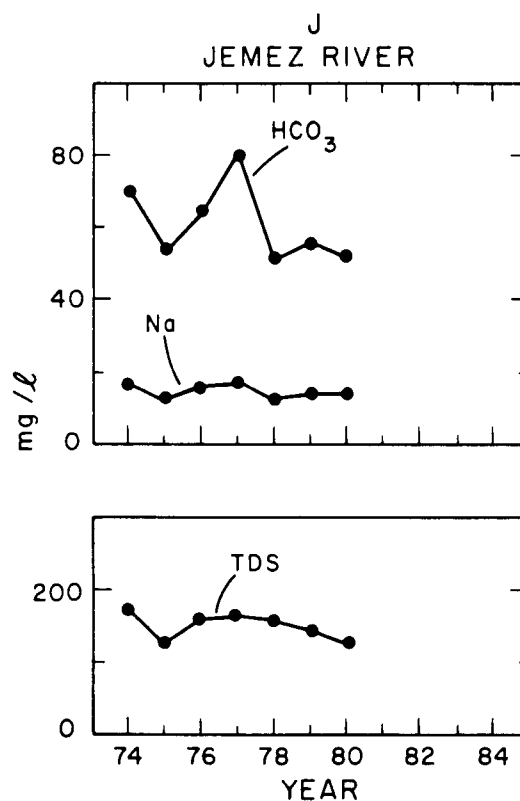


Fig. 6. Sodium, bicarbonate, and TDS in surface water at Location J, 1974-1980.

TABLE II

ARSENIC, BORON, CADMIUM, AND LITHIUM  
IN SURFACE WATER, 1980  
(average two analyses in mg/l)

Station	Location	Arsenic	Boron	Cadmium	Lithium
F	Sulphur Creek	<0.002	0.08	<0.001	0.11
J	Jemez River	0.003	0.05	<0.001	0.07
N	San Antonio Creek	0.003	0.12	<0.001	0.02
Q	Rio Guadalupe	0.002	0.17	<0.001	0.02
R	Jemez River	0.048	0.34	0.002	0.67
S	Jemez River	0.081	0.34	0.003	0.72
T	Rio Cebolla	0.001	0.09	0.002	<0.01
U	Redondo Creek	0.002	0.15	<0.001	0.14
V	Sulphur Creek	0.002	0.02	<0.001	0.03
LF-1	Lake Fork Canyon	<0.001	0.11	<0.001	<0.01
LF-2	Lake Fork Canyon	<0.001	0.13	<0.001	0.02
LF-3	Lake Fork Canyon	<0.001	0.01	<0.001	0.01
LF-4	Lake Fork Canyon	<0.001	0.01	<0.001	0.13

the chemical quality of water at each station can vary widely with change in discharge. The comparison of the chemical quality of surface water from 1974 through 1980 reflects these variations in chemical composition; however, the variations are as anticipated under these conditions (Figs. 3 through 6).

## B. Ground Water

Ground water locations sampled during 1980 include five mineral and thermal springs, five natural springs, and seven wells. The station locations are shown by a capital letter followed by a number or by a number alone (Figs. 1 and 2) and are keyed to detailed analyses presented in Appendix B. Three types of ground water, categorized by predominate ions, occur at ground water stations. The principal types of water are (1) sodium and bicarbonate, (2) sodium and chloride, and (3) calcium and bicarbonate.

Sodium and bicarbonate waters are found at Locations JS-2,-3, JS-4,-5, 4, 6, 27, 31, and 47 and in waters from thermal springs RV-2, RV-4, and RV-5 (Table III). Location JS-2, -3 and JS-4,-5 are springs located on the walls of Jemez Canyon. These springs furnish the water supply for the village of Jemez Springs. Location 4 is a spring that supplies water to some residents of La Cueva, Location 6 is a spring at La Cueva, Location 27 is an unused well, and Location 31 is a spring near the mouth of Lake Fork Canyon (Fig. 1). Location 47 is a well in La Cueva. Thermal springs RV-2, RV-4, and RV-5 discharge from recent volcanic rocks west and south of the Valles Caldera along San Antonio Creek and the east fork of the Jemez River (Fig. 1).

Sodium and chloride waters are found at Locations JF-1 and JF-5 (Table IV). Locations JF-1 and JF-5 are thermal and mineral springs that discharge from along the Jemez Fault into the Jemez River. A series of springs in this reach of Jemez Canyon affect the quality of water in the river, changing it from a sodium and bicarbonate water, as found at Location J, to a sodium and chloride water, as found downgradient from the springs at Locations R and S (Fig. 1).

Calcium and bicarbonate are found at a spring at Location 39, a stock tank in Lake Fork Canyon, two wells at Locations 42 and 48 in La Cueva, and two wells along Sulphur Creek (Table V). The wells along Sulphur Creek, Locations 53 and 54, are being monitored for the first time this year.

The thermal and mineral springs at JF-1 and JF-5 (Soda Dam) along the Jemez Fault contained concentrations of arsenic that ranged from 0.002 to 0.847 mg/l, boron from 1.85 to 4.65 mg/l, and lithium from 3.16 to 13.2 mg/l. Cadmium was 0.008 and <0.001 mg/l, respectively (Table VI). Water from the thermal and mineral springs along the Jemez Fault discharges into the Jemez River. Water from these springs is responsible for the quality of the surface water downstream at Locations R and S on the Jemez River as shown by the concentrations of arsenic, boron, and lithium. Trace amounts of arsenic, boron, cadmium, and lithium occur at natural levels at other ground water locations.

The chemical quality of ground water, springs, or wells reflects the type of rock and length of time the water has been in contact with it from recharge to discharge (spring or well). Seasonal fluctuations in the quality of ground water sources occur as the result of changes in rates of recharge to ground water bodies. Comparison of data from 1974 through 1979 with 1980 reflect normal chemical changes (Tables III through V).

## III. FENTON HILL SITE

The Fenton Hill Site is located on a narrow mesa on the western flank of the Valles Caldera. It is a gently sloping southwest-trending mesa, which is bounded on the east by San Antonio Creek and on the west and northwest by the Rio Cebolla (Fig. 1). Lake Fork Canyon, to the south, drains the immediate area of the site and is tributary to the Rio Cebolla. Adjacent to the site, Lake Fork Canyon and the canyon north of the site contain intermittent streams. Only during periods of heavy precipitation or snowmelt does water reach the Rio Cebolla from these canyons. The lower 5 km of Lake Fork Canyon above the confluence with the Rio Cebolla contains perennial flow from springs and seeps (Fig. 1). Discharges from the ponds at the Fenton Hill site are regulated so that they do not comingle with perennial streams.

### A. Fenton Hill Water Supply (FH-1)

The water supply for Fenton Hill is furnished by a well completed at a depth of about 137 m into a perched aquifer. The aquifer in the Abiquiu Tuff is perched on clays and siltstones of the Abo Formation. The aquifer is

TABLE III

PREDOMINATE IONS OF SODIUM AND  
BICARBONATE IN GROUND WATER  
(analyses in mg/l)

Station	Year	No. of Analyses	Na	HCO <sub>3</sub>	TDS
JS-2,3 (Springs)	1974-79	16	15 ± 2	76 ± 12	182 ± 13
	1980	2	18 ± 5	77 ± 1	182 ± 8
JS-4,5 (Springs)	1974-79	16	15 ± 2	77 ± 13	170 ± 20
	1980	2	17 ± 6	71 ± 4	166 ± 3
Loc. 4 (Spring)	1974-79	16	16 ± 2	67 ± 6	167 ± 25
	1980	2	19 ± 2	60 ± 3	178 ± 17
Loc. 6 (Spring)	1978-79	4	16 ± 2	86 ± 8	188 ± 19
	1980	2	20 ± 2	82 ± 3	210 ± 51
Loc. 27 (Well)	1974-79	13	115 ± 14	387 ± 32	483 ± 52
	1980	2	108 ± 5	302 ± 34	442 ± 65
Loc. 31 (Spring)	1974-79	16	13 ± 3	64 ± 6	148 ± 49
	1980	2	13 ± 3	57 ± 4	129 ± 13
Loc. 47 (Well)	1978-79	4	209 ± 44	514 ± 25	643 ± 23
	1980	2	230 ± 42	536 ± 6	664 ± 20
RV-2 (Spring)	1975-79	5	23 ± 2	50 ± 4	155 ± 22
	1980	1	25	48	182
RV-4 (Spring)	1975-79	6	49 ± 2	117 ± 7	243 ± 23
	1980	1	63	108	172
RV-5 (Spring)	1975-79	6	19 ± 2	74 ± 5	151 ± 27
	1980	1	23	72	172

evidently of limited extent, being terminated to the east along the canyon cut by San Antonio Creek. The movement of water in the aquifer is to the southwest, where a part is discharged through seeps and springs along the lower part of Lake Fork Canyon and the Rio Cebolla.

The production from supply well FH-1 increased  $8.9 \times 10^6 \ell$  from  $18.4 \times 10^6 \ell$  in 1979 to  $27.3 \times 10^6 \ell$  in 1980. The monthly production during 1980 ranged from

a low of  $0.07 \times 10^6 \ell$  (November) to  $5.8 \times 10^6 \ell$  (March). The pumpage from the well during the 10-day aquifer test in October was  $4.9 \times 10^6 \ell$ . Methods used and results of the test are described elsewhere.<sup>11</sup> Cumulative total production from the well since 1976 has been  $76.5 \times 10^6 \ell$ . Water level decline from 1976 through December 1980 has been about 2 m.

TABLE IV

**PREDOMINATE IONS OF SODIUM AND  
CHLORIDE IN GROUND WATER**  
(analyses in mg/l)

<u>Station</u>	<u>Year</u>	<u>No. of Analyses</u>	<u>Na</u>	<u>Cl</u>	<u>TDS</u>
Loc. JF-1	1974-79	16	262 ± 59	389 ± 86	1245 ± 156
(Spring)	1980	2	301 ± 203	417 ± 279	1337 ± 575
Loc. JF-5	1974-79	17	815 ± 158	1444 ± 65	3688 ± 268
(Spring)	1980	2	922 ± 60	1512 ± 95	3904 ± 76

Note: Thermal and mineral springs along the Jemez Fault.

TABLE V

**PREDOMINATE IONS OF CALCIUM AND  
BICARBONATE IN GROUND WATER**  
(analyses in mg/l)

<u>Stations</u>	<u>Year</u>	<u>No. of Analyses</u>	<u>Ca</u>	<u>HCO<sub>3</sub></u>	<u>TDS</u>
Loc. 39	1978-79	4	13 ± 3	38 ± 18	96 ± 15
(Spring)	1980	2	14 ± 2	44 ± 6	81 ± 10
Loc. 42	1978-79	4	10 ± 1	73 ± 3	168 ± 16
(Well)	1980	2	12 ± 0	76 ± 0	169 ± 10
Loc. 48	1978-79	3	22 ± 2	90 ± 0	182 ± 4
(Well)	1980	2	22 ± 0	92 ± 6	213 ± 32
Loc. 53	1980	2	45 ± 4	139 ± 2	331 ± 64
(Well)					
Loc. 54	1980	1	61	268	418
(Well)					

TABLE VI

ARSENIC, BORON, CADMIUM, AND  
LITHIUM IN GROUND WATER, 1980  
(average two analyses in mg/l)

Station	Location	Arsenic	Boron	Cadmium	Lithium
JS-2,3	Jemez Village	0.002	0.01	<0.001	0.01
JS-4,5	Jemez Village	0.001	0.01	<0.001	0.02
JF-1	Jemez Canyon	0.002	1.85	0.008	3.16
JF-5	Jemez Canyon	0.847	4.65	<0.001	13.2
4	La Cueva	<0.001	0.08	<0.001	0.02
6	La Cueva	0.003	0.11	<0.001	0.02
27	La Cueva	<0.001	0.24	<0.001	0.57
31	Lake Fork Canyon	0.002	0.01	<0.001	<0.01
39	Lake Fork Canyon	0.002	0.12	<0.001	<0.01
42	La Cueva	0.001	0.16	<0.001	0.01
47	La Cueva	0.006	0.30	<0.001	0.10
48	La Cueva	0.002	0.07	<0.001	0.01
53	Sulphur Canyon	0.007	0.05	<0.001	0.02
54	Sulphur Canyon <sup>a</sup>	0.008	0.02	<0.001	0.02

<sup>a</sup>One analysis.

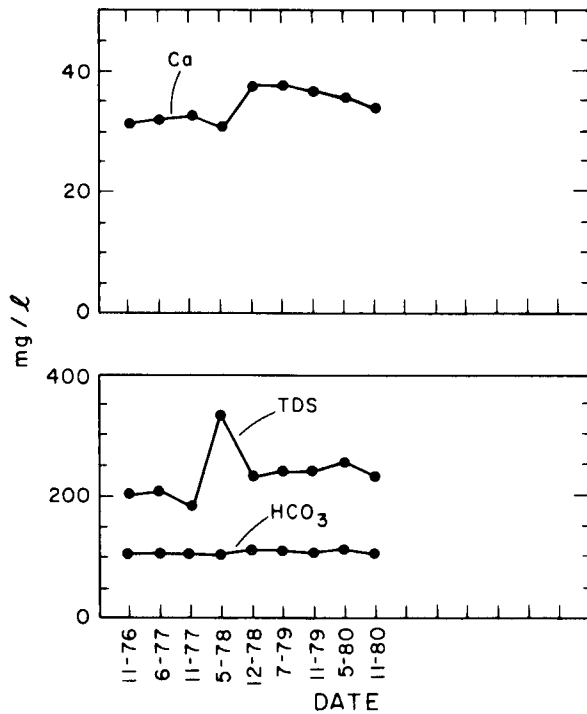


Fig. 7. Calcium, bicarbonate, and TDS from supply well FH-1, Fenton Hill (TA-57), 1976-1980.

Calcium and bicarbonate are the predominate ions in water from well FH-1 (Fig. 7). The concentrations of these ions have shown no significant change from 1976 to 1980. Total dissolved solids have varied, in general, increasing slightly.

Water from the well was analyzed for chemical and radiochemical constituents for comparison with standards set for municipal or domestic use by the USEPA and the State of New Mexico.<sup>12,13</sup> A comparison of the analytical results of water from the well with federal and state standards shows that the water is well below limits set for municipal use (Table VII).

Two test holes were drilled and cased into the same aquifer as FH-1. The water from both wells contains principally ions of calcium and bicarbonate. Total dissolved solid from FH-2 was 206 mg/l and FH-3 was 560 mg/l. The analyses from well FH-3 are probably not representative of the water in the aquifer as the sample was collected during development. Complete analyses of water from the test holes FH-2 and FH-3 are shown in Appendix B.

TABLE VII

**CHEMICAL AND RADIOCHEMICAL  
CONCENTRATIONS IN WATER FROM  
SUPPLY WELL FH-1, 1980**  
(analyses in mg/l)

Chemical (mg/l)	Supply Well FH-1	Standard or Criteria <sup>a</sup>
Ag	<0.003	0.05
As	0.002	0.05
Ba	0.086	1.0
Cd	0.0003	0.010
Cl	15	250
Cr	<0.002	0.05
F	0.1	2.0
Hg	<0.0005	0.002
Na	12	250
NO <sub>3</sub>	1.3	45
Pb	0.003	0.05
Se	<0.005	0.01
TDS	236	1000
<b>Radiochemical (pCi/l)</b>		
<sup>3</sup> H		20
<sup>137</sup> Cs	30	200
<sup>238</sup> Pu	<0.02	15
<sup>239</sup> Pu	<0.03	15
Gross alpha	2.0	15

<sup>a</sup>References 12 and 13.

### B. Storage Ponds

Three ponds have been used at various times to store water from experimental operations in the circulation loop and from drilling operations. During 1980, the volume and surface area of the upper pond (GTP-1) was enlarged. The middle pond (GTP-2) was filled with soil and tuff, so that at the end of 1980, only two storage ponds remained at the site, the upper (GTP-1) and lower (GTP-3).

The ponds were sampled in May, June, and November 1980. The results of the analyses are shown in Appendix C.

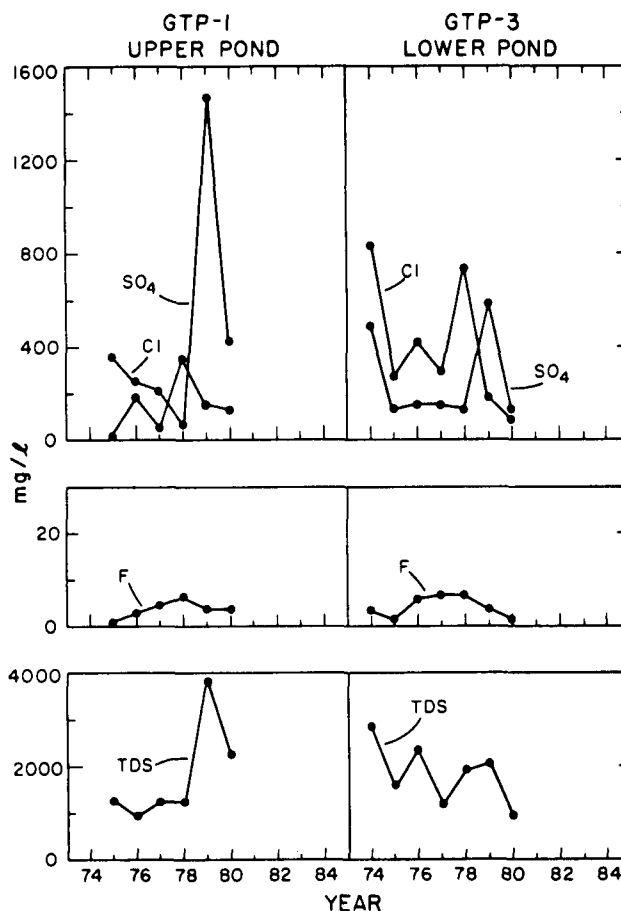


Fig. 8. Sulfate, chloride, fluoride, and TDS at Ponds GTP-1 and GTP-3, Fenton Hill (TA-57), 1974-1980.

Concentrations of sulfate, chlorides, fluorides, and TDS have varied in the ponds for the period of record, reflecting the type of test being conducted or drilling operations in progress at the time the samples were collected (Fig. 8). In general, the TDS in the two ponds, GTP-1 and GTP-3, declined in 1980 compared with the 1979 data, as did most other constituents.

Arsenic, boron, and lithium are present in the pond water. These constituents are from the operation of the circulation loop or additives to drilling fluids (Table VIII). Cadmium was low, at or below limits of detection.

Water from the site was released during two periods in 1980. The first release occurred October 22 through 28 when  $1.13 \times 10^6$  l of water was released during the aquifer test of FH-1, with some release of fluids from the lower pond GTP-3. Fourteen chemical constituents were

TABLE VIII

**ARSENIC, BORON, CADMIUM, AND LITHIUM  
IN PONDS AT FENTON HILL (TA-57)  
(analyses in mg/l)**

<u>Station</u>	<u>Location</u>	<u>Date (1980)</u>	<u>Arsenic</u>	<u>Boron</u>	<u>Cadmium</u>	<u>Lithium</u>
GTP-1	Upper Pond	5-27	0.019	1.15	0.001	0.97
		6-9	0.018	0.78	0.002	0.53
	East	11-18	0.116	1.80	<0.001	1.59
	West	11-18	0.112	2.29	0.001	1.63
GTP-2	Middle Pond <sup>a</sup>	5-27	0.018	1.18	0.008	0.23
GTP-3	Lower Pond	5-27	0.024	1.06	0.007	1.10
		11-18	0.014	0.32	<0.001	<0.01

<sup>a</sup>Pond filled with soil and tuff, July 1980.

measured during the release (Table IX). About 840 kg of TDS were released into the canyon with the water.

The second release of about  $1.87 \times 10^6$  l was from December 18 through 31. The release was not from the ponds but was vented directly from the circulation loop. The discharge was highly mineralized, carrying 4170 kg of total dissolved solids into the canyon. Water released from the site in 1980 infiltrated into the alluvium of the canyon within 300 m of the site.

Chemical concentrations in water from Locations 39 (Spr), LF-1, LF-2, LF-3, LF-4 (SW), 31 (Spr), and T (SW) downgradient from the Fenton Hill Site Ponds in Lake Fork Canyon were in the normal range found in natural waters. The concentrations from these locations showed no effects of water released from the site.

### C. Vegetation and Soil Analysis

Samples of vegetation and soil from the canyon bottom and the bank of the channel below GTP-3 have been collected semiannually since 1978. These samples have been analyzed for As, B, Cd, F, and Li. The sampling locations are about 100, 200, 400, and 1000 m down the canyon. An additional sample is collected far down the

canyon at its junction with Lake Fork Canyon. The available data from these analyses are presented in the 1980 Annual Surveillance Report.<sup>14</sup>

Although the analytical results to date are scanty, there is some indication in the lithium and boron data that there might be elevated concentrations in vegetation in the stream channel in the upper part of the canyon. The results are consistent with the conclusion that the discharge from the ponds infiltrates into the alluvium within 400 m of the point of discharge.

### IV. SUMMARY

During 1980, the quality of surface and ground water within the drainage area of Fenton Hill Site varied slightly, which was attributed to normal seasonal fluctuations. The quality was within previously measured concentrations.

Water in ponds at the site is used in drilling operations and experiments in the circulation loop. Little water was discharged from the ponds during 1980. The two releases of water, about  $3.0 \times 10^6$  l, that did occur were from an aquifer test of the supply well and direct venting of water from the circulation loop. The second release, from the

TABLE IX

**CHEMICAL QUALITY AND ESTIMATED AMOUNT OF CHEMICALS  
DISCHARGED INTO CANYON, OCTOBER AND DECEMBER 1980**

Analyses	mg/l				Estimated Amount (kg)
	Min	Max	$\bar{x}$	s	
<u>October 22-28<sup>a</sup></u>					
SiO <sub>2</sub>	70	195	95	56	107
Ca	17	35	31	8	35
Mg	1	4	3	1	3
Na	12	770	163	338	184
CO <sub>3</sub>	0	0	0	0	0
HCO <sub>3</sub>	106	1140	312	462	353
SO <sub>4</sub>	7	580	122	256	138
Cl	14	216	56	89	63
F	0.3	4.3	1.1	1.8	1
TDS	230	2730	743	1111	840
As	<0.001	0.024	0.005	0.111	<0.1
B	0.1	3.6	1.0	1.5	1
Cd	<0.002	---	---	---	<0.1
Li	0.01	1.8	0.39	0.79	0.4
<u>December 18-31<sup>b</sup></u>					
SiO <sub>2</sub>	218	240	232	7	434
Ca	34	69	54	13	101
Mg	<1	36	17	15	32
Na	465	650	564	62	1055
CO <sub>3</sub>	0	0	0	0	0
HCO <sub>3</sub>	384	470	438	28	819
SO <sub>4</sub>	178	240	218	18	408
Cl	361	777	584	154	1092
F	7.0	11	9.4	1.4	18
TDS	1754	2575	2230	283	4170
As	0.125	0.385	0.269	0.087	0.5
B	5.5	9.5	7.7	1.4	14
Cd	<0.002	0.032	0.005	0.009	<0.1
Li	7.6	10.6	8.8	2.1	16

<sup>a</sup>Five analyses; amount discharged  $1.13 \times 10^6$  l.

<sup>b</sup>Twelve analyses; amount discharged  $1.87 \times 10^6$  l.

circulation loop, was highly mineralized. Monitoring of surface water and spring discharge downgradient (6065 to 9420 m) from the site failed to detect any effect of the previous releases.

#### ACKNOWLEDGMENTS

Field work was done by Max Maes, Chris Tafoya, and Bill Purtymun (H-8). Typesetting and compiling of the finished report was done by Kathy Derouin (H-8).

#### REFERENCES

1. W. D. Purtymun, F. G. West, and W. H. Adams, "Preliminary Study of the Quality of Water in the Drainage Area of the Jemez River and Rio Guadalupe," Los Alamos Scientific Laboratory report LA-5595-MS (April 1974).
2. W. D. Purtymun, "Geology of the Jemez Plateau West of the Valles Caldera," Los Alamos Scientific Laboratory report LA-5124-MS (February 1973).
3. W. D. Purtymun, F. G. West, and R. A. Pettitt, "Geology of Geothermal Test Hole GT-2 Fenton Hill Site, July 1974," Los Alamos Scientific Laboratory report LA-5780-MS (November 1974).
4. W. D. Purtymun, W. H. Adams, and J. W. Owens, "Water Quality in Vicinity of Fenton Hill Site, 1974," Los Alamos Scientific Laboratory report LA-6093 (December 1975).
5. W. D. Purtymun, W. H. Adams, A. K. Stoker, and F. G. West, "Water Quality in Vicinity of Fenton Hill Site, 1975," Los Alamos Scientific Laboratory report LA-6511-MS (September 1976).
6. W. D. Purtymun, W. H. Adams, and A. K. Stoker, "Water Quality in the Vicinity of Fenton Hill Site, 1976," Los Alamos Scientific Laboratory report LA-7307-MS (May 1978).
7. W. D. Purtymun, A. K. Stoker, W. H. Adams, and J. W. Owens, "Water Quality in Vicinity of the Fenton Hill Site, 1977," Los Alamos Scientific Laboratory report LA-7468-PR (September 1978).
8. W. D. Purtymun, R. W. Ferenbaugh, A. K. Stoker, W. H. Adams, and J. W. Owens, "Water Quality in the Vicinity of Fenton Hill Site, 1978," Los Alamos Scientific Laboratory report LA-8217-PR (January 1980).
9. W. D. Purtymun, R. W. Ferenbaugh, A. K. Stoker, and W. H. Adams, "Water Quality in the Vicinity of Fenton Hill, 1979," Los Alamos Scientific Laboratory report LA-8424-PR (June 1980).
10. "Methods for Chemical Analysis of Water and Wastes," U.S. Environmental Protection Agency, Office of Technology Transfer, EPA-600 4-79-020, Washington, D.C. (1979).
11. N. M. Becker, W. D. Purtymun, and W. C. Ballance, "Aquifer Evaluation at Fenton Hill, October and November 1980," Los Alamos National Laboratory report (in preparation).
12. U.S. Environmental Protection Agency, "Scientific Interim Primary Drinking Water Regulations," EPA-570/9-76-003, EPA, Office of Water Supply (1976).
13. New Mexico Environmental Improvement Department, "Water Supply Regulations," New Mexico Environmental Improvement Department, Santa Fe, New Mexico (1977).
14. Environmental Surveillance Group, "Environmental Surveillance at Los Alamos During 1980," Los Alamos National Laboratory report LS-8810-ENV (April 1981).

APPENDIX A  
SURFACE WATER QUALITY

Station	Location	Date 1980	mg/l													Total Hard	Specific Cond (umho)	pH	Temp °C
			SiO <sub>2</sub>	Ca	Mg	Na	CO <sub>3</sub>	HCO <sub>3</sub>	SO <sub>4</sub>	Cl	F	NO <sub>3</sub>	TDS						
F	Sulphur Creek	5-27	31	16	3	6	0	14	29	7	0.4	<1	170	51	215	6.7	2		
		11-18	35	34	5	32	0	22	64	56	0.5	<1	262	106	385	7.0	2		
J	Jemez River	5-27	32	12	2	7	0	32	14	2	0.5	<1	118	36	100	7.2	3		
		11-18	51	12	3	21	0	72	8	4	0.8	<1	130	42	155	7.8	4		
N	San Antonio Creek	5-27	34	12	2	6	0	42	6	2	0.5	<1	120	39	180	7.3	3		
		11-18	57	14	2	22	0	66	12	2	1.2	<1	118	46	170	7.8	3		
Q	Rio Guadalupe	5-27	29	24	3	26	0	76	12	24	0.5	<1	204	72	240	7.6	7		
		11-18	27	51	7	19	0	158	11	4	0.7	<1	182	155	350	7.9	5		
R	Jemez River	5-27	26	24	2	23	0	68	12	23	0.5	<1	178	69	230	7.6	7		
		11-18	46	52	7	105	0	180	17	118	1.1	<1	412	158	750	8.4	6		
S	Jemez River	5-27	28	24	3	26	0	70	14	29	0.6	<1	222	70	280	7.6	7		
		11-18	49	51	6	113	0	180	16	128	1.1	<1	436	154	790	8.3	6		
T	Rio Cebolla	5-27	32	11	2	7	0	44	1	2	0.3	<1	104	35	90	7.0	10		
		11-18	37	17	2	15	0	66	6	2	0.6	<1	150	53	150	7.1	2		
U	Redondo Creek	5-27	27	12	2	9	0	30	6	10	0.2	<1	120	38	125	7.0	2		
		11-18	33	27	4	29	0	38	19	62	0.4	<1	174	84	310	7.2	1		
V	Sulphur Creek	5-27	35	18	3	7	0	0	26	2	0.4	<1	198	57	205	4.1	3		
		11-18	48	60	11	25	0	0	274	4	0.5	<1	480	196	570	3.8	4		
LF-1	Lake Fork (6065)*	6-9	24	14	2	5	0	44	14	2	0.3	<1	92	45	100	5.6	---		
LF-2	Lake Fork (7285)*	11-18	39	16	3	12	0	64	10	4	0.5	<1	138	54	160	5.6	2		
		6-9	32	23	3	10	0	80	3	2	0.3	<1	134	70	150	6.6	---		
LF-3	Lake Fork (8500)*	6-9	56	17	3	13	0	70	6	3	0.6	<1	122	54	150	6.4	---		
		11-18	58	13	2	15	0	56	6	3	0.9	1.3	118	39	130	6.6	11		
LF-4	Lake Fork (9420)*	6-9	38	20	3	14	0	82	4	3	0.7	<1	148	62	170	6.8	---		
		11-18	61	16	3	10	0	70	7	3	0.9	<1	144	51	170	6.7	1		

\*Numbers indicate meters below Lower Pond (GTP-3) in Lake Fork Canyon.

APPENDIX B

GROUND WATER QUALITY

Station	Location	Date 1980/	mg/l													Specific Cond.		Temp °C
			SiO <sub>2</sub>	Ca	Mg	Na	CO <sub>3</sub>	HCO <sub>3</sub>	SO <sub>4</sub>	Cl	F	NO <sub>3</sub>	TDS	Total Hard	pH			
JS-2,3	Jemez Village (Spr)	5-27	62	15	3	14	0	68	<1	3	0.5	2	188	51	160	7.4	12	
		11-18	34	20	3	21	0	78	10	4	0.5	2	176	62	190	7.5	12	
JS-4,5	Jemez Village (Spr)	5-27	71	14	3	13	0	68	<1	2	0.5	1	168	48	140	7.5	9	
		11-18	34	18	3	21	0	74	5	2	0.5	1	164	57	170	7.8	11	
FH-1	Fenton Hill (Well)	5-27	66	36	5	13	0	112	10	12	0.2	1	252	110	250	7.4	16	
		11-19	70	33	4	15	0	94	7	26	0.4	1	218	101	270	7.2	6	
FH-2	Fenton Hill (Well)	1-31	56	31	3	12	0	104	14	8	0.3	3	206	90	265	7.8	---	
		5-21	44	84	18	14	0	426	12	8	0.3	<1	560	284	800	6.0	---	
JF-1	Jemez Canyon (Hot Spr)	5-27	37	99	10	157	0	394	28	220	2.2	<1	930	290	1380	6.8	12	
		11-18	45	79	17	445	0	520	31	615	2.3	1	1744	267	2940	7.3	16	
JF-5	Jemez Canyon (Hot Spr)	5-27	43	142	20	880	0	1220	41	1445	3.5	<1	3850	437	6000	6.3	42	
		11-18	44	136	27	965	0	1100	38	1580	3.3	<1	3958	450	6200	6.6	46	
RV-2	San Antonio (Hot Spr)	11-18	76	4	<1	25	0	48	7	2	0.7	2	182	11	120	7.7	43	
RV-4	Spence (Hot Spr)	11-18	60	8	2	63	0	108	20	6	0.7	<1	172	28	280	7.9	40	
RV-5	McCauley (Hot Spr)	11-19	53	9	5	23	0	72	6	2	1.1	2	172	42	160	7.6	32	
Loc. 4	La Cueva (Well)	6-4	84	10	3	18	0	62	<1	3	0.5	2	190	35	130	6.9	15	
		11-18	81	10	3	20	0	58	7	3	0.2	1	166	36	140	7.3	14	
Loc. 6	La Cueva (Spr)	6-4	72	14	4	18	0	84	<1	3	0.7	2	246	54	180	6.7	13	
		11-18	71	15	4	21	0	80	5	3	0.4	1	174	54	180	7.0	16	
Loc. 27	La Cueva (Well)	6-4	65	26	8	112	0	326	22	4	0.8	<1	488	95	560	6.9	14	
		11-18	66	26	6	105	0	278	6	3	0.7	<1	396	92	580	7.1	21	
Loc. 31	Lake Fork Canyon (Spr)	5-27	48	14	2	11	0	54	<1	3	1.0	1	138	43	130	6.5	10	
		11-19	50	14	2	15	0	60	5	2	0.8	1	120	43	140	6.4	1	
Loc. 39	Lake Fork Tank (Spr)	6-9	26	12	2	5	0	40	14	2	0.3	<1	88	41	100	5.7	---	
		11-19	25	15	3	6	0	48	14	1	0.3	<1	74	50	120	5.9	10	

## APPENDIX B (cont)

Station	Location	Date 1980	mg/l													Specific Cond. (µmho)	pH	Temp °C
			SiO <sub>2</sub>	Ca	Mg	Na	CO <sub>3</sub>	HCO <sub>3</sub>	SO <sub>4</sub>	Cl	F	NO <sub>3</sub>	TDS	Total Hard				
Loc. 42	La Cueva (Well)	6-4	72	12	3	11	0	76	9	3	0.3	<1	176	54	150	6.3	14	
		11-18	71	12	6	15	0	76	5	1	0.4	<1	162	55	170	6.5	10	
Loc. 47	La Cueva (Well)	6-4	23	8	2	200	0	532	37	3	2.0	2	678	30	920	7.9	16	
		11-18	19	6	4	260	0	540	22	2	2.1	<1	650	32	1020	8.2	6	
Loc. 48	La Cueva (Well)	6-4	62	22	4	20	0	88	12	5	0.4	2	190	72	200	6.6	5	
		11-18	58	22	5	21	0	96	10	6	0.7	<1	236	75	230	6.7	7	
Loc. 53	Sulphur Creek (Well)	6-4	66	42	5	18	0	140	5	3	0.4	9	376	126	300	6.5	14	
		11-18	62	48	2	18	0	138	13	3	0.5	3	286	130	305	6.7	6	
Loc. 54	Sulphur Creek (Well)	11-18	64	61	11	45	0	268	22	5	0.4	8	418	198	550	6.9	---	

## APPENDIX C

## WATER QUALITY OF PONDS AT FENTON HILL (TA-57)

Station	Location	Date 1980	mg/l													Specific Cond. (µmho)	pH
			SiO <sub>2</sub>	Ca	Mg	Na	CO <sub>3</sub>	HCO <sub>3</sub>	SO <sub>4</sub>	Cl	F	NO <sub>3</sub>	TDS	Total Hard			
GTP-1	Upper Pond	5-27	115	25	5	630	0	860	36	121	1.6	<1	2440	83	2400	7.2	
		6-9	79	36	6	354	0	420	256	76	1.3	<1	1496	114	1370	8.0	
		11-18	121	16	2	740	0	780	710	167	5.5	<1	2526	48	3100	7.3	
GTP-2	Middle Pond*	11-18	124	16	2	760	0	860	680	166	6.0	<1	2604	46	3210	8.2	
		5-27	97	30	3	550	0	680	53	130	1.9	<1	2180	89	2100	7.4	
GTP-3	Lower Pond	5-27	69	32	3	325	0	530	101	128	1.9	<1	1376	91	1600	6.8	
		11-18	69	32	4	18	0	164	120	34	0.8	<1	456	95	610	7.0	

\*Pond filled with soil and tuff. July 1980.

APPENDIX B

Aquifer Evaluation at Fenton Hill October and November,  
1980 LA-8964-MS, Los Alamos National Laboratory

LA-8964-MS

UC-66e

Issued: October 1981

**Aquifer Evaluation at Fenton Hill,  
October and November 1980**

N. M. Becker  
W. D. Purtymun  
W. C. Ballance \*

\*Consultant. 179 La Cueva, Los Alamos, NM 87544.

**Los Alamos** Los Alamos National Laboratory  
Los Alamos, New Mexico 87545

AQUIFER EVALUATION AT FENTON HILL,  
OCTOBER AND NOVEMBER 1980

by

N. M. Becker, W. D. Purtymun, and W. C. Ballance

ABSTRACT

An aquifer test at the Fenton Hill Geothermal Site was performed on a volcanic aquifer used for water supply. The test was made to determine the yield from the aquifer and to predict the amount of depletion that would occur with increased production during the period 1981-1985. A step-discharge test indicated the aquifer would comfortably yield 100 gal per min (gpm) without excessive water level drawdown in the pumping well. Drawdown test results indicated that the average aquifer transmissivity and storage coefficient are 5000 gal per day per foot (gpd/ft) and 0.07, respectively. Using these parameters, a drawdown was estimated to be at least 42 ft at the pumping well due to a withdrawal of 500 acre-ft of water over 5 yr. However, the presence of ground water boundaries indicates the aquifer is of limited extent, and because of this, the water level decline would probably be much greater. Past water level data indicate that there is little recharge to the aquifer and that the ground water is being depleted.

---

I. INTRODUCTION

The Fenton Hill Site (TA-57) of the Los Alamos National Laboratory is located about 40 mi west of Los Alamos, New Mexico, on the western flank of the Valles Caldera, where investigations are in progress to extract heat from dry geothermal reservoirs.<sup>1</sup>

The development of the geothermal reservoir systems, drilling, fracturing to form the reservoirs, filling the reservoirs for the circulation tests, and supplying makeup water for losses incurred during circulation requires a water supply. Since late 1976, a part of the water supply has come from a well completed in the Cenozoic volcanics while the remainder has been hauled to the site. Therefore, evaluation of the volcanic aquifer was made to determine if it could furnish expected future requirements.

The evaluation consisted of a stepped-drawdown test and a 10-day constant-discharge aquifer-drawdown test

and recovery in October and November 1980. The data from the step and aquifer test were used to determine hydrogeologic parameters to evaluate the performance of the aquifer with the anticipated increased production. This report presents this evaluation and also summarizes previous hydrologic studies.

Two hydrogeologic parameters that frequently will be referred to are aquifer transmissivity and storage coefficient. The transmissivity (T), which is a measure of the ease with which the aquifer transmits water, may be defined

$$T = Kb,$$

where

K = hydraulic conductivity  
b = saturated thickness

the storage coefficient ( $s$ ) may be defined

$$s = \frac{-V_{wr}}{-V_a}$$

where

$-V_{wr}$  = volume of water released or taken into storage

$-V_a$  = volume of aquifer; cross sectional area under unit decline in potentiometric head.

Using a model for radial flow in an infinite, homogeneous, confined aquifer under nonequilibrium conditions, the aquifer test data were used to compute a transmissivity  $T$  of 5000 gpd/ft (gal per day per foot) and a storage coefficient  $s$  of 0.07 (dimensionless). During the 10-day test, at least five hydrologic boundaries were present. These boundaries indicate the aquifer is of limited spatial extent. Records of water level decline indicate that there is little or no recharge to this aquifer, and that the ground water is being mined. A projection of water level decline due to the withdrawal of 500 acre-ft of water over 5 yr was made using  $T = 5000$  gpd/ft and  $s = 0.07$ ; a drawdown of 41.6 ft at FH-1 (the pumping well) and 19.4 ft at FH-3 (located 90 ft from FH-1) was computed. However, due to the presence of aquifer boundaries, the actual decline is expected to be greater than the computed decline.

### A. Geohydrology

The Fenton Hill Site is located near the eastern end of a narrow southwest-trending mesa on the western side of the Valles Caldera. The surface of the mesa slopes gently to the southwest terminating in cliffs and steep slopes above the Rio Cebolla (Fig. 1). Lake Fork Canyon slopes to the south drains the immediate area of the site and is tributary to the Rio Cebolla. Lake Fork Canyon contains intermittent streams in the upper reach; however, near the Rio Cebolla, the ground water discharges to form perennial streams that reach the Rio Cebolla. The eastern edge of the mesa is terminated by a canyon cut by San Antonio Creek, which drains to the south (Fig. 1).

The elevation of the site is about 8700 ft. The average annual precipitation in the area ranges from 14 in. at lower elevations to about 22 in. of precipitation in the mountains east of the site. Average annual air temperature ranges from 40 to 50°F with annual reservoir evaporation at about 46 in.<sup>2</sup>

The upper surface of the mesa is formed by the Bandelier Tuff which, in turn, is underlain by the Paliza Canyon Formation and Abiquiu Tuff.<sup>3-6</sup> The volcanic aquifer is within the Abiquiu Tuff and lower part of the Paliza Canyon Formation. The aquifer is underlain by the Abo Formation that perches the aquifer in the volcanics.<sup>7</sup>

The Bandelier Tuff is a series of ashflows of moderately welded to welded rhyolite tuff. The tuff ranges from light to dark gray and consists of quartz and sanidine crystals with crystal and lithic fragments of

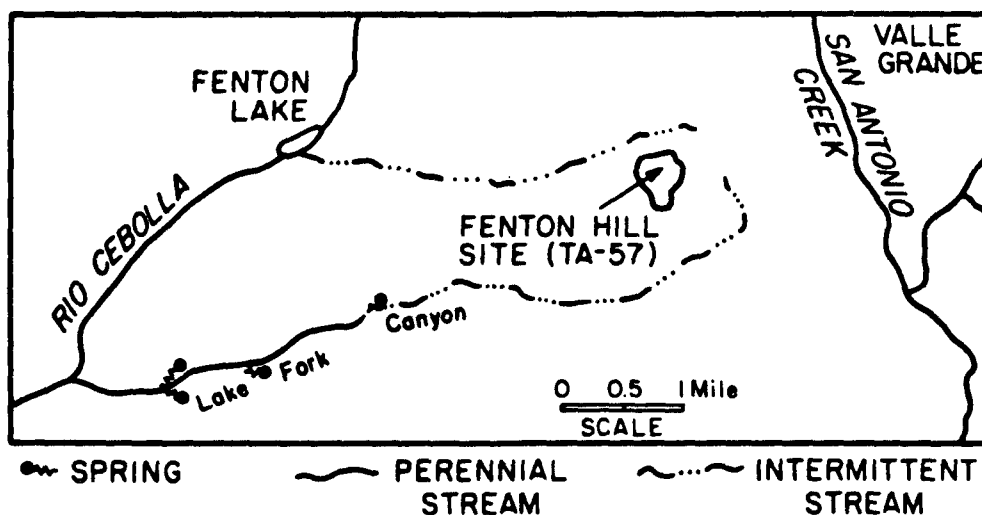


Fig. 1. Location of TA-57 on the west side of the Valle Grande.

latite and rhyolite in an ash matrix. The thickness at the site is about 50 ft.

The Paliza Canyon Formation underlies the Bandelier Tuff. The formation is composed of andesite and basalt andesite breccias that are interbedded with sand and gravels. The thickness at the site is about 310 ft. The Abiquiu Tuff underlies the Paliza Canyon and is composed of a light gray, friable tuffaceous sandstone. The sandstone is composed of quartz, chalcedony, and fragments of the rhyolite and quartzite in a tuffaceous matrix. The upper part of the section is interbedded with angular fragments of basalts. The lower part contains rock fragments and pebbles derived from Precambrian crystalline rocks. The thickness of the Abiquiu Tuff is about 90 ft at the site.<sup>8</sup>

The Abo Formation underlying the Abiquiu Tuff is composed of clay, shale, siltstones, fine-grained sandstones and some thin lenses of limestone. The Abo Formation is relatively impermeable.

The upper surface of the Abo Formation has been fluted and dissected by erosion before the deposition of the volcanics. These erosional channels in the Abo, which were subsequently filled with volcanic debris, comprise the aquifer that has supplied water to the site. The amount of storage in this aquifer is determined mainly by the width and spatial extent of the channels. Topographic highs of the Abo surface limits the aquifer's thickness and lateral extent, and will "disconnect" portions of the aquifer where the Abo surface is above the saturated section.<sup>7</sup>

Generalized contours on the top of the Abo Formation in the area of Fenton Hill indicate the formation dips to the southwest at about 80 ft/mi (Fig. 2). The general movement of water is toward the southwest where a series of springs and seeps discharge from the volcanics into the middle and lower reaches of Lake Fork Canyon (Fig. 1).

The depth to the top of the aquifer at the site is about 370 ft. Water level measurements in observation wells in the immediate area of the site indicate that the water table is near flat.

## B. Supply, Exploratory, and Observation Wells

The presence of water in the volcanics overlying the siltstones and shales of the Abo Formation was determined in 1974 from drilling conditions and geophysical logs of Geothermal Test Hole GT-2.<sup>9</sup> It was recommend-

ed at that time that an exploratory well be drilled and completed as a supply well if tests indicated an adequate yield.

Supply well FH-1 was completed in 1976 at a depth of 450 ft with the water level at an elevation of 8308 ft or about 366 ft below land surface (see Fig. 3). The aquifer was artesian because the water rose in the well about 10 ft after the aquifer was perforated. The well did not penetrate the entire thickness of the aquifer (Table I).

Aquifer tests in January 1978 indicated the well had a specific capacity of about 137 gpm (gal per min) per ft of drawdown after 122 h at a pumping rate of 44 gpm (drawdown 0.32 ft). A second test indicated a specific capacity of 191 gpm per ft of drawdown at a pumping rate of 38 gpm after 25 min of pumping (drawdown 0.20 ft). Based on the specific capacity, a transmissivity (T) of the aquifer was estimated at 100 000 gpd/ft. The total production from the well from November 1976 through December 1980 has been  $20 \times 10^6$  gal.

Test hole FH-2 was drilled in late December 1979 and completed with a torch-slotted 16-in. casing. The test hole encountered the Abo Formation at a depth of 433 ft, or more than 20 ft higher than in supply well FH-1. FH-2 was completed at a depth of 450 ft. The water level elevation was 8321 ft, or 371 ft below land surface. A test on February 4, 1980, indicated a specific capacity of 0.8 gpm per ft of drawdown at a pumping rate of 20 gpm after 2.25 h of pumping (drawdown 25 ft).<sup>10</sup> At that time, the pumping rate was increased to 40 gpm and the water level dropped 49 ft to the top of the pump setting. The specific capacity at the end of 40 min at the rate of 40 gpm was about 1 gpm per ft of drawdown. Using the drawdown at a pumping rate of 20 gpm, a value of T was calculated to be about 600 gpd/ft, whereas from the water level recovery, the T was about 300 gpd/ft.<sup>11</sup> The storage coefficient was  $1 \times 10^{-5}$ . The poor yield at the time was attributed to the reduced thickness of the aquifer.

A third test hole, FH-3, was drilled in March 1980 near FH-1. Well FH-3, completed at a depth of 460 ft, penetrated the top of the Abo Formation. The water level was at about 373 ft with the hole penetrating 85 ft of the aquifer. The hole was completed using torch-cut slots in the casing. Three bailing tests were made of the aquifer to determine characteristics. These tests gave a specific capacity of less than 1 gpm per ft of drawdown.<sup>10</sup>

Inspection of the wellbore with a downhole TV camera showed that the torch slots in both FH-2 and FH-3 were plugged with silt and clay. The results of the

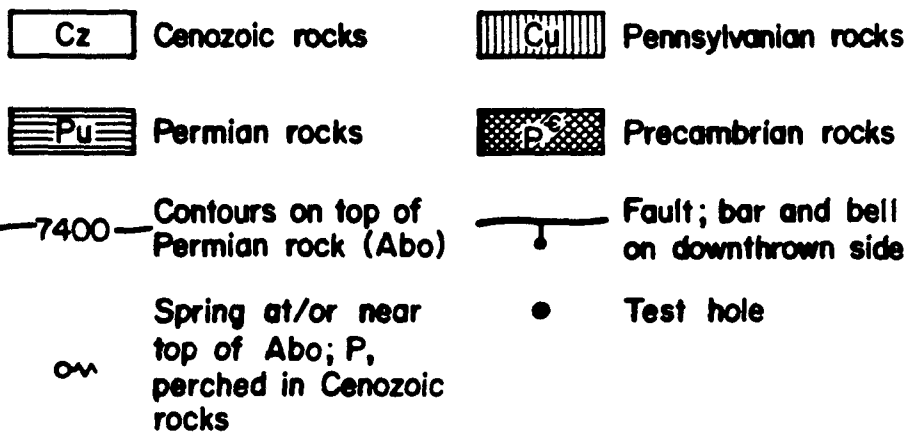
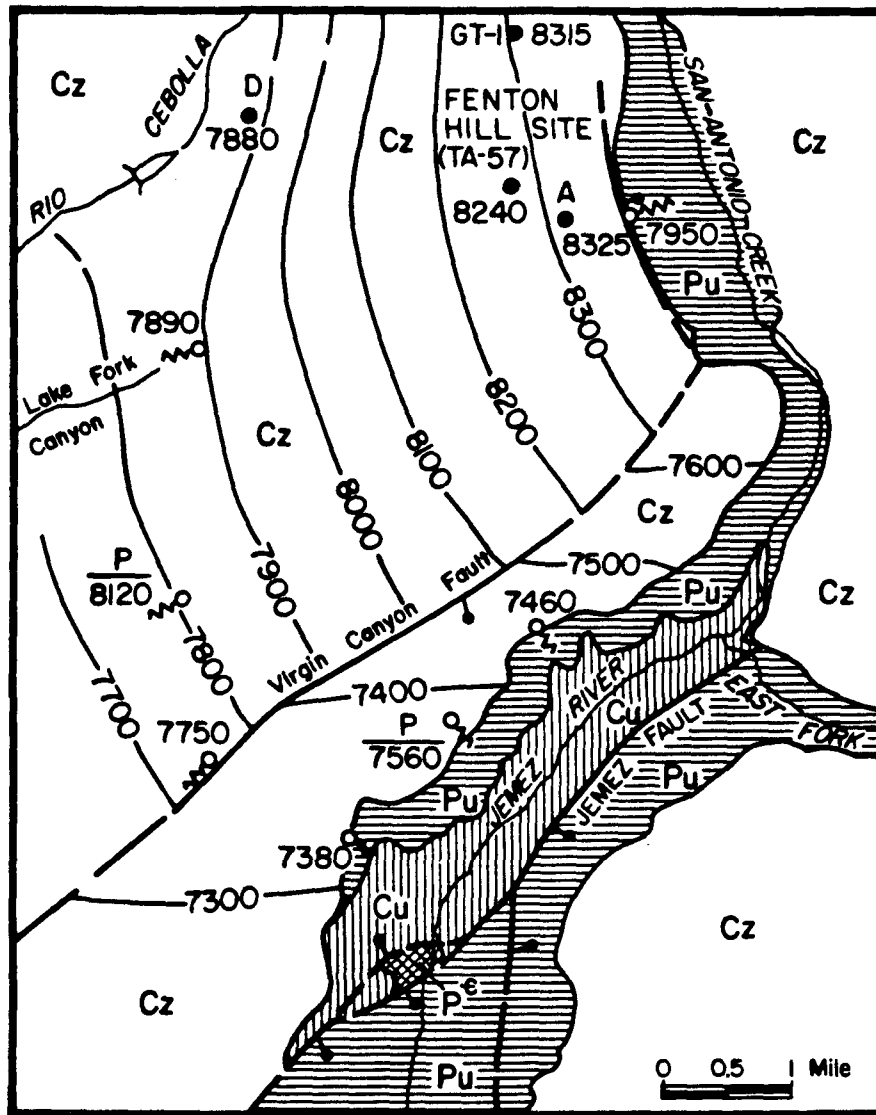


Fig. 2. Generalized geologic map of the Fenton Hill Site (TA-57) showing the erosional surface on top of the Abo Formation (base of the aquifer in volcanics).

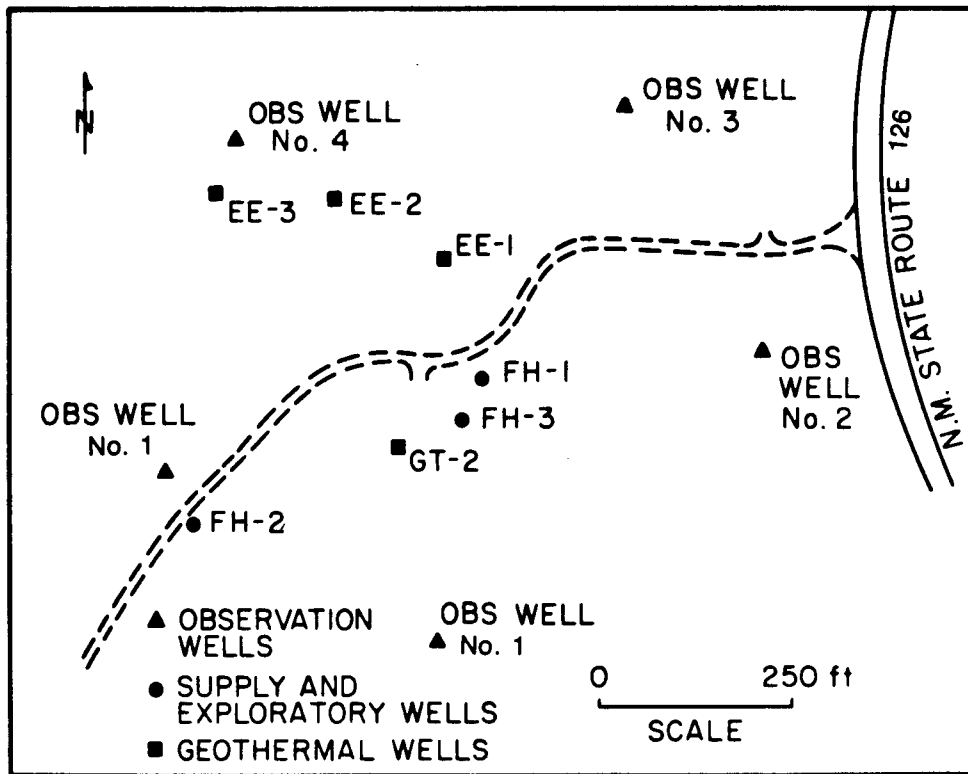


Fig. 3. Site map of Fenton Hill showing location of observation, supply, exploratory, and geothermal wells.

TABLE I

WELL CONSTRUCTION FH-1, FH-2, AND FH-3

	<u>FH-1</u>	<u>FH-2</u>	<u>FH-3</u>
Diameter of Casing (in.)	7 <sup>a</sup>	16	16
Depth Cased (ft)	450	450	460
Depth to Water (ft)	372	371	373
Elevation of Water Surface (ft)	8314	8321	8319
Thickness of Aquifer (ft)	78+	63	85
Length of Screen or Slots (ft)	60 <sup>b</sup>	59 <sup>c</sup>	69 <sup>c</sup>
Specific Capacity (gpm/ft)	100+	≈1	<1

<sup>a</sup>Set with screen on liner 5-1/2 in.

<sup>b</sup>Slotted screen 0.025-in. slots.

<sup>c</sup>Torch-slotted casing.

Note: Water levels (1980).

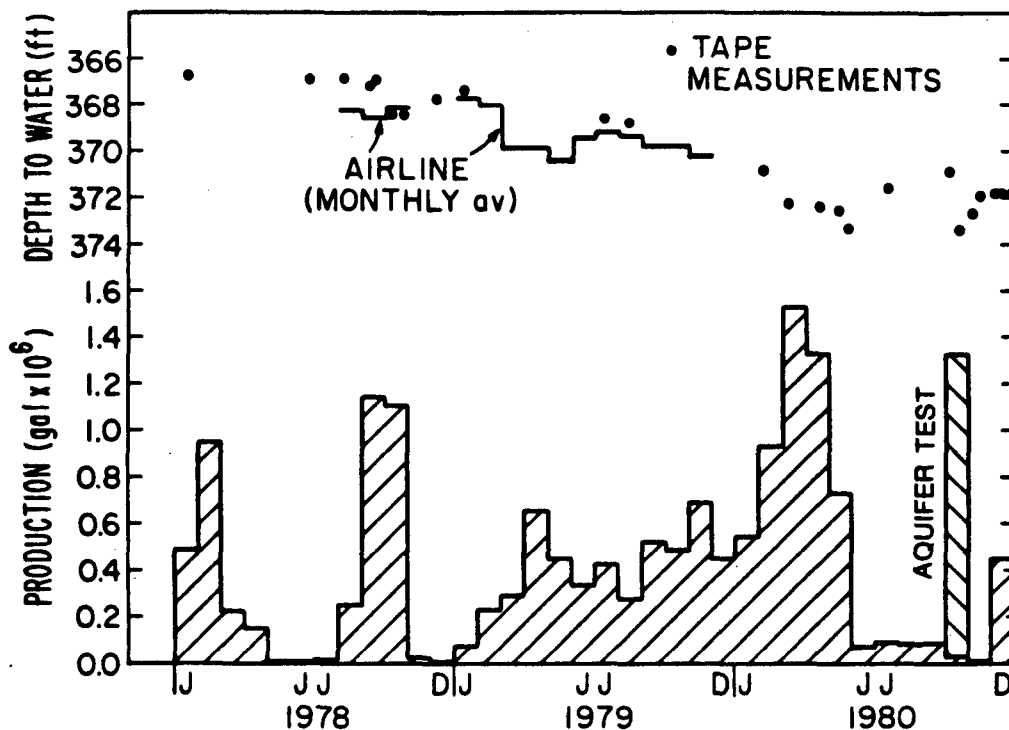


Fig. 4. Water levels and monthly production from Well FH-1, 1978-1980.

aquifer test in FH-2 and bailing tests of FH-3 were consistent with such plugging. The large (16-in.) diameter of the casing precluded cleaning out the slots by conventional methods.

Five observation holes (slim) were drilled to a depth of 450 ft in December 1979 and January 1980 (Fig. 3). The holes are cased with 1-1/2 in. casing.<sup>12</sup> During the drilling of the holes, no geologic or hydrologic logs were kept and the holes were not properly developed. Thus, their usefulness as observation wells is questionable.

### C. Production and Water Levels in Well FH-1

Production from FH-1 has fluctuated a great deal since November 1976 (Fig. 4) because there has been varied demand. The water is supplied for geothermal (deep) well drilling and experiments in the system and for domestic supply onsite. During 1979 and 1980, the monthly production varied from  $0.08 \times 10^6$  gal in January 1979 to  $1.54 \times 10^6$  gal in March 1980. The production of  $1.3 \times 10^6$  gal in October 1980 was mainly for the 10-day aquifer test. During the summer of 1980, the production fell to under  $0.1 \times 10^6$  gal per month.

Cumulative production from FH-1 from November 1976 through December 1980 is  $20 \times 10^6$  gal (Fig. 5).

Water levels in the well were recorded by an airline and continuous airline recorder until November 1979 (Fig. 4). Because the water levels do not fluctuate more than 1 ft during pumping, these airline records can only approximate long-term trends. Supplemental measurements were taken with a steel tape. Since October 1980, measurements have been made using the airline and a Wallace-Tiernan pressure gauge (accurate to about 0.02 ft of water). The average monthly water level has declined approximately 6 ft since January 1978.

### D. Aquifer Evaluation by American Ground Water Consultants, Inc., Spring 1980

During the spring and early summer of 1980, American Ground Water Consultants, Inc. (AGW) conducted an aquifer evaluation program.<sup>13,14</sup> Their primary objective was to determine the aquifer transmissivity and storage coefficient to predict the effect on the nearby streams or rivers caused by pumping the aquifer. The following paragraphs summarize their results.

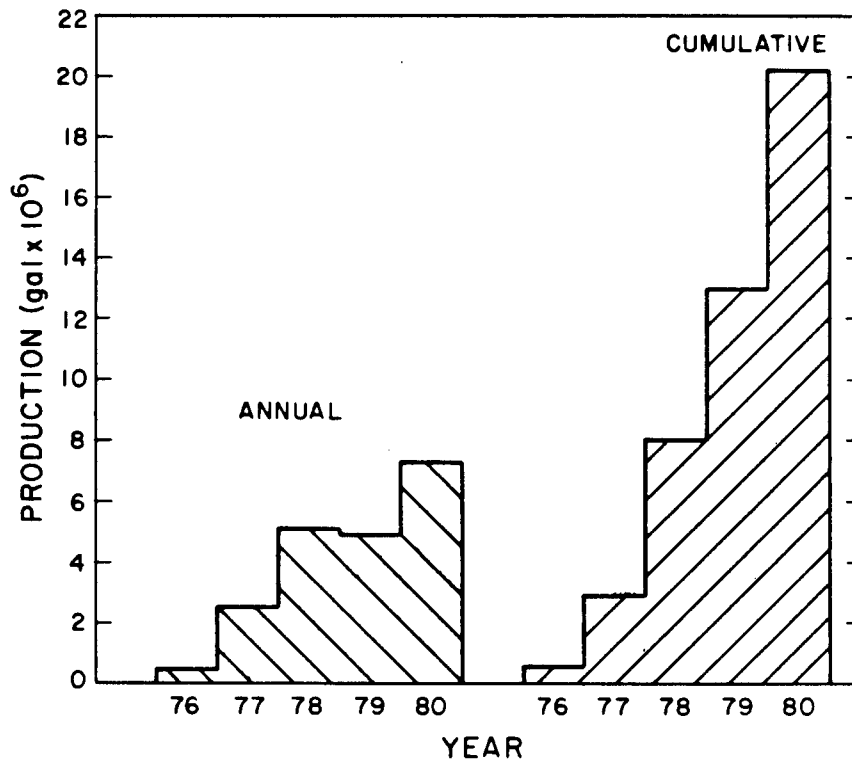


Fig. 5. Annual and cumulative production from Well FH-1, 1976-1980.

After analyzing the results of injection tests in the five slim holes, a 200-min aquifer test in FH-1 where  $Q = 40$  gpm, and the results of a 240-min aquifer test in FH-2 conducted in February 1980,<sup>12,15</sup> aquifer transmissivity was determined to be 7000 gpd/ft.<sup>13</sup> The aquifer storage coefficient was assumed to be  $1 \times 10^{-5}$ , after Purtymun.<sup>11</sup> Assuming a withdrawal rate of 10 acre-ft/yr for a 10-yr period from the aquifer, AGW calculated a surface water depletion in the Rio Cebolla for a 20-yr period (Table II).

Later in 1980, AGW refined their results on aquifer transmissivity using a standard, two-dimensional, steady-state, finite-difference computer model for ground water flow.<sup>14</sup> They reestimated the transmissivity to be 1740 gpd/ft, and made the following assumptions: (1) the aquifer's eastern outcrop and the Virgin Canyon fault south of Fenton Hill were assumed to be impermeable boundaries, (2) streams were assumed to be in hydraulic contact with the aquifer in all locations, (3) the transmissivity and storage coefficients were assumed to be uniform throughout the aquifer, and (4) a ground water recharge (and hence soil infiltration) rate was assumed to be 200 acre-ft/mi<sup>2</sup> annually. Using this

TABLE II  
EVALUATION OF STREAM DEPLETION  
FROM GROUND WATER DISCHARGE TO  
WELLS AT FENTON HILL  
(after AGW 1980, Ref. 13)

Year After Discharge Begins	Surface Water Depletion (acre-ft/yr)
1	0.06
5	6.9
10	15.0
20	6.3

revised transmissivity, the effects on nearby stream flow by ground water pumpage were recomputed for cases of a confined and unconfined aquifer. These calculations assumed a pumping schedule of 70 acre-ft the first 10

months, and 15 acre-ft for the following 6 yr. In a confined aquifer, the effect on the streams would reach a maximum after 5 months of pumping; 95% of the water that would otherwise replenish streamflow would be diverted. After 10 months, stream flow depletion would then equal the current pumping rate. In contrast, in an unconfined aquifer, the stream flow would be decreased by 4% of total flow after 6 yr of ground water pumping. Assumed storage coefficients of  $1 \times 10^{-4}$ , and  $5 \times 10^{-2}$  were used for the confined and unconfined cases, respectively.

## II. AQUIFER EVALUATION BY LOS ALAMOS NATIONAL LABORATORY, FALL 1980

During October and November 1980, the Laboratory conducted an aquifer evaluation at Fenton Hill. The purpose for this was twofold: to determine an optimal discharge rate  $Q$  for the new, higher capacity pump set in FH-1 in September 1980, and to determine if the aquifer would produce the amount of water required for the next 5 yr. The evaluation consisted of both step discharge and constant discharge drawdown tests.

### A. Step Discharge Test

The results of the step discharge test, conducted on October 9, 1980, indicated that the optimal discharge rate  $Q$  for the FH-1 pump would be 100 gpm, which is near the pump's design discharge limit. Pump discharge rates of 50, 60, 80, 100, and 108 gpm were run in successive 60-min segments. At the end of the 5-h test, the cumulative drawdown was 0.3 ft. Five minutes after the pump was shut off, the water level returned to the pretest level. Because of the small drawdown associated with the pump's maximum rate, a  $Q$  of 100 gpm was chosen for the aquifer drawdown test.

### B. Drawdown Test

An aquifer drawdown test using a constant discharge rate of 100 gpm from well FH-1 began October 16, 1980. The well was pumped at a constant rate until the morning of October 25 when the pump was shut off. Water level recovery was then monitored until November 12. A total of  $1.3 \times 10^6$  gal (4 acre-ft) of water was produced.

The water level in the pumping well FH-1 was measured using an airline and a Wallace-Tiernan pressure gauge. The water level in the well was also checked with a steel tape before and after the test.

During the test, wells FH-2 and FH-3 were used for observation wells. A float recorder on FH-2 recorded continuous water level changes, whereas an electrical conductivity water level indicator was used to measure the water level in FH-3. A microbarograph operated continuously during the drawdown and recovery period so that the water level data could be corrected for barometric changes using standard methods described in Ref. 16. The barometric efficiency of the aquifer was calculated to be 44%, using water level and barometric data which had been collected from both heavy and light pumping periods.<sup>17</sup>

1. **Transmissivity and Storage Coefficient.** The water level in FH-1 declined 2.37 ft by the end of the pumping period, October 25. By the end of the recovery period, November 12, the water level had recovered 1.19 ft. The water level declined 1.96 ft in FH-3 and recovered approximately 1 ft at the end of the recovery period. There was a great deal of fluctuation in FH-2 even after correction for barometric effects. The net drawdown from pumping was about 0.2 ft.

Using these water level drawdown and recovery data from FH-1 and FH-3, the transmissivity ( $T$ ) and storage coefficient ( $s$ ) were computed (Table III).<sup>17</sup> Two independent methods were used to determine the transmissivity:

1. **Jacob Straight-Line Approximation.** A semilogarithmic plot of drawdown versus time for FH-1 and FH-3 is used (Figs. 6 and 7).<sup>18,19</sup> A straight line is fitted to the data and the  $T$  is computed over one log cycle. Latest time data were chosen for the line fits because they are considered to be most conservative and reflect the largest possible zone of influence. The transmissivity was computed to be 5000 gpd/ft for FH-1 and 5000 gpd/ft for FH-3. This was repeated using the water level recovery data and a dimensionless time. The transmissivity was calculated to be 5000 gpd/ft, and 5300 gpd/ft for FH-1 and FH-3, respectively (Figs. 8 and 9).<sup>18,19</sup>
2. **Theis Nonequilibrium Formula.** This classic technique uses a log-log plot of drawdown versus time. Matching an artesian, nonleaky type curve to the plot, both the transmissivity and storage coefficient can be computed.<sup>20</sup> Using this method, with FH-3

TABLE III

TRANSMISSIVITY AND STORAGE COEFFICIENTS

Transmissivity	Data Well	T (gpd/ft)
Residual Drawdown	FH-1	5000
Straight Line Solution (SLS)	FH-3	5000
	FH-1 (recovery)	5000
	FH-3 (recovery)	5300
Theis Nonequilibrium Formula	FH-3	2100

Storage Coefficient		s (Dimensionless)
Residual Drawdown, SLS	FH-3	$6.5 \times 10^{-2}$
Theis Nonequilibrium Formula	FH-3	$7.5 \times 10^{-2}$

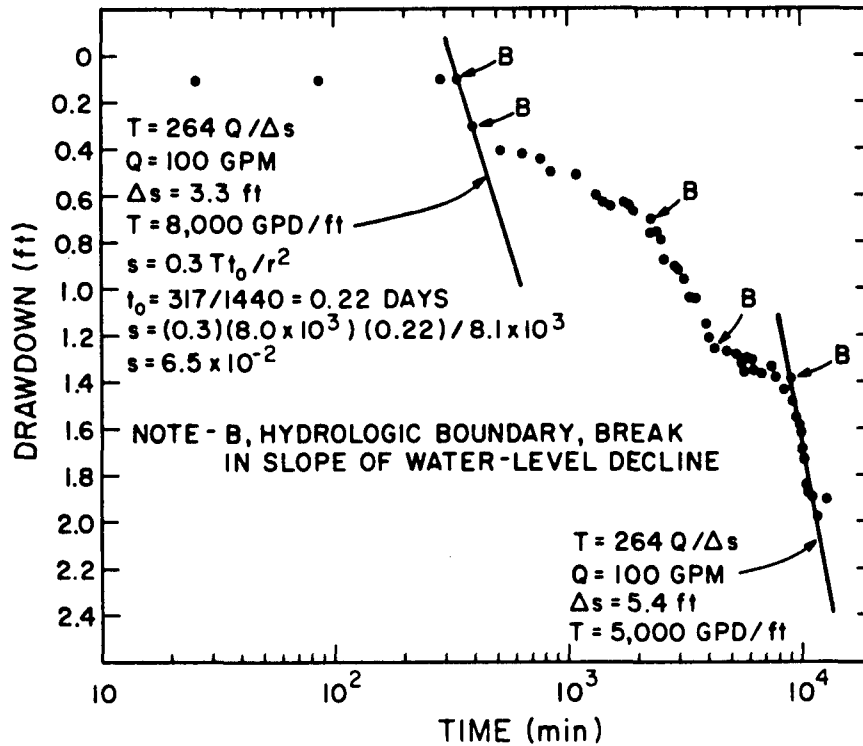


Fig. 6. Water level drawdown in Well FH-3 during pumping, October 16-25, 1980.

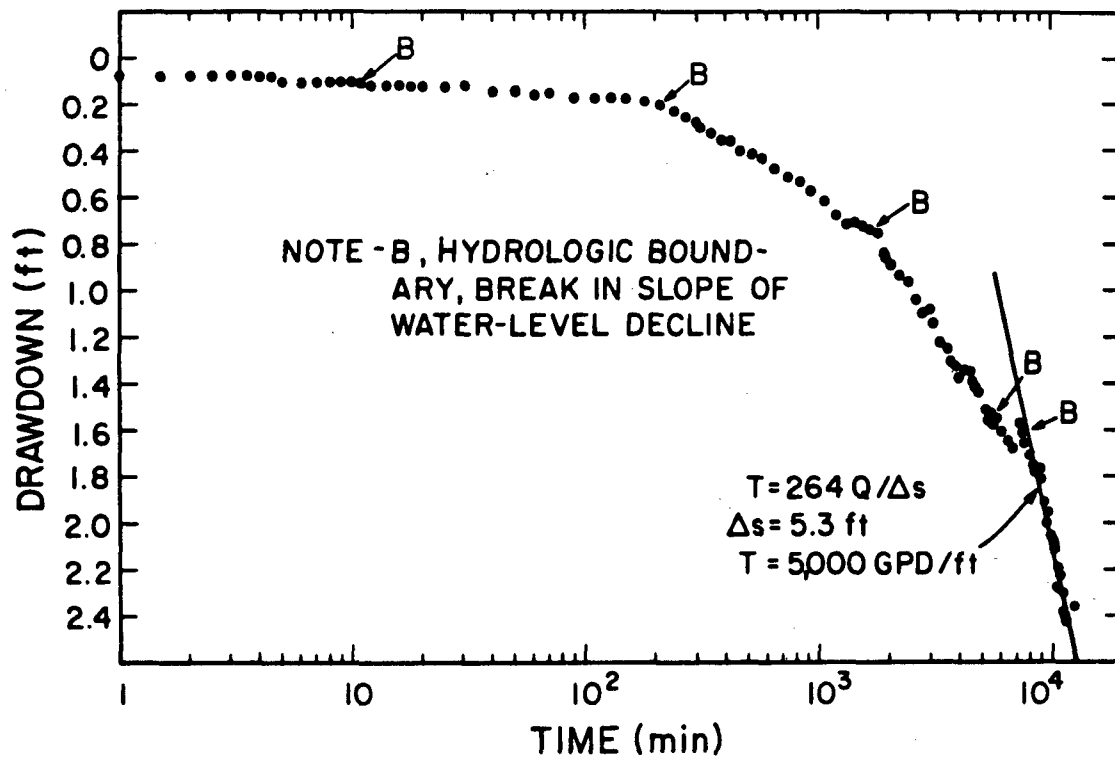


Fig. 7. Water level drawdown in Well FH-1 during pumping, October 16-25, 1980.

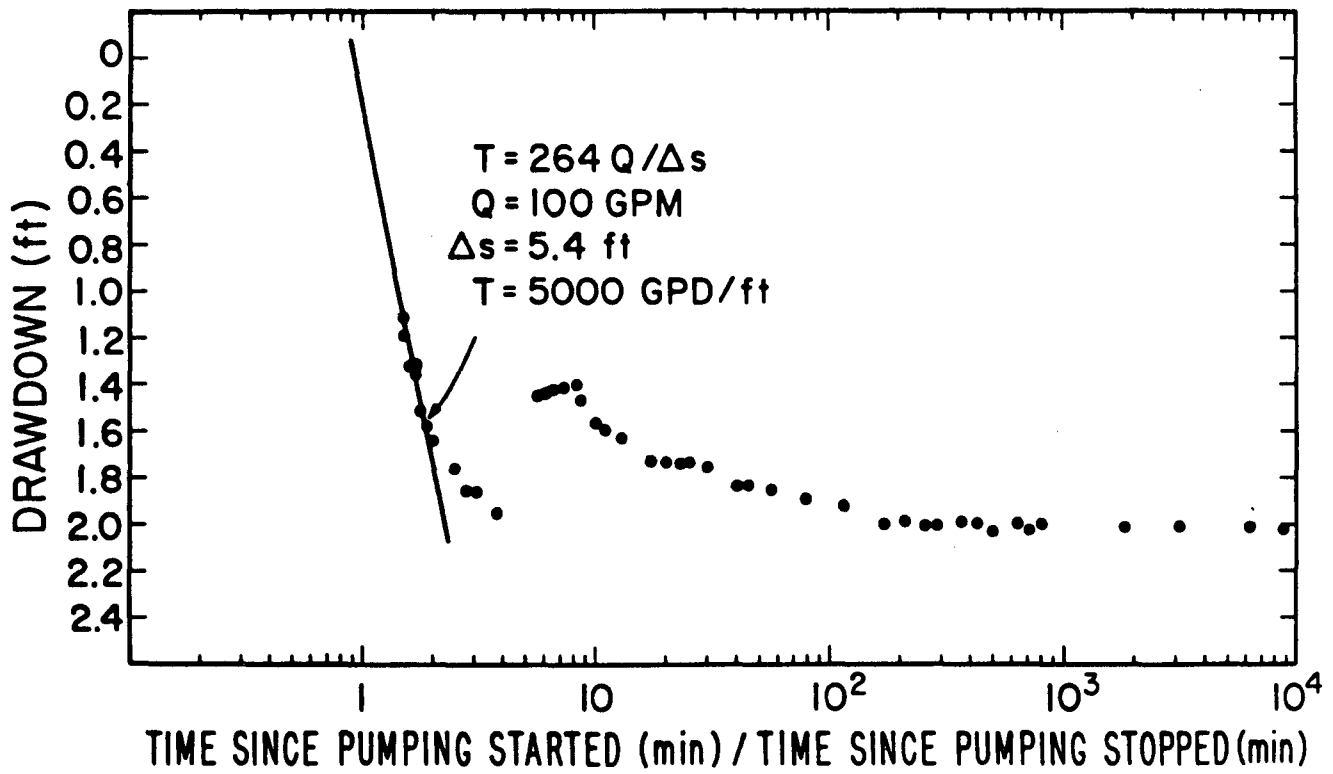


Fig. 8. Water level recovery in Well FH-1 after pumping ended, October 25-November 12, 1980.

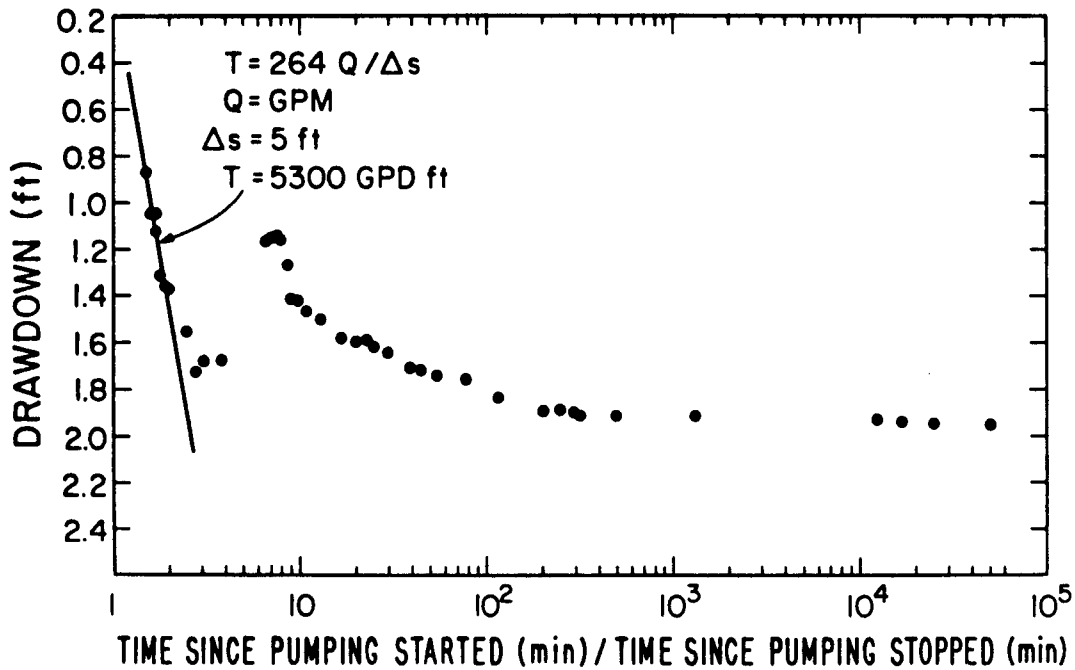


Fig. 9. Water level recovery in Well FH-3 after pumping ended, October 25-November 12, 1980.

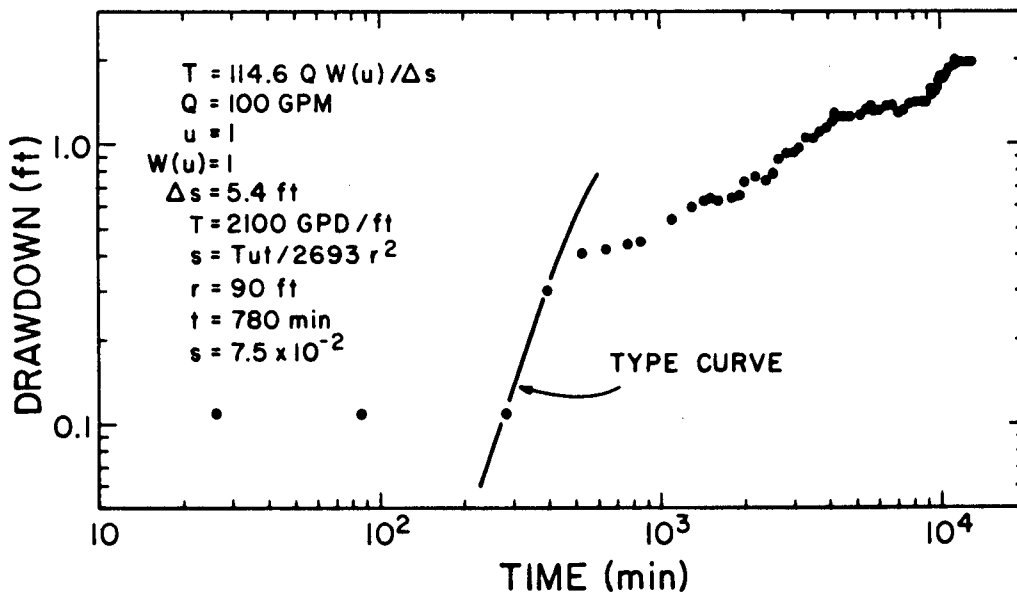


Fig. 10. Nonleaky-type curve solution based on drawdown of water levels in Well FH-1.

data fitted to the early time drawdown before any indication of interferences, a  $T$  of 2100 gpd/ft was computed (Fig. 10).

Two methods were used to determine the storage coefficient, the residual drawdown straight-line solution, and the Theis nonequilibrium formula using the type curve.

1. *Residual Drawdown Straight-Line Solution.* The straight-line portion of the curve in the Jacob Straight-Line Approximation is used to find the time where the drawdown is zero,  $t_0$ . Using the computed transmissivity and the distance  $r$  between

the pumping well and the observation well, the storage coefficient  $s$  may be determined by  $s = 0.3Tt_v/r^2$ , where the units are gpd/ft, days, and ft, respectively. An  $s$  of  $6.5 \times 10^{-2}$  was obtained from the FH-3 data.<sup>19,21</sup>

2. *Theis Nonequilibrium Formula Using the Type Curve.* A log-log plot of drawdown versus time was prepared using the data from FH-3 and fit to a nonleaky artesian aquifer type curve. Using the standard formula,  $s = Tu/2693 r^2$ , where  $u$  is the argument of the well function,  $s$  was computed to be  $7.5 \times 10^{-2}$ . The type curve was fit using the early time data because there were interferences during the later stages.<sup>20</sup>

Averaging the results from these methods, the aquifer has a transmissivity of about 5000 gpd/ft and a storage coefficient of 0.07 (Table III).

2. **Discussion of the Values of Transmissivity and Storage Coefficient.** As described earlier, the aquifer was artesian when it was first penetrated in 1976—the water rose about 10 ft above the top of the saturated section. With continued removal of water, the potentiometric surface of the aquifer will decline until it falls below the top of the saturated section, and the aquifer will then behave as an unconfined, or water table, aquifer. However, pumping of FH-1 results in an almost instantaneous response in water level decline in FH-3 indicating the aquifer is still under artesian pressure.

The computed values for transmissivity and storage coefficient were checked by computing drawdowns and comparing them to the measured drawdowns of 1976-1980. The Theis nonequilibrium formulas for radial flow in a confined aquifer were applied using superposition to compute the drawdown in FH-1, along with the known annual discharge volumes for the years 1976-1980 (Fig. 5). Values of  $T = 5000$  gpd/ft and  $s = 0.07$  were used, and the drawdown at FH-1 was computed to be 5.7 ft.<sup>22</sup> This is compared to a measured 6 ft of drawdown over the same period of time. This close agreement between computed and measured drawdown infers one or both of these conclusions; first, the computed values for the transmissivity and storage coefficient must be in the proper (actual) range, and second, the assumption that the aquifer is still confined is valid. The Laboratory determined transmissivity ( $T = 5000$  gpd/ft) value is of comparable magnitude to those obtained by AGW using a different method ( $T = 1740$  to  $7000$  gpd/ft).

3. **Ground Water Boundaries.** During the drawdown portion of the aquifer test, considerable interference of ground water flow toward the well was apparent with the changes in slope of water levels when plotted against time (Figs. 6 and 7). This interference took place during both drawdown and recovery phases.

The water level drawdown of FH-1 and FH-3 indicated no barriers between the two wells. The first barrier appeared at accelerated drawdown in FH-1 at 200 min and FH-3 at 350 min after pumping began (Figs. 6 and 7). The drawdown data of FH-1 and FH-3 during the 10-day test indicate as many as five boundaries in the aquifer. These boundaries reflect the channels cut in the Abo formation, as previously described. From the number of boundaries intercepted, it may be deduced that the aquifer is limited in its spatial extent. It is highly probable that with continued pumping, more barriers will become apparent and accelerated water level declines will occur in FH-1.

### III. PROJECTED AQUIFER RESPONSE TO FUTURE PUMPING

A water usage schedule for 5 yr of operation of the Phase II system has been formulated (Table IV).<sup>23</sup> Water level decline due to this pumping in FH-1 (assumed pumping well) and FH-3 (90 ft from FH-1) has been calculated over the same time frame (Table V). The Theis

TABLE IV  
PROJECTED WATER USE FROM  
1981 THROUGH 1985

Year	Annual Usage (gal)	Annual Usage (acre-ft)
1981	$6 \times 10^6$	18.41
1982	$13 \times 10^6$	39.90
1983	$30 \times 10^6$	92.07
1984 and 1985	$113 \times 10^6$	346.81
Total	$162 \times 10^6$	497.19

TABLE V

## WATER LEVEL DECLINE AT FH-1 AND FH-3

Year	FH-1 (ft)	FH-3 (ft)
1981	4.2	1.8
1982	9.2	4.1
1983	21.3	9.5
1984	40.3	18.2
1985	41.6	19.4

nonequilibrium equations together with superposition were used to determine the ground water decline.<sup>20,24</sup> The transmissivity and storage coefficients derived from the 1980 aquifer test were used in these computations. After 5 yr of pumping, a decline of approximately 42 ft of water in FH-1 and 20 ft in FH-3 was computed.

These calculations are nonconservative in that they do not account for any additional impermeable aquifer boundaries that may be encountered during pumping. Geologic information is not presently available to be able to project such effects in the calculation. It would be likely for boundaries to appear because the aquifer is apparently spatially limited. The effect of additional impermeable boundaries would be a more rapid lowering and greater decline of the water level in all wells onsite. It is clear that withdrawal to date had exceeded recharge to the aquifer because the water level has declined 6 ft since January 1978. From the aquifer test performed in October 1980, it is also apparent that ground water is being depleted: since the removal of  $1.3 \times 10^6$  gal, the water table has not returned to pretest levels.

If pumping in the future is sufficient to deplete aquifer to the point where it behaves under water-table (unconfined) conditions, then drawdown would also be greater than that projected by these computations.

## IV. CHEMICAL QUALITY

Water from the well FH-1 was analyzed for chemical and radiochemical constituents to compare with standards set for municipal or domestic use by the U.S. Environmental Protection Agency and State of New Mexico standards.<sup>25,26</sup> A comparison of the analytical results

TABLE VI

## CHEMICAL AND RADIOCHEMICAL CONCENTRATIONS IN WATER FROM SUPPLY WELL FH-1, 1979

Chemical (mg/l)	Supply Well FH-1	Standard or Criteria <sup>a</sup>
Ag	<0.001	0.05
As	<0.001	0.05
Ba	<0.5	1.0
Cd	<0.01	0.010
Cl	19	250
Cr	<0.002	0.05
F	0.3	2.0
Hg	<0.0005	0.002
NO <sub>3</sub>	1.5	45
Pb	0.002	0.05
Se	0.005	0.01
TDS	244	1000
<b>Radiochemical (pCi/l)</b>		
<sup>3</sup> H	<0.6	20
<sup>137</sup> Cs	<80	200
<sup>238</sup> Pu	<0.03	15
<sup>239</sup> Pu	<0.04	15
Gross alpha	2.3	15
Total U	1.9	1800

<sup>a</sup>References 25 and 26.

of water from the well to federal and state standards show that the water is below limits set for municipal use (Table VI).<sup>27</sup>

During the 10-day aquifer test, water samples collected at frequent time intervals were analyzed to determine if changes occurred with production. Of the nine samples analyzed, the major constituents, calcium, sodium, chloride, bicarbonate, and TDS, varied slightly from one sample to another, but showed no significant change during the test (Fig. 11). The variations in concentrations were within the range of analytical error. Water temperature during the test remained constant at 27°C.

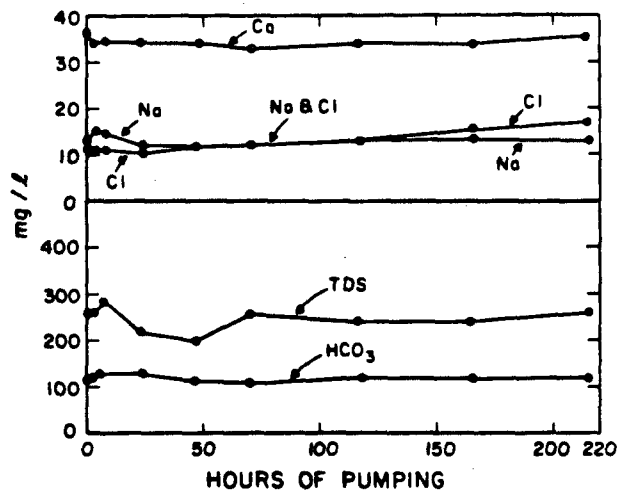


Fig. 11. Select chemical constituents in water from Well FH-1 during aquifer test, October 16-25, 1980.

## V. SUMMARY

1. The main potable aquifer at Los Alamos National Laboratory's Fenton Hill Geothermal Site is in the lower part of the Paliza Canyon Formation and the Abiquiu Tuff, which is a friable, tuffaceous sandstone 90 ft thick at the site.
2. A 10-day aquifer test was performed during October and November 1980. Measurements were taken from one pumping well and two observation wells. Results indicate that the aquifer has a transmissivity of about 5000 gpd/ft and a storage coefficient of about 0.07.
3. These values for transmissivity and storage coefficient were checked by using them to predict drawdown at FH-1 from 1976 through 1980 and comparing the predicted drawdown with that measured. The predicted and measured drawdown agreed to within 5% error.
4. Aquifer test results also indicate a number of impermeable, hydrologic boundaries. It is clear that the aquifer is limited spatially, and likely that more boundaries will become apparent with continued pumping.
5. From a withdrawal of 500 acre-ft over 5 yr (Table IV) from the aquifer, it was calculated that the water level in pumping well FH-1 will decline a minimum of nearly 42 ft; however, due to the presence of ground water boundaries, the water

level decline will be much greater and may result in depletion of the aquifer.

6. The chemical quality of the aquifer water has remained essentially constant from 1976 through 1980.
7. The aquifer in the Abiquiu Tuff was artesian when originally drilled. The aquifer discharges generally to the southwest in Lake Fork Canyon in a series of seeps and springs. The top of the aquifer is relatively flat at the site.
8. The step discharge test indicated that the aquifer could produce 100 gpm with minimum drawdown.
9. Cumulative water production from the aquifer from November 1976 through December 1980 is  $20 \times 10^6$  gal.

## REFERENCES

1. Hot Dry Rock Program Staff, "Hot Dry Rock Geothermal Energy Development Program, Annual Report—Fiscal Year 1979," Los Alamos Scientific Laboratory report LA-8280-HDR (1980).
2. W. E. Hale, L. J. Reiland, and J. P. Beverage, "Characteristics of Water Supply in New Mexico," New Mexico State Engineering Tech report 31 (1965).
3. R. L. Smith, R. A. Bailey, and C. S. Ross, "Structural Evolution of the Valles Caldera, New Mexico, and Its Bearing on Emplacement of Ring Dikes," U.S. Geol. Sur. Prof. Paper 424-D (1961).
4. C. S. Ross, R. L. Smith, and R. A. Bailey, "Outline of Geology of the Jemez Mountains, New Mexico," New Mexico Geol. Soc. Twelfth Field Conf., Albuquerque, New Mexico (1961).
5. R. A. Bailey, R. L. Smith, and C. S. Ross, "Stratigraphic Nomenclature of the Volcanic Rocks in the Jemez Mountains, New Mexico," U.S. Geol. Sur. Bull. 1274-P (1969).
6. R. L. Smith, R. A. Bailey, and C. S. Ross, "Geologic Map of the Jemez Mountains, New Mexico," U.S. Geol. Sur. Misc. Geol. Inv. Map I-571 (1970).

7. W. D. Purtymun, F. G. West, and R. A. Pettitt, "Geology of Geothermal Test Hole GT-2, Fenton Hill Site, July 1974," Los Alamos Scientific Laboratory report LA-5780-MS (November 1974).
8. W. D. Purtymun, "Geology of the Jemez Plateau West of the Valles Caldera," Los Alamos Scientific Laboratory report LA-5124-MS (February 1973).
9. W. Purtymun and F. West, "Exploratory Test Hole in Volcanics with Possible Completion as a Small Yield Water Supply," Los Alamos Scientific Laboratory memorandum H8-74-140 to M. Smith (April 2, 1974).
10. N. Becker and W. Purtymun, "Hydrologic Data Related to Supply Well FH-1, FH-2, and FH-3 at TA-57," Los Alamos Scientific Laboratory memorandum G-5/H-8 to Distribution (June 23, 1980).
11. W. Purtymun, "Hydrologic Characteristics of Supply Well FH-2," Los Alamos Scientific Laboratory memorandum H8-80-247 to N. Becker and D. Miles (April 4, 1980).
12. W. Purtymun, N. Becker, and D. Miles, "Water Supply at Fenton Hill," Los Alamos Scientific Laboratory memorandum H8-80-184 to Distribution (March 12, 1980).
13. American Ground Water Consultants, Inc., "Hydrogeology of the Hot Dry Rock Site at Fenton Hill, Sandoval County, New Mexico," Submitted to Los Alamos Scientific Laboratory (June 1980).
14. American Ground Water Consultants, Inc., "Results of Ground Water Model Studies at Fenton Hill, Sandoval County, New Mexico," Submitted to Los Alamos Scientific Laboratory (July 1980).
15. Dan Miles, "Pumping Test on Water Well #2," Los Alamos Scientific Laboratory memorandum G-4 to G. Nunz, Morris, and Purtymun (Feb. 5, 1980).
16. Bureau of Reclamation, "Ground Water Manual," U.S. Government Printing Office, Washington, D.C. (1977).
17. W. C. Ballance, N. M. Becker, and W. D. Purtymun, "Pumping Test of Well FH-1, Fenton Hill, October 16—November 12, 1980," Los Alamos National Laboratory report (in preparation).
18. L. K. Wenzel, "Methods for Determining Permeability of Water-Bearing Materials," U.S. Geol. Sur. Water-Supply Paper 887 (1942).
19. R. H. Brown, "Selected Procedures for Analyzing Aquifer Test Data," Am. Water Works Assoc. J. 45, No. 8 (1953).
20. C. V. Theis, "The Relation Between the Lowering of the Piezometric Surface and the Rate and Duration of Discharge of a Well Using Ground-Water Storage," Am. Geophys. Union Trans. (1935).
21. Jack Bruin and H. E. Hudson, Jr., "Selected Methods for Pumping Test Analysis," Illinois State Water Survey, Report of Investigation 25, third printing (1961).
22. N. Becker, "Computation of Drawdown at FH-1 Using Superposition," Los Alamos National Laboratory memorandum H8-81-309 to W. D. Purtymun (May 15, 1981).
23. H. N. Fisher, "Water Losses for Phase II System: 1981 Through 1985," Los Alamos Scientific Laboratory memorandum G-6 to J. Hill and R. W. Spence (Dec. 9, 1980).
24. D. K. Todd, "Ground Water Hydrology," John Wiley and Sons, Inc., New York (1959).
25. U.S. Environmental Protection Agency, "National Interim Primary Drinking Water Regulations," EPA-570/9-76-003, Environmental Protection Agency, Office of Water Supply (1976).
26. New Mexico Environmental Improvement Department, "Water Supply Regulations," New Mexico Environmental Improvement Department, Santa Fe, New Mexico (1977).
27. W. Purtymun, R. W. Ferenbaugh, A. K. Stoker, and W. H. Adams, "Water Quality in the Vicinity of Fenton Hill, 1979," Los Alamos Scientific Laboratory report LA-8424-PR (1980).

APPENDIX C

Geology of the Jemez Plateau west of Valles Caldera  
LA-5124-MS, Los Alamos National Laboratory

Geology of Geothermal test hole GT-2, Fenton Hill Site,  
LA-5780-MS, Los Alamos National Laboratory

LA-5124-MS

Geology of the Jemez Plateau  
West of Valles Caldera



**los alamos**  
**scientific laboratory**

of the University of California

LOS ALAMOS, NEW MEXICO 87544



LA-5124-MS

UC-51

ISSUED: February 1973



# Geology of the Jemez Plateau West of Valles Caldera

by

William D. Purtymun

GEOLOGY OF THE JEMEZ PLATEAU  
WEST OF VALLES CALDERA

by

William D. Purtymun

ABSTRACT

The Jemez Plateau at the site proposed for a geothermal-energy study forms an apron around the west side of the Valles Caldera. Five test holes were drilled on the plateau for geologic information, temperature data, and to investigate drilling problems. Four of the test holes, ranging in depth from 500 to 750 ft, penetrated volcanic rocks of Cenozoic Age and were completed into the sediments of Permian Age. A deep test hole, drilled 2575 ft, penetrated the volcanic rocks of Cenozoic Age and sediments of Permian and Pennsylvanian Age, and is completed into the rocks of Precambrian Age. The basic part of the study is to be made in the Precambrian rocks. Test drilling and measured sections indicate a small north-south trending basin near the center plateau in which the sediments thicken. The basin may be structural in part or erosional where the upper surface of Precambrian rocks was cut to form a small valley before deposition of the sediments. The geologic logs of the five test holes are included.

---

I. INTRODUCTION

The site tentatively selected for the first major geothermal-energy study proposed by the Los Alamos Scientific Laboratory is on the Jemez Plateau, about 20 miles west of Los Alamos, New Mexico (Fig. 1). It was chosen principally on the basis of preliminary geologic investigations and geothermal-gradient measurements made in a series of shallow test holes drilled in the region of the Valles Caldera. These indicated that in the area west of the caldera, the geology and geologic structure were least complicated. Also, competent rock (Precambrian basement) at temperatures needed for the experiment could be reached easily by conventional drilling methods (at depths varying from 8000 to 10,000 ft).

Four test holes ranging in depth from 500 to 750 ft were drilled in this area during April 1972. They were cored and cased for geologic investigations and heat-flow measurements. A deeper test hole was drilled during May and June 1972 to obtain additional geologic information and temperature data and to investigate drilling problems in the area. It reached a depth of 2575 ft and was completed in the Precambrian basement rocks.

This report describes the geology and geologic structure of the proposed experimental site on the basis of data obtained from test drilling in the area during April through June 1972. These data are supplemented by the results of other investigations made in the area, including those made by the authors, listed below.

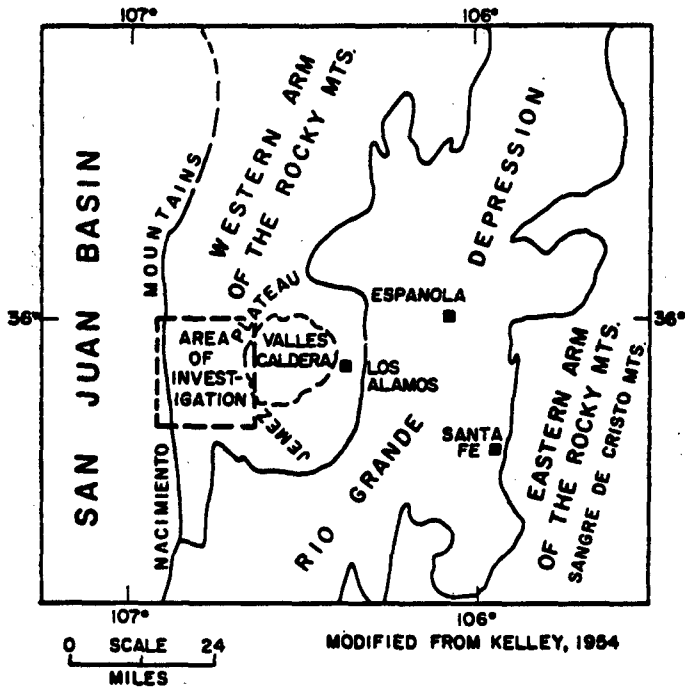


Fig. 1. Major structural features and area of investigation in north-central New Mexico.

The geology of this region was first described by Renich,<sup>1</sup> and has since been described by Woods and Northrop,<sup>2</sup> Smith et al.,<sup>3</sup> Ross et al.,<sup>4</sup> and Bailey et al.<sup>5</sup> A regional geologic map was published by Smith et al.<sup>6</sup> Fitzsimmons<sup>7</sup> describes some of the Precambrian rocks in the area, and Doell et al.<sup>8</sup> present data on the age-dating and paleomagnetism of the volcanic rocks in the Jemez region.

## II. GEOGRAPHY

The proposed experimental site is located on the Jemez Plateau, which is a part of the western arm of the Rocky Mountains that extends into northern New Mexico from southern Colorado. The surface of the plateau is formed by volcanic ash extruded during the volcanic activity that produced the Valles Caldera.

The caldera is surrounded by mountains formed during this same period of active volcanism. The volcanic ash forms an apron around the caldera, which laps onto the flanks of these mountains.

The Jemez Plateau is the western part of this apron (Fig. 1). The north-south-trending Nacimiento Mountains form the western boundary of the area of investigation.

The altitudes of mountains bounding the Jemez Plateau on the east and west range from about 10,000 ft at the westernmost dome in the caldera (San Antonio Mountain) to a little over 9000 ft along the crest of the Nacimiento Mountains. The major drainage in the area is the Rio de Las Vacas and Jemez Creek, with its tributary, San Antonio Creek (Fig. 2). The proposed experimental site is on the plateau between the Rio de Las Vacas and San Antonio Creek. A high ridge along the western part of the plateau is parallel to San Antonio Creek. Otherwise the surface of the plateau slopes gently downward to the west and southwest. The altitude of the area ranges from 8000 to 9000 ft along the crest of the ridge to about 7000 to 8000 ft where the plateau terminates in steep slopes or cliffs above the Rio de Las Vacas. The plateau surface is cut into a number of mesas by southwest-trending streams

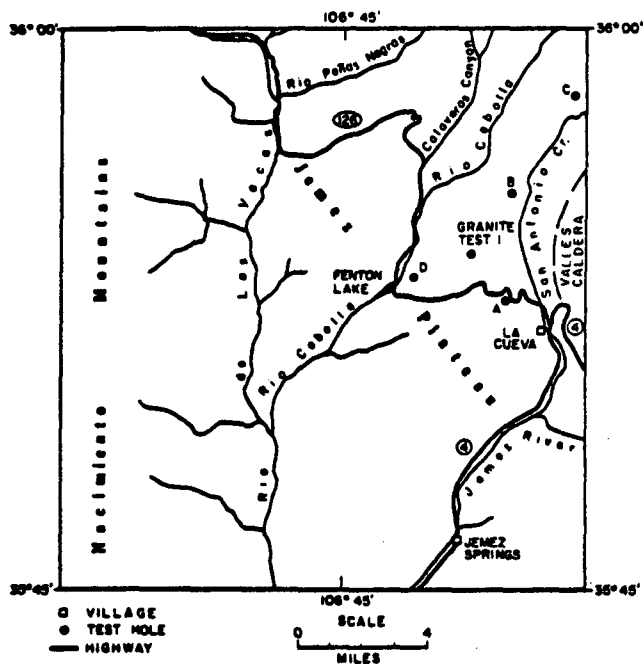


Fig. 2. Cultural and drainage features and locations of test holes in the area of investigation.

that are tributary to the Rio de Las Vacas, the largest of which is the Rio Cebolla.

West of the Rio de Las Vacas the eastern flanks of the Nacimientos rise gently to the crest and then break abruptly in a steep slope into the San Juan Basin.

The average annual precipitation in the area is estimated to range from about 14 in. at lower elevations to about 22 in. in the mountains. Average annual air temperatures range from 40 to 50°F (Ref. 9).

The high mountain slopes are forested mainly with ponderosa pine and some fir and spruce. Groves of aspen and live oak are found in the higher canyons, with some willow and poplar along the streams at the lower elevations. About 5000 acres of the forest, west of La Cueva and south of State Road 126, were burned in a forest fire in 1971.

Access to the area from Los Alamos is on State Highway 4 to La Cueva and State Road 126 northwest to Fenton Lake and Cuba. Logging and service roads off State Road 126 provide additional access to the Jemez Plateau.

### III. GEOLOGY

The area of investigation is a part of the southern extension of the Rocky Mountains that lies between the structural features of the San Juan Basin to the west and the Rio Grande Depression to the east (Fig. 1). Precambrian, Pennsylvanian, Permian, Mesozoic, and Cenozoic rocks outcrop in the area (Fig. 3).

### IV. STRATIGRAPHY

Precambrian rocks of granite and gneiss outcrop along the flanks and crest of the Nacimiento Mountains. These are overlain by Pennsylvanian and Permian limestones, sandstones, and shales. Mesozoic sediments outcrop in the northwest part of the area and on the western slopes of the Nacimiento Mountains, but because they do not extend beneath the Jemez Plateau they are not further

considered in this report. The Cenozoic volcanic rocks form the upper surface of the Jemez Plateau, overlying the Permian, Pennsylvanian, and Precambrian rocks.

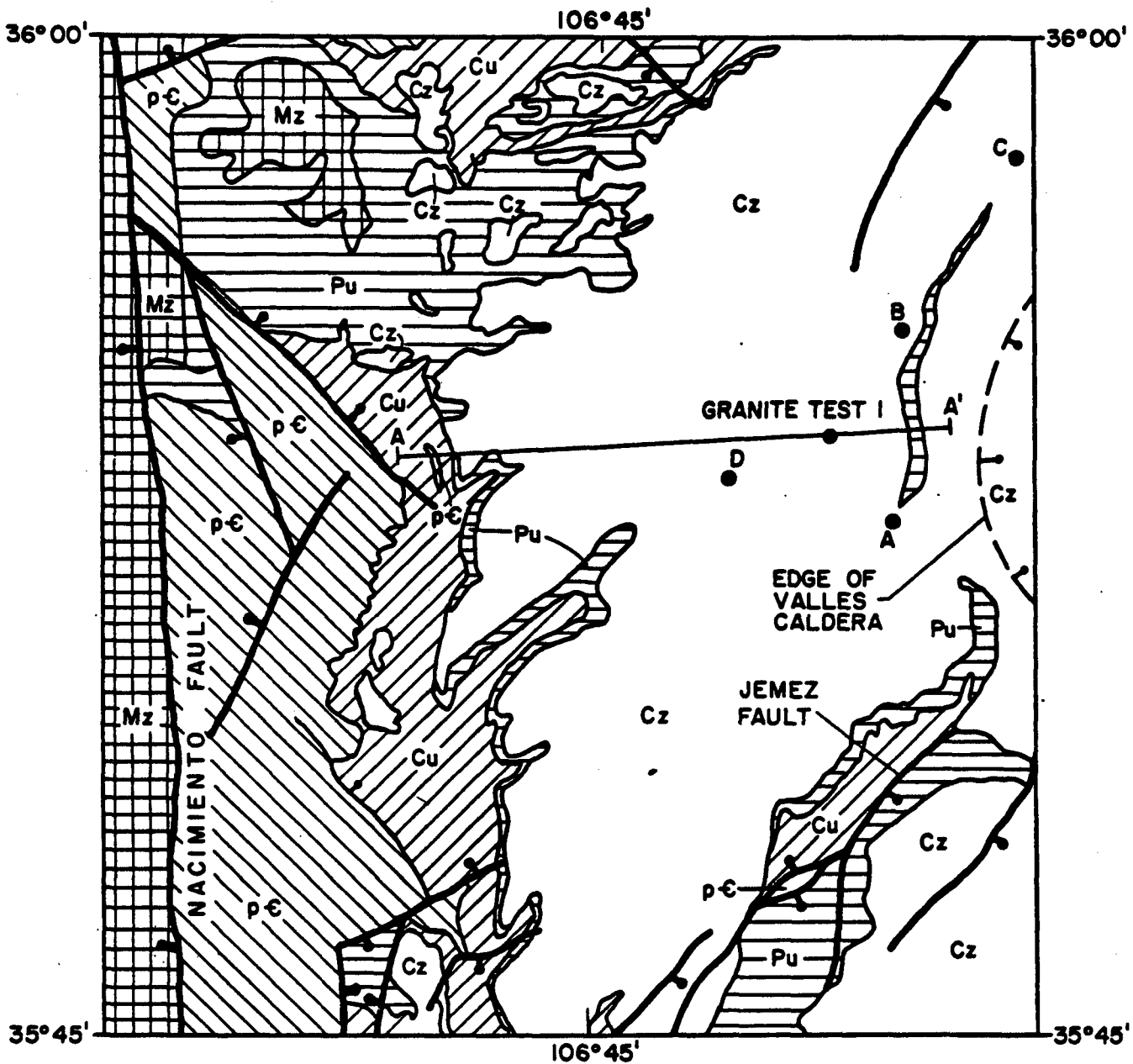
### V. PRECAMBRIAN ROCKS

The Precambrian rocks are particularly important to the proposed geothermal-energy experiment because it is intended that they will contain the pressurized-water circulation system.

Granite is the most abundant type of Precambrian rock. This granite is coarse-grained with large insets of microcline. Microcline is the dominant feldspar, although albite-oligoclase is usually also present in smaller amounts. Quartz is abundant, with biotite a common mafic mineral.

Quartz-feldspar gneiss is common. The feldspar consists mainly of microcline. However, oligoclase-andesine is also abundant, although it is finer-grained and more uniformly spread throughout the rocks. The quartz shows moderate straining. Accessory minerals are hornblende, biotite, and epidote, and some sphene, apatite, zircon, and magnetite. Granite Test 1 penetrated augen-gneiss in which the augen ("eyes") were of microcline (Table I). The gneiss is lenticular, with planes of foliation. The foliation has a general, characteristic northeast trend, which has also been observed to the southeast in the Sandia, Manzanito, and Manzano Mountains--as if deformation and metamorphism had taken place in a single major event with forces acting at right angles to the foliation (Ref. 7).

Associated in a few places with the granite is a black intrusive rock, mostly in dikes. Also cutting the granite in many places are quartz veins, most of which are less than 6 in. in width (Ref. 1). Granite Test 1 penetrated a dark gray amphibolite consisting mainly of amphibole and plagioclase. A few small outcrops occur in the Precambrian along the Rio de Las Vacas.



<b>Cz</b>	CENOZOIC ROCKS	<b>Cu</b>	PENNSYLVANIA ROCKS
<b>Mz</b>	MESOZOIC ROCKS	<b>pε</b>	PRECAMBRIAN ROCKS
<b>Pu</b>	PERMIAN ROCKS		FAULT, BAR & BALL ON DOWN THROWN SIDE

0 SCALE 4  
MILES

A A' LINE OF GEOLOGICAL SECTION SHOWN ON FIG. 4

GEOLOGY MODIFIED FROM WOODS, NORTHROP, SMITH AND OTHERS.

Fig. 3. Generalized geologic map of the area of investigation.

There are no apparent outcrops of pegmatites or greenstone schists, although there are a few outcrops of mica schist into which the granites have been intruded.

The color of the granites ranges from brownish gray to red, whereas the predominant color of the gneiss ranges from pinkish gray to red. The granites weather to spheroidal boulders and hummocks. The gneiss weathers to rounded knolls and undulating uplands.

## VI. PENNSYLVANIAN ROCKS

The Pennsylvanian rocks are dominantly massive limestones, shales, and arkose. In the area of investigation these rocks comprise the Magdalena Group, which includes the lower Sandia formation and overlying Madera limestone. Although these strata are combined on the map (Fig. 3), the cross section (Fig. 4) in the area of the experimental site shows individual units within the two formations.

The Sandia Formation is divided into the lower limestone member and the upper clastic member. The lower limestone member is a dark gray, siliceous limestone, whereas the overlying clastic member consists of dark brown to brownish-green sandstone and arenaceous shale and limestone. The lower limestone member is discontinuous, so that in some areas the upper clastic member rests on the Precambrian rocks (Ref. 2). Both clastic member and lower limestone member were present in Granite Test 1 (Table I).

The Madera limestone is composed of a lower, gray limestone member and an upper arkosic limestone member. The lower gray limestone consists of a dark gray limestone interbedded with gray shale and a few sandstone beds. The upper arkosic limestone member is of limestone and arkosic limestone, alternating with gray and red arkosic shale.

The thickness of the Pennsylvanian rocks of the Magdalena Group varies, and in some places

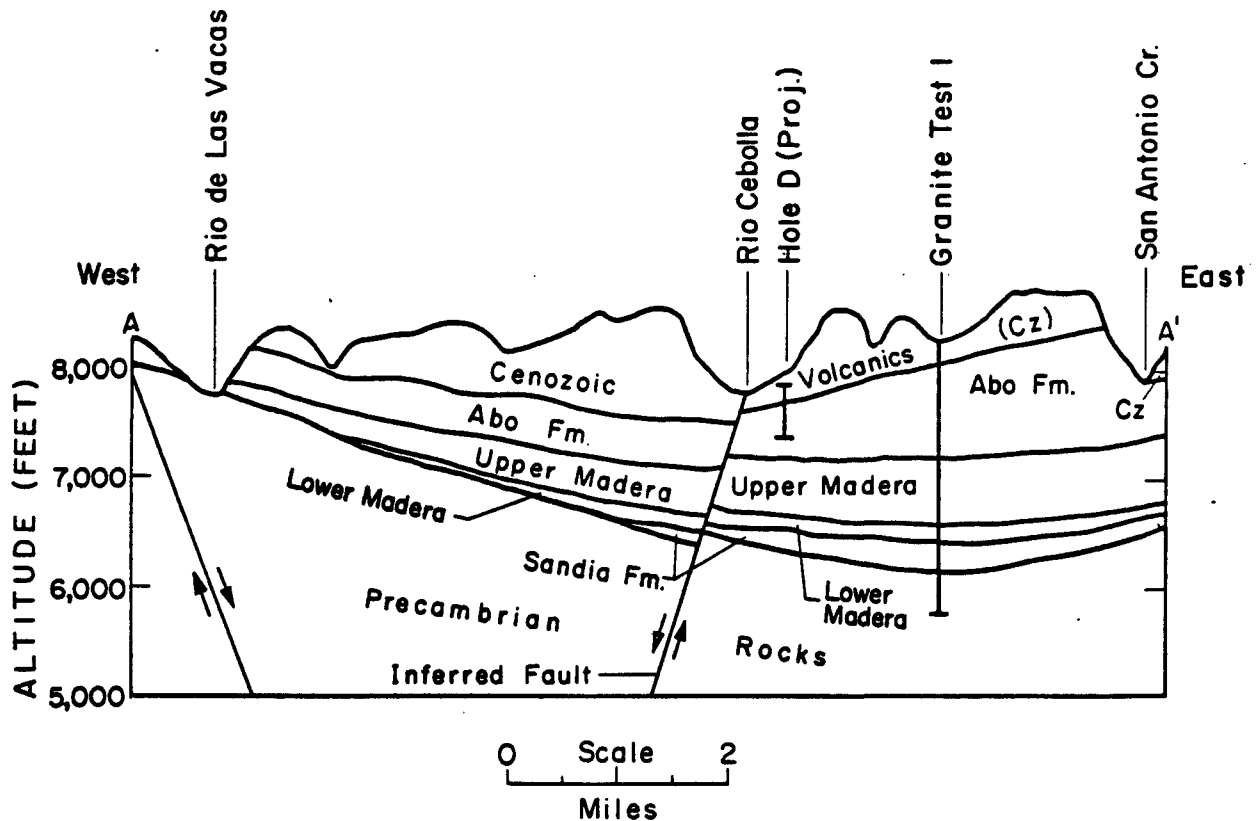


Fig. 4. Geologic section from the Rio de Las Vacas to San Antonio Creek.

they are not present--either because they were removed by erosion before deposition of the overlying Permian rocks or because they were never deposited. Shown below are the thicknesses of sections measured elsewhere and the thicknesses penetrated by Granite Test 1.

<u>Location Reference</u>	<u>Section Thickness in Feet</u>				
	<u>1</u>	<u>2</u>	<u>3</u>	<u>4</u>	<u>5</u>
<b>Madera Limestone</b>					
Arkosic limestone	610	230	340	410	590
Gray limestone	120	200	-	-	155
<b>Sandia Formation</b>					
Upper clastic	200	210	-	-	235
Lower limestones	30	30	-	-	55

1. Rio de Las Vacas, 5 miles southwest of Jemez Springs.
2. Jemez Creek, near Jemez Springs.
3. Rio de Las Vacas, 5 miles west of Fenton Lake.
4. Ten miles northwest of Fenton Lake.
5. Granite Test No. 1, LASL.

Sections 1, 2, 3, and 4 were measured in the field (Ref. 2) and rest directly on the Precambrian rocks. Section 5, Granite Test 1, did penetrate into the Precambrian rocks.

## VII. PERMIAN ROCKS

The Permian rocks were deposited on an old flood plain that may have been flooded periodically by marine waters, although the irregular bedding in the sandstones suggests a fluvial mode of deposition for most of the rocks, in a continental environment.

In the area of investigation the Permian rocks are of the Abo Formation. The formation consists of arkosic siltstone, sandstone, and shale. The sandstone is fine-grained with occasional lenses of pebbly conglomerate. Lenses of clay also occur, as well as some minor and thin lenses of arkosic limestone. The formation is made up of alternating layers of shale, siltstone, sandstone, and clay, with the shales making up the larger part of the section. Quartz grains are numerous in coarser-bedded material; however, some feldspar is also

present, as well as small particles of igneous rock. The Abo in the lower part of the section may contain some reworked material from the Magdalena Group. The color of the formation is predominantly various shades of red, from light to very dark. There are some calcareous lenses that range in color from white to dark gray.

The upper surface of the Abo was heavily eroded prior to the deposition of the Cenozoic volcanics. Thus the thickness of the Abo varies, due to this irregular surface. Various thicknesses in the area are presented in the following table. Test Hole A (Table II), Test Hole B (Table III), Test Hole C (Table IV), and Test Hole D (Table V) did not penetrate the complete section of the Abo but are completed 335, 210, 170, and 380 ft, respectively, into the upper part of the formation.

<u>Location Reference</u>	<u>Section Thickness in Feet</u>		
	<u>1</u>	<u>3</u>	<u>5</u>
Abo Formation	590	700	910

## VIII. CENOZOIC ROCK

The Cenozoic rocks are made up of volcanics or sediments derived from volcanic rocks. The older Cenozoic rocks--the Abiquiu Tuff and the Tachicoma Formation--are exposed in the west wall of the canyon cut by San Antonio Creek north of La Cueva, whereas the younger rocks--the Banelier Tuff--form the upper part and surface of the Jemez Plateau (Fig. 3).

The Abiquiu Tuff lies in the topographically low areas in the eroded surface of the Abo Formation. It is composed mainly of white to light gray tuffaceous sandstone and conglomerate, which includes a basal gravel member that includes pebbles and sand derived from the Precambrian crystalline rocks. Test Hole A (Table II), Test Hole C (Table IV), and Granite Test 1 penetrated the Abiquiu Tuff at 125, 340, and 100 ft, respectively.

The Tschicoma Formation overlies the Abo Formation and a part of the Abiquiu Tuff along the west wall of the canyon cut by San Antonio Creek. The formation is a thin pyroclastic flow of dark gray latite that, in places, contains some thin lenses of light gray clay. The formation contains phenocrysts of plagioclase and some smaller crystals of quartz, biotite, hornblende, and augite, in a fine grained gray matrix. Test Hole B (Table III) penetrated about 60 ft of the Tschicoma above the Abo Formation.

The Bandelier Tuff forms the upper part and the surface of the Jemez Plateau overlying the older volcanic rocks of the Tschicoma Formation-- Abiquiu Tuff and, in places, the sediments of the Abo Formation. The Bandelier Tuff ranges from a nonwelded to a welded rhyolite tuff, with colors from light gray to dark gray. The tuff is made up of crystals and crystal fragments of quartz and sanidine, glass shards, and some mafic minerals as well as rock fragments, pumice, latite, and rhyolite in a fine-grained ash matrix. The Bandelier Tuff thins to the west and southwest away from the source area, the Valles Caldera. Test Holes A, B, C, and D, and Granite Test 1 penetrated thicknesses ranging from 30 to 380 ft of the Bandelier Tuff (Tables I through V).

The ages of the volcanic rocks in the area of investigation and in adjacent areas were determined by potassium-argon methods (Refs. 5 and 8). The ages presented here are not for correlation of geologic formations but to show the time span of volcanic activity in the Valles Caldera Region. The Abiquiu Tuff is associated with older volcanic centers to the north. It is much older than rocks in the Valles Region, ranging in age from 25 to 35 million years.

The ages of the El Cajete member and the Blanca Bonita member are estimated older than 42,000 years before present (BP), and younger than 0.1 millions of years (MY). Thus, in the area of investigation, the youngest to oldest volcanic

rocks are the Bandelier Tuff (1.1 to 1.4 MY) and Tschicoma Formation (3.7 to 6.7 MY). However, in the Valles Caldera the intracaldera domes range from 0.4 to 1.0 MY, with the oldest volcanic activity associated with the Valles Caldera beginning about 9 million years ago. The westernmost intracaldera dome (San Antonio Mountain) adjacent to the site on the plateau has an age of 0.5 MY.

Volcanic Rocks (Unit Name)	K-Ar Age (Millions of Years)
Canvoas Canyon Rhyolite	8.5 to 9.1
Plaza Canyon Formation	8.5 to 9.1
Labato Basalt	7.4
Tschicoma Formation	3.7 to 6.7
El Rechuelos Rhyolite	2.0
Bandelier Tuff	
Upper Member	1.1
Lower Member	1.4
Valle Grande Member	
Intracaldera Domes	0.4 to 1.0
Battleship Rock Member	0.5

## IX. STRUCTURE

The area of investigation is in the western arm of the Rocky Mountains between the Rio Grande Depression on the east and the San Juan Basin on the west (Fig. 1). The San Juan Basin, a part of the Colorado Plateau, is a large structural basin that extends from the western edge of the north-south-trending Nacimiento Mountains into northwestern New Mexico. The deepest part of the basin contains over 18,000 ft of Mesozoic and Cenozoic sediments. The Rio Grande Depression to the east is a structural depression that extends from southern Colorado through central New Mexico into northern Mexico (Ref. 10). Near Los Alamos, the depression, formed by north-south-trending faults, contains over 12,000 ft of sediments above the Precambrian rocks (Ref. 11). The western arm of the Rocky Mountains is a high mountain chain that lies

between the structural basin to the east and the depression to the west.

The area of investigation lies between the smaller structural features of the western arm of the Rockies, the Nacimiento Mountains or uplift, and the Valles Caldera. The Valles Caldera is a depression about 12 to 15 miles in diameter, formed by eruption of a large volume of volcanic ash. The central part of the caldera collapsed and was later intruded by volcanics, which formed a series of intracaldera domes.

The Nacimiento Mountains were formed by faulting that took place to the west of the main mountain mass (Fig. 3). Renich<sup>1</sup> described the fault as an overthrust with most fault planes in this shear zone dipping to the east, showing that the mountain mass has been overthrust to the west toward the San Juan Basin. The overthrust is not a single fault; movement has taken place along several planes of shear. The fault has thrust the Precambrian rocks upward to a position in which they are adjacent to the younger Mesozoic rocks to the west. The stratigraphic displacement along the fault ranges from 3000 to 3500 ft.

Numerous smaller faults on the flanks of the mountains are contemporaneous with the overthrust, as is the Jemez fault along the southeastern edge of the area (Fig. 3). This northeast-trending fault parallels Jemez Creek, and is covered by younger volcanics to the north where it continues into the caldera. Near Jemez Springs the fault brings to the surface an outcrop of Precambrian gneiss.

Smith et al.<sup>3</sup> have indicated through work in the area that the Valles Caldera is bounded by ring faults in which the intracaldera blocks dropped down into the center of the caldera. The exposures of the faults are covered by younger volcanics, but probably constitute a complex fracture zone 2 to 3 miles wide. After this subsidence, intracaldera domes were intruded through this zone of weakness.

The Jemez Plateau is covered by Cenozoic volcanic rocks that obscure most of the structure. The test drilling and measured sections indicate a small north-south-trending basin near the center of the experimental site. The basin is characterized by the thickening of the Pennsylvanian rocks off the flanks of the mountain, and thinning to the east (Fig. 4). The basin may be structural in part (a faulted area) or erosional, where the upper surface of the Precambrian rock was cut to form a small valley. General structural features in the area indicate north-south lineations. The overlying Permian rocks appear to thicken eastward, off the flanks of the mountains. Except in the northwest corner of the area, the Mesozoic rocks were eroded from the Permian rocks before the explosive deposition of the Cenozoic volcanics.

The Precambrian, Pennsylvanian, and Permian rocks are probably arched upward along the outer rim of the caldera by welling of the magma through the central chamber. Within the caldera the eastern edge of the basin is truncated by the down-faulted ring-fault structure.

## X. GEOLOGIC HISTORY

This brief geologic history of the area was condensed from Woods and Northrop<sup>2</sup> and Ross et al.,<sup>4</sup> with minor modifications.

The Precambrian rocks were deformed prior to the deposition of the earlier Paleozoic sediments. Subsequent erosion reduced the rocks to a peneplain, above which rose an occasional monadnock. Either some minor structural deformation occurred or an erosional valley was cut into the Precambrian surface near the center of the experimental area before the deposition of the Pennsylvanian rocks. The lower rocks of the Magdalena Group were deposited into the lowlands and shallow seas. These sediments thickened in the small basin. As the upper part of the Magdalena Group was being deposited, a positive land mass began to rise along the present position of the Nacimiento Mountains.

Subsidence of the basin to the east and west began to occur. Deposition of the Permian rocks (Abo Formation) followed, as sedimentation became continental--due to extensive filling of the basins. Mesozoic and Cenozoic sediments were also deposited.

The folding and deformation along the Nacimiento thrust-faults in the early Cenozoic Era caused the high mountain area to emerge. Subsequent erosion stripped off most of the Mesozoic rocks and all of the early Cenozoic sediments, cutting an irregular surface into the Abo Formation.

Volcanic activity then began in the Valles Caldera (Pliocene Epoch) with the extrusion of basalts, followed by latites and rhyolites. After a period of quiescence and erosion, catastrophic eruptions of hot ash-flows followed, resulting in formation of the Valles Caldera and capping of the Jemez Plateau with the Bandelier Tuff. The intracaldera domes were subsequently formed in the Valles Caldera. The caldera was then filled by lakes that have since been drained by headward erosion of Jemez and San Antonio Creeks. Erosion has modified the Jemez Plateau into a number of narrow mesas as we see it now.

TABLE I  
GEOLOGIC LOG OF GRANITE TEST HOLE NO. 1

Elevation of land surface	-	8475 ft
Depth drilled	-	2575 ft
Hole diameter	-	13-3/4 in. to 280 ft 9-7/8 in. to 1600 ft 6-3/4 in. to 2410 ft 4-1/4 in. to 2575 ft
Casing Schedule	-	10-3/4 in. o.d. to 258 ft 7-5/8 in. o.d. to 1357 ft 5 in. o.d. to 2400 ft Open hole 2400 to 2575 ft
Drilled-Air-Mist Rotary	-	To 2410 ft
Core-Water Rotary	-	2410 to 2575 ft
Date Completed.	-	June 30, 1972

	<u>Thickness</u> (ft)	<u>Depth</u> (ft)
<u>Bandelier Tuff</u> Tuff, gray, moderately welded, rhyolitic; crystals and crystal fragments of quartz and sanidine, rock fragments of pumice, rhyolite and latite, in ash matrix.	60	60
<u>Abiquiu Tuff</u> Sandstone, light gray, with pebbly conglomerate containing rock fragments of pumice, latite and rhyolite, and unidentified rock fragments ranging from light gray and green to dark gray and black.	100	160
<u>Abo Formation</u> Shale and fine-grained sandstone, some clay lenses; predominantly red to dark red in color, with some lenses of white to gray; arkosic with a few thin beds of limestone. Shale, dark red, 160 to 290 ft; sandstone, fine-grained, dark red, 290 to 350 ft; sandstone, fine-grained, alternating with shale, dark red, 350 to 680 ft; shale and sandstone, fine-grained, predominantly red, with lenses of white to gray shale and sandstone, a few thin beds of limestone, 680 to 1030 ft; clay, dark red with minor lenses of shale and sandstone, 1030 to 1070 ft.	910	1070

TABLE I (cont)

	<u>Thickness</u> (ft)	<u>Depth</u> (ft)
<b><u>Magdalena Group</u></b>		
<b>Madera Limestones:</b>		
Upper limestone member consists of limestone alternating with gray and red shales and sandstone, arkosic; limestone, gray, alternating with sandstone, fine-grained red, 1070 to 1250 ft; shale, red with some thin lenses of limestone, gray, 1250 to 1330 ft; limestone, gray, with some lenses of sandstone, fine-grained red, and shale, light red, 1330 to 1440 ft; shale, dark red, with lenses of limestone, dark gray, 1440 to 1530 ft; limestone, gray, with thin lenses of light red and gray sandstone, fine-grained, 1530 to 1670 ft.	590	1660
Lower limestone member consisting of dark gray limestone and thin lenses of white to gray shale and fine-grained sandstone. Limestone, dark gray, with thin lenses of sandstone, fine-grained, white to light gray and shale, dark gray.	155	1815
<b><u>Sandia Formation</u></b>		
Upper clastic member, limestone, gray, with lenses of gray shale and fine-grained sandstone ranging from light gray to light green.	235	2050
Lower limestone member, limestone, dark gray, siliceous, dense.	55	2105
<b><u>Precambrian Rocks</u></b>		
Augen gneiss, brownish gray, with inclusions of pink plagioclase, 2105 to 2430 ft; granite, reddish brown, medium-grained, 2430 to 2480 ft; gneiss, reddish brown, medium-grained, foliated, 2480 to 2520 ft; amphibolite, dark gray, fine-grained, 2520 to 2575 ft.	470	2575

TABLE II  
GEOLOGIC LOG OF HOLE A

Elevation of land surface	- 8450 ft
Depth drilled	- 590 ft
Hole diameter	- 9-5/8 in. to 100 ft 6-1/4 in. to 590 ft
Casing schedule	- 7 in. o.d. to 97 ft 4-1/2 in. o.d. to 578 ft
Drilled - Mud, rotary	
Date completed	- April 10, 1972

	<u>Thickness</u> (ft)	<u>Depth</u> (ft)
<b><u>Bandelier Tuff</u></b>		
Tuff, light gray, nonwelded to moderately welded, rhyolitic; crystals and crystal fragments of sanidine and quartz, with rock fragments of pumice and latite, in gray ash matrix.	30	30
<b><u>Abiquiu Tuff</u></b>		
Sandstone, light gray, tuffaceous, friable; mafic minerals and a few quartz crystals; rock fragments of pumice, latite, and rhyolite in a fine ash matrix with mafic mineral altered to stain matrix light yellow, 50 to 100 ft. Conglomerate, light gray, tuffaceous, friable with rock fragments of quartzite and chalcedony, 100 to 155 ft.	125	155

TABLE II (cont)

	<u>Thickness</u> (ft)	<u>Depth</u> (ft)
<u>Abo Formation</u>		
Shale and silty sandstone, predominantly brownish-red to dark red in color, with some lenses of white and dark gray; arkosic, with minor amounts of quartz grains. Silty sandstone, brownish-red, 155 to 260 ft; shale, dark red, 260 to 320 ft; silty sandstone, red, 320 to 380 ft; shale, red, 380 to 460 ft; shale, dark red, 460 to 590 ft.	335	590

TABLE III  
GEOLOGIC LOG OF HOLE B

Elevation of land surface	-	8625 ft		
Depth drilled	-	650 ft		
Hole diameter	-	9-5/8 in. to 100 ft 6-1/4 in. to 650 ft		
Casing schedule	-	7 in. o.d. to 97 ft 4-1/2 in. o.d. to 566 ft		
Drilled - Mud, rotary				
Date completed	-	April 13, 1972		
			<u>Thickness</u> (ft)	<u>Depth</u> (ft)
<u>Bandelier Tuff</u>				
Tuff, light gray to gray, nonwelded to moderately welded, rhyolitic, containing crystals and crystal fragments of quartz and sanidine and rock fragments of pumice, latite, and rhyolite in an ash matrix. Tuff, gray, moderately welded, 0 to 140 ft; tuff, light gray, moderately welded, 140 to 230 ft; tuff, light gray, nonwelded, made up mostly of pumice, 230 to 380 ft.			380	380
<u>Tschicoma Formation</u>				
Latite, dark gray, vugs in places, with some calcite crystals; some thin lenses of light gray clay.			60	440
<u>Abo Formation</u>				
Shale and silty sandstone, dark red in color, with some lenses and clots of white and gray to dark gray, arkosic. Shale, dark red, 440 to 560 ft; silty sandstone, dark red, 560 to 650 ft.			210	650



TABLE V  
GEOLOGIC LOG OF HOLE D

Elevation of land surface - 7900 ft  
 Depth drilled - 500 ft  
 Hole diameter - 9-5/8 in. to 100 ft  
                   6-1/4 in. to 500 ft  
 Casing schedule - 7 in. o.d. to 97 ft  
                   4-1/2 in. o.d. to 500 ft  
 Drilled - Mud, rotary  
 Date completed - April 18, 1972

	Thickness (ft)	Depth (ft)
<u>Bandelier Tuff</u>		
Tuff, gray, moderately welded, rhyolitic, containing crystals and crystal fragments of quartz and sanidine, mafic minerals, rock fragments of pumice, rhyolite and latite, in gray ash matrix.	120	120
<u>Abo Formation</u>		
Shale, fine-grained sandstone and clay, ranging from tan to dark red, with stringers and lenses of white and gray. Clay, dark gray, 120 to 190 ft; clay, tan, some mafic stains, and light pinkish clots, 190 to 200 ft; shale, light red with gray clay lenses, 200 to 240 ft; shale, red, with dark gray lenses of white shale, 240 to 280 ft; shale, red, with dark gray lenses of sandstone, 280 to 320 ft; shale, dark red, with lenses of white to gray shale, 320 to 390 ft; shale, dark red, 390 to 430 ft; sandstone, fine-grained, dark red, with lenses of dark gray, 430 to 460 ft; shale, dark red, 460 to 500 ft.	380	500

REFERENCES

1. B. C. Renich, "Geology and Ground-Water Resources of Western Sandoval County, New Mexico," U. S. Geol. Survey Water-Supply Paper 620 (1931).
2. G. H. Woods, Jr., and S. A. Northrop; "Geology of the Nacimiento Mountains, San Pedro Mountains, and Adjacent Plateaus in Parts of Sandoval and Rio Arriba Counties, New Mexico," U. S. Geol. Survey Oil and Gas Inv. Prelim. Map 57 (1946).
3. R. L. Smith, R. A. Bailey, and C. S. Ross, "Structural Evolution of the Valles Caldera, New Mexico, and Its Bearing on Emplacement of Ring Dikes," U. S. Geol. Survey Prof. Paper 424-D (1961).
4. C. S. Ross, R. L. Smith, and R. A. Bailey, "Outline of Geology of the Jemez Mountains, New Mexico," New Mex. Geol. Soc. Twelfth Field Conf., Albuquerque Country (1961).
5. R. A. Bailey, R. L. Smith, and C. S. Ross, "Stratigraphic Nomenclature of the Volcanic Rocks in the Jemez Mountains, New Mexico," U. S. Geol. Survey Bull. 1274-P (1969).
6. R. L. Smith, R. A. Bailey, C. S. Ross, "Geologic Map of the Jemez Mountains, New Mexico," U. S. Geol. Survey Misc. Geol. Inv. Map I-571 (1970).
7. J. P. Fitzsimmons, "Precambrian Rocks of the Albuquerque Country," New Mex. Geol. Soc. Twelfth Field Conf., Albuquerque Country (1961).
8. R. R. Doell, G. B. Dalrymple, R. L. Smith, and R. A. Bailey, "Paleomagnetism, Potassium-Argon Ages, and Geology of the Rhyolites and Associated Rocks of the Valles Caldera, New Mexico," Geol. Soc. America Mem. 116 (1968).
9. W. E. Hale, L. J. Reiland, and J. P. Beverage, "Characteristics of Water Supply in New Mexico," New Mex. State Eng. Tech Rept. 31 (1965).
10. V. C. Kelley, "Tectonic Map of a Part of the Upper Rio Grande Area, New Mexico," U. S. Geol. Survey Oil and Gas Inv. Map OM-157 (1954).
11. M. D. Keller, "Geologic Studies and Material Properties Investigations of Mesita de Los Alamos," Los Alamos Scientific Laboratory report, LA-3728 (1968).

LA-5780-MS  
Informal Report

UC-11  
Reporting Date: October 1974  
Issued: November 1974

Geology of Geothermal Test Hole GT-2  
Fenton Hill Site, July 1974

by

W. D. Purtymun  
F. G. West  
R. A. Pettitt

The logo consists of a central circle containing a cross, surrounded by a larger circle with several small dots on its circumference. A vertical line passes through the center, and a wavy line extends upwards from the top of the logo.

**los alamos**  
**scientific laboratory**

of the University of California

LOS ALAMOS, NEW MEXICO 87544

UNITED STATES  
ATOMIC ENERGY COMMISSION  
CONTRACT W-7405-ENG. 36

In the interest of prompt distribution, this LAMS report was not edited by the Technical Information staff.

Printed in the United States of America. Available from  
National Technical Information Service  
U.S. Department of Commerce  
5285 Port Royal Road  
Springfield, VA 22151  
Price: Printed Copy \$4.00 Microfiche \$2.25

## GEOLOGY OF GEOTHERMAL TEST HOLE GT-2

FENTON HILL SITE, JULY 1974

by

W. D. Purtymun, F. G. West, and R. A. Pettitt

### ABSTRACT

The test hole GT-2, drilled at the Fenton Hill Site, was completed at a depth of 6346 ft (1934.3 m) below land surface. The hole penetrated 450 ft (137.2 m) of Cenozoic volcanics, 1945 ft (592.8 m) of sediments of Permian and Pennsylvanian age and 3951 ft (1204.3 m) of granitic rocks of Precambrian age. This report presents the field geologic log of the hole and hydrologic data compiled during the drilling phase of the program.

### I. INTRODUCTION

The second geothermal exploratory hole, GT-2, drilled by the Los Alamos Scientific Laboratory, is located on Fenton Hill about 2 miles (3.2 km) northwest of La Cueva, New Mexico (Fig. 1). The area is designated as the Fenton Hill Site, TA-57. The location of the site was based on investigations made in the area by the Laboratory.

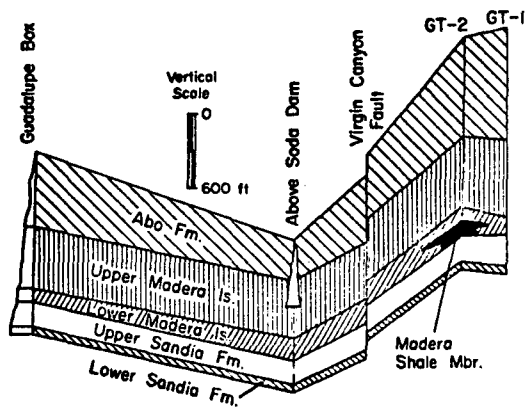
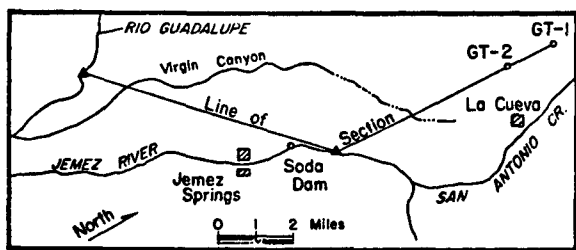
This report presents data obtained during the test drilling phase through the volcanic, sedimentary and granitic sections of GT-2. The field geologic log and a brief description are presented of the stratigraphy, structure, and hydrology of the area. A regional description of geology and/or hydrology is found in Renick,<sup>1</sup> Woods and Northrop,<sup>2</sup> Smith et al.,<sup>3</sup> Ross et al.,<sup>4</sup> Bailey et al.,<sup>5</sup> Purtymun,<sup>6</sup> West,<sup>7</sup> and Purtymun et al.<sup>8</sup> The petrology of rock types of Precambrian age penetrated by test hole GT-1 are described by Perkins,<sup>9</sup> while Fitzsimmons<sup>10</sup> presents a general description of Precambrian rocks in the area. A regional geologic map was published by Smith et al.<sup>11</sup>

The drilling contractor and drilling support units do not use the metric system. As this report is prepared to be used as a working document by contractors for the drilling and construction of additional energy extraction holes, English units are used first to avoid confusion. Metric units are shown in parentheses. Depth measurements in the report are referred to land surface elevation of 8690 ft (2648.7 m).

### II. GEOLOGY

This report describes the volcanic rocks of Cenozoic age, sediments of Permian and Pennsylvanian age, and granitic rocks of Precambrian age.

The log interpretation in the volcanic and sedimentary section was based on microscopic examination of the cuttings collected while using mud or air-mist-mud as a cuttings carrier (Table I). The log interpretation of the Precambrian section was based on microscopic examination of cuttings collected while using air and/or soap to a depth of 3550 ft (1082 m) and water and



Diagrammatic Section

Fig. 1. Location of Test Hole GT-2 and diagrammatic section showing Permian and Pennsylvanian rock overlying Precambrian rocks.

drilling mud to a depth of 6346 ft (1934.3 m). Geophysical logs were used to adjust the contact between the different rock types (Table I).

A. Stratigraphy

Rock units penetrated by the test hole were (youngest to oldest) the Bandelier Tuff, the Paliza Canyon Formation, the Abiquiu Tuff, the Abo Formation, and the Madera Limestone and Sandia Formation of the Magdalena Group. Granitic and metamorphic rocks were penetrated in the Precambrian section.

1. Cenozoic Volcanics. The Bandelier Tuff forms the surface and upper part of the Jemez Plateau at the Fenton Hill Site. The tuff ranges from moderately welded to welded ashflows of rhyolitic tuff with an ash-fall of gray pumice. The tuff ranges in color from light to dark gray and consists of quartz and sanidine crystals with crystal fragments and lithic fragments of latite and pumice in an ash matrix. The pumice is

composed of minor amounts of quartz and sanidine crystal fragments with some lithic inclusions of latite and rhyolite in a cellular structure of glass. The thickness of the Bandelier Tuff penetrated by GT-2 was 350 ft (106.7 m) (Table I).

The Paliza Canyon Formation underlies the Bandelier Tuff at the site. The Paliza Canyon Formation is composed of andesite and basaltic andesite breccias that are interbedded with sand and gravel. A part of the formation outcrops in a road cut in the canyon to the north of the site. The thickness of the formation penetrated by GT-2 was 50 ft (15.2 m).

The Abiquiu Tuff underlies the Paliza Canyon and is composed of a light gray, friable tuffaceous sandstone. In the upper part of the section, the sandstone is interbedded with angular fragments of basalt. The sandstone is composed of quartz, chalcedony, and fragments of rhyolite and quartzite in a tuffaceous matrix. The lower part contains rock fragments and pebbles derived from Precambrian crystalline rocks. The thickness penetrated by GT-2 was 50 ft (15.2 m).

2. Permian Rocks. The Abo Formation underlies the Abiquiu Tuff and is composed of a sequence of shales, siltstones and fine-grained sandstones with some clay lenses. The color of the sediments ranges from brownish-red to dark red, with the clays ranging from white to gray. Near the base of the formation are dark red lenses of clay interbedded with gray limestone. The thickness of the Abo penetrated by GT-2 was 780 ft (237.7 m).

3. Pennsylvanian Rocks. The Magdalena Group is composed of the Madera Limestone and the Sandia Formation, which at GT-2 are separated by a shale member.

The Madera Limestone is made up of an upper limestone and a lower limestone member. The upper limestone is composed of gray limestone and arkosic limestone alternating with gray and red arkosic shale. The thickness of the upper member at GT-2

was 610 ft (185.9 m). The lower limestone is a dark gray dense limestone with thin lenses of gray shale and white to gray fine-grained siltstone and sandstone. The thickness of the lower limestone at GT-2 was 115 ft (35.1 m).

The lower member of the Madera is underlain by a shale which has not been described in previous reports on the area. The shale has tentatively been placed in the lower part of the Madera. The shale member is dark gray shale with lenses of gray siliceous limestone and some lenses of gray clay and reddish-brown fine-grained sandstone. The shale is probably of only local extent and is equivalent in part to the lower limestone member of the Madera. The thickness of the shale member penetrated by GT-2 was 180 ft (54.9 m).

The Sandia Formation consists of an upper clastic member and a lower limestone member. The clastic member is a gray limestone and reddish-brown fine- to coarse-grained sandstone with lenses of brown shale and brown to greenish-gray clays. The thickness of the clastic member at GT-2 was 205 ft (62.5 m).

The lower limestone member consists of a light gray siliceous dense limestone with a few lenses of fine- to coarse-grained sandstone and light gray siltstone. The lower limestone overlies the Precambrian granitic rocks. There appears to be little if any weathering of the top granite immediately underlying the sediments. The thickness of the lower limestone at GT-2 was 55 ft (16.8 m).

4. Precambrian Rocks. As identified from the cuttings, the granitic rocks penetrated represent three general types: granites, granodiorites and monzonites. The identification is based on percentages of quartz, potassic feldspar (microcline, orthoclase), and sodic feldspar (plagioclase).

The following criteria were used for identification of cuttings:

Granite: quartz >10%  
potassic feldspar primary  
plagioclase, secondary

Granodiorite: quartz >10%  
potassic feldspar = or <plagioclase

Monzonite: quartz <10%  
potassic feldspar = plagioclase  
or if quartz >10%, the rock is a quartz monzonite.

Biotite is the major mafic mineral with minor amounts of hornblende. The metamorphic rocks penetrated in the lower section of the hole consisted of biotite-hornblende schist associated with some granitic gneiss. A thin section of amphibolite was penetrated in the lower section of the hole. Also identified in the cuttings were dikes or veins that were mainly biotite with hornblende and sodic feldspar.

Granites in general had the slowest drilling rates of 4 to 6 ft/h (1.2 to 1.8 m/h). The coarse-grained granites drilled slower than the fine-grained granites. Granodiorites had similar drilling rates, while the monzonites and schists were cut at 8 to 12 ft/h (2.4 to 3.7 m/h).

The granites tend to cut to the gauge of the bit except in sections containing large crystals of orthoclase or at contacts between units. The sections of the hole through the granodiorites, monzonites, schists, and thicker dikes tend to enlarge slightly due to erosion from the circulating fluids used as cutting carriers.

A comparison of the geologic log with the gamma log indicates a greater level of gamma activity in the granite than in other rock types. Coarse-grained granites (large orthoclase crystals) had higher gamma activity. Contacts between rocks of different textures (coarse- to fine- or medium-grained) had an observed gamma activity indicating the chill margin associated with emplacement of the granitic rocks.

The cores showed two major sets of joints or fractures. One set was nearly horizontal and another set was about 60° from vertical. Some joints were plated with calcite or epidote; others appeared closed, with no mineralization. The granitic cores contained a slight gneissic structure which appeared nearly vertical.

The cores, each ranging from 5 to 20 ft (1.5 to 6.1 m) long, showed several textural or lithologic changes within the section of core. The descriptions of the rock types given on Table I are based on observations of cuttings. Small features such as textural changes, thin veins or dikes, joints or fractures, or slight lithologic changes could not always be characterized from the cuttings nor represented in this summary form.

#### B. Structure

The upper surface of the Jemez Plateau at the Fenton Hill Site is dissected into elongated mesas by the southwest-trending intermittent streams. The site is located on one of these mesas and is underlain by the Bandelier Tuff. The tuff thins to the west and southwest from the source area (Valles Caldera) which lies to the east of the site.

The upper surface of the Abo Formation was deeply eroded prior to the emplacement of the overlying Cenozoic volcanics. Since the Abiquiu Tuff and Paliza Canyon Formations were deposited on this irregular surface, they vary in thickness across the area and in some locations may be absent.

Generalized contours on top of the Abo Formation (using test holes GT-1, GT-2, A and D for control, as well as outcrop elevations) show that the surface of the Abo dips gently to the southwest (Fig. 2).

A north-south trending normal fault occurs east of the site along the west wall of the canyon cut by San Antonio Creek. The fault is downthrown to the east with an apparent throw that ranges from 300 to 400 ft (91.4 to 121.9 m).

Along the Jemez River to the southeast of the site, the base of the volcanics is 300 to 500 ft (91.4 to 152.4 m) below the basal contact at the site. This displacement is due in part to the erosion of the top of the Abo prior to the emplacement of the volcanics and in part to a fault along Virgin Canyon that is downthrown to the east. The fault has had some apparent reverse movement since the emplacement of the Bandelier Tuff. The tuff that forms the elongated mesa to the southeast of Virgin Canyon is about 50 ft (15.2 m) higher than the surface of the mesa to the northwest of the canyon. The Abo thickens to the north and northwest of the site and thins to southwest and southeast of the site (Fig 1). Thicknesses of the section are shown in Table II.

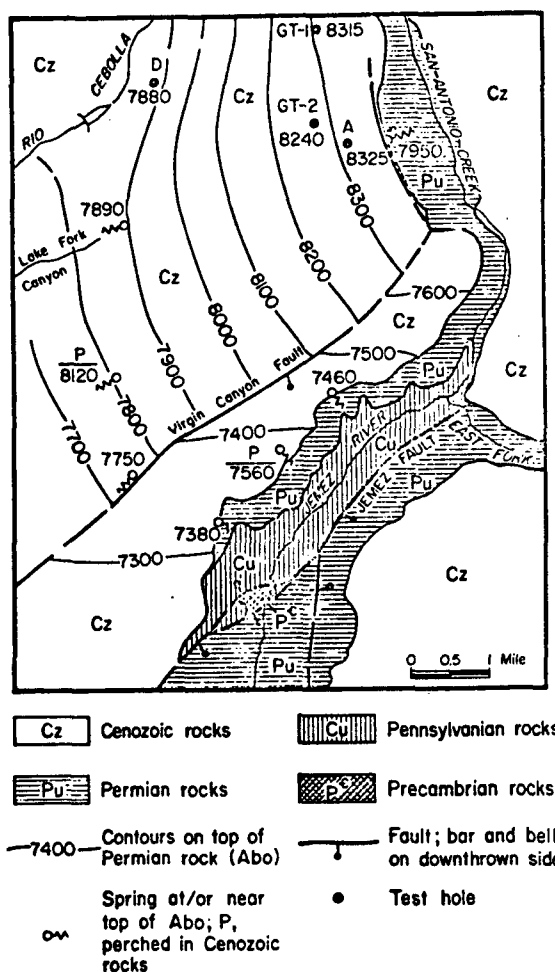


Fig. 2. Geologic map of area with structure contours on top of Abo Formation.

The members of the Madera Limestone and Sandia Formation vary in thickness, but in general thin rapidly to the west from the western edge of an old depositional basin and to the east and south of the site at Fenton Hill. The site is located near the axis of the north-south trending depositional basin that is truncated by the ring-fault structure formed by the Valles Caldera to the east (Fig. 3). The basin may be either structural in origin as the result of faulting or erosion of the granitic rocks prior to the deposition of the sediments of Pennsylvanian age.

The Jemez Fault trends northeast along the east side of the Jemez River (Fig. 3). It is one of the major faults in the area, being a normal fault that is downthrown to the east. Renick estimated the throw to be about 8000 ft (2438.4 m) in an area about 12 miles (19.3 km) to the south.<sup>1</sup> The throw

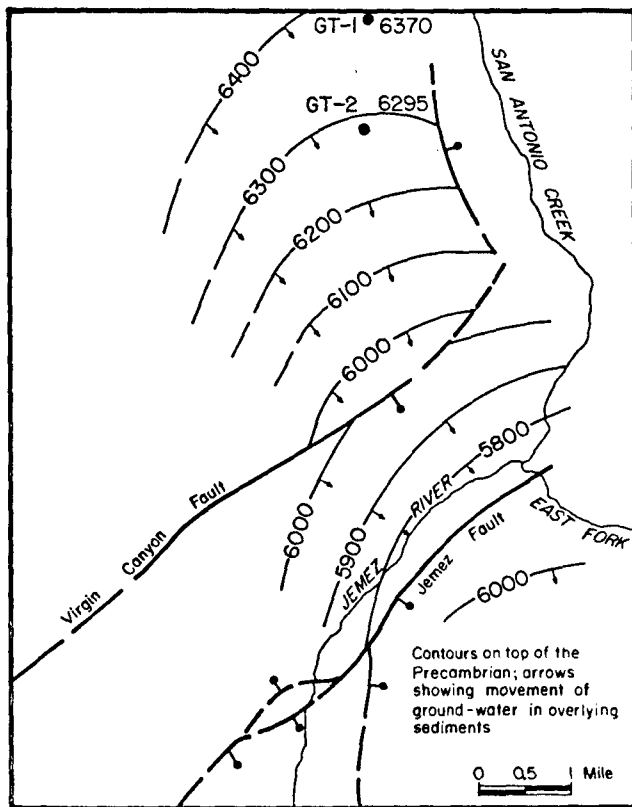


Fig. 3. Structure contours on top of Precambrian rocks showing direction of groundwater movement in overlying sediments.

along the Jemez River is about 800 to 1000 ft (243.8 to 304.8 m) based on displacement of the Permian and Pennsylvanian sediments.

### III. HYDROLOGY

The hydrologic interpretation is based on geophysical logs in the volcanic and sedimentary sections. Perched water was encountered in the Cenozoic volcanics, the Abo Formation, and the upper limestone member of the Madera Limestone. The zone of saturation occurred in the lower limestone and shale member of the Madera and in the Sandia Formation. Fracture zones in the Precambrian rocks may contain small amounts of water.

#### A. Cenozoic Volcanics

Geophysical logs indicated a 40-ft (12.2 m) saturated section of the Abiquiu Tuff from a depth of 410 to 450 ft (125.0 to 137.1 m). The Bandelier Tuff and the Paliza Canyon Formations, which lie above the Abiquiu Tuff, did not contain perched water. Water in the Abiquiu is perched on the underlying shale, siltstone, and fine-grained sandstone of the Abo Formation.

The Abiquiu Tuff is a loosely consolidated, friable tuffaceous sandstone. The caliper log through the Abiquiu section indicated an enlarged hole with considerable washout of the friable material. The electric log indicated porosity filled with fresh water. Water in the volcanics moves downslope filling the low areas, while some of the high areas of the Abo may be above the water table.

Generalized contours on top of the Abo, in the area of the Fenton Hill Site, indicate that the surface of the formation dips to the west-southwest at about 80 ft/mi (15 m/km) (Fig. 2). Thus, the water in the volcanics perched on the Abo will move in that direction. The spring-seeps in Lake Fork and Virgin Canyons discharge from the volcanics overlying the Abo. This discharge forms perennial streams that flow into the Rio Cebolla and Rio Guadalupe. The spring at elevation 8120 ft (2475 m) is perched in

the volcanics. Test hole D contains water in the volcanics which rises to a depth of ~30 ft (9.1 m) below land surface (Fig. 2). The hole was cased to 100 ft (30.5 m) leaving about 20 ft (6.1 m) of the hole open in the volcanic section above the Abo.

The groundwater divide in the volcanics between the Fenton Hill Site and the valley cut by San Antonio Creek occurs along a north-south trending fault (Fig. 2). The spring at the base of the volcanics on the downthrown side at elevation 7950 ft (2423 m), Horseshoe Springs, discharges from the base of the volcanics.

The groundwater divide in the volcanics to the south and southeast of the Fenton Hill Site occurs along the Virgin Canyon Fault. Here, the base of the volcanics is 300 to 500 ft (91.4 to 152.4 m) below the basal contact at the site. Springs at elevations 7300 ft (2225 m) and 7460 ft (2274 m) discharge from the base of the volcanics while the spring at 7560 ft (2304 m) discharges from a perched zone in the volcanics.

The springs at elevations 7300 ft (2225 m) and 7460 ft (2274 m) are used for water supply at Jemez Springs. The quality of water in the volcanics is good, dissolved solids concentration is less than 500 mg/l.

#### B. Abo Formation

Geophysical logs indicated several perched zones of water in the Abo Formation. The water is in fine-grained sandstones which are underlain by shales. The permeability of the fine-grained sandstones is low, probably less than 10 gpd/ft<sup>2</sup> (0.41 m/d). The saturated intervals are 30 ft (9 m) or less in thickness and would yield very little water to a well. The electric logs indicate that the saturated intervals occur at depths of 780 to 800 ft (237.7 to 243.8 m); 970 to 995 ft (295.7 to 303.3 m); 1005 to 1015 ft (306.3 to 309.4 m), and 1100 to 1120 ft (335.3 to 341.4 m) below land surface at GT-2.

The total dissolved-solids concentration of the water in the Abo may range

from 300 to 1000 mg/l, based on data collected on quality of water in the area.

#### C. Magdalena Group

The Magdalena Group contains several perched water zones in the Upper Madera Limestone, while the Lower Madera, the shale member, and the Sandia Formation are in the zone of saturation above the Precambrian granitic rocks.

1. Madera Limestone. Geophysical logs indicate six perched zones in the upper limestone member above the main zone of saturation overlying the granitic rocks. No hydrologic characteristics of the water in these zones were determined, as the hole was drilled using mud as the cuttings carrier. The electric logs indicate that the perched zones occur at depths of 1245 to 1260 ft (379.5 to 384.0 m), 1290 to 1295 ft (393.2 to 394.7 m), 1320 to 1345 ft (402.3 to 410.0 m), 1595 to 1620 ft (486.2 to 493.8 m), 1715 to 1745 ft (522.7 to 531.9 m), and 1780 to 1790 ft (542.5 to 545.6 m) below land surface. The lithologic logs show that these water zones are in limestone that is probably underlain by shales or clays. The perched zones are of limited extent and comprise thicknesses of less than 25 ft (7.6 m).

When drilled to a depth of 1905 ft (580.6 m) the hole was cased to a depth of 1590 ft (484.6 m) below land surface. The three water-bearing zones above 1590 ft (484.6 m) were sealed off when the casing was cemented by pumping cement through a packer set near the casing shoe.

The dense limestone of the lower limestone member was encountered at a depth of 1840 ft (560.8 m). At a depth of 1905 ft (580.6 m) the carrier fluid was lost and circulation of fluid could not be regained to drill to the granitic basement until a number of cement plugs were placed.

The zone of saturation above the granitic rocks is in the lower limestone and shale members of the Madera and Sandia Formation. The water level after the casing was set at 1590 ft (484.6 m) was about

1750 ft (533.4 m). This probably reflects the artesian head in the zone of saturation which was encountered in the lower limestone member at a depth of 1840 ft (560.8 m). The slight variation of water levels at 1750 ft (533.4 m), measured after the casing was set at 1590 ft (484.6 m), indicated that water in the limestone is under artesian head.

The water in the zone of saturation is moving to the southeast on top of the Precambrian granitic rocks (Fig. 3). The small displacement of the Virgin Canyon Fault has little effect on the movement of water; however, the Jemez Fault that lies to the east of the Jemez River and intersects the river at Soda Dam forms a discharge boundary for water in the zone of saturation. The fault is downthrown to the east and down-drops the relatively impermeable sediments of the Abo Formation against the permeable rocks in the zone of saturation to the west. The discharge of water from the zone of saturation occurs along the Jemez River from the confluence of San Antonio Creek and the East Fork of the Jemez to Soda Dam. The major part of the discharge occurs at Soda Dam. The discharge along the Jemez Fault from the zone of saturation (Lower Madera Limestone and Sandia Formation) is  $\approx 5$  cfs (142 l/sec) based on records from U. S. Geological Survey gaging stations on the Jemez River.

Fluid loss in the lower limestone member indicated a field coefficient of permeability of about 1000 gpd/ft<sup>2</sup> (4.1 m/d), and an estimated transmissibility of about 115 000 gpd/ft (1426 m<sup>2</sup>/d) of the 115 ft (35.1 m) section of dense limestone. The permeability is due to open fractures or joints.

The velocity of water in the lower limestone aquifer can be estimated using the field coefficient of permeability, the hydrologic gradient of the aquifer, and the porosity by means of a method described by Wenzel.<sup>12</sup>

$$V = \frac{PI}{p}$$

where V = velocity in ft per day  
P = field permeability, gpd/ft<sup>2</sup>  
I = hydrologic gradient, ft per ft  
p = porosity of the aquifer, percent.

The hydrologic gradient is about 100 ft/mi (18.9 m/km). The porosity of the limestone (fracture) is estimated to be about 20%. Thus the velocity is computed as follows

$$V = \frac{(1000)(.017)}{(0.20)(7.48)}$$

or

$$V = \sim 11 \text{ ft/d (3.4 m/d) or } 4015 \text{ ft/yr (1224 m/yr).}$$

Using a velocity of 4000 ft/yr (1219 m/yr), it would take about 6 yr for the water in the aquifer at GT-2 to move into the discharge area along the Jemez River.

2. Sandia Formation. The Sandia Formation lies within the zone of saturation above the granitic rocks. Geophysical logs to indicate water-bearing characteristics were not run through the Sandia section, nor were there any hydrologic tests made in the section.

3. Quality of Water. The water in the Madera Limestone is high in total dissolved solids (Table III). Shown in the table is the quality of water from a spring discharging from the Upper Madera, the zone of saturation in the Lower Madera limestone, and the thermal spring at Soda Dam (zone of saturation). As the water moves down-gradient to the discharge area, it becomes highly mineralized. Temperatures in the zone of saturation are high. The aquifer would be classified as thermal.

#### D. Precambrian Rocks

The test hole had been drilled with air (or air and soap) to a depth of 3510 ft (1069.8 m) when the cement broke loose from casing set into the granite. This allowed water from the sediments to enter the hole.

Fracture zones in the granitic rock above 3510 ft (1069.8 m) also yielded some water. Drilling was continued with air and/or air and water to about 4020 ft (1225.3 m); the remainder of the hole was drilled using water with added drilling mud.

**1. Fracture Zones.** Geophysical logs (nuclear, 3-D velocity, density, electric, and caliper) were used to identify fracture zones (Table IV). Drilling mud and lost-circulation material was added to the circulation fluids at a depth of 4020 ft (1225.3 m). Fluid loss prior to addition of mud and lost-circulation material was ~10 gpm (0.6 l/sec). After the mud program was introduced, the losses decreased ~1-2 gpm (0.06 l/sec). Temperature anomalies indicate nine zones were taking drilling fluids on July 13 (Table IV). These were at depths of 3185 ft (970.8 m); 3214 ft (979.6 m); 3410 ft (1039.4 m); 3550 ft (1082.0 m); 3574 ft (1089.4 m); 3590 ft (1094.2 m); 4198 ft (1279.6 m); 4352 ft (1326.5 m); and 4458 ft (1358.8 m). The other zones were plugged with drilling mud or cement; however, a reduction of fluid head in the hole will probably result in re-opening the fracture and allow fluid entrance into the hole.

The coefficient of transmissibility in the granite section of the hole was estimated by the Slug-Injection Test in a method described by Ferris and Knowles.<sup>13</sup> The method utilizes fluid decline with time. The initial test was made at a depth of 4010 ft (1222.2 m) when water was being used as a cuttings carrier. The remainder of the tests were made after drilling mud was added to the fluid carrier. Except during the first test when declines were measured with a sounder, the remainder of the measurements were taken with a transducer which was attached to the bottom hole temperature sonde. The results of the test are shown in the following table.

Zone Tested (ft)		Estimated Coefficient of Transmissibility
From*	To	
2520 (768.1 m)	4010 (1222.2 m)	4.4 gpd/ft (.055 m <sup>2</sup> /d)
2520 (768.1 m)	4545 (1385.3 m)	2.6 gpd/ft **(.032 m <sup>2</sup> /d)
2520 (768.1 m)	5210 (1588.0 m)	2.2 gpd/ft (.027 m <sup>2</sup> /d)
2520 (768.1 m)	5470 (1667.3 m)	2.5 gpd/ft (.031 m <sup>2</sup> /d)
2520 (768.1 m)	5980 (1822.7 m)	3.7 gpd/ft (.046 m <sup>2</sup> /d)

\* Bottom of casing set in granite.

\*\*Average of two slopes in curve; 4.2 gpd/ft decreased to 1.1 gpd/ft after 5 hours of decline.

In general an increase in thickness of interval tested did not change the transmissibility significantly. The drilling mud decreased the permeability of the fracture zones as the drilling of the hole progressed. The transmissibilities are very low, indicating a very low permeability in the granitic rocks.

**2. Bulk Permeability.** The lower section of the hole contains schists and quartz monzonites which were intruded by a small mass of granitic rocks. Geophysical logs indicated two permeable sections from depths of 5600 to 5690 ft (1706.9 to 1734.3 m) and from 6000 to 6050 ft (1828.8 to 1844.0 m). These zones may contain some water or the anomalies may instead indicate the invasion of drilling fluids into these slightly permeable schists and monzonites. Temperature anomalies obtained through these sections on July 13 showed that the rocks were taking drilling fluids.

**3. Quality of Water.** Several samples of water were collected from the granitic section. However, there may have been either some contamination with drilling fluids or some change in concentration of solids by evaporation as the fractures were releasing small amounts of water into the hole while drilling was being done with air. Partial analyses are shown in Table V, with two analyses of drilling fluid for comparison. In general, the mineral concentrations decreased with depth although they still are considered quite high.

REFERENCES

1. B. C. Renick, "Geology and Ground-Water Resources of Western Sandoval County, New Mexico," U. S. Geol. Survey Water-Supply Paper 620 (1931).
2. G. H. Woods, Jr. and S. A. Northrop, "Geology of the Nacimiento Mountains, San Pedro Mountains, and Adjacent Plateaus in Parts of Sandoval and Rio Arriba Counties, New Mexico," U. S. Geol. Survey Oil and Gas Inv. Prelim. Map 57 (1946).
3. R. L. Smith, R. A. Bailey, and C. S. Ross, "Structural Evolution of the Valles Caldera, New Mexico, and Its Bearing on Emplacement of Ring Dikes," U. S. Geol. Prof. Paper 424-D (1961).
4. C. S. Ross, R. L. Smith, and R. A. Bailey, "Outline of Geology of the Jemez Mountains, New Mexico," New Mex. Geol. Soc. Twelfth Field Conf., Albuquerque Country (1961).
5. R. A. Bailey, R. L. Smith, and C. S. Ross, "Stratigraphic Nomenclature of the Volcanic Rocks in the Jemez Mountains, New Mexico," U. S. Geol. Survey Bull. 1274-P (1969).
6. W. D. Purtymun, "Geology of the Jemez Plateau West of the Valles Caldera," Los Alamos Scientific Laboratory report LA-5124-MS (1973).
7. F. G. West, "Regional Geology and Geophysics of the Jemez Mountains," Los Alamos Scientific Laboratory report LA-5362-MS (1973).
8. W. D. Purtymun, F. G. West, and W. H. Adams, "Preliminary Study of the Quality of Water in the Drainage Area of the Jemez River and Rio Guadalupe," Los Alamos Scientific Laboratory report LA-5595-MS (1974).
9. P. C. Perkins, "Petrology of Some Rock Types of the Precambrian Basement Near the Los Alamos Scientific Laboratory Geothermal Test Site, Jemez Mountains, New Mexico," Los Alamos Scientific Laboratory report LA-5129 (1973).
10. J. P. Fitzsimmons, "Precambrian Rocks of the Albuquerque Country," New Mex. Geol. Soc. Twelfth Field Conf., Albuquerque Country (1961).
11. R. L. Smith, R. A. Bailey, and C. S. Ross, "Geologic Map of the Jemez Mountains, New Mexico," U. S. Geol. Survey Misc. Geol. Inv. Map I-571 (1970).
12. L. K. Wenzel, "Methods for Determining Permeability of Water Bearing Materials," U. S. Geol. Survey Water-Supply Paper 887 (1942).
13. J. G. Ferris and D. B. Knowles, "The Slug-Injection Test for Estimating the Coefficient of Transmissibility of an Aquifer," in "Methods of Determining Permeability, Transmissibility and Drawdown," U. S. Geol. Survey Water-Supply Paper 1536-I (1963).

TABLE I  
FIELD GEOLOGIC LOG OF TEST HOLE GT-2  
ELEVATION OF LAND SURFACE 8690 FT (2648.7 m)

	<u>Thickness</u> (ft)	<u>Depth</u> (ft)
<u>Bandelier Tuff</u> Tuff, dark gray, moderately welded to welded, rhyolitic crystal and crystal fragments of quartz and sanidine, lithic fragments of pumice, rhyolite, and latite in ash matrix. Pumice, light gray with lithic fragments of light to dark gray rhyolite. Moderately welded tuff 0 to 110 ft; pumice 110 to 250 ft; welded tuff 250 to 295 ft; moderately welded tuff 295 to 325 ft; welded tuff 325 to 350 ft.	350 (106.7 m)	350 (106.7 m)
<u>Paliza Canyon Formation</u> Andesites and basaltic andesite breccia, dark gray, with interbedded sands and gravels.	50 ( 15.2 m)	400 (121.9 m)
<u>Abiquiu Tuff</u> Sandstone, light gray tuffaceous, friable, with angular basalt in upper part of section, crystal fragments of quartz, sanidine, and chalcedony; lithic fragments of rhyolite and quartzite in tuffaceous sand matrix.	50 ( 15.2 m)	450 (137.1 m)
<u>Abo Formation</u> Shale, siltstone, and fine-grained sandstone, brownish-red to dark red, with lenses of white to gray shale; clay lenses, dark red, with thin limestone lenses, gray, near base. Shale, dark red with thin lenses of white to gray shale and clay, 450 to 495 ft; siltstone and fine-grained sandstone, brownish-red, arkosic, 495 to 600 ft; shale, dark red, alternating with lenses of silty sandstone and siltstone and thin lenses of white to gray shale, 600 to 775 ft; sandstone, dark red, fine-grained, 775 to 800 ft; shale, dark red, alternating with lenses of silty sandstone and siltstone, 800 to 965 ft; sandstone, dark red, fine-grained, 965 to 1005 ft; shale, brownish-red, alternating with fine-grained silty sandstone, and thin lenses of limestone, gray, 1005 to 1095 ft; sandstone, red, fine-grained with lenses of thin limestone, gray, 1095 to 1130 ft; shale, red with lenses of fine-grained sandstone, thin lenses of white to gray shale and limestone, gray, 1130 to 1230 ft.	780 (237.7 m)	1230 (374.9 m)
<u>Magdalena Group</u> Upper limestone member consists of limestone, alternating with shale, fine-grained sandstone, and clay. Limestone, gray, alternating with thin lenses of sandstone, reddish-brown, fine-grained, and shale, red, 1230 to 1360 ft; clay, gray with thin lenses of limestone, gray, dense, 1360 to 1390 ft; limestone, gray, dense, arkosic, and shale, reddish-brown, with thin lenses of sandstone, reddish-brown, fine-grained, 1390 to 1580 ft; limestone, gray, dense, arkosic, 1580 to 1625 ft; clay, gray, with thin lenses of limestone, gray, dense, 1625 to 1650 ft; limestone, gray, dense with thin lenses of sandstone, reddish-brown, fine-grained, 1650 to 1700 ft;		

TABLE I (Continued)

	<u>Thickness</u> (ft)	<u>Depth</u> (ft)
<u>Magdalena Group (continued)</u>		
limestone, gray, dense, alternating with shale, dark red, sandstone, fine-grained, brown-red, and clay, dark gray, 1700 to 1840 ft.	610 (185.9 m)	1840 (560.8 m)
Lower limestone member consists of limestone, dark gray, dense, with thin lenses of shale, dark gray, and sandstone, white to gray, fine-grained.	115 ( 35.1 m)	1955 (595.9 m)
Shale member, (not previously described in area) shale, dark gray with thin lenses of limestone, gray, dense, siliceous, and siltstone, reddish-brown and clay, dark gray.	180 ( 54.9 m)	2135 (650.8 m)
<u>Sandia Formation</u>		
Upper clastic member consists of limestone, gray with sandstone, reddish-brown, fine- to coarse-grained, with shales, brown, and clays brown to greenish gray.	205 ( 62.5 m)	2340 (713.2 m)
Lower limestone member consists of limestone, light gray, siliceous, dense, with a few thin lenses of sandstone, fine- to coarse-grained, and siltstone, light gray.	55 ( 16.8 m)	2395 (730.0 m)
<u>Precambrian Rocks</u>		
Granites, granodiorites, monzonites, quartz monzonites, gneiss, schist and amphibolites with dikes of biotite-hornblende-pagioclase. Granite, light pinkish-red, 2395 to 2540 ft; granodiorite, light gray, 2540 to 2600 ft; granite, light pink coarse-grained, 2600 to 2615 ft; granodiorite, light pink, 2715 to 2730 ft; granodiorite, light gray, 2730 to 2745 ft; granite, pink, coarsed-grained, 2745 to 2765 ft; granodiorite, gray, 2765 to 2805 ft; granite, pink, coarse-grained, 2805 to 2930 ft; granodiorite, gray, 2930 to 2990 ft; monzonite, light gray, 2990 to 3030 ft; granodiorite, gray (dike ~3120 to 3123 ft), 3030 to 3175 ft; granite, pink, coarse-grained, 3175 to 3195 ft; granodiorite, gray, 3195 to 3260 ft; granite, pink, coarse-grained (dike ~3260 to 3265 ft), 3260 to 3340 ft; granodiorite, light gray, 3340 to 3375 ft; granite, pink (dike ~3495 to 3500 ft), 3375 to 3520 ft; granite, light pink, coarse-grained, alternating with granite, gray, fine-grained, 3520 to 3695 ft; granite, light gray, fine-grained, 3695 to 3755 ft; granite, light pink to light gray, 3755 to 3855 ft; granite, light gray with intervals of granite, pink, coarse-grained, 3855 to 3915 ft; granite, light pinkish-gray, 3915 to 3980 ft; granite, gray, 3980 to 4010 ft; granite, pink, coarse-grained, 4010 to 4030 ft; granite, light pinkish-gray, 4030 to 4210 ft; granite, light pink to light gray, coarse-grained [altered (weathered?) 4285 to 4290 ft]; 4210 to 4290 ft; granite, dark gray (thin dikes in interval), 4290 to 4350 ft; granite, gray, 4350 to 4480 ft; granite, light pinkish-gray, 4480 to 4610 ft; granite, light gray, 4610 to 4685 ft; granite, light pink, 4685 to 4750 ft; granite,		

TABLE I (Continued)

	<u>Thickness</u> (ft)	<u>Depth</u> (ft)
<u>Precambrian Rocks (continued)</u>		
light gray, 4750 to 4965 ft; granite, pink, coarse-grained, 4965 to 5000 ft; granite, light pinkish-gray, 5000 to 5095 ft; granite, gray, 5095 to 5165 ft; granite, light pinkish-gray, 5165 to 5240 ft; granite, light pink, coarse-grained, 5240 to 5265 ft; granite, dark gray, fine-grained, 5265 to 5275 ft; granite, pink, 5275 to 5335 ft; granite, dark gray, fine-grained, 5335 to 5345 ft; granite, light pink, 5345 to 5400 ft; granite, brownish-gray, coarse-grained, 5400 to 5410 ft; granite, light pink, 5410 to 5430 ft; granite, light pinkish-gray, 5430 to 5480 ft; granite, light pink, 5480 to 5520 ft; granite, light gray, 5520 to 5530 ft; granite, pink, coarse-grained, 5530 to 5545 ft; schist, biotite, hornblende, dark gray, 5545 to 5580 ft; granite, light pink, coarse-grained, 5580 to 5590 ft; schist, biotite, hornblende, dark gray, 5590 to 5605 ft; granite, light pink, coarse-grained, 5605 to 5615 ft; schist, biotite, hornblende, dark gray, 5615 to 5680 ft; amphibolite, olive gray, 5680 to 5705 ft; granite, light gray, 5705 to 5770 ft; granite, light pink, 5770 to 5800 ft; schist, biotite, hornblende, dark gray, 5800 to 5815 ft; granite, pink, coarse-grained, 5815 to 5825 ft; granite, light gray, 5825 to 5845 ft; dike, biotite, hornblende, plagioclase-orthoclase, 5845 to 5850 ft; granite, light gray, 5850 to 5875 ft; granite, gray, 5875 to 5895 ft; granite, pink, coarse-grained, 5895 to 5910 ft; schist, biotite, hornblende, gray, 5910 to 5950 ft; granite, pink, coarse-grained, 5950 to 5960 ft; gneiss, gray, alternating with schist, dark gray, 5960 to 5990 ft; quartz monzonite, light pinkish-gray, altered, 5990 to 6050 ft; quartz monzonite, pink, 6050 to 6145 ft; schist, biotite, hornblende, gray, 6145 to 6170 ft; granite, light pinkish-gray, 6170 to 6220 ft; granite, light pink, 6220 to 6245 ft; gneiss, gray, 6245 to 6255 ft; granite, light pink, 6255 to 6346 ft.	3951 (1204.3 m)	6346 (1934.3)

TABLE II  
THICKNESS OF GEOLOGIC FORMATION

Geologic Formation	Section Thickness in Ft				
	GT-1	GT-2	Above Soda Dam	Guadalupe Box	Seven Mi (11.2 km) West of GT-2
Abo Formation	910 (277.4 m)	780 (237.7 m)	300 ( 91.4 m)	590 (179.8 m)	700 (213.4 m)
Madera Limestone					
Upper Ls. Mbr.	590 (179.8 m)	610 (185.9 m)	450 (137.2 m)	610 (185.9 m)	340 (103.6 m)
Lower Ls. Mbr.	155 ( 47.2 m)	115 ( 35.1 m)	200 ( 61.0 m)	120 ( 36.6 m)	--
Shale Mbr.	--	180 ( 54.9 m)	--	--	--
Sandia Formation					
Upper Clastic Mbr.	235 ( 71.6 m)	205 ( 62.5 m)	210 ( 64.0 m)	200 ( 61.0 m)	--
Lower Ls. Mbr.	55 ( 16.8 m)	55 ( 16.8 m)	30 ( 9.1 m)	30 ( 9.1 m)	--

TABLE III  
CHEMICAL QUALITY OF WATER

	JF-1	GT-2	Soda Dam
Analysis	3-29-74	3-18-74	3-29-74
Silica (mg/l)	40	115	42
Calcium (mg/l)	115	78	320
Magnesium (mg/l)	10	42	16
Sodium (mg/l)	210	550	850
Carbonate (mg/l)	0	0	0
Bicarbonate (mg/l)	464	1230	1200
Sulfate (mg/l)	30	200	38
Chloride (mg/l)	290	400	1480
Fluoride (mg/l)	2.6	3.1	3.3
Nitrate (mg/l)	0	0	0
Hardness (mg/l)	330	370	860
Total Dissolved Solids (mg/l)	1100	2500	4000
Conductance (µmhos)	1700	2920	5900
pH	6.9	7.4	6.6
Temperature (°C)	16	56	46

JF-1 - Spring Upper Madera Limestone, Jemez River

GT-2 - Lower Madera Limestone

Soda Dam - Thermal Spring on Jemez Fault (Zone of Saturation)

TABLE IV  
 FRACTURE ZONES CONTAINING FLUIDS  
 (POTENTIAL AQUIFERS)

<u>Internal (ft)</u>		<u>Thickness (ft)</u>	<u>Temp. Anomalies</u>		
<u>From</u>	<u>To</u>		<u>6-25</u>	<u>7-8</u>	<u>7-13</u>
2710 ( 826.0 m)	2718 ( 828.4 m)	8 (2.4 m)			
2930 ( 893.1 m)	2948 ( 898.6 m)	18 (5.5 m)			
2980 ( 908.3 m)	3008 ( 916.8 m)	28 (8.5 m)			<u>1/</u>
3012 ( 918.1 m)	3024 ( 921.7 m)	12 (3.6 m)			<u>1/</u>
3065 ( 934.2 m)	3070 ( 935.7 m)	5 (1.5 m)			
3082 ( 939.4 m)	3092 ( 942.4 m)	10 (3.0 m)			
3105 ( 946.4 m)	3113 ( 948.8 m)	8 (2.4 m)			
3185 ( 970.8 m)	3198 ( 974.8 m)	13 (4.0 m)	<u>1/</u>	<u>1/</u>	<u>1/</u>
3214 ( 979.6 m)	3232 ( 985.1 m)	18 (5.5 m)	<u>1/</u>	<u>1/</u>	<u>1/</u>
3410 (1039.4 m)	3424 (1043.6 m)	14 (4.2 m)			<u>1/</u>
3550 (1082.0 m)	3560 (1085.0 m)	10 (3.0 m)	<u>1/</u>	<u>1/</u>	<u>1/</u>
3574 (1089.4 m)	3580 (1091.2 m)	6 (1.8 m)	<u>1/</u>	<u>1/</u>	<u>1/</u>
3590 (1094.2 m)	3600 (1097.2 m)	10 (3.0 m)	<u>1/</u>	<u>1/</u>	<u>1/</u>
3645 (1111.0 m)	3658 (1114.0 m)	13 (4.0 m)	<u>1/</u>		
3732 (1137.5 m)	3738 (1139.3 m)	6 (1.8 m)	<u>1/</u>		
3848 (1172.9 m)	3858 (1175.9 m)	10 (3.0 m)	<u>1/</u>		
4008 (1221.6 m)	4012 (1222.8 m)	4 (1.2 m)			
4198 (1279.6 m)	4220 (1286.3 m)	22 (6.7 m)	<u>1/</u>	<u>1/</u>	<u>1/</u>
4352 (1326.5 m)	4384 (1336.2 m)	32 (9.7 m)	<u>1/</u>	<u>1/</u>	<u>1/</u>
4458 (1358.8 m)	4470 (1362.4 m)	12 (3.6 m)	<u>1/</u>	<u>1/</u>	<u>1/</u>
4510 (1374.6 m)	4540 (1383.8 m)	30 (9.2 m)			
4940 (1505.7 m)	4960 (1511.8 m)	20 (6.1 m)	<u>1/</u>	<u>1/</u>	
5340 (1627.6 m)	5352 (1631.2 m)	12 (3.6 m)	<u>1/</u>	<u>1/</u>	
5548 (1691.0 m)	5562 (1695.2 m)	14 (4.2 m)			<u>2/</u>
5664 (1726.4 m)	5676 (1730.0 m)	12 (3.6 m)			
5846 (1781.9 m)	5852 (1783.7 m)	6 (1.8 m)			
5885 (1793.8 m)	5895 (1796.8 m)	10 (3.0 m)			<u>2/</u>
5986 (1824.5 m)	6014 (1833.0 m)	28 (8.5 m)			<u>2/</u>
6025 (1836.4 m)	6030 (1837.9 m)	5 (1.5 m)			<u>2/</u>
6042 (1841.6 m)	6048 (1843.4 m)	6 (1.8 m)			<u>2/</u>
6062 (1847.7 m)	6068 (1849.5 m)	6 (1.8 m)			
6084 (1854.4 m)	6088 (1855.6 m)	4 (1.2 m)			

1/ Temperature anomalies indicate cooling as drilling fluid moves into the fractures. LASL temperature log 6-25-74 run to a depth of 5484 ft (1671.5 m); LASL temperature log 7-8-74 run to a depth of 6118 ft (1864.8 m); Birdwell temperature log run to a depth of 6344 ft (1933.6 m).

2/ Temperature anomalies ~5500 to 5650 ft (~1674 to 1722 m) and ~6000 to 6050 ft (~1829 to 1844 m) due to change in rock type and invasion of drilling fluids.

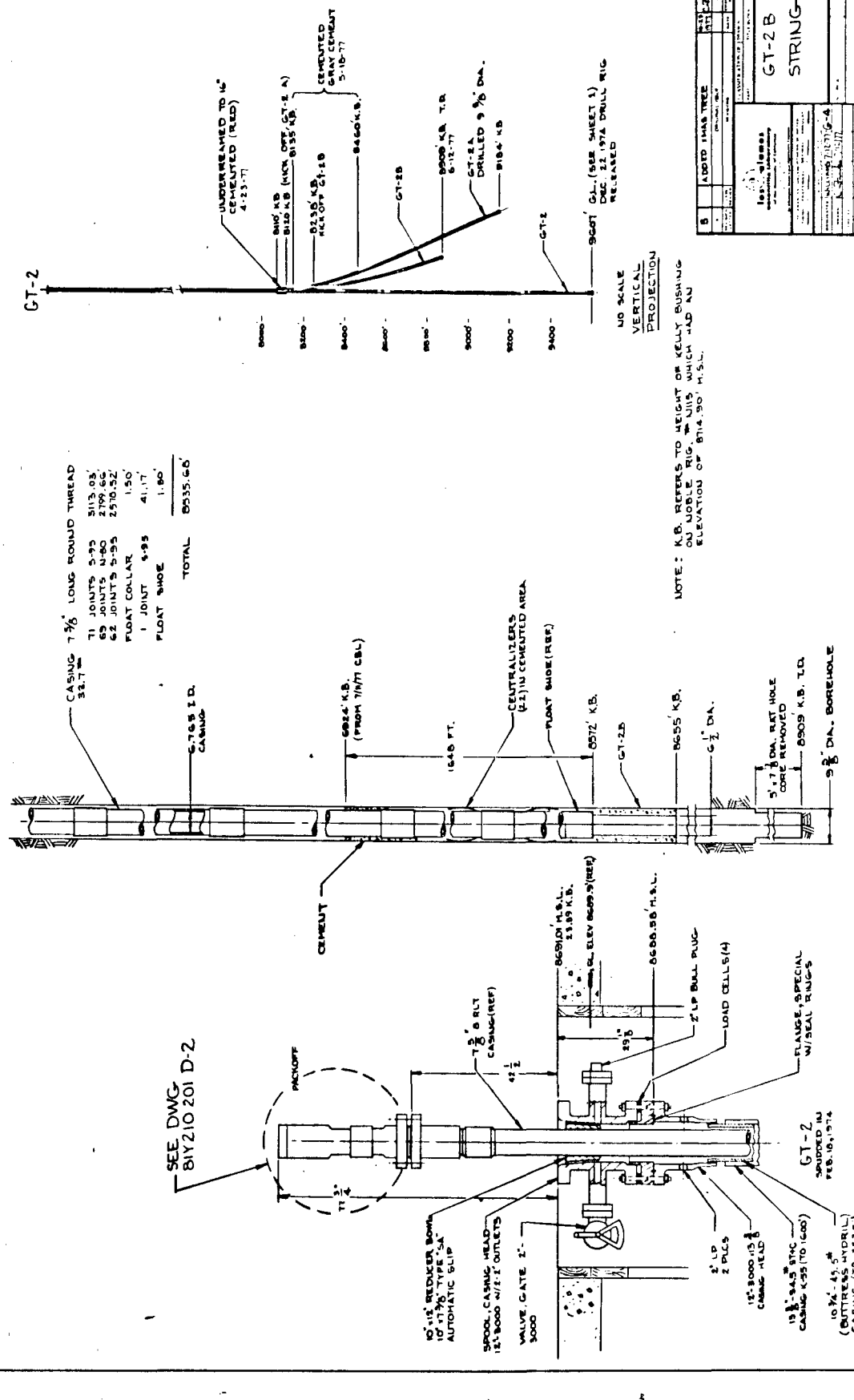
TABLE V  
QUALITY OF WATER

<u>Date</u>	<u>Depth (ft)</u>	<u>Conductance (<math>\mu</math>mhos)</u>	<u>Dissolved Solids (mg/l)</u>	<u>Chloride (mg/l)</u>
4-16	<u>1/</u>	5080	4230	1200
4-23	2800 (853.4 m)	21900	--	3400
4-27	<u>1/</u>	6400	--	--
5-3	2400 (731.5 m)	18800	14900	2750
5-14	3200 (975.4 m)	12800	8800	3800

1/Drilling Fluid

APPENDIX D

As completed well and pipe string sections



CASING 7 7/8" LONG ROUND THREAD  
32.7' W

71 JOINTS 5-75	5113.03'
69 JOINTS 4-80	2799.66'
62 JOINTS 5-55	2570.52'
FLOAT COLLAR	1.50'
1 JOINT 5-95	41.17'
FLOAT SHOE	1.80'
<b>TOTAL</b>	<b>8535.60'</b>

SEE DWG  
81Y210 201 D-2

NO SCALE  
VERTICAL  
PROJECTION

NOTE: K.B. REFERS TO HEIGHT OF KELLY BUSHING  
ON MOBILE RIG. THE J115 WHICH HAD AN  
ELEVATION OF 8714.90' H.S.L.

NO.	REV.	DATE	BY	CHK.
1				
2				
3				
4				
5				
6				
7				
8				
9				
10				

APPROVED: [Signature]

DATE: [Date]

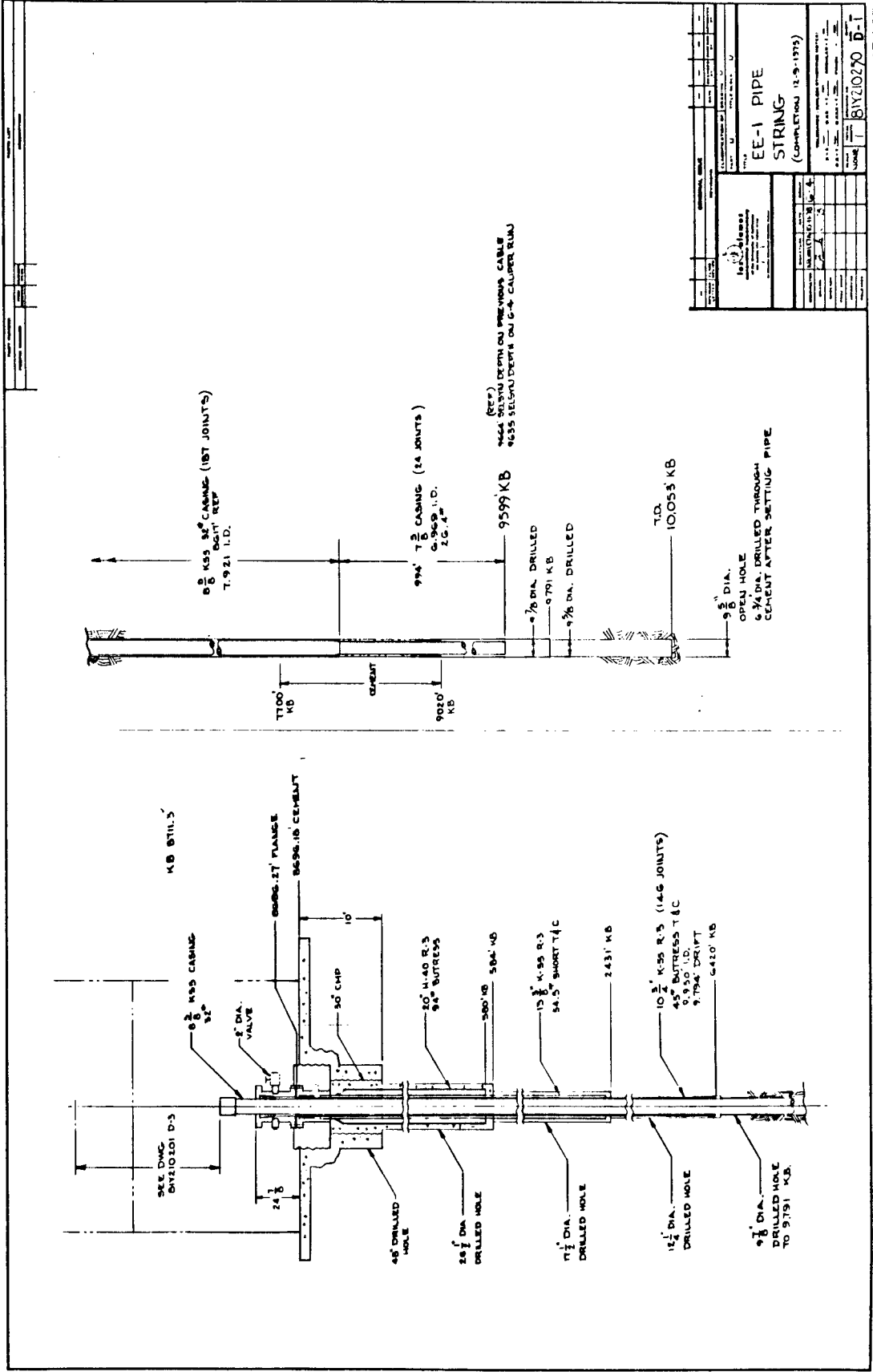
PROJECT: [Project Name]

SCALE: [Scale]

81Y210 201 D-2

GT-2 B  
STRING

81Y210 201 D-2



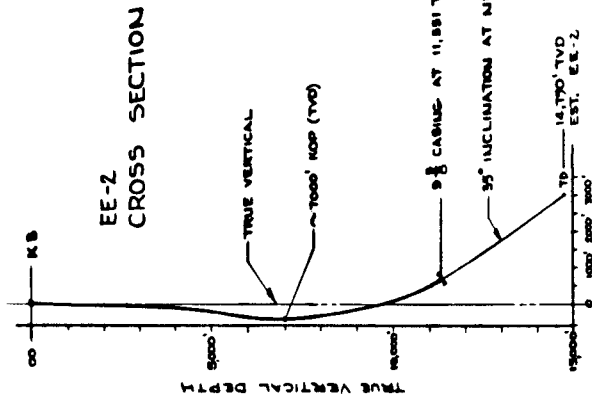
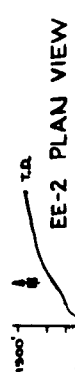
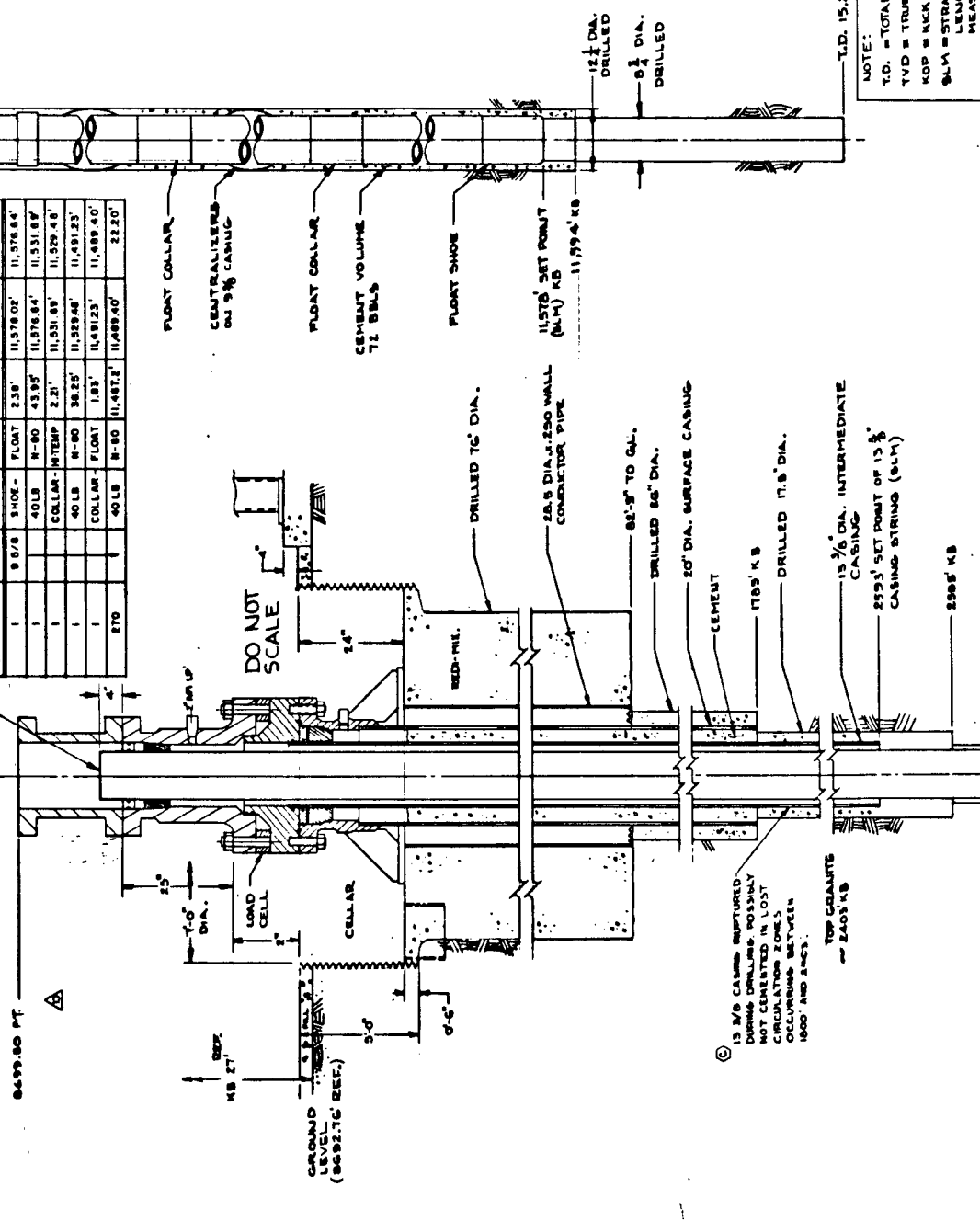
DATE	11-9-1977
BY	81Y20270
CHECKED	
APPROVED	
SCALE	
PROJECT	
WELL NO.	
SECTION	
DATE	
BY	
CHECKED	
APPROVED	
SCALE	
PROJECT	
WELL NO.	
SECTION	
DATE	
BY	
CHECKED	
APPROVED	
SCALE	
PROJECT	
WELL NO.	
SECTION	
DATE	
BY	
CHECKED	
APPROVED	
SCALE	
PROJECT	
WELL NO.	
SECTION	
DATE	
BY	
CHECKED	
APPROVED	
SCALE	
PROJECT	
WELL NO.	
SECTION	
DATE	
BY	
CHECKED	
APPROVED	
SCALE	
PROJECT	
WELL NO.	
SECTION	
DATE	
BY	
CHECKED	
APPROVED	
SCALE	
PROJECT	
WELL NO.	
SECTION	
DATE	
BY	
CHECKED	
APPROVED	
SCALE	
PROJECT	
WELL NO.	
SECTION	
DATE	
BY	
CHECKED	
APPROVED	
SCALE	
PROJECT	
WELL NO.	
SECTION	
DATE	
BY	
CHECKED	
APPROVED	
SCALE	
PROJECT	
WELL NO.	
SECTION	
DATE	
BY	
CHECKED	
APPROVED	
SCALE	
PROJECT	
WELL NO.	
SECTION	
DATE	
BY	
CHECKED	
APPROVED	
SCALE	
PROJECT	
WELL NO.	
SECTION	
DATE	
BY	
CHECKED	
APPROVED	
SCALE	
PROJECT	
WELL NO.	
SECTION	
DATE	
BY	
CHECKED	
APPROVED	
SCALE	
PROJECT	
WELL NO.	
SECTION	
DATE	
BY	
CHECKED	
APPROVED	
SCALE	
PROJECT	
WELL NO.	
SECTION	
DATE	
BY	
CHECKED	
APPROVED	
SCALE	
PROJECT	
WELL NO.	
SECTION	
DATE	
BY	
CHECKED	
APPROVED	
SCALE	
PROJECT	
WELL NO.	
SECTION	
DATE	
BY	
CHECKED	
APPROVED	
SCALE	
PROJECT	
WELL NO.	
SECTION	
DATE	
BY	
CHECKED	
APPROVED	
SCALE	
PROJECT	
WELL NO.	
SECTION	
DATE	
BY	
CHECKED	
APPROVED	
SCALE	
PROJECT	
WELL NO.	
SECTION	
DATE	
BY	
CHECKED	
APPROVED	
SCALE	
PROJECT	
WELL NO.	
SECTION	
DATE	
BY	
CHECKED	
APPROVED	
SCALE	
PROJECT	
WELL NO.	
SECTION	
DATE	
BY	
CHECKED	
APPROVED	
SCALE	
PROJECT	
WELL NO.	
SECTION	
DATE	
BY	
CHECKED	
APPROVED	
SCALE	
PROJECT	
WELL NO.	
SECTION	
DATE	
BY	
CHECKED	
APPROVED	
SCALE	
PROJECT	
WELL NO.	
SECTION	
DATE	
BY	
CHECKED	
APPROVED	
SCALE	
PROJECT	
WELL NO.	
SECTION	
DATE	
BY	
CHECKED	
APPROVED	
SCALE	
PROJECT	
WELL NO.	
SECTION	
DATE	
BY	
CHECKED	
APPROVED	
SCALE	
PROJECT	
WELL NO.	
SECTION	
DATE	
BY	
CHECKED	
APPROVED	
SCALE	
PROJECT	
WELL NO.	
SECTION	
DATE	
BY	
CHECKED	
APPROVED	
SCALE	
PROJECT	
WELL NO.	
SECTION	
DATE	
BY	
CHECKED	
APPROVED	
SCALE	
PROJECT	
WELL NO.	
SECTION	
DATE	
BY	
CHECKED	
APPROVED	
SCALE	
PROJECT	
WELL NO.	
SECTION	
DATE	
BY	
CHECKED	
APPROVED	
SCALE	
PROJECT	
WELL NO.	
SECTION	
DATE	
BY	
CHECKED	
APPROVED	
SCALE	
PROJECT	
WELL NO.	
SECTION	
DATE	
BY	
CHECKED	
APPROVED	
SCALE	
PROJECT	
WELL NO.	
SECTION	
DATE	
BY	
CHECKED	
APPROVED	
SCALE	
PROJECT	
WELL NO.	
SECTION	
DATE	
BY	
CHECKED	
APPROVED	
SCALE	
PROJECT	
WELL NO.	
SECTION	
DATE	
BY	
CHECKED	
APPROVED	
SCALE	
PROJECT	
WELL NO.	
SECTION	
DATE	
BY	
CHECKED	
APPROVED	
SCALE	
PROJECT	
WELL NO.	
SECTION	
DATE	
BY	
CHECKED	
APPROVED	
SCALE	
PROJECT	
WELL NO.	
SECTION	
DATE	
BY	
CHECKED	
APPROVED	
SCALE	
PROJECT	
WELL NO.	
SECTION	
DATE	
BY	
CHECKED	
APPROVED	
SCALE	
PROJECT	
WELL NO.	
SECTION	
DATE	
BY	
CHECKED	
APPROVED	
SCALE	
PROJECT	
WELL NO.	
SECTION	
DATE	
BY	
CHECKED	
APPROVED	
SCALE	
PROJECT	
WELL NO.	
SECTION	
DATE	
BY	
CHECKED	
APPROVED	
SCALE	
PROJECT	
WELL NO.	
SECTION	
DATE	
BY	
CHECKED	
APPROVED	
SCALE	
PROJECT	
WELL NO.	
SECTION	
DATE	
BY	
CHECKED	
APPROVED	
SCALE	
PROJECT	
WELL NO.	
SECTION	
DATE	
BY	
CHECKED	
APPROVED	
SCALE	
PROJECT	
WELL NO.	
SECTION	
DATE	
BY	
CHECKED	
APPROVED	
SCALE	
PROJECT	
WELL NO.	
SECTION	
DATE	
BY	
CHECKED	
APPROVED	
SCALE	
PROJECT	
WELL NO.	
SECTION	
DATE	
BY	
CHECKED	
APPROVED	
SCALE	
PROJECT	
WELL NO.	
SECTION	
DATE	
BY	
CHECKED	
APPROVED	
SCALE	
PROJECT	
WELL NO.	
SECTION	
DATE	
BY	
CHECKED	
APPROVED	
SCALE	
PROJECT	
WELL NO.	
SECTION	
DATE	
BY	
CHECKED	
APPROVED	
SCALE	
PROJECT	
WELL NO.	
SECTION	
DATE	
BY	
CHECKED	
APPROVED	
SCALE	
PROJECT	
WELL NO.	
SECTION	
DATE	
BY	
CHECKED	
APPROVED	
SCALE	
PROJECT	
WELL NO.	
SECTION	
DATE	
BY	
CHECKED	
APPROVED	
SCALE	
PROJECT	
WELL NO.	
SECTION	
DATE	
BY	
CHECKED	
APPROVED	
SCALE	
PROJECT	
WELL NO.	
SECTION	
DATE	
BY	
CHECKED	
APPROVED	
SCALE	
PROJECT	
WELL NO.	
SECTION	
DATE	
BY	
CHECKED	
APPROVED	
SCALE	
PROJECT	
WELL NO.	
SECTION	
DATE	
BY	
CHECKED	
APPROVED	
SCALE	
PROJECT	
WELL NO.	
SECTION	
DATE	
BY	
CHECKED	
APPROVED	
SCALE	
PROJECT	
WELL NO.	
SECTION	
DATE	
BY	
CHECKED	
APPROVED	
SCALE	
PROJECT	
WELL NO.	
SECTION	
DATE	
BY	
CHECKED	
APPROVED	
SCALE	
PROJECT	
WELL NO.	
SECTION	
DATE	
BY	
CHECKED	
APPROVED	
SCALE	
PROJECT	
WELL NO.	
SECTION	
DATE	
BY	
CHECKED	
APPROVED	
SCALE	
PROJECT	
WELL NO.	
SECTION	
DATE	
BY	
CHECKED	
APPROVED	
SCALE	
PROJECT	
WELL NO.	
SECTION	
DATE	
BY	
CHECKED	
APPROVED	
SCALE	
PROJECT	
WELL NO.	
SECTION	
DATE	
BY	
CHECKED	
APPROVED	
SCALE	
PROJECT	
WELL NO.	
SECTION	
DATE	
BY	
CHECKED	
APPROVED	
SCALE	
PROJECT	
WELL NO.	
SECTION	
DATE	
BY	
CHECKED	
APPROVED	
SCALE	
PROJECT	
WELL NO.	
SECTION	
DATE	
BY	
CHECKED	
APPROVED	
SCALE	
PROJECT	
WELL NO.	
SECTION	
DATE	
BY	
CHECKED	
APPROVED	
SCALE	
PROJECT	
WELL NO.	
SECTION	
DATE	
BY	

KB 8119.76 M.S.L. ←

8699.80 PF

PRODUCTION CASING 9 5/8 BUTTRESS THREAD, N80  
 40,395 WALL, 8,935 I.D.

NO. OF JOINTS	SIZE	WEIGHT	GRADE	LENGTH	S.L.M.	KB
1	9 5/8	40 LB	N-80	2.38'	11,578.02'	11,578.84'
1	COLLAR-INTMP	2.31'			11,531.89'	11,529.40'
1	COLLAR-FLOAT	1.83'			11,491.23'	11,489.40'
1	40 LB N-80	38.25'			11,453.00'	11,451.23'
1	40 LB N-80	38.25'			11,414.75'	11,413.00'
1	40 LB N-80	38.25'			11,376.50'	11,374.75'
1	40 LB N-80	38.25'			11,338.25'	11,336.50'
1	40 LB N-80	38.25'			11,300.00'	11,298.25'
1	40 LB N-80	38.25'			11,261.75'	11,259.50'
1	40 LB N-80	38.25'			11,223.50'	11,221.75'
1	40 LB N-80	38.25'			11,185.25'	11,183.50'
1	40 LB N-80	38.25'			11,147.00'	11,145.25'
1	40 LB N-80	38.25'			11,108.75'	11,107.00'
1	40 LB N-80	38.25'			11,070.50'	11,068.75'
1	40 LB N-80	38.25'			11,032.25'	11,030.50'
1	40 LB N-80	38.25'			10,994.00'	10,992.25'
1	40 LB N-80	38.25'			10,955.75'	10,954.00'
1	40 LB N-80	38.25'			10,917.50'	10,915.75'
1	40 LB N-80	38.25'			10,879.25'	10,877.50'
1	40 LB N-80	38.25'			10,841.00'	10,839.25'
1	40 LB N-80	38.25'			10,802.75'	10,801.00'
1	40 LB N-80	38.25'			10,764.50'	10,762.75'
1	40 LB N-80	38.25'			10,726.25'	10,724.50'
1	40 LB N-80	38.25'			10,688.00'	10,686.25'
1	40 LB N-80	38.25'			10,649.75'	10,648.00'
1	40 LB N-80	38.25'			10,611.50'	10,609.75'
1	40 LB N-80	38.25'			10,573.25'	10,571.50'
1	40 LB N-80	38.25'			10,535.00'	10,533.25'
1	40 LB N-80	38.25'			10,496.75'	10,495.00'
1	40 LB N-80	38.25'			10,458.50'	10,456.75'
1	40 LB N-80	38.25'			10,420.25'	10,418.50'
1	40 LB N-80	38.25'			10,382.00'	10,380.25'
1	40 LB N-80	38.25'			10,343.75'	10,342.00'
1	40 LB N-80	38.25'			10,305.50'	10,303.75'
1	40 LB N-80	38.25'			10,267.25'	10,265.50'
1	40 LB N-80	38.25'			10,229.00'	10,227.25'
1	40 LB N-80	38.25'			10,190.75'	10,189.00'
1	40 LB N-80	38.25'			10,152.50'	10,150.75'
1	40 LB N-80	38.25'			10,114.25'	10,112.50'
1	40 LB N-80	38.25'			10,076.00'	10,074.25'
1	40 LB N-80	38.25'			10,037.75'	10,036.00'
1	40 LB N-80	38.25'			9,999.50'	9,997.75'
1	40 LB N-80	38.25'			9,961.25'	9,959.50'
1	40 LB N-80	38.25'			9,923.00'	9,921.25'
1	40 LB N-80	38.25'			9,884.75'	9,883.00'
1	40 LB N-80	38.25'			9,846.50'	9,844.75'
1	40 LB N-80	38.25'			9,808.25'	9,806.50'
1	40 LB N-80	38.25'			9,770.00'	9,768.25'
1	40 LB N-80	38.25'			9,731.75'	9,730.00'
1	40 LB N-80	38.25'			9,693.50'	9,691.75'
1	40 LB N-80	38.25'			9,655.25'	9,653.50'
1	40 LB N-80	38.25'			9,617.00'	9,615.25'
1	40 LB N-80	38.25'			9,578.75'	9,577.00'
1	40 LB N-80	38.25'			9,540.50'	9,538.75'
1	40 LB N-80	38.25'			9,502.25'	9,500.50'
1	40 LB N-80	38.25'			9,464.00'	9,462.25'
1	40 LB N-80	38.25'			9,425.75'	9,424.00'
1	40 LB N-80	38.25'			9,387.50'	9,385.75'
1	40 LB N-80	38.25'			9,349.25'	9,347.50'
1	40 LB N-80	38.25'			9,311.00'	9,309.25'
1	40 LB N-80	38.25'			9,272.75'	9,271.00'
1	40 LB N-80	38.25'			9,234.50'	9,232.75'
1	40 LB N-80	38.25'			9,196.25'	9,194.50'
1	40 LB N-80	38.25'			9,158.00'	9,156.25'
1	40 LB N-80	38.25'			9,119.75'	9,118.00'
1	40 LB N-80	38.25'			9,081.50'	9,079.75'
1	40 LB N-80	38.25'			9,043.25'	9,041.50'
1	40 LB N-80	38.25'			9,005.00'	9,003.25'
1	40 LB N-80	38.25'			8,966.75'	8,965.00'
1	40 LB N-80	38.25'			8,928.50'	8,926.75'
1	40 LB N-80	38.25'			8,890.25'	8,888.50'
1	40 LB N-80	38.25'			8,852.00'	8,850.25'
1	40 LB N-80	38.25'			8,813.75'	8,812.00'
1	40 LB N-80	38.25'			8,775.50'	8,773.75'
1	40 LB N-80	38.25'			8,737.25'	8,735.50'
1	40 LB N-80	38.25'			8,699.00'	8,697.25'
1	40 LB N-80	38.25'			8,660.75'	8,659.00'
1	40 LB N-80	38.25'			8,622.50'	8,620.75'
1	40 LB N-80	38.25'			8,584.25'	8,582.50'
1	40 LB N-80	38.25'			8,546.00'	8,544.25'
1	40 LB N-80	38.25'			8,507.75'	8,506.00'
1	40 LB N-80	38.25'			8,469.50'	8,467.75'
1	40 LB N-80	38.25'			8,431.25'	8,429.50'
1	40 LB N-80	38.25'			8,393.00'	8,391.25'
1	40 LB N-80	38.25'			8,354.75'	8,353.00'
1	40 LB N-80	38.25'			8,316.50'	8,314.75'
1	40 LB N-80	38.25'			8,278.25'	8,276.50'
1	40 LB N-80	38.25'			8,240.00'	8,238.25'
1	40 LB N-80	38.25'			8,201.75'	8,199.99'



DEPARTURE		ADDED RLV. AND SPOOL	
1	ADDED NOTE	2	2
2	ADDED CROSS SECT. & PISC.	3	3
3	ADDED 9 5/8 CASING	4	4
4	ORIGINAL TITLE	5	5
5		6	6
6		7	7
7		8	8
8		9	9
9		10	10
10		11	11
11		12	12
12		13	13
13		14	14
14		15	15
15		16	16
16		17	17
17		18	18
18		19	19
19		20	20
20		21	21
21		22	22
22		23	23
23		24	24
24		25	25
25		26	26
26		27	27
27		28	28
28		29	29
29		30	30
30		31	31
31		32	32
32		33	33
33		34	34
34		35	35
35		36	36
36		37	37
37		38	38
38		39	39
39		40	40
40		41	41
41		42	42
42		43	43
43		44	44
44		45	45
45		46	46
46		47	47
47		48	48
48		49	49
49		50	50
50		51	51
51		52	52
52		53	53
53		54	54
54		55	55
55		56	56
56		57	57
57		58	58
58		59	59
59		60	60
60		61	61
61		62	62
62		63	63
63		64	64
64		65	65
65		66	66
66		67	67
67		68	68
68		69	69
69		70	70
70		71	71
71		72	72
72		73	73
73		74	74
74		75	75
75		76	76
76		77	77
77		78	78
78		79	79
79		80	80
80		81	81
81		82	82
82		83	83
83		84	84
84		85	85
85		86	86
86		87	87
87		88	88
88		89	89
89		90	90
90		91	91
91		92	92
92		93	93
93		94	94
94		95	95
95		96	96
96		97	97
97		98	98
98		99	99
99		100	100

NOTE:  
 T.D. = TOTAL DEPTH  
 TVD = TRUE VERTICAL DEPTH  
 KOP = KICK OFF POINT  
 S.L.M. = STRAPPED LENGTH MEASUREMENT  
 KB = KELLY BUSHING

**USA**  
 UNITED STATES GEOLOGICAL SURVEY  
 WASHINGTON, D.C. 20540

EE-2  
 AS COMPLETED  
 ON MAY 12, 1980

8120275 D-1

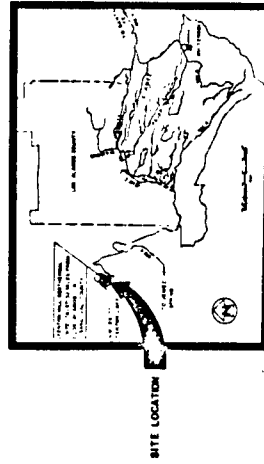


APPENDIX E

As Built Drawings - 5.7 M gal reservoir

# U.S. DEPARTMENT OF ENERGY

## WATER STORAGE POND TA-57



VICINITY MAP

### INDEX OF DRAWINGS

- 1 TITLE SHEET
- 2 SITE PLAN
- 3 STORAGE POND GRADING PLAN
- 4-7 PLAN & PROFILE SHEETS
- 8 PUMP HOUSE PLAN
- 9 ELECTRICAL DIAGRAM
- 10-11 PUMP HOUSE PIPING DETAILS
- 12 SECTIONS & DETAILS
- 13 FENCE DETAILS
- 14 STORAGE POND GRADING PROFILE

AS BUILT

NO. 1	DATE	REVISION	BY
1	10/1/57	AS BUILT	AS
2			
3			
4			
5			
6			
7			
8			
9			
10			
11			
12			
13			
14			

DESIGNED BY	DATE	BY
AS	10/1/57	AS
CHECKED BY	DATE	BY
AS	10/1/57	AS
APPROVED BY	DATE	BY
AS	10/1/57	AS

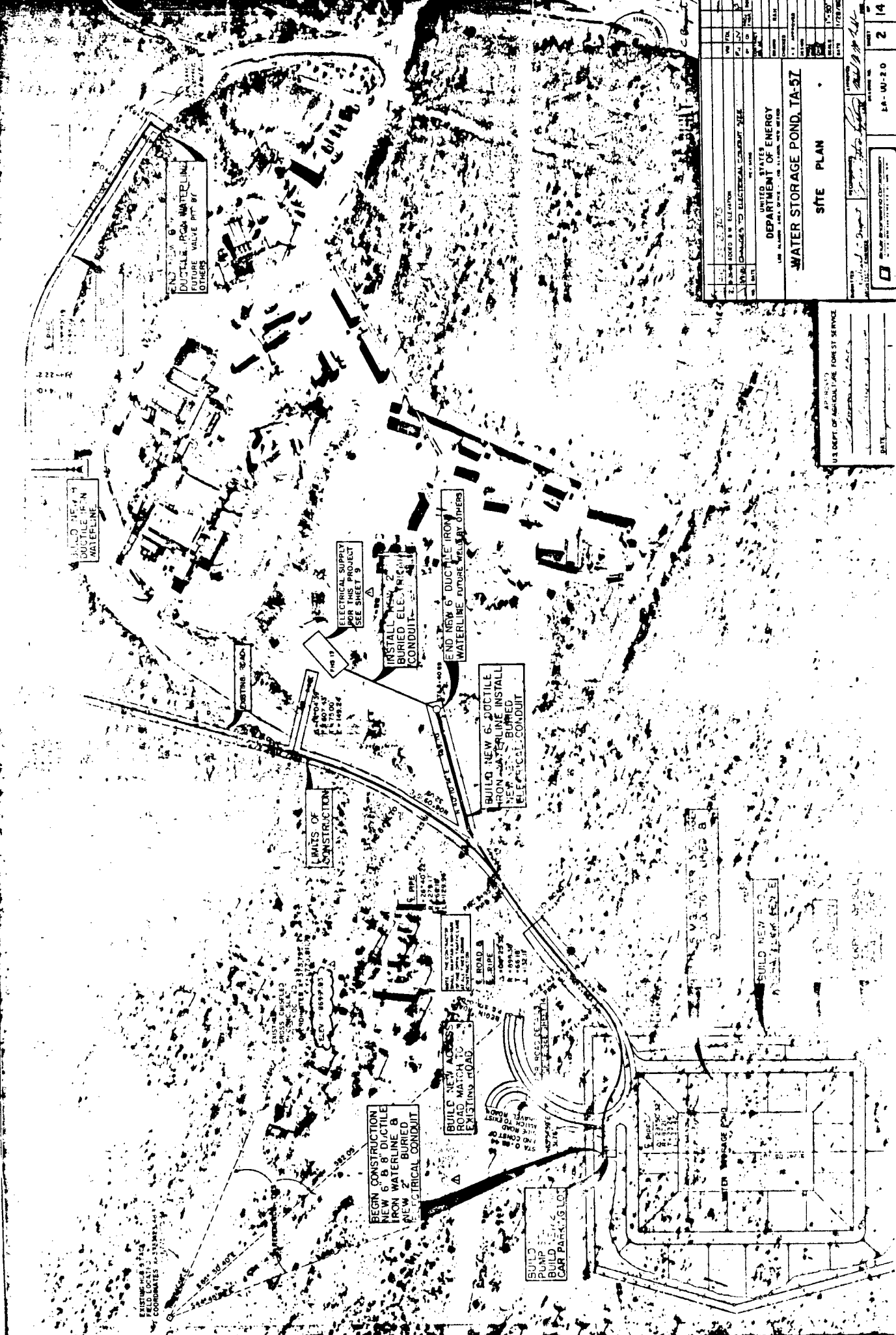
U.S. DEPARTMENT OF ENERGY  
 WATER STORAGE POND, TA-57  
 TITLE SHEET

U.S. DEPARTMENT OF AGRICULTURE FOREST SERVICE  
 APPROVED  
 DATE

PROJECT NO. LA-00-10  
 SHEET 1 OF 14

**Boyle Engineering Corporation**





NO. 1	NO. 2	NO. 3	NO. 4	NO. 5	NO. 6	NO. 7	NO. 8	NO. 9	NO. 10	NO. 11	NO. 12	NO. 13	NO. 14	NO. 15	NO. 16	NO. 17	NO. 18	NO. 19	NO. 20
UNITED STATES DEPARTMENT OF ENERGY WATER STORAGE POND, TA-57										SITE PLAN									
U.S. DEPT. OF AGRICULTURE FOREST SERVICE																			

U.S. DEPT. OF AGRICULTURE FOREST SERVICE  
 APPLICANT'S NAME: \_\_\_\_\_  
 PROJECT NO.: \_\_\_\_\_  
 DATE: \_\_\_\_\_

S. PIPE  
 4.0  
 22.2

END NEW 6" DUCTILE IRON WATERLINE  
 FUTURE VALUE PPT BY OTHERS

BUILD NEW 6" DUCTILE IRON WATERLINE

ELECTRICAL SUPPLY FOR THIS PROJECT SEE SHEET 9

INSTALL BURIED ELECTRICAL CONDUIT

END NEW 6" DUCTILE IRON WATERLINE FUTURE VALUE BY OTHERS

BUILD NEW 6" DUCTILE IRON WATERLINE INSTALL BURIED ELECTRICAL CONDUIT

LIMITS OF CONSTRUCTION

EXISTING ROAD

NEW ROAD

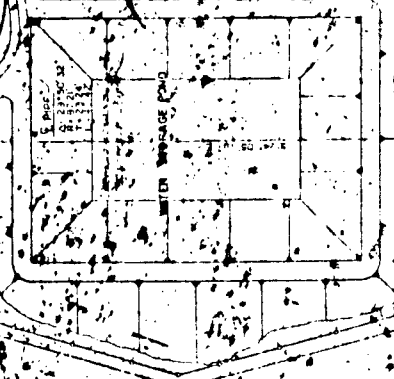
BEGIN CONSTRUCTION NEW 6" & 8" DUCTILE IRON WATERLINE & NEW 2" BURIED ELECTRICAL CONDUIT

BUILD NEW AGES ROAD MATCH TO EXISTING ROAD

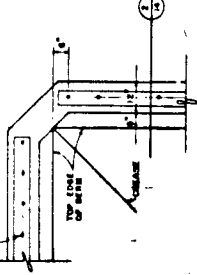
BUILD PUMP BUILD CAR PARKING LOT

BUILD NEW 6" DUCTILE IRON WATERLINE TO BE LINED B

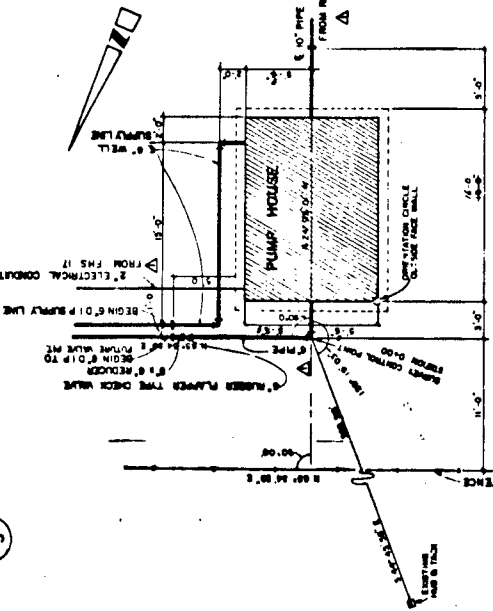
BUILD NEW 6" DUCTILE IRON WATERLINE



NOTES: 1. ALL DIMENSIONS TO BE CHECKED BY MANUFACTURER.  
2. ALL DIMENSIONS TO BE CHECKED BY CONTRACTOR.  
3. ALL DIMENSIONS TO BE CHECKED BY CONTRACTOR.



1 CURB CORNER DETAIL



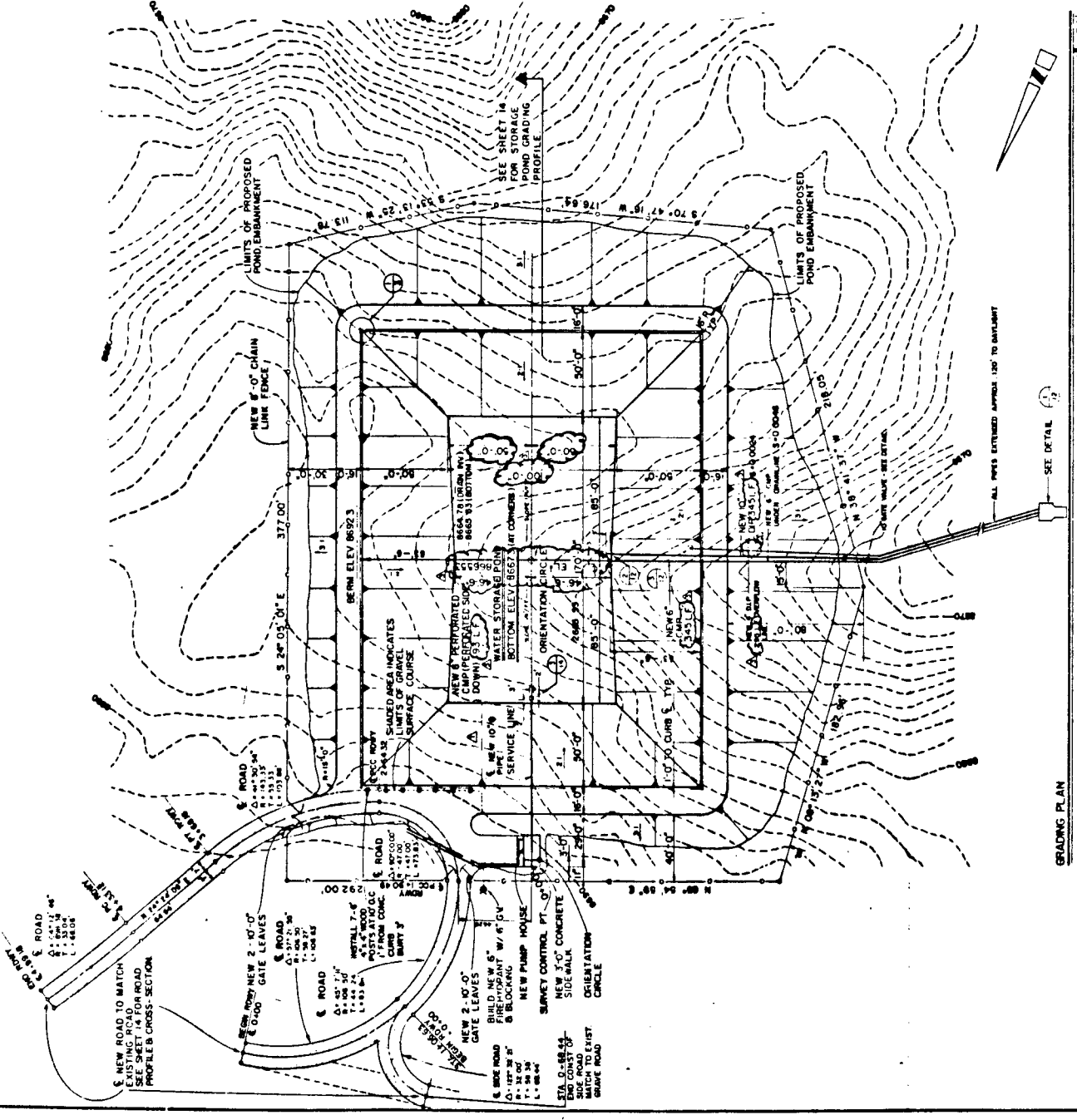
PUMP HOUSE CONTROL LAYOUT PLAN

GENERAL NOTES:  
1. Reserve 2' of topsoil inside limits of proposed pond embankment and stockpile in an area as designated on Sheet 2.  
2. All denuded areas including outer berm of Reservoir shall be covered with a layer of topsoil and reseeded with native grasses.  
3. Additional borrow material is available on site if required by Contractor.

AS BUILT

DATE	1/23/70
BY	AS BUILT
CHECKED	
APPROVED	
SCALE	AS SHOWN
TITLE	WATER STORAGE POND, TA-57
PROJECT	UNITED STATES DEPARTMENT OF ENERGY
OFFICE	WATER RESOURCES DIVISION
LOCATION	WATER STORAGE POND, TA-57
PROJECT NO.	LA-UU-30
SHEET NO.	3

APPROVED  
RICHARD C. BERGANT  
U.S. DEPT. OF AGRICULTURE, FOREST SERVICE



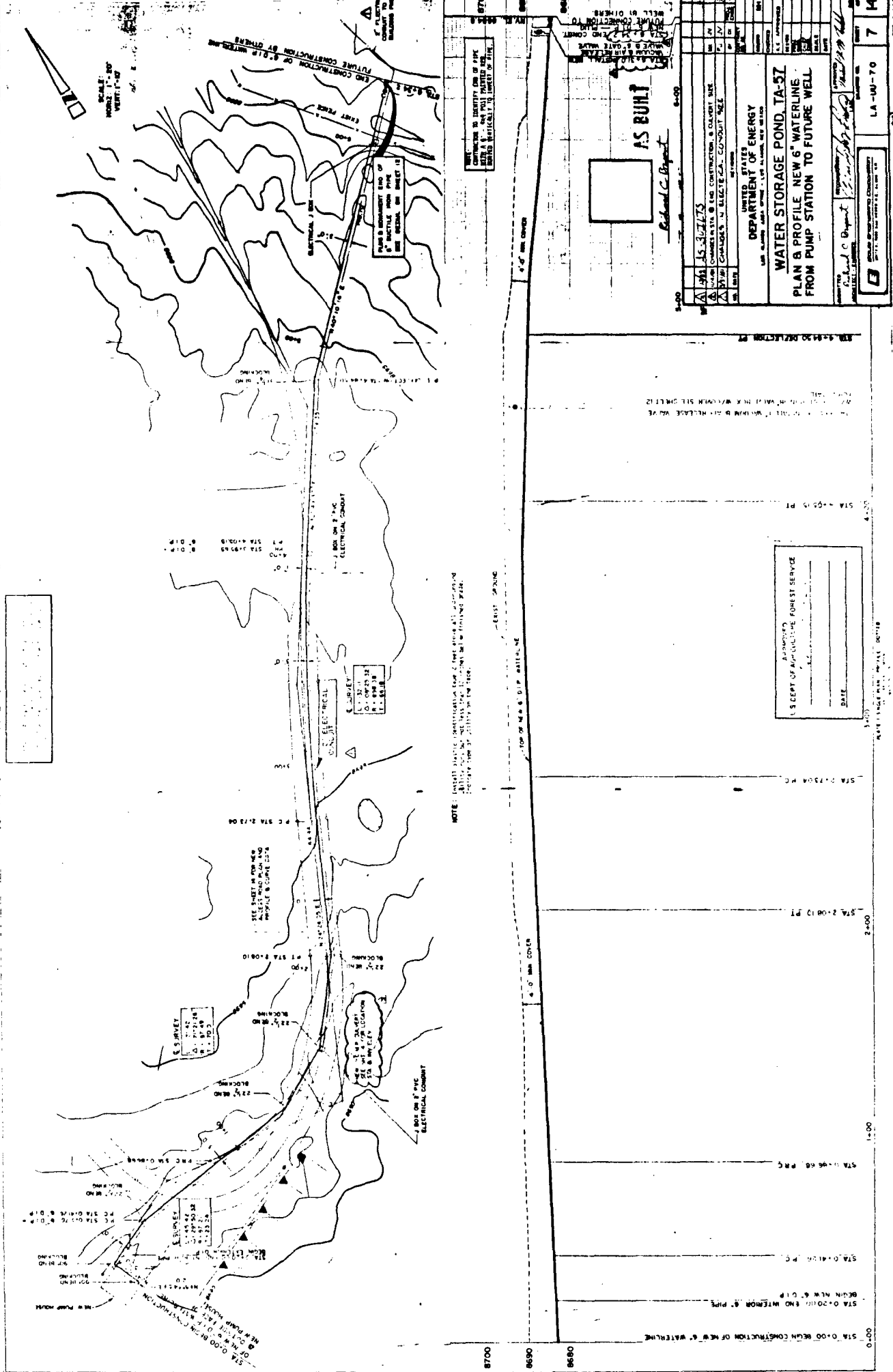
GRADING PLAN

1:20









AS BUILT

AS BUILT

PROJECT NO. 15-307275 DRAWN BY: [Name] CHECKED BY: [Name] DATE: [Date]	
UNITED STATES DEPARTMENT OF ENERGY WATER STORAGE POND, TA-57 PLAN & PROFILE NEW 6" WATERLINE FROM PUMP STATION TO FUTURE WELL	
SHEET NO. 1 OF 1	DRAWING NO. LA-100-70 SCALE: 1" = 40'

NOTE: (Small) Electric investigation line 2 feet above all underground utility lines. See also the notes on the following page.

APPROVED FOR CONSTRUCTION

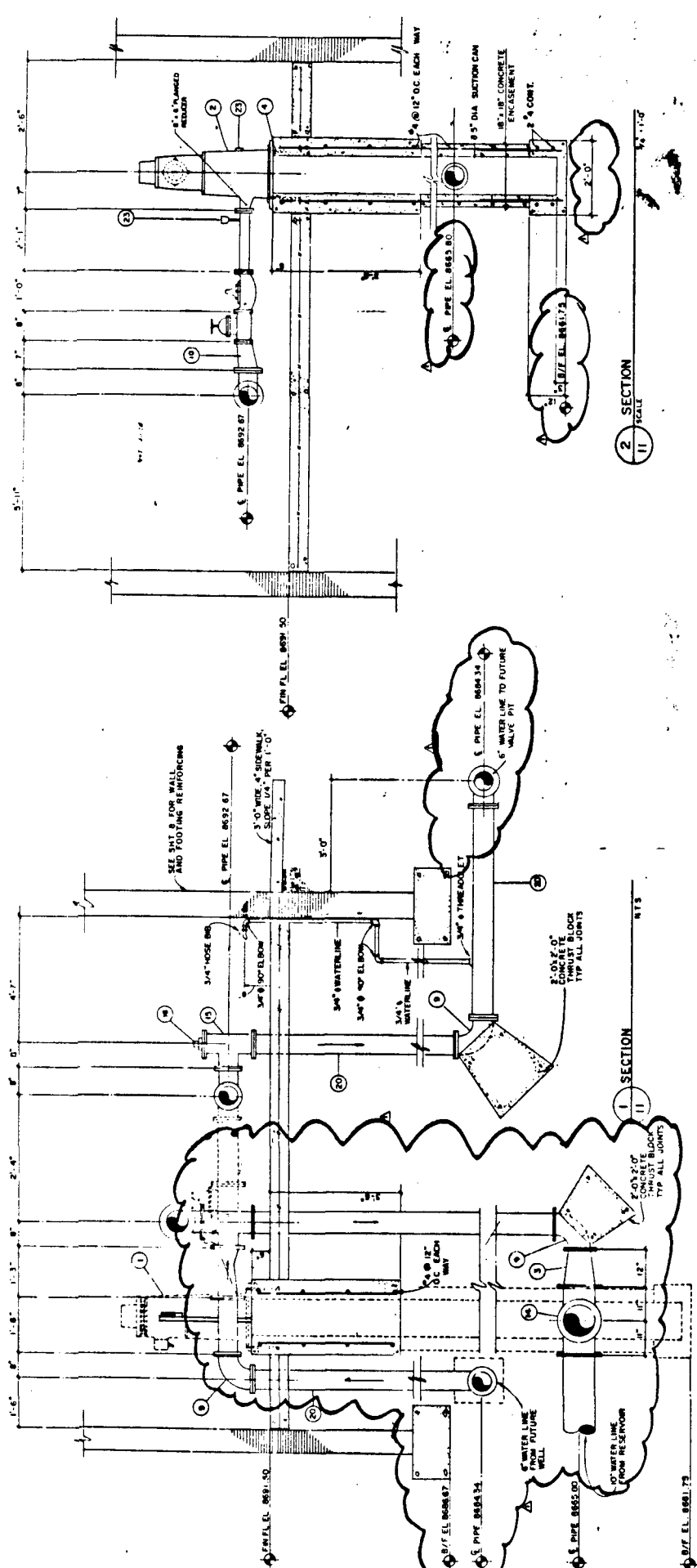
DATE: \_\_\_\_\_

NO.	DESCRIPTION
1	PLAN

NO.	DESCRIPTION
1	PLAN







SEE ALL DIMENSIONS

1. All pipe assemblies in this drawing shall be in accordance with the latest edition of the ASME B31.1 Code for Pressure Piping.

2. All pipe assemblies shall be installed in accordance with the latest edition of the ASME B31.1 Code for Pressure Piping.

3. All pipe assemblies shall be installed in accordance with the latest edition of the ASME B31.1 Code for Pressure Piping.

4. All pipe assemblies shall be installed in accordance with the latest edition of the ASME B31.1 Code for Pressure Piping.

5. All pipe assemblies shall be installed in accordance with the latest edition of the ASME B31.1 Code for Pressure Piping.

6. All pipe assemblies shall be installed in accordance with the latest edition of the ASME B31.1 Code for Pressure Piping.

7. All pipe assemblies shall be installed in accordance with the latest edition of the ASME B31.1 Code for Pressure Piping.

8. All pipe assemblies shall be installed in accordance with the latest edition of the ASME B31.1 Code for Pressure Piping.

9. All pipe assemblies shall be installed in accordance with the latest edition of the ASME B31.1 Code for Pressure Piping.

10. All pipe assemblies shall be installed in accordance with the latest edition of the ASME B31.1 Code for Pressure Piping.

11. All pipe assemblies shall be installed in accordance with the latest edition of the ASME B31.1 Code for Pressure Piping.

12. All pipe assemblies shall be installed in accordance with the latest edition of the ASME B31.1 Code for Pressure Piping.

13. All pipe assemblies shall be installed in accordance with the latest edition of the ASME B31.1 Code for Pressure Piping.

14. All pipe assemblies shall be installed in accordance with the latest edition of the ASME B31.1 Code for Pressure Piping.

15. All pipe assemblies shall be installed in accordance with the latest edition of the ASME B31.1 Code for Pressure Piping.

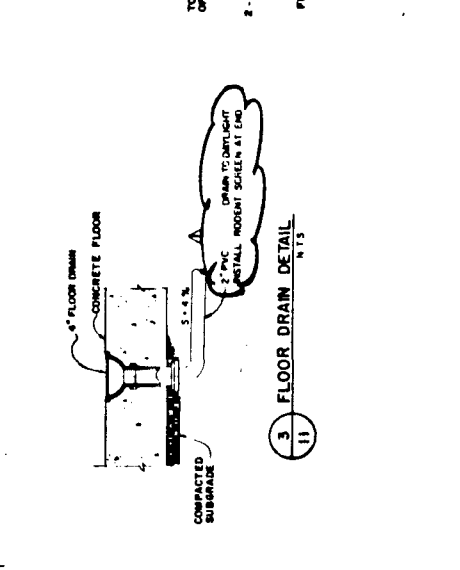
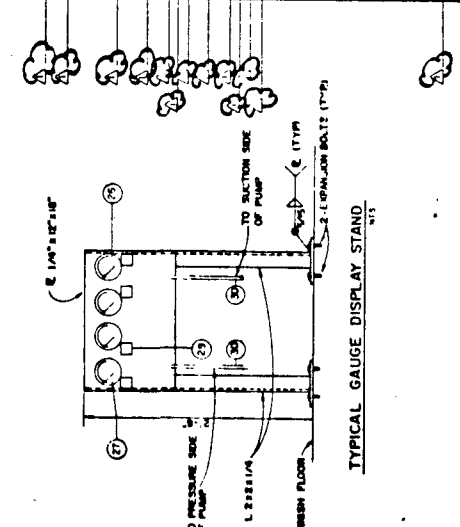
16. All pipe assemblies shall be installed in accordance with the latest edition of the ASME B31.1 Code for Pressure Piping.

17. All pipe assemblies shall be installed in accordance with the latest edition of the ASME B31.1 Code for Pressure Piping.

18. All pipe assemblies shall be installed in accordance with the latest edition of the ASME B31.1 Code for Pressure Piping.

19. All pipe assemblies shall be installed in accordance with the latest edition of the ASME B31.1 Code for Pressure Piping.

20. All pipe assemblies shall be installed in accordance with the latest edition of the ASME B31.1 Code for Pressure Piping.



*Richard C. Bryant*

**AS P-43**

APPROVED  
U.S. DEPT. OF AGRICULTURE FOREST SERVICE

DATE: \_\_\_\_\_

NO.	DATE	BY	REVISION
1	1/25/73	AS P-43	ISSUED FOR CONSTRUCTION
2	1/25/73	AS P-43	CHANGE TO SCHEDULE OF EQUIPMENT

UNITED STATES  
DEPARTMENT OF ENERGY

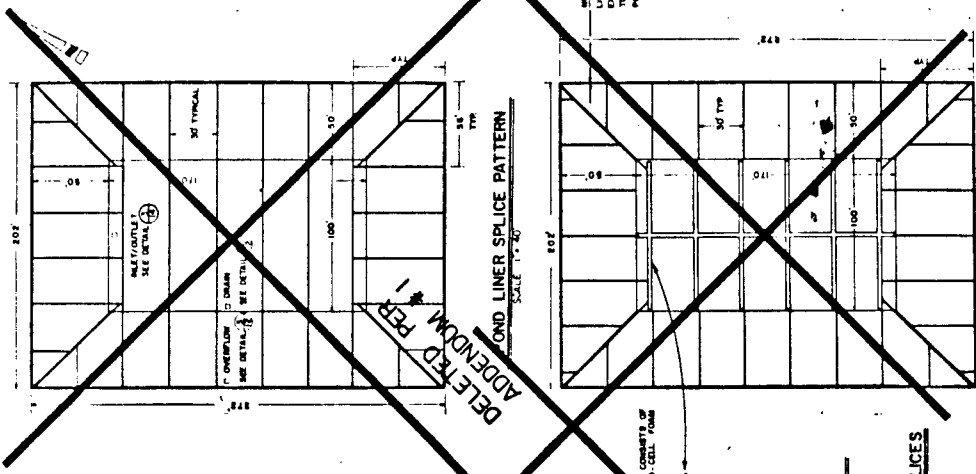
**WATER STORAGE POND, TA-57**

PUMP HOUSE PIPING DETAILS

DRAWN BY: *[Signature]*  
CHECKED BY: *[Signature]*  
DATE: 1/25/73

SCALE: \_\_\_\_\_  
NOTED: \_\_\_\_\_  
DATE: 1/25/73

PROJECT NO. \_\_\_\_\_  
SHEET NO. \_\_\_\_\_ OF \_\_\_\_\_  
LA-UD-110

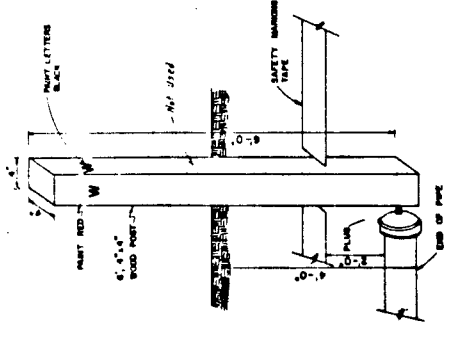


Richard C. Bay

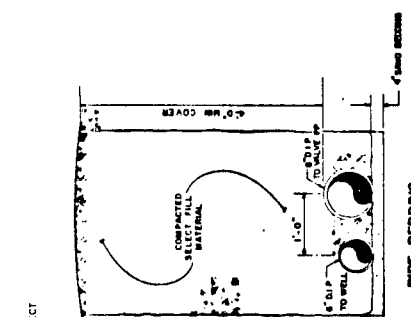
NO.	DATE	REVISIONS
1	10/1/57	ISSUED FOR CONSTRUCTION
2	10/1/57	REVISED DETAILS FOR 2-D
3	10/1/57	REVISED DETAILS FOR 2-D
4	10/1/57	REVISED DETAILS FOR 2-D
5	10/1/57	REVISED DETAILS FOR 2-D
6	10/1/57	REVISED DETAILS FOR 2-D
7	10/1/57	REVISED DETAILS FOR 2-D
8	10/1/57	REVISED DETAILS FOR 2-D
9	10/1/57	REVISED DETAILS FOR 2-D
10	10/1/57	REVISED DETAILS FOR 2-D
11	10/1/57	REVISED DETAILS FOR 2-D
12	10/1/57	REVISED DETAILS FOR 2-D

UNITED STATES  
DEPARTMENT OF ENERGY  
WATER STORAGE POND, TA-57  
SECTIONS & DETAILS

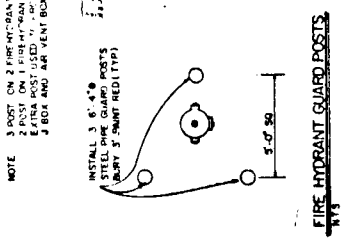
LA-UU-120 12



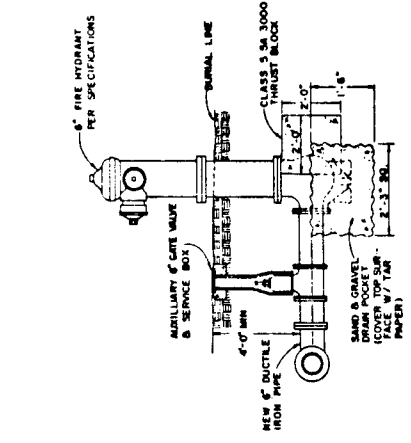
4" x 4" x 6'-0" END OF PIPE MONUMENT  
WOOD POST BORED IN INLET  
SCALE 1/2" = 1'-0"



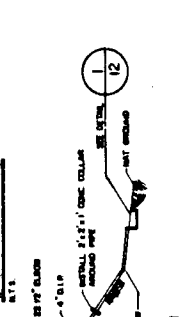
PIPE BEDDING  
BACKFILL DETAIL  
N.T.S.



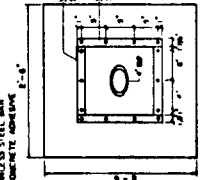
FIRE HYDRANT GUARD POSTS  
N.T.S.



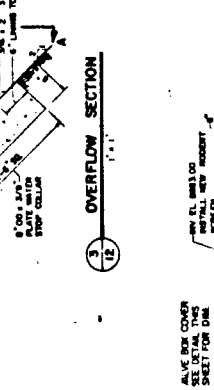
FIRE HYDRANT SETTING WITH BLOCKING  
N.T.S.



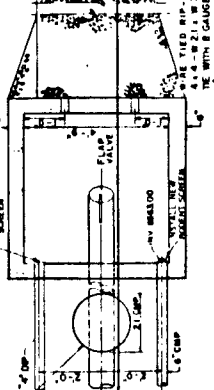
OVER FLOW SECTION  
N.T.S.



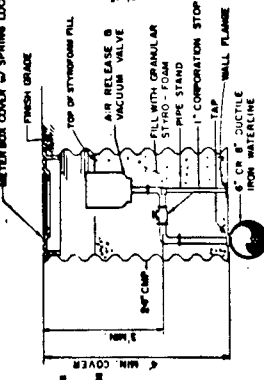
OVERFLOW PLAN  
SECTION A-A  
N.T.S.



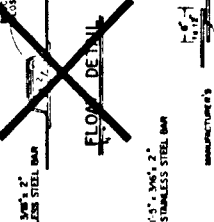
OVERFLOW SECTION  
N.T.S.



EMERGENCY DRAIN HEADWALL PLAN  
N.T.S.



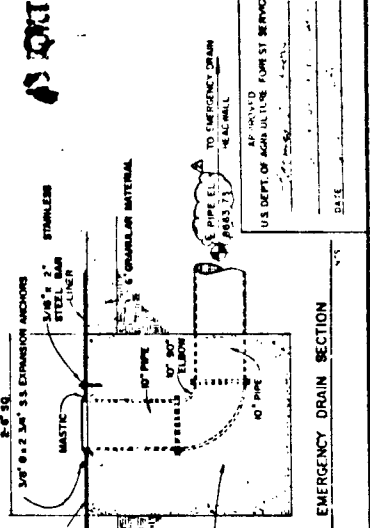
EMERGENCY DRAIN PLAN  
1\"/>



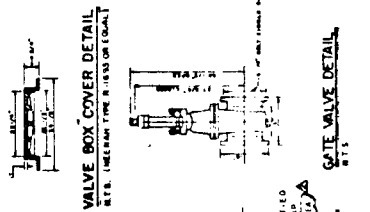
FLOW DETAIL  
N.T.S.



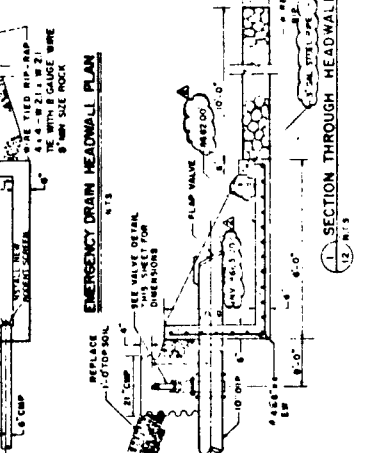
TYPICAL SPLICES  
N.T.S.



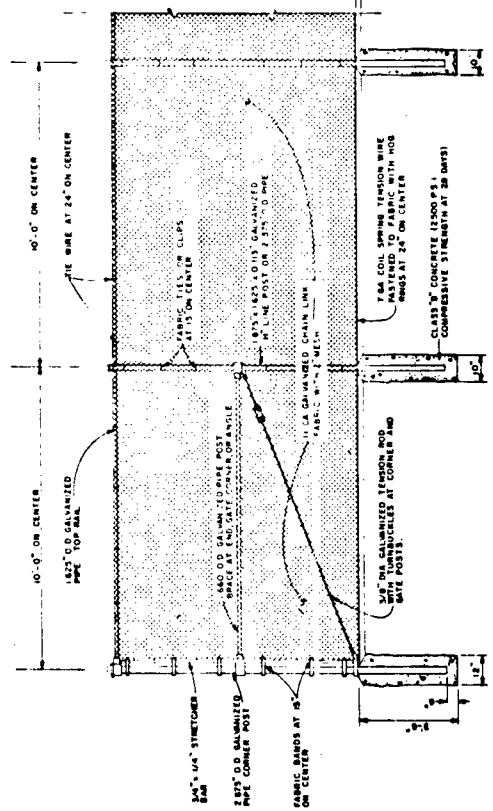
EMERGENCY DRAIN SECTION  
N.T.S.



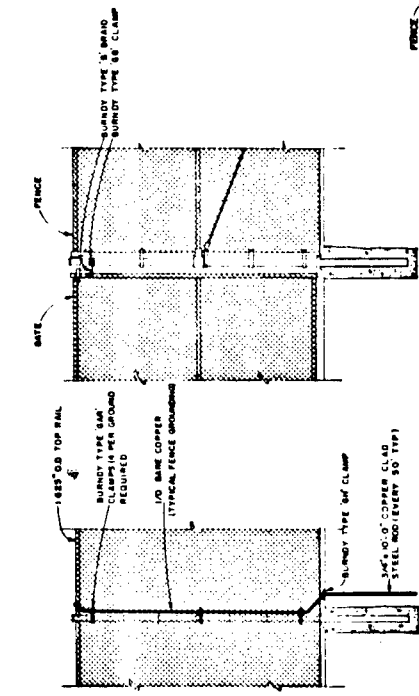
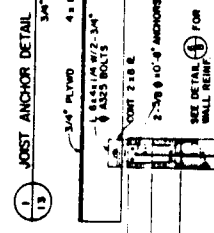
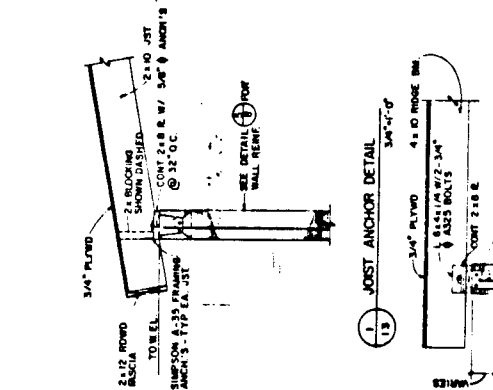
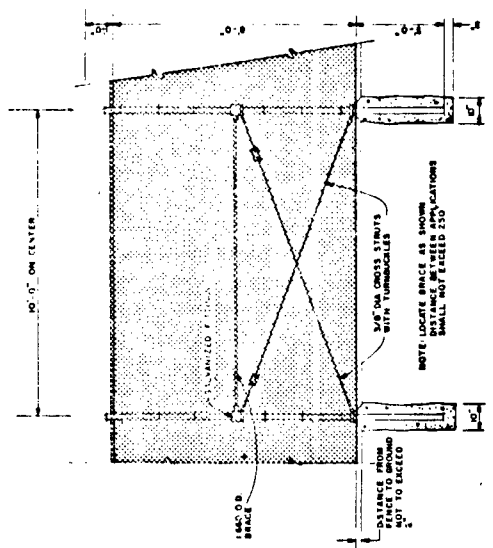
VALVE BOX COVER DETAIL  
N.T.S. (INDICATE TYPE & BRAND OR EQUIV.)



SECTION THROUGH HEADWALL  
N.T.S.

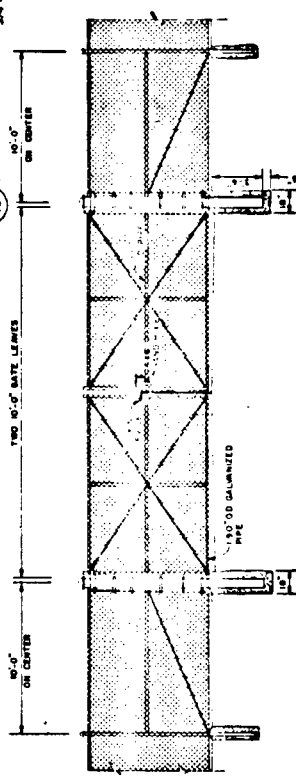


TYPICAL FENCE DETAILS  
N13

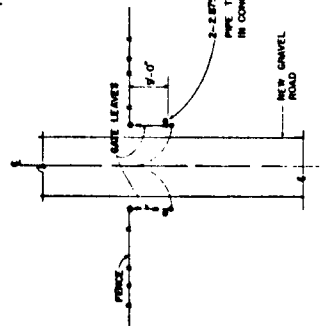


FENCE GROUNDING DETAILS  
N15

- NOTE: FENCES SHALL BE ANCHORED AS FOLLOWS:
- AT EACH END OF EVERY GATE
  - AT POINTS APPROX. 100' ON EACH SIDE OF HIGH TENSION LINE (EXCEPT HIGH TENSION BRACE ARE WITHIN 20' AND 50' PARALLEL TO FENCE)
  - EVERY 100' WATER FENCES ARE LOCATED IN
  - EVERY 100' WATER IN CLOSE PROXIMITY (100' OR LESS) TO PAVEMENT, HIGHWAYS, AND BUILDINGS



GATE DETAIL  
N14



TYPICAL GATE TIE BACKS  
N15

AS-BUILT School Capital

NO.	DATE	BY	CHKD.	APPV.
1	11/15/13	AS-BUILT		
2				
3				
4				
5				
6				
7				
8				
9				
10				
11				
12				
13				
14				

UNITED STATES  
DEPARTMENT OF ENERGY  
WASHINGTON, D.C. 20545-0001

WATER STORAGE POND, TA-57  
FENCE DETAILS

APPROVED FOR CONSTRUCTION  
DATE: 11/15/13

U.S. DEPT. OF AGRICULTURE FOREST SERVICE



APPENDIX F

Site Maps of Fenton Hill

RECEIVED

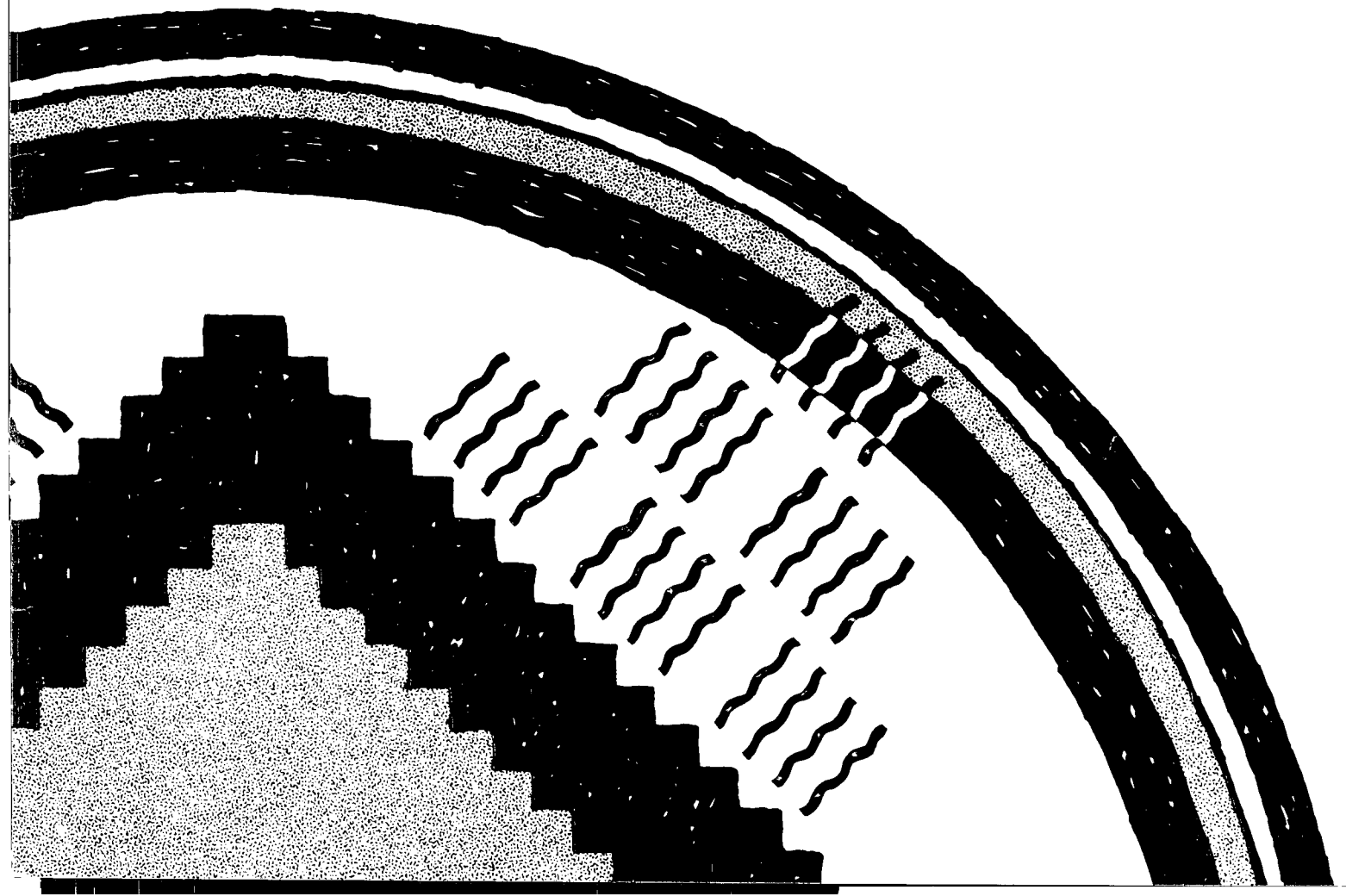
AUG 10 1984

OIL CONSERVATION DIVISION  
SANTA FE

LA-10661-HDR

*Hot Dry Rock Geothermal Energy  
Development Program*

*Annual Report  
Fiscal Year 1984*



The four most recent reports in this series, unclassified, are LA-8855-HDR, LA-9287-HDR, LA-9780-HDR, and LA-10347-HDR.

This work was supported by the US Department of Energy, Division of Geothermal and Hydropower Technologies; Kernforschungsanlage Jülich GmbH, Federal Republic of Germany; and New Energy Development Organization, Japan.

DISCLAIMER

This report was prepared as an account of work sponsored by an agency of the United States Government. Neither the United States Government nor any agency thereof, nor any of their employees, makes any warranty, express or implied, or assumes any legal liability or responsibility for the accuracy, completeness, or usefulness of any information, apparatus, product, or process disclosed, or represents that its use would not infringe privately owned rights. Reference herein to any specific commercial product, process, or service by trade name, trademark, manufacturer, or otherwise, does not necessarily constitute or imply its endorsement, recommendation, or favoring by the United States Government or any agency thereof. The views and opinions of authors expressed herein do not necessarily state or reflect those of the United States Government or any agency thereof.

UNITED STATES  
DEPARTMENT OF ENERGY  
CONTRACT W-7405-ENG. 36

**The cover design by John Paskiewicz is based on motifs found in Native American pottery decoration and painting. It depicts the movement of heat from deep within the earth toward the surface. Exploiting this immense global reservoir of heat is the goal of HDR research.**

# Hot Dry Rock Geothermal Energy Development Program

---

## Annual Report Fiscal Year 1984

P. R. Franke, D. W. Brown, M. C. Smith, and K. L. Mathews

### Contents

ABSTRACT . . . . .	1
EXECUTIVE SUMMARY . . . . .	1
INTRODUCTION . . . . .	3
FENTON HILL SITE OPERATIONS . . . . .	6
SCIENTIFIC AND ENGINEERING SUPPORT . . . . .	10
RESERVOIR ENGINEERING . . . . .	12
TECHNOLOGY TRANSFER . . . . .	25
PROGRAM MANAGEMENT . . . . .	26
PLANS FOR FISCAL YEAR 1985 . . . . .	28
REFERENCES . . . . .	30

## ABSTRACT

The Hot Dry Rock Program in FY84 concentrated on achieving a connection between the two Phase II injection and production wells. Two massive hydraulic fracturing (MHF) experiments were conducted. The first MHF occurred in December 1983 when 21 300 m<sup>3</sup> (5.63 × 10<sup>6</sup> gal) of water were injected into well EE-2. The experiment was terminated by equipment failure, but a huge reservoir was created. The other fracturing experiment was conducted in well EE-3 when 7570 m<sup>3</sup> (2 × 10<sup>6</sup> gal) of water were injected. Neither experiment brought about a connection between the two wells. Improvements in seismic mapping techniques were notable during the year. These techniques identified the size and parameters of the big reservoir created by the MHF. Development has continued on the family of "slimline" downhole instruments. A "cross-well acoustic transceiver" has been developed for investigation of rock structures between wellbores, and chemically reactive tracers are proving useful to observe temperature changes in the system. Other related activities have included development of an analytical method for measuring radon concentration in vented gases, studies of geochemical reactions, potassium-argon dating of Fenton Hill cores and cuttings, and a laboratory study of natural convection in an inclined wellbore.

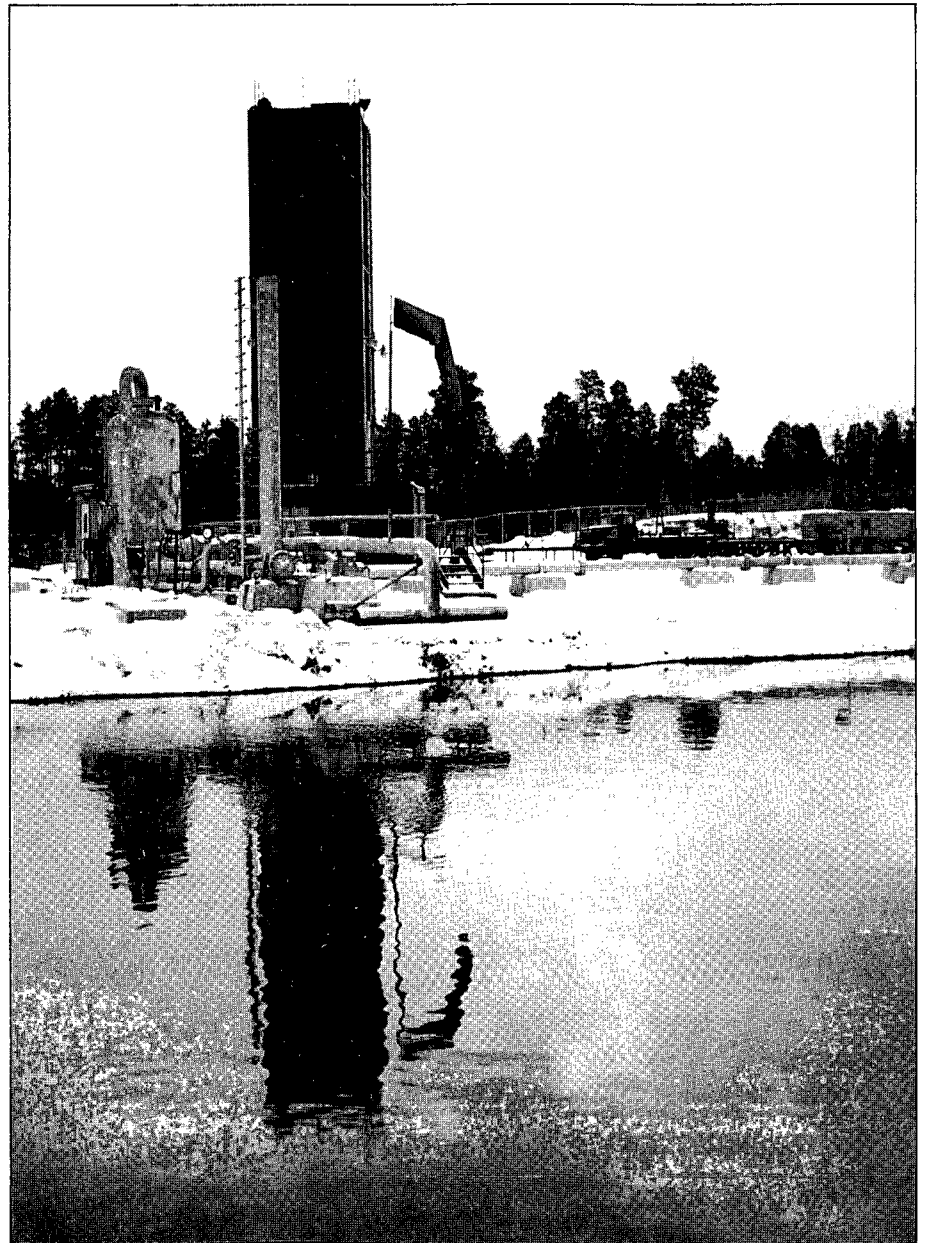
## EXECUTIVE SUMMARY

Fiscal Year 1984 was primarily a year of field operations, with emphasis on achieving a connection between the injection and production wells of the Phase II Hot Dry Rock (HDR) system. As a result of earlier hardware failures due to stress corrosion and higher pressures, a new low-alloy steel fracturing string had to be specially ordered. It arrived at the beginning of this fiscal year.

In December, a massive hydraulic fracturing (MHF) experiment was conducted wherein 21 300 m<sup>3</sup> (5.63 × 10<sup>6</sup> gal) of water were injected into well EE-2 in a total of 61 hours (Fig. 1). The experiment was terminated by fatigue failure of a connection between a flow line and a wellhead

flange. The resulting rapid vent returned about 54% of the injected fluid and delivered thermal energy to the surface at rates estimated to have been 100 MW(t) initially and averaged 60 MW(t) over a 2-day period of rapid venting. No connection was made to the other well, and there was damage to both the well casing and the fracturing string. However, the continued advancements in microseismic mapping indicated the existence of a very large fracture system created by the MHF, and the amount and rate of fluid return indicated that the system was tightly contained and well connected.

*Figure 1. Wellhead tower during MHF experiments.*



The source locations of microseismic signals generated by this hydraulic fracturing operation were mapped by three separate systems. Several geophone instruments were emplaced in two Fenton Hill wells which acquired data for mapping by the hodogram method; a "Precambrian Net" of instruments in three other wells permitted location of acoustic sources by triangulation; and a series of surface seismic stations provided additional data for mapping and for fault-plane solutions (Fig. 2).

At the conclusion of the massive hydraulic fracturing experiment in well EE-2, it was known only that it had failed to produce a hydraulic connection to the other well and that preliminary acoustic maps indicated that there was a seismically quiet region around the EE-3 wellbore. A series of experiments was therefore conducted to investigate the behavior of this quiet region, determine whether it could be penetrated by a hydraulic-fracture (which might intersect the fracture system created from EE-2), and provide an opportunity for improvement of acoustic fracture-mapping equipment and techniques.

In another major hydraulic fracturing experiment, 7570 m<sup>3</sup> (2 × 10<sup>6</sup> gal) of water

were pumped into EE-3 at 44.4 MPa (6440 psi). Early in the experiment, a pressure rise in the annulus between the fracturing string and the casing indicated that there was a connection between the open-hole sections below and above the liner. Subsequent temperature, pressure-vent, and radioactive tracer tests showed that this was a direct fracture short circuit with very small volume, which permitted some unknown fraction of the injected fluid to bypass the liner and enter the fluid-loss zone near the casing shoe. A temperature tool stationed in EE-2 showed no evidence of a hydraulic connection to the other well.

In addition to field operations, maintenance, and environmental monitoring at Fenton Hill, a wide variety of supporting activities has continued there and in the facilities at Los Alamos National Laboratory. Among the more significant accomplishments of these activities are the following.

The precision and accuracy of locating the sources of microseismic signals that accompany fracturing events have been increased, together with improvements in the analysis of those signals. The original single-tool hodogram technique for source location has been greatly improved by development of a "partial two-tool" technique, and further improvement is expected from use of a "complete two-tool" technique in which directional as well as distance information from a second downhole instrument will be utilized. Work has also been initiated to better understand the three-component geophone package and, in particular, how its design affects hodogram results. The Precambrian Net has been expanded. Station calibrations have been improved by use of a downhole explosive tool designed specifically to permit detonation of relatively large explosive charges at known depths and under high-temperature conditions in the Fenton Hill wells. Good progress has been made in investigation of source mechanisms by spectral analysis of seismic wave forms. Further studies of seismic data will be facilitated by use of a new digital data-acquisition system. Software required to detect and record microseismic events is currently being developed for use with this system.

Development has continued of a new

*Figure 2. HDR Staff monitor incoming data during MHF experiment.*



family of "slimline" downhole instruments. A slimline explosive tool, usually used to fire small (2.66 g) detonator charges for geophone calibration, has been modified to permit firing of "string shots" containing up to 100 g of high explosive and has been used successfully at depths greater than 3 km (10 000 ft). A slimline geophone package that used high-temperature electronics (with no dewar or heat sink) operated continuously for 84 hours during Experiment 2042 at a depth of 3.4 km (11 200 ft) in well EE-2. Final design of a slimline high-temperature digital borehole acoustic televiewer is nearing completion, and component procurement and shop fabrication are in progress.

While it has not yet been temperature hardened, a "crosswell acoustic transceiver" has been developed for investigation of rock structure between wellbores. The system was tested at shallow depths in the Fenton Hill wells, then used successfully to investigate reservoir structure in a natural-gas field in Colorado.

Chemically reactive tracers with temperature-dependent reaction rates offer a possible means of observing the progress of cooling of reservoir rock away from the injection well, and thus of predicting useful lifetime of the fractured reservoir long before there is a measurable decrease in temperature of the fluid produced from it. Hydrolysis reactions of ethyl acetate, hexyl acetate, iso-pentyl acetate, and ethyl propionate have been found potentially useful for such investigations at temperatures up to about 150°C, and acetamide and ethyl pivalate for temperatures around 200°C. They would be used individually in injection-flowback ("huff-puff") experiments in the injection well, or a series of them with different temperature dependencies would be flowed through the reservoir.

Related recent activities have included development of a rapid analytical method for radon in vented gases, now used routinely at Fenton Hill; studies of the recrystallization of montmorillonite drilling mud and of the effects of carbon dioxide partial pressure and reactant ratios on the reaction of quartz and calcite to form wollastonite; potassium-argon dating of cores and cuttings from the Fenton Hill

wells; and a laboratory study of natural convection in an inclined wellbore.

In other program areas, a plan for transition of Hot Dry Rock Technology to the private sector has been drafted. In addition, other promising areas in the country have been identified and cooperative work investigated between the Hot Dry Rock Program Office and various state agencies. These include the Clear Lake area in northern California, Roosevelt Hot Springs in southern Utah, and Long Island, New York. Close interaction continued in FY84 with HDR research and development programs in other countries including West Germany, Japan, Great Britain, and Australia.

## INTRODUCTION

### The HDR Concept

The Hot Dry Rock Program is a continuing research and development program whose overall goal is to demonstrate the commercial feasibility of energy derived from hot crustal rock characterized by the absence of thermal fluids, or "hot, dry rock." It is based on closed-loop circulation of pressurized water through a man-made fracture system created by hydraulically fracturing hot rock (of low initial permeability) between two wellbores. The useful heat from superheated water is recovered at the surface through heat exchangers, and the cooled water is reinjected to recirculate through the underground loop.

### Synopsis of the HDR Program Through FY83

This HDR concept originated at Los Alamos National Laboratory in 1970. During 1971, background information was collected on the equipment and techniques required to create such a system and on the geology, hydrology, and terrestrial heat flow in the vicinity of the Valles Caldera just west of Los Alamos, an area of geologically recent silicic volcanism that appeared well suited

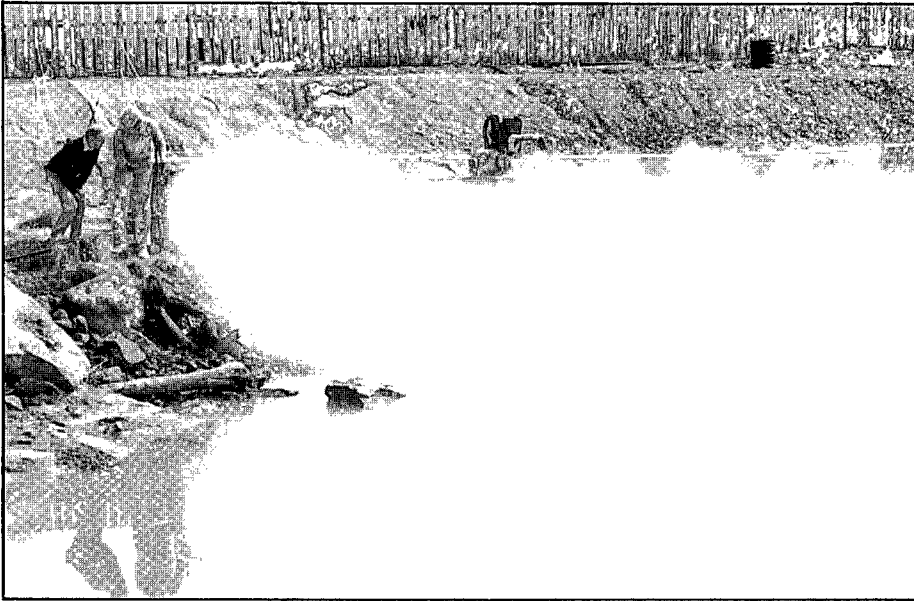


Figure 3. Steam venting from Phase I HDR system.

for HDR field experiments. In 1972, a slim exploratory hole (GT-1) was drilled in Barley Canyon on the western volcanic apron of the caldera. It reached a depth of 785 m (2576 ft), a rock temperature of 100.4°C, and penetrated 143 m (469 ft) of Precambrian crystalline basement. Experiments in GT-1 during 1973 showed that the basement rock could be fractured hydraulically at moderate pressures, that its permeability was low enough to contain pressurized water with very little loss, and that the fractures produced were essentially vertical with an approximately northwest-southeast orientation.

In 1974, a second exploratory hole (GT-2) was drilled at Fenton Hill, a more accessible and convenient location about 2.5 km (1.5 mi) south of GT-1. Final depth was 2929 m (9610 ft) in a granodiorite intrusive, where the rock temperature was 197°C. Experiments in GT-2 confirmed the results of similar experiments in GT-1 but at greater depth and higher temperature.

In 1975, well EE-1 was directionally drilled in an attempt to intersect a hydraulic fracture made from near the bottom of GT-2. It reached a final depth of 3064 m (10 053 ft) and a rock temperature of 105°C, but did not intersect that fracture. However, another hydraulic fracture made from EE-1 did permit enough flow through the rock between the two fractures to make useful experiments possible.

By 1977 there had been significant improvements in equipment, instrumentation, and wellbore- and fracture-mapping techniques, and the lower part of well GT-2 was directionally redrilled in an attempt to intersect the hydraulic fracture made from EE-1. Apparently it did so, but at a point too near the upper edge of the fracture, so that flow impedance between the two wells was still very high. Therefore GT-2 was again redrilled, along a lower trajectory, and a connection with reasonably low flow impedance was achieved. With the two well-heads connected at the surface through an air-cooled heat exchanger, this became the Fenton Hill "Phase I" (or "Research") HDR system (Fig. 3).

The Phase I system was convincing with regard to the feasibility of creating and operating an HDR heat-extraction loop and using the heat that it produced. However, while it could have heated several hundred homes, it did not produce heat at a temperature or rate that could support a commercial electrical power plant. To more nearly approach the requirements of that higher temperature application, a larger, hotter "Phase II" system has been planned and is now being developed at the same site. Its design was of course based on experience in constructing and operating the Phase I system.

To avoid the problems anticipated in accurately mapping a series of horizontally and vertically separated fractures and then directionally drilling through a specific point on each of them, it was decided to develop the Phase II system by drilling both holes and then extending the hydraulic fractures from one wellbore to the other.

The injection well, EE-2, was completed as planned in May 1980 at a vertical depth of 4389 m (14 400 ft) where the rock temperature was 320°C. (This was about 50°C hotter than had been predicted by extrapolating temperature gradients measured in the Phase I wells, presumably because the inclined section of EE-2 was drilled toward a magmatic heat source underlying the Valles Caldera.) The production well, EE-3, was completed in August 1981 at a vertical depth of 3977 m (13 049 ft) and in its inclined section is about 370 m (1215 ft) above EE-2. Approximately 1000 m (3000 ft) at the bottom of each well were left uncased.

The first two hydraulic fracturing attempts in the Phase II system were made by pumping water through inflatable open-hole packers set about 90 m (300 ft) off bottom in EE-2. In both cases the packers failed before there was evidence that a hydraulic fracture of significant size had been produced. Therefore a steel liner 11.4 cm (4.5 in.) in outside diameter, terminating at its upper end in a polished-bore receptacle (PBR), was cemented in place with its lower end 136 m (447 ft) off bottom. With a sliding seal at the end of drill pipe or pressure tubing inserted into the PBR, water was pumped through the liner into the open-hole section below it. In five pumping operations, four of which were terminated by equipment problems, a total of 8820 m<sup>3</sup> (2.33 × 10<sup>6</sup> gal) of water was injected into this region.

Formation breakdown was observed at a wellhead pressure of 33 MPa (4800 psi). Mapping the source locations of acoustic signals generated by subsequent fracturing events indicated growth of a set of large hydraulic fractures, initially as planar features sloping upward toward the east at about 45°. Thereafter the microseismic events were distributed throughout an oblate volume containing those planar features and having a similar strike and dip. The fracture system appeared to pass below and beyond the bottom of well EE-3 and made no hydraulic connection to it. Because it seemed unlikely that further pumping would produce a connection, it was decided to make the next attempt higher in the hole, where the relative positions of the open-hole sections of the two wellbores increased the probability that an inclined fracture would intersect EE-3.

In addition to this unexpected fracturing behavior, which was quite different from that observed a few thousand feet higher in the Phase I wells, hydraulic fracturing resulted in the evolution of large quantities of gas from the reservoir formation. Its presence resulted in a long series of stress-corrosion-cracking failures of downhole tubular goods and long and expensive fishing jobs and programmatic delays. To isolate an open-hole section higher in the EE-2 wellbore, a sand and gel plug was emplaced in it, initially to a well depth of

3 638 m (11 935 ft).

In the first hydraulic fracturing operation in this open-hole section of EE-2, 903 m<sup>3</sup> (239 000 gal) of water were injected and three fracture zones were created—about 30 m (100 ft) apart along the wellbore. Pumping was terminated by a drill-pipe failure, as were two subsequent pumping operations. In one of them, an additional 42.8 m<sup>3</sup> (11 300 gal) of water were injected. After failures of a packer and then a coupling on the frac string, the next successful fluid injection was accomplished during the first week of FY83.

During Fiscal Year 1983, attention was focused on hydraulic fracturing experiments at depths around 3.5 km (11 473 ft) in the two inclined wells of the Phase II system and on improved facilities and techniques for mapping the source locations of acoustic signals generated by the fracturing events. Mathematical modeling of the fracture systems produced in these and earlier experiments was given additional emphasis as was development of a family of "slimline" high-temperature downhole instruments that can be used within or through relatively small-diameter pressure tubing.

Almost from its beginning, the HDR Program has operated at, or beyond, the limits of existing downhole technology with regard to equipment, instruments, and experimental techniques. It has therefore been necessary to work with industrial manufacturers, service companies, other laboratories, universities, or independently, to improve such things as high-temperature drilling, drill-guidance and well-completion equipment, borehole-surveying instruments, well-logging and downhole-monitoring tools, and the equipment and techniques for a variety of tests and innovative experiments. Many of these items are now finding useful applications outside of the HDR Program. Recent progress in several of these areas is described below.

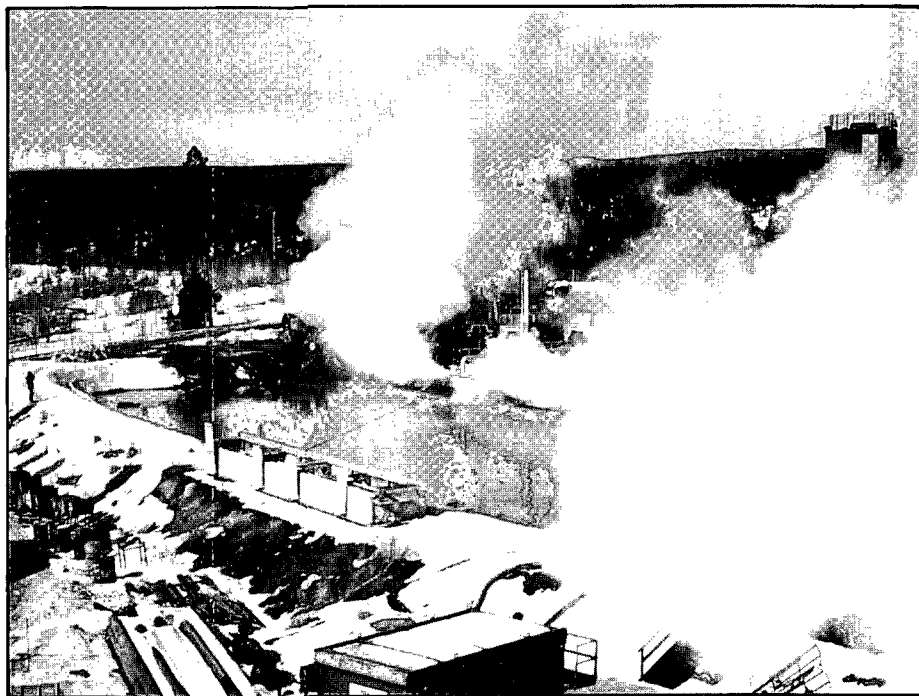
Similarly, until recently, there has been little interest in analyzing and modeling the thermal, hydraulic, and mechanical behavior of fractured geothermal systems. There has also been important progress in this area in the HDR Program.

Because hot dry rock represents an essentially inexhaustible supply of thermal

energy almost everywhere, the U.S. HDR Program has attracted international interest ever since it was first publicly announced. Parallel and complementary programs have since been initiated in several other countries, notably in the Federal Republic of Germany, Japan, Great Britain, Sweden, and France. Under an International Energy Agency (IEA) Agreement, agencies of the Governments of West Germany and Japan (KFA-Jülich and NEDO) now participate directly in the Fenton Hill Project. This involves partial financial support, membership in its International Steering Committee (ISC), and long-term assignment of scientists and engineers from both countries to the HDR staff at Los Alamos. Under a bilateral agreement between the U.S. DOE and the Italian Energy Agency (ENEL), a close relation with geothermal programs in Italy has been maintained. There is continuing informal cooperation and information exchange with individuals and organizations in other countries.

The precision and accuracy of locating the sources of acoustic signals detected during hydraulic fracturing operations have been increased by improvements in equipment, drilling of another deep hole for geophone emplacement, and additional station calibrations. Analysis of the signals has

*Figure 4. Steam venting from HDR reservoir after termination of MHF pump.*



also been improved and broadened.

Development of slimline downhole instruments has included a detonator tool used to fire small explosive charges for geophone calibration, a geophone package using high-temperature electronics and requiring no temperature protection, and final design of a high-temperature borehole acoustic televiewer. A "crosswell acoustic transceiver" has also been developed for investigating rock type and structure between wellbores.

These and other activities in the Hot Dry Rock Program are discussed in this Annual Report for Fiscal Year 1984.

## FENTON HILL SITE OPERATIONS

### Phase II Energy Extraction System

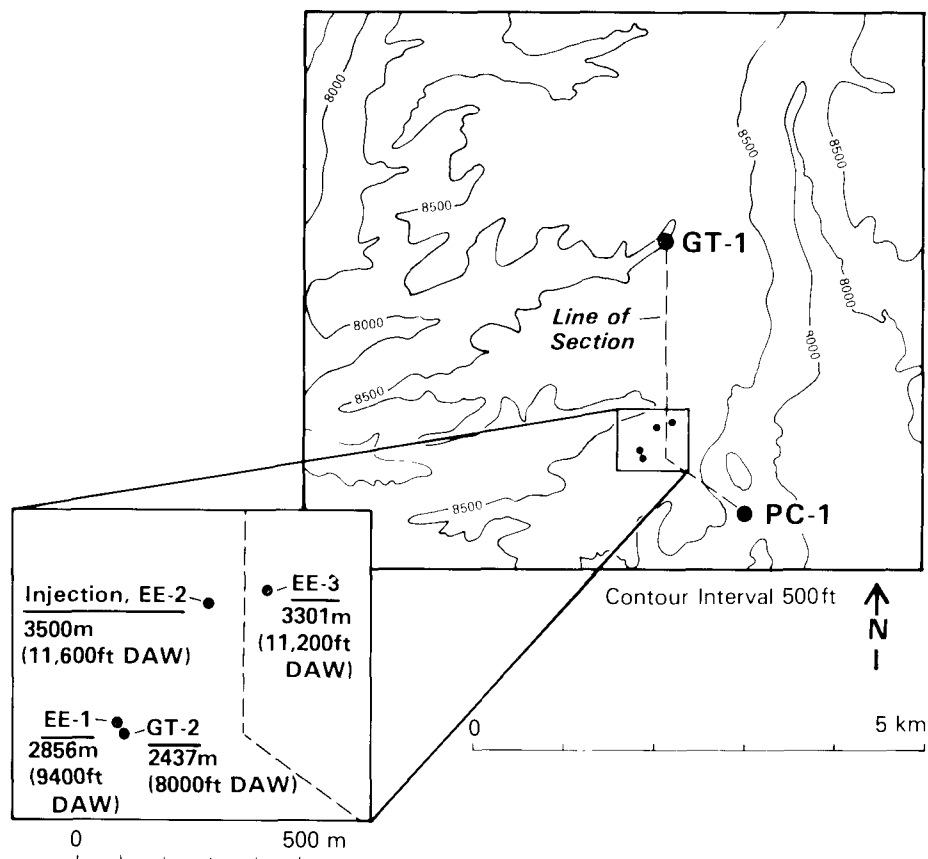
At the end of October 1983, a new 140-mm (5.5 in.) diameter low-alloy steel fracturing string for well EE-2 had been received and preparations were being made for a very large fluid injection into well EE-2, the MHF Experiment 2032. In preparation for this very large fracturing test, well EE-2 was cleaned to a depth of 3660 m (12 000 ft), 131 m (430 ft) below the casing shoe at 3529 m (11 578 ft), and a series of diagnostic logs was run. Repeated small fluid injections with temperature logging showed that a major fracture about 3 to 6 m (10 to 20 ft) below the casing shoe accepted about 50% of the injected water; another about 97 m (320 ft) below the casing shoe accepted about 30% of the water; and there were smaller fluid-acceptance zones about 43 m (140 ft) below the casing shoe and in the bottom 30 m (100 ft) of the open-hole section. To confine subsequent fluid injections to a single fracture zone, the top of the previously emplaced sand plug was raised to a point 21 m (69 ft) below the casing shoe.

A specially designed casing packer, penetrated by the new tubing string, was set in the casing at a depth of 3456 m (11 340 ft)

and was successfully pressure tested by pumping  $360 \text{ m}^3$  (95 000 gal) of water through it with differential pressures across the packer up to 31.4 MPa (4550 psi).

After final preparations of the MHF test, a total of  $21,300 \text{ m}^3$  ( $5.63 \times 10^6$  gal) of water was injected into the open-hole section of EE-2 in 61 hours, from December 6 to 9, 1983. Pumping pressures up to 48.3 MPa (7000 psi) were used to maintain flow rates up to 132  $\ell/\text{s}$  (2090 gpm). The experiment was terminated by fatigue failure of a threaded connection between a high-pressure flow line and a flange at the wellhead. The resulting rapid vent returned to the surface about 54% of the water that had been injected, and delivered thermal energy to the surface at rates estimated to have been 100 MW(t) initially and an average of 30 MW(t) over the 3.3-day period of rapid venting (Fig. 4). No connection was made to the other well, and there was damage to both the well casing and the fracturing string. However, both the volume of fluid injected and the seismic map described below indicated that a very large fracture system had been created; the amount and rate of fluid return indicated that the fracture system was tightly contained and well connected; and the high rate of energy production indicated that heat was extracted effectively from the fractured reservoir rock back through well EE-2.

The source locations of microseismic signals generated during the MHF test, as determined by triangulation using data collected by the Precambrian Net (Fig. 5), occupy a roughly tabular volume about 900 m (3000 ft) high, 1000 m (3300 ft) wide, and 400 m (1300 ft) thick, which strikes about  $\text{N}8^\circ\text{W}$ , is inclined at about  $20^\circ$  to the vertical and is roughly centered around the injection interval in well EE-2. The total seismic moment released was only about 0.1% of that which present theory indicates should have been released, suggesting that a large fraction of the energy supplied by pumping was expended in the aseismic opening of tensile fractures. With the assumptions that it did and that the shear signals whose source locations were plotted reflect the approximate dimensions of the fractured volume, numerical models—based on injection and venting



behavior—were constructed, representing the thermal-energy potential of the fractured reservoir. These suggest that the MHF zone is potentially capable of producing 35 MW(t) at temperatures above  $195^\circ\text{C}$  for 20 years. Uncertainties in these calculations are large, but they at least indicate that a thermal reservoir extensive enough to be commercially useful has been opened.

Samples of the fluid vented at the end of this experiment contained 430 ppm of silica (corrected for flashing), which is consistent with equilibrium in the dissolution of quartz by water at  $216^\circ\text{C}$ . This agrees well with the temperatures both of the formation at the depth of the fractured reservoir and the temperature of the superheated water, before flashing, in the later stages of venting.

At the conclusion of the massive hydraulic-fracturing experiment in well EE-2, it was known only that it had failed to produce a hydraulic connection to the other well and that preliminary acoustic maps indicated that there was a seismically quiet

Figure 5. Map view showing locations of precambrian network seismic stations used during Experiment 2032.

region around the EE-3 wellbore. A series of experiments was therefore conducted to investigate the behavior of this quiet region, determine whether it could be penetrated by a hydraulic fracture (which might intersect the fracture system created from EE-2), and provide an opportunity for improvement of acoustic fracture-mapping equipment and techniques. So that preheating of the water used in these experiments would not be necessary, tension in the EE-3 well casing was released before fluid injection began.

Temperature and radioactive-tracer logging of EE-3 showed that, when it was pressurized, most of the injected fluid left the wellbore in the water-loss zone just below the casing. The open-hole section containing this zone was therefore bypassed by emplacing a packer in the cemented-in liner below it. The downhole assembly was tested by pumping about 95 m<sup>3</sup> (25 000 gal) of water through the liner into the open-hole section below it, at a wellhead pressure of 39 MPa (5700 psi). Then, in Experiment 2042, another 7570 m<sup>3</sup> (2 × 10<sup>6</sup> gal) of water were injected at an average flow rate of 53 l/s and at a pumping pressure of 41.4 MPa (6000 psi). Early in the experiment, a pressure rise in the annulus between the fracturing string and the casing indicated that there was a connection between the open-hole sections below and above the

liner. Subsequent temperature, pressure-vent, and radioactive-tracer tests showed that this was a direct fracture short-circuit with very small volume, which permitted some unknown fraction of the injected fluid to bypass the liner and enter the fluid-loss zone near the casing shoe. A temperature tool stationed in EE-2 showed no evidence of a hydraulic connection to the other well.

Seismic maps, based on Experiment 2042 data from the Precambrian Net (stations in GT-1, GT-2, EE-1, EE-2, and PC-1), indicated that the source locations of microseismic events during Experiment 2042 occupied another roughly tabular volume about 1150 m (3800 ft) high, 670 m (2200 ft) wide, and 150 m (492 ft) thick, striking about N4°W and inclined toward the east at about 35° to the vertical. It followed the EE-3 wellbore along the sand-packed interval essentially to bottom, and in its upper part was connected to a smaller feature above and to the east of the main seismic cloud—which appeared to represent fracture extension from the water-loss zone near the bottom of the casing.

Spectral analysis of 50 well-located microseismic events that occurred during Experiment 2042 suggests stress drops of 1 to 10 bars (15 to 150 psi), rupture radii of 2 to 10 m (7 to 30 ft), shear displacements of 10 to 100 μm (0.0004 to 0.004 in.), and seismic moments of about 10<sup>16</sup> dyne-cm (7 × 10<sup>8</sup> ft-lb). Again, the total seismic moment was very low, only about 1% of theoretical, suggesting occurrence of much aseismic tensile fracturing.

Since hydraulic fracturing from the two wells of the Phase II system in this deeper and more volcanically associated structural setting failed to connect them hydraulically, it was concluded that a more promising method of completing the underground flow connection would be that initially used to complete the Phase I system: redrilling of one well into the fracture system produced from the other well. Accordingly, a tentative drilling trajectory was designed to sidetrack deep in well EE-3 toward the very large fracture system created from EE-2 during the MHF test and—with a minimum of expensive directional drilling—extend it through as much as possible of that fracture system.

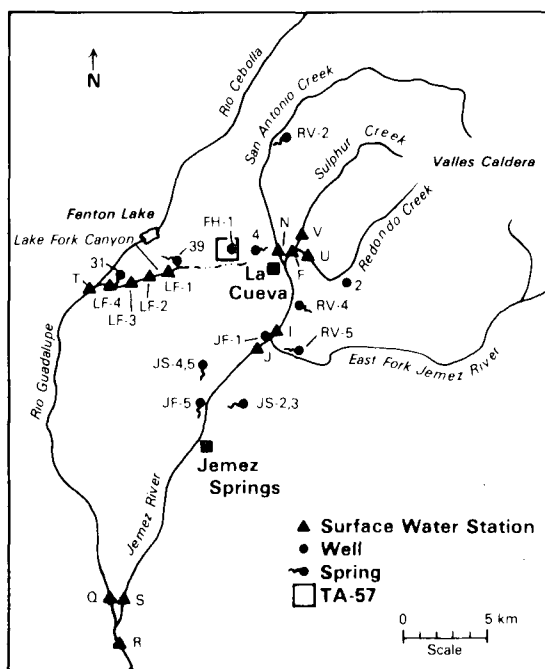


Figure 6. Map of the Fenton Hill area showing environmental monitoring sample collection locations.

## Phase II Ancillary Activities

### Diagnostic Logging

A number of borehole surveys were run in the Phase II system wellbores (EE-2/EE-3) at Fenton Hill. Many of these surveys were used to determine the condition of the boreholes and the associated well-completion equipment that had been deployed in each well. Several surveys were made with a clearance gage attached to the instrument sonde to verify the possibility of deployment of other wireline equipment within liners and packers. A brief description of the surveys is given in Table I.

### Environmental Monitoring

Activities were concentrated in collection of water samples in the vicinity of the Fenton Hill HDR site and in an effort to obtain an approved Groundwater Discharge Plan (GWDP). A small leak at the base of the six-million-gallon storage reservoir constituted the only discharge of fluid into the environment.

Samples from the domestic well and the large ponds were collected and analyzed at regular intervals. During late November and early December of 1984, 32 additional samples were collected at established locations (Fig. 6) as part of a continuing study.<sup>1,8</sup> Information obtained from these samples will be published later in a formal Laboratory report.

The effort started in 1983 to obtain approval from the New Mexico Oil Conservation Division (OCD) for a GWDP was continued. In February 1984, comments were received on a draft plan that had been submitted for review in June 1983. The February comments requested two minor modifications and indicated that the plan should be approvable upon enactment of the changes. The changes were made and the plan was printed in final format and sub-

Table I. Summary of Diagnostic Logging Surveys

Survey	Well	Purpose
Temperature Survey	EE-3	Measure insulating effect of pumping nitrogen foam in annulus.
Borehole Televiwer (Sandia)	EE-3	Run televiwer in open hole of EE-3
Borehole Televiwer (Sandia)	EE-2	Run televiwer in open hole of EE-2.
Temperature/Clearance	EE-3	Liner-patch integrity and clearance gage for new slimline detonator tool.
Temperature/Clearance	EE-3	Fluid-flow paths and clearance gage for new slimline geophone package.
Spinner Temperature	EE-2	Determine fluid-flow paths.
Magnetic Survey	EE-2	Determine exact location of lower packer.
Flowing Temperature	EE-2	Detection of new fluid-flow paths following the 5 000 000-gal hydraulic-fracturing experiment.
Gamma Survey	EE-2	Determine fluid flow in wellbore and possible intrusion into annulus with active gamma-tracer injection ( $Br^{82}$ ).
Flowing Temperature	EE-3	Detect new flow paths with wellbore pressurized.
Flowing Temperature	EE-3	Repeat of above survey following 22 h of pressurization.
Temperature/Clearance	EE-2	Check pressure integrity and clearance in 5-1/2-in. frac string.
Gamma Survey	EE-3	Obtain better definition of fluid-flow paths above and below cemented-in liner using injected tracer ( $Br^{82}$ ).
Temperature Survey	EE-3	Test PBR seals and hardware associated with Otis packer deployed in liner.
Magnetic Survey	EE-2	Test for possible damage to 9-5/8-in. casing.
Temperature Survey	PC-1	Background temperature log.

mitted to the OCD in August. In September a request for additional information was received that stated a new staff had been appointed within the OCD to review the GWDP and previous documents indicating approval should be disregarded, as all plans were being reviewed by new OCD personnel. Negotiations with the OCD resulted in a due date of April 15, 1985, for the requested information in draft form. Upon OCD approval the GWDP will be reprinted and resubmitted in final form.

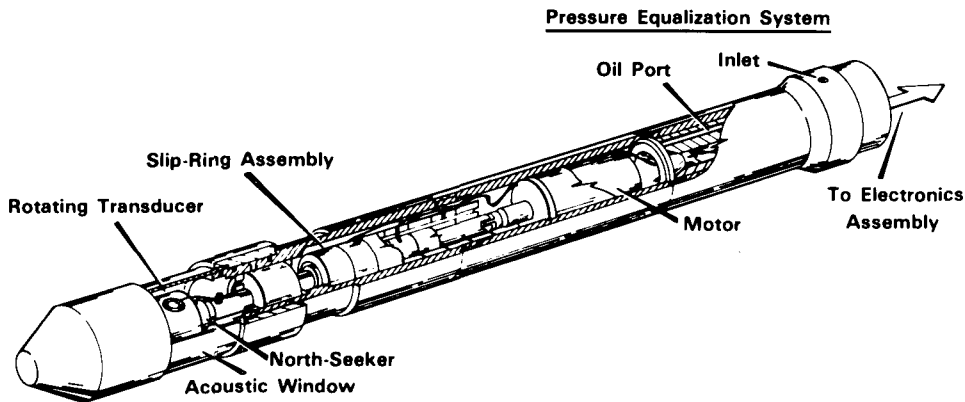


Figure 7. WBK/Los Alamos-developed borehole acoustic televiewer (BAT).

## Test Site Support and Utilities

A contract was continued with CJC, Inc. to provide site maintenance support and water supply. This contract provided snow removal, custodial and minor maintenance services in addition to occasional pipe handling, welding and miscellaneous services for the workover operations. The availability of water and haulage to the site was utilized in preparation for the large fracturing experiments.

A water collection-return system was added to the 21 300 m<sup>3</sup> (5.63 × 10<sup>6</sup> gal) pond to handle seepage water from the lined pond. The seepage, as high as 0.2 l/s (3 gpm), is a direct function of water depth in the pond.

The site was prepared for the resumption of workover operations immediately after the beginning of FY85.

## SCIENTIFIC AND ENGINEERING SUPPORT

### Tools and Instrumentation

Currently, the Westfälische Berggewerkschaftskasse (WBK) of West Germany and the Los Alamos National Laboratory of the United States are jointly developing a high temperature, digital data,

borehole acoustic televiewer for use in geothermal wellbores. The new version not only will be temperature hardened for geothermal applications but will incorporate several new concepts.

The borehole acoustic televiewer (BAT) (Fig. 7) can be broken into five subsystems. The acoustic section transmits and receives each acoustic pulse used to map the borehole wall. The reflected signal is processed by the downhole electronics. Resulting data are PCM-encoded and transmitted to the surface via a logging cable. Once the data arrive at the surface, the uphole control unit records the data on tape as well as provides the user with real-time outputs. Since the data will reside on tape, mission-specific off-line processing procedures are easily applied.

In addition to mentioned design specifications, two other criteria have been addressed. The acoustic part of the tool has been placed as far forward on the tool as possible in order to provide a "look-down" perspective. Also subassemblies have been modularly designed to aid in field assembly.

## Acoustic Measurements During Hydraulic Fracture Experiments

Preparations were made for the large hydraulic fracturing experiment to deploy an array of acoustic-detection instruments in several wellbores. The triaxial-geophone systems were stationed in three wellbores adjacent to the pressurized EE-2 borehole to record microseismic events generated throughout the 21 300 m<sup>3</sup> (5.63 × 10<sup>6</sup> gal) fluid-injection experiment. Two standard geophone packages with the associated electronics housed in the thermal-protection subassembly were stationed at 2865 m (9400 ft) in EE-1 and 2438 m (8000 ft) in GT-2 respectively. The new slimline geophone system with all temperature-hardened components was stationed at 3414 m (11 200 ft) in EE-3. The data from each triaxial geophone package were transmitted to an on-line processing unit and used to determine the location of acoustic

events produced by the fluid pressurization, resulting in a "map" of the hydraulic fracture system. The downhole geophone detector in EE-3 recorded the acoustic events continuously for a total of 80 hours during the fluid injection. Data were also recorded from a vertical-axis geophone set at a depth of 731 m (2400 ft) in GT-1.

The new slimline detonator tool was fired at depths of 2774 m (9100 ft) and 3109 m (10 200 ft) through the frac string to calibrate the geophone arrays before the pressurization experiment.

The second large hydraulic fracture experiment was performed by pressurizing EE-3 with 7570 m<sup>3</sup> ( $2 \times 10^6$  gal) of water. Again, an array of downhole geophone instruments was deployed in GT-2, EE-1, and EE-2. This time a vertical geophone package was also inserted in the new PC-1 Precambrian borehole to complement the vertical phones in GT-1 in what was termed the Precambrian Net. The slimline geophone package operated continuously throughout 72 hours of pressurization at a depth of 3350 m (11 000 ft) in EE-2. A temperature survey was run immediately following the pressurization experiment.

## Instrument-Development Tests

Several instrument-development tests took place in the Fenton Hill wellbores to test new tools in the high-temperature environment. The crosswell-transceiver sondes were run in the EE-1 and GT-1 boreholes to test overall performance. The slimline detonator tool was deployed in EE-2 to test increasing detonator loads up to 10 g of explosive charge. This test required deployment of the triaxial-geophone arrays in Wellbores EE-1, EE-2, and EE-3. Three separate trips were made in EE-2 to fire two detonators per trip.

## Cooperative Development Programs

The high-temperature equipment developed for the Hot Dry Rock Project was

used in conjunction with other DOE programs. A high-temperature spinner/temperature/pressure logging tool designed by Denver Research, Inc., under another DOE-funded program, was tested at Fenton Hill using the Los Alamos high-temperature armored cable and associated draw works. All surface signal-conditioning and data-acquisition electronics, including computer interface and appropriate software, was provided with the well-logging equipment.

Los Alamos logging equipment and field crews supported the Sandia National Laboratories work in the Salton Sea area in the Imperial Valley (Fig. 8). The Sandia televiewer was used to survey several wells for Union Geothermal. Temperature logs were run using the Los Alamos equipment prior to running the Sandia televiewer. Temperatures encountered in these wells reached 260°C.

A crosswell-acoustic experiment was performed at Rifle, Colorado, to collect data for a comprehensive tomographic imaging of sand channels in the coastal zone sediments. Crosswell surveys were successfully run in three wells over a 10-day period. The transceiver equipment performed exceptionally well with a very high signal-to-noise ratio.

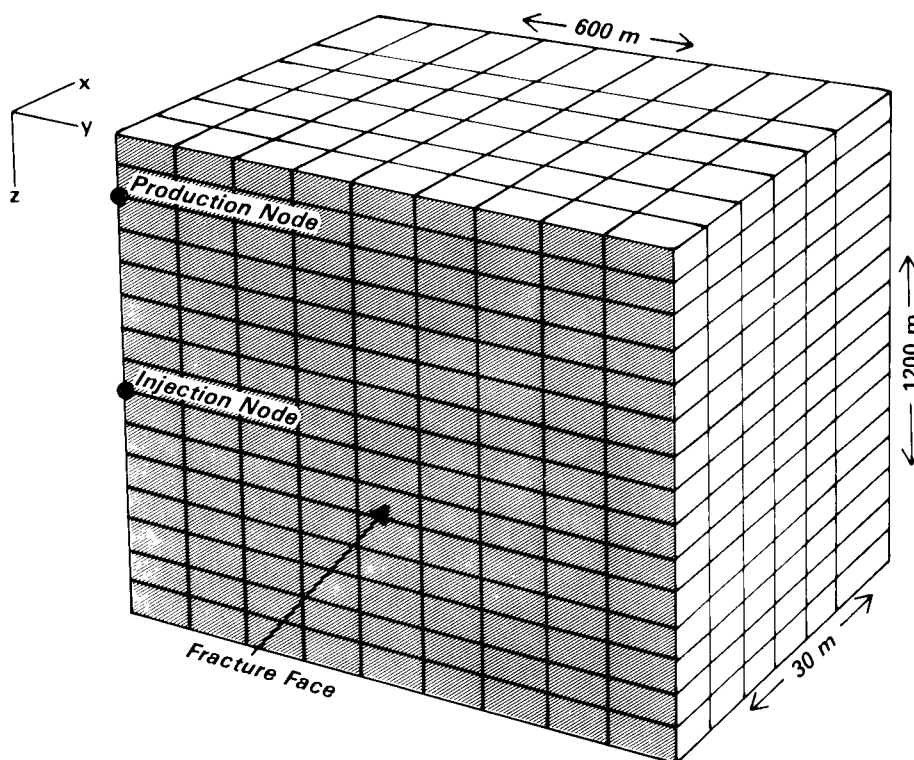
*Figure 8. Los Alamos high-temperature logging equipment in use at a Salton Sea geothermal site.*



## RESERVOIR ENGINEERING

The reservoir engineering effort during Fiscal Year 1984 consisted of six major tasks. These were reservoir analysis, microseismic analysis, tracer development, rock-mechanics research, geochemistry, and computer-code application and development. Highlighted in the reservoir analysis section is work supporting the existence of large [2-mm (0.08-in.) aperture] tensile fractures and work sizing the reservoir created in the large fracturing experiment in EE-2. It appears that the system is large enough to sustain 35-MW(t) production over 20 years. The microseismic section gives details of the analysis carried out for the MHF experiments in EE-2 and EE-3 and contrasts the results of different location techniques. The tracer work during 1984 dealt primarily with reactive tracers, which show promise of predicting early-time reservoir-temperature distributions. The rock-mechanics work during the past year was wide ranging. It dealt with the analysis of the Fenton Hill stress field in the general regional setting as

Figure 9. Computational grid for fracture model.



well as projects to determine pressurization schemes that minimize the effort in hydraulically connecting EE-2 and EE-3. Geochemistry research was highlighted by work on geochemical kinetics. The kinetic approach, as opposed to the equilibrium approach, to geochemistry can be used to predict reservoir lifetimes far in advance of thermal breakthrough. The computer-code work consisted of getting a coupled fluid-flow/rock-mechanics code (ROCMAS) to work on the Los Alamos computing system and then running verification problems. Improvements were made on the reservoir-simulation model FEHM to make it run substantially faster.

## Reservoir Design and Analysis

In Fiscal Year 1984, several experiments were performed in the Phase II wellbores EE-2 and EE-3. These included pumping tests, temperature logs (flowing and static), and radioactive-tracer experiments. Because of space considerations, we report here on the reservoir analysis of only two major experiments. These were massive hydraulic fractures in EE-2 and EE-3 (Experiments 2032 and 2042, respectively). In this section an analysis of fracture apertures will be presented for the experiments, and then a detailed reservoir-size assessment will be presented for Experiment 2032. Finally, a comparison of the pressures and impedances in Experiments 2032 and 2042 is made to previous Phase II pumping experiments.

## Fracture-Aperture Calculations

The high volume fracturing operations of Experiment 2032 and Experiment 2042 produced high-volume reservoirs. Microseismic-event mapping showed that much of the fluid went into creating shear fractures. These fractures have small apertures. Tensile fractures have large apertures but are difficult to identify using seismic techniques. Therefore a technique of analyzing

the flow rate and pressure was used to investigate the tensile fracture possibilities of these reservoirs.

## Aperture Equations

Aperture/pressure equations can be derived, for example:

$$a = 3\sqrt{\left[\frac{6\dot{m}\dot{Q}}{\pi\Delta P}\ln\left(\frac{r}{r_w}\right)\right]} \quad (1)$$

if it is assumed that the fracture is radial and the flow is laminar. Similar equations can be derived for radial/turbulent flow and linear fractures. In the above equation,  $\dot{Q}$  is the flow rate,  $\Delta P$  the pressure drop,  $\dot{m}$  the viscosity,  $r$  the radius,  $r_w$  the wellbore radius and the aperture. Using the formulas and data for the experiment, apertures of the order of 0.002 m (0.08 in.) were obtained for Experiment 2032 and apertures of 0.001 m (0.04 in.) were obtained for Experiment 2042. The experimental data and aperture sizes are summarized in Table II.

Table II. Summary of Experiments 2032 and 2042

Experiment	2032	2042
Flow rate, M <sup>3</sup> /s	0.111	0.025
$\Delta P$ MPa	13.7	13.2
BHT °C (during flow)	12.8	38.6
Cumulative Injected, m <sup>3</sup>	21 330	750
Apertures, mm	1-2.3	0.3-1
Calculated Fracture extent, m	400-600	400-600

is given here. A value of the aperture from this analysis [0.002 m (0.08 in)] was used as the maximum fracture aperture during Experiment 2032 at 80 MPa (11 600 psi). A finite-element-based geothermal reservoir simulator<sup>10</sup> was then used to model the pumping and flowback during the fracturing experiment. To model the rapid opening of the fracture, the aperture dependence with pressure was modeled by an exponential function

$$w = 2 \times 10^{-4} \exp(9.21 \Delta P/44) \quad (2)$$

where  $\Delta P$  is the difference between the current pressure and the initial pressure. With Eq. (2)  $w = 2 \times 10^{-4}$  at  $\Delta P = 0$  and  $w = 0.002$  m (0.08 in) at  $\Delta P = 44$  MPa (6400 psi), the observed fracturing pressure difference. Other forms of aperture law could be used and indeed the experiment results would indicate an even faster opening law. The form used here was near the limit of computational stability. The permeability was allowed to vary according to the usual parallel-plate model

$$k = \frac{w^2}{12} \quad (3)$$

The computational grid for the simulator runs is shown in Fig. 9. A less complex mesh could have been used to model the fracturing experiment, but this mesh was also used for the long-term drawdown simulations. Other parameters used in the computer input are shown in Table III.

## Reservoir Analysis of Exp. 2032

Experiment 2032 was carried out on December 6-9, 1983, and 21 330 m<sup>3</sup> (5.63 × 10<sup>6</sup> gal) of water were injected. A variety of data was available. These data included flow rate, bottom-hole pressure, and seismic-event mapping. Upon flowback of the injected fluid, geochemical and temperature data and volume of retained fluid estimates were obtained to assess the size of the reservoir created in Experiment 2032. A technique was developed to utilize the data mentioned above. This has been reported previously.<sup>9</sup> A brief summary of the method

Table III. Experiment 2032 Simulation

Parameter	Symbol	Value
Permeability, m <sup>2</sup>	k	10 <sup>-18</sup> matrix
Fracture (maximum)		10 <sup>-8</sup>
Thermal conductivity, W/m°C	K	2.7
Porosity	φ	0.001 matrix 1.0 fracture
Rock density, kg/m <sup>3</sup>	ρ <sub>t</sub>	2700
Rock specific heat, J/kg°C	C <sub>r</sub>	1000
Fracture radius, m	—	500
Fracture width, m	—	0.0024
Initial pressure, MPa	P <sub>ij</sub> <sup>o</sup>	hydrostatic
Initial temperature, °C	T <sub>ij</sub> <sup>o</sup>	216
Injection rate kg/s	—	111

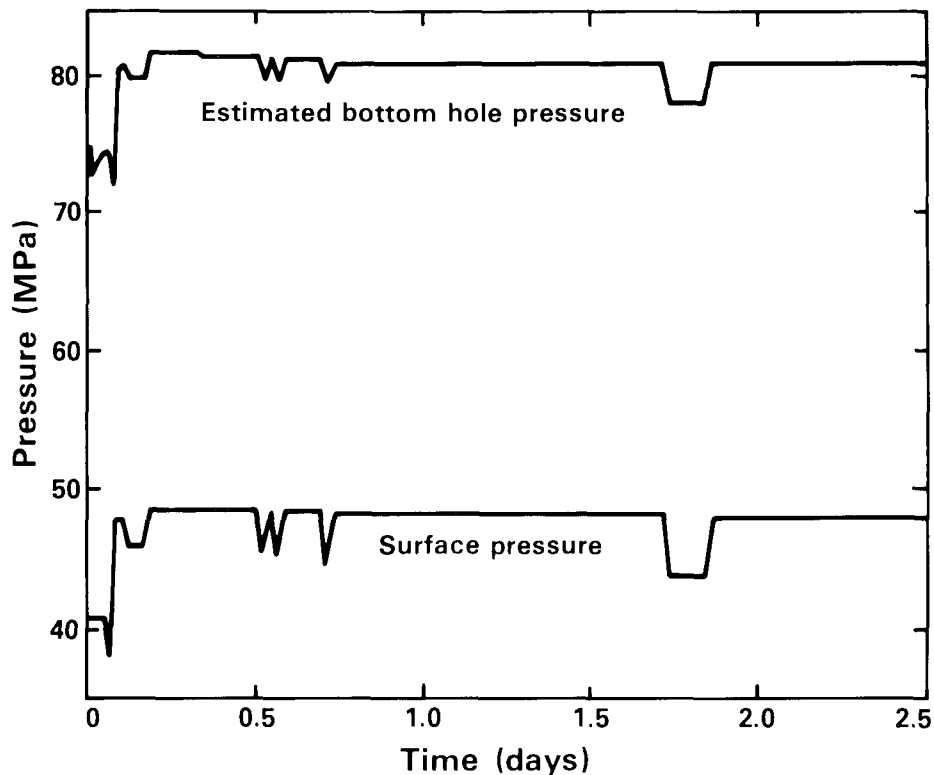
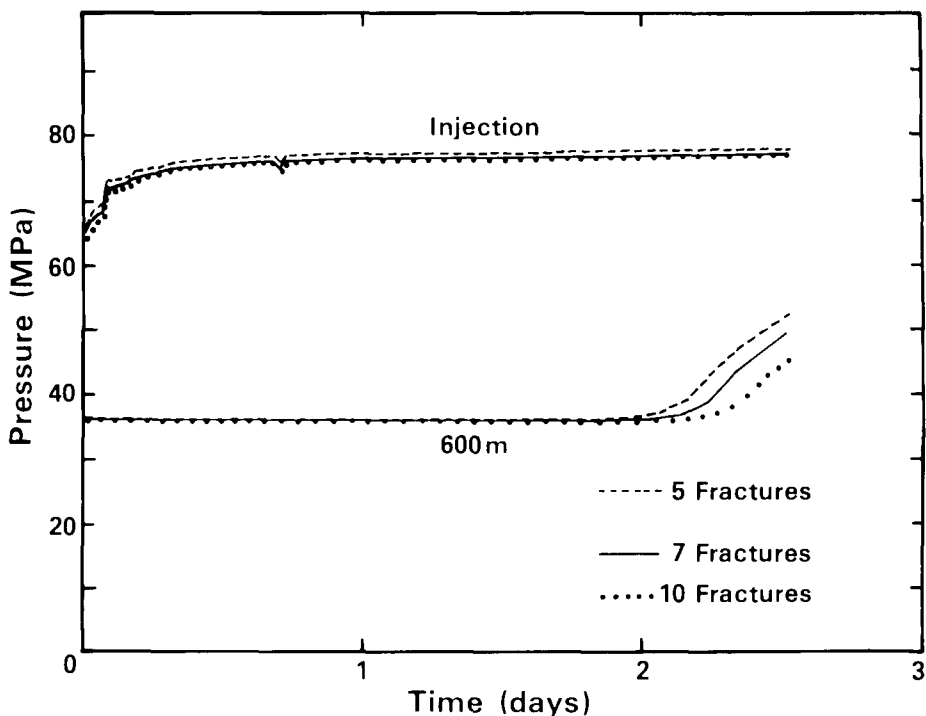


Figure 10. Pressure history during Experiment 2032.

Figure 11. Model pressure history during Experiment 2032.



## Model Results

To model the results of Experiment 2032 several preliminary calculations were made. The seismic surveillance put bounds on the dimensions of the computational grid. Since there were no events recorded 500 m (1600 ft) or farther from the injection point, the limit of the flow extent was placed at 600 m (2000 ft). The minimum thickness of the seismic-event cloud was 200 m (660 ft) (orthogonal to the fractures). This distance was used to bound the spacing between fractures. The unit-fracture concept was used whereby the flow was divided into  $n$  parallel fractures each carrying  $1/n$  of the total flow with associated volume of bounding porous media. This concept leads to optimistic values of the water loss in an HDR system due to inability to represent the permeation from the end fractures; however, for the small times involved in the fracturing process, little error would result. A material balance of the injected fluid would yield about 13 fractures of 0.002-m (0.08 in.) aperture and 500-m (1600-ft) radius. However there are probably less than this number of "large-aperture" fractures due to permeation along orthogonal joints and the fact that the seismic results indicated a preponderance of shear events which would yield aperture along the sheared surfaces many times smaller. In this work it is assumed that the larger tensile fractures carry the bulk of the fluid and that the small shear fractures can be accounted for by permeation. The permeability in the direction orthogonal to the large fractures was set to a value of several microdarcies (the *in situ* permeability) but allowed to increase to a value determined by parallel-plate theory for an aperture of 0.0002 m (0.008 in.).<sup>4</sup> This value was then averaged over the mean joint spacing orthogonal to the main fractures. This joint spacing was taken as 1 m (3.3 ft) from surface-outcrop observations. This gave the effective maximum permeability in the direction orthogonal to the fracture of about  $10^{-14}$  m<sup>2</sup> (0.01 darcy). The behavior of the orthogonal joints with pressure is very uncertain.

Figure 10 shows Experiment 2032 pressure responses. Figure 11 shows the computer-generated response. From the figure it is evident that all the fracture cases show a significant pressure rise at a point 600 m (2000 ft) from the injection point. So far heat transfer was not included in the modeling process. The computer-generated temperature near the injection point showed a rapid rise to initial conditions upon flowback. This may be compared to a value of the return temperature inferred from geochemical analysis of the return fluid, which also indicated a rapid temperature rise to the temperature of the fluid at the injection point (216°C).

The last piece of information used to verify the model is the amount of fluid return after pumping, and it is speculative. It was estimated that about 50% of the injected fluid returned in 3 days following the end of pumping. Fig. 12 shows the flow rate calculated by the computer model. Using the area under the curve as an indicator, it is evident that the model returns the required amount of fluid after the end of pumping.

## Summary of Modeling Results

The model needed to fit the data consisted of

1. an aperture law of the form  
 $w = 2 \times 10^{-4} \exp. (9.21 \Delta P / 44)$ ,
2. a permeability law of the form  
 $k = w^2 / 12$
3. 10 fractures, and
4. fracture spacing of 20 m.

## Application of Long-Term Reservoir Simulation

With the reservoir model validated against the fracturing experiment, the model was run with an extraction flow rate of 20 BPM (barrels per minute) (840 gpm). The reservoir proved capable of sustaining 35 MW(t) for 20 years.

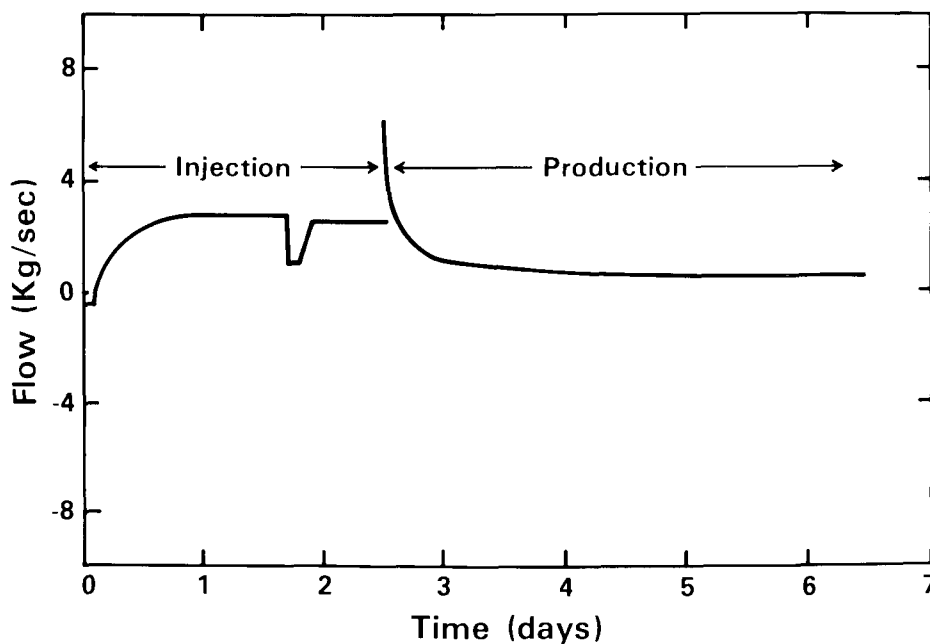
## Pressure Dependence in Fenton Hill Stimulation Experiments

It has been found that for the flow in fractures the pressure (P) scales with the square root of the flow rate  $\dot{Q}$  for turbulent flow according to the formula:

$$P = A + B \dot{Q}^{-0.5}$$

where A is the zero flow rate pressure and B is related to the impedance of the fracture.<sup>11</sup> In Table IV, all the hydraulic fracture experiments at Fenton Hill are summarized. As is seen from this table, these experiments can be classified into four groups according to the well and depth. In each experiment, Eq. (1) holds the data well. One remarkable result from Table IV is that the impedance of the reservoir of each group decreases with time. While the long term decrease in impedance observed in Fenton Hill reservoirs is thought to be due to thermal contraction effects, this short term behavior may be due to self-propping of the reservoir.

Figure 12. Flowrate during Experiment 2032.



## Microseismology

During 1984, data from two major pumping experiments were analyzed using numerous techniques. In addition, three seismic calibration experiments were conducted in an attempt to measure the travel time from the region where seismic events were occurring to the various stations that comprise the Precambrian seismic network. Results of these calibration experiments allow us to locate reliably the positions of the seismic events relative to the location of the calibration shots. Another effort undertaken in 1984 was aimed at improving the acquisition of data during injection experiments. A new digital data-acquisition system was purchased that is capable of recording up to

48 channels of data, some at rates as high as 50 000 samples/sec. Efforts are now under way to obtain software to do event-detection on the incoming data and store waveforms of the microearthquakes.

### Experiment 2032

During hydraulic fracturing Experiment 2032, waveforms from nearly 2000 microearthquakes were digitally recorded using the current seismic data acquisition scheme. Events were located using the partial double-tool hodographic technique, an extension of the hodographic technique where travel times from a second seismic sensor supplement the travel-time and particle-motion data used in the normal hodographic technique; a travel-time technique that employs the arrival times measured at five downhole sensors that comprise the Precambrian network; and a travel-time technique that uses travel times measured at stations set up on the surface near Fenton Hill.

Figure 5 is a map showing the locations of the stations that compose the downhole Precambrian network. Data from the station located in EE-1 were used in the conventional hodographic location technique, and data from stations EE-1 and EE-3 were used in the partial double-tool hodographic technique. Fig. 13 shows locations of events calculated using the Precambrian travel-time location technique. Locations calculated using the hodographic and surface-network travel-time techniques are similar to those shown in Fig. 13.

Fault-plane solutions were calculated for some of the events that were located using the surface seismic-network data. Most events fell into two groups, based on their fault-plane solution. These groups are designated Group I and Group II. Fig. 14 shows the locations of Group I and II events and the fault-plane solutions for these two groups. Interestingly, most of these events fall in a tight cluster.

Spectra of P-waveforms were calculated to determine source parameters of events. Three-component waveforms measured in EE-1 during an event were rotated into the radial and horizontal tangential directions.

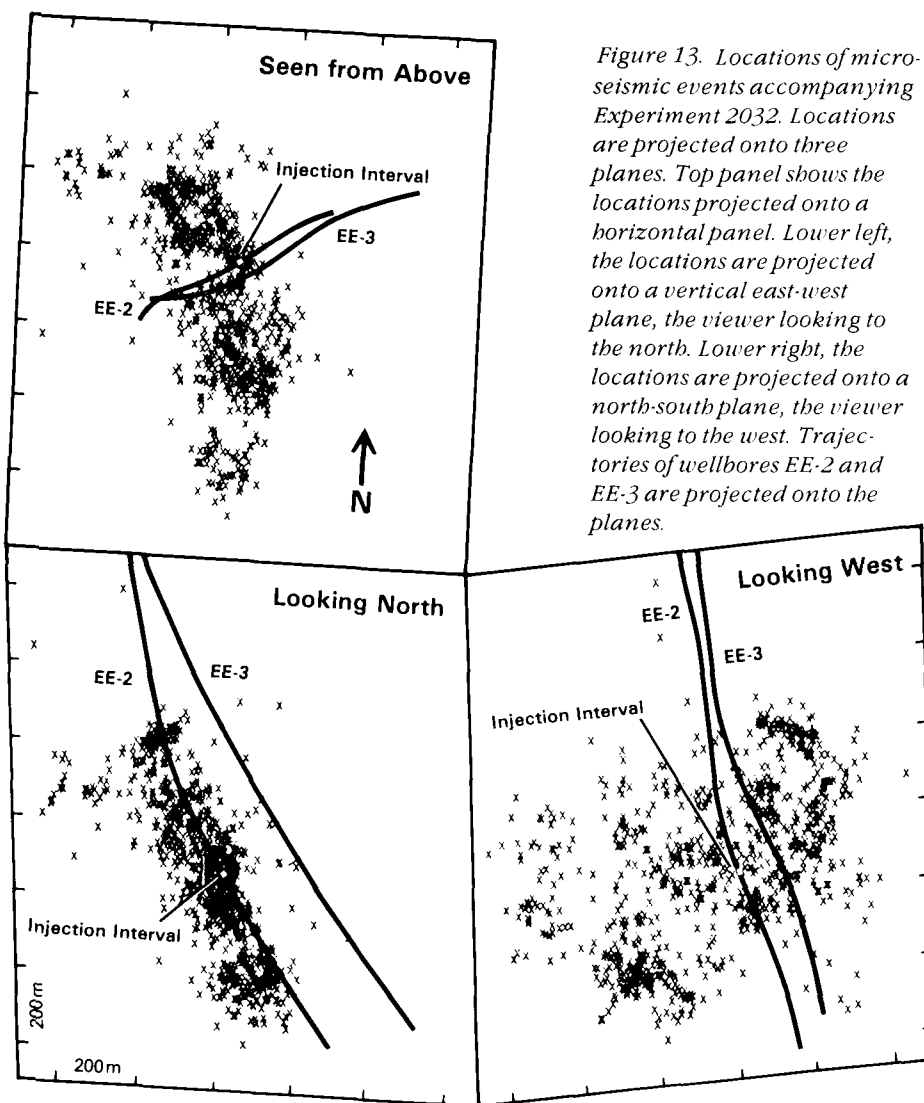


Figure 13. Locations of microseismic events accompanying Experiment 2032. Locations are projected onto three planes. Top panel shows the locations projected onto a horizontal panel. Lower left, the locations are projected onto a vertical east-west plane, the viewer looking to the north. Lower right, the locations are projected onto a north-south plane, the viewer looking to the west. Trajectories of wellbores EE-2 and EE-3 are projected onto the planes.

The spectrum of the P-wave was calculated from the radial-component seismogram. Fig. 15 is a plot of seismic moment vs source radius of earthquakes as calculated from measurements on the spectra. For the events studied, source radii range between 2 and 20 m (7 and 70 ft), stress drops range from 5 to 50 bars (70 to 700 psi), and average slip ranges from 6 to 1000 microns (0.000,2 to 0.04 in.).

Fig. 16 is a plot of the total seismic moment of all events recorded by the surface network up to a given time plotted against the total volume of water injected up to that time. For injected volumes greater than 4000 m<sup>3</sup> (10<sup>6</sup> gal), the seismic moments of all events increased linearly with increased injected-fluid volume.

### Experiment 2042

Seismic monitoring of Experiment 2042 was nearly identical to that in 2032. The slimline geophone package was moved from its location in wellbore EE-3 for Experiment 2032 to EE-2 for this experiment. This location is shown in Fig. 5. Analysis of

**Table IV. Hydraulic Fracturing Tests at Fenton Hill**

Experiment Number	Well	Date	Injection Zone Top Depth (Ft)	Total Water Volume Injected (bbls)	Regression Coefficients	
					A (psi)	B (psi/gpm <sup>1/2</sup> )
2007	EE-3	81/ 2/17	10 374	3 500	6 334	92
2023	EE-3	81/11/ 8	10 374	930	5 914	28
2033	EE-3	83/ 9/28	10 374	4 700	—	—
2025	EE-3	82/12/14	11 400	3 600	8 904	81
2042	EE-3	84/ 5/15	11 400	48 000	9 632	60
2018	EE-2	82/ 7/19	11 575	5 700	9 058	125
2020	EE-2	82/10/ 6	11 575	20 000	9 765	49
2032	EE-2	83/11/30	11 575	2 300	8 005	179
2032	EE-2	83/12/ 6	11 575	130 000	10 361	39
2011	EE-1	81/ 5/30	14 700	3 300	8 945	259
2012	EE-1	82/ 6/ 4	14 700	20 000	11 321	37
2016	EE-2	82/ 6/20	14 700	3 000	10 841	63

data for this experiment is currently in progress. Fig. 17 shows the locations of micro-earthquakes calculated using the travel-time technique and arrival times measured at the Precambrian network stations. Fig. 18 shows the integrated seismic moment plotted against injected-fluid volume. It is interesting to note that the sum of the seismic moments of all events recorded during Experiment 2032 is approximately ten times that of Experiment 2042 although approximately 3 times more fluid was injected during Experiment 2032 than during 2042.

Spectral analysis of waveforms as well as locations and fault-plane solutions calculated using surface network data are all in progress.

### Calibration Experiments

Three seismic-calibration experiments were carried out in 1984. The goal was to place an explosive at a known location in one of the boreholes and measure travel times to each of the five stations that comprise the Precambrian seismic network. In this way, the variations in the average acoustic velocity from the source to the various stations can be accounted for by implementation of travel-time corrections to each station. The travel-time corrections resulting from the three experiments are listed in Table V.

**Table V. Station Corrections**

Station	P - Correction (ms)	S - Correction (ms)
EE-1	+0.6	2.3
EE-3	-0.5	-1.5
GT-2	-1.4	-2.1
GT-1	-0.5	+10.9
PC-1	+17.4	+32.8

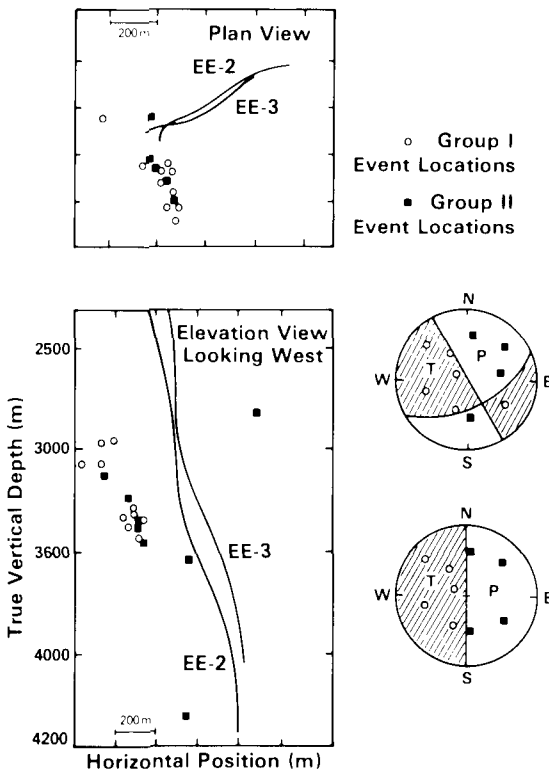


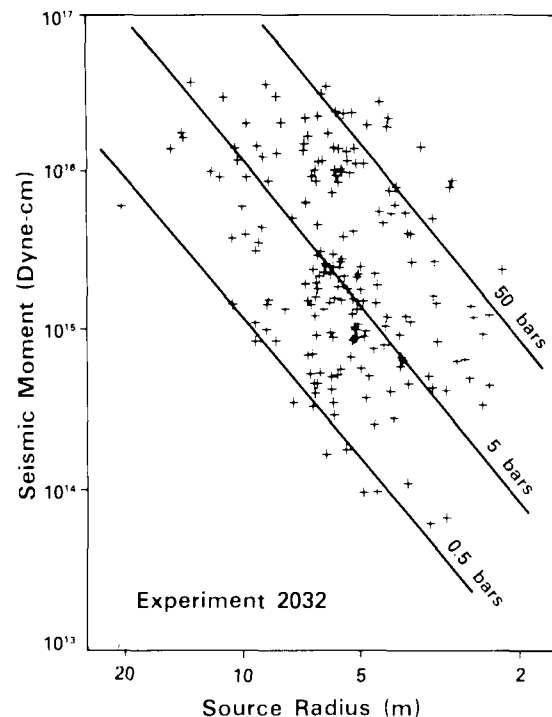
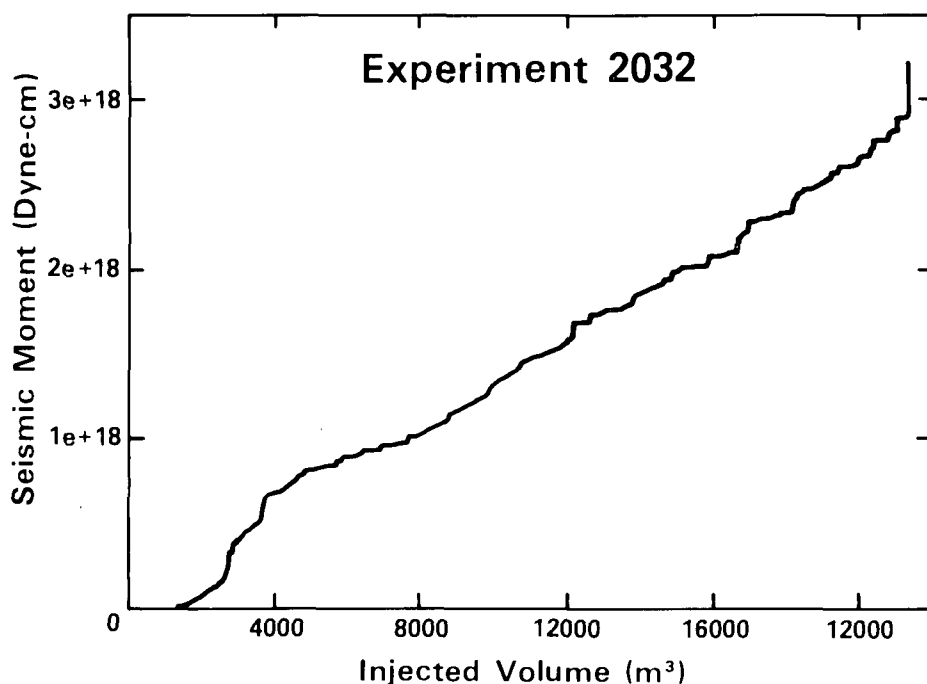
Figure 14. The two most common fault-plane solutions found to accompany Experiment 2032. Locations of events studied that had these fault-plane solutions are also shown.

Figure 15. Seismic moment vs. source radius for individual seismic events accompanying Experiment 2032. Lines of constant state stress drop are indicated by solid lines.

## Tracer Studies

The development and improvement of techniques for using both nonreacting and chemically reacting tracers were pursued throughout the year. Tracer tests are regarded as extremely important. Nonreacting tracer tests already have given essential information about flow patterns and volumes in the Phase I system and will be relied on similarly when the Phase II system is operational. Chemically reacting tracer tests have the potential of measuring temperature patterns between wells in HDR reservoirs and following the changes in these patterns as the reservoirs are exploited. Such temperature measurement is almost indispensable for making an accurate forecast of a reservoir's life. Two experimental approaches are being pursued—one which involves flow-through experiments and the other using reverse-flow techniques. A reverse-flow test would be more difficult to carry out and would interfere more with normal operation. On the other hand, there would be greater accuracy during the earlier part of reservoir exploitation than would be given by a flow-through test, and thus there would be an earlier indication of thermal draw-down. Each of the two experimental approaches can, in turn, take either of two

Figure 16. Seismic moment vs. injected fluid volume for Experiment 2032.



alternative forms: one involving a single reaction and the other using several reactions. Developments in the single-reaction approach were presented in last year's report; this year's mathematical advances were primarily in the multiple-reaction approaches. The year's progress in the development of nonreactive tracer methods and the two approaches in reacting-tracer methods are presented below, and the results of early kinetic studies of candidate tracer reactions are summarized.

**Nonreactive tracer tests.** A plot versus time of the experimental output concentration data from most nonreactive tracer tests involving fractured media usually possesses a "tail," which is a long period of low tracer concentrations during the later phases of the experiment, declining slowly toward zero. The data in this tail are usually not accurate, and it has been the custom to ignore the tail and treat only the earlier portion of the response curve. Unfortunately, the tail may represent a significant portion of the total volume in an HDR reservoir, so not considering it here may lead to significant error. No satisfactory methods of treating these data were offered by the literature, so a method of using the tail was developed during the past year. Two

items were needed: the flow rate through the portion of the reservoir penetrated by the tracer tail and the volume of this portion. Obtaining the flow rate was straightforward. Investigation showed that the volume was insensitive to several reasonable functional forms used for the tail, so any reasonable functional form could be used for the tail and a reliable value for the volume would result. Thus this study developed a reliable method for determining both flow rate through the portion of the reservoir penetrated by the tail of the tracer response curve and its volume.

**Flow-through experiments with chemically reactive tracers.** During Fiscal Year 1984, principles were developed further for using reacting tracers to measure temperature characteristics of HDR reservoirs by flow-through multiple-reaction experiments. In these tests, a suite of perhaps 10 reactions is the tracer, and a vector of conversions is obtained for each residence time sampled. Two approaches have been devised for determining a temperature profile from a conversion vector. The first involves parameter optimization using postulated functional forms for the profile. If there is insufficient knowledge of the temperature profile for the function form to be postulated, then a temperature-distribution function  $\eta(T)$  may be defined and the temperature distribution obtained by solution of the associated Fredholm integral equation. The solution of the Fredholm equation is approximate and gives only the principal characteristics of  $\eta(T)$ , as shown in Fig. 19. With these characteristics, though, a functional form for  $T$  can then be postulated and the first approach used. The experimental variable in both approaches is the activation energy of the chemical reaction, so different reactions must have differing activation energies. Optimal ranges of activation energies have been identified for both approaches. The resulting series of  $\eta(T)$ 's can be extremely helpful in developing a set of severe model constraints.

**Reverse-flow tests.** The use of a single-reaction reverse-flow tracer test has been shown to give information sufficient to establish the temperature profile in the principal flow path of the reservoir. During the

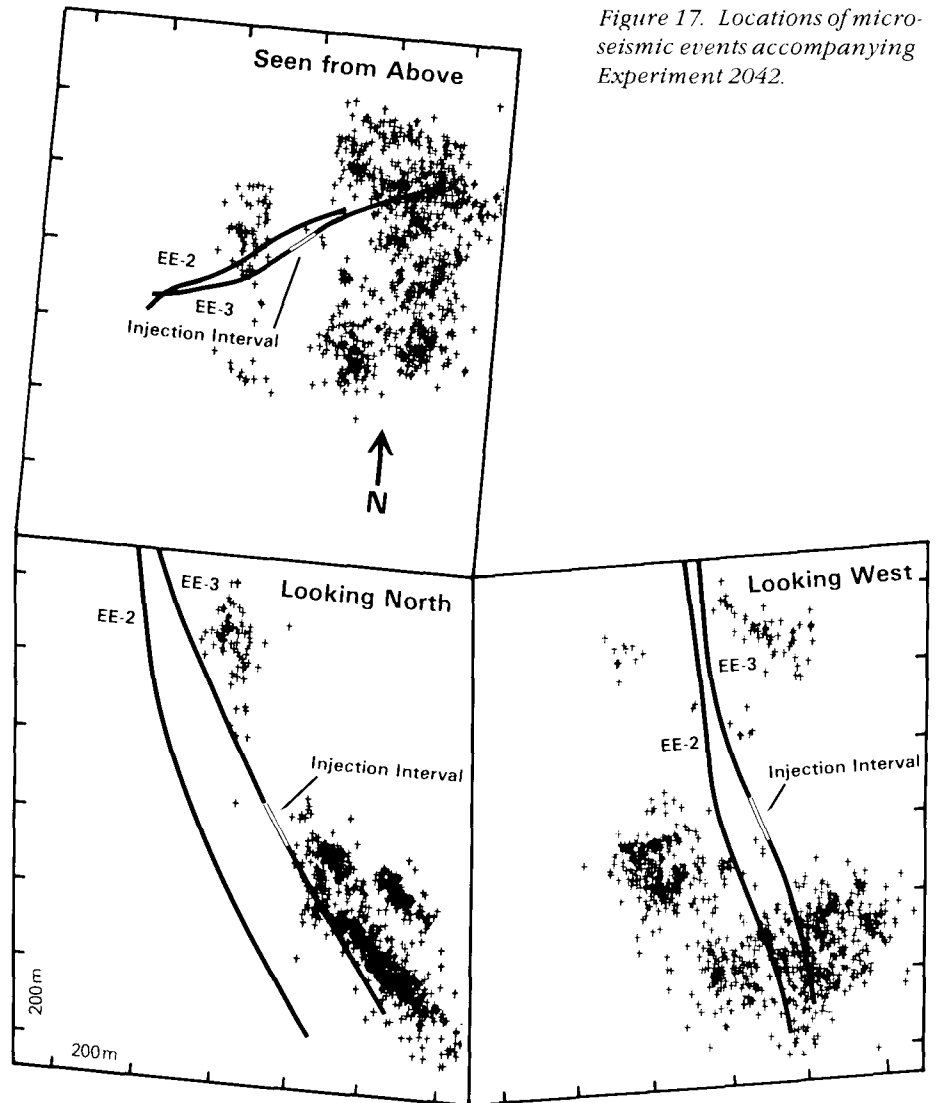


Figure 17. Locations of microseismic events accompanying Experiment 2042.

past year, the use of multiple reactions for reverse-flow tests was considered, and it was shown that the use of multiple reactions could give the temperature profiles of several flow paths simultaneously. The mathematics of this approach were developed to a significant degree during the year.

**Kinetics of candidate tracer reactions.**

Laboratory kinetic experiments also are being carried out to find suitable reacting tracers for different reservoir conditions. The reaction rate, activation energy, and pre-exponential factor must be such that the "half-life" of reaction is on the order of the average fluid-residence time in the reservoir mathematically, and whose reactants and products are soluble in water, nonsorbing,

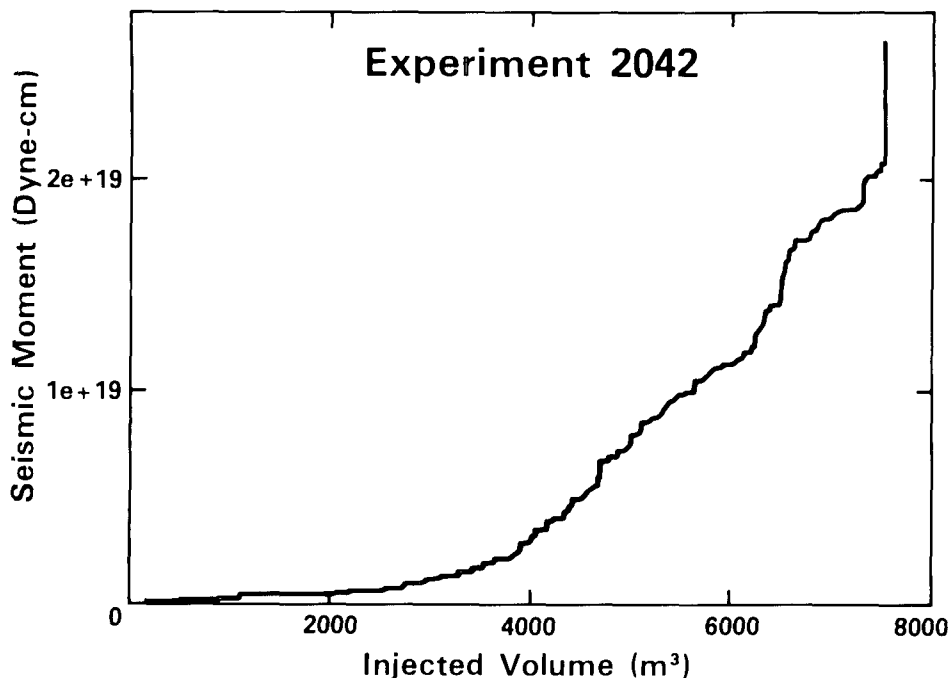


Figure 18. Seismic moment vs. injected fluid volume for Experiment 2042.

and analyzable to the desired precision. Two classes of reactions are being investigated at the present time—ester hydrolysis and amide hydrolysis. Both of these classes appear to include reactions which have the desired properties. Fig. 20 presents some of the kinetic data obtained during the past year. The reaction time  $\tau_r$  is the time required for the reactant concentration to proceed to  $1/e$  of its original value. To choose the appropriate tracer,  $\tau_r$  should equal the typical fluid residence time in the reservoir.

## Rock Mechanics

Two phenomena in the Phase II reservoir were investigated in an effort to understand the fractures. These were increase in water pressure in the cracks and pores around EE-3 and simultaneous stimulation of EE-2 and EE-3. This latter phenomenon is thought to improve the chance of connecting these two holes hydraulically.

The water level in EE-3 has been maintained at about 200 m (650 ft) above the unperturbed standing-water level for the past 2 years. This excess water pressure inflates the pores in the rock and causes an increase of 0.3-0.6 MPa (50-100 psi) in total

stresses out to about 50 m (160 ft) from EE-3. Such stress changes are thought to be just large enough to stop a conventional tensile hydraulic fracture from penetrating this zone around EE-3 and prohibit a hydraulic connection between the two wells.

Using a finite-element program, simultaneous and sequential stimulation of EE-2 and EE-3 were investigated assuming that many joints around each hole are involved in the stimulation. Simultaneous stimulation of both holes as well as merely pressurizing a previously stimulated region around EE-3 during stimulation of EE-2 encourages the stimulated region around EE-2 to grow toward EE-3. Consequently, sequential and simultaneous stimulations are useful procedures for hydraulically connecting two wells in a jointed rock mass.

Hydraulic injection processes at Fenton Hill involve three regions:

- (1) A source region, where downhole fluid pressures cause inflation, or jacking of joints, probably aseismically.
- (2) A nearfield region, or seismic cloud, or yield zone, where permeation through the joint network reduces effective shear stress, and microseismic events represent failure under a combination of source and farfield stresses, exponentially reversible.
- (3) A farfield region, or country rock, outside the seismic envelope, where strains generated in regions (1) and (2) are absorbed elastically, reversibly.

There are several ways to approach such a problem. One is to construct theoretical models of increasing complexity and determine the operative parameters by successive approximation. A second is to search for "asymptotic" conditions, that is, experiments where some of the parameters appear in degenerate or simple form.

Investigations in 1984 have followed the second approach, with studies of *in situ* material properties, the *in situ* stress field, and the relation of microseismicity to injection pressures. The result has been the estimation of some of the governing parameters, such as macroscopic structure, farfield stress, yield strength, and stress within the seismic envelope. These may now be sufficiently well known to proceed

to inversion of microseismicity for processes in the source region, which is required for delineation of the reservoir.

## Macroscopic Material Properties

Radiometric (K-Ar) age dates from Fenton Hill gneiss show a bimodal distribution which reproduces that from the Tusas Mountains to the north and Picuris Range to the east, enabling a country correlation of the gneiss between the subcrop which forms the reservoir country rock at Fenton Hill and those distant outcrops.

The correlation of metamorphic ages indicates that there are two different gneisses at Fenton Hill, which may be termed "isochemical" and "metasomatized." The Phase I system was constructed in a granodiorite intrusive at the base of the isochemical gneiss. The boundary between the two gneisses is an inclined surface at the base of the granodiorite, a "metamorphic front," with a dip of approximately 30°. The Phase II system is in the younger, metasomatized gneiss underneath this contact.

Methods of structural characterization from televiewer logs are operational, but some numerical problems remain. Preliminary results enable a structural correlation between Fenton Hill and the Picuris Range. This indicates that natural fractures are controlled by the foliations S2 (a gneissosity) and S3 (a crenulation cleavage), so that the approximating second-order permeation tensor probably has a principal plane striking N-S, near-vertical, with the long axis plunging obliquely south at between 30 and 60°.

## Farfield Stress

Experience at geothermal sites in Japan and Britain indicates that farfield stresses at the site can be satisfactorily estimated by interpolation from a regional pattern of *in situ* stress measurements.

There is no pattern of *in situ* stress measurements for northern New Mexico so,

as a substitute, data were used from Aldrich and Laughlin.<sup>12, 13</sup> These were horizontal stress trajectories determined from the morphology of magmatic intrusions dating back 5 million years. Some 77 estimates of the minimum horizontal stress direction in northern New Mexico, west Texas, and southern Colorado were used as a basis for reconstructing the regional stress field.

Figure 19. Assumed and calculated chemical distributions for the multiple chemically reacting tracer technique.

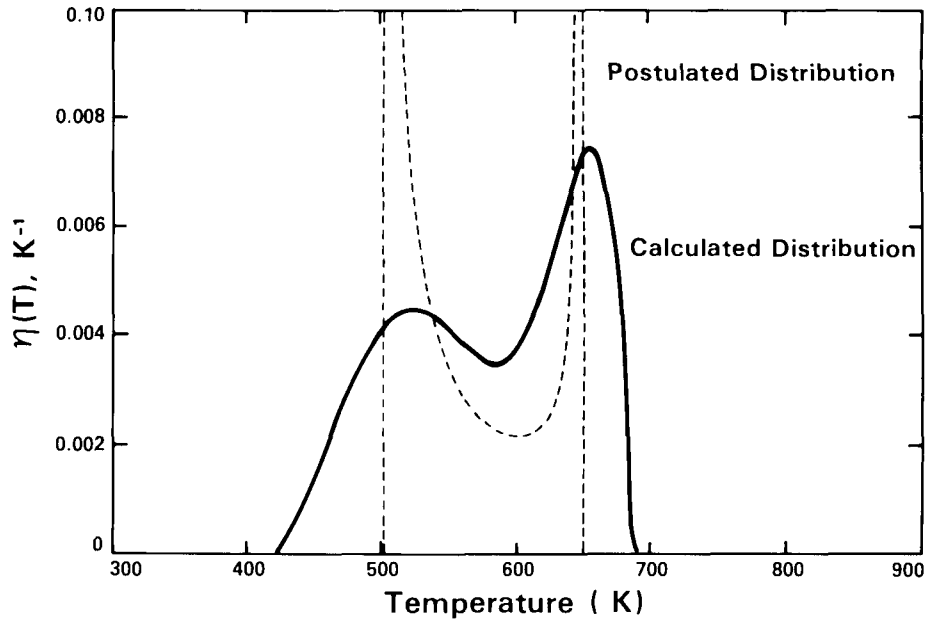
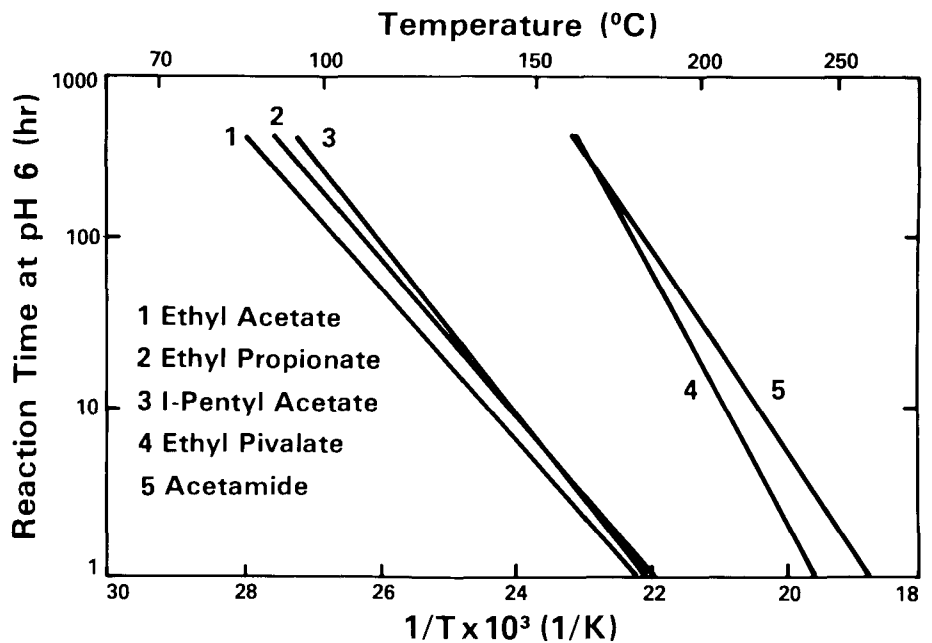


Figure 20. Experimental kinetic data for the hydrolysis of various organic esters and amides.



A new type of numerical tectonophysical model was developed by adaption of dislocation models from mining. The field points of Aldrich and Laughlin<sup>13</sup> are dilatational dislocations, inflated by injection of magmatic fluid. The numerical method sought to invert the stress features at these field dislocations by finding which regional structural features could be sources of the field. An inefficient, supervised search procedure was used, partly conjugate gradients (to select candidate sources and their segmentation) and partly steepest descent (to refine source parameters).

The tectonophysical model found that the regional stress field can be wholly explained by a dislocation at the Jemez lineament, a seismic zone some 20 km west of Fenton Hill. The sense of the dislocation vector is sinistral contraction. The source magnitude increases linearly south from the junction of the Jemez lineament and Chama fault at a rate proportional to the accumulated horizontal displacement (opening angle) of the Rio Grande Rift.

Some 47 different models gave an estimate of the minimum horizontal stress trajectory at Fenton Hill ranging from 83 to 106° E of N, with a mode at 100.5°. In support, the Valles Caldera, formed synchronously with this stress field, has a long axis trending 092°, within 10° of the estimate.

This estimate conflicts with previous estimates at Fenton Hill.

- a) Hydraulic fracturing at a depth between 1983 and 2042 m (6500 and 6750 ft) in GT-2 determined the trend of vertical fractures at 035 ± 5° E of N.<sup>14</sup> If an extensive fracture, the indicated direction of minimum horizontal stress is 125° E of N, 15° away from the present estimate.
- b) The large hydraulic fracture in GT-2 was initially estimated to trend NE-SW, but packer impressions from EE-1 caused that estimate to be revised to NW-SE.<sup>15</sup> This was subsequently confirmed. The indicated direction of minimum horizontal stress is 045° E of N.

These two estimates are 15 and 35° on either side of the tectonophysical model estimate. The discrepancies are explained by shear-dilatation failure of pre-existing joints.

## Yield Strength

An asymptotic model for the seismic envelope assumes a spherical source region in equilibrium with farfield stresses with an intervening "plastic" zone of yield in shear.

Using the size and shape of the seismic cloud from Experiment 2033 and an estimate of the radius of an equivalent spherical source from Murphy's general relation between injected volume and size of the seismic envelope, the yield strength in shear of the rock in the seismic envelope was estimated at 11.5 MPa (1670 psi).

This figure is much lower than the shear strength of intact rock, which indicates that seismicity is generated by failure on pre-existing joints.

## Shape of Seismic Cloud

The shape of the microseismic cloud in experiments preceding and including 2020 is an ellipsoid with a steeply dipping, N-S striking, principal plane and long axis inclined obliquely south.

## Propagation of Seismic Envelope

Comparison of the shape of the seismic envelope in Experiment 2020 with downhole injection pressures indicated a reversible, time dependent transition at 76.15 MPa (11 000 psi) and a reversible, instantaneous transition at 77 MPa.

The first is interpreted as working of joints within the seismic envelope, the second as expansion of the outer boundary of the yield zone against the farfield.

There is thus a small difference between the downhole pressure required to reactivate previously slipped joints and that required to cause failure on unslipped joints.

This result is not inconsistent with Spence and Turcotte<sup>16</sup> who suggested that downhole fluid pressure would be unaffected by the stress-intensity factor required

to extend the fluid-filled joints, as the process and material properties are different.

## Stress Field in the Seismic Envelope

The microseismic radiation patterns have been interpreted in terms of quadrantal nodal planes.

A numerical procedure was developed for inversion of the nodal planes to yield an estimate of the stress field within the seismic envelope. The procedure assumes a random distribution of joint orientations and takes into account the effect of normal stress on the yield criterion.

A Coulomb-Navier failure criterion was fitted to the seismic nodal planes from Experiments 2012, 2016, 2032. This yielded the stress ratio within the seismic cloud.

## Seismic Source Mechanism

The microseismic null vectors from Experiments 2012, 2016, 2032 have been found to be consistent, all lying on a small circle.

The cause of this is a common source mechanism, possibly Ishimoto's inflated-dike source<sup>17, 18, 19</sup> which could be due to a single inflated fracture or set of parallel fractures.

## Tests for Consistency

A test for consistency is through two "asymptotic" models.

(a) Permeation Model:

The relation between the inferred fracture anisotropy and the shape of the seismic cloud described above supports a permeation model of the reservoir at low injection volumes, that is, the seismicity is due to pore-pressure reduction of effective shear strength. This agrees with explanations of microseismicity accompanying fluid injection at the Denver arsenal and at Fenton Hill<sup>20</sup> with the modification that diffusion is

not planar but three-dimensional, controlled by a permeation tensor which is, approximately, second-order. There is no other explanation for the substantial plunge of the long axis of the seismic cloud.

This asymptotic condition would be expected to break down for larger injected volumes, due to the increased magnitude of tractions applied by the injected fluid to joint faces in the source region.

(b) Jacking Model:

The stress field in the seismic envelope is the superposition of farfield stresses and tractions due to fluid pressures in the source region. Burns<sup>21</sup> used as input:

- horizontal stress trajectories from the tectonophysical model described above,
- estimate of stress ratio from seismic first motions in Experiments 2012, 2016, 2032, described above,
- a single, tabular, inflated fracture, or set of parallel fractures, as inferred above, and
- estimates of lithostatic and hydrostatic load.

The model yields an estimate of the orientation of the fracture as striking N13° E, dipping 42° SE, and a peak dilatation in the seismic cloud at 4.7 E-4. This is consistent with an independent estimate of an average dilatation in the seismic cloud of 2.30 E-4.

A synthesis is that at low injection volumes, pore-pressure diffusion "softens" the rock by lowering the effective shear strength of the conducting joints, with the seismic envelope representing a region which is yielding as a "soft" inclusion under the initial load. This is the permeation phase. At higher injection volumes, the dilating joints in the source region apply tractions to the yield zone, re-orienting the stress field and producing a more complex microseismic response. Equilibrium considerations require that the reservoir be inside the seismic cloud but the distribution of fluid content need not resemble the distribution of microseismic sources.

## Geochemistry

In this fiscal year, research was initiated in the area of geochemical kinetics for reservoir analysis. This new work is an extension of the geochemical modeling of the Phase I

HDR system,<sup>22, 23</sup> and it bears the same relationship to the geochemical modeling that the chemically reacting tracer research, also discussed in this report, bears to the inert tracer experiments. That is, the geochemical kinetics and the chemically reactive tracers both will be used to interpret internal temperature distributions within an HDR reservoir, while the geochemical modeling and tracer studies were used only for interpreting internal flow characteristics in a reservoir. These advanced methods take advantage of the fact that the rates of chemical reactions are exponential functions of temperature, and thus can be used to "predict" reservoir lifetime far in advance of thermal breakthrough.

A major accomplishment in the geochemical kinetics studies is the development of a formal kinetics model for complex networks of multi-phase reactions.<sup>24</sup> This model has been tested mathematically against example problems given by Wei and Prater<sup>25</sup> and has proved to be significantly more efficient in estimating rate constants without the restrictions imposed by the Wei-Prater approach. The model is now being tested with experimental data.

Following the suggestion of Anthony Batchelor of the British HDR program, we have found that, under certain conditions of residence time and Peclet number, the radon concentration in the production fluid can be used to estimate mean fracture apertures. The minimum value of mean residence time for which this analysis is appropriate is approximately 100 hours, and the analysis is not sensitive to Peclet numbers above about 5 (essentially the Peclet number of the Phase I system). Fracture apertures calculated by this technique were compared with fracture apertures calculated from pressure-drop measurements for the Fenton Hill Phase I system and for the British Phase II system. In the British system, where the mean residence time is  $\sim 200$  hours, the "radon" aperture is  $39 \mu\text{m}$  (0.001,5 in.), which is good agreement with the hydraulic width. For the Fenton Hill system, however, the mean residence time is  $\sim 12$  hours and the "radon" aperture is  $30 \mu\text{m}$  (0.001,2 in.) significantly less than the 1-5 mm (0.04-0.20 in.) aperture esti-

mated from pressure-drop calculations. This technique will certainly be applicable for estimating fracture apertures in the Phase II system.

In conjunction with the redrilling of the Phase II system, Los Alamos personnel have assumed major responsibility for the drilling-mud chemistry. This includes formulation, analysis, and testing of mud properties, and maintaining inventories of the appropriate drilling-fluid additives. It is expected that with increased awareness of the drilling mud, mud-related problems with the redrilling effort will be significantly reduced.

## Computer Program Development

### ROCMAS

The ROCMAS computer code, developed at Lawrence Berkeley Laboratory, solves the differential equations governing the coupled fluid-flow/deformation behavior of fractured porous rock.<sup>26</sup> Biot's<sup>27</sup> poroelastic law is used for calculation of the behavior of the porous medium, while the fractures (joints) are represented by the force-displacement relations described by Goodman et al.<sup>28</sup> The code is based on a finite-element discretization of a Gurtin-type variation integral; the nonlinear behavior of the joints is accounted for by a stiffness-matrix perturbation technique.<sup>29</sup> To make an evaluation of the computer output easier, a postprocessor for ROCMAS has been written to display the results graphically.

ROCMAS allows for a detailed computation of the interaction of pumping a reservoir and the stress induced by this in a plane or symmetrical geometry. Currently, the case of two joints pumped simultaneously from one wellbore is being investigated in order to get more information concerning the circumstances in which the two joints may influence each other, e.g., the joint with the larger initial aperture might tend to close the other one.

## FEHM

The code FEHM,<sup>10</sup> the three-dimensional, finite-element-based reservoir simulator, has undergone development of the solution scheme to improve the efficiency of the code. An incomplete LU decomposition scheme with ORTHOMIN acceleration was implemented in a novel way. The code allows for "adapting" the degree of factorization so a high degree may be used in difficult areas and a lower degree may be used in other areas. Improvements in speed of up to two orders of magnitude compared to the standard Gauss elimination has been observed for three-dimensional problems.

## TECHNOLOGY TRANSFER

### Transition Plan

At the request of the Division of Geothermal and Hydropower Technologies (DGHT) of the U.S. Department of Energy (DOE), a formal plan for "Transition of Hot Dry Rock Technology to the Private Sector" has been drafted, reviewed, and submitted to the DOE for possible publication in FY85. In addition to completion of Fenton Hill experiments in FY88 and active programs of technical publication and public information, it is intended to encourage private-sector interest in constructing a 5- to 10-MW<sub>e</sub> power plant at Fenton Hill as one of several options. In addition, private interests will be sought for independent HDR experiments elsewhere.

### Candidate Sites

Many promising areas have been identified at which HDR projects might be undertaken. Of particular interest are the following.

- The Clear Lake geothermal area in northern California, separated by the Col-

layomi Fault from the Geysers steam field. Exploratory drilling by several energy companies has demonstrated that, over a large area, high temperatures exist at relatively shallow depths in low-permeability rock that does not produce natural steam or hot water. Interest in expanding California's indigenous energy resource has led to discussions in FY84 between the California Energy Commission and the HDR Program Office of possible arrangements for cooperation among the Commission, the Laboratory, and the owner of a hot, dry well for an HDR experiment in the Clear Lake area. The feasibility, desirability, and details of such an arrangement may be decided in FY85.

- The Milford Valley in southern Utah, separated by the Opal Mound Fault from the Roosevelt Hot Springs hot-water hydrothermal field. Here also, there is a large area in which exploratory holes have reached high temperatures in low-permeability rock at relatively shallow depths, without encountering fluid production. During FY84 there have been discussions with representatives of the Utah State Legislature concerning the possibility of arranging a cooperative experiment in the Milford Valley similar in concept to that being discussed with the California Energy Commission in the Clear Lake Area. These discussions will also continue in FY85.
- Mountain Home, Idaho. The margins of the Snake River Plain in southwestern Idaho represent one of the most promising HDR geothermal areas in the northwestern United States. During FY84, an investigation of an area east of Mountain Home, on the northern margin of the Plain, was completed with detailed examination of cuttings from a 2949 m (9676-ft) oil and gas wildcat well drilled there and correlation of stratigraphy with that elsewhere on the Plain. It was determined that, contrary to an earlier report by others, the well bottomed in silicic volcanics and (from geophysical studies) that it is underlain by something like 3 km (10 000 ft) of basalt. It was concluded that other areas, underlain by the granites of the Idaho batholith, are more promising

- for HDR development.
- Long Island, New York. Under sponsorship of the New York State Energy Research and Development Authority and others, it was planned, during FY84, to deepen an existing 326-m- (1070-ft) deep temperature-gradient hole at Terryville into the basement rock in order to investigate the technical feasibility of developing an HDR space-heating system for the State University of New York at Stony Brook. The Los Alamos contribution was to have been *in situ* stress determinations by strain-relaxation measurements on oriented cores, as a guide to hydraulic-fracturing behavior. Unfortunately, the hole had been junked so badly by the original driller that deepening it proved impractical. However, there is continuing interest in possible HDR experiments there or elsewhere on Long Island, and discussions of the Laboratory's participation will continue in FY85.
  - Other countries. Close interaction continued during FY84 with HDR research and development programs in other countries—particularly those in West Germany, Japan, and England. There were also discussions and information exchanges with three Australian organizations interested in possible commercial HDR development in that country for generating electricity and for direct use of geothermal heat.

## Field Support of Other Programs

In addition to testing new equipment, instruments, and components at the Laboratory and in the Fenton Hill wells, the HDR program is occasionally called on to field its logging trucks and special downhole instruments in support of other programs elsewhere. Two such operations of special interest conducted during FY84 were the following.

- In support of the Multi-Well Experiment of the Western Gas Sands Program, managed by Sandia National Laboratories, the

- improved Los Alamos crosswell-acoustic-transceiver (CAT) system was used at Rifle, Colorado, to evaluate crosswell imaging as a technique for investigation of lenticular gas sands. A series of acoustic scans was run between three well pairs 1800 to 2000 m (6000 to 6500 ft) deep and 37 to 67 m (121 to 221 ft) apart. Strong, high-quality signals were recorded, which were still being analyzed at the end of FY84. The equipment and technique appear very promising for investigating rock type and structure between gas, oil, and geothermal wells.
- In support of a successful field test of Sandia National Laboratories' borehole televiewer, a Los Alamos logging truck, support van, instrument cable, and temperature probe were used to log three Union 76 hydrothermal wells in the Salton Sea geothermal area.

## PROGRAM MANAGEMENT

### Program Organization

During FY84, some organizational and personnel changes occurred in the management structure of the Hot Dry Rock Program. J. E. Rannels replaced A. J. Jelacic as HDR Program Director in the DOE Division of Geothermal and Hydropower Technologies. Within the Los Alamos National Laboratory, under the Chemistry, Earth and Life Sciences Directorate, the program is now managed from the office of the Deputy Associate Director for Alternate Energy Sources. R. A. Benson joined this office in the capacity of HDR Program Manager. His supporting management staff are members of the Earth and Space Sciences Division.

The present programmatic organizational structure is depicted in Fig. 21. As indicated, the HDR Program continues to be field-managed jointly by Los Alamos, as described above, and the Energy Technologies Division of the DOE Albuquerque Operations Office with support from the Los Alamos Area Office, under the overall

purview of the HDR Program Director in the DOE Division of Geothermal and Hydropower Technologies (DGHT).

Progress of the program is reviewed by its International Steering Committee, which has jurisdiction over resolution of major programmatic problems and approval of proposed changes with significant schedule and/or fiscal impact.

The program is also reviewed annually by the HDR Program Development Council, an advisory body to Los Alamos whose membership comprises representatives of industry, academia, and the U.S. Geological Survey. This group is chartered to provide guidance to program management in the development of a commercializable technology.

### FY84 PDC Meeting

The HDR Program Development Council's Executive Committee met for the ninth time on Friday, 31 August 1984. Present were Committee members G. V. Keller (chairman), S. K. Bazant, R. Grider, and L. J. P. Muffler, together with *ex officio* Los Alamos and DOE members and visitors from Sandia, West Germany, and Japan.

Los Alamos presented an overview of technical programs since the previous meeting, with considerable detail on the massive hydraulic fracturing experiment and the developments in microseismic reservoir analysis. Plans for the workover/redrilling effort were then discussed.

A deep and far-ranging discussion ensued about the future of the technology development and its possible near-term commercialization. Specifically addressed were the utilization of the Fenton Hill wells when Phase II testing is completed; development of a second site elsewhere in the US; and the most appropriate means of expeditiously transferring the technology to industry. It was noted that a formal transition plan is being prepared for commercialization of HDR-derived energy.

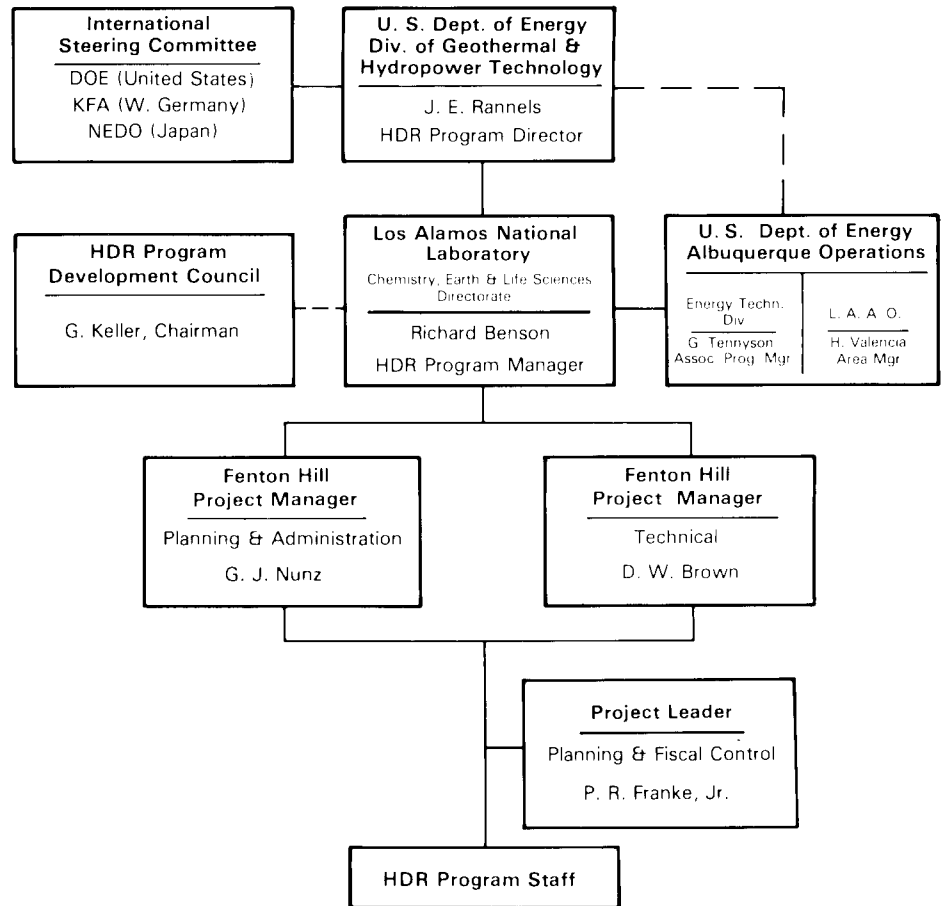
## International Energy Agency (IEA) Hot Dry Rock Program—

### International Steering Committee (ISC)

The ISC met twice during FY1984, once in early March and once in early October (actually a few days after the end of the US fiscal year). Committee members present at both meetings were J. Bresee (DOE), chairman; W. P. Grace (DOE); K. Kusunoki (NEDO); and W. Schloemer (KFA).

The eighth regular ISC meeting was held on March 6-7, 1984, at the Los Alamos National Laboratory's University House. The Committee was briefed on the results and

Figure 21. HDR Program organization.



preliminary analyses of the recently completed MHF experiment; FY83 financial summary; current FY84 schedule and fiscal status; and plans for FY85 and beyond. The ISC agreed that the flowback evidence from the MHF seemed to indicate a reservoir region so large that the distinction between an "interim" and "final" configuration has become moot. Hence, the serial Phase II system development will be eliminated in future planning. It was also agreed that an intensive effort would be devoted to analysis of the microseismic data, in light of their importance to redrilling plans.

The ninth ISC meeting was hosted by NEDO and held at NEDO Headquarters in Tokyo. Los Alamos presented the results of comprehensive analysis of data from the MHF and subsequent experiments (especially the microseismic data); recent developments in downhole instruments and equipment; FY84 and 85 financial updates; a preliminary trajectory for the redrilling of well EE-3; and a discussion of the commercial transition planning. T. Watamori, NEDO's president, addressed the group and stressed the importance of the Fenton Hill project. W. Schloemer gave a presentation on the two German HDR field experiments

in Falkenberg, Bavaria, and Urach, Swabia. N. Nagata discussed the Japanese Yakedake project. A tour of the Japanese geothermal projects followed the meeting.

## PLANS FOR FISCAL YEAR 1985

The primary objective for the HDR Project during FY85 is to complete the Phase II reservoir connection and to begin flow testing the resulting reservoir. This includes development of a scientific understanding of the Phase II fractured region.

Since previous massive hydraulic fracturing attempts from the two Phase II wells have failed to connect them hydraulically, it has been decided to complete the underground flow connection by redrilling one well (EE-3) into the fracture system produced from the other well (EE-2). The drilling trajectory is being designed to sidetrack deep in well EE-3 toward the very large fracture system created from EE-2 during the massive hydraulic fracturing (MHF) test and—with a minimum of expensive directional drilling—extend it through as

much as possible of that fracture system.

At the outset of FY85, a workover/drilling rig will be mobilized at the Fenton Hill Test Site first to repair the EE-2 wellbore and then (after the redrilling trajectory has been selected) to initiate the directional drilling of EE-3A by kicking out of the present EE-3 wellbore at a depth of about 2800 m (9300 ft); after which the rig will be dismissed. The repair of EE-2 is necessitated by damage incurred to the casing and frac strings during the rapid vent following Experiment 2032.

In March 1985, after extensive planning, a larger drilling rig will be mobilized over EE-3 to complete redrilling of the optimized EE-3A wellbore trajectory through the seismic zone associated with the MHF test.

After completing EE-3A as the Phase II reservoir injection hole, a series of flow tests—beginning with the 70-hour Run Segment ER-1—will be conducted to establish the initial reservoir flow impedance, outlet temperature, and fluid geochemistry.

Additional design modifications or improvements in the basic downhole instruments being used in the Phase II wells will continue to be made as necessary. Develop-

ment of the prototype thermally upgraded digital borehole acoustic televiewer (BAT) tool will continue as a cooperative effort between Los Alamos and a research institute (WBK) of the Federal Republic of Germany. Development will also continue on a family of high-temperature explosively activated tools needed in both the Phase II reservoir completion and interrogation stages during FY85.

## Acknowledgments

We thank the many individuals who contributed to the content of this report: D. Brown, L. Brown, K. Burns, G. Cocks, D. Counce, Z. Dash, B. Dennis, T. Dey, D. Dreesen, M. Fehler, C. Grigsby, R. Hendron, B. Hoffers, L. House, J. Miller, H. Murphy, G. Nunz, B. Robinson, J. Schillo, J. Skalski, and G. Zyvoloski.

We also thank the following for their assistance with the preparation of this report: M. Findley, R. Johnson, and P. Valencia, word processors; J. Paskiewicz and R. Robichaud, illustrators. We also thank J. Paskiewicz for his cover design, and G. Sharp and M. Wilson for their valuable consultation.

## REFERENCES

1. Purtymun, W. D., W. H. Adams, and J. W. Owens, "Water Quality in Vicinity of Fenton Hill Site, 1974," Los Alamos Scientific Laboratory report LA-6093-MS (December 1975).
2. Purtymun, W. D., W. H. Adams, A. K. Stoker, and F. G. West, "Water Quality in the Vicinity of Fenton Hill Site, 1975," Los Alamos Scientific Laboratory report LA-6511-MS (September 1976).
3. Purtymun, W. D., W. H. Adams, and A. K. Stoker, "Water Quality in the Vicinity of Fenton Hill Site, 1976," Los Alamos Scientific Laboratory report LA-7307-MS (May 1978).
4. Purtymun, W. D., A. K. Stoker, W. H. Adams, and J. W. Owens, "Water Quality in Vicinity of Fenton Hill Site, 1977," Los Alamos Scientific Laboratory report LA-7468-PR (September 1978).
5. Purtymun, W. D., R. W. Ferenbaugh, A. K. Stoker, W. H. Adams, and J. W. Owens, "Water Quality in the Vicinity of Fenton Hill Site, 1978," Los Alamos Scientific Laboratory report LA-8217-PR (January 1980).
6. Purtymun, W. D., R. W. Ferenbaugh, A. K. Stoker, and W. H. Adams, "Water Quality in the Vicinity of Fenton Hill Site, 1979" Los Alamos Scientific Laboratory report LA-8424-PR (June 1980).
7. Purtymun, W. D., R. W. Ferenbaugh, and W. H. Adams, "Water Quality in the Vicinity of Fenton Hill Site, 1980," Los Alamos National Laboratory report LA-9007-PR (September 1981).
8. Purtymun, W. D., R. W. Ferenbaugh, N. M. Becker, W. H. Adams, and M. N. Maes, "Water Quality in the Vicinity of Fenton Hill Site, 1981 and 1982," Los Alamos National Laboratory report LA-9854-PR (September 1983).
9. Zvoloski, G., "The Sizing of a Hot Dry Rock Reservoir from a Hydraulic Fracturing Experiment," 26th U.S. Symposium on Rock Mechanics, Rapid City, South Dakota, 1985.
10. Zvoloski, G., "Finite Element Methods for Geothermal Reservoir Simulation," *Int. J. Num. Meth. Geomech.* 7, (1983), 75-83.
11. Dash, Z. and H. Murphy, "Variation of Fracturing Pressures with Depth Near the Valles Caldera," *Proc. 9th Workshop Geothermal Reservoir Engineering, Stanford University, Palo Alto, California, December 1983.*
12. Aldrich, M. J. and A. W. Laughlin, "Orientation of Least-Principal Horizontal Stress: Arizona, New Mexico, and the Trans-Pecos Area of West Texas," Los Alamos National Laboratory report LA-9158-MAP (February 1982).
13. Aldrich, M. J. and A. W. Laughlin, "A Model for the Tectonic Development of the Southeastern Colorado Plateau," *J. Geophys. Res.* 89(B12), 10207-10218 (1984).
14. Aamodt, R. L., "Hydraulic Fracture Experiments in GT-1 and GT-2, Los Alamos Scientific Laboratory report LA-6712-MS, (February 1977).

15. Pettitt, R. A., "Planning, Drilling, Logging, and Testing of Energy Extraction Hole FF-1, Phases I and II," Los Alamos Scientific Laboratory report LA-6906-MS (August 1977).
16. Spence, D. A. and D. L. Turcotte, "Magma-Driven Propagation of Cracks," *J. Geophys. Res.* **90**(B1), 575-580 (1985).
17. Ishimoto, M., "Existence of a Quadrupole Source at the Seismic Focus According to the Study of the Distribution of the Initial Movements of Seismic Shocks," *Bull. Earthquake Res. Inst. Univ. Tokyo* **10**, 449 (1932).
18. Julian, B. R., and R. S. Cockerham, "Mechanisms of the May 1980 Earthquakes Near Long Valley Caldera, California. Evidence for Dike Injection," *Earthquake Notes* **54**, 88 (1983).
19. Aki, K., "Evidence for Magma Intrusion During the Mammoth Lakes Earthquakes of May 1980 and Implications of the Absence of Volcanic (Harmonic) Tremor," *J. Geophys. Res.* **89**(B9), 7689-7696 (1984).
20. Pearson, C., "The Relationship Between Microseismicity and High Pore Pressure During Hydraulic Stimulation Experiments in Low Permeability Granitic Rocks," *J. Geophys. Res.* **86**(B9), 7855-7864 (1981).
21. Burns, K., "Reconstruction of the Stress field at Fenton Hill," in "Recent Research of the Valles Caldera," DOE/OBES, October 15-18, 1984.
22. Grigsby, C. O., "Geochemical Behavior of a Hot Dry Rock System: Reservoir Simulation and Modeling," MS thesis, Dept. of Chemical Engineering, MIT, 134 pp. (1983).
23. Grigsby, C. O., F. Goff, P. Trujillo, and D. Counce, "Geochemical Behavior of a Hot Dry Rock Geothermal System," *New Mexico Geological Society, 35th Field Conference Guidebook*, 265-270 (1984).
24. Grigsby, C. O., "Kinetics of Rock-Water Reactions," proposal for Ph.D. thesis research, Dept. of Chemical Engineering, MIT, 48 pp. (1984).
25. Wei, J., and C. Prater, "The Structure and Analysis of Complex Reaction Systems," *Adv. Catalysis* **13**, 203-392 (1962).
26. Noorishad, J., M. S. Ayatollahi, and P. A. Witherspoon, "A Finite-Element Method for Coupled Stress and Fluid Flow Analysis in Fractured Rock Masses," *Int. J. Rock Mech. Min. Sci. and Geo-mech.*, Abstr. **19**, 185-193 (1983).
27. Biot, M. A., "General Theory of Three-Dimensional Consolidation," *J. Appl. Phys.* **12**, 155-164 (1941).
28. Goodman, R. E., R. L. Taylor, and T. L. Brekke, "A Model for the Mechanics of Jointed Rock," *J. Soil Mech. Found. Eng., Proc. Am. Soc. Civ. Eng.* 1968, 637-659 (1968).
29. Gurtin, M. E., "Variational Principles for Linear Elastodynamics," *Archive. Rat. Mech. Anal.* **16**, 34-50 (1964).

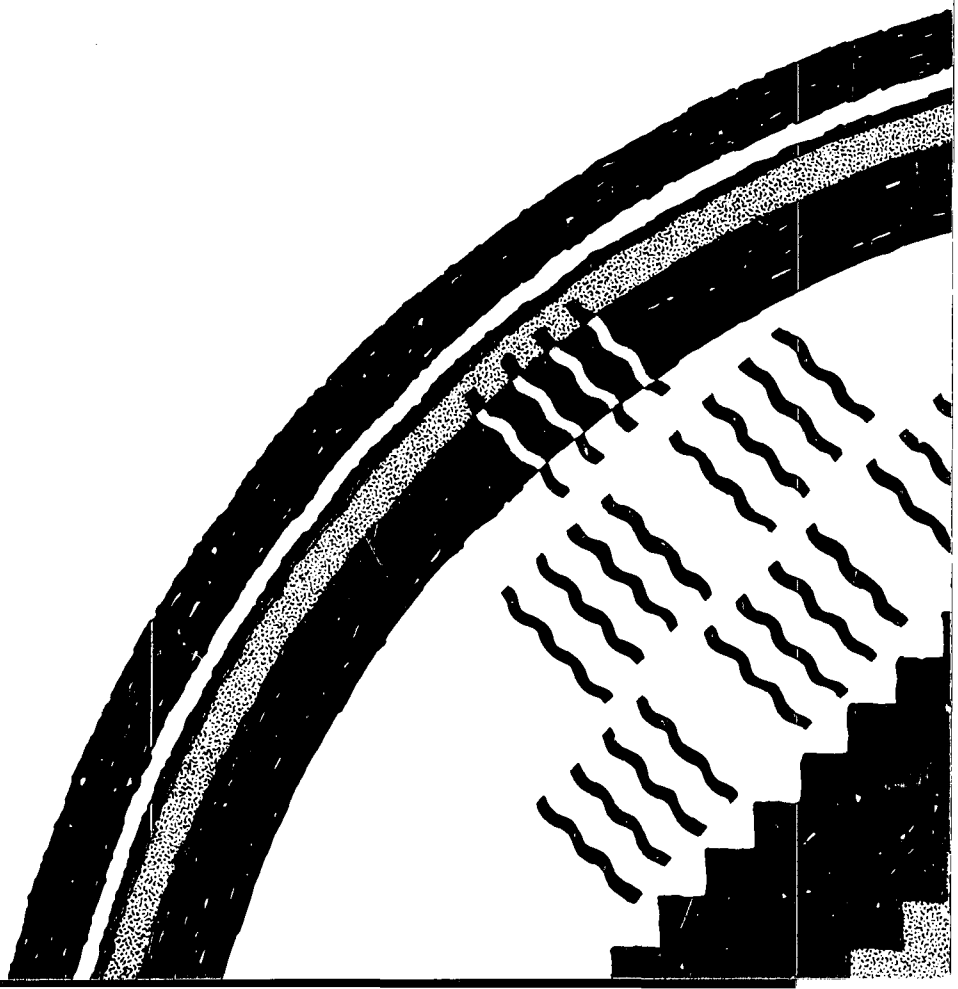
Printed in the United States of America  
Available from  
National Technical Information Service  
US Department of Commerce  
5285 Port Royal Road  
Springfield, VA 22161

Microfiche (A01)

Page Range	NTIS Price Code						
001-025	A02	151-175	A08	301-325	A14	451-475	A20
026-050	A03	176-200	A09	326-350	A15	476-500	A21
051-075	A04	201-225	A10	351-375	A16	501-525	A22
076-100	A05	226-250	A11	376-400	A17	526-550	A23
101-125	A06	251-275	A12	401-425	A18	551-575	A24
126-150	A07	276-300	A13	426-450	A19	576-600	A25
						601 up*	A99

\*Contact NTIS for a price quote.

Los Alamos  
Los Alamos National Laboratory  
Los Alamos, New Mexico, 87545



**LA-7771-MS**

Informal Report

**Hot Dry Rock Energy Extraction Field Test:  
75 Days of Operation of a Prototype  
Reservoir at Fenton Hill**

**Segment 2 of Phase I**

University of California



**LOS ALAMOS SCIENTIFIC LABORATORY**

Post Office Box 1663 Los Alamos, New Mexico 87545

This report was prepared as an account of work sponsored by the United States Government. Neither the United States nor the United States Department of Energy, nor any of their employees, nor any of their contractors, subcontractors, or their employees, makes any warranty, express or implied, or assumes any legal liability or responsibility for the accuracy, completeness, or usefulness of any information, apparatus, product, or process disclosed, or represents that its use would not infringe privately owned rights.

LA-7771-MS  
Informal Report  
UC-66a  
Issued: April 1979

**Hot Dry Rock Energy Extraction Field Test:  
75 Days of Operation of a Prototype  
Reservoir at Fenton Hill  
Segment 2 of Phase I**

Edited by  
Jefferson W. Tester  
James N. Albright



## CONTENTS

ABSTRACT . . . . .	1
1. INTRODUCTION AND SCOPE . . . . .	1
2. EQUIPMENT DESCRIPTION AND OPERATING PARAMETERS . . . . .	4
2.1 Equipment . . . . .	4
2.2 Operations . . . . .	7
2.3 Operational Problems . . . . .	8
System Perturbations . . . . .	8
3. RESERVOIR HEAT EXTRACTION CHARACTERISTICS . . . . .	12
3.1 Measurements and Data . . . . .	12
3.2 Thermal Drawdown Analysis . . . . .	14
3.3 Heat Extraction . . . . .	15
4. RESERVOIR FLOW CHARACTERISTICS AND MODELS . . . . .	19
4.1 Flow Impedance . . . . .	19
4.2 Fracture System Size and Degree of Mixing . . . . .	24
4.3 Fluid Loss and Storage . . . . .	30
4.4 Injection and Production Zones . . . . .	34
4.5 Flow Models . . . . .	36
5. FLUID GEOCHEMISTRY . . . . .	42
5.1 Major Element Analysis . . . . .	42
Procedures . . . . .	42
Results . . . . .	43
Preliminary Interpretation - Reservoir . . . . .	56
Preliminary Interpretation - Surface Equipment . . . . .	64
5.2 Trace Element Analysis . . . . .	67
5.3 Strontium Isotope Ratio Measurements . . . . .	72
5.4 Radon . . . . .	77
6. MONITORING FOR INDUCED SEISMIC EFFECTS . . . . .	87
7. SUMMARY OF SYSTEM PERFORMANCE AND MODELS . . . . .	89
APPENDIX A: FRACTURE OPENING BY COOLING . . . . .	99
APPENDIX B: THERMAL EFFECTS IN SPHERICALLY COOLED REGIONS . . . . .	103

HOT DRY ROCK ENERGY EXTRACTION FIELD TEST:  
75 DAYS OF OPERATION OF A PROTOTYPE RESERVOIR AT FENTON HILL

SEGMENT 2 OF PHASE I

Edited by

Jefferson W. Tester  
James N. Albright

ABSTRACT

Results from the first extensive field test of a man-made hot dry rock (HDR) geothermal reservoir in low permeability crystalline rock are presented. A reservoir with a small heat transfer area was utilized to study the characteristics of a prototype HDR system over a shortened lifetime. The resulting accelerated thermal drawdown was modeled to yield an effective area of 8000 m<sup>2</sup>. In addition to the thermal effects, this test provided an opportunity to examine equipment operation, water permeation into the formation, geochemical interaction between the circulating fluid and the rock and flow characteristics including impedance and residence time distributions. Continuous monitoring for induced seismic effects showed that no activity to a Richter threshold of -1.0 was detected during the 75-day experiment.

---

1. INTRODUCTION AND SCOPE

The major prerequisite for full-scale testing of the Los Alamos Scientific Laboratory's (LASL) Hot Dry Rock concept was achieved. By redrilling the production well, GT-2, at the Fenton Hill site along a planned trajectory, we intersected a low-impedance hydraulic fracture that directly communicated with the injection well, EE-1. It should be emphasized that the redrilling program of GT-2 was designed to produce the largest heat transfer surface area possible with the inherent geometric limitations of the wellbores and with an acceptable initial flow impedance of less than 21 bar-ℓ/s (20 psi/gpm). Having achieved this, the Hot Dry Rock (HDR) concept could be tested by establishing a high-flow

rate between wells at low wellhead differential pressures. Previously, the only communication with EE-1 had been through and between high-impedance fractures, and flow was insufficient to evaluate the heat-extraction concept.

In September, with much of the work on the surface plant of the energy-extraction loop nearly complete, a preliminary test of the entire system which includes the surface plant and downhole flow paths was conducted. During 96 h of closed-loop circulation, fluid total dissolved solids remained low (<400 ppm), water losses continually decreased, and no induced seismic activity occurred. The operating power level was 3.2 MW (thermal), and fluid temperature reached 130°C at the surface. This test demonstrated for the first time that heat could be extracted at a usefully high rate from hot dry rock at depth and transported to the surface by a manmade system. The test further indicated a high probability that no significant problem would be encountered during sustained operation of the system.

Full-scale operation of the loop occurred from January 27 to April 13, 1978. This part of Phase I is referred to as Segment 2 and was designed to examine the thermal drawdown, flow characteristics, water losses, and fluid geochemistry of the system in detail. In addition, the experimental area was closely monitored for induced seismic activity. Results of these studies are the major topic of this report.

Because the anticipated effective heat transfer surface area was small (<10 000 m<sup>2</sup>), the Segment 2 test was structured to examine reservoir performance in a compressed time scale with accelerated thermal drawdown. From a practical point of view, a rapid drawdown rate will hasten the development of thermal stress cracks and hence our evaluation of the concept. To induce cracks into the fracture surface under the Fenton Hill reservoir stress conditions, an excess of 75°C of cooling is required to produce cracks wide enough to provide low-impedance flow paths.<sup>1,2</sup>

It was planned that circulation flow rates would be maintained at their maximum values as determined by the system impedance and the maximum possible drop across the reservoir. With an initial impedance of 11-16 bar-s/ℓ (10-15 psi/gpm), circulating flows of about 6-10 ℓ/s (100-150 gpm) were anticipated. With this flow rate and an active fracture surface area of 10 000 m<sup>2</sup>, about 90°C of cooling might occur after 60 days with no change in reservoir size due to thermal stress cracking or other effects. Consequently,

the difference between observed and calculated thermal drawdown could be used to identify changes in reservoir size. In addition, changes in fluid chemistry, water losses, residence time, flow impedance and production zones in GT-2 would be used to correlate with observed thermal effects.

The major purpose of the Phase I test was to evaluate hot dry rock reservoir engineering concepts in a prototype system. This evaluation will improve reservoir design and modeling capabilities to aid in the development of larger in-situ surface areas required for future commercial systems. The plans for Phase II are to enlarge the present reservoir to a capacity of 20-50 MW(t) with extended lifetime by directionally drilling to a deeper region ( $\sim 250^{\circ}\text{C}$ ) and produce a multiply fractured system between two high-angle inclined wellbores.

This report is divided into seven sections. The surface circulation loop equipment and instrumentation are described in Section 2. Thermal behavior of the reservoir and associated heat extraction modeling results are presented in Section 3, with flow characteristics and water permeation effects covered in Section 4. Major and trace element geochemistry and kinetic flow models appear in Section 5, while reconnaissance data for induced seismic effects are discussed in Section 6. Section 7 summarizes the physical, geometric, and chemical behavior of the reservoir. In order to develop a consistent model the effects of hydraulically activated, parallel, natural joints are coupled to a vertical fracture system producing the existing flow connections between EE-1 and GT-2B. This report assumes that the reader is familiar with the chronological drilling sequence. It also assumes a familiarity with the geometry of the wellbores including the original EE-1 wellbore and the GT-2 wellbore with its sidetracked trajectories GT-2A and GT-2B. Readers who need a review of this background information should read Section 7 as a further introduction to the preceding sections.

2. EQUIPMENT DESCRIPTION AND OPERATING PARAMETERS (J. H. Hill, R. H. Hendron, E. Horton, B. R. Dennis, and the Geothermal Operations Staff)

2.1 Equipment

Equipment used in this segment of Phase I included the makeup system, the main circulating pumps, the control valve, the heat exchanger, the surface piping, the vent system, pressure lock system, and flow meters. The schematic of the loop (Fig. 2-1) shows the component locations. Pressure, temperature, and flow measurements are indicated by P, T, and F symbols respectively.

The makeup system furnished the initial water to fill the entire loop and any makeup water required during the run. The principal feature was a two-stage centrifugal pump capable of 8.2-l/s (130-gpm) flow at ~13.1 bar (190 psi). The water was drawn from the EE-1 reserve pond with a capacity of  $1.5 \times 10^6$  liters (400 000 gal). Makeup water was supplied at a maximum rate of ~2.5 l/s (40 gpm) from a 122-m (400-ft) deep well.

Each centrifugal circulating pump module had seven vertical stages capable of raising the pressure 41 bar (600 psi). Two pumps were used in series

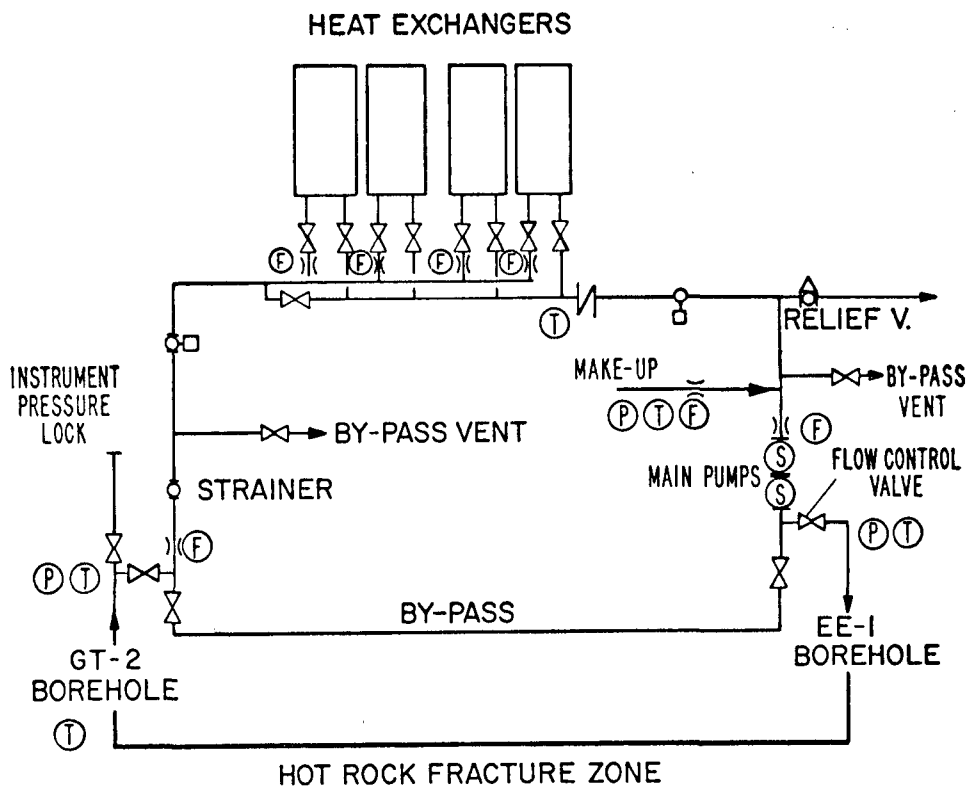


Fig. 2-1.  
Schematic of the Fenton Hill circulation loop.

with an inlet pressure of 12 bar (175 psi) to produce a discharge pressure of 95 bar (1375 psi). Each pump module was driven by a 200-hp electric motor and on the flat part of the performance curve could deliver up to 32  $\ell/s$  (500 gpm). The final control element, located at the EE-1 wellhead, was a 5.0-cm (2-in.), linear trim, high-pressure, hand-controlled valve with an operating characteristic  $C_v$  of 14.6.

The water-to-air heat exchanger units were arranged for vertical forced draft across aluminum-finned, carbon steel tubes. The straight-tube sections with plugged headers may be mechanically or chemically cleaned in the event of scaling. Design point conditions were: 172 bar (2500 psi) working pressure; 12.1 MW(t) per bay of two tube bundles with an inlet water temperature of 250°C and a 65°C outlet, air inlet at 21°C, and a total flow of 18.3  $\ell/s$  (290 gpm) per module. Each bay was cooled by two axial flow fans driven by 30-hp motors. The louvers were automatically controlled to maintain a specified exit temperature.

The majority of the surface piping was 10 cm (4 in.) Schedule 160 carbon steel with a working pressure of 172.4 bar (2500 psi). The last 1 m of piping at the EE-1 borehole was 5.0-cm Schedule 160 and included the control valve mentioned above. The bypass vent system immediately downstream of the GT-2 wellhead leading to the GT-2 pond was included for start up, and the 5.0-cm line could isolate the flow from the heat exchangers, if required. The instrument pressure-lock system for the wellheads enabled borehole logging, tool retrieval, and reinsertion of a tool during operation of the system. Other equipment used in this system were a 15-cm (6-in.) gate valve, a water-cooled section of 19-cm (7 5/8-in.) casing, and a "control head" to pack off the cable. Seven venturi flow meters were placed throughout the loop to measure flow. In addition a totalizer (water meter) integrated the makeup water.

The Control and Data Acquisition System (CDA) used a Hewlett Packard 3050 B data acquisition system that consisted of a Hewlett Packard 9830 calculator and its peripheral equipment as shown in Fig. 2-2. During the 75-day run, 20 channels of loop information were recorded: 7 flow rates, 8 pressures (3 in line and 5 differential across heat exchanger tube bundles) and 5 temperatures. In addition to the loop instrumentation, 80 channels of thermocouple data were recorded. These thermocouples were strategically located on the heat exchanger to study possible scaling or fouling problems.

## CONTROL AND DATA ACQUISITION BLOCK DIAGRAM

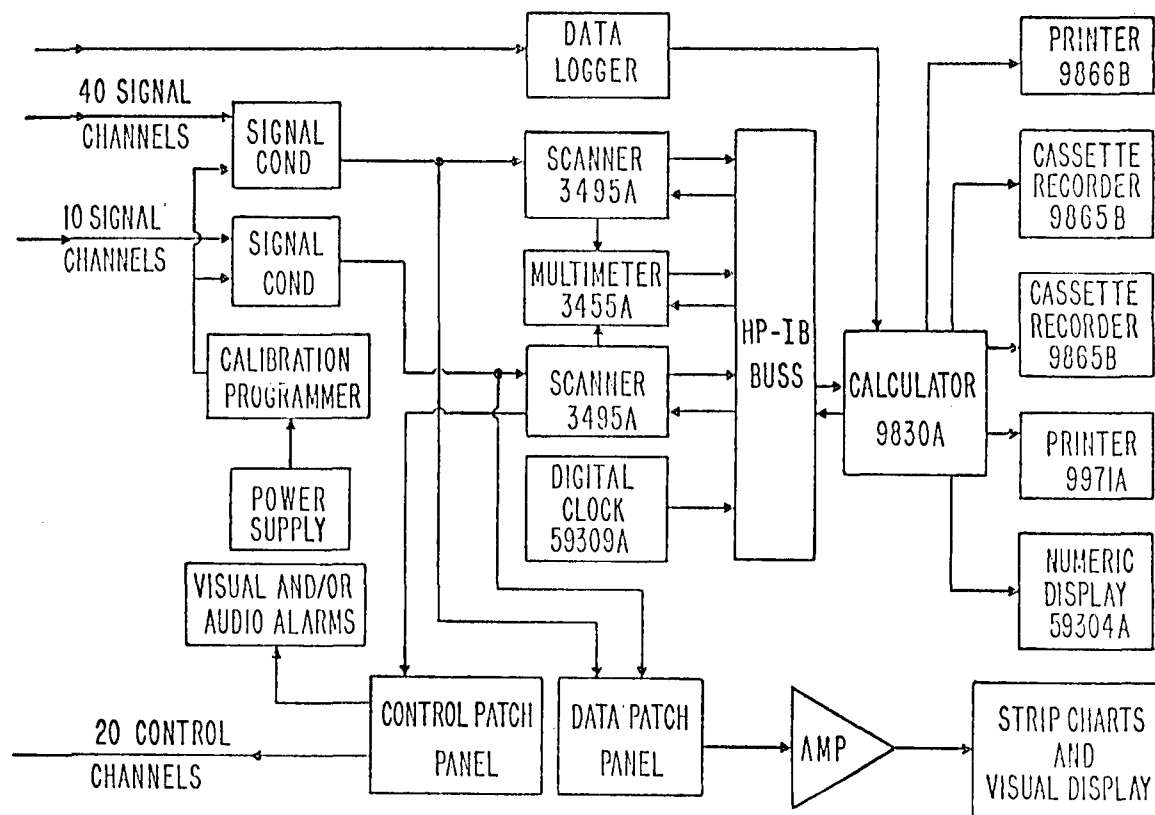


Fig. 2-2.  
Schematic diagram of Control and Data Acquisition System.

Flow rates were measured with venturi meters using differential pressure transducers. Pressures were measured with pressure transducers, and Chromel-Alumel thermocouples monitored the temperatures.

All loop signals were hard-wired from the transducers and thermocouples to the signal conditioners, which provided power, shunt calibration, and balance networks for the transducers. The outputs of the signal conditioner were connected to an HP 3495 A scanner consisting of six decades of low thermal relays and two decades of actuators (control relays). The calculators controlled each relay individually allowing the HP 3455 A multimeter to read any selected data channel. The multimeter then passed the voltage reading upon command to the calculator via the HP-IB buss. The HP 9830 calculator then performed the necessary calculations and transmitted the reduced data to the 59304 A numeric displays and the 9971 A line printer, while the raw data went to the HP 9865 B cassette recorders.

In addition, the 80 heat-exchanger thermocouple channels were hard-wired directly to a data logger, which entered the data into a buffer. On command, individual thermocouple outputs were transmitted to the HP 9830 calculator in ASCII code.

Control functions for the Phase I loop during this run were minimal. The CDA operator could manually start and stop four fans on the heat exchanger and manually stop the makeup pumps and main circulating pumps. The HP 9830 was programmed to check all measurements for predetermined minimum and maximum values. If these parameters were exceeded, the calculator would sound an alarm and define the problem with a printed statement. If the problem could possibly result in damage to the pumps, the calculator would also turn off all pumps automatically.

The numeric displays were updated every 15 seconds. All data channels were recorded on magnetic tape and on the line printer at 15-minute intervals. If any one of the predetermined parameters mentioned was exceeded, the recording interval changed to one minute. In addition, certain experiments during the loop operation required more frequent output.

An uninterruptible power supply backed up the local power to prevent loss of data.

## 2.2. Operations

Operation began with the pumps drawing makeup water from the EE-1 storage pond. Within a few minutes, the output pressure at GT-2 reached 12 bar (175 psi) and the main circulating pumps were turned on. This level of back pressure was used to avoid flashing in the system. Fluid was injected into the EE-1 borehole, pumped through the fracture system, and out of GT-2, where the flow was vented to the GT-2 pond to clean out the system in an initial purge. After approximately 150 000 liters (40 000 gal.) of water had been vented and the outlet total dissolved solids was <400 ppm, the flow was then routed through the heat exchangers and back to the main pumps. The closed loop was then in operation. The inlet pressure to the main pumps was controlled by the makeup pump pressure, which in turn was controlled by a back pressure valve. This valve was set at 12 bar (175 psi), and it automatically diverted the makeup flow to the EE-1 holding pond when that pressure was exceeded. As the return flow from the heat exchanger gradually increased, the makeup flow was proportionately reduced. The EE-1 borehole pressure was kept below 90 bar (1300 psi) to avoid fracture extension. As the pressure approached 90 bar, flow was throttled at the control

valve. After a few days the pressure and flow had stabilized at  $\sim 90$  bar and  $7.9 \text{ l/s}$  ( $125 \text{ gpm}$ ). (A schematic of the surface facility is shown in Fig. 2-3.

After three weeks of operation in this mode, the impedance of the fracture system started to decrease. This created a demand for a higher injection flow rate to maintain the wellhead pressure at  $1300 \text{ psi}$ . The control valve was opened to increase the rate. Finally, the control valve was wide open, with the injection rate at approximately  $17 \text{ l/s}$  ( $270 \text{ gpm}$ ), and the  $90\text{-bar}$  injection pressure could not be maintained as the impedance continued to decrease. At that time, we decided to control the flow rate at  $14.5 \text{ l/s}$  ( $230 \text{ gpm}$ ). This was a compromise due to our concern for the inordinately high fluid velocities in the  $5.0\text{-cm}$  piping at EE-1, and also for the desired flow and what could be achieved. The loop was operated under these constraints until it was "shut in" on April 13, 1978. This condition was maintained for 10 days, and then the system was vented.

### 2.3. Operational Problems

The operation of the system for the 75-day period was without major problems with a total of only 2% down time. Figure 2-4 indicates the shutdown periods greater than 1 h occurring during the 75-day run. Following are some of the specific problems.

The main pump seals failed within the first few days of operation. The seals were changed in the field by the pump manufacturer on day 18 and have since operated without mishap. The total downtime was  $\sim 6$  hours. The seals on the makeup pump failed near the end of the test, and a substitute pump was temporarily connected to carry the operation through the last 3 days. The turbine meter failed after 4 days, then operated intermittently during the remainder of the test. The control head on the pressure lock system leaked excessively  $>38 \text{ l/min}$  ( $>10 \text{ gpm}$ ) after 65 days of operation because of progressive degradation caused by repeated temperature logging performed almost daily during that period. The temperature probe had to be removed from the hole, and the control head rebuilt.

Power to the site was furnished by Jemez Electric COOP. Most of the run was conducted during the winter months, and there were frequent momentary power interruptions, which caused pump failure for short periods. More serious power failures occurred on two occasions when power was out in excess of 12 hours. Because these outages occurred during winter storms, special efforts were needed to prevent freezing the exposed plumbing.

System Perturbations. The loop operation was perturbed at times by excessive flow. Ordinarily, the fracture system acts as a large ( $>38,0\text{-m}^3$ ) accumulator

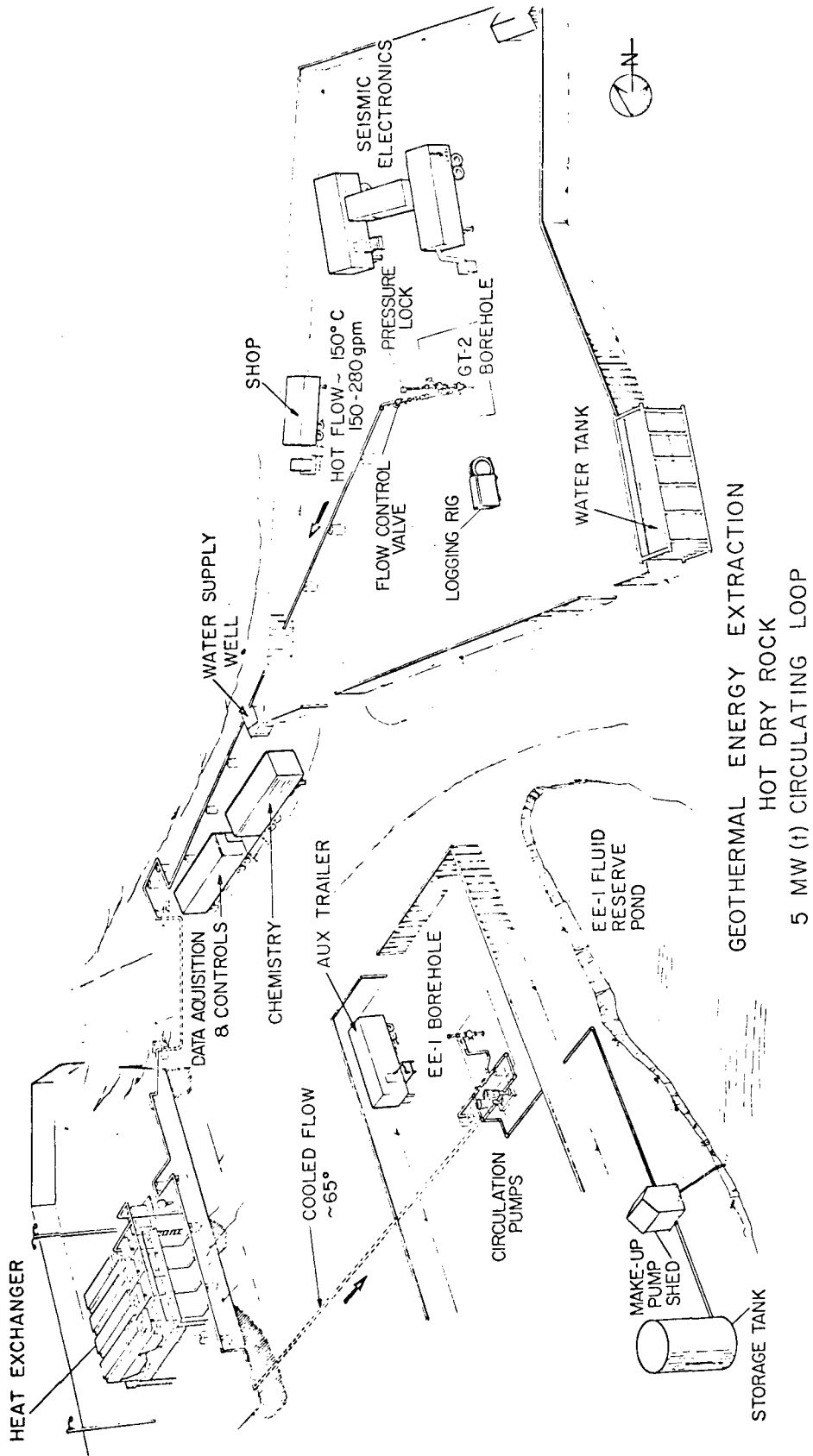


Fig. 2-3.  
Fenton Hill surface facility showing major components and structures.

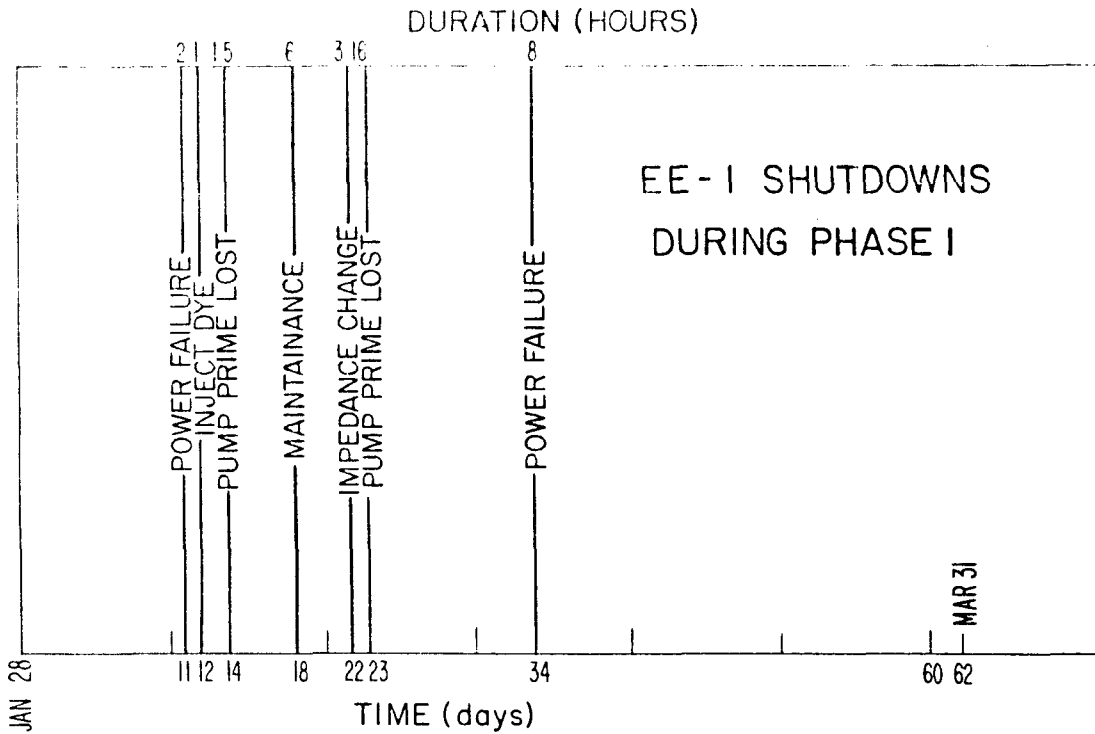


Fig. 2-4.  
Indicated shutdowns during Phase I greater than 1 h in duration.

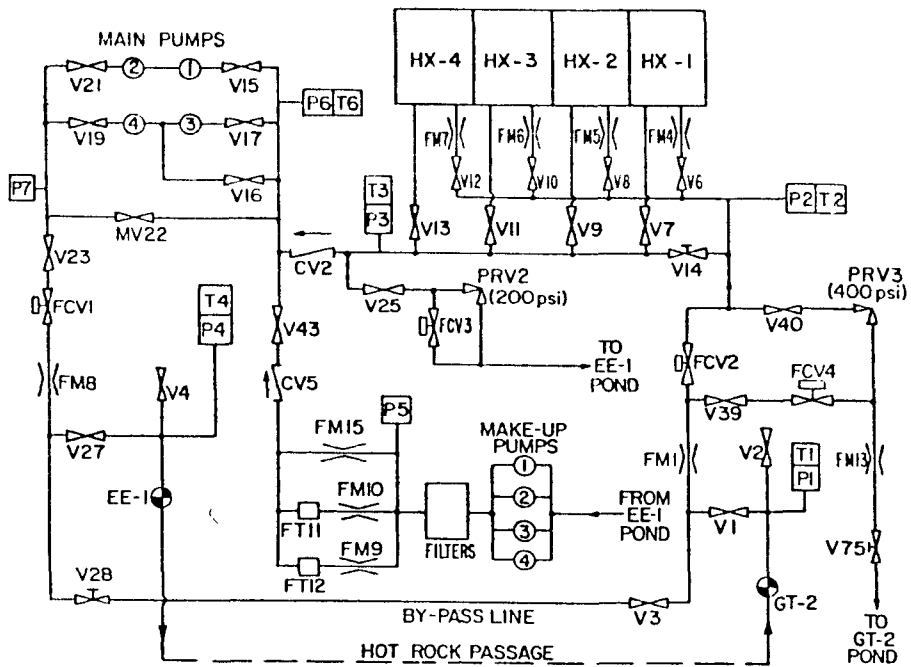


Fig. 2-5.  
Schematic of the Fenton Hill circulation system with modifications.

where the output flows through a restriction or impedance. If this restriction is suddenly reduced, a higher flow out of the reservoir will result. This occurred several times, and twice the change in impedance was sufficient to cause problems in loop operation. At these times there were increases in the flow from the production wellbore, the flow and temperature to the heat exchanger, and the heat exchanger exit flow and temperature. When the pump inlet pressure exceeds the makeup limiting discharge pressure, the makeup flow ceases. When the heat exchanger output temperature (pump inlet temperature) exceeds the specified limit for the seals, the pumps are programmed to shut down. In two instances, the loop was shut down automatically by these perturbations, at one time for as long as 3 h as shown in Fig. 2-4. It took many hours to get the system running smoothly after a large change in impedance. This involved adjusting flow rates, makeup pressures, heat exchanger louver settings, and throttle valve settings.

To streamline operation and increase injection flow capacity, several modifications to the loop have been made as shown on Fig. 2-5. These are (1) the installation of a new makeup pumping system with a capacity of  $\sim 14.2$  l/s (225 gpm), (2) the addition of flow control valves at GT-2 (FCV2 and FCV4) to maintain smooth operation when perturbations in reservoir impedance or flow occur, (3) the installation of two new multistage centrifugal pump units to increase circulation rate capacity to  $\sim 32.6$  l/s (500 gpm) at a differential pressure of 93 bar (1350 psi), (4) the addition of an antifreeze circulation system to avoid freeze up during emergency shutdowns, and (5) installation of a larger capacity flow control valve and piping at EE-1 to accommodate up to 40 l/s. A pressure lock system was also installed at the EE-1 wellhead to allow logging in EE-1 during operation.

### 3. RESERVOIR HEAT EXTRACTION CHARACTERISTICS (H. Murphy)

#### 3.1. Measurements and Data

Injection and production flow rates were measured with venturi meters and differential pressure transducers. Surface injection and production temperatures were measured by thermocouples inserted into the wellheads. In addition, a temperature surveying tool with a  $0.05^{\circ}\text{C}$  resolution employing a thermistor was positioned downhole in the GT-2B production well for almost the entire duration of the test. A total of 58 logs or surveys were taken during the 75-day run. Between surveys the tool was stationed at 2.6 km (8600 ft), just above all the known producing zones in GT-2B. In this fashion the mean temperature due to the mixed fluid flows converging upon GT-2B was continuously monitored.

A typical set of temperature surveys is presented in Fig. 3-1. Only the downhole region where the produced fluid enters the well is shown. The uppermost survey was obtained on February 4, 1978, 7 days after the start of power production, while the middle and lower surveys were obtained after 12 and 16 days, respectively. Even a cursory look at these surveys indicates a complex reservoir-to-production well connectivity. The major temperature changes at the depths indicated with arrows are associated with flow connections identified in earlier testing.<sup>3</sup> (See Section 4.4 also). These earlier results showed that 20% and 80% of the flow enter the deepest and next deepest of these four main connections whereas the flow rates in the upper two were too small to be measured. The more precise logs taken during Segment 2, in which digitized temperature data were obtained every 0.15 m, showed that even these major connections seemed to have fine structures that changed with time. For example, both major connections 1 and 2 actually consist of two connections each. At connection 2, a colder flow rate entered at the bottom, but 2 meters farther up, water at least  $5^{\circ}\text{C}$  hotter entered the well. The second survey and even more visibly the third survey show the development of new flow connections located between the previously established major connections 1 and 2, and in fact, the magnitude of the temperature change at 2.68 km (8800 ft) suggests that a major connection has developed there. In Section 4.4 this information along with flowing spinner surveys and radioactive tracer logs are used to characterize the production and injection zones.

Figure 3-2 presents the variation of temperature at 2.6 km (8500 ft) with time. As stated earlier, the measurement is made above all the flow connections

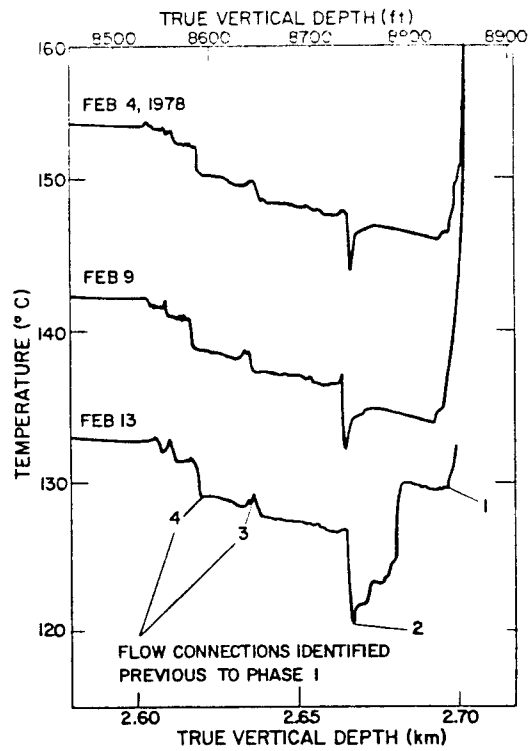


Fig. 3-1.

Three temperature surveys taken in the bottom section of GT-2B during Phase I.

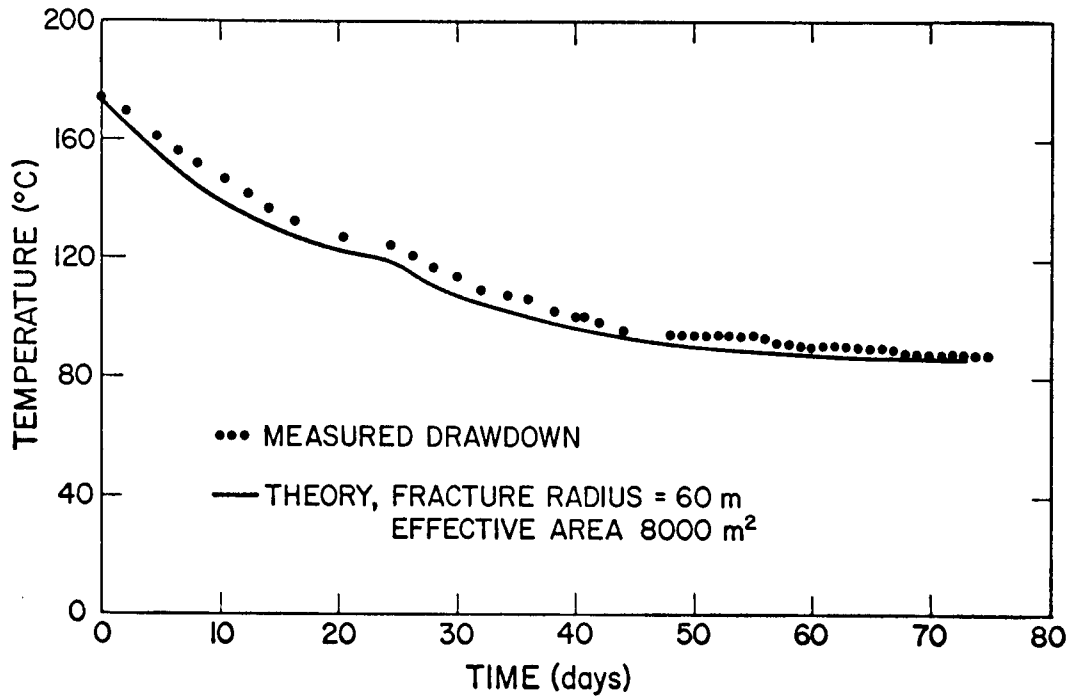


Fig. 3-2.

Thermal drawdown of produced fluid measured at a 2.6 km (8500 ft) depth in GT-2B.

so that the temperature represents the mean temperature of the mixed fluid in the production wellbore and thus provides an indication of the overall thermal drawdown of the reservoir. Figure 3-2 also shows the predicted drawdown for a reservoir with a surface area (one side only) of  $8000 \text{ m}^2$  ( $8.6 \times 10^4 \text{ ft}^2$ ). These theoretical results are described in the next section. The "scallop" in Fig. 3-2 results from a doubling of the production flow rate.

Figure 3-3 presents the net thermal power produced using a constant  $25^\circ\text{C}$  surface reinjection temperature in the calculation. Despite the declining production temperatures, the increasing flow rate allowed the power to be kept roughly constant for the last 40 days. Peak power was 5 MW(t).

### 3.2. Thermal Drawdown Analysis

To interpret the drawdown results of Fig. 3-2 in terms of effective heat transfer area it was assumed that the fracture system could be described as a single circular fracture. This is indeed an approximation -- the actual fracture need not be circular, and in fact multiple fractures may be possible,<sup>3</sup> but our

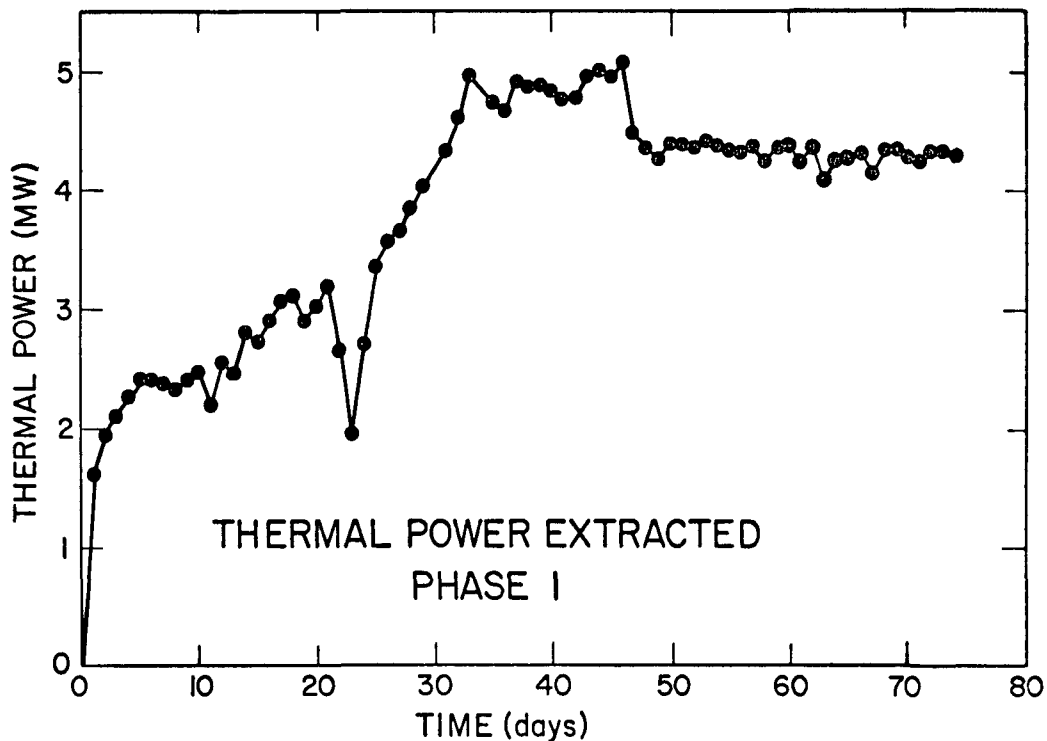


Fig. 3-3.  
Net thermal power extracted during Phase I.

intent is to provide an estimate of the fracture area effective for heat transfer; thus the assumption of a single circular fracture is reasonable for a first estimate.

Because the hydraulic fracture itself is much more permeable than the surrounding rock, it was assumed that fluid was confined to the fracture and that heat from the rock was transported to the fluid in the fracture only by means of thermal conduction in the rock. (The possible enhancement of the heat transfer area because of thermal stress cracking is not considered in this model.) In fact, a small amount of fluid did penetrate the surrounding rock, particularly at very early times as evidenced by the makeup losses. (See Section 4.3.) To correct for this effect fluid loss was assumed to occur uniformly over the fracture area. Thus the permeation effect can be approximated by assuming that on the average, heat was removed from the reservoir by all of the produced water flow and half the difference between the injected and produced water flows.

### 3.3. Heat Extraction

To model the heat extraction process, several equations related to the fluid in the fracture and the surrounding rock are important. In the fracture plane, the horizontal coordinate is taken as  $x$ , the vertical coordinate as  $y$ . Solid rock heat conduction takes place along the  $z$ -coordinate, perpendicular to the  $x$ - $y$  fracture plane. Using Darcy's law for flow in the open fracture with a permeability or hydraulic conductivity of  $\frac{w^2}{12}$ , the flow velocities  $u$  and  $v$  in the  $x$  and  $y$  directions are, respectively:

$$u = - \frac{w^2}{12\mu} \frac{\partial P}{\partial x} \quad \text{and} \quad (3-1)$$

$$v = - \frac{w^2}{12\mu} \left[ \frac{\partial P}{\partial x} - \rho g \beta (T - T_0) \right], \quad (3-2)$$

in which

- $w$  = fracture aperture or width
- $P$  = pressure
- $\mu$  = viscosity
- $t$  = time
- $T_0$  = reference temperature, eg. fluid injection temperature
- $T$  = temperature of the fluid
- $T_r$  = initial equilibrium rock temperature

- $g$  = acceleration of gravity  
 $\beta$  = volumetric expansion coefficient of fluid  
 $\lambda$  = thermal conductivity of rock  
 $\theta$  = temperature of the rock  
 $\rho$  = fluid density  
 $e$  = the flux of energy delivered to the fluid by one rock surface  
 evaluated as  $e(t) = \lambda \frac{\partial \theta}{\partial z} (x, y, z = 0, t)$   
 $c$  = specific heat capacity of fluid,

and where the last term in the equation for  $v$  represents the effects of buoyancy.

By making the Boussinesq approximation, the equations of conservation of mass and energy in the flowing fluid are:

$$\frac{\partial}{\partial x} \left( \frac{w^3}{\mu} \frac{\partial P}{\partial x} \right) + \frac{\partial}{\partial y} \left[ \frac{w^3}{\mu} \left( \frac{\partial P}{\partial y} - \rho \beta g (T - T_0) \right) \right] = 0 \quad \text{and} \quad (3-3)$$

$$\rho c w u \frac{\partial T}{\partial x} + \rho c w v \frac{\partial T}{\partial y} - 2e = 0 \quad , \quad (3-4)$$

Finally, the rock conduction equation is

$$\frac{\partial \theta}{\partial t} = \frac{\lambda}{\rho_r c_r} \frac{\partial^2 \theta}{\partial z^2} \quad , \quad (3-5)$$

where  $\rho_r$  and  $c_r$  are the density and heat capacity of the rock, respectively. Equation (3-5) is subject to the initial and boundary conditions

$$\theta(x, y, z, t=0) = T_r \quad , \quad (3-6)$$

$$\theta(x, y, z=0, t) = T(x, y, t) \quad , \text{and} \quad (3-7)$$

$$\theta(x, y, z \rightarrow \infty, t) = T_r \quad . \quad (3-8)$$

These coupled nonlinear partial differential equations are solved numerically.<sup>4,5</sup>

In the calculations, the observed time variations of production and injection flow rates as well as the reservoir injection temperature were used. Initial equilibrium rock temperatures and their variation with depth were determined from borehole equilibrium temperature surveys. The downhole temperature variation was calculated by the WELLBOR code.<sup>6</sup> Heat transfer causes this variation by radial conduction to the convecting fluid as it is pumped down the injection well. The measured wellhead temperature and injection flow rate at

EE-1 were used as initial conditions. The accuracy of this estimate of fluid injection temperature as it enters the reservoir at 2760 m (9050 ft) can be assessed in Fig. 3-2, where the predicted downhole temperature variation in GT-2B is in good agreement with measurements. This calculation was performed using the measured downhole temperature (2.6 km or 8500 ft) on day 0 and the production flow rate, as initial conditions.

As hot fluid flows into the production wellbore and rises to the surface, it is cooled as the formation surrounding the wellbore is heated. The rate of wellbore heat loss declines continuously as the circulation continues. Consequently if fluid enters the production zone at a constant temperature, a monotonic increase in wellhead temperature approaching the production zone temperature is observed. When thermal drawdown occurs, it is superimposed on this wellbore heat loss effect. In the present system the production surface temperature peaked after 6 days because of the coupled effect of reservoir thermal drawdown and wellbore heat loss.

For these reservoir simulations, a constant value of 0.2 mm was assumed for fracture aperture (width), which results in an overall fracture impedance of 3 bar-s/l ( $\sim$  3 psi/gpm). During the early phases of the experiment, the impedance of the total system was actually as high as 16 bar-s/l (15 psi/gpm) before being reduced to the former value. Earlier testing<sup>2</sup> showed that the total system impedance was composed of a main fracture impedance of 4 bar-s/l (3.7 psi/gpm) and a fracture-to-production well impedance of 8 to 12 bar-s/l (7.3 to 11 psi/gpm). This latter impedance resulted because the re-drilled production hole did not directly intersect the main fracture. The observed reduction of total impedance may simply reflect a reduction of this latter component, rather than a reduction of fracture impedance itself. Certainly, the new flow connections indicated in the production well temperature survey, Fig. 3-1, and the spinner survey results given in Section 4.4 suggest that the reduction occurred in the fracture-to-wellbore impedance.

Using the above data and assumptions, the simulator was run for several assumed fracture radii until the complete thermal drawdown history could be matched. The results for a 60-m (200-ft) radius fracture agreed quite well with the measurements, as previously shown in Fig. 3-2. Because of hydrodynamic flow inefficiencies, only about 75% of the fracture area actively transferred heat; so the effective heat transfer area was only 8000 m<sup>2</sup>.

We emphasize that this is not a measure of the total fracture area accessible to water. The effective heat transfer area is strongly influenced by the vertical separation of the fracture water inlet and outlet locations. Because fracture flow impedances are  $\sim 3-4$  bar-s/ $\ell$  buoyant forces will not significantly affect flow patterns within the fracture, and the water only partially fans out between the inlet and outlet points. Thus the effective heat transfer area swept by this flow is a direct function of the inlet and outlet spacing. In the present case the spacing between the inlet located at 2.76 km (9050 ft) in the injection well and the production well connection with the highest flow capacity is approximately 100 m. Roughly speaking, then, the effective area would be defined by a circle 50 m in radius, with an area of 7900 m<sup>2</sup>, very close to that derived with the simulator.

The possibilities of reducing flow impedances and enhancing heat transfer area by means of thermal cracking as the reservoir cools and contracts were discussed by Murphy.<sup>1</sup> Subject to large uncertainties in our knowledge of the maximum horizontal earth stress, it was estimated that the effects of thermal cooling might be apparent after a cooling of about 75°C or more. A close scrutiny of the temperatures in Fig. 3-2 shows that starting at 48 days there is a period of 8 days in which the temperature was constant. Additional constant temperature intervals are noted starting at day 58, and then again on day 68. Each of these plateaus was terminated by stepwise decreases in temperature. Such behavior may have resulted from thermal stress cracking or possibly the enlargement of the heat transfer area by pore-pressure induced fracturing. Murphy suggested that a state might be sustained in which continued power production was matched by the continual creation of new heat transfer area, so that the temperature would remain essentially constant. To verify this hypothesis, an extended circulation period at the rate of 14.5  $\ell/s$  (230 gpm) would be required. Furthermore at this drawdown rate, a quasi-steady state condition exists where the decline rate is very small, making it difficult to discern changes due to fracture extension by thermal cracking or other effects. Future tests at higher circulation rates are planned as well as evaluation of the concept in deeper, hotter reservoirs where induced thermal stress would be higher.

#### 4. RESERVOIR FLOW CHARACTERISTICS AND MODELS

##### 4.1. Flow Impedance (R. L. Aamodt and R. M. Potter)

For the circulation system, the flow impedance is defined as the pressure drop through the fracture system connecting two wellbores divided by the flow rate. There is some ambiguity in the definition because the injected flow differs from the produced flow because of the fluid permeation rate into the rock surrounding the fracture. Conservatively, we adopted the production flow rate in the definition.

Since there were no downhole pressure gauges, the downhole pressure drop through the fracture system was obtained from the measured surface pressure difference between EE-1 and GT-2, corrected for the difference in fluid density between wells. This buoyancy correction requires a knowledge of the temperature distribution in each well. The corrections shown in Fig. 4-1 were derived from calculated wellbore temperatures during the first 3 weeks of operation as well as estimates based on surface and downhole temperature measurements at later times, with a few periodic checks obtained from GT-2B temperature logs over the entire wellbore.

The downhole temperature changed slowly at late times, as shown in Fig. 3-2. In addition, the injection well temperature fluctuated, but was generally lower in the last 6 weeks. As a result, the buoyancy correction remained almost constant during this time. A possible 20% error in buoyancy is reflected as less than 5% error in impedance, since the buoyancy correction was never more than 25% of the total measured pressure difference between EE-1 and GT-2B.

Figure 4-2 shows the measured impedance during the first 4 hours of the test. After a few minutes, the impedance oscillates between 14 and 17.5 bar-s/l (13-16 psi/gpm), very near the steady state value of 17.5 bar-s/l, which was observed on the second day through the sixth. This indicates that a large fraction of the initial flow came along a direct path with little or no diffusion in series with the path.

As seen in Fig. 4-3, the impedance began to fall after one week of flow. Figure 4-4 is an idealized graph of the flow and pressure history in EE-1. The maximum flow into EE-1 was limited by surface plumbing to less than 16 l/s (250 gpm), and as the impedance dropped, it became impossible to maintain a constant injection pressure. Consequently it was decided to keep the injection flow rate constant at  $\sim 14$  l/s ( $\sim 230$  gpm). This was generally done during the second

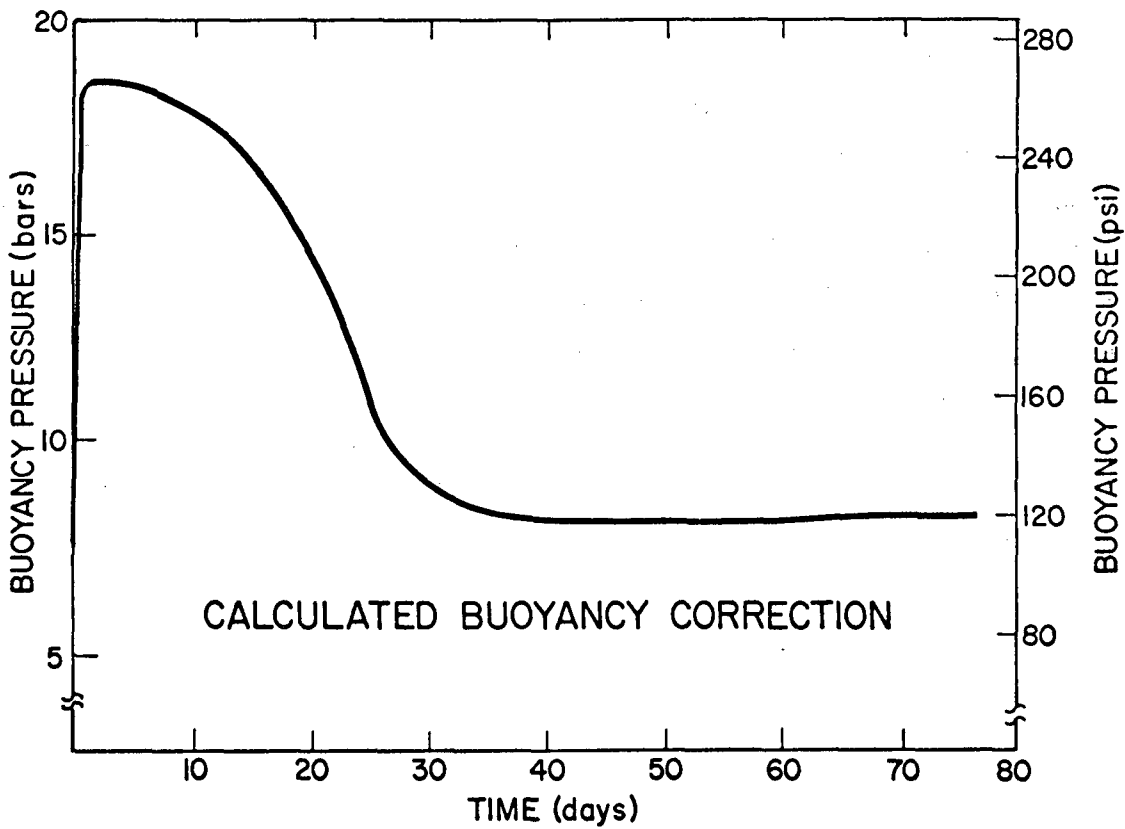


Fig. 4-1.

Calculated buoyancy correction between the GT-2B production and the EE-1 injection wellbores.

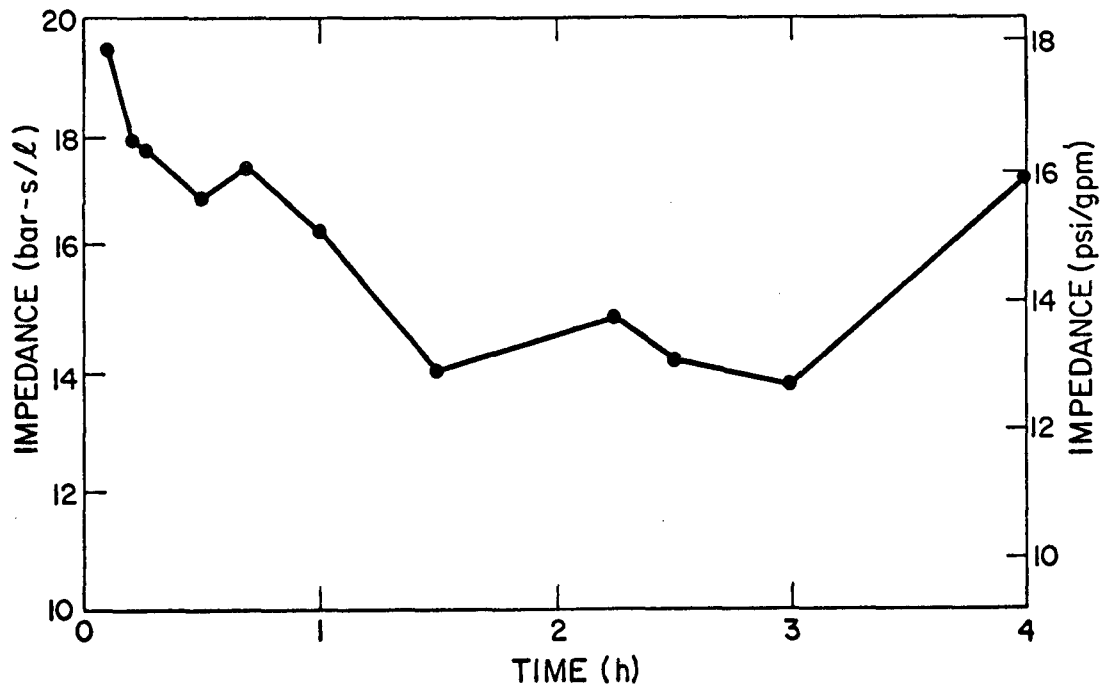


Fig. 4-2.

Early net flow impedance with buoyancy corrections included.

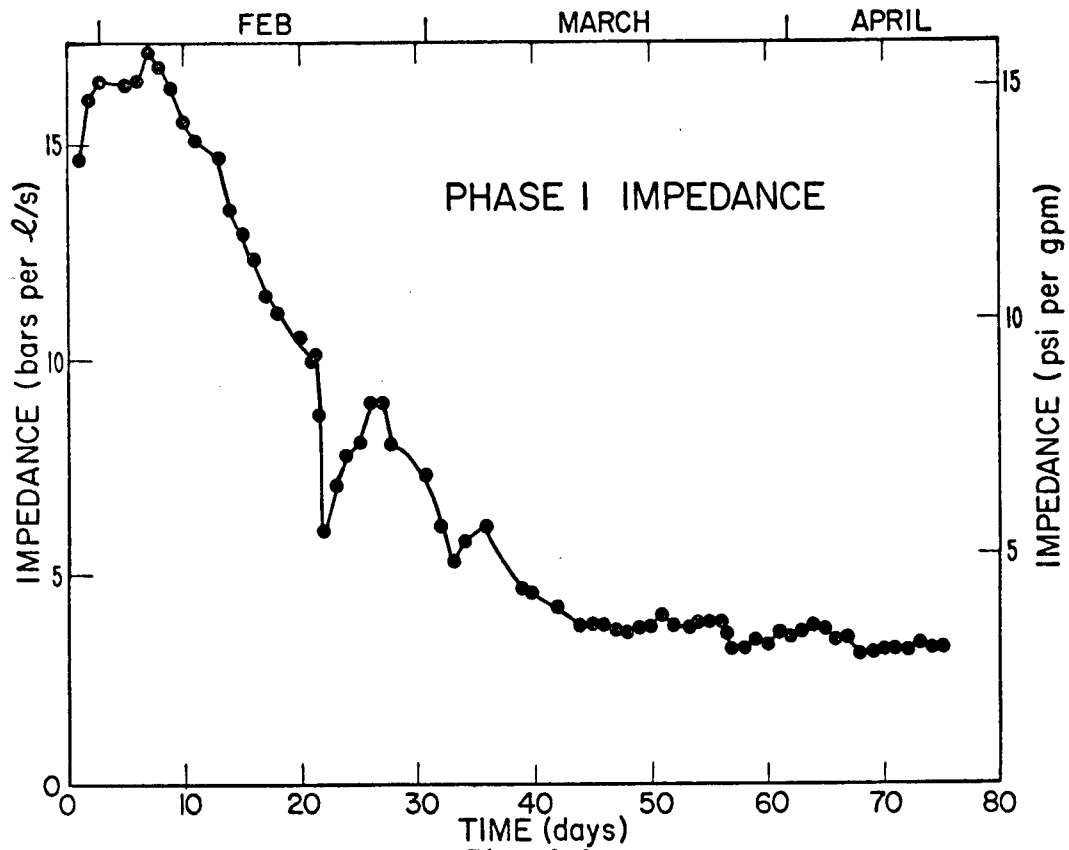


Fig. 4-3.

Net flow impedance between the GT-2B production and EE-1 injection wellbores with buoyancy corrections included.

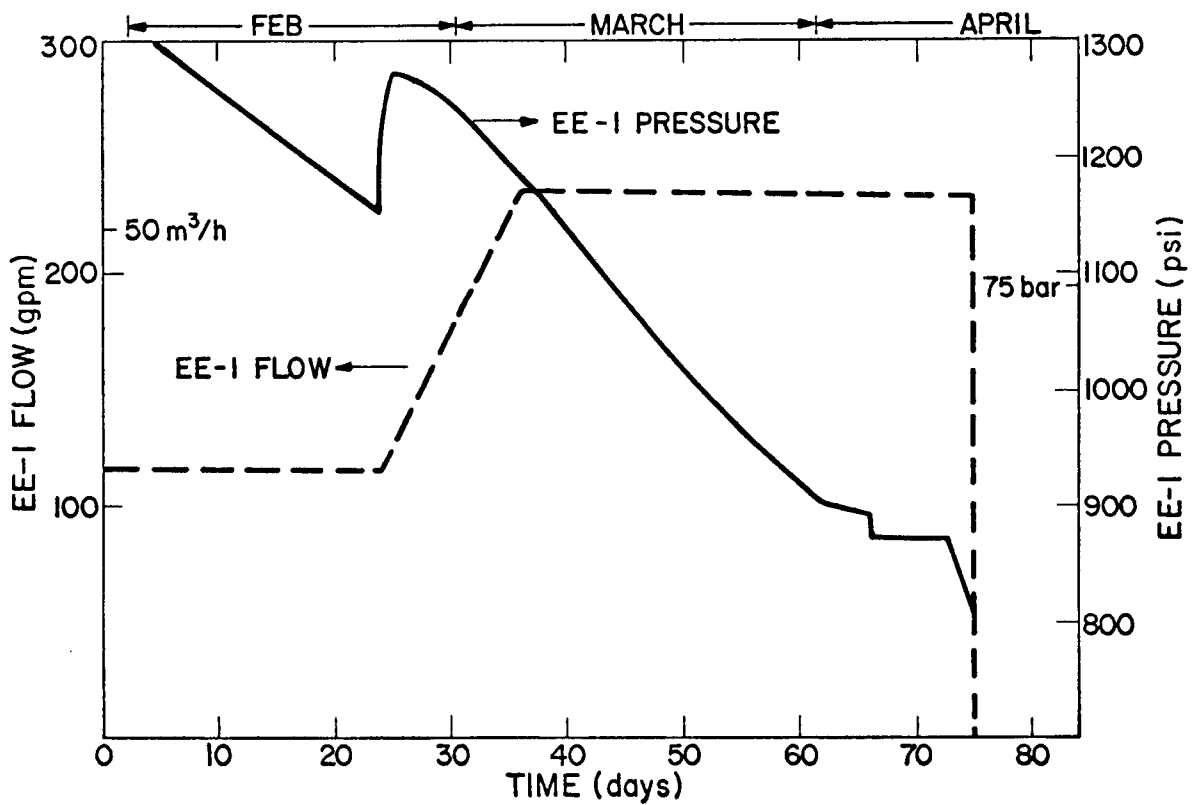


Fig. 4-4.

Idealized pressure and flow history at the EE-1 injection wellhead.

half of the test, as seen in Fig. 4-4. The impedance decreased to less than 1/3 the original value in the first 40 days, but decreased only 25% more from day 40 to the end of the run at day 75.

Events of continuous or abrupt nature, which result in impedance changes, can occur in a mass of rock that is cooled, pressurized, or both. Appendix A discusses an idealized case of the shrinkage of fracture faces away from each other, caused by cooling and pressurization. Separation of fracture faces should occur gradually as heat is extracted, rather than abruptly. Appendix B discusses changes in the compressive stresses inside a spherical region of rock, caused by uniform cooling or pressurization. When the stresses in the rock decrease together, so that the stress differences do not change, the normal stresses across many of the fractures will decrease, while the shear stress remains constant, and one fracture face may slip across the other. Because the pre-existing fractures were not truly planar, this slippage may result in a partially open crack, supported by small irregularities along the faces. Such an event would cause an abrupt change in flow impedance.

The real reservoir must be much more complex than any of these simple models, with both irregular regions of cooling and irregular regions of pressurization (not necessarily the same regions). Stresses will be relieved in some regions and concentrated in others, possibly leading to extensive localized rubbleization of the rock.

Temperature logs, like those shown in Fig. 4-5, were made in the open hole portion of GT-2B during the early portion of the run. Leakage problems in the pressure lock system from cable packoff eventually made it necessary to omit these logs. Those that were recorded were informative. Places where sudden changes in wellbore temperature occur are assumed to be producing zones, and a change in the magnitude of a step increase or decrease of temperature from one log to another probably represents a change in the flow along a particular path. In the absence of such changes, the shape of the logs was quite reproducible from day-to-day, as seen in Fig. 4-5, which is actually a superposition of two logs made on successive days. The next day's log, as seen in Fig. 4-6, showed an increased influx of hot water near 2680-m (8800-ft) depth.

Examination of the downhole temperature, surface pressure and produced flow data over the time span between the last two temperature logs showed that an increase in flow rate, accompanied by changes in EE-1 and GT-2B pressure and

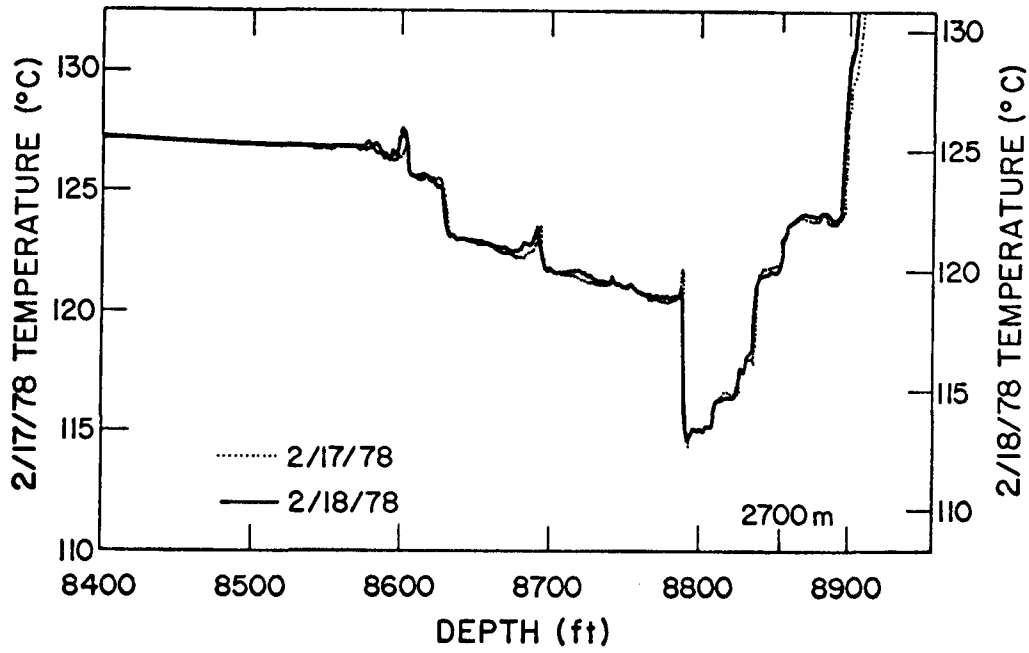


Fig. 4-5.  
Temperature logs from the bottom section of GT-2B taken on February 17 and 18, 1978.

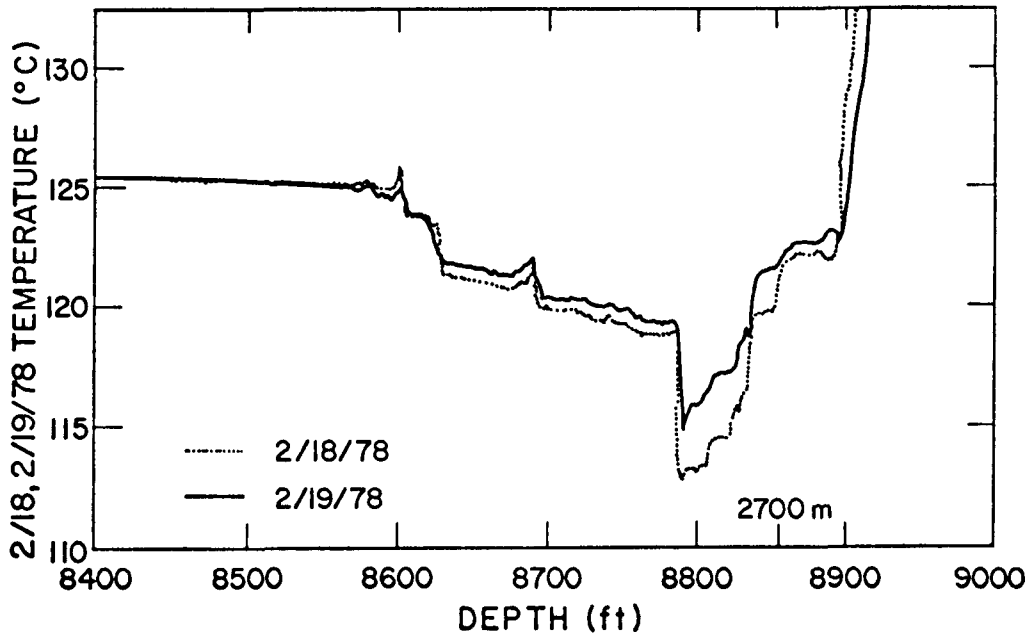


Fig. 4-6.  
Temperature logs from the bottom section of GT-2B taken on February 18 and 19, 1978.

downhole temperature, occurred within a 15-min time span (the data-recording interval) just before 0100 in the morning of the second log. These changes are shown in Fig. 4-7 and 4-8. A number of such events were found in the records. When the logarithm of the number of events with step flow increases above a certain size was plotted against the logarithm of the size of the increase (Fig. 4-9), a straight line with a slope of -1 was obtained. Many small events must have been missed, but those which were observed were sufficient to account for over half the flow increase observed during the run. Thus, many of the events causing impedance changes took place within a short time span, possibly only fractions of a second. We concluded therefore that the rock may have undergone considerable dislocation during the 75-day test.

#### 4.2. Fracture System Size and Degree of Mixing (J. W. Tester)

Dye tracer techniques developed previously<sup>2</sup> were used to characterize the fracture system volume and fluid residence-time distribution (RTD) within the reservoir during circulation. In the four experiments run during the 75-day test, a 200-ppm, 400-liter (100-gal) pulse of sodium-fluorescein dye was injected into the EE-1 wellhead, pumped down EE-1 and through the fractured region, and up the GT-2B wellbore. Dye concentration in the produced fluid was monitored spectrophotometrically at the surface as a function of time and volume throughput.

To evaluate the experimental residence time distributions several simple normalization procedures were used. The results of the four experiments and their statistical analysis are summarized in Table 4-I and Fig. 4-10. The distributions have been characterized using integral (first moment) mean volumes, median volumes, integral mean volumes using a trimmed section of the distribution, and variances of the normalized distributions. These can be expressed using the following equations and definitions:

$$C_{\theta} = C_i / \left[ \frac{1}{V} \int_0^{\infty} C_i dV \right] = \text{normalized concentration} \quad (4-1)$$

$$\langle V \rangle = \int_0^{\infty} VC_i dV / \left[ \int_0^{\infty} C_i dV \right] = \text{integral mean volume} \quad (4-2)$$

FEB 19, 1978 EVENT

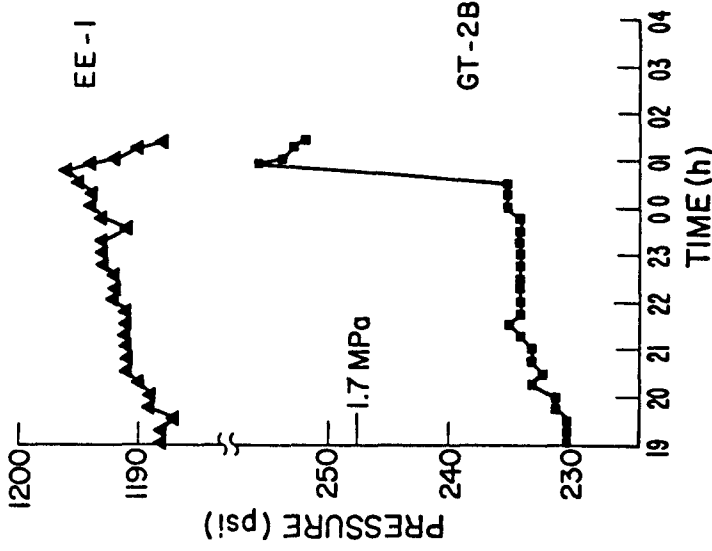


Fig. 4-7.  
GT-2B and EE-1 surface pressure histories near the February 19, 1978 event.

FEB 19, 1978 EVENT

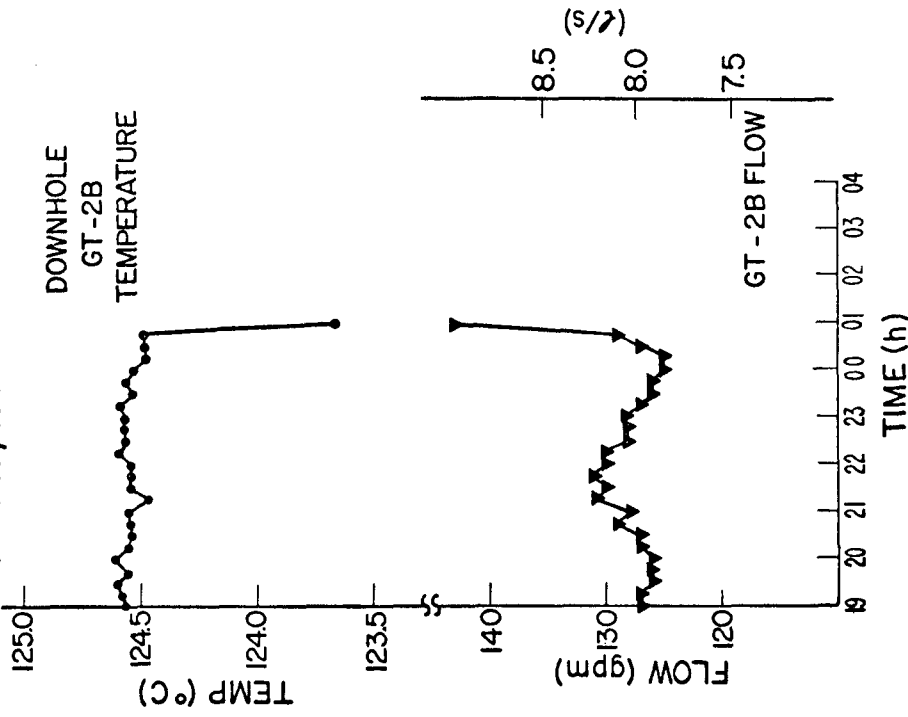


Fig. 4-8.  
Downhole temperature at 2.8 km (8500 ft) in GT-2B and production flow histories near the February 19, 1978 event.

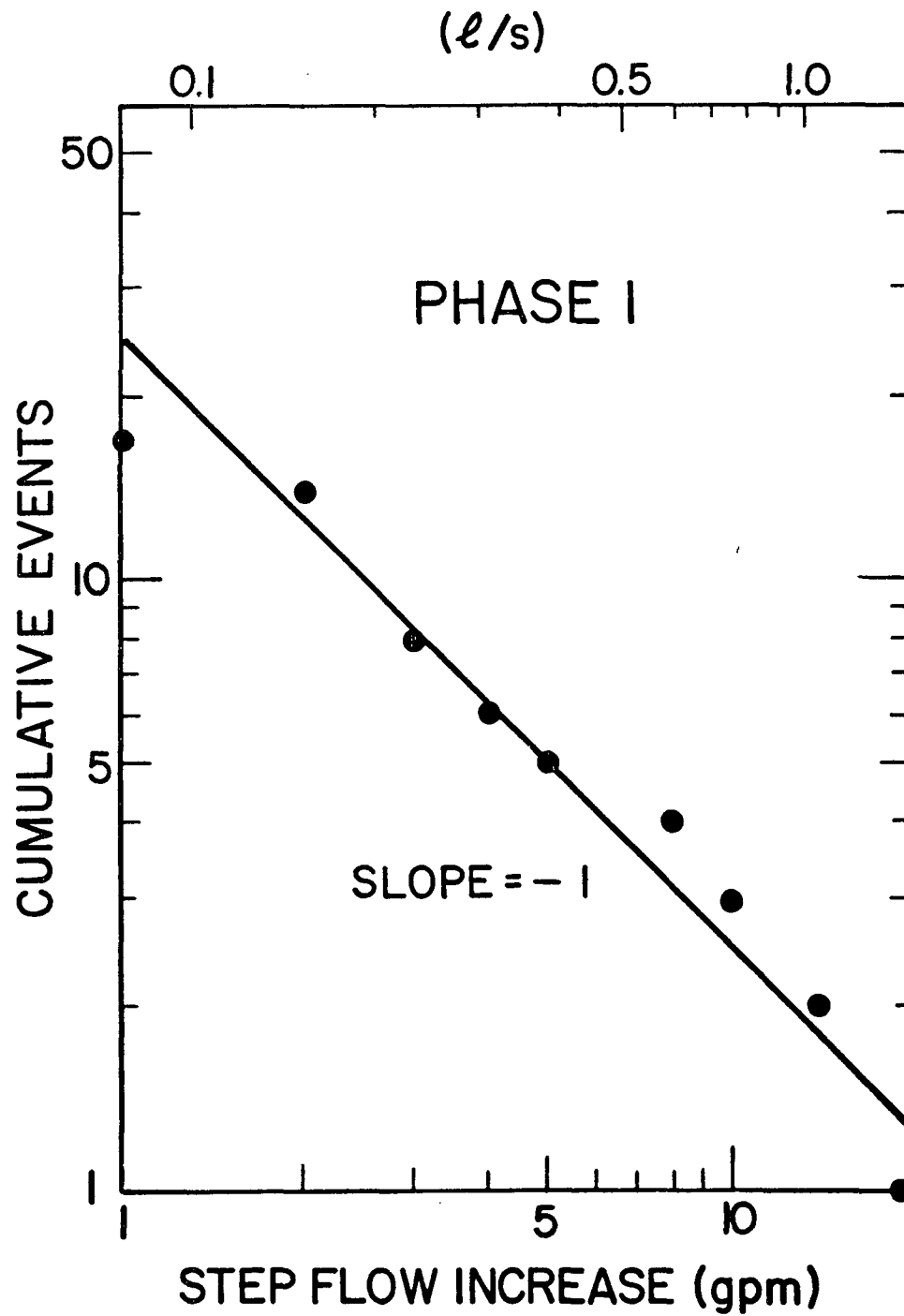


Fig. 4-9.  
Correlation of the frequency of events to the size of the production flow increase in GT-2B.

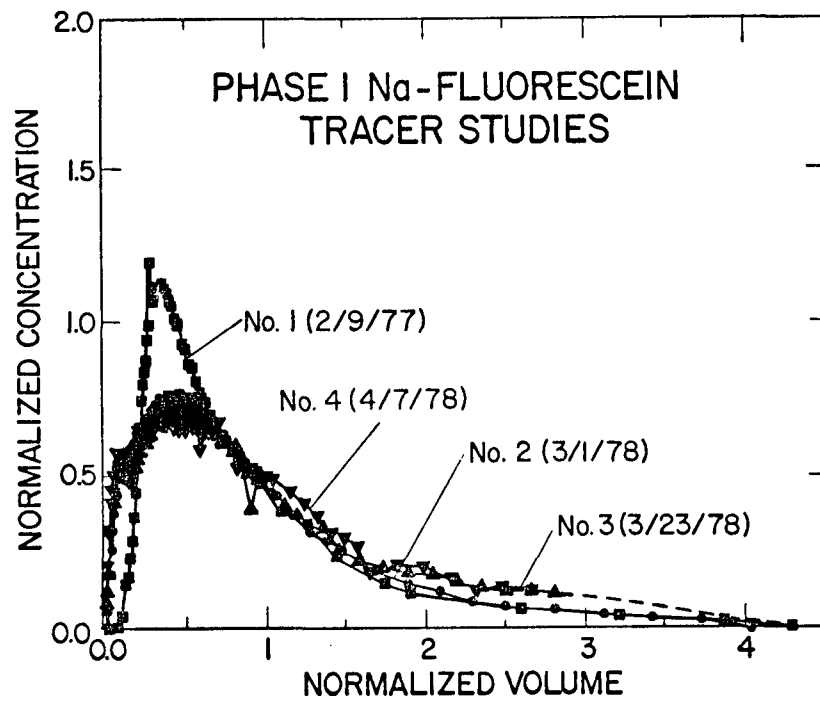


Fig. 4-10A.

Normalized tracer concentration as a function of normalized fracture system volume.

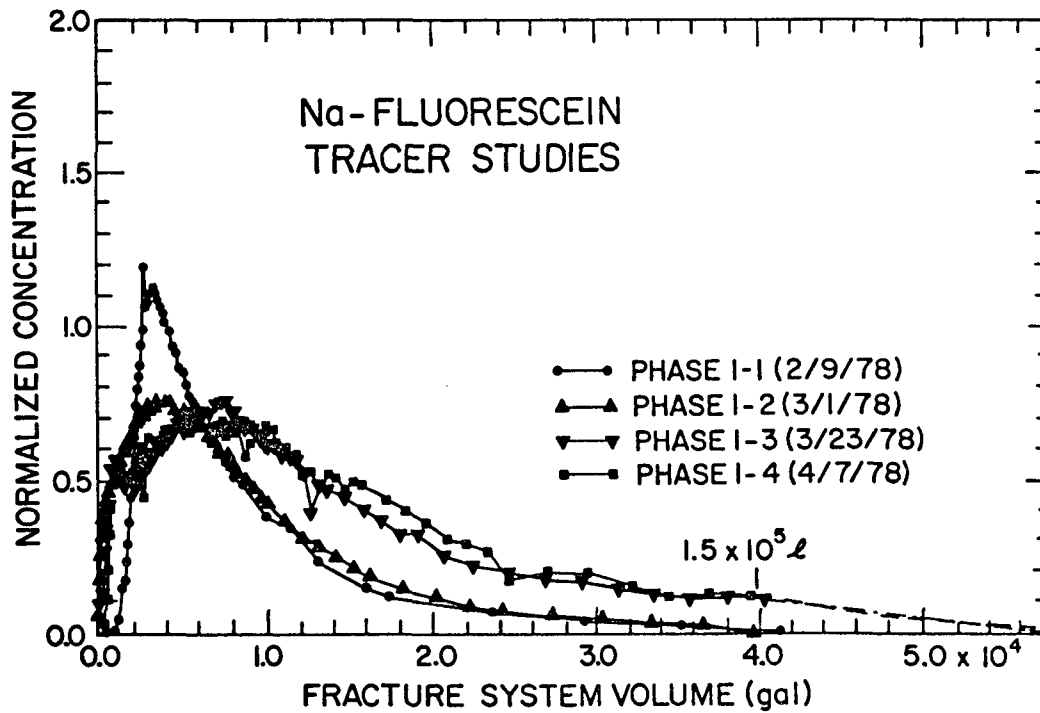


Fig. 4-10B

Normalized tracer concentration as a function of fracture system volume.

TABLE 4-I  
RESIDENCE-TIME DISTRIBUTION RESULTS

EXPERIMENT	$Q$ 10 <sup>6</sup> gallons	$\bar{q}$ gpm <sup>b</sup>	dye recovery (%)	$\langle V \rangle$ gal <sup>c</sup>	[V] gal	V  at 90% gal	$\sigma_{\theta}^2$	$\sigma_{\theta}^2$ (90%)	$Pe^{*-1d}$
Phase 1-1 (2/9/78)	2.1	115	69	9089	6753	7728	0.65	0.44	0.591
Phase 1-2 (3/1/78)	6.9	208	65	9899	7644	8160	0.62	0.43	0.942
Phase 1-3 (3/23/78)	15.1	220	71 <sup>a</sup>	14446	11904	12218	0.51	0.42	0.944
Phase 1-4 (4/7/78)	20.0	240	> 65 <sup>a</sup>	14855	12786	12998	0.47	0.39	1.120

<sup>a</sup>Estimated from extrapolation of the RTD tail shown in Fig. 4-9; actual recovery to 40 000 gal was 63% for 1-3 and 57% for 1-4.

<sup>b</sup>1 gpm = 6.31 x 10<sup>-2</sup> liters/s (L/s).

<sup>c</sup>1 gal = 3.785 liters.

<sup>d</sup> $Pe^{*-1} = D/u\ell$  = inverse Peclet number.

$$[V] = \text{median volume} \int_0^{[V]} C_i dV / \left[ \int_0^{\infty} C_i dV \right] = 0.5 \quad (4-3)$$

$$|V| = \int_0^{V^*} VC_i dV / \left[ \int_0^{V^*} C_i dV \right] = \text{trimmed mean volume.} \quad (4-4)$$

$$\bar{\tau} = \langle V \rangle / \bar{q} = \text{integral mean residence time, and} \quad (4-5)$$

$$\sigma_{\theta}^2 = C_{\theta} \text{ distribution variance} = \int_0^{\infty} V^2 C_i dV / \left[ \langle V \rangle^2 \int_0^{\infty} C_i dV \right] - 1, \quad (4-6)$$

where

$C_i$  = measured output dye concentration

$V$  = fracture system volume corresponding to  $C_i$

$\bar{q}$  = mean flow rate through the fracture system

$V^*$  = truncation point in the trimmed distribution.

Flow in the fracture system can be described as well-mixed with no major short circuits. Dispersion of flow in a single hydraulic fracture does not account for all of the mixing. Because of this and the known existence of multiple flow paths between EE-1 and GT-2B, the observed shape of the RTD is caused by dispersion within individual flow paths as well as superposition from mixing of various production flows in the wellbore (see also Section 4.4 and 4.5). Consequently, several statistical quantities are needed to describe flow in the system. The median volume probably adequately represents the flow through the major production paths in GT-2B, while the increase in the spread of the distribution to larger volumes as evidenced by an increasing integral mean and variance are indicative of longer residence time paths possibly through more circuitous routes in the rock. The results of the RTD studies have been incorporated into a general flow model, which is discussed in detail in Section 4.5. However at this time, several general comments can be made: (1) The fracture flow system has grown considerably in size during the 75-day test, the integrated mean fracture system volume  $\langle V \rangle$  increased to 56 400 ℓ (14 900 gal), up from 37 500 ℓ (9900 gal) on March 1, and the median volume became larger, 48 500 ℓ (12 800 gal) vs 28 800 ℓ (7600 gal). (2) Development of additional flow paths, was evident because of different arrivals of dye with smaller and larger residence times (or volumes), increasing the spread of the distribution. (3) The

apparent degree of mixing or dispersion (D) is virtually unchanged between the March 1 and April 7 experiments as shown by the similar shapes of the phase 1-2, 1-3, and 1-4 curves on the normalized coordinates of Fig. 4-9 and the similar inverse Peclet numbers ( $Pe^{*-1} = D/u\ell$ ,  $u$  = velocity,  $\ell$  = flow path length, and  $D$  = dispersion coefficient) resulting from homogeneous dispersed porous zone fits to the data of 0.942 (March 1, 1978), 0.944 (March 23, 1978) and 1.120 (April 7, 1978). (4) The increase in apparent  $Pe^{*-1}$  observed between the phase 1-1 and subsequent tests (1-2, 1-3, 1-4) cannot be explained by an increase in flow rate from 7.3 to  $\sim 14.5$   $\ell/s$  (115 to  $\sim 230$  gpm). Because we are operating in the freely turbulent region for porous media flow, one would expect a linear dependence of  $D$  on  $u$  and therefore a constant  $Pe^*$ . Additional flow paths or a change in the character of flow in existing paths is a more likely cause of the change in apparent  $Pe^*$  between the early and late tests.

#### 4.3. Fluid Loss and Storage (H. Fisher)

The water loss, or the difference between the EE-1 injected flow and the GT-2B produced flow is determined by the fracture geometry, and an appropriate average permeability and pore (or reservoir) compressibility associated with all types of porosity accessible to the flow. The fracture area involved is not necessarily the same as the heat transfer area determined by the GT-2B temperature drawdown (see Section 3). There are other fractures intersecting the EE-1 wellbore. The fractures connected to the GT-2 and GT-2A wellbore could also contribute to the water storage and loss to permeation. Any fractures directly connected to the GT-2B wellbore did not contribute significantly to the loss, because they were maintained at close to hydrostatic pressure during Phase I. The observed permeability is an average over the large scale permeability opened by previous pressurizations, any welded joints, and the microporosity. Similarly the reservoir compressibility, or the ability of the reservoir to store water, includes the compressibility of the main fractures as well as the microporosity.

The data from past pressurization and flow experiments can be fit by a model in which the fluid pressure ( $P$ ) in the reservoir is governed by a non-linear diffusion equation (Refs. 2 and 7),

$$\nabla \cdot \left( \frac{k}{\mu} \nabla P \right) = \beta \frac{\partial P}{\partial t} \quad (4-7)$$

This equation can be derived from the conservation of fluid mass and the assumption of Darcy-type flow in all forms of porosity.

The permeability  $k$  and the compressibility  $\beta$  are functions of  $P$ , but the viscosity can be considered a constant. The  $k$  and  $\beta$ , which best fit past data, can be obtained from a porosity  $\phi$  with a pressure dependence given by

$$\phi = \frac{\phi_0}{(1-C_3P)^{0.6}} \quad (4-8)$$

The compressibility,  $\beta = (\partial\phi/\partial P)_T$  is, then

$$\beta = \frac{\beta_0}{(1-C_3P)^{1.6}} \quad (4-9)$$

Since the permeability is determined by the confining stress, and the two horizontal earth stresses are not necessarily equal, two components of permeability are used. Each is related to some portion of the porosity by the Karmen-Kozeny relation for small porosity  $k_i \propto \phi_i^3$ . Then  $k_3$ , perpendicular to the minimum earth stress  $S_3$ , is

$$k_3 = \frac{k_0}{(1-C_3P)^{1.8}} \quad (4-10)$$

and  $k_2$ , perpendicular to the intermediate horizontal earth stress  $S_2$ , is

$$k_2 = \frac{k_0}{(1-C_2P)^{1.8}} \quad (4-11)$$

The exponents in Eqs. (4-9), (4-10), and (4-11) have been determined from previous experiments, as have  $C_2$  and  $C_3$ . The best results are obtained for  $C_3 \approx 5.0 C_2$ . With  $C_2$  and  $C_3$  constant, Eqs. (4-9), (4-10), and (4-11) are an approximation that holds only for  $P < C_3^{-1}$ . True singularities in Eqs. (4-9), (4-10), and (4-11) do not exist because  $P \rightarrow S_3$ ,  $C_3$ , and  $C_2$  become functions of  $P$ . This pressure dependence of  $C_2$  and  $C_3$  occurs when  $P$  contributes significantly to the local value of the total stress, and complete solutions can be obtained only if Eq (4-7) is coupled with the stress-strain relations. During much of

the 75-day test the pressure was near the minimum estimates of  $S_3$  and some adjustment of  $C_3$  is necessary to obtain good fits to the data.

As in past experiments, the pressure and flow were calculated for a disk-shaped fracture with the diffusion code AYER.<sup>8</sup> Because multidimensional permeation flow was anticipated for long pumping times, two-dimensional axially symmetric problems were used. However, only one-dimensional flow was observed for the entire 75-day pumping period. The one-dimensional portion of the flow can be characterized by the magnitude of the diffusion parameter  $\alpha = A\sqrt{k\beta}$  at hydrostatic pressure. If multidimensional flow develops, then the time constant  $\tau = A\mu\beta/k$  is needed. Here  $A$  is the effective diffusion area of the fracture.

Fluid loss data were examined in two stages. Figure 4-11 shows the loss rate  $\dot{q}$  and the EE-1 surface pressure  $P$  for the first 10 days of the test. For analysis purposes, either can be used as input, and the other results from the calculation. For the first 5 days, the input was taken to be a linear approximation of the fluid loss rate shown in Fig. 4-11. The calculated downhole pressures were then converted to equivalent surface pressures by subtracting the hydrostatic change of pressure in the wellbore corrected for temperature changes. The fit shown is for an  $A\sqrt{k_0\beta_0} = 8.1 \times 10^5 \text{ m}^3 \text{ MPa}^{-1/2}$  (or  $160 \text{ cm}^3$  when normalized to  $\beta_0 = 2.7 \times 10^{-5} \text{ MPa}^{-1}$ ) at hydrostatic pressure and at  $C_3^{-1} \approx 8.9 \text{ MPa}$ . (1 MPa = 10 bar.) Most of the discrepancy at early times (0.5 days) is probably due to the initial spike in loss rate  $q$  that was not included in the input.

For the calculation of longer term water losses (times > 5 days), the EE-1 downhole pressure was used as input to AYER. The surface pressure was approximated by the straight line segments as in Fig. 4-12, and converted to a downhole pressure by adding the temperature-corrected hydrostatic pressure in the wellbore. Figure 4-13 shows the fluid loss data as recorded on the makeup pump venturi. The dashed line is the result of the AYER calculation for the model described earlier. The data of Fig. 4-14 show totalized makeup flow as recorded on the makeup-pump Crane meter. These data have been corrected for a large vent (5300 m<sup>3</sup> or 140 000 gal) on the 23rd day. Both the loss rate data of Fig. 4-13 and the integral data of Fig. 4-14 have been corrected for the EE-1 annulus leak occurring after the 35th day. The solid curve of Fig. 4-14 is the result of the same AYER calculation as was used to match the loss rate. Because of the pressure transient at the start of pumping, the calculated lines in Figs. 4-13 and 4-14, which are a response to a step function input, begin on the third

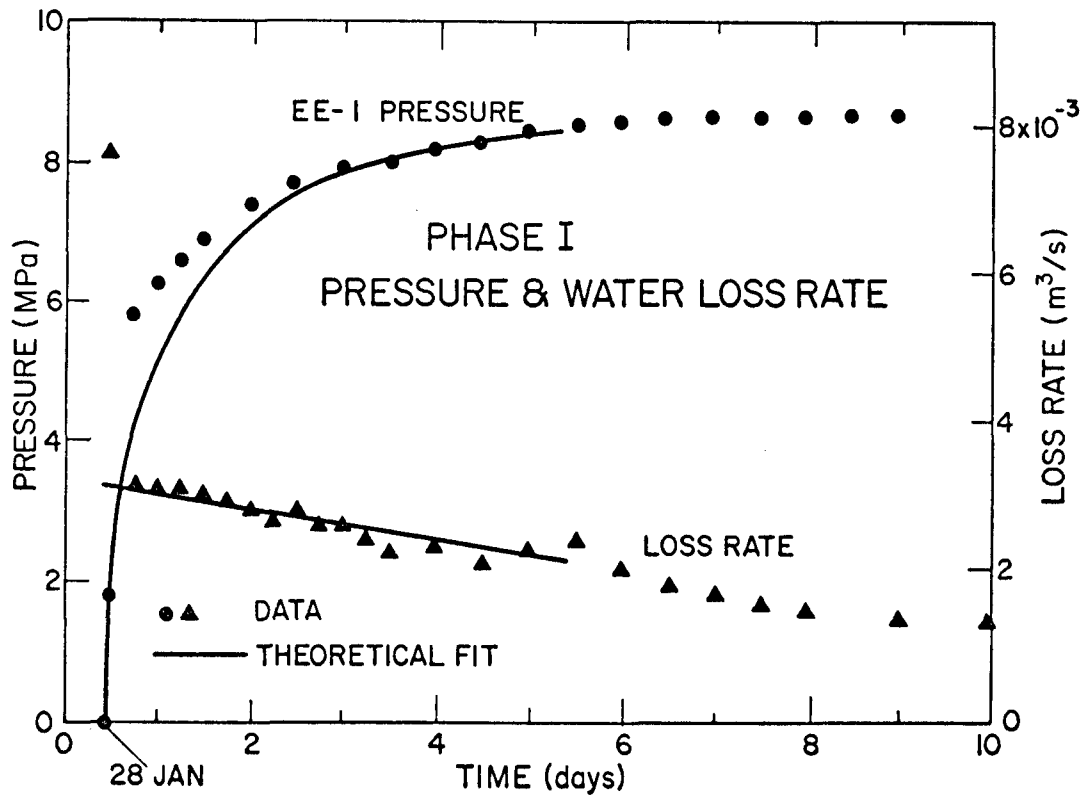


Fig. 4-11.  
Early histories of surface injection pressure and water loss rate.

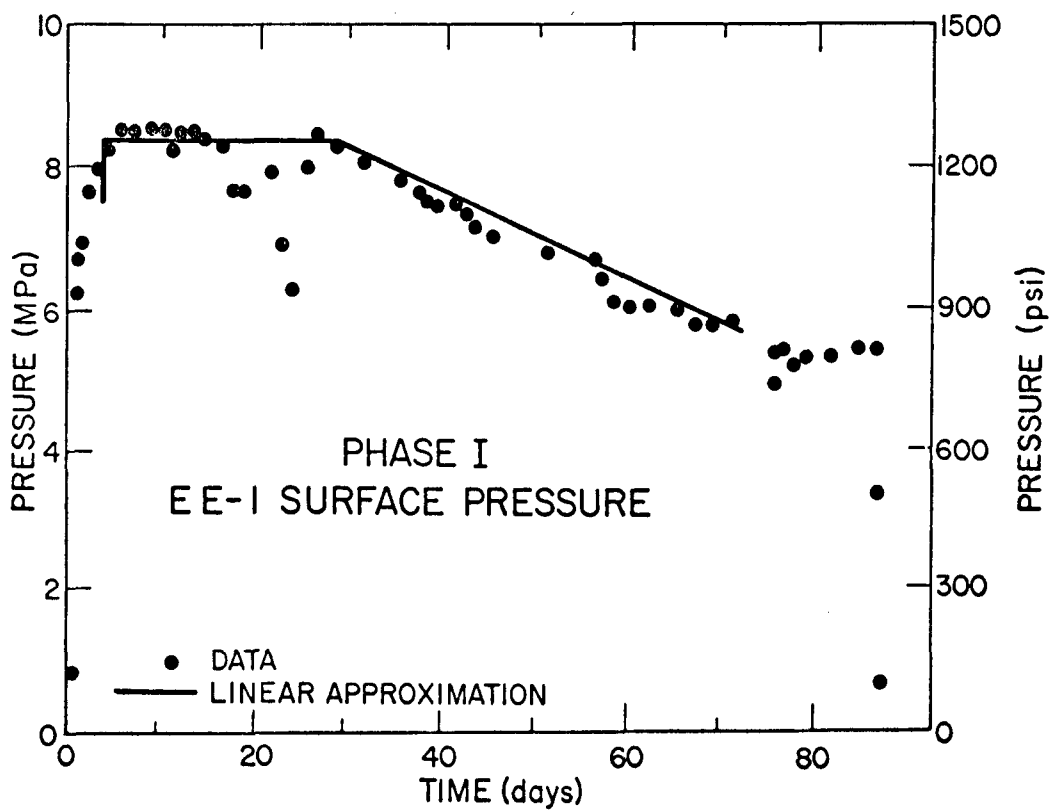


Fig. 4-12.  
EE-1 surface injection pressure and modeling approximations used.

day. The parameters in the long-term calculations are  $A\sqrt{k_0\beta_0} = 7.0 \times 10^{-7} \text{ m}^3 \text{ MPa}^{-1/2}$  (or  $137 \text{ cm}^3$  when normalized to  $\beta_0 = 2.7 \times 10^{-5} \text{ MPa}^{-1}$ ) at hydrostatic pressure and  $C_3^{-1} = 9.3 \text{ MPa}$ . The time constant  $\tau = A\mu\beta/k$  in the calculations was increased to such large values that changes in it did not significantly effect the results. Because of the sensitivity of the fits to the exact pressure dependence of  $k$  and  $\beta$  it is difficult to attach significance to the difference in the values of  $A\sqrt{k_0\beta_0}$  as used in the short- and long-term analysis. We concluded that only a one-dimensional flow was observed in the 75-day experiment.

#### 4.4. Injection and Production Zones (R. M. Potter, H. D. Murphy, and S. Faas)

The temperature history in the open hole region of GT-2B obtained during the Phase I operation has shown both numerous production zones and changes in the relative temperatures of the produced fluid (see Figs. 4-5 and 4-6). Unfortunately, because of the complexity of the flow, the specific flow rate in each production zone cannot be determined from the temperature alone. A velocity-measuring tool (spinner) was purchased from the Worth-Well Company in order to measure relative flow at various depths in GT-2B. Its initial test deployment was carried out on April 12, 1978 just one day before shut-in. Because of the importance that any estimate of the relative values of production flows would provide, a temporary system of recording the data was devised.

Three runs were made over the region of interest using a constant downward logging velocity of  $\sim 0.8 \text{ m/min}$  (29 ft/min). Inspection of the output voltage signal from the spinner circuit plotted against depth showed several distinct step changes. Actual flow increases could be calculated from the relative values of velocity and the measured GT-2B production flow. Table 4-II shows the position and magnitude of these detectable flow points.

The rather large level of fluctuation in the production zone did not allow detection much below a flow fraction of  $\sim 0.05$ . Inspection of a typical temperature log in GT-2B during this period (Fig. 4-15) shows that in addition to the steps detected by the spinner, there are several additional temperature steps that are not correlated with observable flow changes.

Because flow enters the reservoir behind the casing in a poorly cemented 180-m (600-ft) section of EE-1 from 2740 to 2930 m, relative injection flows in this well cannot be measured with a spinner tool but have been deduced from radioiodine injection and flowing temperature logs.

Figure 4-16 is the June 2, 1978 temperature survey of EE-1. The dashed upper lines represent the radial conduction-dominated recovery of the wellbore

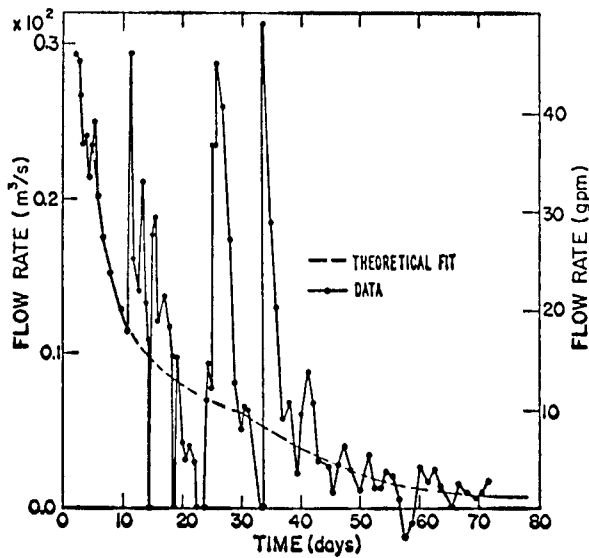


Fig. 4-13.  
 Makeup water loss rate as recorded on the makeup venturi flow meter.

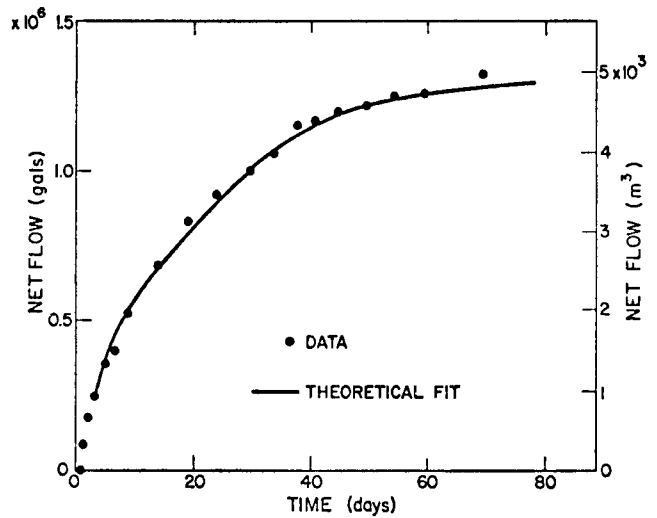


Fig. 4-14.  
 Total accumulated water loss in storage as recorded on the makeup Crane meter.

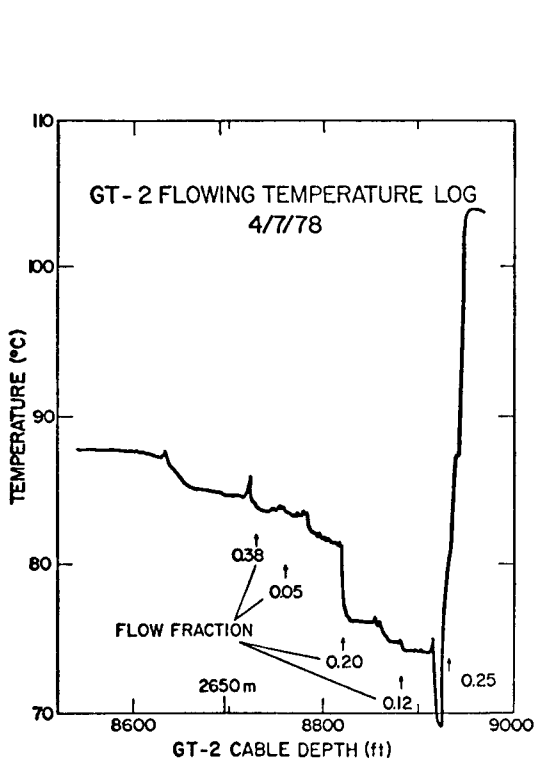


Fig. 4-15.  
 GT-2B flowing temperature log taken on April 7, 1978.

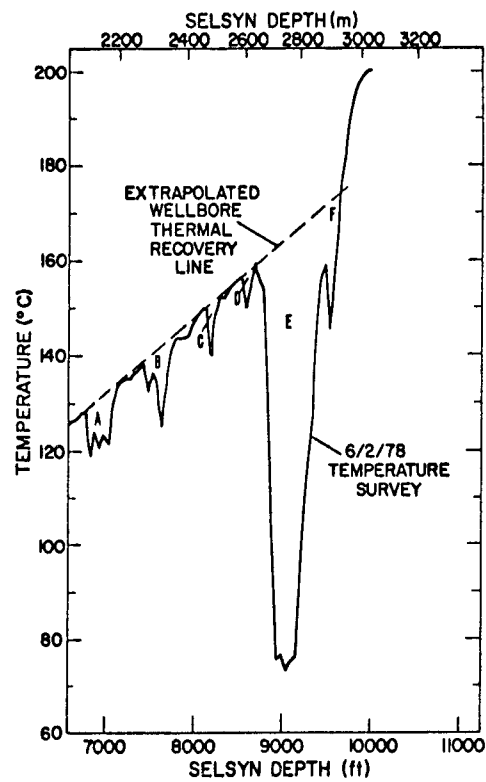


Fig. 4-16.  
 Shut-in temperature log taken in EE-1 on June 2, 1978.

temperature following shut-in. Departures from this line are caused by water infiltration into the formation. The principal temperature depression anomalies are labeled A through F. Subject to certain assumptions, it is possible to estimate the relative water flows into each zone corresponding to a temperature depression simply by measuring the area of each depression and normalizing by the total area of all the depressions. This was done with a planimeter, and the results are given in Table 4-III.

About 81% of the flow goes into Anomaly E, which is centered about 2760 m (9050 ft). Only 5% enters Anomaly F at ~ 2930 m. It is this latter connection, which may provide a relatively high-temperature source of dissolved silica as discussed in Section 5.1. At the end of the 75-day test the net system impedance for the combined flow paths between EE-1 and GT-2B was 3 psi/gpm. Since only 1/20 of the total flow appears to be via the 2930-m path, the impedance between the 2930-m injection zone in EE-1 and GT-2B must have been about 60 psi/gpm.

#### 4.5. Flow Models (R. M. Potter and J. W. Tester)

A two-fracture flow model based on the following assumptions has been developed. First, there is a high conductance flow path (fracture) that supplies all measurable flow increases as indicated by the spinner survey. The temperature of the fluid in this fracture with depth will be calculated. This fracture lies between GT-2B and EE-1. Secondly, there is another fracture or secondary flow path that has several small connecting fractures of high impedance that allow relatively isothermal flows into the GT-2B borehole along its length. Assuming a value for the fluid temperature, we can calculate the magnitude of these flows. This secondary flow path lies in the region beyond GT-2B opposite EE-1.

The previous analysis of the spinner survey has indicated five distinct and measurable flow changes, which are coincident with temperature steps. In addition, a measured flow near the bottom of the GT-2B borehole requires at least two flows, each with temperatures significantly different. The temperature log taken on April 7 (Fig. 4-15) shows at least four temperature steps that have no measurable (via spinner survey) accompanying flow changes. This behavior suggests two sources for the flows, one that provides relatively high flow at moderate temperature and another with flows below the limit of resolution but whose temperatures are great enough to produce measurable temperature changes.

TABLE 4-II  
 POSITION AND MAGNITUDE OF GT-2B EXIT FLOWS

<u>GT-2B LASL Cable Depth (m)</u>	<u>GT-2B LASL Cable Depth (ft)</u>	<u>Voltage Change (mv)</u>	<u>Flow Frac- tion</u>	<u>Absolute Flow (gpm)</u>	<u>ℓ/min</u>
2660-2661	8726-8729	6.0	.38	92	348
2671-2672	8764-8765	0.8	.05	12	45
2686-2688	8812-8820	3.2	.20	48	182
2705-2706	8876-8879	1.8	.12	29	110
2719	8920	3.9	.25	61	231
	<u>Total</u>	<u>15.7</u>	<u>1.00</u>	<u>242</u>	<u>916</u>

TABLE 4-III  
 POSITION AND MAGNITUDE OF RELATIVE EE-1 INJECTION FLOWS

<u>Anomaly</u>	<u>Cable Depth Interval (m)</u>	<u>Cable Depth Interval (ft)</u>	<u>Flow Fraction</u>
A	2073-2179	6800-7150	0.05
B	2271-2377	7450-7800	0.06
C	2484-2530	8150-8300	0.01
D	2606-2652	8550-8700	0.01
E	2652-2896	8700-9500	0.81
F	2896-2957	9500-9700	0.05
			<u>Total</u> 1.00

Figure 4-17 provides an explanation for these observations, which use the measured flows and the observed GT-2B wellbore temperature profile (Fig. 4-15) along with an assumed 180°C temperature in the secondary fracture flow path. All the calculated flows from this secondary zone are less than the resolution of the spinner survey. In addition, the derived temperature gradient profile shown in Fig. 4-18 appears to be consistent with the drawdown of a 100-m-diam fracture.

This temperature choice comes from the pre-test unperturbed rock temperature in this region and from geochemical data that indicate a steady flow with a quartz saturation temperature of ~180-190°C (see Section 5.1). Figure 4-19 shows a temperature log of GT-2B after shut-in. The maximum temperature at a depth of 2640 m (~ 8660 ft) coincides with the point of maximum flow from the assumed second fracture or flow path.

Table 4-IV gives the measured average flows and pressures in the two boreholes during this experiment along with calculated values of impedance for the various flow connections. It is assumed that there is no significant pressure drop in the entire EE-1 system except at the GT-2B connecting fractures. Also shown are the initial values of impedance on January 30, 1978 before the start of the major flow test. This table shows the original main fracture in GT-2B (at 2686-2688 m) that carried a smaller fraction of the total flow with a significantly smaller impedance.

The location of this secondary flow path or fracture system that provides hot fluid entering GT-2B is uncertain. Figure 4-20 presents a hypothetical case in plan view showing two wellbores (GT-2B and EE-1) connected by main and secondary vertical fractures, which leave the EE-1 wellbore at 2758 and 2940 m (9050 and 9650 ft) respectively. Both fractures are oriented in a northwest-southwest direction. A number of early fracturing experiments in EE-1 activated the fracture zone at 2940 m, while degradation of the casing cement between 2940 m eventually led to the activation of a lower impedance flow path leaving EE-1 at 2758 m. If the proposed fracture at 2940 m extended vertically for 305 m (~ 1000 ft), it would come very close to the uncased GT-2B wellbore. Furthermore, if this fracture is connected to GT-2B at 2690 m (8660 ft) via a high angle conductive joint, it would serve as the source of "hot water" as shown in Fig. 4-19.

The flow model described above can also be used to explain the residence time distribution and geochemistry results described in Sections 4.2 and 5.1.

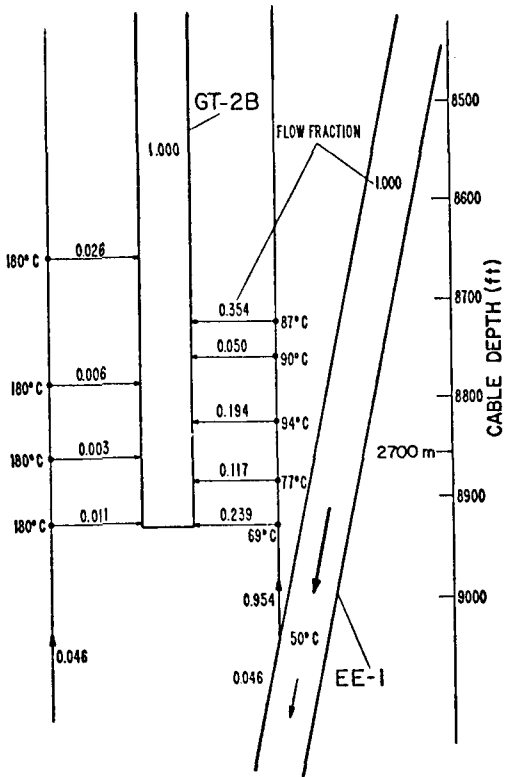


Fig. 4-17.

Conceptual flow model for the GT-2B/EE-1 system.

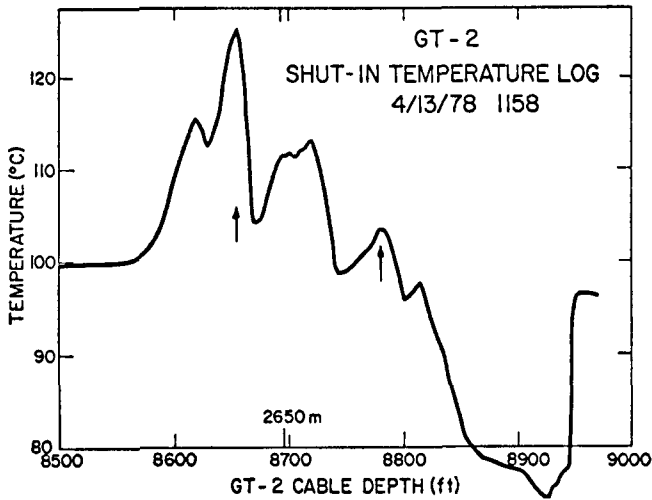


Fig. 4-19.

GT-2B shut-in temperature log taken on April 13, 1978

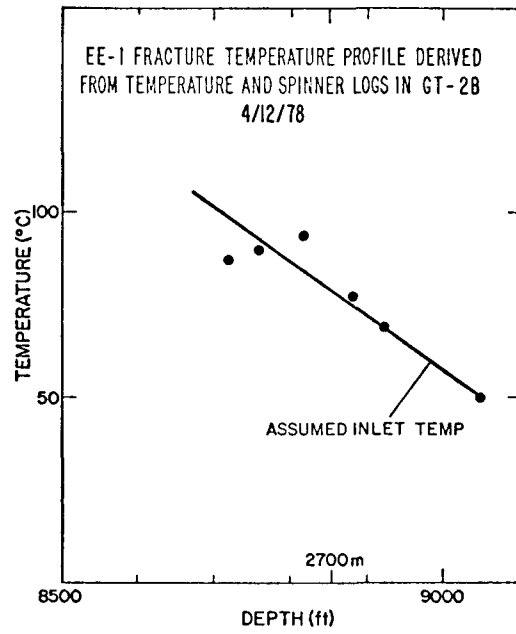


Fig. 4-18.

Derived temperature gradient profile for GT-2B.

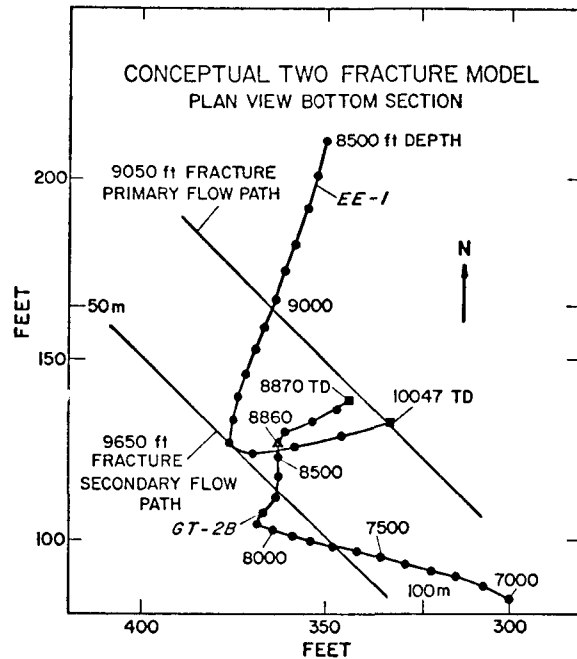


Fig. 4-20.

Conceptual model of primary and secondary flow paths in the GT-2B/EE-1 system.

TABLE 4-IV

## VARIOUS IMPEDANCES IN EE-1/GT-2B SYSTEM

(m)	Fracture Depth (ft) in GT-2B	Flow Impedance bar-s/l (psi/gpm)			
		Jan. 30, 1978		April 12, 1978	
		Main	Secondary	Main	Secondary
2640	8660				126 (115)
2660	8728			8.2 (7.5)	
2670	8760			66 (60)	
2677	8784				541 (495)
2688	8820	22 (20)		16.7 (15.3)	
2703	8867				1082 (990)
2707	8882			27.8 (25.4)	
2719	8920				295 (270)
2720	8925	87 (80)		13.6 (12.4)	
	Fracture set	17 (16)		3.4 (3.12)	71 (65)
	Entire system	17 (16)			3.26 (2.98)

On April 12, 1978 EE-1 pressure = 55.9 bar (810 psi)

GT-2 pressure = 14.5 bar (210 psi)

Buoyancy = 8.3 bar (120 psi)

System pressure drop = 49.7 bar (720 psi)

GT-2 flow = 15.9 l/s

respectively. Figure 4-21 presents a simplified version of the flow model with primary and secondary flow paths. The primary path flows each have a small degree of dispersion but widely different residence times in the main fracture between a fixed injection point in EE-1 and the production zone in GT-2B. These flows are mixed to produce an apparent high level of dispersion. Also, a secondary "matrix-like" flow is present, empirically characterized by a volume plug flow in series with a well-mixed volume. Thus the overall RTD observed during the later period of the 75-day test is a combination of all flow paths as shown in Fig. 4-22.

The discussion has illustrated the complex relationships that exist between the geometric, thermal, and chemical properties of the fracture system. A unique model consistent with all the data does not exist, at least with the information we now have on the properties of the reservoir. In fact, we have selected simple models and tested their consistency rather than try to improve our fit to the data by adding unnecessary complexity.

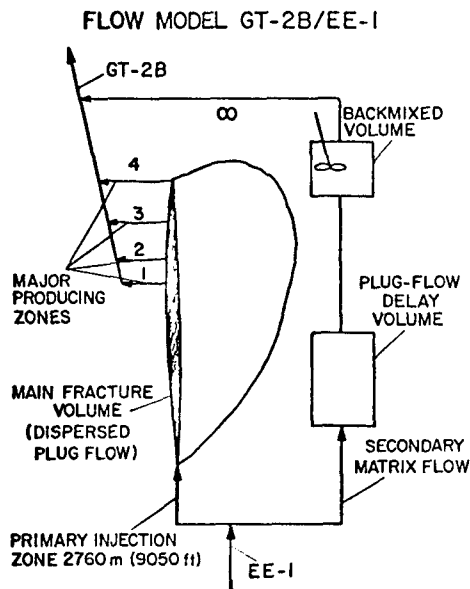


Fig. 4-21.

Simplified schematic depicting dispersed plug flow in the main fracture and "matrix-like" flow in secondary fracture system.

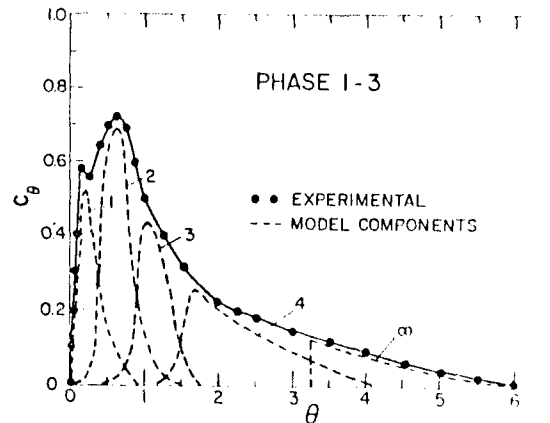


Fig. 4-22.

Normalized residence time distribution (RTD) with individual flow zone contributions shown from the model of Fig. 4-21.

## 5. FLUID GEOCHEMISTRY

### 5.1. Major Element Analysis (C. O. Grigsby, J. Abbott, L. Blatz, C. Holley, and J. W. Tester)

During the 75-day period, a gradual rise in the concentration of dissolved species approached steady state levels corresponding to the concentrations observed for water which remains in contact with the reservoir for an extended period. The effects of mixing among various flow paths and mass transfer strongly influenced the observed concentration change of dissolved species with time.

#### Procedures

Liquid samples were collected during Phase I Segment 2 at four points: Samples designated "G" were collected at the GT-2 producing wellhead by cooling the fluid through a 15-m 1.27-cm (50-foot 1/2-in.) O.D. copper tube, which was immersed in a 0.2-m<sup>3</sup> (55-gal) drum of cold water. The sampling tube was open to atmospheric pressure at all times, and the pressure drop from GT-2 wellhead pressure to atmospheric pressure was taken across a ball valve. Samples were collected in 1-l nalgene LPE bottles, which were rinsed 2 or 3 times with geothermal fluid just prior to actual sample collection. Before each bottle was rinsed, the sampling tube was flushed with 3.8 l (~ 1 gal) of water to remove the stagnant water from the previous sampling. For the first month of operation, the valve was left open at a flow rate of 3.8 l/min (~ 1 gpm) to prevent freezing in the tube. This continual flow caused the deposition of calcite on the inside of the tube, which eventually plugged the sample tube. The sample tube was replaced, and the new tube did not develop any observable calcite scale as the danger of freezing had passed, and the valve was closed between sample collections.

Samples designated "E" were collected between pumps #1 and #2. As described in Section 2 these samples represent the fluid injected into the geothermal system at EE-1.

Makeup water samples, labeled "M", were collected from the manifold at the exit of the 100-micron filters. The makeup water was supplied from a 122-m (400-ft) well on site to a 1.5 x 10<sup>6</sup> l (400 000-gal) holding pond near EE-1 where the water was stored and where in emergency situations water from the circulating system was discharged. (See Fig. 2-3.) The pond was at all times open to the atmosphere and exposed to rain, snow and runoff.

About halfway through the 75-day run, the EE-1 annulus began to leak and samples of the fluid were collected for analysis. These samples are labeled "A".

The following analytical techniques were used in the determination of chemical composition of the fluids: standard pH electrode and meter;  $\text{HCO}_3^-$ , titration with 0.02N  $\text{H}_2\text{SO}_4$  to a pH of 4.5 endpoint using a pH meter; conductivity with a Hach conductivity probe and meter;  $\text{F}^-$ , Orion solid state selective electrode with Beckman millivolt meter;  $\text{SiO}_2$ , ammonium molybdate spectrophotometric technique;  $\text{Cl}^-$ , argentometric titration;  $\text{SO}_4^{=}$ , spectrophotometer measurement after precipitation with  $\text{BaCl}_2$ ; and Ca, Na, K, Si, Li by atomic absorption with a Perkin-Elmer Model 460AA.

### Results

The concentration-time history of various dissolved species collected from the production (GT-2) and injection (EE-1) wellheads is presented in Figs. 5-2 through 5-11. In addition, plots of total dissolved solids and solution conductivity are also presented (Figs. 5-12 and 5-13). There are several features common to all of the graphs. First, the initial samples had high concentrations of each of the species measured. During the early pumping period when makeup rates were high these high concentrations dropped very rapidly due to dilution and mixing with the relatively pure makeup water (see Figs. 5-1, 5-5, 5-8, 5-9, 5-11, 5-12, and 5-13). These initial samples reflect the nature of the water, which had been contained in the reservoir for approximately 3 months. After an initial flushing of the 230 000-ℓ (~60 000-gal) system in which the water produced at GT-2 was discharged, the system was operated as a closed loop with the makeup water flow supplying water lost to permeability storage in the reservoir. As makeup flow rates dropped, the dilution effect was lessened, and the concentrations of dissolved material began to rise to steady state values.

There were several emergencies that forced the shutdown of the system for various lengths of time. The most noticeable of these was the sudden change in downhole impedance on day 21-1/2. At that time, the GT-2 pressure rose rapidly causing an unacceptably high inlet pump pressure. Consequently a fraction of the produced fluid was vented to the EE-1 storage pond to control the pressure. However the high flow rate through the heat exchangers resulted in an outlet temperature that was too high to operate the pumps. The pumps were shut down, and all of the GT-2 flow was vented to the EE-1 storage pond. Because of the pressure decline in the fracture system, water stored in the permeable rock returned to the wellbore and then to the surface carrying more dissolved material

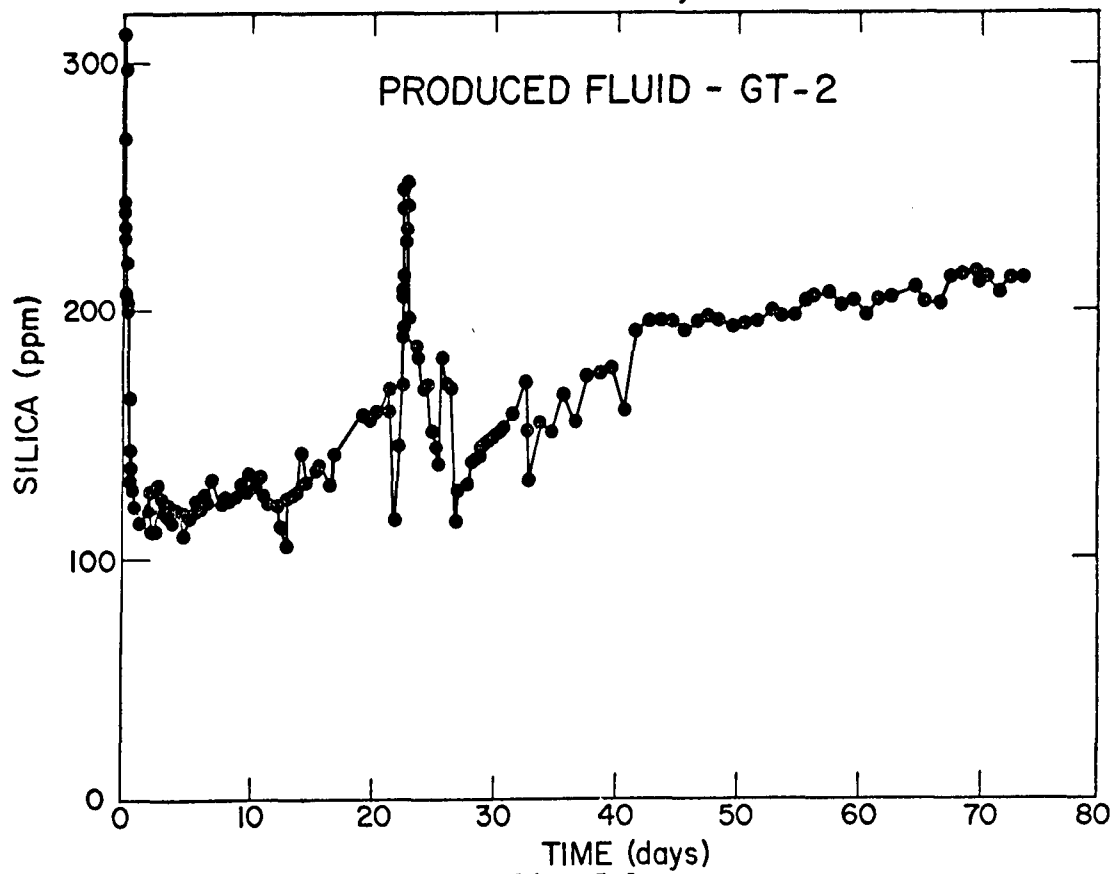
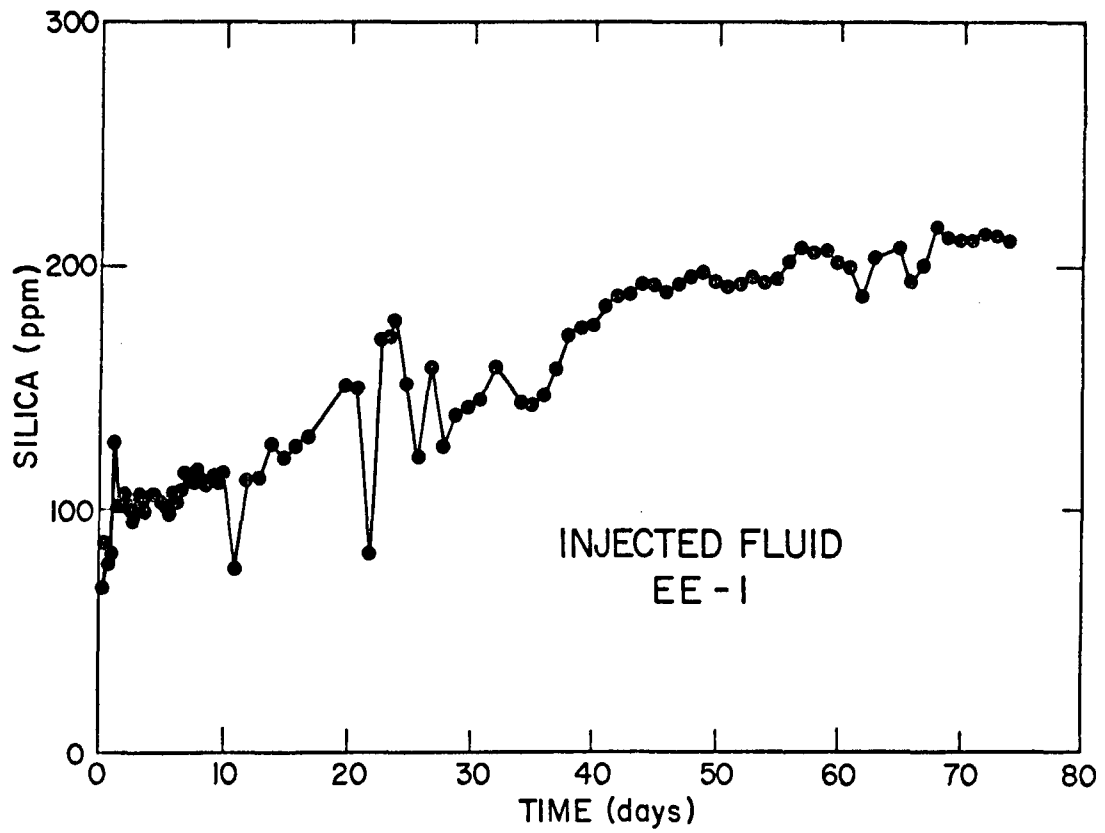


Fig. 5-1.  
Dissolved silica in the injected and produced fluids.

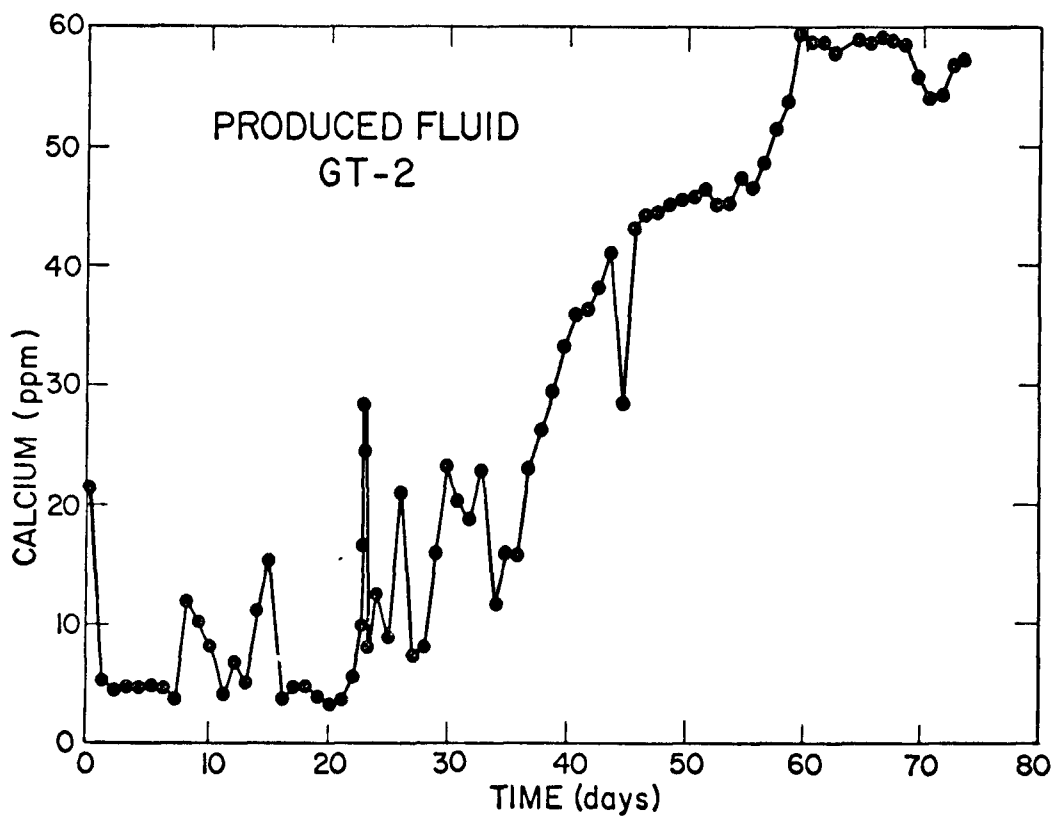
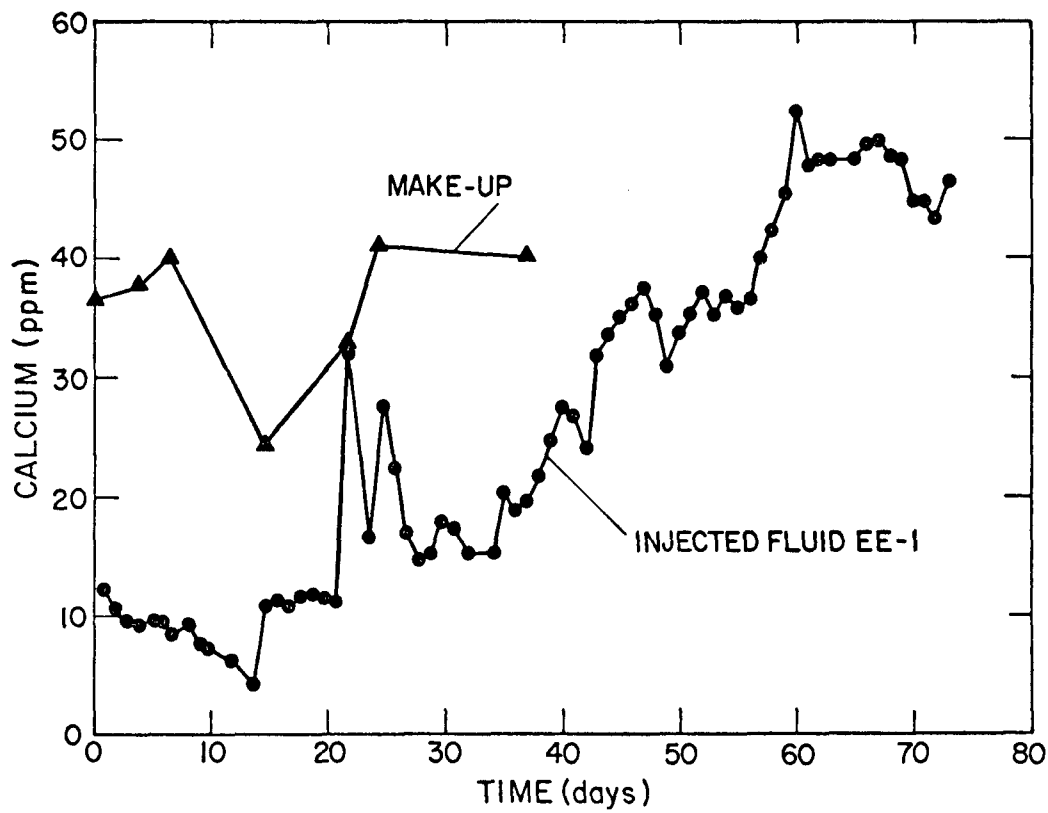


Fig. 5-2.  
Calcium concentration in the injected, produced, and make-up fluids.

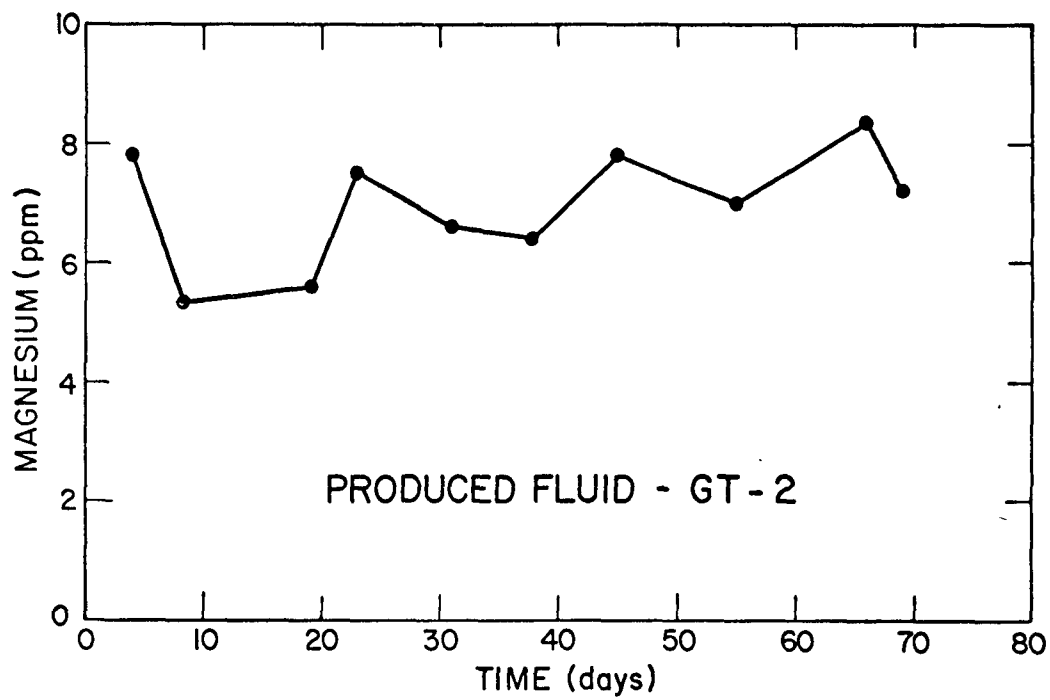
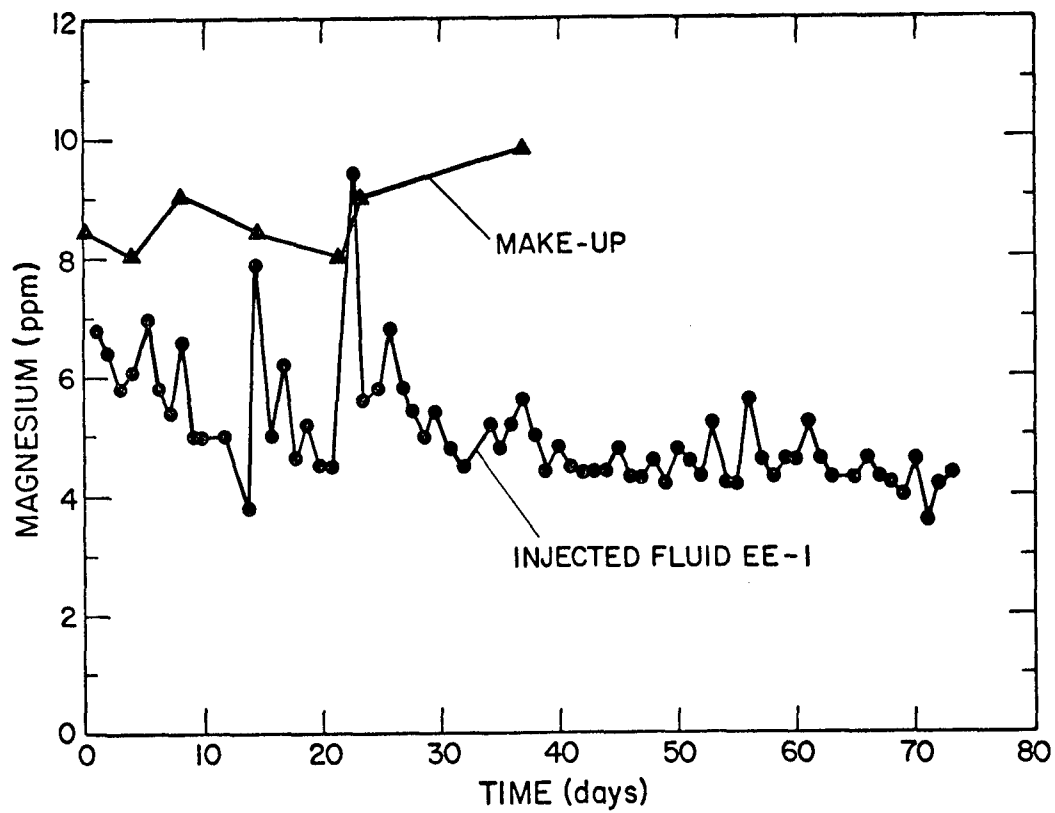


Fig. 5-3.  
Magnesium concentrations in the injected, produced, and make-up fluids.

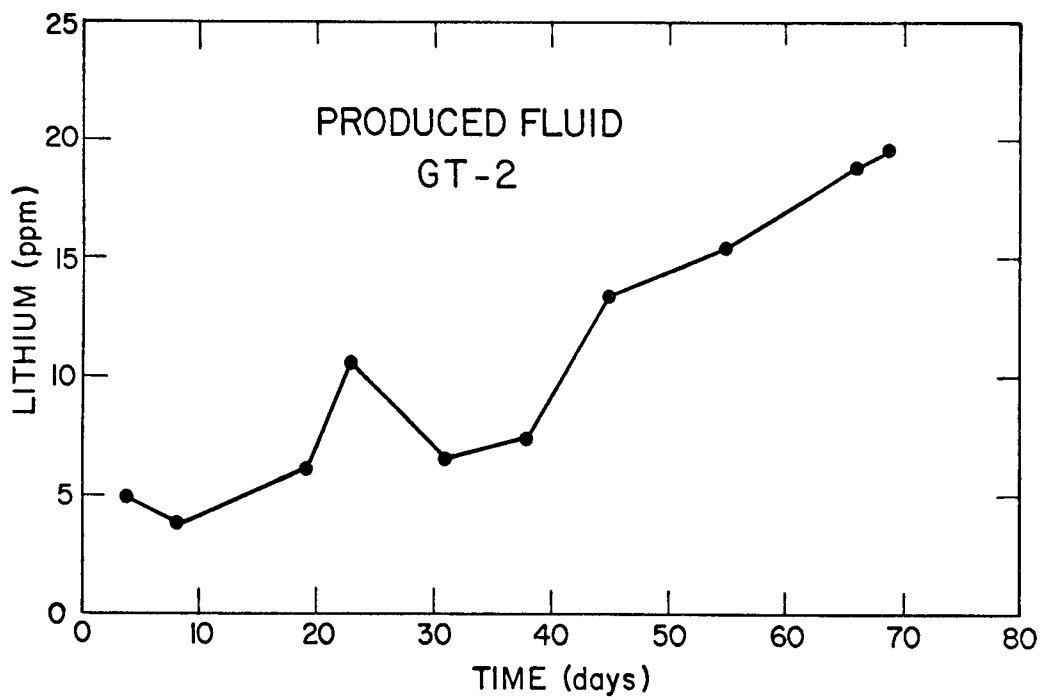
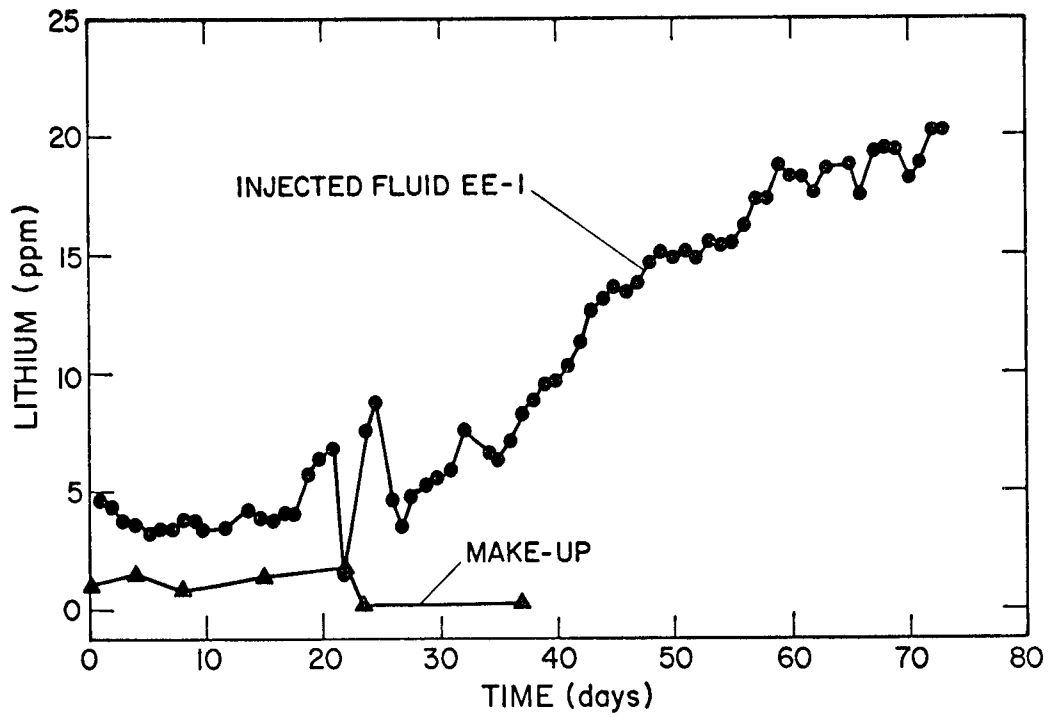


Fig. 5-4.  
Lithium concentrations in the injected, produced, and make-up fluids.

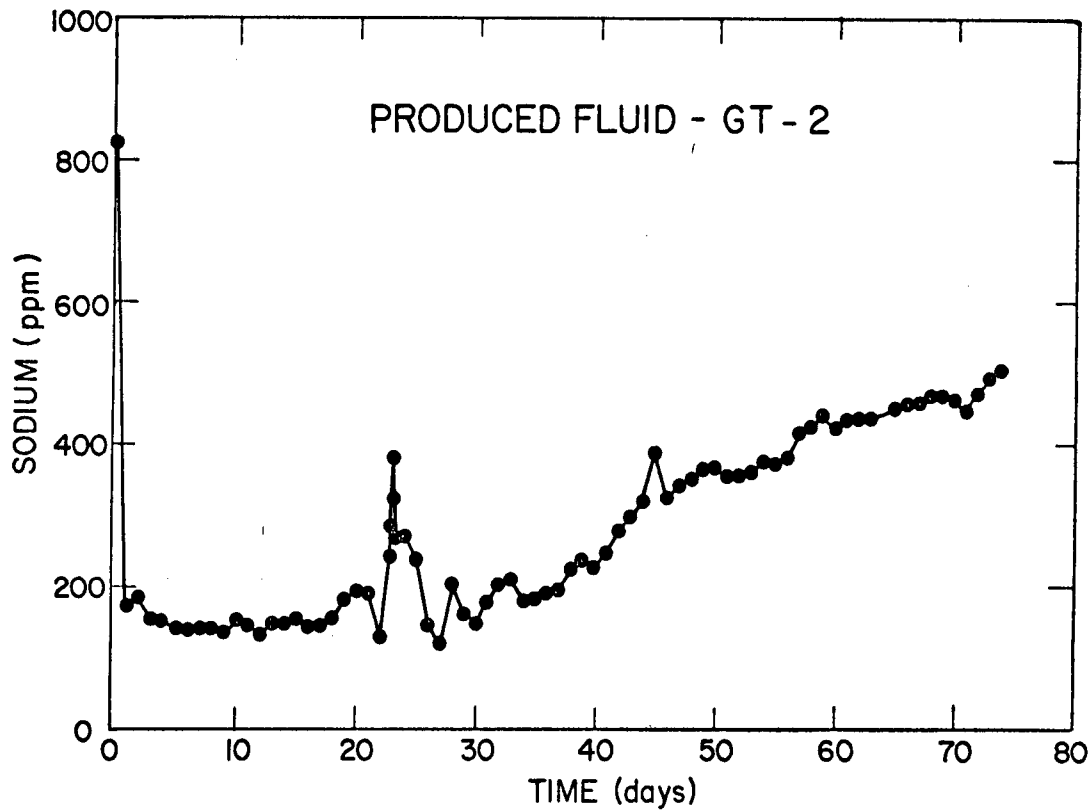


Fig. 5-5.  
Sodium concentration in the produced fluid.

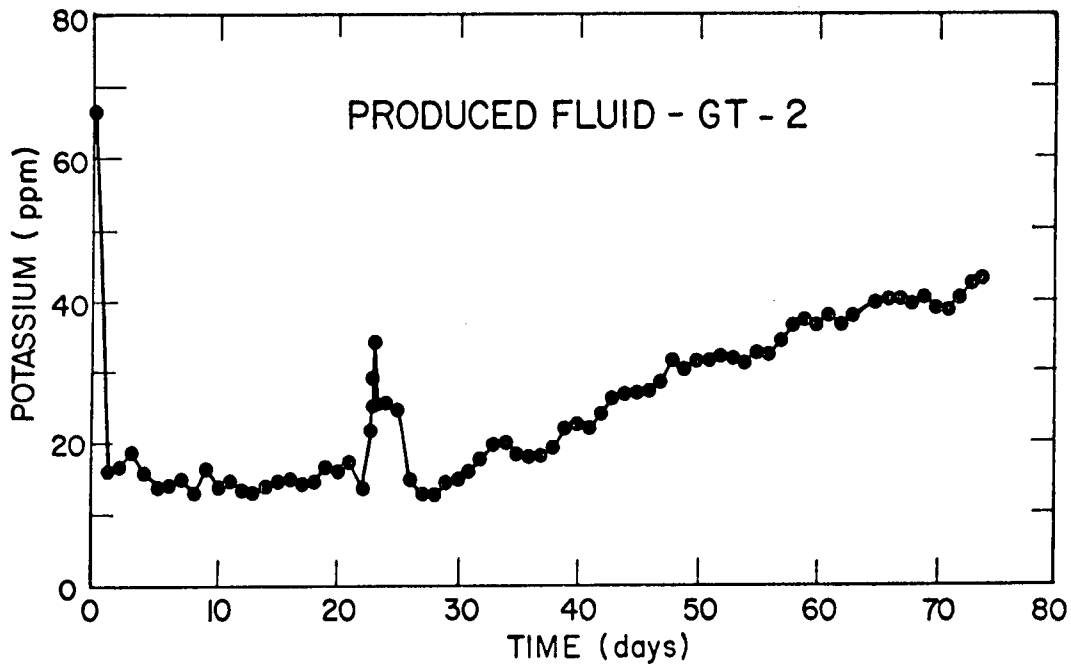


Fig. 5-6.  
Potassium concentration in the produced fluid.

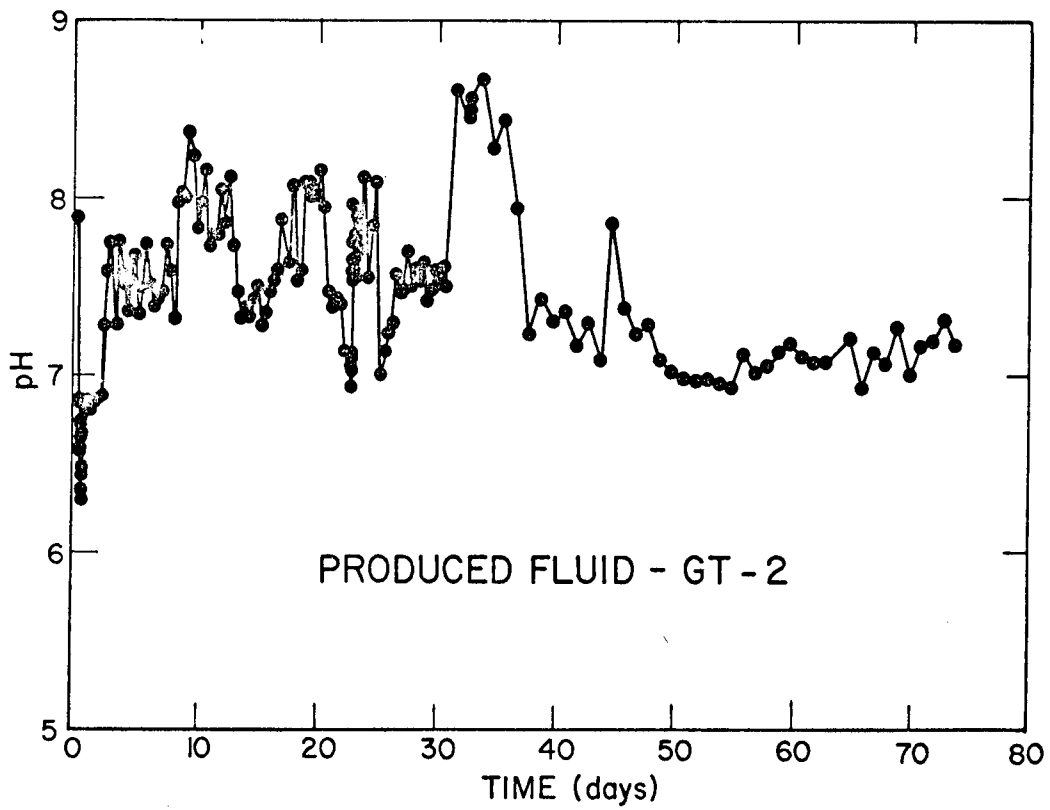
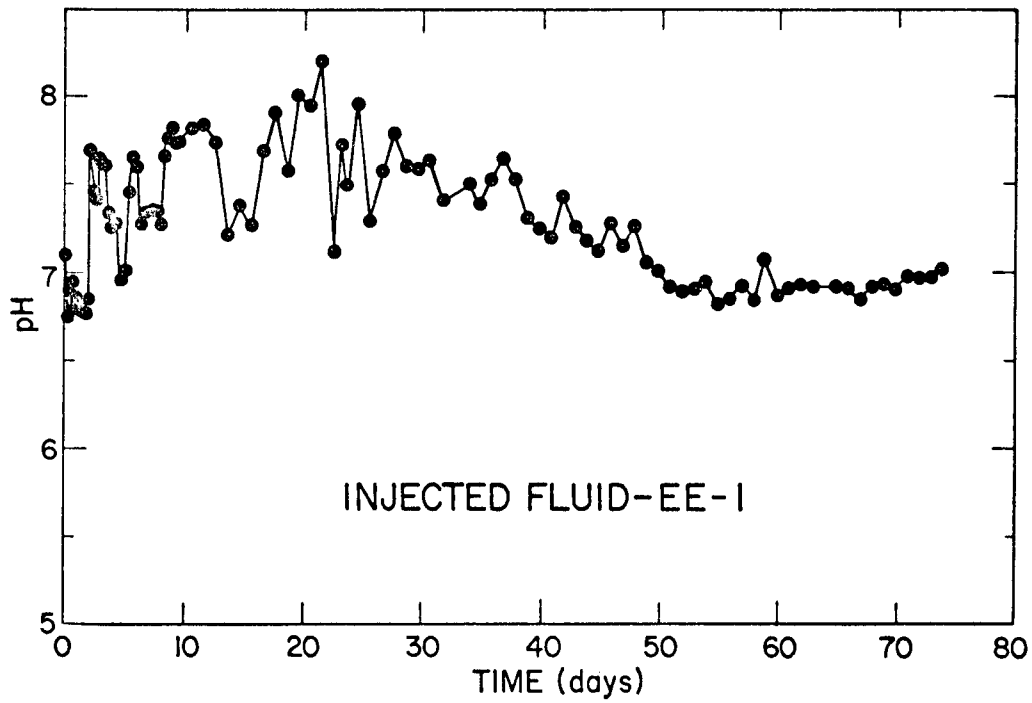


Fig. 5-7.  
Hydrogen ion concentrations expressed as pH in the injected and produced fluids.

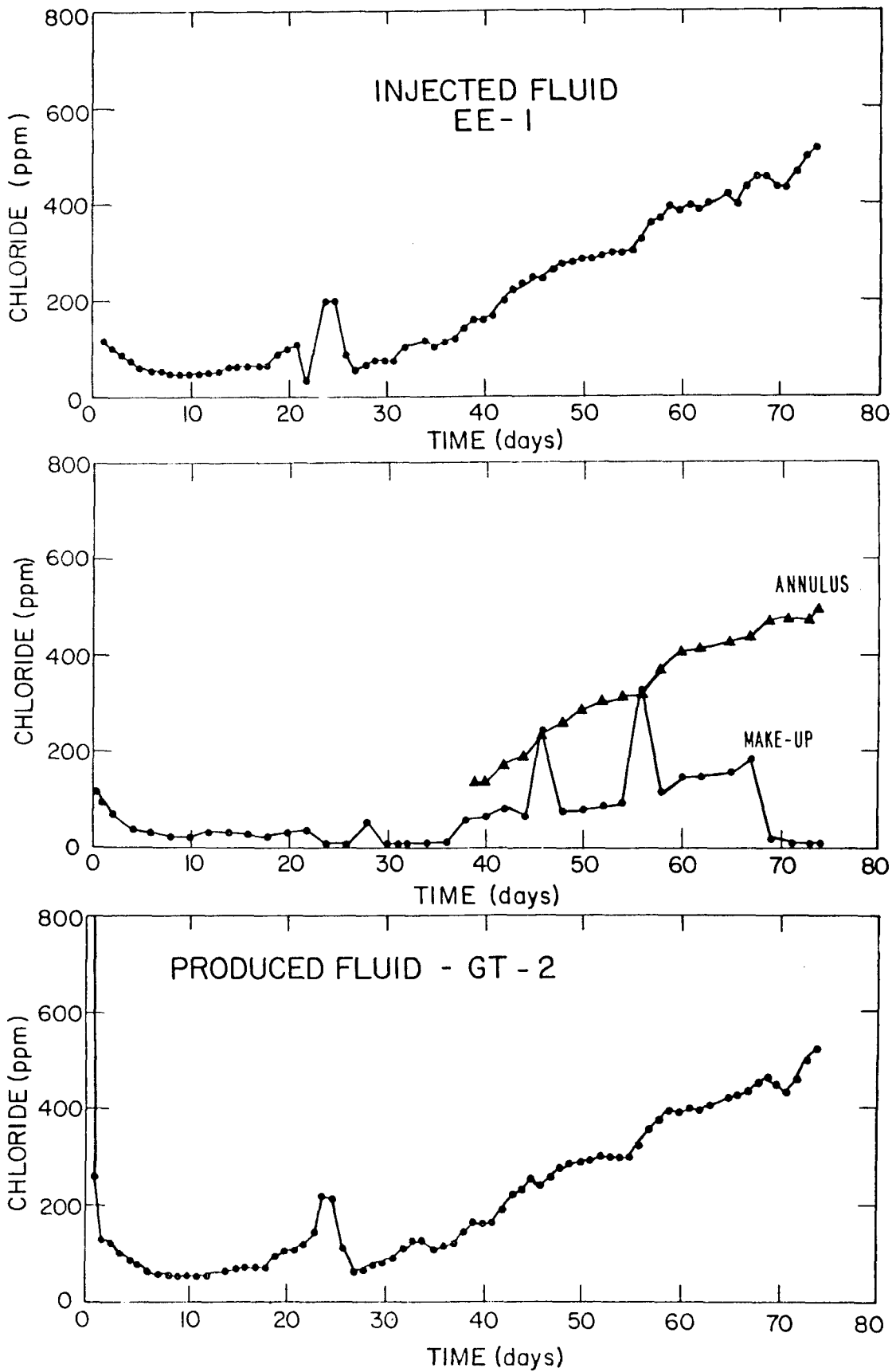


Fig. 5-8.

Chloride concentrations in the injected, produced, make-up, and EE-1 annulus fluids.

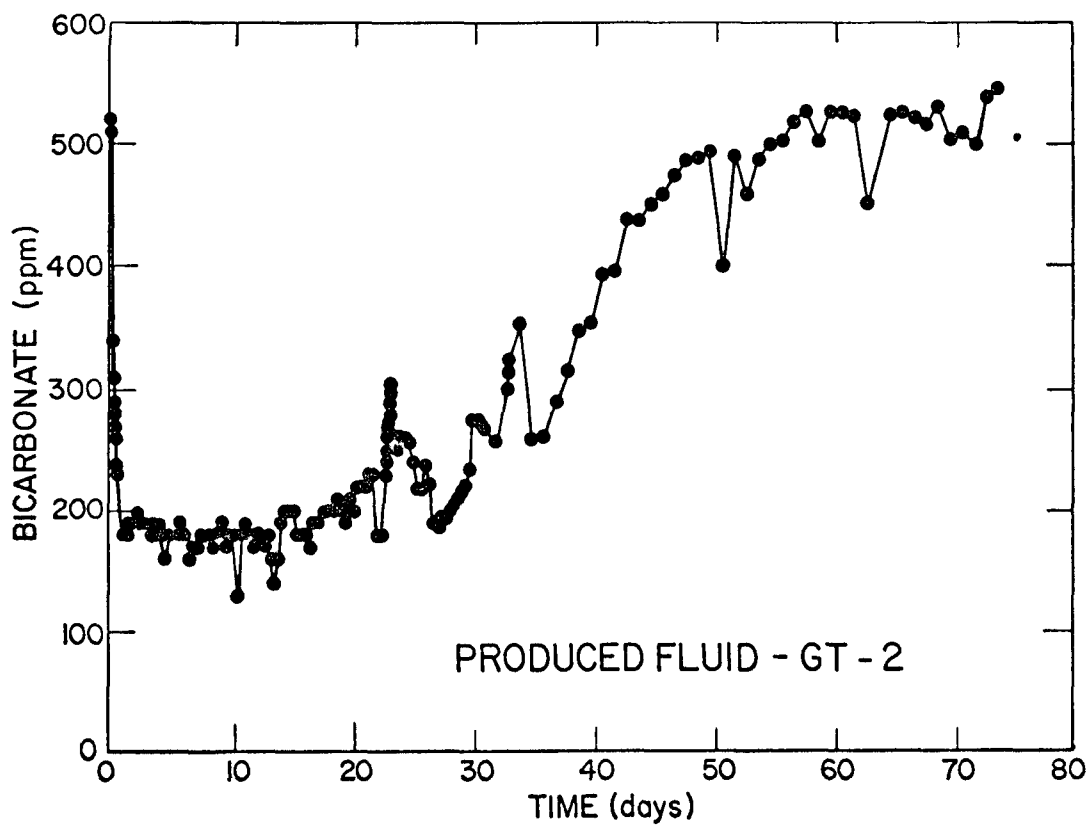
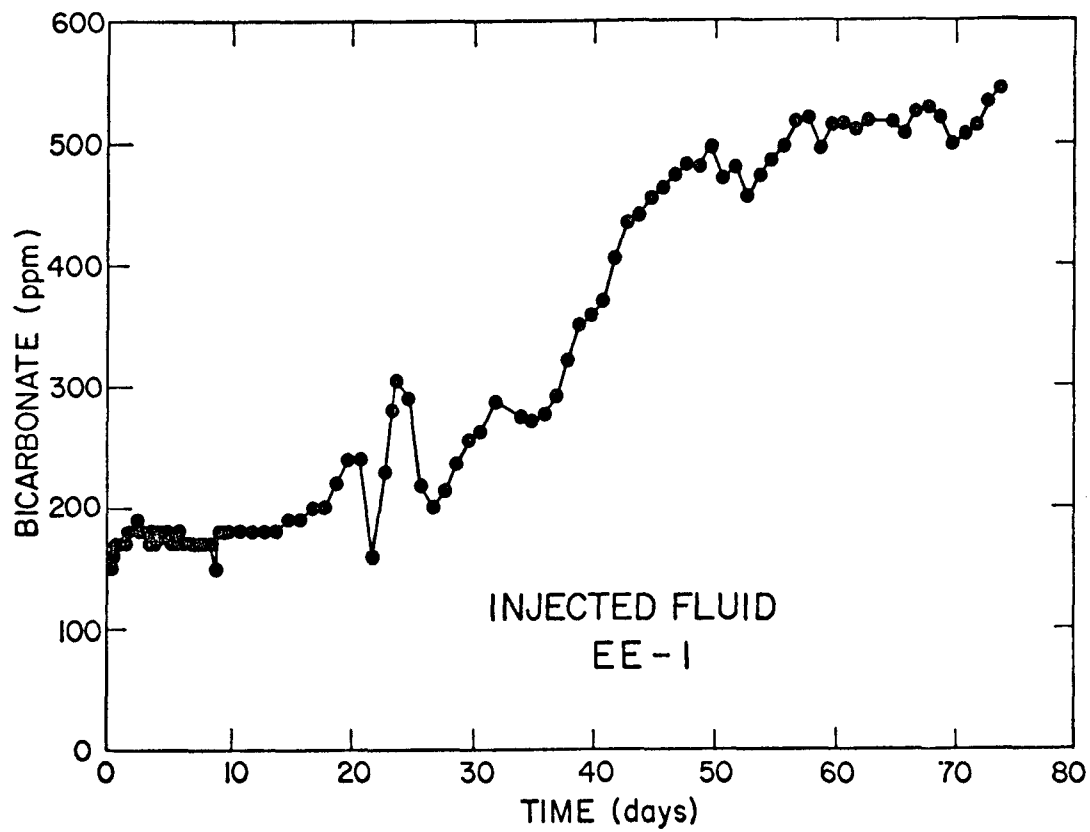


Fig. 5-9.  
Bicarbonate concentrations in the injected and produced fluids.

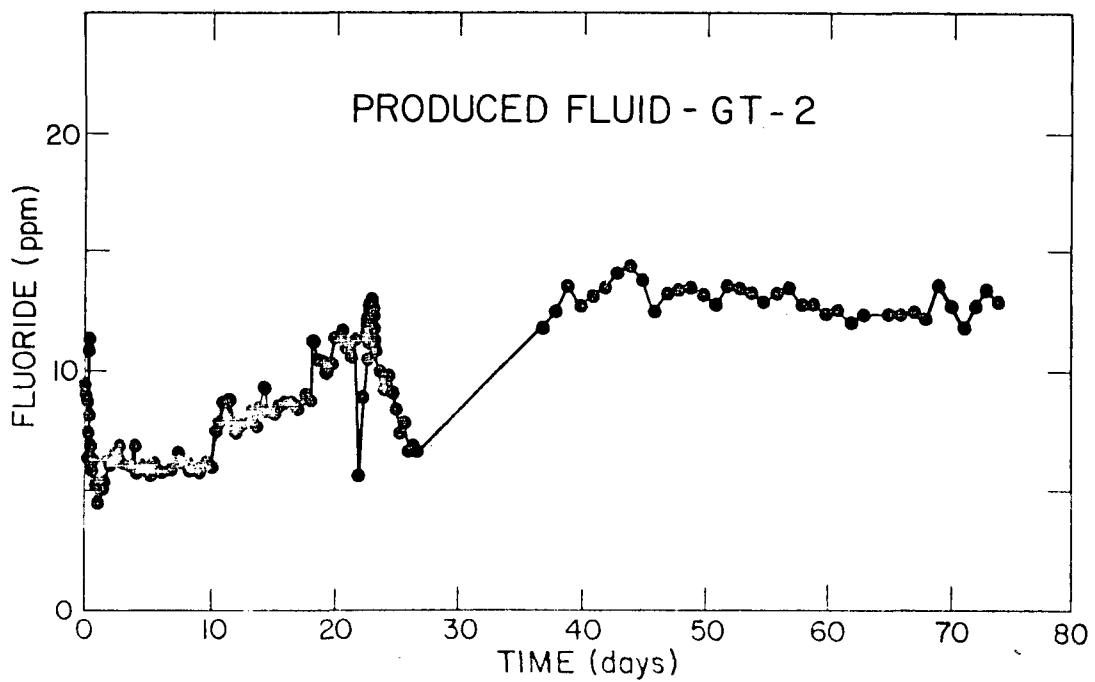
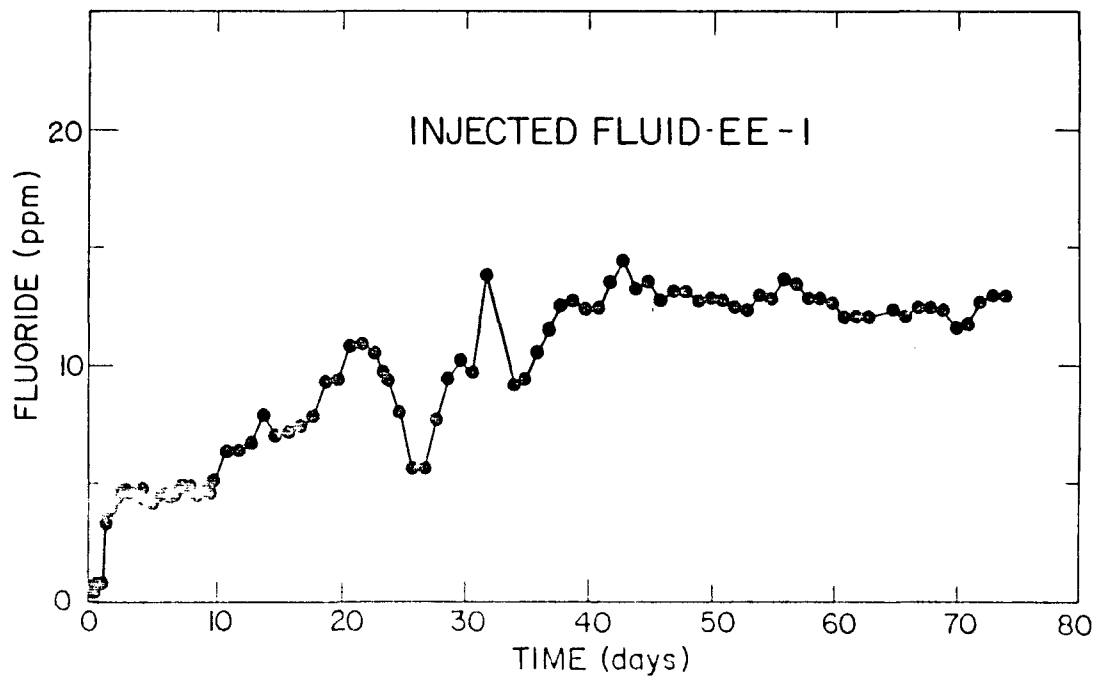


Fig. 5-10.  
Fluoride concentrations in the injected and produced fluids.

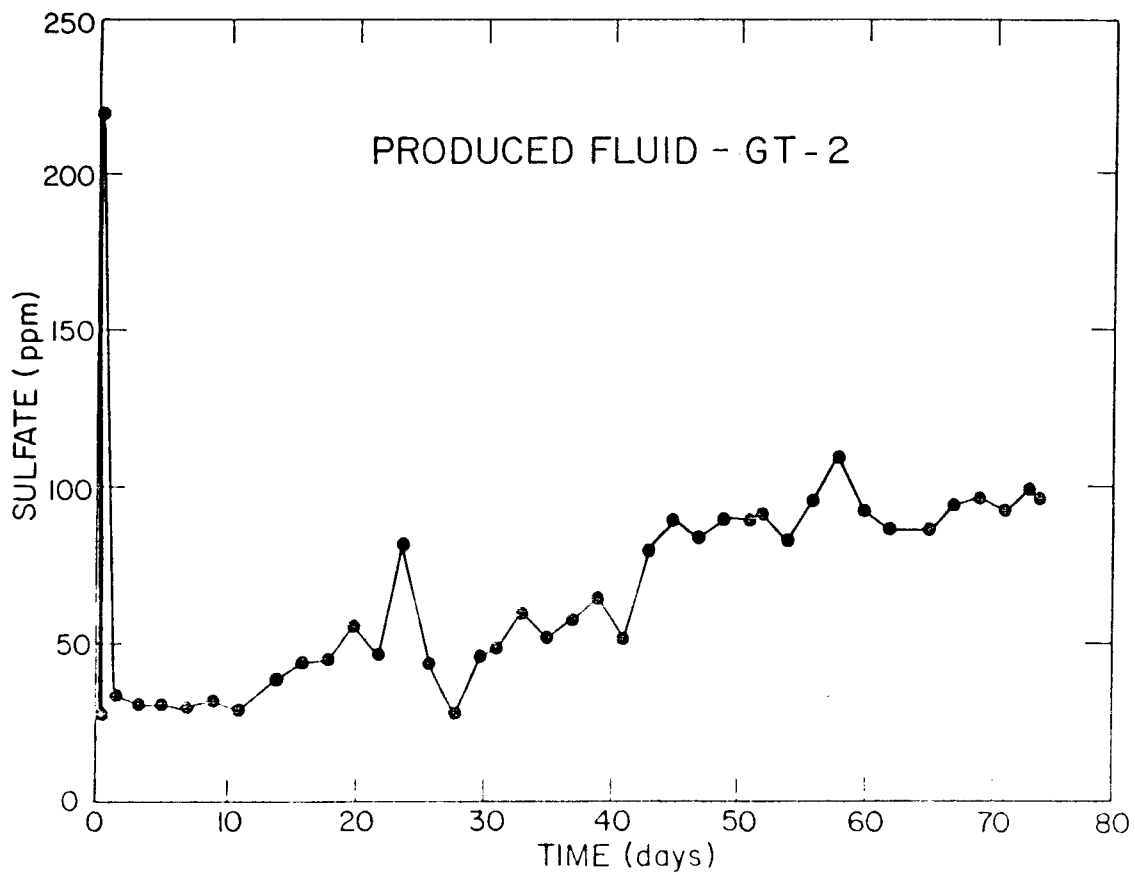
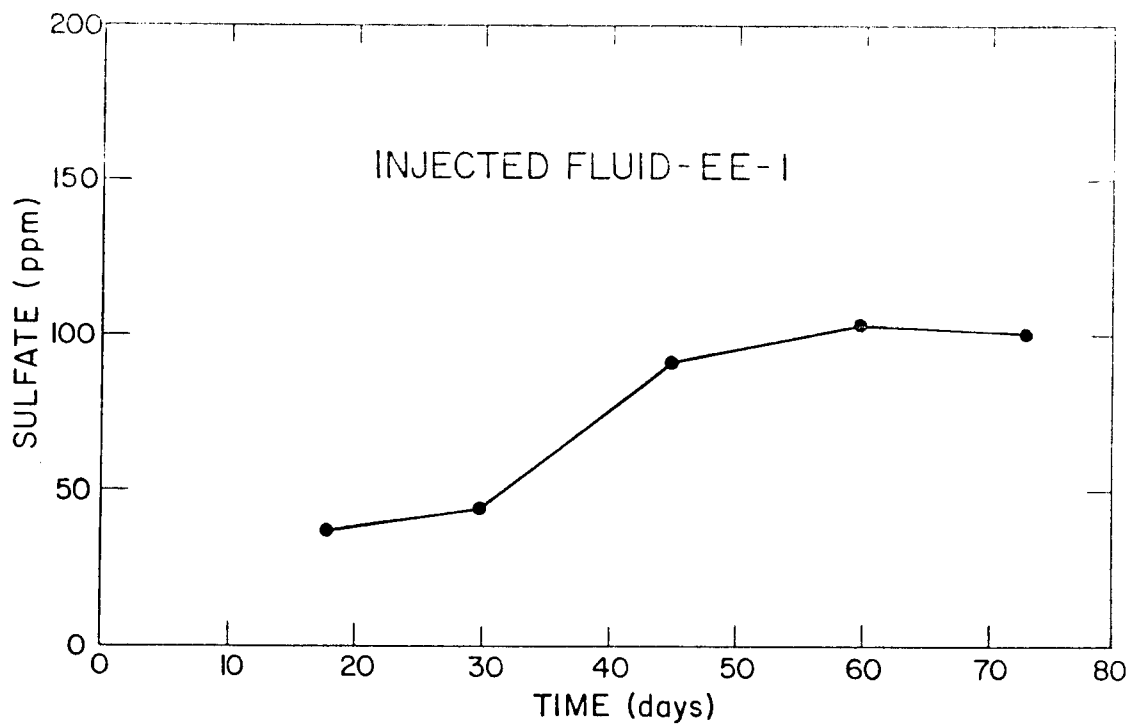


Fig. 5-11.  
Sulfate concentrations in the injected and produced fluids.

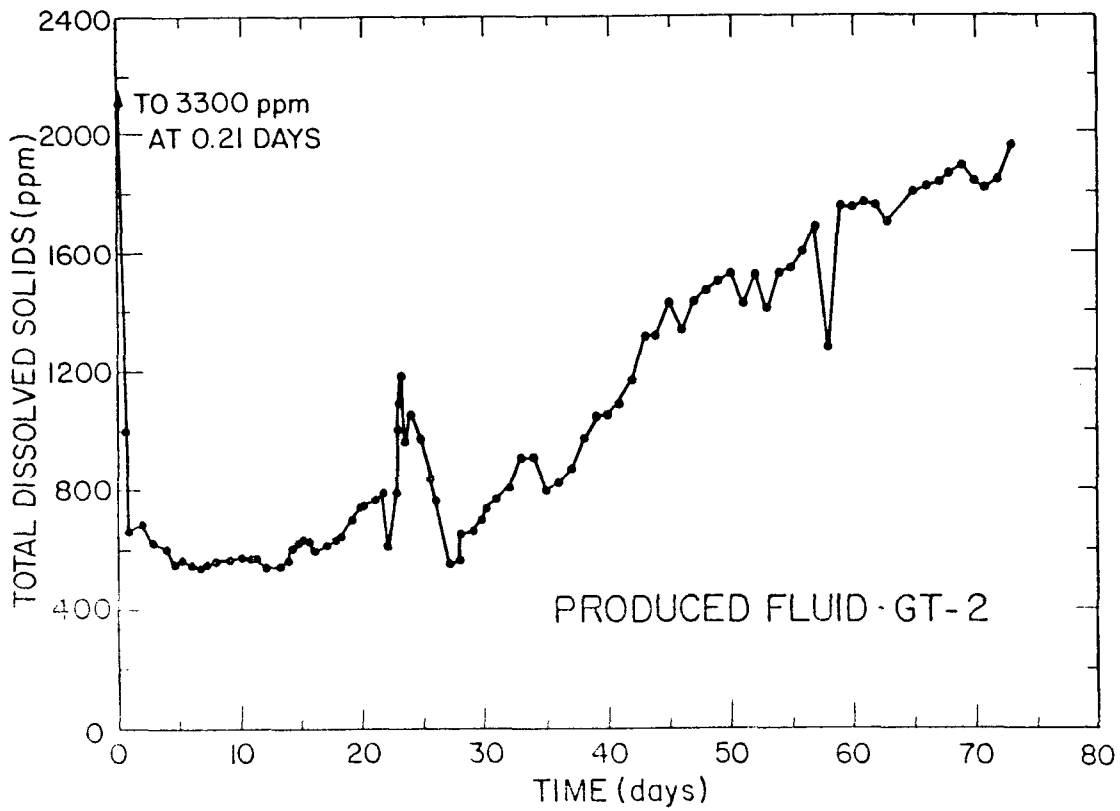


Fig. 5-12.  
Calculated total dissolved solids for produced fluid.

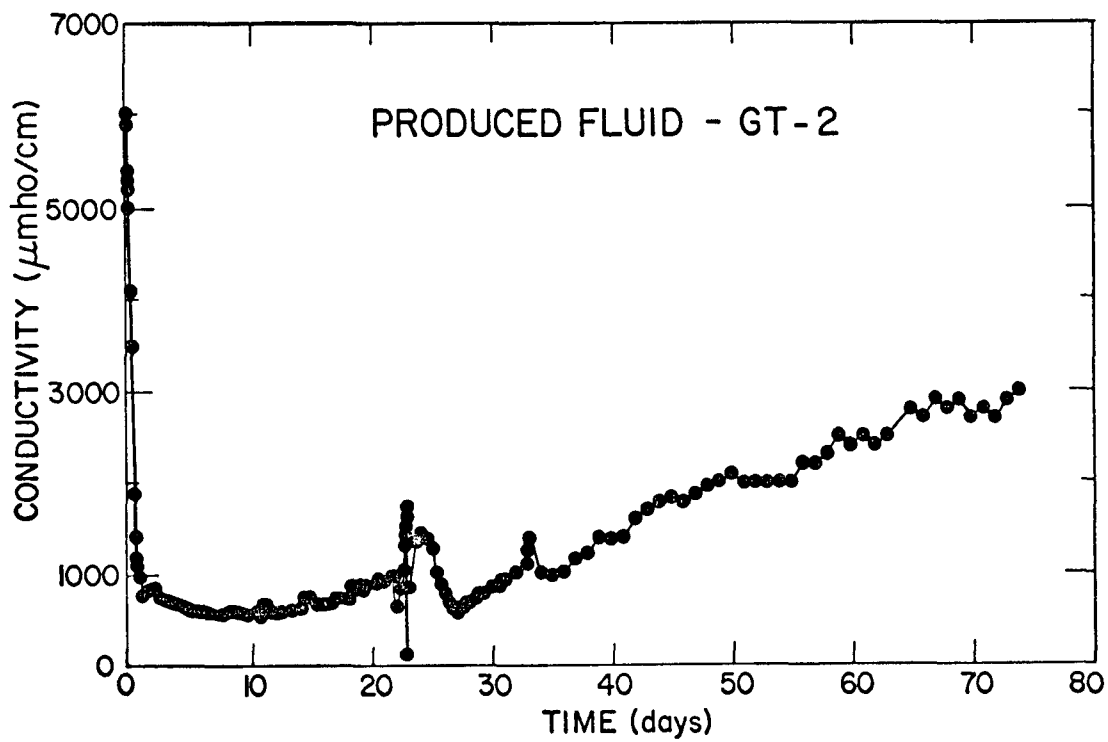
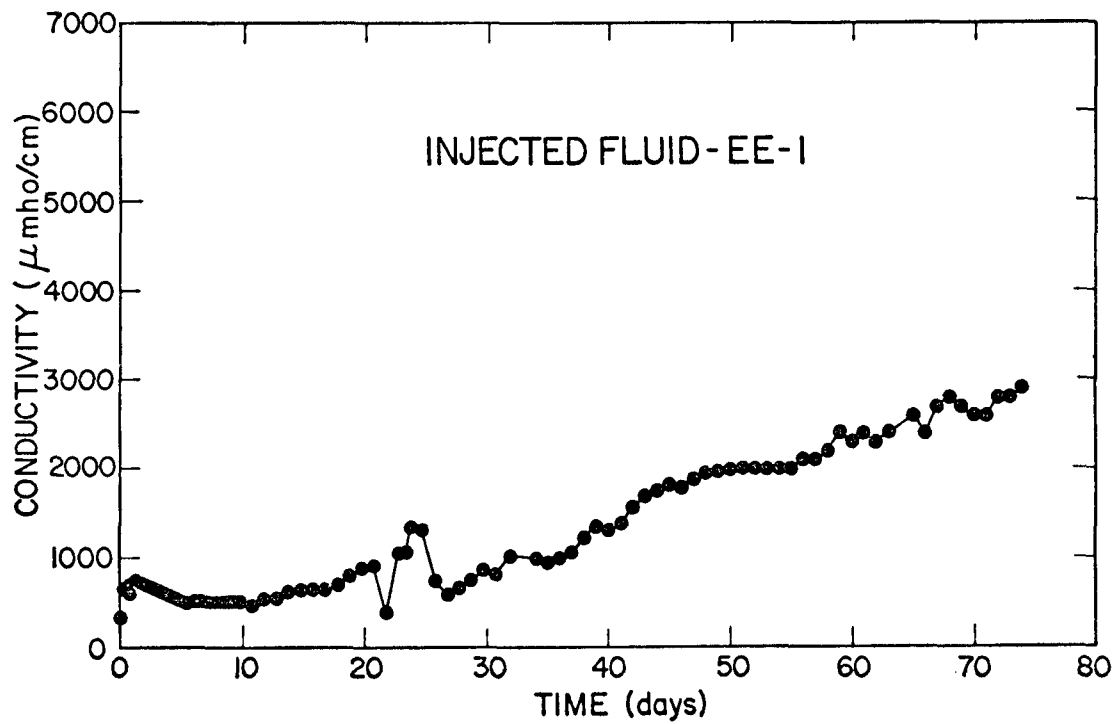


Fig. 5-13.  
Solution electrical conductivity for injected and produced fluids.

because of the longer contact times with the rock and higher rock temperatures. This is seen as a local maximum on each graph at day 23. As the system was restored to operating pressures, makeup fluid replaced the fluid that had returned from the permeability storage. This large amount of makeup had a strong dilution effect as seen in the local minimum just after the 23rd day.

Dissolution, mixing, and transport of minerals continued to approach "steady state" conditions toward the end of the 75-day run. Several curves began to level off starting somewhere between day 40 and 50.

At the completion of the 75-day test only one successful gas analysis was achieved. A 3 l-atm gas sample was separated from 140 l of H<sub>2</sub>O at 200-mm Hg total pressure. One liter-atm was scrubbed yielding the following analysis: 0.7 mg H<sub>2</sub>S; 223 mg CO<sub>2</sub>; O<sub>2</sub> and N<sub>2</sub> in a normal atmospheric ratio make up the bulk; N<sub>2</sub>O trace; and NH<sub>3</sub> not detected.

#### Preliminary Interpretation - Reservoir

When the silica concentration exceeded the quartz saturation value at the measured temperature of the fluid entering the GT-2 wellbore, we sought explanations for the "high" SiO<sub>2</sub> concentrations. One mechanism requires that a small fraction of the fluid actually circulates through a portion of the reservoir, which is still at the initial reservoir temperature as described in the flow model of Section 4.5. According to this model, the change in silica concentration with time for that fraction of the flow corresponds to a first order rate depending on the difference between the silica saturation value of the highest reservoir temperature in contact with flowing fluid and the average silica concentration at any particular time:

$$\frac{d(\overline{\text{SiO}_2})}{dt} = k\bar{a}^* \left[ \left( \text{SiO}_2 \right)_{T=T_{\text{max}}}^{\text{sat}} - \left( \overline{\text{SiO}_2} \right) \right] , \quad (5-1)$$

where  $k\bar{a}^*$  is a constant that includes relevant mass transfer rates, dissolution kinetics rates, and a rock surface area to fluid volume parameter.

There are two distinct flow paths through the reservoir: one major path (~95% of the flow) through the main fracture system with its connected joints to GT-2B, and a secondary path (~5% of the flow) through a hot region that may be a highly fractured matrix-like section with a large effective volume and large

contact area. Thus information in Figs. 4-17 and 4-21 can be used in an equation to describe the rate of SiO<sub>2</sub> buildup. If no further dissolution or reprecipitation occurs in the cooler main flow path, then a differential material balance shows that the rate of accumulation of SiO<sub>2</sub> is due to three principal effects: the relative volumes of each flow path, the fluid loss rate to permeation, and the production of SiO<sub>2</sub> from active dissolution and/or displacement in the hot region. This is approximated in the following equation, assuming that the circulating time  $t$  is large compared to the mean residence time  $\tau = (V_T/\dot{q}_T)$  in the system:

$$V \frac{d\bar{C}}{dt} = \dot{q}_T (C_{in} - \bar{C}) + \dot{q}_2 (1 - e^{-ka^* \tau_2 f}) (C^\infty - C_{in}) \quad (5-2)$$

where

$$C_{in} = \frac{\dot{q}_T - \dot{q}_{loss}}{\dot{q}_T} \bar{C} + \frac{\dot{q}_{loss}}{\dot{q}_T} C^M \quad (5-3)$$

and

$V_T$  = total system volume (fracture and wellbores),

$V$  = total volume of all fracture flow paths =  $V_1 + V_2$ ,

$V_2$  = volume of hot region flow path,

$C^M$  = (SiO<sub>2</sub>) makeup = concentration of SiO<sub>2</sub> in the makeup water,

$C^\infty$  = (SiO<sub>2</sub><sup>sat</sup>)<sub>T=T<sub>max</sub></sub> = quartz controlled saturation concentration of SiO<sub>2</sub> at T<sub>max</sub>,

$\bar{C}$  = ( $\overline{SiO_2}$ ) = average concentration of SiO<sub>2</sub> at time  $t$ ,

$k$  = dissolution mass transfer coefficient, cm/s,

$a^*$  = rock surface area to fluid volume ratio, cm<sup>-1</sup>,

$\dot{q}_2$  = fluid circulation rate through hot region at time  $t$ ,

$\dot{q}_T$  = total fluid circulation rate at time  $t$ ,

$\dot{q}_{loss}$  =  $\dot{q}_{makeup}$  = fluid loss rate to permeation at time  $t$ ,

$\tau_2$  = mean residence time in hot region =  $V_2/\dot{q}_2$ , and

$f$  = fraction of plug flow conversion = function of dispersion in hot region ( $0 \leq f \leq 1$ ).

By assuming all parameters on the right-hand side of Eq. (5-2) are approximately constant except  $\bar{C} = (\overline{SiO_2})$ , the equation can be integrated analytically to yield the time dependence of  $\bar{C}$ :

$$\bar{C} = C^{**} - (C^{**} - C_0 \chi) e^{-\dot{q}_2 t / V}, \quad (5-4)$$

with constants:

$$C^{**} = (C^\infty - B) (1 - e^{-ka^* \tau_2 f}) - B \dot{q}_T / \dot{q}_2,$$

$$\chi = - \frac{(A-1) \dot{q}_T}{\dot{q}_2} + A (1 - e^{-ka^* \tau_2 f}),$$

$$A = (\dot{q}_T - \dot{q}_{1\text{loss}}) / \dot{q}_T,$$

$C_0 = (\text{SiO}_2) = \text{initial silica concentration, and}$

$$B = \frac{\dot{q}_{1\text{loss}}}{\dot{q}_T} C^M.$$

In the extreme case of low water loss ( $A \approx 1$ ,  $B \approx 0$ ) and rapid reaction in the hot region ( $ka^* \tau_2 f \gg 1$ ), Eq. (5-4) reduces to

$$\bar{C} = C^\infty - (C^\infty - C_0) e^{-\dot{q}_2 t / V} = C^\infty - (C^\infty - C_0) e^{-\xi t}, \quad (5-5)$$

By using the solution to this equation for a negligible water-loss rate and fast kinetics with  $\xi = 0.04 \text{ s}^{-1}$ ,  $C^\infty = \text{SiO}_2^{\text{sat}}_{T=180^\circ\text{C}} = 220 \text{ ppm SiO}_2$  and  $C_0 = \text{SiO}_2 \left. \begin{matrix} (t=0) \\ \text{initial} \end{matrix} \right\} = 80 \text{ ppm}$  (the  $\text{SiO}_2$  concentration of the initial EE-1 injected water), the predicted  $\text{SiO}_2$  time history is given in Fig. 5-14. Rate equations of the same form were applied to the fluoride, sulfate, and the  $^{87/86}\text{Sr}$  data (Figs. 5-15, 1-16, and 5-17) with the same success. Remarkably, the value of  $\xi$  is in each case  $0.04 \text{ s}^{-1}$ . Since in all probability more than one mineral is dissolving to contribute  $\text{SiO}_2$ ,  $\text{SO}_4^{2-}$ ,  $\text{F}^-$ , and  $\text{Sr}$  to the solution; this would imply that all dissolution rates were equal. Thus it appears that mass transfer rates, specifically mixing rates between various flow fractions, control the concentration history of these particular species in solution.

The possibility remains that saturated pore fluid is merely being displaced from the hot region at a rate  $\dot{q}_2$ . Further investigation is under way to consider the difference between active dissolution and pore fluid displacement by examining the time dependence of ratios of various ions including  $\text{Na}^+/\text{K}^+/\text{Li}^+/\text{Cs}^+$  and  $\text{Cl}^-/\text{Br}^-/\text{I}^-$ .

As seen in Fig. 5-8 chloride concentrations also show a marked increase in time possibly indicating displacement and/or mixing with "saturated" pore fluid because no solid mineral source of chloride should exist with these reservoir

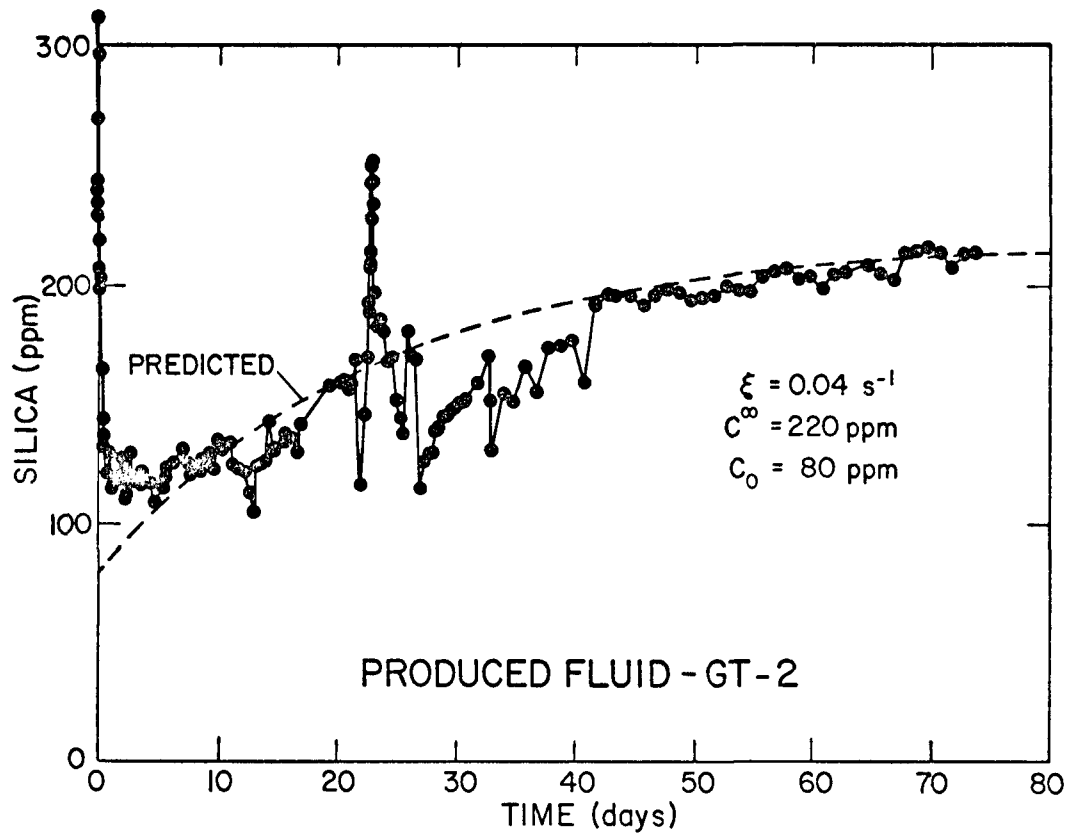


Fig. 5-14.

Observed and predicted silica concentrations in the produced fluid.

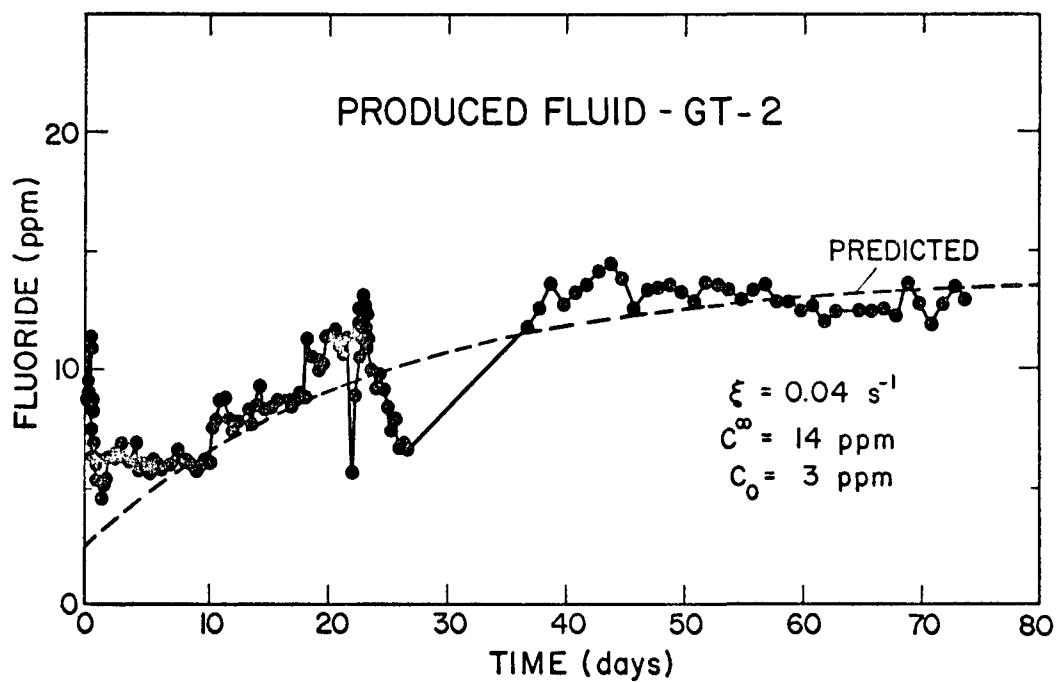


Fig. 5-15.

Observed and predicted fluoride concentrations in the produced fluid.

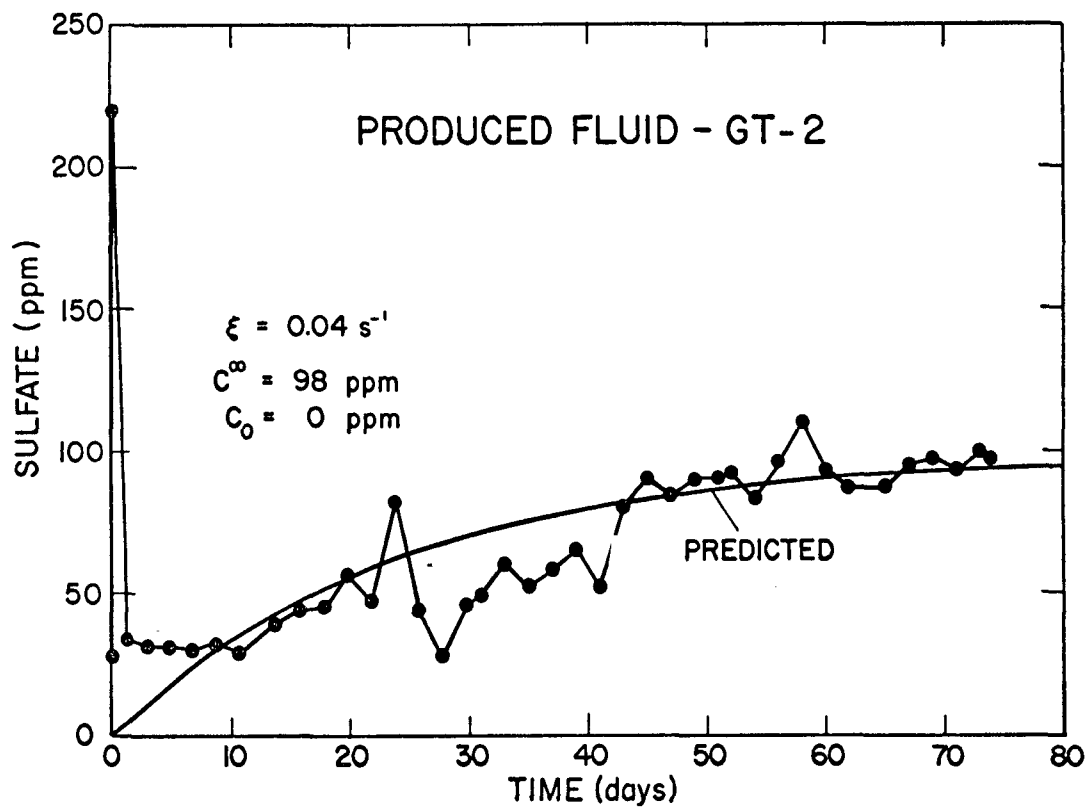


Fig. 5-16.

Observed and predicted sulfate concentrations in the produced fluid.

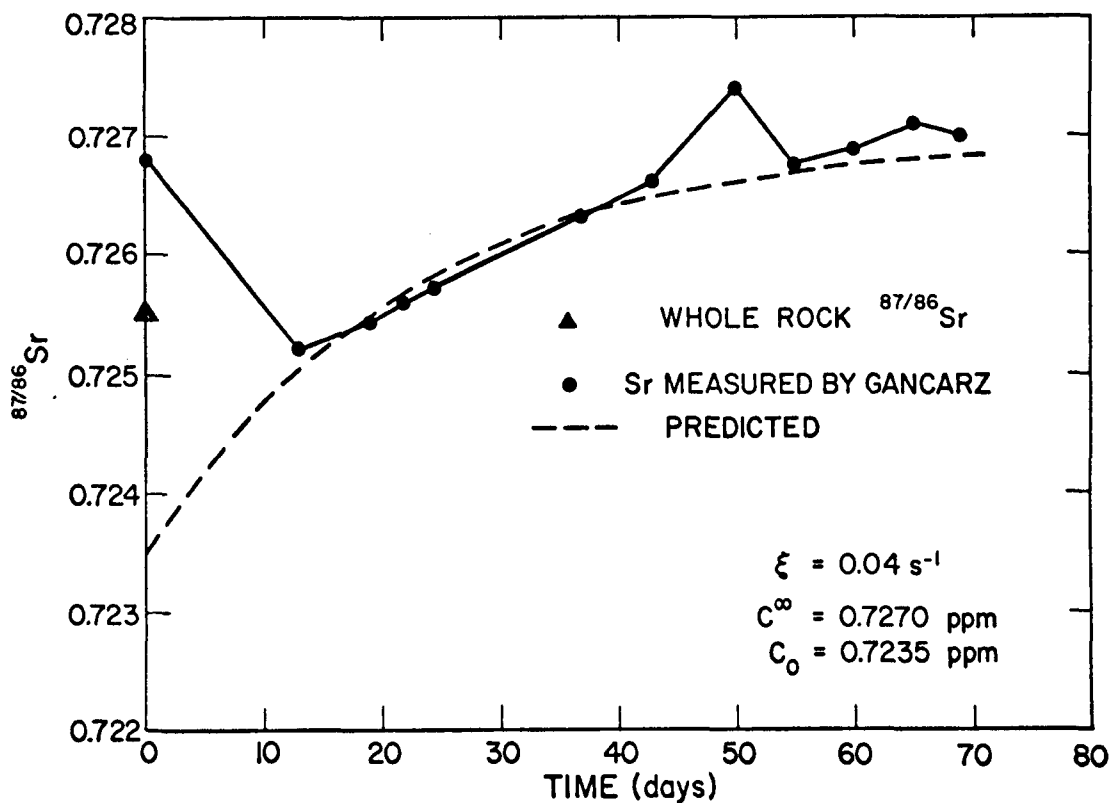


Fig. 5-17.

Observed and predicted  $^{87/86}\text{Sr}$  concentrations in the produced fluid.

conditions. In addition, the rate of increase of  $\text{Cl}^-$  agrees with the empirical model proposed to explain  $\text{SiO}_2$  buildup if a variable concentration source of  $\text{Cl}^-$  is being supplied to the flow path through the hot region.

We are determining the distribution of chloride in the GT-2 core samples by microprobe. If chloride is concentrated along calcite-filled fractures, the  $\text{Cl}^-$  concentration in solution could be dependent on calcite dissolution. The presence of  $\text{Cl}^-$  in fractures would indicate the  $\text{Cl}^-$  accompanied the carbonate-rich water, which migrated in and filled the fractures with calcite.

In the case of the bicarbonate concentration vs time, different conditions prevail. Calcite ( $\text{CaCO}_3$ ) -- the principal contributor of  $\text{CO}_3^{--}$  in solution -- has a retrograde solubility with temperature at constant  $P_{\text{CO}_3}$ .<sup>9</sup> Hence the lowest temperature of the reservoir may control the bicarbonate dissolution, and this lowest temperature is encountered in the main flow path as shown by temperatures measured at the EE-1-to-fracture system connection. As the fluid passes through the reservoir, however, it heats up and possibly reprecipitates calcite. In fact, there is some evidence of Ca depletion (see Fig. 5-2). If precipitation occurs, the highest temperature in the major flow connections will be the "equilibrium temperature" for  $\text{Ca}^{++}$  and  $\text{HCO}_3^-$  in solution. Figure 5-18 is a graph of observed ( $\text{HCO}_3^-$ ) history along with the time dependent ( $\text{HCO}_3^-$ )<sup>sat</sup> at the EE-1 fracture connection temperature (see Section 3) and ( $\text{HCO}_3^-$ )<sup>sat</sup> at the measured 2621-m (8600-ft) temperature in the producing wellbore GT-2B. Possibly, only minor amounts of calcite are available to the fluid as it passes through the wellbore, and therefore the average reservoir temperature may control calcite solubility. In the first 35 days of the run the calcite solubility appears to be controlled by the temperature of the mixed production flow in GT-2B. The changes in bicarbonate concentration with time can be fit into Eq. (5-5) employed previously with  $\xi = 0.04 \text{ s}^{-1}$  and  $\text{HCO}_3^- \text{ sat} = 325 \text{ ppm}$  (determined by the reservoir drawdown temperature at 70 days). During the last 40 days of this run, however, the bicarbonate concentration approaches saturation corresponding to the EE-1 calculated injection temperature. The change in bicarbonate concentration with time after 26 days can be fit to the empirical rate in Eq. (5-5) if the time constant is changed to  $0.07 \text{ s}^{-1}$  with a saturation concentration of 540 ppm (Fig. 5-19). Since this behavior was not observed for other major solution species, the change in the rate of ( $\text{HCO}_3^-$ ) buildup may be caused by the shift to a new controlling mechanism. One possibility for the apparent shift in control of the calcite solubility to the EE-1 injection temperature is the major

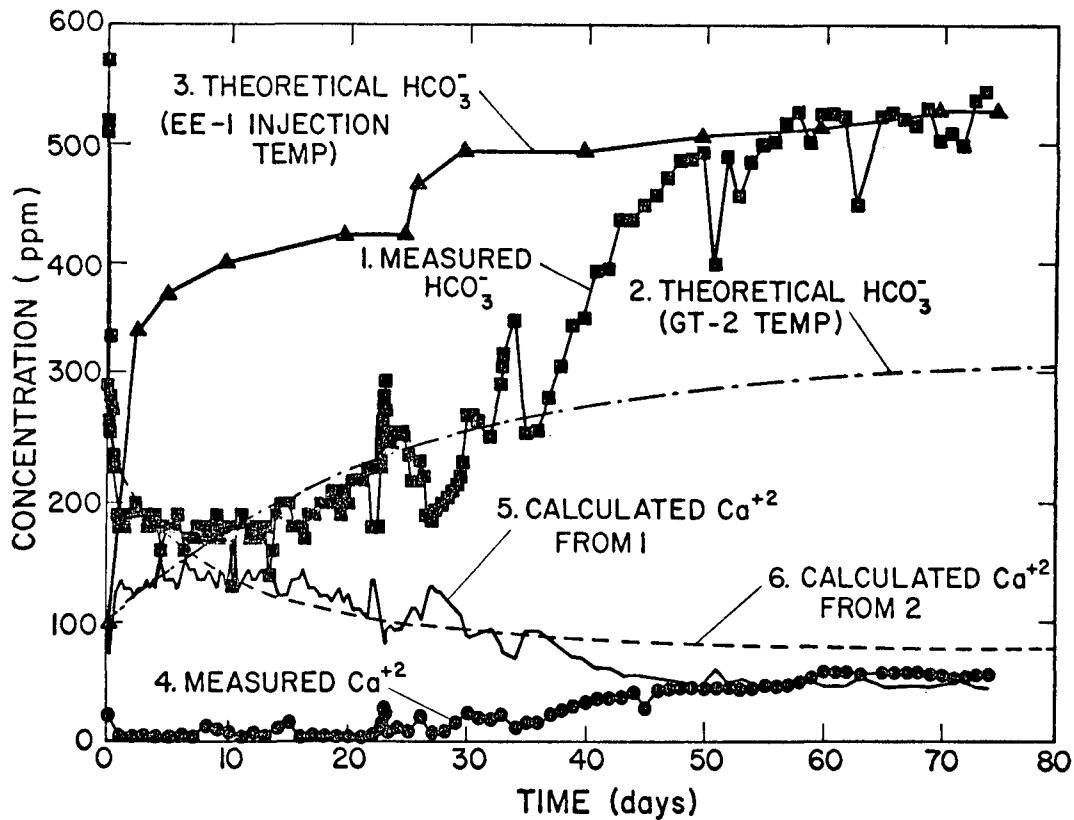


Fig. 5-18.

Observed and predicted  $\text{Ca}^{+2}$  and  $\text{HCO}_3^-$  concentrations in the produced fluid.

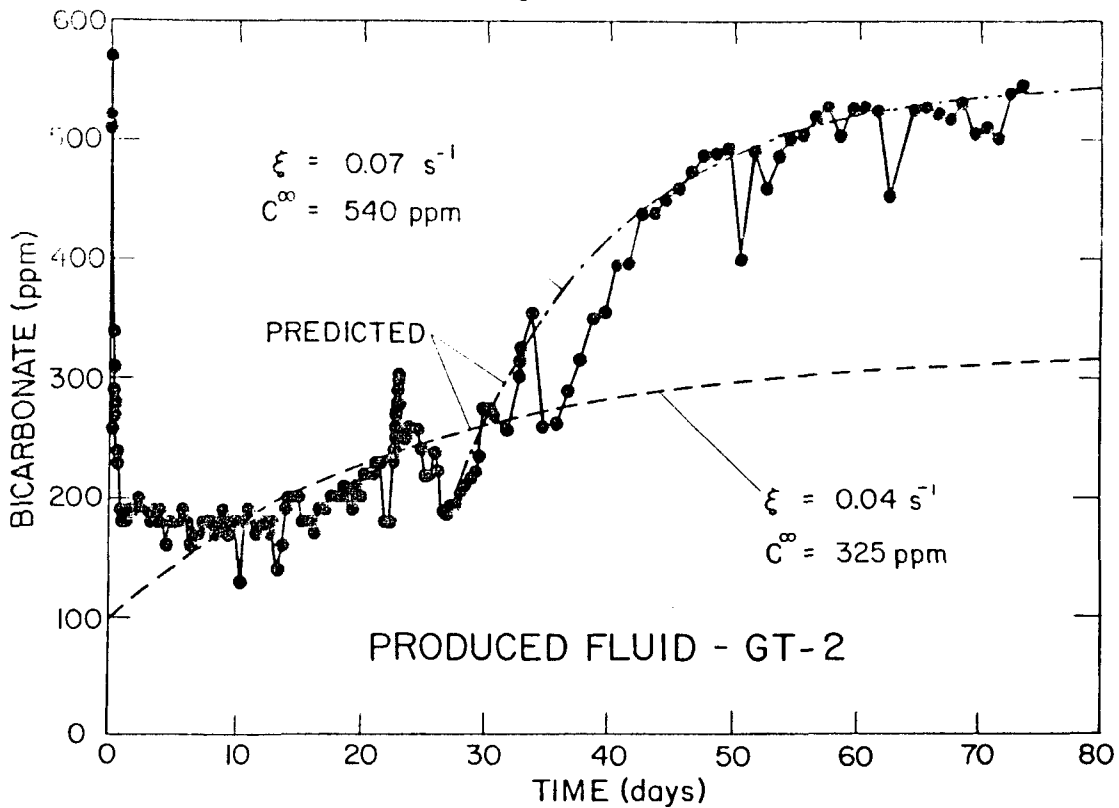


Fig. 5-19.

Observed and predicted bicarbonate concentration in the produced fluid.

change in downhole impedance and a doubling of the EE-1 flow rate that was observed during this period. If the impedance change is due to opening up of pre-existing fractures, the strategic position of calcite as a primary fracture-filling material could certainly increase the amount of calcite exposed to the fluid.

Calcium concentrations in equilibrium with calcite and  $(\text{HCO}_3^-)$  were calculated in the following manner from the thermodynamic data (equilibrium constants from Garrels and Christ)<sup>9</sup> assuming unit activity coefficients:

$$\frac{[\text{Ca}^{++}] [\text{CO}_3^{--}]}{[\text{CaCO}_3]} = 10^{-8.3} \quad (5-6)$$

$$\frac{[\text{H}^+] [\text{CO}_3^{--}]}{[\text{HCO}_3^-]} = 10^{-10.3} \text{ or } [\text{CO}_3^{--}] = \frac{10^{-10.3}}{10^{\text{pH}}} [\text{HCO}_3^-] \quad (5-7)$$

$$[\text{Ca}^{++}] = \frac{\text{Ca ppm}}{40.1} \times 10^{-3} \quad (5-8)$$

$$[\text{HCO}_3^-] = \frac{\text{HCO}_3^- \text{ ppm}}{61} \times 10^{-3} \quad (5-9)$$

$$\text{Ca}^{++} \text{ ppm} = \frac{61 (40.1) 10^{2-\text{pH}}}{\text{HCO}_3^- \text{ ppm} \times 10^{-6}} \quad (5-10)$$

Temperature corrections are made according to Frear and Johnston.<sup>10</sup>  $\text{Ca}^{++}$  ppm corresponding to values of  $\text{HCO}_3^-$  observed and saturation concentration of  $\text{HCO}_3^-$  at the GT-2 production temperature are also plotted in Fig. 5-18. Notice that the calculated  $\text{Ca}^{++}$  based on observed  $\text{HCO}_3^-$  approaches the  $\text{Ca}^{++}$  observed at day 45. Until that time, however, the  $\text{Ca}^{\text{calc}}$  is much higher than the  $\text{Ca}^{\text{observed}}$ . For every 3 ppm  $\text{CO}_3^{--}$  in solution contributed by calcite, there are 2 ppm  $\text{Ca}^{++}$  by stoichiometry. Assuming that all the  $\text{HCO}_3^-$  originally came from calcite, the observed  $\text{Ca}^{++}$  is an order of magnitude too low during the first 25 days of operation. This could be the result of precipitation of a noncarbonate calcium-rich mineral such as phillipsite  $(\text{K}_2, \text{Na}_2, \text{Ca})\text{Al}_2\text{Si}_4\text{O}_{12} \cdot 4.5 \text{H}_2\text{O}$ . Charles<sup>2,11</sup> observes phillipsite as an overgrowth on plagioclase in his experimental apparatus at 200°C, and Deer, Howie, and Zussman<sup>12</sup> list phillipsite with other calcic zeolites,

which occur in either undersaturated or saturated SiO<sub>2</sub> environments. If phillipsite is indeed precipitating, we might see the effects of its precipitation in the N-K-Ca ratios in the fluid. Figure 5-20 is a triangular diagram showing the Na-K-Ca ratios for the produced Fenton Hill fluid. The time history moves along a constant K line, and although they become richer in Ca relative to Na with time, the sense of the trend cycles up and down as if calcite is dissolved (and therefore increasing the Ca/Na ratio) followed by dissolution of albite (which lowers the Ca/Na ratio along the constant K line). The thermodynamics of dissolution and precipitation in this system have not been examined to see if phillipsite is indeed stable under these conditions, and there is inconclusive evidence that phillipsite exists in the Fenton Hill reservoir.

In the Na-K-Ca triangular diagram of Fig. 5-21, the changes in fluid and mineral compositions with time are shown. In addition, composition changes were observed by Charles<sup>2,11</sup> in a laboratory circulating system at 200°C using a biotite granodiorite from GT-2 and initially distilled water. In his circulating system, the fluid composition changes away from the Na-K-Ca ratios of the whole rock toward the starting solution values for the Fenton Hill reservoir. Apparently, the laboratory rock-water system has not achieved the same degree of reaction completion as is observed at the Fenton Hill reservoir. Therefore, changes in solid phases may correspond to early changes in the solid phases in the Fenton Hill reservoir.

#### Preliminary Interpretation - Surface Equipment

There were no indications of any solid deposition or corrosion in any surface piping during the Phase I, Segment 2 run. This statement is based on visual observation by J. Skalski. However, he does mention the presence of a "chalky" material produced by evaporation on some exterior components, which dissolves in acid with effervescence and is presumed to be calcite.

During the week of February 20, a crystalline material had filled the 7.94-mm (5/16-in.) stainless steel line, which had not yet been used for gas sampling. (The line had been left running to prevent its freezing.) The material was analyzed by x-ray diffraction and by electron microprobe and was found to be calcite with minor amounts of Sr (probably substituting for Ca). No silica was found.

According to Johnston and Williamson<sup>13</sup> the solubility of calcite in water at 16°C at  $P_{CO_2} = 7.63 \times 10^{-5}$  atm is 0.040 g/l. Frear and Johnston<sup>10</sup> report that "the temperature coefficient of solubility is, within the accuracy of the

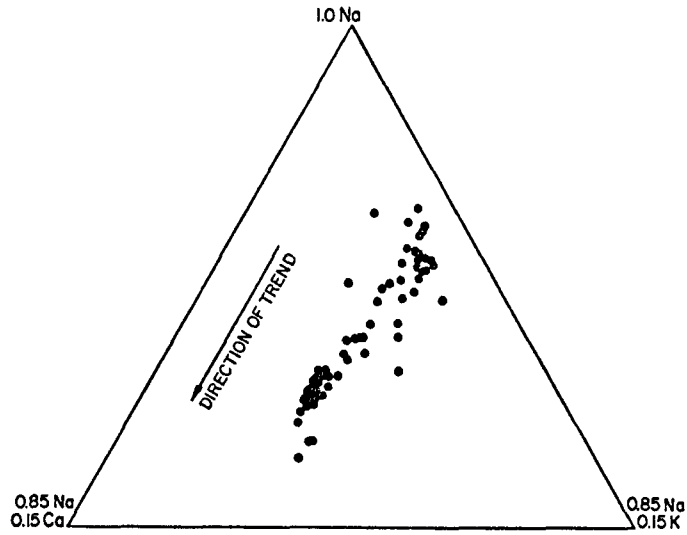


Fig. 5-20.  
Na-K-Ca ratios observed in the produced fluid during Phase I.

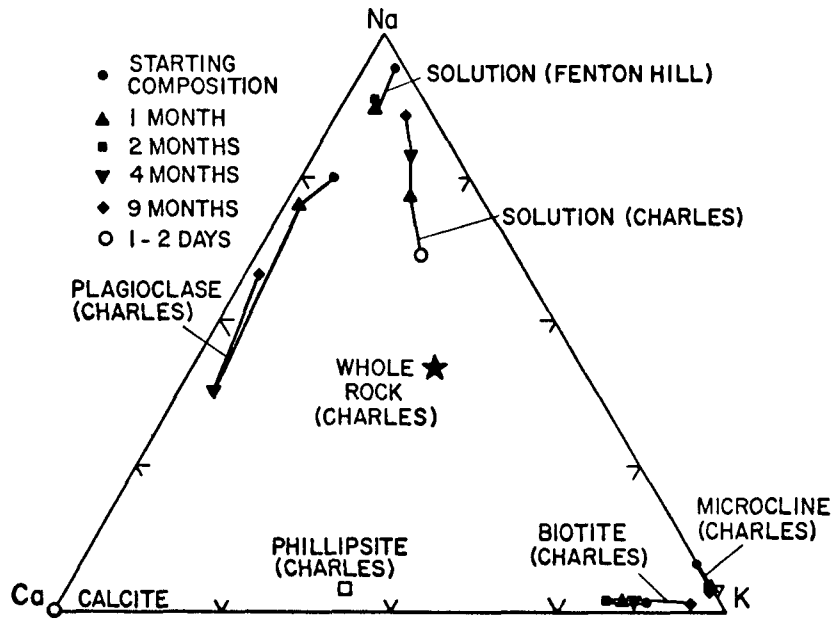


Fig. 5-21.  
Comparison of laboratory and field measurements for rock and solution samples using biotite granodiorite as the starting material.

measurements independent of the partial pressure of carbon dioxide particularly in the range of 0.003 to 1 atm; consequently it suffices to give the ratio  $r$  of the solubility at  $T$  to that at  $25^\circ\text{C}$ ." The ratio  $r$  is calculated by the formula:

$$\log r = (830/T^\circ\text{K}) - 2.78 \quad . \quad (5-11)$$

By assuming Eq. (5-11) to hold at the measured  $P_{\text{CO}_2}$  in the Fenton Hill geothermal fluid of  $6.152 \times 10^{-5}$  atm, for  $T = 140^\circ\text{C}$ ,  $r = 0.17$ . The solubility of calcite at  $P_{\text{CO}_2} = 7.63 \times 10^{-5}$  atm and  $25^\circ\text{C}$  is  $0.0323$  g/l, therefore, the solubility of calcite at  $140^\circ\text{C}$  and  $P_{\text{CO}_2} = 7.63 \times 10^{-5}$  atm is  $0.00548$  g/l. The calculated  $\text{Ca}^{++}$  concentration is then  $0.00219$  g/l or  $2.19$  ppm. The measured  $\text{Ca}^{++}$  concentration at day 20 is  $3.3$  ppm (see Fig. 5-2). According to the calcite equilibria cited earlier, the following equations develop:

$$\frac{[\text{Ca}^{++}] [\text{CO}_3^{--}]}{[\text{CaCO}_3]} = 10^{-8.3} \quad (5-12)$$

$$[\text{CO}_3^{--}] = \frac{10^{-10.3} [\text{HCO}_3^-]}{[\text{H}^+]} = 10^{-10.3} 10^{-6.4} 10^{-1.47} \frac{P_{\text{CO}_2}}{[\text{H}^+]^2} \quad (5-13)$$

$$[\text{HCO}_3^-] = 10^{-6.4} \frac{[\text{H}_2\text{CO}_3]}{[\text{H}^+]} \quad (5-14)$$

$$[\text{H}_2\text{CO}_3] = 10^{-1.47} P_{\text{CO}_2} \quad , \quad (5-15)$$

or

$$\frac{[\text{Ca}^{++}] P_{\text{CO}_2}}{[\text{CaCO}_3] [\text{H}^+]^{-2}} = 10^{9.87} \quad \text{at } 25^\circ\text{C} \quad . \quad (5-16)$$

If at constant pH and constant  $[Ca^{++}]$ , the  $P_{CO_2}$  drops (as it would when the gas phase separates from geothermal fluid at an expansion valve); the  $CaCO_3$  solubility would also have to drop enough to cause precipitation.

5.2. Trace Element Analysis (T. Beddoe, I. Binder, E. A. Bryant, A. J. Gancarz, J. S. Gilmore, R. J. Vidale, and R. A. Williams)

Precise, sensitive chemical analyses for trace elements found in the fluids flowing through the Fenton Hill reservoir were conducted to provide reconnaissance information concerning changes within the system that might be useful in determining the extent of rock-water interaction. Neutron activation analysis was chosen because of its great sensitivity for some elements and its capability of yielding data on many elements from the analysis of one sample.

This method involves exposing a sample to a high dose of neutrons, such as can be obtained in a nuclear reactor, and then measuring the resulting radioactivities to determine what was produced and how much. From this information one can calculate the amounts of elements present for those that produce suitable radioisotopes.

Freeze drying has been used to reduce approximately a 200-ml fluid sample taken at Fenton Hill to a solid mass that could be conveniently irradiated in the Omega West Reactor at LASL. This method increases the concentrations of trace species in the sample to increase sensitivity but also may introduce some contamination and inhomogeneity. All sampling and processing apparatus was carefully washed before use. Polyethylene equipment was used to reduce the introduction of additional inorganic elements. Freeze drying removes water by sublimation and reduces the chance that any solid will redissolve.

In addition to the Fenton Hill liquid samples, a 500-g rock core obtained at a depth of 2714 m (8904 ft) was treated to obtain samples of the component minerals. The rock was initially disaggregated by numerous cycles of rapid cooling to the liquid nitrogen temperatures ( $-196^{\circ}C$ ), followed by rapid warming to room temperature. The mixture was sieved to obtain a 50-200 mesh fraction between several of the cycles. The properly sized mixture was then separated by use of a hand magnet, a Frantz magnetic separator at several field strengths, and heavy liquids that separate fractions according to density differences by a sink-float technique. The six resulting mineral fractions represent apatite, biotite, magnetite, combined plagioclase and quartz, potassium feldspar, and sphene. An optical examination of the fractions showed the mineral purity to range from better than 50% to exceeding 95% for the desired component.

Either about 100 mg of freeze-dried solids or 20-350 mg of mineral separates were loaded into a special polyethylene vial for the reactor irradiation. These very clean plastic vials show a significant amount of chromium-51 radioactivity following irradiation, causing a background that accounted for all the chromium found in most of the samples. The irradiations were carried out in the Thermal-Column-Rabbit-2 position of the Omega West Reactor for approximately 7 h. The neutron dose received by the sample was monitored by an accompanying chromium wire.

After allowing the intense activities to decay to an acceptable level, the samples were individually examined using a calibrated, large-volume Ge(Li) gamma-ray detector coupled to a multi-channel pulse-height analyzer. The spectral data were immediately analyzed by computer program RAYGUN and recorded on magnetic tape for later computer evaluation with GAMANAL.<sup>14</sup> Such spectral measurements were made several times for each sample.

Using published neutron-capture cross sections, the resulting identifications and measurements were converted into the mass of each element found in the sample, and the fraction of the total solid mass was irradiated and analyzed. Initial results are given in the accompanying tables for several fluid samples (Table 5-I) and the mineral separates (Table 5-II) for the 2714-m (8904-ft) core sample. Values for the whole rock are also given for neutron activation as well as wet chemical analysis. Individual mineral compositions for the 2714-m (8904-ft) core sample are given in Table 5-III.

In addition, delayed neutron counting on activated liquid samples was used to determine uranium concentrations in the produced GT-2 fluid. Concentrations ranged from 0.1 to 2.0 ppb.

It is premature to arrive at any significant conclusions based upon the limited data presently available, but we are encouraged at the general consistency for the concentrations of several elements and similar results obtained for injected EE-1 and produced fluid GT-2 collected at similar times. Two samples in particular stand out as not conforming to the general pattern: N-1b and 66G. For N-1b this is likely due to the extended residence time in contact with rock for the water that first was produced at GT-2. However, this does not apply to sample 66G, which was obtained during continuous operation. Measurements will be repeated for 66G along with others collected shortly before and afterwards.

TABLE 5-I

CONCENTRATIONS OF ELEMENTS IN GEOTHERMAL WELL FLUID SAMPLES AS DETERMINED BY NEUTRON ACTIVITIES<sup>a</sup>  
 ng/gH<sub>2</sub>O (ppb)

Sample <sup>b</sup>	Time Collected	Na	Ca	Sc	Fe	Co	Zn	As	Br	Sr	Mo	Sb	Cs	Ba	Eu
N-1b	28 Jan 78 1845	8,224			1,860	0.27	1,270		5,603	1,223		1.88	1,043	87	0.080
33G	2 Feb 78 1500	107,100	4,505	0.46	50	0.75	11	60	440	125	14.3	1.85	178	29	0.016
36G	3 Feb 78 1500	6,890		0.050	85		9.9		445	747		1.5	195		0.015
56G	6 Feb 78 2300						1.9			156		1.15	184	62	
56G	10 Feb 78 0700									210		1.3	183		0.015
66G	13 Feb 78 1500	25,200	12,900	0.25	459	0.16	131	386	382	356		114	169	48	0.010
75G	16 Feb 78 1500								524	220		1.3	228		0.016
84G	19 Feb 78 1500		5,400	0.057					437	221		1.5	239	41	0.018
130E	6 Mar 78 1200														
130G	6 Mar 78 1200														
137G	13 Mar 78 1200	333,000	78,840		219			324	1,460	637	55		400		
141E	17 Mar 78 1200	363,000	42,900		563	0.13		224	1,606	801	46		423	132	
141G	17 Mar 78	349,000	45,400		373			266	1,670	585	45		429		

<sup>a</sup> No entry does not necessarily indicate a non-detectable concentration. Additional results will be added to this tabulations based on further analysis of spectra.

<sup>b</sup> Sample #'s correspond to major element sample # except N-1b which was taken between 9G and 10G at the producing GT-2B wellhead.

TABLE 5-II

ELEMENTAL COMPOSITION OF MINERAL SEPARATES  
AND WHOLE ROCK FROM CORE 2714 M (8904 FT)  
ppm ( $\mu\text{g/g}$ )

Element	Whole Rock	Av. Biotite Granodiorite <sup>a</sup>	Zircon	Sphene	Apatite	Plagioclase	K-feldspar	Biotite	Magnetite
Na	22,800	24,600	202	~0	1,260	63,150	8,830	~0	294
Mg	-	8,380	-	-	-	-	-	-	-
Al	71,000	76,600	-	-	-	-	-	-	-
K	38,000	35,000	~0	~0	~0	~0	130,000	84,200	443
Ca	20,000	22,200	~0	176,000	375,000	41,500	2,590	~0	~0
Sc	1,310	-	282	348	35.2	53.1	7.15	1,360	20
V	45.9	-	-	-	-	-	-	-	-
Cr	109	-	-	-	-	-	-	-	-
Mn	570	705	54.4	1,520	727	367	122	6,790	1,420
Fe	27,700	43,400 <sup>b</sup>	~0	15,400	4,470	4,530	1,030	18,000	730,000
Co	7.29	-	~0	1.69	0.86	1.76	0.18	69.7	44
Zn	88.9	-	~0	~0	~0	54.3	~0	1,120	70
As	1.38	-	~0	11.7	276	4.47	~0	~0	1.0
Br	~0	-	40.6	~0	~0	~0	~0	~0	8.97
Sr	430	372	~0	~0	~0	303	735	~0	638
Zr	~0	-	495,000	~0	24,800	~0	~0	~0	44,000
Mo	10.1	-	298	378	275	~0	4.62	~0	~0
Ag	~0	-	~0	~0	~0	1.43	~0	~0	-
Sb	0.263	-	~0	1.77	14	0.41	~0	1.29	~0
Cs	4.85	-	~0	~0	~0	2.18	3.00	43.1	~0
Ba	1,520	-	~0	1,030	896	~0	6,700	549	~0
La	68.0	-	~0	1,020	336	17.3	3.54	60.0	14
Ce	145	-	~0	5,860	981	~0	10.2	~0	38.6
Nd	48.5	-	443	3,270	321	~0	0.85	~0	~0
Eu	1.30	-	8.13	88.6	4.99	~0	0.19	~0	-
Tb	1.80	-	3.76	179	1.83	~0	0.25	~0	0.43
Dy	11.7	-	35.5	950	~0	~0	1.42	~0	2.0
Tm	1.032	-	~0	91.2	63.6	~0	0.11	~0	~0
Yb	4.57	-	399.0	1,920	24.3	~0	2.79	~0	7.8
Lu	1.75	-	47.1	143	6.71	~0	0.23	~0	0.90
Hf	9.50	-	2,880	63.8	80.2	13.0	128	42.0	26
Ta	3.38	-	56.0	206	1,040	6.68	1.36	~0	2.0
W	~0	-	39.4	~0	183	~0	~0	~0	~0
Th	13.2	-	49.5	458	172	~0	0.66	6.17	2.16

<sup>a</sup> From Laughlin and Eddy (1977)

<sup>b</sup> Large variation from sample to sample.

No entry means that the element was not detected because its concentration was below the sensitivity of the method.

- Not observable with this method.

TABLE 5-III

MINERAL COMPOSITION OF GT-2 CORE SPECIMEN FROM 2714 m (8904 FT)

	<u>Modal Volume %</u>	<u>Calculated Weight %</u>
Quartz	26	26
Plagioclase	37	37
K-feldspar	20	19
Biotite	10	11
Sphene	2.0	2.6
Chlorite	0.2	0.2
Magnetite	1.5	3.0
Zircon	~0.05	~0.1
Apatite	2.0	2.0
Calcite	0.3	0.3
Epidote	2.2	2.8

A substantial amount of data remains to be evaluated to supplement presently available results, and further water samples will be processed and analyzed. Of special interest will be water samples collected for both EE-1 and GT-2 at the same time and a sample of the makeup water.

A more accurate calibration for the neutron activation of various elements will be made by irradiating and analyzing a U. S. Geological Survey standard rock sample for which the composition has been well determined. Not all the elements detected in the water samples have been precisely measured in the USGS standards, and for these elements individual standards will have to be prepared.

### 5.3. Strontium Isotope Ratio Measurements (A. J. Gancarz)

Different minerals have different rubidium-to-strontium (Rb/Sr) ratios, and as a consequence of the radioactive decay of  $^{87}\text{Rb}$  they have different  $^{87}\text{Sr}/^{86}\text{Sr}$ . This, coupled with the evidence of the rock-water chemical interaction in the actual field operation and the differential reactivity of minerals observed in laboratory experiments,<sup>2,11</sup> suggests that it might be possible to detect in the field experiment which minerals are reacting preferentially by monitoring the isotopic composition of Sr in the circulating water. Strontium isotopic data were measured for water collected during the 75-day operation. In this unique application, Sr has been used apparently for the first time as a hydrologic tracer. Mixing of fluids from different sources and the interactions of the water with the rocks were observed by monitoring the isotopic compositions.

Three types of water samples were analyzed for Sr isotope ratios: (1) heated water produced at GT-2, designated G; (2) a mixture of cooled water and makeup water, designated E, which is pumped back into the hot-rock reservoir; and (3) filtered makeup water from the holding pond, designated M. In general, all three types of samples were collected simultaneously at various times throughout the 75 days. Thirty-ml aliquots were evaporated and processed to separate the Sr sample. The Sr was analyzed on a National Bureau of Standards type 15.2-cm (6-in.) mass spectrometer. The analytical data are presented in Table 5-IV and illustrated on Fig. 5-22.

Strontium isotope data for each of the three types of fluids (G, E, and M) are presented in Fig. 5-22. For any set of samples collected at a given time, we observe in all cases that the  $^{87}\text{Sr}/^{86}\text{Sr}$  in the fluid produced from the hot-rock reservoir is greater than that in the cooled injected fluid being cycled back down into the rock reservoir. Furthermore, the  $^{87}\text{Sr}/^{86}\text{Sr}$  in the injected

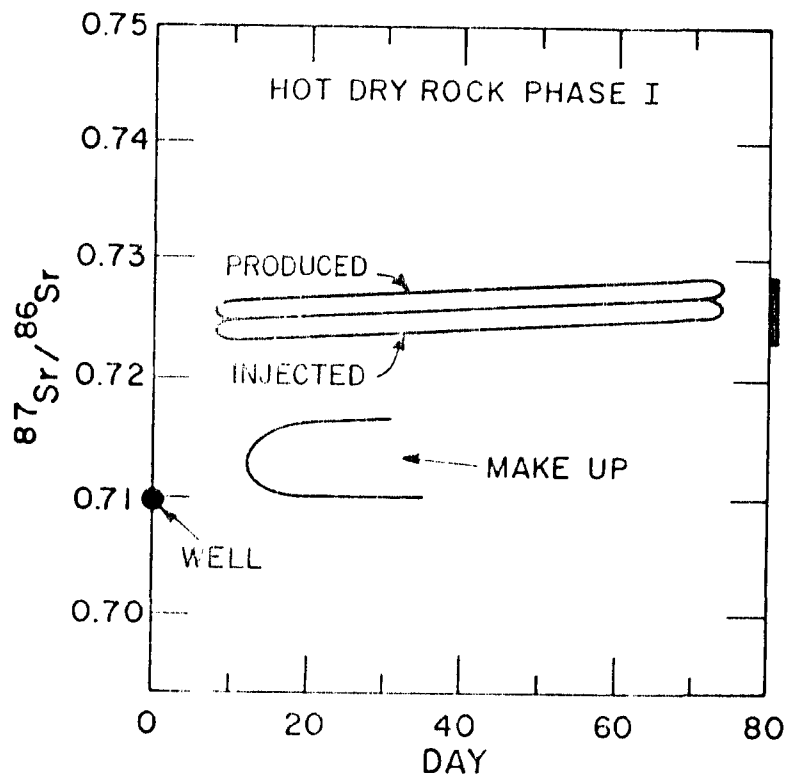


Fig. 5-22.

$^{87}\text{Sr}/^{86}\text{Sr}$  ratio history during Phase I for injected, produced, and make-up fluids.

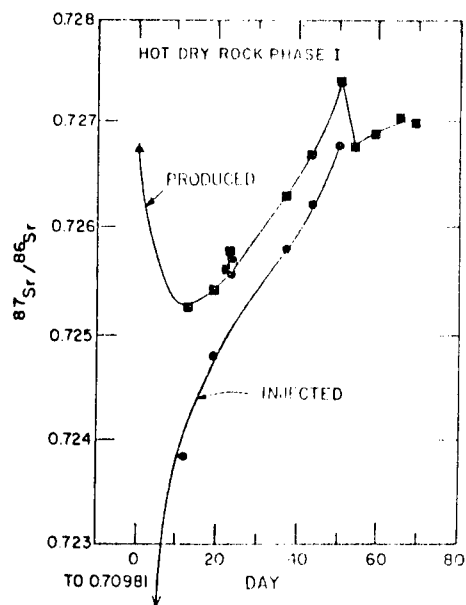


Fig. 5-23.

$^{87}\text{Sr}/^{86}\text{Sr}$  ratio history during Phase I in the injected and produced fluids.

which the rate of addition of  $^{87}\text{Sr}$ -rich Sr from the reservoir is constant. This implies a constant net rate of chemical interaction between rock, circulating fluid, and indigenous pore fluid.

The injected fluid datum for day 23 is not included in the E curve. At this time a sharp drop in impedance occurred and because of associated pumping difficulties the injected water plus a significant fraction of permeation flow returned up GT-2, was passed through the heat exchange modules, and was directed into the EE-1 holding pond. Consequently, the 23E sample does not represent produced water mixed with makeup water as supplied by the 122-m-deep water well.

Between days 50 and 55 there is a decrease in the  $^{87}\text{Sr}/^{86}\text{Sr}$  of G water. In this period there were no significant changes in flow rates or impedances. But as pointed out earlier in Section 4.3, the declining average fracture inflation pressure caused a flow-back phenomenon from permeation, which reduces the nominal water loss rate and provides a new source of fluid. The observed  $^{87}\text{Sr}/^{86}\text{Sr}$  decrease may indicate a change in the rock-pore fluid interaction. Furthermore, other effects such as pore pressure induced fracturing and/or thermal stress cracking may expose a fraction of the circulating fluid to new rock surfaces as well as indigenous pore fluid. "Fresh" rock exposed by the cracking may result in this case in the preferential dissolution of  $^{87}\text{Sr}/^{86}\text{Sr}$ -poor and consequently, low Rb/Sr mineral(s). The apparent rapid change in the Sr ratio after day 55 suggests that these  $^{87}\text{Sr}/^{86}\text{Sr}$ -poor minerals react rapidly with the water, and by day 55 a different rock-water interaction regime is established.

However, because of the complexity of the downhole environment these postulated effects should be viewed with an appropriate degree of caution. The only unequivocal fact that remains from the Sr isotope data is that distinct changes occurred in  $^{87}\text{Sr}/^{86}\text{Sr}$  during the 75-day experiment and these appear to correlate well with other observed changes.

As noted earlier the average temperature of the produced fluid at the end of segment 2 was only  $90^\circ\text{C}$  as compared to an initial value of  $175^\circ\text{C}$ . Laboratory experiments on rock samples conducted at  $300$  and  $200^\circ\text{C}$  show not only slower dissolution rates and solubilities at the lower temperatures but also changes in the order of the reactivity of the minerals.<sup>2,11</sup> Extrapolating to temperatures below  $200^\circ\text{C}$ , these data may suggest that changes in the isotopic ratios could occur solely because of temperature effects.

Unresolved is the following question: what mineral-water interaction is dominating the observed rock-water Sr isotopic effects? The average of

$^{87}\text{Sr}/^{86}\text{Sr}$  of 15 "whole-rock" biotite granodiorite samples from the cores is  $0.7255 \pm 40$ . This value and its error include the whole range of  $^{87}\text{Sr}/^{86}\text{Sr}$  fluid values observed. If we accept 0.7255 as the whole-rock value (indicated by the symbol  $\blacktriangle$  on Fig. 5-23), then we conclude that the Sr from rock-water interactions is dominated by minerals with  $^{87}\text{Sr}/^{86}\text{Sr}$  greater than the average rock. Biotite is a likely candidate and the measured  $^{87}\text{Sr}/^{86}\text{Sr}$  of biotite separated from the rock is  $0.80278 \pm 0.000010$ . This is, however, in marked contrast to the laboratory experiments, which indicate biotite is among the least reactive phases. Another possible mineral is potassium feldspar, which in some rocks is enriched in  $^{87}\text{Sr}/^{86}\text{Sr}$  relative to the average rock. Laboratory experiments show this mineral is among the most reactive and thus would appear more reasonable as the mineral providing the Sr and dominating the isotopic effects.

In summary, the Sr isotopic measurements have successfully been used to monitor mixing of fluids from different sources and to indicate when rock-water interactions in a continuously circulating system are in "steady-state" with respect to the production and depletion of Sr. Furthermore, there is some evidence that Sr data record changes in rock-water interaction regimes due to temperature changes or exposure, or both, of "fresh" rock due to thermal or mechanical cracking.

Experiments to determine Sr element abundances in the water and minerals and to determine the isotopic composition of Sr in the minerals composing the Fenton Hill reservoir rock are in progress. These data will facilitate quantitative mass balance calculations for rock-water interactions in the reservoir.

#### 5.4. Radon (P. Kruger\*, L. Semprini\*, G. Cederberg\*, R. Potter)

Radon measurements are useful for obtaining two types of geothermal reservoir data: (1) structural properties of the reservoir as they affect the emanation of radon from rock to pore fluids, and (2) fluid flow properties of the reservoir as they affect radon transport to the wellhead.

Radon has a set of properties which make it a useful internal reservoir tracer. First, radon is the radioactive noble gas produced in nature from decay of radium dispersed in the earth's crust. The principal isotope of radon is 3.83-day  $^{222}\text{Rn}$  resulting from alpha-particle emission from 1600-yr  $^{226}\text{Ra}$ , which in turn is produced in the natural uranium series originating with a  $4.5 \times 10^9$   $^{238}\text{U}$ . Since radon is produced essentially "forever" in the reservoir but decays

---

\* Stanford University, Stanford, California

with its characteristic 3.83-day half-life when separated from its radium parent radionuclide in the formation, it introduces a "time element" in tracer studies. This property of radon contrasts sharply with the stable gas components of geothermal fluids, such as CO<sub>2</sub>, H<sub>2</sub>S, and O<sub>2</sub> isotopes.

Radon concentration in geofluids depends on several reservoir parameters, primarily the concentration and distribution of radium in the reservoir formation, the conditions for emanation and diffusion into the pore and circulating fluids, and the transport properties of the convecting fluids from the reservoir emanation sites to the producing wellhead. These parameters, in turn, are related to different geologic factors. Radium is found rather uniformly distributed in sedimentary and igneous rocks at an average concentration of about 1 pg/g. Its distribution depends on the local thermodynamic and hydrochemical history of the formation. Since radium is a chemical homolog of the alkaline earth elements calcium, strontium, and barium, it can become redistributed with these elements in hydrothermal regions.

The emanation of radon in rock matrices depends on the chemical, mineral, structural, and thermodynamic properties of the rock. The recoil energy of <sup>222</sup>Rn on alpha decay of <sup>226</sup>Ra is 86 keV, sufficient to migrate about 1 μm in rock. The emanation from the rock is thus strongly dependent on the surface area exposed, the porosity, and the composition of the cementing materials in the rock, as noted by Andrews and Wood.<sup>15</sup> It is also dependent on the pressure, temperature, and density of the pore fluid in the formation. The transport of radon depends on its solubility in the convecting fluid and the hydrodynamic properties of the reservoir, such as permeability-thickness, reservoir pressure gradients, and flow rate.

Two general types of information may be obtained with radon as an internal reservoir tracer. Under steady flow conditions, changes in reservoir properties will result in changes in radon concentration in the produced geofluids. Under steady emanation conditions, changes in flow regime will also result in changes in radon concentration. A discussion of some of the types of information that can be obtained from radon measurements was given by Kruger, Warren, and Honeyman.<sup>16</sup> The challenge of successfully applying radon transient analysis to geothermal reservoir engineering rests with the ability to show the relationships between changes in reservoir or flow properties and changes in radon concentration. Sufficient data are needed to separate the changes due to each effect.

In a particular case, radon measurements were used to study changes in fracture permeability in geothermal systems as noted by Stoker and Kruger.<sup>17</sup>

This section reviews the experimental radon data obtained during the first 75 days of the LASL Phase I experiment and is the first attempt to study radon emanation in a hydraulically-fractured geothermal reservoir. During the 75-day period, five samples were collected at the producing wellhead and shipped to the nuclear civil engineering laboratory at Stanford, where the radon concentration was measured by the method developed by Stoker and Kruger.<sup>17</sup> The system was shut in for 11 days after the flow test period and then vented. Two samples of wellhead fluid were collected during this latter venting period. To obtain a background value of radon due to radium dissolved in the makeup water, one sample of makeup water was collected during the flow test period.

The concentration of  $^{226}\text{Ra}$  in the formation rock was reported by L. M. Marple and R. M. Potter as  $1.7 \pm 0.18$  pCi/g determined by gamma-ray spectroscopy at LASL. To determine the fraction of radon due to dissolved radium in the recirculating fluid, double-extraction measurements of radon were made in one of the five flow-test samples and in the makeup water sample. In this method, the fraction of radon in the original wellhead sample due to dissolved radium is determined by complete initial removal of the radon from the sample, then allowing radon to reestablish equilibrium with the dissolved radium, and removing the radon a second time for measurement.

The wellhead conditions and the radon concentration values for the samples analyzed during the Phase I test are given in Table 5-V. Readily apparent over the 73 days of the flow period is the marked increase in radon concentration coupled with the continuous decrease in wellhead fluid temperature and the continuous increase in flow rate. Also apparent in the data is the rapid decrease in radon concentration during the 3 days of venting the system. Table 5-V also shows that the radon concentration due to dissolved radium in the GT-2 produced sample of day 65 was 0.0083 nCi/l compared to a total radon concentration of 1.7 nCi/l. Thus dissolved radium accounts for only 2% of the total radon observed in the wellhead fluid. The double-extraction method for radon in the makeup water sample showed a total radon concentration of 0.0075 nCi/l (corrected to time of sampling) with dissolved radium contributing 0.0018 nCi/l ( $\sim 24\%$ ).

The experimental data in Table 5-V show a quasi-exponential growth of radon concentration in the recirculated fluid over the 75-day flow test period, a

TABLE 5-V

RADON DATA - PHASE I TEST  
JANUARY 28 - APRIL 27, 1978

CIRCULATING SYSTEM  
(GT-2 PRODUCING WELL SAMPLES)

Test Day	T (°C)	$\dot{q}$ ℓ/min (gpm)	$Q^a$ $10^6 \ell$ ( $10^6$ gal)	(Rn) (nCi/ℓ)
0.3	~170	208 (~55)	0.08 (0.02)	0.17 ± 0.02
18.9	130	424 (112)	10.6 (2.8)	0.10 ± 0.10
38.2	100	852 (225)	35.2 (9.3)	0.58 ± 0.05
65.9	90	897 (237)	69.3 (18.3)	1.7 ± 0.2
73.1	90	927 (245)	77.6 (20.5)	2.8 ± 0.3

VENTING SYSTEM (GT-2 WELL SAMPLES)

86.1	80	416 (110)	80.3 (21.2)	2.3 ± 0.2
89.2	80	≤95 (≤25)	85.2 (22.5)	0.50 ± 0.06

MAKEUP WATER

65.9	-	-	-	0.0075
------	---	---	---	--------

RADIUM CONTENT (RADON DUE TO DISSOLVED RADIUM)

65.9 (for GT-2 produced fluid)	80	897 (237)	69.3 (18.3)	0.0083
65.9 (for makeup)	-	-	-	0.0018

<sup>a</sup> Total produced fluid volume.

rapid decrease in radon concentration during the venting period, and a low concentration of dissolved radium in both the makeup and circulating fluid.

The radon concentration growth history during the flow period and the decay history during the venting period are shown in Fig. 5-24. The first sample, collected 6 h after initiation of the flow test period, represents water that was resident in the fracture system during the ~3-month shut-in period prior to the test. Since the shut-in period was longer than 1 month (large compared to the 3.83-day half-life of  $^{222}\text{Rn}$ ), the radon concentration should have been in equilibrium with the radon emanation from the fractured rock surface. The initial concentration of  $0.17 \pm 0.02$  nCi/ $\ell$  can be considered representative of the radon concentration in the main fracture volume of the large hydraulic fracture system. The second sample was collected after 20 days of flow during which time the flow rate increased by a factor of two and the average reservoir temperature declined steadily from 170 to 130°C. This sample showed a radon concentration of  $0.10 \pm 0.10$  nCi/ $\ell$ , smaller than the initial sample. The uncertainty of this sample is very large ( $\pm 100\%$ ) due to an unfortunate delay in shipping between collection and analysis, resulting in an alpha-particle measurement close to counter background and a large-decay correction factor to sampling time. However the measured concentration may be correct, and the lower value of 0.1 nCi/ $\ell$  may represent the effect of dilution of the shut-in volume of water with makeup water, which is noted during this period to have exceeded 151  $\ell/\text{min}$  (40 gpm) when the flow rate was reaching 379  $\ell/\text{min}$  (100 gpm).

The third sample, collected on day 38 when the system dynamics were reaching steady state, shows the initiation of a rapid rise in radon concentration up to the end of the Phase I flow test at day 75. The rise is shown in Fig. 5-25 as an exponential growth, given by the equation

$$[\text{Rn}] = [\text{Rn}]_0 e^{+kt} \quad , \quad (5-17)$$

where  $[\text{Rn}]_0$  = initial fracture-volume concentration (0.17 nCi/ $\ell$ ) uncorrected for dilution with makeup water, and  $k$  = growth constant for the system function of (Q, T, P).

Although the radon concentration exhibits an exponential growth pattern during the test period, it cannot continue to rise indefinitely, but must reach some steady-state concentration given by maximum emanation of radon from the

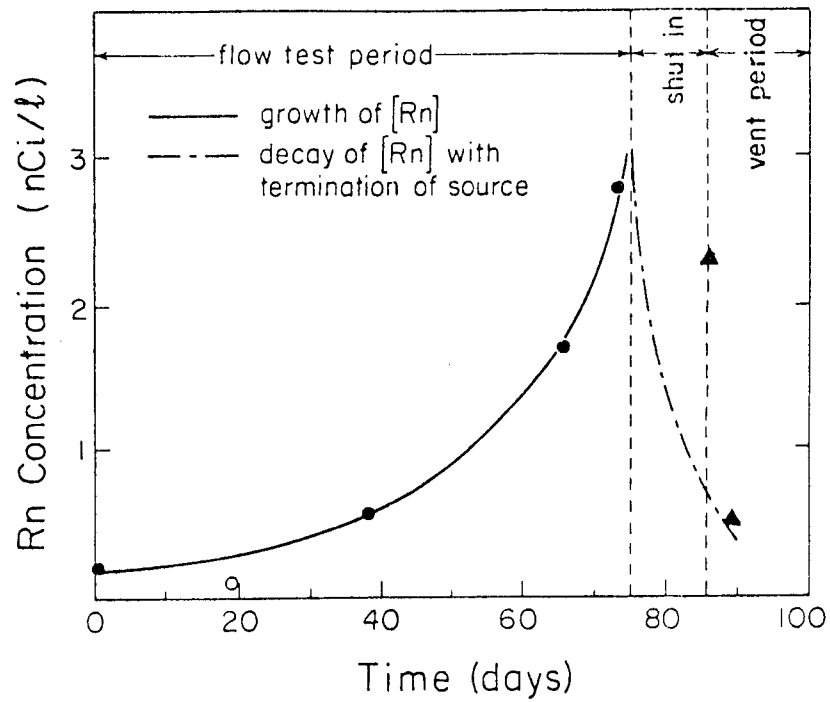


Fig. 5-24.  
Radon concentration in the produced fluid.

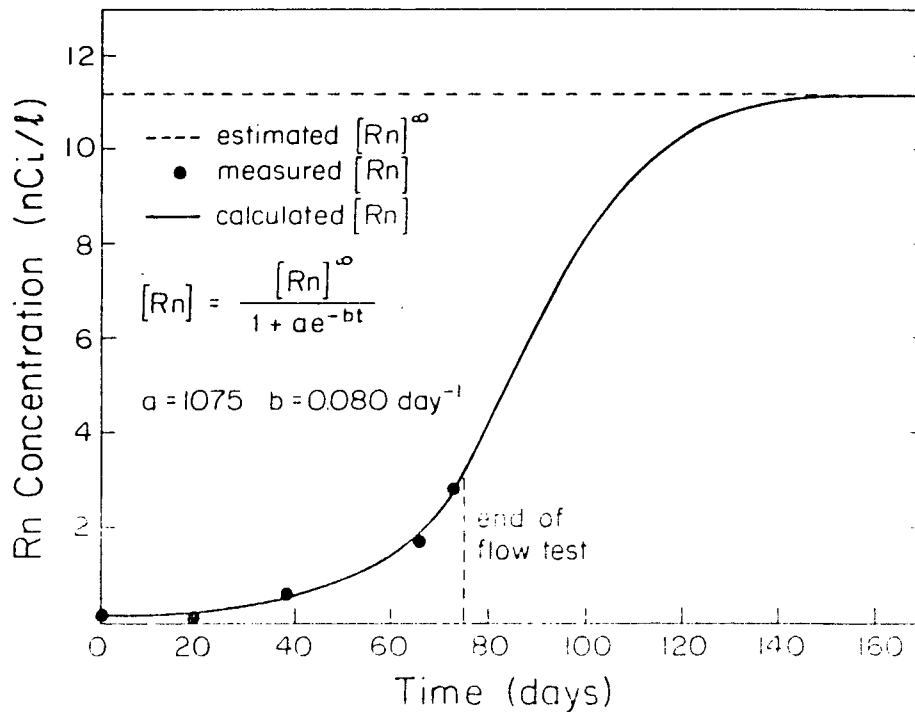


Fig. 5-25.  
Observed and predicted radon concentration in the produced fluid.

radium concentration in the formation rock. The trend toward saturation is noted in the nonconstancy of the growth constant,  $k$ , and its counterpart, the growth half-life,  $\tau$ , given by  $\tau = \ln 2/k$ , as shown below:

<u>Sample Range</u>	<u>k</u> <u>(day<sup>-1</sup>)</u>	<u><math>\tau</math></u> <u>(days)</u>
1 - 3	0.032	21.8
1 - 4	0.035	19.9
1 - 5	0.038	18.1
3 - 4	0.039	17.8
4 - 5	0.071	9.7

Several mechanisms could potentially explain the observed quasi-exponential rise in radon concentration over the 75-day Phase I flow period. They include: (a) continuous dissolution of radium from the exposed rock surfaces into the recirculating water, (b) increase in solubility of radon in the circulating fluid as the temperature of the rock-water system decreases, (c) increase in the emanating power of the radon by recoil or diffusion from the fractured rock to the circulating fluid, and (d) increase in the area of the fractured rock surface (at constant emanating power) through increased fracturing of the formation by the recirculating fluid pressure and temperature differential.

Table 5-V showed that the dissolved radium concentration in the day 65 wellhead sample accounted for only about 2% of the total radon present in the sample; the value was not much larger than the radium initially present in the makeup water. Both radium values are sufficiently small to preclude the dissolution of radium from fractured rock as the reason for the observed growth in radon concentration over the Phase I flow test period.

The solubility of radon in water is significant at low temperature and decreases rapidly with temperatures above 0°C.<sup>18</sup> The value of 86 cm<sup>3</sup>/ℓ at 70°C and 1 atm pressure does not change greatly in the temperature range of 90 to 170°C. Table 5-V notes the decrease in wellhead temperature from 170 to 90°C during the 75-day flow test. This temperature drop might affect the radon concentration in two ways: an increase in emanating power of radon and an increase in its solubility. Since the emanating power is expected to increase with the larger diffusion coefficients at increased temperature (at constant pressure and pore fluid density), it is difficult to accept the inverse

relationship. And unless there is a stagnant volume in the system where degassed gaseous components can accumulate or bypass the wellhead collection site, it is difficult to visualize how a potential for degassing in the closed recirculation system could occur. Therefore, the growth in radon concentration over the flow test period cannot, at this time, be attributed to the decrease in reservoir temperature.

The distinction between increased emanating power and increased fracture surface area is difficult to make. There are few experimental data available on emanating power of radon from geothermal rock mediums. Research is currently underway as part of the Stanford Geothermal Program to determine the dependence of radon emanation power on the thermodynamic conditions of pressure, temperature, and pore fluid density in fractured rock formations.

A reasonable speculation at this time is that the most likely factor contributing to the observed increase in radon concentration is the increase in new surface area created during the experiment. Based on downhole spinner and temperature measurements in GT-2B and compositional changes occurring in other critical chemical species such as  $\text{SiO}_2$ , Cl, Na, K, and  $\text{HCO}_3$ , a fraction of the circulating fluid is being exposed to additional surface area by newly created flow paths, which apparently penetrate into hot regions of the reservoir rock containing indigenous pore fluid. At this time, it is difficult to say whether pressure fracturing, thermal stress cracking, or permeation is the source of these new flow paths. If the surface area of new fractures or flow paths increases at a rate greater than the increase in fracture volume (and assuming even a constant emanating power under these conditions), the radon concentration in the recirculating water would be expected to increase. As noted earlier, however, a saturation concentration would eventually be reached, given by a logistics equation

$$[\text{Rn}] = \frac{[\text{Rn}]^\infty}{1 + ae^{-bt}} \quad , \quad (5-18)$$

where

$[\text{Rn}]^\infty$  = infinite-time steady-state radon concentration for finite radium concentration and constant emanating and thermodynamic conditions  
a,b = empirical constants.

An attempt to fit the measured radon concentrations with an estimated  $[Rn]^\infty$  value is shown in Fig. 5-25. The value for  $[Rn]^\infty$  was obtained from the relation

$$[Rn] = \frac{[Ra] (EP)}{\phi} \quad (5-19)$$

where

$[Rn]$  = radium concentration

(EP) = emanating power

$\phi$  = porosity.

From the LASL value of 1.7 pCi/g for the radium concentration in the rock, and assumed values of (EP)  $\approx$  0.1 and  $\phi \approx$  0.01, a rock density of 2.5 g/cm<sup>3</sup>, the radon concentration in the fracture volume would be  $[Rn] = 42.5$  nCi/l. For a dilution based on values of the main fracture volume  $\approx$  54 883l (14 500 gal) and total circulation volume  $\approx$  208 175l (55,000 gal), the radon concentration in the wellhead fluid would be  $[Rn]^\infty = 11.2$  nCi/l.

A least squares fit of Eq. (5-18) to the data in Fig. 5-25 gives values to the two empirical constants of  $a = 1075$  and  $b = 0.080 \text{ day}^{-1}$ . The curve, based on the estimated value of  $[Rn]^\infty = 11.2$  nCi/l, indicates that equilibrium would have been achieved if the test had run an additional 2 months. It will be interesting to confirm the values of the empirical constants  $a$  and  $b$  in future flow tests in the EE-1/GT-2 system.

Figure 5-24 also shows the results of the radon measurements made during the venting part of the Phase I test. The first of the two post-flow samples represents water in the main fracture on day 86 of the test with pressure maintained in the shut-in system. The radon concentration remained at an elevated value of 2.3 nCi/l 11 days after shut in, as contrasted to an expected value of 0.67 nCi/l based on radioactive decay of the dissolved radon if the mechanism for the growth during the flow period were cut off with shut-in of the system. The implication is that the source of radon continued under the pressure conditions reached during the flow period to shut-in. However, the second sample on day 89, collected after fluid pressure reduction shows a radon concentration of 0.5 nCi/l consistent with radioactive decay to pre-flow conditions. The wellhead water obtained for this sample however may not represent fluid from the fracture system due to gas fractionation at the wellhead resulting from depressurization.

An explanation for the sustained high value of Rn may be a flow from permeation into the GT-2B open hole exiting then to the EE-1 annulus through the main flow system. This permeation flow would carry additional Rn to compensate partially for the decay of Rn in the wellbore fluid.

Downhole samples taken later in the vent period on July 27, 1978 showed considerably higher Rn concentrations of 3.3 nCi/l. Samples were taken with the downhole water sampler at the 2590-m (8500-ft) depth in GT-2B which is 46 m (150 ft) above the highest producing zone.<sup>2</sup> This was done to avoid the long borehole residence time and subsequent decay at the low venting rate of 8 l/min (~2 gpm). In addition, 1900l (~500 gal) of fluid was pumped into EE-1 with GT-2 vented, and another sample was taken; this time the Rn concentration had decreased to 1.4 nCi/l. Because the experimental error is  $\leq 10\%$ , the difference in concentration between the two samples is real. One possible mechanism is dilution between EE-1 wellbore fluid and fluid which has equilibrated with the fracture system. Because the venting Rn concentration of 3.3 nCi/l is drastically higher than the initial Rn concentration of 0.17 nCi/l, an alternate source of Rn is suggested. During the latter venting period, a very small return flow rate of 8-19 l/min (2-5 gpm) was observed in the GT-2B wellbore. This fluid is returning as permeation stored fluid quite likely in contact with the fine-grained rock matrix of the reservoir, whereas the original flow sample collected on day 0 (see Fig. 5-24) consisted of fluid contained in a self-propped hydraulic fracture system with little or no returned flow from permeation. Consequently, the higher Rn concentration observed is probably caused by a higher effective emanation power of radium exposed to fluid returning via matrix flow.

6. MONITORING FOR INDUCED SEISMIC EFFECTS (C. Newton, J. Albright, R. Potter, and R. Butler)

During Phase I, Segment 2 of the HDR geothermal demonstration, seismic monitoring was done to detect local seismic sources and to discriminate among several possible source types, such as man-made disturbances, earthquakes, and rock failure induced by the pressurized fluid injection into the inlet well of the HDR system.

The monitoring array consisted of seven surface stations at distances up to 750 m from the wells, two shallow borehole stations ( $\sim$ 125-m deep) at about 1 and 3 km, and stations of the LASL regional seismic network -- the nearest of which is about 10 km away. The two borehole stations were positioned a few meters below the Permian sandstone - Quaternary tuff interface.

The only local earthquakes identified during the loop operation were located by the regional array near a fault 15 km west of the HDR geothermal site (see Fig. 6-1). These three events, and a fourth that occurred in May, were in the same epicentral zone as a swarm of earthquakes that were observed in late September 1975. The largest event observed to date had a local magnitude,  $M_L = 3.2$ . These small earthquakes may be premonitory activity to a much larger earthquake (whose magnitude and time of occurrence are not yet predictable), which might occur sometime in the next few years. Figure 6-1 shows the capability of the regional network to locate microearthquakes in the vicinity of Fenton Hill. For  $M_L > 0.0$  more than five stations can be used to locate the epicenter (Fig. 6-1 a,b,d), but as the magnitude approaches  $-1.0$  the existing network is close to its location-limiting threshold (Fig. 6-1 c).

There were many blasts, sonic booms, and earthquakes observed with more distant epicenters. Some of the smaller of these acoustic signals needed positive identification by the seismograms of the regional network.

The background noise was generally high during the day, beginning with sunrise thermal expansion of the metal buildings, which shelter the surface seismic stations. These amplitudes of noise bursts frequently exceeded levels expected for  $M_L = 1.0$  earthquakes. At night, however, the background noise was nearly always below signal levels for  $M_L = -1.0$  earthquakes.

Although it is likely that  $M_L < 0.0$  earthquakes would not have been identified during the daytime, the absence of detectable, induced earthquakes with  $M_L > -1.0$  at night is reasonable evidence that none with  $M_L > 0.0$  occurred during the loop operation. Although the stress alterations to the reservoir during the

nearly 3 months of the loop operation were significant but not overwhelming [5 677 500ℓ (1 500 000 gal) of water in situ, pressures to 1400 psi above hydrostatic, and nearly 250 MW-days of thermal energy removed] the absence of detectable earthquakes (i.e.,  $M_L > -1.0$ ) is an encouraging observation. The seismic monitoring will continue with an improved network during future flow experiments.

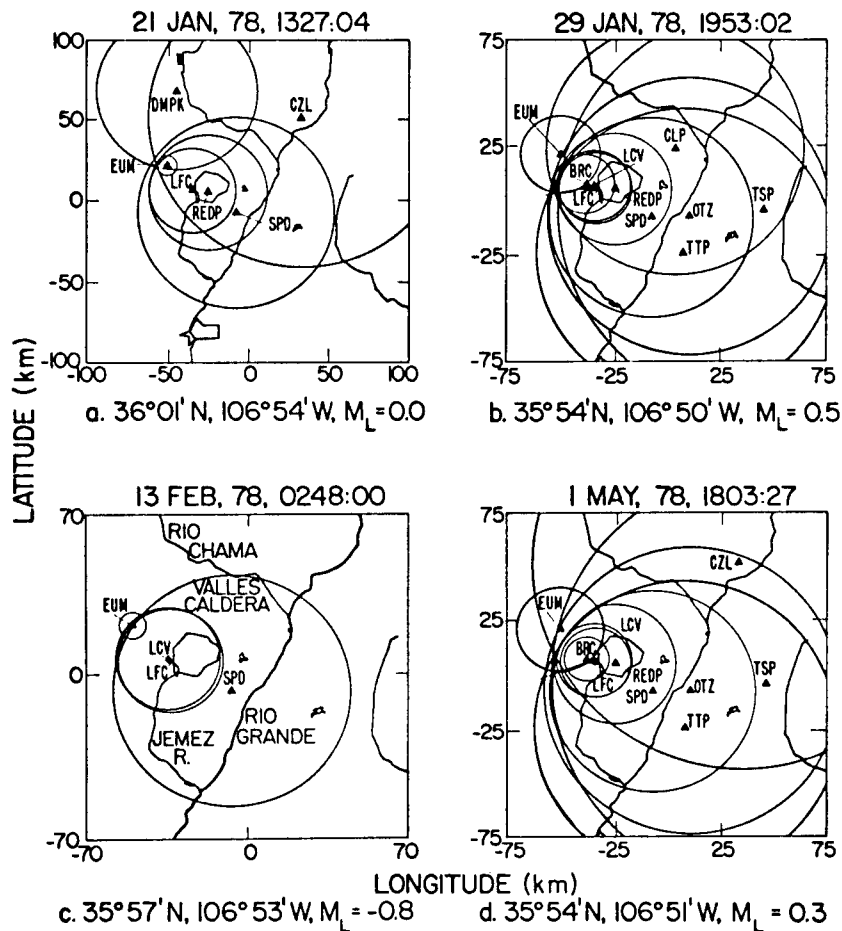


Fig. 6-1.  
Calculated epicenters for four earthquakes near Señorita, New Mexico.

## 7. SUMMARY OF SYSTEM PERFORMANCE AND MODELS (J. W. Tester and J. N. Albright)

A brief review of the redrilling program at Fenton Hill, which culminated in the completion of the present GT-2B/EE-1 connected fracture system, is presented in Figs. 7-1 through 7-4. Projections showing the bottom sections of EE-1 and GT-2 with GT-2A and GT-2B, the sidetracked hole sections, are shown in Figs. 7-1 and 7-2. The redrilling was completed in the following sequence: GT-2 (December 1974), EE-1 (November 1975), GT-2A (May 1977), and GT-2B (June 1977). A complete description of the drilling activity between 1975 and 1977 is contained in Project reports (LASL HDR Project Staff, 1978<sup>2</sup>). GT-2B is cased through the sidetrack points from GT-2 and GT-2A. Figure 7-3 is a horizontal projection to a vertical plane parallel to the most probable direction of a main hydraulically induced fracture (NW-SE) and perpendicular to the least principal horizontal stress. A low impedance flow between wells was finally achieved by the redrilling, which entered a region of the reservoir with increased permeability due to hydraulic fracturing. Because of the low formation breakdown pressures (100 bar or 1500 psi) encountered, previously sealed natural fractures were probably opened.

The current production system at Fenton Hill is represented schematically in Fig. 7-4. GT-2B terminates at 2707 m (8882 ft) and EE-1 at 3050 m (10 007 ft), a greater depth than represented in the figure. Both wells penetrate basement rocks at approximately 732 m (2400 ft) and terminate in biotite granodiorite. Four fractures in GT-2B account for 90% of production. In order of decreasing flow, the fractures are located at 2661 m (35%), 2719 m (25%), 2687 m (20%), and 2706 m (12%). GT-2B is cased to 2603 m (8541 ft) and openhole from there to the bottom. The bottom of the casing in EE-1 is at 2919 m (9578 ft), but 90% of the flow moves behind casing in a poorly cemented region from 2919 to 2759 m (9578 to 9050 ft) where it enters the reservoir through a hydraulic fracture. Water then moves vertically 64 m (210 ft) before the lowest entry point in GT-2B is reached. Several other fractures over the depth interval of 2134-2941 m (7000-9650 ft) accepted water on pressurization of EE-1, but this accounts for only a small percentage of the injection into the reservoir. The injection zone at 2941 m (9650 ft) accepts up to 5% of the flow.

A synthesis of geophysical logging data, core studies, and pertinent results of the pressure, temperature, and flow measurements acquired to date at Fenton Hill are presented in Fig. 7-5. Shown is the projection of the four wellbore sections onto a northeasterly striking vertical plane. Bulk rock properties of

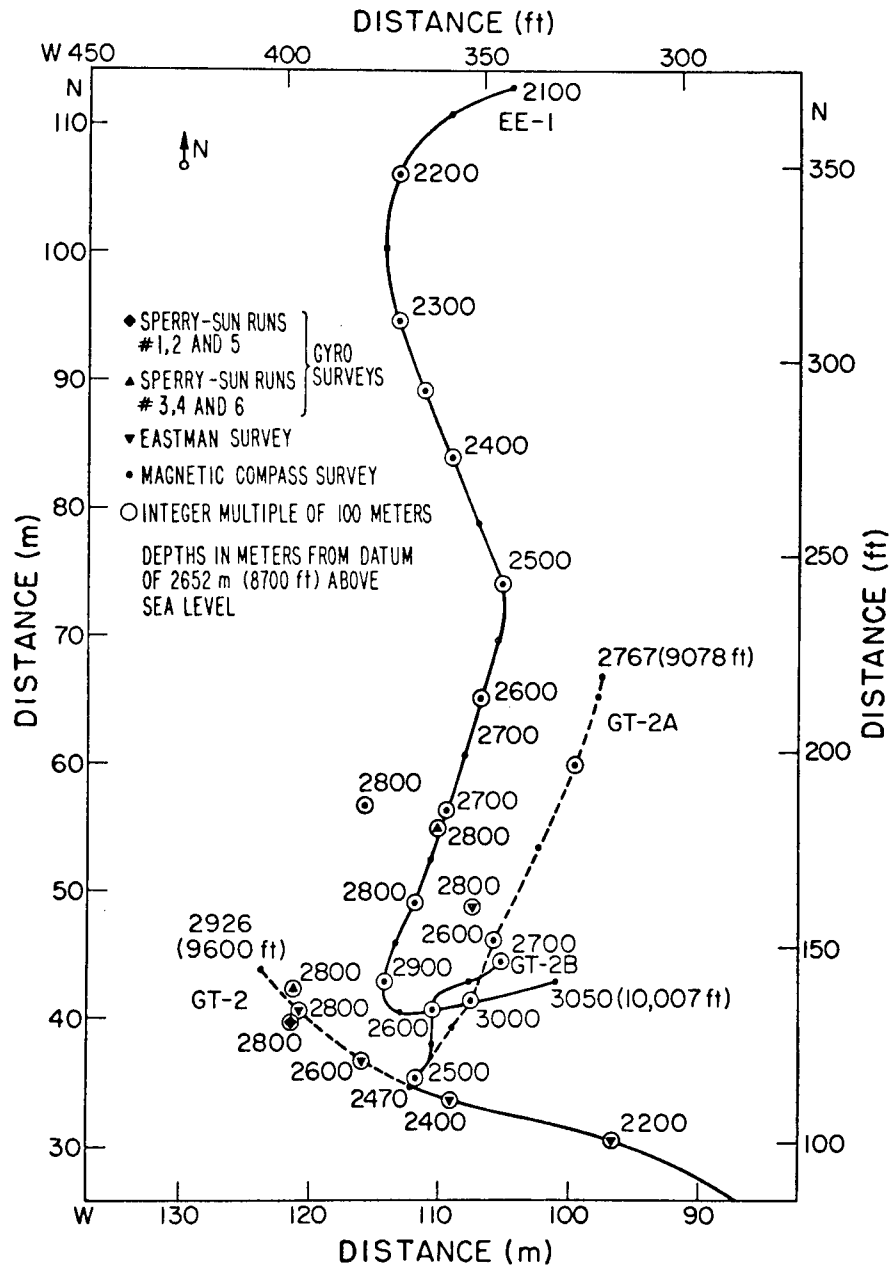


Fig. 7-1.  
Plan view projections of the lower sections of the GT-2 and EE-1 wellbores.

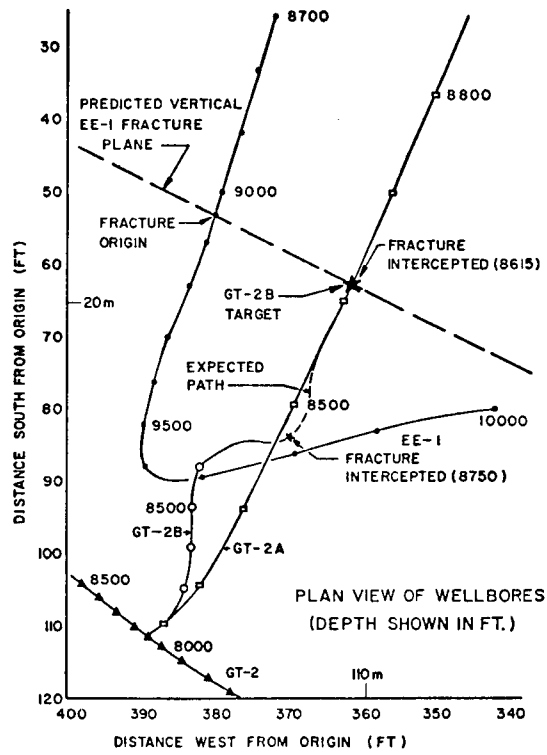


Fig. 7-2.  
Enlarged plan view of the lower sections of the GT-2 and EE-1 wellbores.

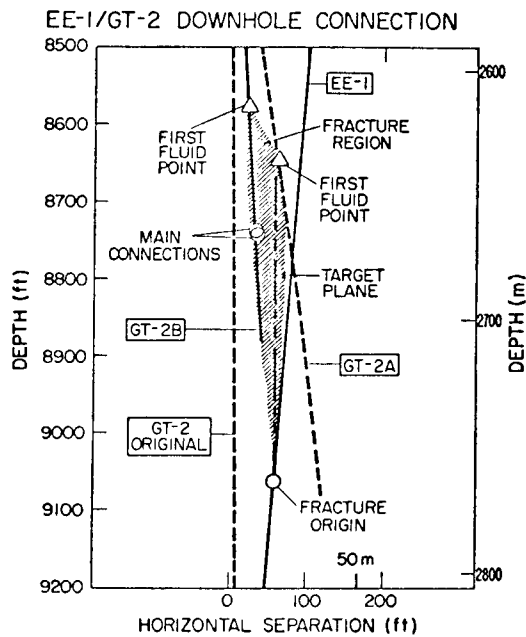


Fig. 7-3.  
Elevation view of the GT-2 and EE-1 wellbores parallel to the NW-SE direction.

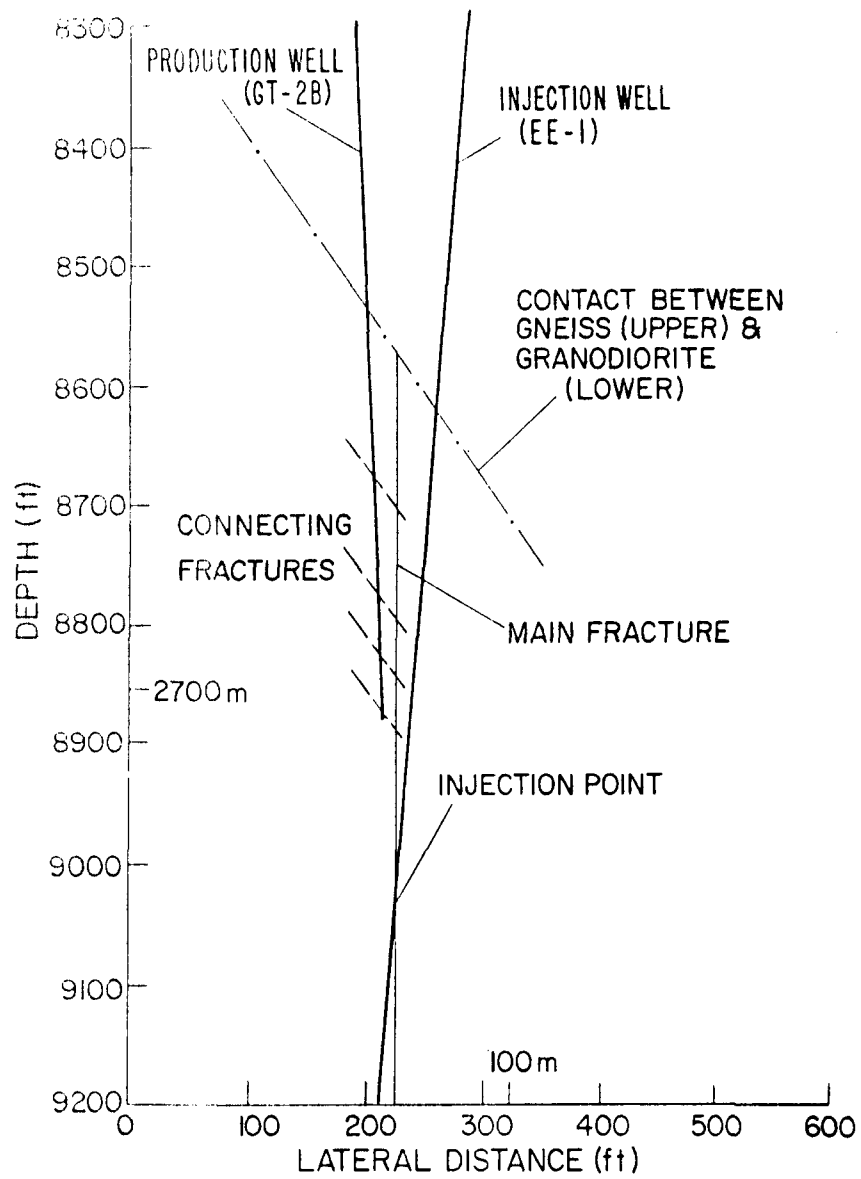


Fig. 7-4.  
Simplified schematic of the GT-2B/EE-1 connected fracture system.

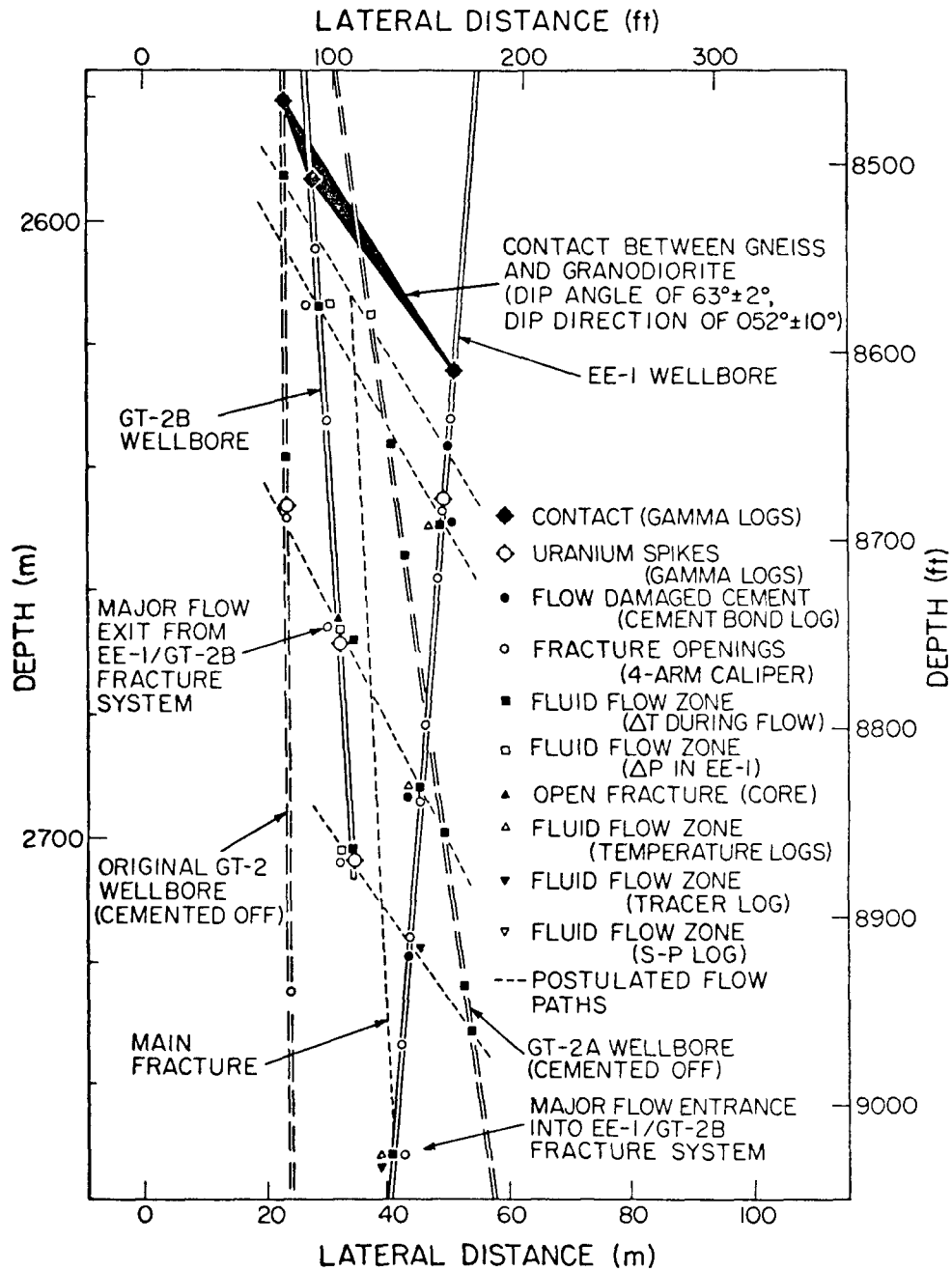


Fig. 7-5.  
Elevation view showing GT-2, GT-2A, GT-2B, and EE-1 wellbores with geophysical information shown and the fracture model depicted with dotted lines.

the reservoir have been determined through pressure and flow testing, analysis of cores,<sup>19</sup> and geophysical logs.<sup>2</sup> The properties of individual fractures accepting or producing fluids were established, where and when possible, in terms of flow fraction, temperature, trace of wellbore intersection, and probable secondary mineralization.

The principal geologic feature in the reservoir is a contact between granitic gneiss and granodiorite lithology, which effectively caps the region of heat extraction. Hydraulic stimulation of the reservoir has resulted in gaining access to a system of at least two definable sets of previously existing fractures for use as heat exchange surfaces. The first may consist of vertical fractures that are parallel, uniformly spaced ( $\sim 10$  m), and northwesterly striking. They are characterized by low flow impedance at intersections with wellbores as well as low internal impedance due to self propping. Injection into the reservoir is principally through an incompletely isolated member of this set. A second set of fractures, as steep as  $60^\circ$ , are roughly coplanar with the gneiss-granodiorite contact and have an order of magnitude higher impedance to flow. GT-2B production comes from several of these high angle fractures. Very little is known about the spatial relationships between fractures not penetrated during drilling because of the inherent complexity of the reservoir; therefore details of the flow between wells in the fracture system can only be inferred. The path for the current production (Fig. 7-5, dashed lines) satisfies established criteria. In addition, temperature logs, fluid geochemistry, and fluid residence time studies suggest that a secondary flow path exists, with a possible entrance passing through a hydraulic fracture originating at 2940 m (9650 ft) in EE-1. This secondary flow path may provide a source of hot fluid, which contains a relatively high concentration of silica, chloride, bicarbonate, and radon thus explaining the rise in concentration observed during the 75-day run. Because the final silica concentration was saturated with quartz at approximately 185 to  $200^\circ\text{C}$ , fluid of at least this temperature must be entering the GT-2B wellbore. The high chloride concentration suggests a mechanism of pore fluid displacement and mixing before entering the GT-2B wellbore, because the origin of chloride is most likely not caused by dissolution of the rock.

Although a model that uniquely describes all facets of the data from Phase I and earlier experiments cannot be specified at this time, the results of the 75-day test have provided an extremely valuable experience with a prototype hot

dry rock system in low permeability rock, and it will facilitate expansion to a much larger capacity Phase II system.

The main observations, in fact, suggest a very optimistic future for hot dry rock. Reservoir flow impedance decreased from an initial 16 bar-s/ℓ (15 psi-gpm) to about 3.3 bar-s/ℓ (3 psi/gpm) by both continuous and discontinuous drops in impedance with an increase in reservoir volume as shown by tracer studies. Permeation water-loss rate quickly decreased to less than 0.19 ℓ/s (3 gpm) which is <1-1/2% of circulation rate and could be modeled by one-dimensional transient flow in a homogeneous reservoir. Geofluid chemistry is most acceptable, with 1550-2000 ppm total dissolved solids and no evidence of scaling in main flow passages in the reservoir or surface equipment. Thermal drawdown for the first small prototype system followed the theoretical prediction for an 8000-m<sup>2</sup> system. The surface facilities and data acquisition systems proved sufficient for a short-term test. There is no evidence of any measurable seismicity induced at the site.

From early experience at Fenton Hill, we thought that flow impedance was going to present a formidable problem because high mass flows of >9.5 ℓ/s (>150 gpm) were not possible with impedances of 11 bar-s/ℓ (10 psi/gpm) and a formation breakdown pressure of 100 bar (~1500 psi). The 75-day test demonstrated that extended periods of fluid pressurization could significantly lower the impedance without an increase in flow short-circuiting. The dye tracer indicated that well-mixed flow occurs in the fractured region and that the average size or volume of the system increased. Periodic initiation and activation of new flow paths from pore-pressure-induced cracking or thermal stress cracking or both may have caused the observed decline in impedance as well as the change in the apparent system volume. Whatever the mechanism, the reservoir has responded in a dynamic manner. The impedance changes did not however represent significant changes in either the effective heat transfer or effective fluid-permeating area. Thermal drawdown and fluid permeation were adequately modeled with one-dimensional heat and fluid diffusion into the rock from the two-dimensional pressurized fracture of fixed area. Because permeating areas inferred from an acceptable range of average compressibilities and permeabilities for the reservoir are much larger than the 8000-m<sup>2</sup> effective heat transfer area and because flow communication was observed from a hotter region of the reservoir, the potential heat exchange area must be considerably greater.

Further tests of the present reservoir will be aimed at characterizing methods for activation of this larger region of hot rock.

## ACKNOWLEDGMENTS

The authors would like to acknowledge M. Brown, G. Nunz, and the late A. Blair for their helpful suggestions and comments in reviewing the manuscript. B. Ramsay and D. Elsner are thanked for their aid in the preparation.

## REFERENCES

1. H. D. Murphy, "Thermal Stress Cracking and the Enhancement of Heat Extraction from Fractured Geothermal Reservoirs," Los Alamos Scientific Laboratory report LA-7235-MS (April 1978).
2. LASL HDR Project Staff, "Hot Dry Rock Geothermal Energy Development Project - Annual Report FY 1977," Los Alamos Scientific Laboratory report LA-7109-PR (February 1978).
3. H. D. Murphy and R. M. Potter, "Fracture and Borehole Mapping Technique Development," in Hot Dry Rock Geothermal Energy Development Project - Annual Report FY 1977, (Los Alamos Scientific Laboratory report LA-7109-PR February 1978), pp. 126-128.
4. R. D. McFarland and H. D. Murphy, "Extracting Energy from Hydraulically Fractured Geothermal Reservoirs," Proceedings of 11th Intersociety Energy Conversion Engineering Conference, State Line, Nevada, 1976.
5. F. H. Harlow and W. E. Pracht, "A Theoretical Study of Geothermal Energy Extraction," Journ. Geophy. Res., 77, (35), 7038 (1972).
6. R. G. Lawton, "WELLBOR - Wellbore Heat Transmission Code," unpublished results (1976).
7. H. N. Fisher, "An Interpretation of the Pressure and Flow Data for Two Fractures of the Los Alamos Hot Dry Rock (HDR) Geothermal System," Proc. of the 18th U. S. Symposium on Rock Mechanics, Keystone, Colorado, June 22, 1977.
8. R. G. Lawton, "The AYER Heat Conduction Computer Program," Los Alamos Scientific Laboratory report LA-5613-MS (May 1974).
9. R. M. Garrels and C. L. Christ, Solutions, Minerals and Equilibria (Harper and Row, New York, 1965), pp. 403-428.
10. G. L. Frear and J. Johnston, J. Am. Chem. Soc. 51, 2082-2093, in Solubilities of Inorganic and Metal Organic Compounds, Vol. I, 4th ed. (A. Siedell, Am. Chem. Soc., Washington, D. C., 1958), p. 539.
11. R. W. Charles, "Experimental Geothermal Loop: I, 295°C Study," Los Alamos Scientific Laboratory report LA-7334-MS (July 1978).
12. W. A. Deer, R. A. Howie, and J. Zussman, Introduction to Rock Forming Minerals (John Wiley and Sons, Inc., New York, 1966), pp. 400-401.

13. J. Johnston and E. D. Williamson, J. Am. Chem Soc. 38, 975-983, in Solubilities of Inorganic and Metal Organic Compounds, Vol. I, 4th ed. (A. Siedell, Am. Chem. Soc., Washington, D. C., 1958).
14. R. Gunnink and J. B. Niday, "Computerized Quantitative Analyses by Gamma-Ray Spectrometry," Lawrence Livermore Laboratory report UCRL-51061 (March 1972).
15. J. N. Andrews and D. F. Wood, "Mechanism of Radon Release in Rock Matrices and Entry into Groundwaters," Inst. of Mining and Metallurgy Trans/Sec. B, 81, No. 792 (November 1972).
16. P. Kruger, G. Warren, and B. D. Honeyman, "Radon as an Internal Tracer in Geothermal Reservoirs," paper presented at 3rd International Conf. on Nuclear Methods in Environmental and Energy Research, ANS/ERDA, Univ. of Missouri (October 1977).
17. A. Stoker and P. Kruger, "Radon in Geothermal Reservoirs," in Proc. Second United Nations Symp. on the Development and Use of Geothermal Resources San Francisco, California, 1975.
18. A. S. Rogers, "Physical Behavior and Geologic Control of Radon in Mountain Streams," USGS Bulletin 1052-E (1958).
19. A. W. Laughlin and A. Eddy, "Petrography and Geochemistry of Precambrian Rocks from GT-2 and EE-1," Los Alamos Scientific Laboratory report LA-6930-MS (August 1977).

## APPENDIX A

### FRACTURE OPENING BY COOLING

#### A. INTRODUCTION

When a fracture is cooled, thermal stress cracking normal to the fracture face will probably occur. In addition, there is a shrinkage of the rock normal to the fracture face which produces no stress over most of the fracture face because it is free to move.

If the fracture is unpressurized, then after some long time, proportional to the fracture radius, this cooling will cause the fracture to open. If however, the pressure is high enough to open the fracture, its width will begin to increase immediately. The time required to open the fracture is calculated in this appendix under the following assumptions:

- (1) The fracture is penny shaped.
- (2) Heat is withdrawn at the same rate over the entire fracture surface.
- (3) The heat flow is considered to be one-dimensional, normal to the fracture face.
- (4) The rock is impermeable.

#### A.1 Thermal Contraction of Rock Face

When rock is cooled under these assumptions, the contraction of the rock face is proportional to the total heat withdrawn. Let  $\dot{q}(x,t)$  be the net rate of power extraction per unit volume at time,  $t$ , at a distance  $x$  into the rock from the fracture face. The change in temperature of an element of unit area and thickness  $dx$  about  $x$ , at time  $t$ , is

$$- \frac{1}{\rho c} \int_0^t \dot{q} dt ,$$

the shrinkage of  $dx$  is

$$\frac{\delta dx}{dx} = \frac{\alpha}{\rho c} \int_0^t \dot{q} dt ,$$

and the total shrinkage from 0 to  $x$  is

$$\int_0^x \delta dx = - \frac{\alpha}{\rho c} \int_0^x \int_0^t \dot{q} dt dx = - \frac{\alpha Q}{\rho c} \quad (A-1)$$

where, if  $x$  is sufficiently large,  $Q$  is the total energy extracted per unit area of the fracture face. Thus, if energy  $Q$  is withdrawn per unit area, the thermal contraction of the rock face is

$$\delta W = - \frac{\alpha Q}{\rho c} \quad (A-2)$$

where  $\alpha$  is the thermal expansion coefficient of the rock and  $\rho$  and  $c$  are its density and specific heat, respectively.

The equations of elasticity are independent of the sign of the stress, and since the deflection of the walls of the pillbox-shaped cavity in Fig. A-1 will differ only infinitesimally from that of the penny-shaped fracture when  $P > \sigma$  the theory of the penny-shaped fracture<sup>1</sup> may be applied to calculate the inward deflection of the wall when  $P < \sigma$ . This deflection, which must be overcome by thermal contraction before the fracture opens is  $b = 4 (\sigma - P)(1 - \nu^2)R / (\pi E)$ , where  $P$  is the internal pressure,  $\sigma$  the normal earth stress,  $\nu$  is Poisson's ratio,  $R$  the radius, and  $E$ , Young's modulus. A fracture will begin to open when

$$- \frac{\alpha Q}{\rho c} + \frac{4(\sigma - P)(1 - \nu^2)R}{\pi E} = 0 \quad (A-3)$$

Some typical values of these constants for granite are as follows ( $E$ ,  $\nu$ , and  $\rho$  are typical acoustic log values in EE-1 and GT-2;  $\alpha$  and  $C$  are taken from Clark<sup>2</sup>):

$$\begin{aligned} E &= 8 \times 10^4 \text{ MPa} \\ \alpha &= 8 \times 10^{-6} \text{ K}^{-1} \\ \nu &= 0.25 \\ c &= 1000 \text{ J kg}^{-1} \text{ K}^{-1} \\ \rho &= 2700 \text{ kgm}^{-3} \end{aligned}$$

Using these values, (A-3) becomes

$$Q = 5.04 (\sigma - P)R \quad (A-4)$$

If cold water enters near the center of the fracture, at temperature  $T_w$ , and the rock temperature is  $T_R$ , then a reasonable approximation for  $Q$  is

$$Q = \frac{2\lambda(T_R - T_w)}{\sqrt{\pi\kappa}} \sqrt{t} \quad (A-5)$$

from the standard formula for linear heat diffusion with a step function change in temperature. The thermal conductivity  $\lambda$  of granite is near 2.7 w/m-k,<sup>3</sup> so using the definition  $\kappa = \frac{\lambda}{\rho C}$ , with the values of  $\rho$  and  $C$  given above, Eq. (A-5) becomes:

$$A = 2725 (T_R - T_w) \sqrt{t}. \quad (A-6)$$

We may equate Eqs. (A-4) and (A-6) and solve for the ratio  $R/(T_R - T_w)$  vs  $(\sigma - P)$  at fixed  $t$ . Some results are given in Fig. A-2. Since both  $R$  and  $T_R - T_w$  are of the order 100, the most interesting times are those with  $R/(T_R - T_w) \approx 1$ . If  $P \approx \sigma$  (i.e.,  $\sigma - P < 10^5$  Pa) cooling helps on the first day. If  $P \approx 0$  (i.e.,  $\sigma - P > 10^7$  Pa) it takes  $\sim 5$  years to open the fracture by cooling.

#### REFERENCES

1. I. N. Sneddon, "The Distribution of Stress in the Neighborhood of a Crack in an Elastic Solid," Proc. Roy. Soc. London, A187 (1945) p. 229.
2. S. P. Clark, "Rock Properties Related to Rapid Excavation," in Handbook of Physical Constants PB 184, 767.
3. W. L. Sibbitt, J. G. Dodson, and J. W. Tester, "Thermal Conductivity of Crystalline Rocks Associated with Energy Extraction from Hot Dry Rock Geothermal Systems," Jour. Geophys. Research (to be published 1979).

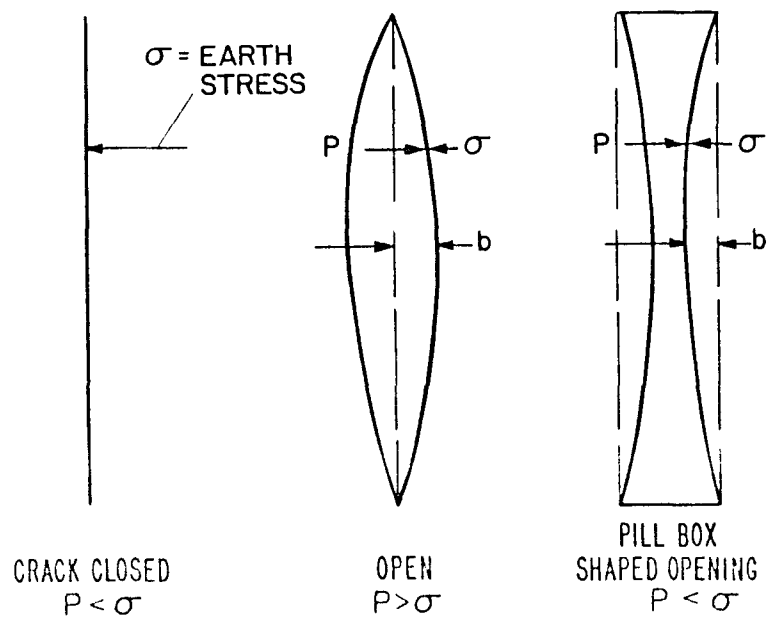


Fig. A-1.  
Cavity geometries.

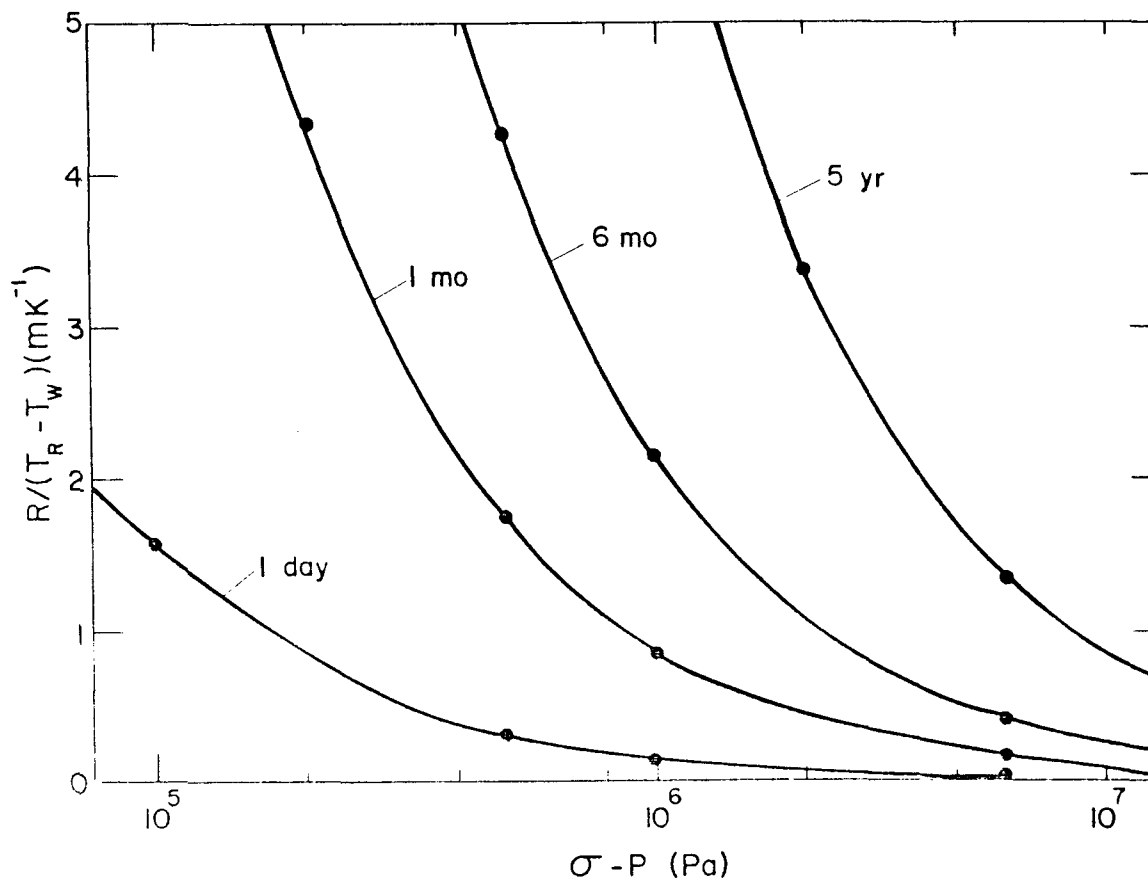


Fig. A-2.  
Curves for deriving time for unpressurized fracture to open by cooling.

## APPENDIX B

### THERMAL EFFECTS IN SPHERICALLY COOLED REGIONS

#### B. INTRODUCTION

Appendix A discussed the opening of a cooled and pressurized penny-shaped crack. This appendix gives an exact solution for the onset of thermal stress cracking when a spherical portion of a large homogeneous mass of rock is cooled below the surrounding rock temperature by an amount  $|\Delta T|$ , and pressurized above the pressure of the surrounding rock by an amount  $P - P_0$  where  $P_0$  is the pore pressure.

As before in Appendix A,  $E$  is Young's modulus,  $\nu$  is Poisson's ratio,  $\sigma$  is a stress in the rock matrix, positive in compression, and  $\alpha$  is the thermal expansion coefficient of the rock.

#### A.1 Displacement at $r = a$

It is convenient to consider the mass of rock in two parts. The external rock may be modeled as a very thick-walled hollow sphere of internal radius  $a$ , with a normal stress  $\sigma$  on the outside and normal stress  $\sigma_1$  on the inside. The remainder of the rock may be treated as a homogeneous sphere of radius  $a$ , subjected to a normal stress  $\sigma_1$  on its surface and cooled by an amount  $|\Delta T|$ . By requiring the displacements  $\delta a$  for the external and internal rock to be equal, we may solve for  $\sigma_1$  for any given  $|\Delta T|$ .

The displacement of the inner surface of the external rock is given by the expression<sup>1</sup>

$$\delta a = \frac{-\sigma(1-2\nu)}{E} a + \frac{(1+\nu)(\sigma_1-\sigma)}{2E} a \quad . \quad (B-1)$$

The displacement of the surface of the inner sphere arising from the normal stress  $\sigma_1$  is easily derived from the compressibility,

$$\beta = \frac{1}{K} = \frac{3(1-2\nu)}{E} - \frac{\delta V}{\sigma_1 V} \approx - \frac{3\delta a}{\sigma_1 a} \quad ,$$

so

$$\delta a = -\sigma_1 \frac{1-2\nu}{E} a$$

from compression. The displacement due to cooling is  $-\delta a |\Delta T|$ , so the total displacement is

$$\delta a = -\sigma_1 \frac{1-2\nu}{E} a - \alpha a |\Delta T| \quad . \quad (B-2)$$

By equating (B-1) and (B-2), we have

$$\sigma - \sigma_1 = \frac{2}{3} \frac{\alpha E}{1-\nu} |\Delta T| \quad . \quad (B-3)$$

In this expression,  $\sigma_1$  represents the stress acting on the rock matrix inside the cooled region. To open an existing fracture under this stress, an internal pressure  $P = \sigma_1$  must be applied to the fracture. If a uniform pore fluid pressure  $P_0$  is present throughout the rock, then  $P - P_0$  must equal  $\sigma_1$  in order to open the fracture, i.e.,  $P = \sigma_1 + P_0 = S_1$ , where  $S_1$  is the total stress inside the cooled region. The expression, Eq. (B-3), may also be written as,

$$\sigma + P_0 - (\sigma_1 + P_0) = S - S_1 = \frac{2}{3} \frac{\alpha E}{1-\nu} |\Delta T| \quad . \quad (B-4)$$

In conclusion, the requirement for a preexisting fracture to open in a region where the fluid pressure is  $P$  is

$$P + \frac{2}{3} \frac{\alpha E}{1-\nu} |\Delta T| = S \quad ,$$

the total stress in the surrounding rock. In a rock with many weakly cemented fractures, this condition may be considered as describing the onset of thermal stress cracking.

#### REFERENCES

1. Raymond J. Roark, Formulas for Stress and Strain (McGraw-Hill, New York, 1965), p. 308.

Printed in the United States of America. Available from  
National Technical Information Service  
U.S. Department of Commerce  
5285 Port Royal Road  
Springfield, VA 22161

Microfiche \$3.00

001-025	4.00	126-150	7.25	251-275	10.75	376-400	13.00	501-525	15.25
026-050	4.50	151-175	8.00	276-300	11.00	401-425	13.25	526-550	15.50
051-075	5.25	176-200	9.00	301-325	11.75	426-450	14.00	551-575	16.25
076-100	6.00	201-225	9.25	326-350	12.00	451-475	14.50	576-600	16.50
101-125	6.50	226-250	9.50	351-375	12.50	476-500	15.00	601-up	

Note: Add \$2.50 for each additional 100-page increment from 601 pages up.

PERMITTEE NAME/ADDRESS (include Facility Name/ Location) **DEPT OF ENERGY**

NAME **MR HAROLD E VALENCIA-AREA MGR**  
 ADDRESS **LOS ALAMOS AREA OFFICE**  
**LOS ALAMOS NM 87544**

FACILITY **R**  
 LOCATION

NATIONAL POLLUTANT DISCHARGE ELIMINATION SYSTEM (NPDES) DISCHARGE MONITORING REPORT (DMR) (17-19)

PERMIT NUMBER **NM0028576**

DISCHARGE NUMBER **001**

Fenton Hill

MONITORING PERIOD					
YEAR	MO	DAY	YEAR	MO	DAY
82	04	01	82	04	30
FROM			TO		
82 04 01			82 04 30		

NOTE: Read instructions before completing this form.

PARAMETER (32-37)	SAMPLE MEASUREMENT PERMIT REQUIREMENT	QUANTITY OR LOADING (46-53)			QUALITY OR CONCENTRATION (54-61)			UNITS	NO. EX (62-63)	FREQUENCY OF ANALYSIS (64-68)	SAMPLE TYPE (69-70)
		AVERAGE	MAXIMUM	UNITS	MINIMUM	AVERAGE	MAXIMUM				
FLOW										8/30	METERED
PH					8.4					8/30	GRAB
BORON						2.53	2.8			8/30	GRAB
ARSENIC						0.0227	0.0260			8/30	GRAB
CADMIUM						0.0009	0.0019			8/30	GRAB
FLUORIDE						1.32	1.48			8/30	GRAB
LITHIUM						0.285	0.303			8/30	GRAB

NAME/TITLE PRINCIPAL EXECUTIVE OFFICER

**WILLIAM CRISMON**

THIS DOCUMENT IS SIGNED WITH RECOGNITION THAT KNOWINGLY MAKING A FALSE CERTIFICATION ON THIS REPORT OR SUPPORTING DOCUMENTS OR INTENTIONALLY TAMPERING WITH ANY MONITORING DEVICE OR METHOD ARE CRIMINAL OFFENSES. SEE 18 U.S.C. § 1001 AND 33 U.S.C. § 1319. (Penalty: Imprisonment of between 6 months and 5 years.)

*William Crismon*  
 SIGNATURE OF PRINCIPAL EXECUTIVE OFFICER OR AUTHORIZED AGENT

TELEPHONE **505 667-5288** DATE **82 07 23**

THERE WERE 8 DISCHARGES DURING THE MONTH OF APRIL

PERMITTEE NAME/ADDRESS (include Facility Name/Location if different)

NATIONAL POLLUTANT DISCHARGE ELIMINATION SYSTEM (NPDES) DISCHARGE MONITORING REPORT (DMR)

Form Approved OMB No. 158-R0073

NAME: WILLIAM CRISMON  
 ADDRESS: 1001 FENSON BLVD  
 FACILITY: FENSON BLVD  
 LOCATION: FENSON BLVD

PERMIT NUMBER: MD000070  
 DISCHARGE NUMBER: 001

MONITORING PERIOD					
YEAR	MO	DAY	YEAR	MO	DAY
11	11	01	11	05	03

NOTE: Read instructions before completing this form.

PARAMETER (2-37)	SAMPLE MEASUREMENT PERMIT REQUIREMENT	QUANTITY OR LOADING (3 Cont Only) (46-53)			QUALITY OR CONCENTRATION (46-53)			UNITS	NO. EX (62-63)	FREQUENCY ANALYSIS (64-68)	SAMPLE TYPE (69-70)
		AVERAGE	MAXIMUM	UNITS	MINIMUM	AVERAGE	MAXIMUM				
FLUORIDE	SAMPLE MEASUREMENT PERMIT REQUIREMENT					0.013	0.013	0.013	1/30	1/30	MG/L
BORON	SAMPLE MEASUREMENT PERMIT REQUIREMENT					6.7	6.7	6.7	1/30	1/30	MG/L
ARSENIC	SAMPLE MEASUREMENT PERMIT REQUIREMENT					6.4	6.4	6.4	1/30	1/30	MG/L
ZINC	SAMPLE MEASUREMENT PERMIT REQUIREMENT					0.13	0.13	0.13	1/30	1/30	MG/L
BRIDE	SAMPLE MEASUREMENT PERMIT REQUIREMENT					1.14	1.14	1.14	1/30	1/30	MG/L
LITHIUM	SAMPLE MEASUREMENT PERMIT REQUIREMENT					4.0	4.0	4.0	1/30	1/30	MG/L

NAME/TITLE PRINCIPAL EXECUTIVE OFFICER: WILLIAM CRISMON

COMMENT AND EXPLANATION OF ANY VIOLATIONS (reference all attachments here)

THIS DOCUMENT IS SIGNED WITH RECOGNITION THAT KNOWINGLY MAKING A FALSE CERTIFICATION ON THIS REPORT OR SUPPORTING DOCUMENTS OR INTENTIONALLY TAMPERING WITH ANY MONITORING DEVICE OR METHOD ARE CRIMINAL OFFENSES. SEE 18 U.S.C. § 1001 AND 33 U.S.C. § 1319. (Penalties under these statutes may be fines up to \$10,000 and/or imprisonment of between 6 months and 5 years.)

SIGNATURE OF PRINCIPAL EXECUTIVE OFFICER OR AUTHORIZED AGENT: [Signature]

TELEPHONE: [Blank] DATE: [Blank]

AREA CODE: [Blank] NUMBER: [Blank] YEAR: [Blank] MO: [Blank] DAY: [Blank]

PERMITTEE NAME/ADDRESS (include Facility Name/ Location if different)  
 NAME  
 ADDRESS  
 LOCATION

MR. KENNETH H. BEZZEL-AREA FOR  
 LOS ALAMOS AREA OFFICE  
 105 ALAMOS NW 87544  
 LOS ALAMOS, NM 87544

NATIONAL POLLUTANT DISCHARGE ELIMINATION SYSTEM (NPDES)  
 DISCHARGE MONITORING REPORT (DMR)  
 (2-16)  
 (17-19)  
 (2-21)  
 (2-23)  
 (2-25)  
 (2-27)  
 (2-29)  
 (2-31)

MM028576  
 PERMIT NUMBER

001  
 DISCHARGE NUMBER

MONITORING PERIOD			
YEAR	MO	DAY	TH
81	09	01	RD
YEAR	MO	DAY	TH
81	09	30	RD

Fenton H111

NOTE: Read instructions before completing this form.

PARAMETER (3-37)	SAMPLE MEASUREMENT PERMIT REQUIREMENT	QUANTITY OR LOADING (3 Card Only) (4-53)		QUALITY OR CONCENTRATION (4-41)		UNITS	NO. OF ANALYSIS (6-48)	FREQUENCY OF SAMPLE TYPE (6-70)
		AVERAGE	MAXIMUM	MINIMUM	AVERAGE			
FLOW						80.0	80.0	1/30
						8.0	8.0	1/30
						8.0	8.0	1/30
						9.0	9.0	1/30
BORON						6.7	6.7	1/30
ARSENIC						5.4	5.4	1/30
CADMIUM						0.013	0.013	1/30
CHLORIDE						1.14	1.14	1/30
LITHIUM						4.8	4.8	1/30

NAME/TITLE-PRINCIPAL EXECUTIVE OFFICER  
 WILLIAM CRISMON  
 TYPED OR PRINTED

THIS DOCUMENT IS SIGNED WITH RECOGNITION THAT KNOWINGLY MAKING A FALSE CERTIFICATION ON THIS REPORT OR SUPPORTING DOCUMENTS OR INTENTIONALLY TAMPERING WITH ANY MONITORING DEVICE OR METHOD ARE CRIMINAL OFFENSES. SEE 18 U.S.C. § 1001 AND 33 U.S.C. § 1319. (Penalties under these statutes may be fines up to \$10,000 and/or imprisonment of between 6 months and 5 years.)

SIGNATURE OF PRINCIPAL EXECUTIVE OFFICER OR AUTHORIZED AGENT

TELEPHONE NUMBER

AREA CODE

CARRIER NUMBER

DATE

TIME

DAY

PERMIT NAME/ADDRESS (include Facility Name/Location if different)  
 DEPT OF ENERGY

NATIONAL POLLUTANT DISCHARGE ELIMINATION SYSTEM (NPDES)  
 DISCHARGE MONITORING REPORT (DMR)

Form Approved  
 OMB No. 158-R0073

NAME: MR KENNETH R BRAZILL-AREA MGR  
 ADDRESS: LOS ALAMOS AREA OFFICE  
 LOS ALAMOS NM 87544  
 FACILITY: FENTON HILL  
 LOCATION: R

PERMIT NUMBER: NM0028576

DISCHARGE NUMBER: 001

FENTON HILL

MONITORING PERIOD			DISCHARGE PERIOD		
YEAR	MO	DAY	YEAR	MO	DAY
80	12	01	80	12	31

NOTE: Read instructions before completing this form.

PARAMETER (32-37)	SAMPLE MEASUREMENT	PERMIT REQUIREMENT	QUANTITY OR LOADING (3 Card Only) (46-53)			QUALITY OR CONCENTRATION (4 Card Only) (38-45)			UNITS	NO. EX (62-63)	FREQUENCY OF ANALYSIS (64-68)	SAMPLE TYPE (69-70)
			AVERAGE	MAXIMUM	UNITS	MINIMUM	AVERAGE	MAXIMUM				
FLOW	SAMPLE MEASUREMENT	PERMIT REQUIREMENT										
	PERMIT REQUIREMENT											
PH	SAMPLE MEASUREMENT	PERMIT REQUIREMENT										
	PERMIT REQUIREMENT											
BOPC	SAMPLE MEASUREMENT	PERMIT REQUIREMENT										
	PERMIT REQUIREMENT											
ARSENIC	SAMPLE MEASUREMENT	PERMIT REQUIREMENT										
	PERMIT REQUIREMENT											
CADMIUM	SAMPLE MEASUREMENT	PERMIT REQUIREMENT										
	PERMIT REQUIREMENT											
FLUORIDE	SAMPLE MEASUREMENT	PERMIT REQUIREMENT										
	PERMIT REQUIREMENT											
THIUM	SAMPLE MEASUREMENT	PERMIT REQUIREMENT										
	PERMIT REQUIREMENT											

NAME/TITLE PRINCIPAL EXECUTIVE OFFICER

I CERTIFY UNDER PENALTY OF LAW THAT I HAVE PERSONALLY EXAMINED AND AM FAMILIAR WITH THE INFORMATION SUBMITTED HEREIN AND BASED ON MY INQUIRY OF THOSE INDIVIDUALS IMMEDIATELY RESPONSIBLE FOR OBTAINING THE INFORMATION, I BELIEVE THE SUBMITTED INFORMATION IS TRUE AND ACCURATE AND I STATE THAT THERE ARE NO SIGNIFICANT PENALTIES FOR SUBMITTING FALSE INFORMATION INCLUDING THE POSSIBILITY OF FINE AND IMPRISONMENT. SEE 19 U.S.C. § 1001 AND 33 U.S.C. § 1319. (Penalties under these statutes may include fines up to \$10,000 and/or maximum imprisonment of between 6 months and 5 years.)

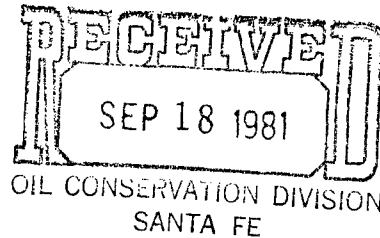
SIGNATURE OF PRINCIPAL EXECUTIVE OFFICER OR AUTHORIZED AGENT: [Signature]  
 TELEPHONE: 505 667-5288  
 AREA CODE: 505  
 NUMBER: 667-5288  
 DATE: 12/31/80



SEP 17 1981

Oscar

Department of Energy  
Albuquerque Operations  
Los Alamos Area Office  
Los Alamos, New Mexico 87544



Mr. Joe Ramey  
State Petroleum Engineer  
Oil Conservation Division  
P. O. Box 288  
Santa Fe, N. M. 87501

Dear Mr. Ramey:

During the past six months Mr. Wally McCorkle, of the Los Alamos National Laboratory staff, has had several conversations with Mr. Nutter and Mr. Ulvog, of your staff, concerning the Laboratory's Hot Dry Rock (HDR) Facility at Fenton Hill. The Department of Energy (DOE) has a National Pollutant Discharge Elimination System (NPDES) Permit #NMO028576 issued by the Environmental Protection Agency (EPA), effective October 15, 1979, authorizing surface water discharges from the Fenton Hill site to Lake Fork Canyon.

As part of the State certification process, the Environmental Improvement Division (EID) required the NPDES permit to contain the following provision:

Quantity of discharge from the outfall point shall be controlled such that no effluent flow, whether alone or commingled with natural runoff, travels beyond the point where the Lake Fork Canyon Road crosses the watercourse receiving the effluent; this point is approximately one mile downstream from the outfall.

Your office was contacted at the direction of the EID as the result of Mr. McCorkle's request concerning specific effluent criteria. Your office was suggested as the appropriate contact point since the discharge is from an "energy production facility". Previous correspondence dated February 22, 1980, informed your office of our intent to construct a water storage facility at Fenton Hill. At that time we stated: "In connection with obtaining our NPDES permit, the EID staff toured Fenton Hill and indicated that NPDES activities did not require submission of a ground water discharge plan".

As requested by Mr. Nutter, enclosed is a copy of the NPDES permit and summaries of the monitoring data for 1979, 1980, and 1981. All four are included as attachments to this letter. The NPDES permit does not contain any numerical effluent limits but does require monitoring for arsenic, boron, cadmium, fluoride, and lithium each time a discharge occurs.

Mr. Joe Ramey

- 2 -

SEP 17 1981

We believe we have complied with all State and Federal environmental regulations regarding water discharges at Fenton Hill. All information and application forms submitted to the EPA have been submitted to the EID. In addition, your office is now included as part of the distribution list for all correspondence regarding environmental concerns at Fenton Hill. As stated in our February 22, 1980 letter, it is our understanding that the HDR activities do not require a ground water discharge plan.

Please advise this office of any requirements that the Oil Conservation Division has regarding the HDR experimental facility at Fenton Hill. You, or members of your staff, are most cordially invited to tour the Fenton Hill Facility. If additional information is needed or to arrange a tour, please contact Mr. William Crismon of my staff at 667-5288, or Mr. Wally McCorkle of the Laboratory staff at 667-7957. We are looking forward to hearing from you.

Sincerely,

  
Gary M. Granere  
Acting Area Manager

Attachments

cc:  
Mr. Joe Pierce, NMEID  
Santa Fe, NM, w/atts.  
Mr. Fred Humke, USEPA  
Dallas, TX, w/atts.

Permit No. NM0028576  
Application No. NM0028576

**AUTHORIZATION TO DISCHARGE UNDER THE  
NATIONAL POLLUTANT DISCHARGE ELIMINATION SYSTEM**

In compliance with the provisions of the Federal Water Pollution Control Act, as amended,  
(33 U.S.C. 1251 et. seq; the "Act"),

Department of Energy  
Los Alamos Area Office  
Los Alamos, New Mexico 87544

is authorized to discharge from a facility located at

TA-57 Geothermal Site  
Sandoval County, New Mexico

to receiving waters named

Lake Fork Canyon and thence  
to the Rio Grande River

in accordance with effluent limitations, monitoring requirements and other conditions set forth  
in Parts I, II, and III hereof.

This permit shall become effective on October 15, 1979

This permit and the authorization to discharge shall expire at midnight, June 30, 1983

Signed this 3rd day of May 1979

  
\_\_\_\_\_  
Diana Dutton  
Director  
Enforcement Division (6AE)

A-1

**EFFLUENT LIMITATIONS AND MONITORING REQUIREMENTS**

During the period beginning effective date and lasting through the expiration of this permit the permittee is authorized to discharge from outfall(s) serial number(s) 001, excess water from the hot rock experiment.

Such discharges shall be limited and monitored by the permittee as specified below:

Effluent Characteristic	Discharge Limitations			Monitoring Requirements		
	kg/day (lbs/day)			Measurement Frequency	Sample Type	
Flow-m <sup>3</sup> /Day (MGD)	Daily Avg	Daily Max	Daily Avg	Daily Max	Daily	Totalized
Arsenic	N/A	N/A	(*) * mg/l	(*) * mg/l	1/day**	Grab
Boron	N/A	N/A	* mg/l	* mg/l	1/day**	Grab
Cadmium	N/A	N/A	* mg/l	* mg/l	1/day**	Grab
Fluoride	N/A	N/A	* mg/l	* mg/l	1/day**	Grab
Lithium	N/A	N/A	* mg/l	* mg/l	1/day**	Grab

\*Report

\*\*During discharge

The pH shall not be less than 6.0 standard units nor greater than 9.0 standard units and shall be monitored 1/day\*\* by grab sample.

There shall be no discharge of floating solids or visible foam in other than trace amounts.

Samples taken in compliance with the monitoring requirements specified above shall be taken at the following location(s):  
At the point of discharge from the TA-57 Geothermal Site.

**B. SCHEDULE OF COMPLIANCE**

1. The permittee shall achieve compliance with the effluent limitations specified for discharges in accordance with the following schedule:

None.

2. No later than 14 calendar days following a date identified in the above schedule of compliance, the permittee shall submit either a report of progress or, in the case of specific actions being required by identified dates, a written notice of compliance or noncompliance. In the latter case, the notice shall include the cause of noncompliance, any remedial actions taken, and the probability of meeting the next scheduled requirement.

**C. MONITORING AND REPORTING****1. Representative Sampling**

Samples and measurements taken as required herein shall be representative of the volume and nature of the monitored discharge.

**2. Reporting**

Monitoring results obtained during the previous 3 months shall be summarized for each month and reported on a Discharge Monitoring Report Form (EPA No. 3320-1), postmarked no later than the 28th day of the month following the completed reporting period. The first report is due on January 28, 1980. Duplicate signed copies of these, and all other reports required herein, shall be submitted to the Regional Administrator and the State at the following addresses:

Diana Dutton, Director  
Enforcement Division (6AE)  
Environmental Protection Agency  
First International Building  
1201 Elm Street  
Dallas, Texas 75270

Ms. Maxine S. Goad, Program manager  
Permits & Regulations Unit  
Water Pollution Control Section  
New Mexico Environmental  
Improvement division  
P. O. Box 968  
Santa Fe, New Mexico 87503

**3. Definitions**

- a. The "daily average" discharge means the total discharge by weight during a calendar month divided by the number of days in the month that the production or commercial facility was operating. Where less than daily sampling is required by this permit, the daily average discharge shall be determined by the summation of all the measured daily discharges by weight divided by the number of days during the calendar month when the measurements were made.
- b. The "daily maximum" discharge means the total discharge by weight during any calendar day.

**4. Test Procedures**

Test procedures for the analysis of pollutants shall conform to regulations published pursuant to Section 304(g) of the Act, under which such procedures may be required.

**5. Recording of Results**

For each measurement or sample taken pursuant to the requirements of this permit, the permittee shall record the following information:

- a. The exact place, date, and time of sampling;
- b. The dates the analyses were performed;
- c. The person(s) who performed the analyses;

- d. The analytical techniques or methods used; and
- e. The results of all required analyses.

6. *Additional Monitoring by Permittee*

If the permittee monitors any pollutant at the location(s) designated herein more frequently than required by this permit, using approved analytical methods as specified above, the results of such monitoring shall be included in the calculation and reporting of the values required in the Discharge Monitoring Report Form (EPA No. 3320-1). Such increased frequency shall also be indicated.

7. *Records Retention*

All records and information resulting from the monitoring activities required by this permit including all records of analyses performed and calibration and maintenance of instrumentation and recordings from continuous monitoring instrumentation shall be retained for a minimum of three (3) years, or longer if requested by the Regional Administrator or the State water pollution control agency.

**A. MANAGEMENT REQUIREMENTS**

**1. *Change in Discharge***

All discharges authorized herein shall be consistent with the terms and conditions of this permit. The discharge of any pollutant identified in this permit more frequently than or at a level in excess of that authorized shall constitute a violation of the permit. Any anticipated facility expansions, production increases, or process modifications which will result in new, different, or increased discharges of pollutants must be reported by submission of a new NPDES application or, if such changes will not violate the effluent limitations specified in this permit, by notice to the permit issuing authority of such changes. Following such notice, the permit may be modified to specify and limit any pollutants not previously limited.

**2. *Noncompliance Notification***

If, for any reason, the permittee does not comply with or will be unable to comply with any daily maximum effluent limitation specified in this permit, the permittee shall provide the Regional Administrator and the State with the following information, in writing, within five (5) days of becoming aware of such condition:

- a. A description of the discharge and cause of noncompliance; and
- b. The period of noncompliance, including exact dates and times; or, if not corrected, the anticipated time the noncompliance is expected to continue, and steps being taken to reduce, eliminate and prevent recurrence of the noncomplying discharge.

**3. *Facilities Operation***

The permittee shall at all times maintain in good working order and operate as efficiently as possible all treatment or control facilities or systems installed or used by the permittee to achieve compliance with the terms and conditions of this permit.

**4. *Adverse Impact***

The permittee shall take all reasonable steps to minimize any adverse impact to navigable waters resulting from noncompliance with any effluent limitations specified in this permit, including such accelerated or additional monitoring as necessary to determine the nature and impact of the noncomplying discharge.

**5. *Bypassing***

Any diversion from or bypass of facilities necessary to maintain compliance with the terms and conditions of this permit is prohibited, except (i) where unavoidable to prevent loss of life or severe property damage, or (ii) where excessive storm drainage or runoff would damage any facilities necessary for compliance with the effluent limitations and prohibitions of this permit. The permittee shall promptly notify the Regional Administrator and the State in writing of each such diversion or bypass.

## 6. *Removed Substances*

Solids, sludges, filter backwash, or other pollutants removed in the course of treatment or control of wastewaters shall be disposed of in a manner such as to prevent any pollutant from such materials from entering navigable waters.

## 7. *Power Failures*

In order to maintain compliance with the effluent limitations and prohibitions of this permit, the permittee shall either:

- a. In accordance with the Schedule of Compliance contained in Part I, provide an alternative power source sufficient to operate the wastewater control facilities;

or, if such alternative power source is not in existence, and no date for its implementation appears in Part I,

- b. Halt, reduce or otherwise control production and/or all discharges upon the reduction, loss, or failure of the primary source of power to the wastewater control facilities.

## B. RESPONSIBILITIES

### 1. *Right of Entry*

The permittee shall allow the head of the State water pollution control agency, the Regional Administrator, and/or their authorized representatives, upon the presentation of credentials:

- a. To enter upon the permittee's premises where an effluent source is located or in which any records are required to be kept under the terms and conditions of this permit; and
- b. At reasonable times to have access to and copy any records required to be kept under the terms and conditions of this permit; to inspect any monitoring equipment or monitoring method required in this permit; and to sample any discharge of pollutants.

### 2. *Transfer of Ownership or Control*

In the event of any change in control or ownership of facilities from which the authorized discharges emanate, the permittee shall notify the succeeding owner or controller of the existence of this permit by letter, a copy of which shall be forwarded to the Regional Administrator and the State water pollution control agency.

### 3. *Availability of Reports*

Except for data determined to be confidential under Section 308 of the Act, all reports prepared in accordance with the terms of this permit shall be available for public

inspection at the offices of the State water pollution control agency and the Regional Administrator. As required by the Act, effluent data shall not be considered confidential. Knowingly making any false statement on any such report may result in the imposition of criminal penalties as provided for in Section 309 of the Act.

#### 4. *Permit Modification*

After notice and opportunity for a hearing, this permit may be modified, suspended, or revoked in whole or in part during its term for cause including, but not limited to, the following:

- a. Violation of any terms or conditions of this permit;
- b. Obtaining this permit by misrepresentation or failure to disclose fully all relevant facts; or
- c. A change in any condition that requires either a temporary or permanent reduction or elimination of the authorized discharge.

#### 5. *Toxic Pollutants*

Notwithstanding Part II, B-4 above, if a toxic effluent standard or prohibition (including any schedule of compliance specified in such effluent standard or prohibition) is established under Section 307(a) of the Act for a toxic pollutant which is present in the discharge and such standard or prohibition is more stringent than any limitation for such pollutant in this permit, this permit shall be revised or modified in accordance with the toxic effluent standard or prohibition and the permittee so notified.

#### 6. *Civil and Criminal Liability*

Except as provided in permit conditions on "Bypassing" (Part II, A-5) and "Power Failures" (Part II, A-7), nothing in this permit shall be construed to relieve the permittee from civil or criminal penalties for noncompliance.

#### 7. *Oil and Hazardous Substance Liability*

Nothing in this permit shall be construed to preclude the institution of any legal action or relieve the permittee from any responsibilities, liabilities, or penalties to which the permittee is or may be subject under Section 311 of the Act.

#### 8. *State Laws*

Nothing in this permit shall be construed to preclude the institution of any legal action or relieve the permittee from any responsibilities, liabilities, or penalties established pursuant to any applicable State law or regulation under authority preserved by Section 510 of the Act.

PART II

Page 9 of 9

Permit No. NM0028576

9. *Property Rights*

The issuance of this permit does not convey any property rights in either real or personal property, or any exclusive privileges, nor does it authorize any injury to private property or any invasion of personal rights, nor any infringement of Federal, State or local laws or regulations.

10. *Severability*

The provisions of this permit are severable, and if any provision of this permit, or the application of any provision of this permit to any circumstance, is held invalid, the application of such provision to other circumstances, and the remainder of this permit, shall not be affected thereby.

PART III

OTHER REQUIREMENTS

- A. The "daily average" concentration means the arithmetic average (weighted by flow value) of all the daily determinations of concentration made during a calendar month. Daily determinations of concentration made using a composite sample shall be the concentration of the composite sample. When grab samples are used, the daily determination of concentration shall be the arithmetic average (weighted by flow value) of all the samples collected during that calendar day.

The "daily maximum" concentration means the daily determination of concentration for any calendar day.

- B. Final definition of BAT limitations for renewal of this permit shall be subject to analysis of data reported under the DMR provisions of this permit, and subsequent regulations and guidelines which may be applicable.
- C. Quantity of discharge from the outfall point shall be controlled such that no effluent flow, whether alone or co-mingled with natural runoff, travels beyond the point where the Lake Fork Canyon Road crosses the watercourse receiving the effluent; this point is approximately one mile downstream from the outfall.

Samples Analyzed in Accordance with EPA Approved Methods  
 Results reported in mg/L  
 1979

8 Discharges                      8 Samples Analyzed

	<u>Min.</u>	<u>Max.</u>	<u>Aver</u>
5.0 Al	0.37	16.33	4.27
As	0.013	0.03	0.018
0.75 B	* 1.75	* 63.00	12.36 *
0.01 Ca	48.0	970.0	170.7
Cd	0.0004	0.0020	0.0012
250 Cl	110.0	* 2200.0	441.0 *
CO	ND*	ND*	ND*
1.6 F	* 4.7	* 7.3	5.5 *
1.0 Fe	* 1.24	* 26.50	* 5.84
HCO	130.0	460.0	231.1
K	18.8	89.2	33.7
Li	1.95	10.73	3.65
Mg	0.27	10.00	3.04
Na	370.0	1900.0	826.0
P	0.67	3.39	1.95
pH	6.2	7.7	
SiO	109.0	208.0	132.9
SO	707.0	739.0	721.8
TDS	* 1812.0	* 4860.0	* 2630.8
TS	1894.0	5096	2874.8
TSS	77.0	950.0	244.0

\*ND = Non Detected

Samples Analyzed in Accordance with EPA Approved Methods  
Results reported in mg/L  
1980

17 Discharges		17 Samples Analyzed	
	<u>Min.</u>	<u>Max.</u>	<u>Aver</u>
6.0 Al	0.02	1.91	0.46
.1 As	0.00001	0.385 *	0.191 *
.75 B	0.10	9.50 *	5.65 *
Ca	17.3	69.0	47.0
.01 Cd	0.0001	0.0320 *	0.0036 *
250 Cl	14.0	777.0 *	428.8 *
CO <sub>3</sub>	ND*	ND*	ND*
1.6 F	0.3	11.30 *	6.98 *
1.0 Fe	0.03	9.42 *	5.34 *
HCO <sub>3</sub>	104.0	1140.0	401.2
K	9.3	77.2	34.0
Li	0.01	10.61	6.31
Mg	0.05	35.80	12.70
Na	12.5	770.0	446.6
P	0.01	275.00	0.23
pH	6.0	10.3 *	
SiO <sub>2</sub>	70.0	240.0	191.9
SO <sub>4</sub>	7.2	580.0	189.0
TDS	230.0	2731.0 *	1782.8 *
TS	231.0	3011.0	1810.8
TSS	1.0	280.0	27.4

\*ND = None Detected

Samples Analyzed in Accordance with EPA Approved Methods  
 Results reported in mg/L  
 1981

52 Discharges

52 Samples Analyzed

	<u>Min.</u>	<u>Max.</u>	<u>Aver</u>
4.0 Al	0.04	14.00 <del>A</del>	0.57
1 As	0.004	0.233 <del>†</del>	0.057
17 B	2.60 <del>‡</del>	14.60 <del>‡</del>	12.02 <del>*</del>
Ca	39.7	271.0	74.4
0 Cd	0.00002	0.006	0.0003
10 Cl	300.0 <del>*</del>	1332.0 <del>*</del>	1083.2 <del>*</del>
CO <sub>3</sub>	ND*	200.0	10.8
6 F	5.9 <del>*</del>	10.0 <del>*</del>	8.1 <del>*</del>
10 Fe	2.79 <del>*</del>	75.50 <del>*</del>	38.57 <del>*</del>
HCO <sub>3</sub>	470.0	795.0	582.5
K	19.0	92.9	69.7
Li	2.96	16.00	12.78
Mg	2.28	26.8	6.63
Na	395.0	1080.0	343.4
P	ND	1.45	0.11
pH	6.0	8.5	
SiO <sub>2</sub>	113.0	244.0	197.8
SO <sub>4</sub>	173.0	491.0	215.4
TDS	1575.0 <del>*</del>	4671.0 <del>*</del>	3150.5 <del>*</del>
TS	1658.0	4709.0	3197.3
TSS	4.0	876.0	47.3

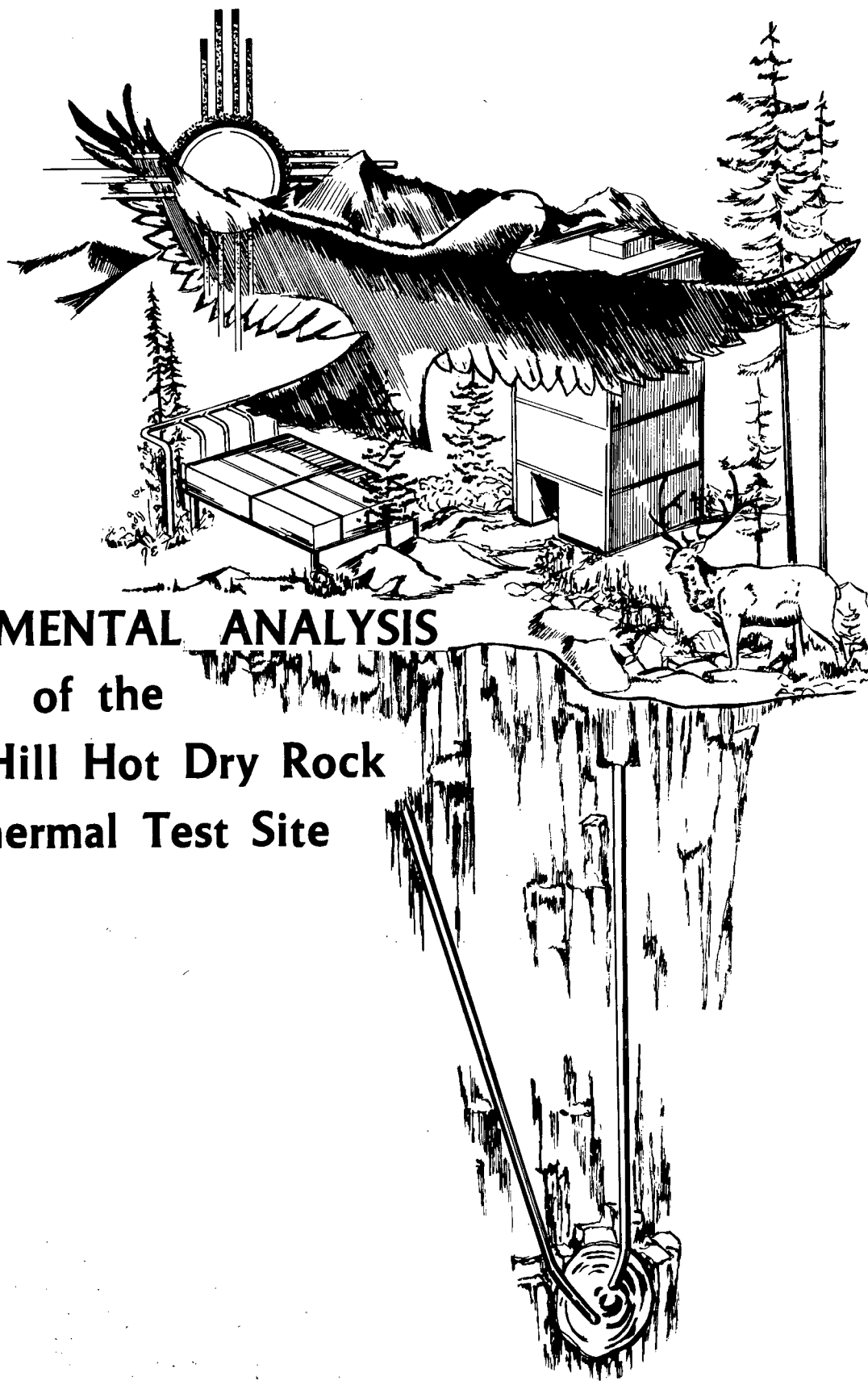
\*ND = Non Detected

RECEIVED

SEP 15 8 24 AM '81

MAIL & RECORDS  
LAAO

LA-7830-HDR



**ENVIRONMENTAL ANALYSIS**  
of the  
**Fenton Hill Hot Dry Rock**  
**Geothermal Test Site**



**LOS ALAMOS SCIENTIFIC LABORATORY**  
**UNIVERSITY OF CALIFORNIA**

**An Affirmative Action/Equal Opportunity Employer**

This work was supported by the US Department of Energy, Division of Geothermal Energy.

This report was prepared as an account of work sponsored by the United States Government. Neither the United States nor the United States Department of Energy, nor any of their employees, nor any of their contractors, subcontractors, or their employees, makes any warranty, express or implied, or assumes any legal liability or responsibility for the accuracy, completeness, or usefulness of any information, apparatus, product, or process disclosed, or represents that its use would not infringe privately owned rights.

**UNITED STATES  
DEPARTMENT OF ENERGY  
CONTRACT W-7408-ENG. 36**

**LA-7830-HDR**  
**UC-66e**  
**Issued: May 1979**

**ENVIRONMENTAL ANALYSIS**  
**of the**  
**Fenton Hill Hot Dry Rock**  
**Geothermal Test Site**

**Compiled and Edited by**

**E. L. Kaufman**  
**and**  
**C. L. B. Siciliano**

## CONTENTS

ABSTRACT-----	1
I. INTRODUCTION AND PROGRAM HISTORY-----	1
II. THE HDR SYSTEM AT FENTON HILL-----	5
A. Site Selection and Preparation-----	5
B. Drilling and Fracturing-----	6
C. Surface Facilities-----	7
III. THE AFFECTED ENVIRONMENT-----	10
A. Land Status and Uses-----	11
B. Physical Factors-----	11
1. Geography and Topography-----	11
2. Geology-----	12
3. Seismology-----	16
4. Hydrology-----	18
a. Surface Water-----	19
b. Ground Water-----	23
5. Climatology-----	28
6. Aesthetics-----	30
C. Biological Factors-----	32
1. Vegetation-----	32
2. Small Mammals-----	34
3. Elk-----	35
4. Birds-----	36
5. Endangered Species-----	37
D. Social and Economic Factors-----	38
IV. EFFECTS OF IMPLEMENTATION-----	40
A. Land Status and Uses-----	40
B. Physical Factors-----	40
1. Geography and Topography-----	40
2. Geology-----	42
3. Seismology-----	42
a. Activities at the Fenton Hill Site-----	42
b. Other Activities in the Area and Adjacent Regions-----	43
4. Hydrology-----	44
a. Water Requirements-----	44
b. Liquid Effluents-----	45
5. Climatology-----	50
6. Aesthetics-----	50
C. Biological Factors-----	51
1. Vegetation-----	51
2. Wildlife-----	51
3. Endangered Species-----	51

D. Environmental Contaminants-----	52
1. Air-----	52
2. Water-----	53
3. Water Treatment Plant-----	53
4. Noise-----	53
E. Social and Economic Factors-----	54
V. SUMMARY-----	54
ACKNOWLEDGMENTS-----	55
REFERENCES-----	56

## FIGURES

1. Index Map.-----	3
2. Schematic of the Fenton Hill Site as it is today.-----	4
3. Structure of an HDR electricity generating plant.-----	7
4. Proposed subsurface array of seismic monitoring stations.-----	9
5. Schematic of LASL seismic network station with radio telemetry.-----	10
6. Generalized geologic map of the area of investigation.-----	13
7. Geologic section from the Rio de Las Vacas to San Antonio Creek.-----	13
8. Location of sampling stations.-----	22
9. Hydrograph to estimate volume of flow near Locations J and Q from US Geological Survey records from gaging station near Location R.-----	23
10. Chemical analysis comparison of surface water, December 1974.-----	26
11. Chemical analysis comparison of ground water discharges from Cenozoic-Volcanic overlying the Abo Formation.-----	27
12. Chemical analysis comparison from thermal and mineral springs.-----	27
13. Schematic casing diagram of GT-2.-----	27
14. Schematic casing diagram of EE-1.-----	27
15. Schematic casing diagram of proposed EE-2.-----	28
16. Location of the weather stations near the site.-----	29
17. View of Fenton Hill Site from Highway 126.-----	31
18. Location of vegetation transects.-----	32
19. Location of small mammal traplines.-----	34
20. Location of elk pellet groups counting plots.-----	36
21. Location of bird counting transects.-----	37
22. Indian reservations in the vicinity of the Site.-----	41

## TABLES

I.	Water Quality Analysis for Horseshoe Spring -----	19
II.	Water Quality Analysis for San Antonio Creek -----	20
III.	Water Quality Analysis for Holding Ponds -----	20
IV.	Temperature, Precipitation, and Wind Summaries for 1976 -----	30
V.	Average Percentage of Ground Cover by Community Type -----	33
VI.	Estimated Nesting Populations at the Well Site and Open Mesa Site During the Summer of 1976 -----	38
VII.	Animal Species Listed as Endangered by the State of New Mexico -----	39
VIII.	Average Chlorides, Fluorides and Total Dissolved Solids (TDS) of Effluents (Ponds) and Water from Sampling Stations, 1978 -----	47
IX.	Chemical Characteristics of Pond Water, Ranges, and Maxima Observed in 1977-78 -----	48
X.	Latest Discharge Analysis Results -----	49

ENVIRONMENTAL ANALYSIS  
OF THE  
FENTON HILL HOT DRY ROCK  
GEOTHERMAL TEST SITE

Compiled and Edited by

E. L. Kaufman and C. L. B. Siciliano

ABSTRACT

Techniques for the extraction of geothermal energy from hot dry rock within the earth's crust were tested at the first experimental system at Fenton Hill and proved successful. Because new concepts were being tried and new uses of the natural resources were being made, environmental effects were a major concern. Therefore, at all phases of development and operation, the area was monitored for physical, biological, and social factors. The results were significant because after several extended operations, there were no adverse environmental effects, and no detrimental social impacts were detected. Although these results are specific for Fenton Hill, they are applicable to future systems at other locations.

---

I. INTRODUCTION AND PROGRAM HISTORY

The Los Alamos Scientific Laboratory (LASL) administered by the University of California has been investigating the feasibility of extracting heat from the very large geothermal resource contained in the hot dry rock within the earth's crust. The technique requires that a borehole be drilled into low-permeability, hot crystalline rock and that a large, hydraulically fractured region be created near the bottom of this borehole. A second borehole is drilled along a trajectory to intersect the fracture and complete the subterranean portion of the circulation loop. Then pressurized fluid, in this case water, is pumped down one borehole to the "reservoir" where it is heated as it flows over rock in the range of 250°C. The water, now at temperatures

in excess of 100°C, is brought to the surface and directed through heat exchangers before being recycled through the system. The thermal energy that is extracted can be used for generating electricity or directly as heat. This is an efficient system, which has minimal water loss, low noise levels, and few of the other environmental problems associated with hydrothermal systems (such as The Geysers in California).<sup>1-3</sup>

Active work on this concept began at LASL in 1970 under sponsorship of the US Atomic Energy Commission (AEC). The Fenton Hill Site, selected in 1973, is located in north-central New Mexico in section 13, T19N, R2E, NMPM, as shown on Fig. 1. Field work was initiated in fiscal year 1974 (FY74), and during the period FY74 through FY76, the two boreholes GT-2 and EE-1 (Geothermal Testhole 2 and Energy Extraction hole 1) were drilled. The necessary surface facilities, such as heat exchangers and water storage, were connected into the system, and energy production tests were conducted. Figure 2 is a schematic of the site as it is today. Because the area chosen for the Hot Dry Rock Geothermal Energy Development Project (HDR Project) is on a part of the Santa Fe National Forest (SFNF), it is under the jurisdiction of the Department of Agriculture, US Forest Service (USFS). A Memorandum of Understanding between the AEC and the Forest Service was written to define the land, the basis of use, and responsibilities of both parties, SFNF (Contract AT 29-1 - 2213, signed November 30, 1973). In addition, the Jemez District Ranger of the Santa Fe National Forest completed an Environmental Analysis Report and determined that initial operations through the drilling phases were acceptable by environmental and public-land-use standards. This report, dated April 3, 1978, states,

"This [Fenton Hill Complex] does not constitute a major federal action. It does not involve an irretrievable commitment of the resource. An Environmental Impact Statement is not needed."

A later Memorandum of Understanding (Contract No. DE-AC32-79AL10001) between the USFS and the Department of Energy (DOE) dated January 3, 1979, provides, in summary, that:

- 1457 hectares (3600 acres) are excluded from Known Geothermal Resource Area leasing for the HDR experimental site, but specifically excluding use for commercial electricity generation;
- Various locations, in addition to the site and subject to approval

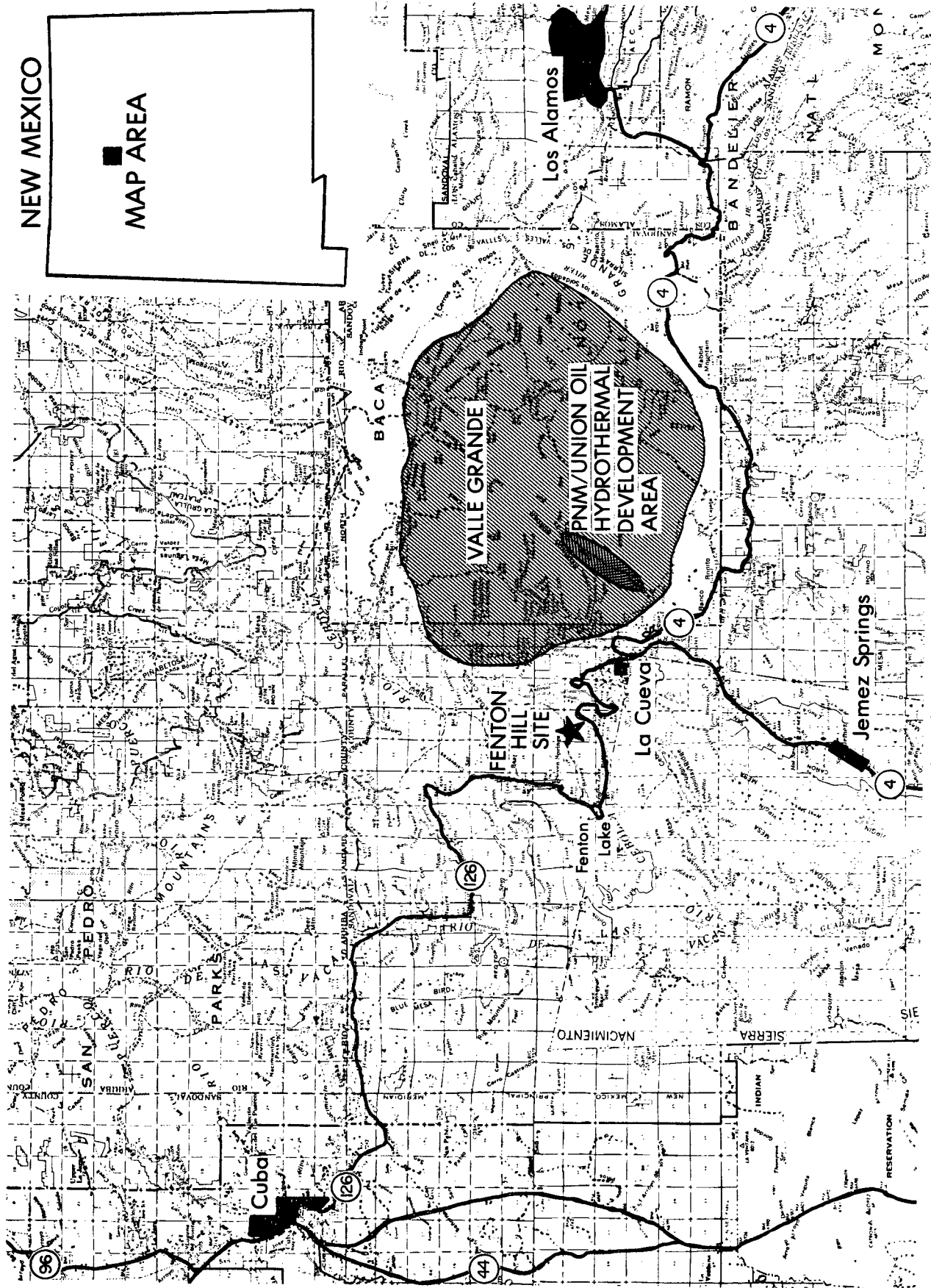


Fig. 1. Index map.

- by the District Ranger, may be used for heat flow, geophysical, geological, and environmental monitoring;
- DOE will take all reasonable precautions to minimize damage to the soil, flora, and fauna, that might result from its operations and will comply with the applicable regulations of the Forest Service;
  - DOE will submit sixty days in advance for written approval by the Forest Supervisor the development plans, layout plans, plans for construction, reconstruction, or alteration or improvement of facilities to be located on Forest Service land. DOE will prepare for the Forest Supervisor appropriate Environmental Analysis Reports so that the Forest Supervisor may assess project impacts and design mitigating measures. Approved activities will then be coordinated through the appropriate District Ranger;
  - DOE will submit in advance for approval by the District Ranger plans and activities of a temporary nature that comply with overall plans and that do not include significant surface disturbance, road building, or drilling in excess of 305 m (1000 ft) deep. DOE will

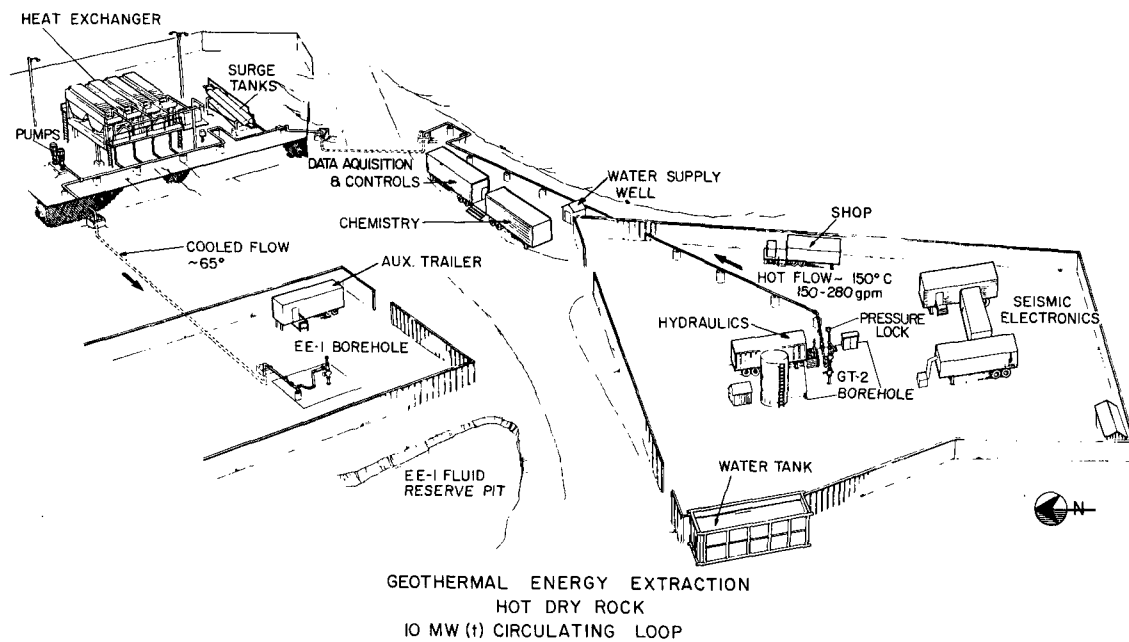


Fig. 2. Schematic of Fenton Hill Site as it is today.

prepare for the District Ranger appropriate Environmental Analysis Reports so that the District Ranger may assess project impacts and design mitigating measures;

- DOE will provide, for Forest Service review and comment, ecological and environmental study plans and will draft manuscripts related to the surface environment and its renewable resources; and,
- All parties shall comply with applicable federal, state, and local laws and regulations.

## II. THE HDR SYSTEM AT FENTON HILL

Analysis of the Fenton Hill Site and its operation will provide the initial guidelines for development of future HDR systems at other locations. The present system was designed to determine the flow parameters and to test operation with accelerated thermal drawdown (the rate at which rock temperatures are reduced). The results were as follows.

- Water loss through permeation in the reservoir rock stabilized at <2% of the circulation rate.
- The circulating water dissolves some of the soluble constituents of the rock, but the concentration of total dissolved solids stabilized at  $\approx$ 2000 ppm, which is near drinking water quality.
- There are no gaseous emissions during operation of the circulation loop. However, during some reservoir and equipment testing, water is diverted to storage and then dissolved gases may be released. The composition of the gas was analyzed as 87% air and 13% carbon dioxide, with only trace amounts of hydrogen sulfide and ammonia.
- Dissolved radioactive elements were minimal, and these had short half-lives that rendered them undetectable after a few days.
- Noise levels during loop operation approximated those of a typical street corner.
- This does not represent a significant depletion of a natural resource.

### A. Site Selection and Preparation

The effects of injecting fluid into artificially created reservoirs are still being studied. During all phases of development and operation, a very

sensitive array of seismometers is used to detect any possible induced micro-earthquakes. But until it is thoroughly demonstrated that this process will not affect the natural tectonics, sites will not be located in earthquake-prone areas or along major geologic faults.

A small surface area of 5.5 hectares (13.5 acres) was cleared to accommodate the Phase I experimental system. This site included both boreholes, the heat exchangers, water storage, and all support facilities required for the extraction of 5 MW of thermal energy. To include a demonstration electricity generating plant, the site may have to be expanded somewhat but would require only the clearing and leveling of the specific land to be used. This is insignificant when compared with the amount and use of land required for the strip mining of coal.

HDR facilities can be located within or near cities without concern for possible hazards or contamination because all effects will be restricted to the site. Furthermore, studies are being made of all federal, state, and local laws and regulations that are applicable to the establishment and operation of these systems.

#### B. Drilling and Fracturing

During the production of the Phase I reservoir, on-site and regional arrays of seismometers were used to record any induced microearthquakes. None were detected, and the creation of the next, Phase II, system at the site will be monitored by additional stations. This reservoir will require drilling a new well, deepening one of the existing wells, and creating a second fracture below the first one. The fracture may be several hundred meters long but only a few millimeters wide. This reservoir will be of a commercially feasible size and will demonstrate the production lifetime of such a system.

The diagnostic and fracture-forming operations will be carried out in the new wellbore (EE-2). The fracture will be formed by injecting water down the cased hole at an adequately high pressure to open the cracks in the granitic rock at the bottom of the hole. A similar method produced the existing system, and pumping and fluid-handling equipment will be temporarily located near the EE-2 wellhead to support these operations. The final configuration of the fracture system will depend on the exact nature of the rock formation encountered at the bottom of the hole. The designation of the present land area of 1457 hectares (3600 acres), which is excluded from the Known

Geothermal Resource Area (KGRA) leasing program, will ensure that the entire subsurface reservoir is confined to the excluded land. Then wellbore EE-1 will be redrilled along a trajectory to intersect the fracture system produced near the bottom of EE-2.

After drilling EE-2, a redrilling operation will be carried out on the remaining well GT-2. The wellbore depth will be increased to 4 km (13 000 ft), and a tower will be erected over the wellhead. The redrilled wellbore will be a downhole facility for a Deep-Wellbore Equipment Test Station (DWETS). A service building or trailer and a cable-handling drawworks will be placed near the wellhead.

### C. Surface Facilities

The support facilities required for operation are minimal. Aside from the trailers for housing equipment and work areas, the main facilities at Fenton Hill are heat exchange modules, 15-m (48-ft) towers over the wellheads, a makeup-water tank, a water storage pond, and a piping system of the circulation loop. A small, electricity generating plant for demonstration may be included. This portable, 60-kVA unit can be patched into the incoming electric utility lines and, when the energy-extraction loop is operating, can provide up to 12% of the site demand. Figure 3 shows the structure of a possible HDR plant for commercial production of electricity. By screening with fencing and trees and by selection of appropriate paint colors, an HDR plant would not greatly affect the aesthetics of the area.

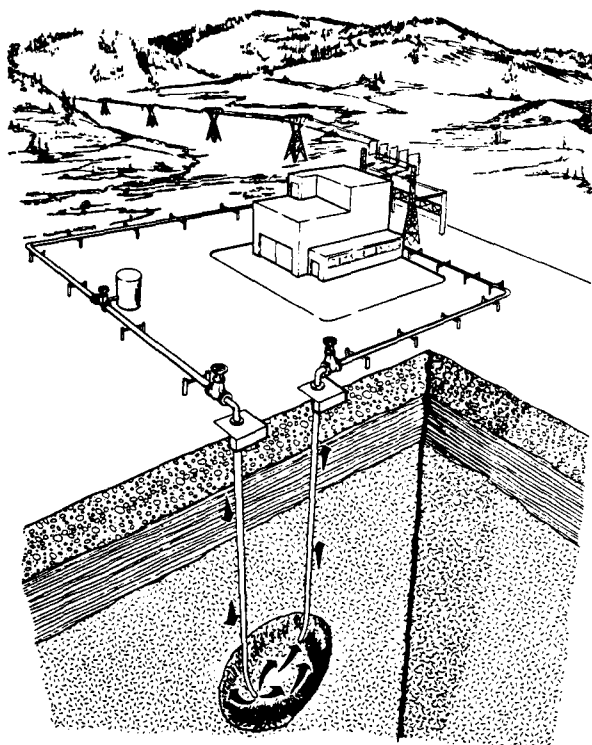


Fig. 3. Structure of an HDR electricity generating plant.

A small (9 by 12 m or 30 by 40 ft) geothermally heated greenhouse might also be installed at Fenton Hill for controlled plant and fish

physiology experiments (such as effects of geofluid uptake). Heating of this unit would be augmented by a passive solar-energy system and by a back-up fossil-fuel heating system for periods when the loop is not operating.

The larger, Phase II reservoir is expected to require additional water storage, treatment, and production facilities. The alternatives for water storage are covered tanks, excavated holding ponds, and earth fill dams. The anticipated storage capacity will range from 22 700 to 45 000 m<sup>3</sup> (5 to 10 Mgal). To store 34 000 m<sup>3</sup> (7.5 Mgal), a pond with dimensions of 91 m (300 ft) in diameter and 3 m (10 ft) deep would be required. The maximum water-surface area would be 0.8 hectares (2 acres). A single tank of 26 000 m<sup>3</sup> (5.7 Mgal) capacity would be 61 m (200 ft) in diameter and 9 m (30 ft) high.

A water treatment facility, if needed, would consist of a number of modular treatment units housed in a suitable weather-protective enclosure. This facility will be used for treatment and conditioning of water circulated in the heat-extraction loop, including possible removal of dissolved minerals, and treatment of water for release from the site to meet Environmental Protection Agency (EPA) effluent limits, pursuant to a National Pollutant Discharge Elimination System (NPDES) permit.

This larger fracture system may require a new water-supply well that would be drilled on the site and produce from a depth interval of 305 to 732 m (1000 to 2400 ft). The well drilling and operation will be pursuant to a New Mexico State Engineer's authorization and will comply with USFS regulations.

Certain experimental observations will be made using facilities to be located in the Santa Fe National Forest outside the test site. An existing array of nine seismic monitoring stations in the area surrounding the geothermal site maintain present surveillance. Seven of these are surface stations lying within an 750-m radius of the site, and the other two are in Holes A and D shown on Fig. 4. Also shown on Fig. 4 are six proposed sites, S1 through S4, GT-1, and Hole B. Of these GT-1 and Hole B were drilled before development of the Fenton Hill Complex. S1 through S4 are intended to be augered holes 15 cm (6 in.) in diameter and 30 m (100 ft) deep. The additional sites will have radio-frequency (rf) telemetry for wireless transmission of seismic signals to recording facilities at the site. These seismic stations will require a very small surface disturbance, limited to only that area

necessary for burying the 30- to 55-gal drums containing the electronic equipment and the area immediately above ground for the solar panels and transmitting antennas as illustrated in Fig. 5.

Another installation will be constructed on Lake Fork Mesa to measure earth strain with equipment of special sensitivity and will be located 1.6 km (1 mi) SW of the geothermal site. The facility will consist of a 10-m-long, 0.5-m-deep, and 0.6-m-wide trench with 180-mm-diam, 3-m-deep holes on both ends. Steel pipes 4.5-in. in diameter will be cemented into each hole. The trench will be filled with insulation, cans of water, and covered with a

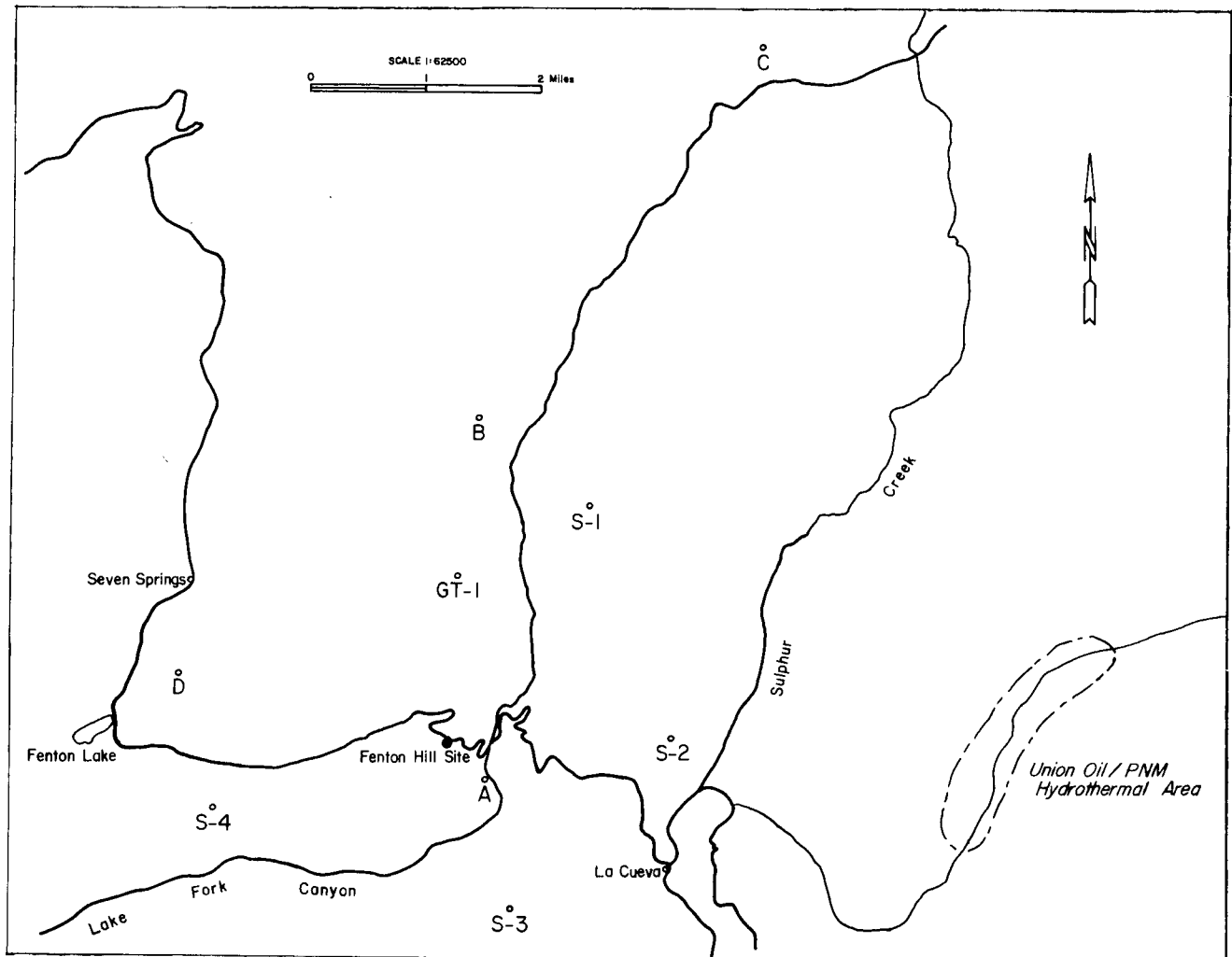


Fig. 4. Proposed subsurface array of seismic monitoring stations.

tarpaulin. At the end of the trench where the equipment is located a portable shed will be erected.

Approval from the USFS will be obtained before fielding any temporary equipment in the area surrounding the geothermal site in accordance with the stipulations of the latest Memorandum of Understanding.

### III. THE AFFECTED ENVIRONMENT

Much information on the existing environment, including documentation of effects resulting from the present facilities, has been gathered by LASL through special studies relating to the HDR Project. These include geologic and geophysical investigations, regional hydrology and water quality studies started in 1971, specially funded environmental studies started in 1975, and monitoring conducted as part of LASL's routine environmental surveillance. Reports from these studies are available and are listed in the references.

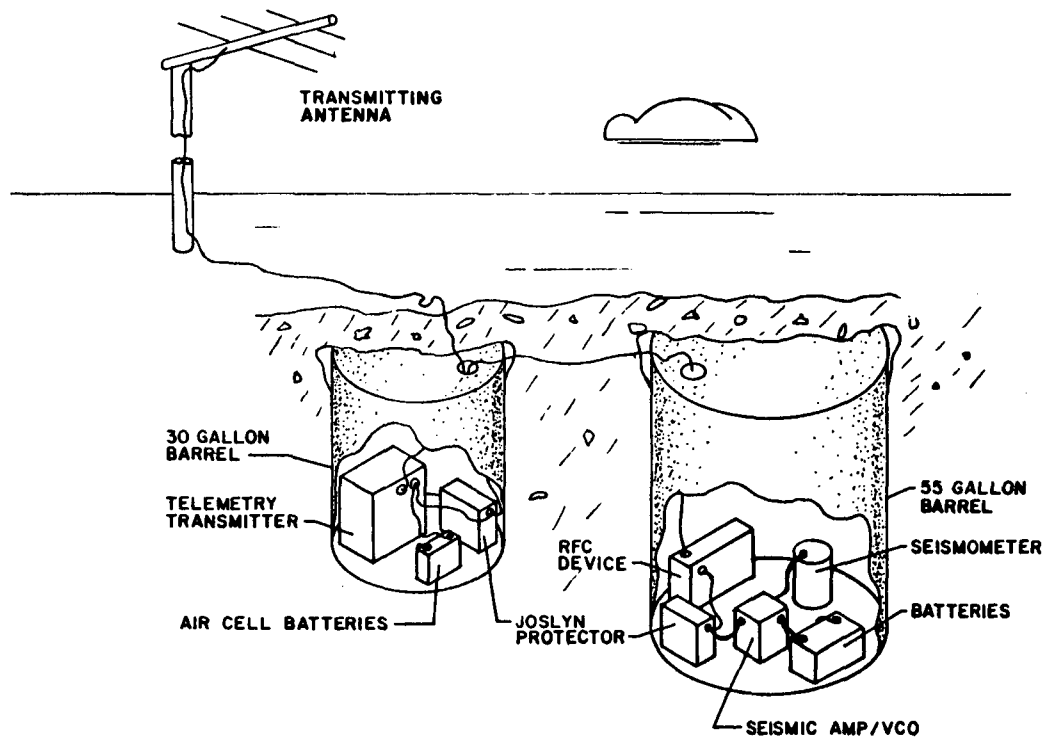


Fig. 5. Schematic of LASL seismic network station with radio telemetry. The solar panels are not shown.

## A. Land Status and Uses

Based upon an administrative charter, this area is dedicated to the preservation of the natural vegetation, wildlife, and scenic beauty as a segment of the forested high-mesa country of the American Southwest.<sup>4</sup> Multiple-use policies in management of public lands have led to the establishment of a USFS fire control helipad on this plateau, planting of tree seedlings, cattle grazing, fuel wood gathering, hunting, picnicking, etc., and finally to the development of a geothermal test facility. The small surface area 5.5 hectares (13.5 acres) containing the facility will be of limited access, but the rest of the plateau will remain under the multiple-use concept.

Because the Valles Caldera is the central feature of the Jemez Mountains and is one of the world's largest calderas, it is deemed worthy of preservation and has been declared a National Natural Landmark. The nearest boundary of the designated area is 5.5 km (3.5 miles) away from Fenton Hill. Therefore, geothermal developments at Fenton Hill will not affect the integrity of the landmark area.

The subsurface area, 1457 hectares (3600 acres), that will contain the geothermal reservoirs is within the western portion of the Valles Caldera KGRA and is excluded from further leasing.

## B. Physical Factors

1. Geography and Topography. The LASL HDR facility is located on the Jemez Plateau 35 km (22 mi) west of Los Alamos, in north-central New Mexico.<sup>3</sup> The Jemez Plateau is a part of the western arm of the Rocky Mountains that extends into northern New Mexico from southern Colorado. The surface of the plateau is formed by volcanic ash extruded during the volcanic activity that produced the Valles Caldera 1.1 Myr ago.<sup>5</sup>

The Valles Caldera is surrounded by mountains formed during this same period of active volcanism. The volcanic ash forms an apron around the caldera that laps onto the flanks of these mountains, and the Jemez Plateau is the western part of this apron. The north-south trending Nacimiento Mountains form the western boundary of the area of investigation.

The altitudes of mountains bounding the Jemez Plateau on the east and west range from about 3048 m (10 000 ft) at the westernmost dome in the

caldera (San Antonio Mountain) to a little over 2743 m (9000 ft) along the crest of the Nacimiento Mountains. The major drainage in the area is the Rio de Las Vacas and Jemez Creek, with its tributary, San Antonio Creek. The Fenton Hill Site is on the plateau between the Rio de Las Vacas and San Antonio Creek. A high ridge along the western part of the plateau is parallel to San Antonio Creek. Otherwise the surface of the plateau slopes gently downward to the west and southwest. The altitude of the area ranges from 2440 to 2740 m (8000 to 9000 ft) along the crest of the ridge to about 2130 to 2440 m (7000 to 8000 ft) where the plateau terminates in steep slopes or cliffs above the Rio de Las Vacas. The plateau surface is cut into a number of mesas by southwest trending streams that are tributary to the Rio de Las Vacas, the largest of which is the Rio Cebolla. West of the Rio de Las Vacas, the eastern flank of the Nacimientos rises gently to the crest, then the slope breaks steeply westward into the San Juan Basin.

2. Geology.<sup>6,7</sup> The site area is a part of the southern extension of the Rocky Mountains and is bounded on the east by the Rio Grande Depression and on the west by the San Juan Basin. Precambrian, Pennsylvanian, Permian, Mesozoic, and Cenozoic rocks outcrop in the area as shown on Fig. 6.

Precambrian rocks of granite and gneiss outcrop along the flanks and crest of the Nacimiento Mountains. These are overlain by Pennsylvanian and Permian limestones, sandstones, and shales. Mesozoic sediments outcrop in the northwestern part of the area and on the western slopes of the Nacimiento Mountains, but because they do not extend beneath the Jemez Plateau they are not further considered. The Cenozoic volcanic rocks form the upper surface of the Jemez Plateau, overlying the Permian, Pennsylvanian, and Precambrian rocks.

The Precambrian rocks are particularly important to the present geothermal energy research because they will contain the pressurized-water circulation system to be created. Granite is the most abundant type of Precambrian rock. The granite is coarse-grained with large insets of microcline. Microcline is the dominant feldspar, although albite-oligoclase is usually present in smaller amounts. Quartz is abundant, with biotite a common mafic mineral.

Quartz-feldspar gneiss is common. The feldspar consists mainly of microcline. However, oligoclase-andesine is also abundant, although it is finer grained and more uniformly spread throughout the rocks. The quartz shows moderate straining. Accessory minerals are hornblende, biotite, epidote,

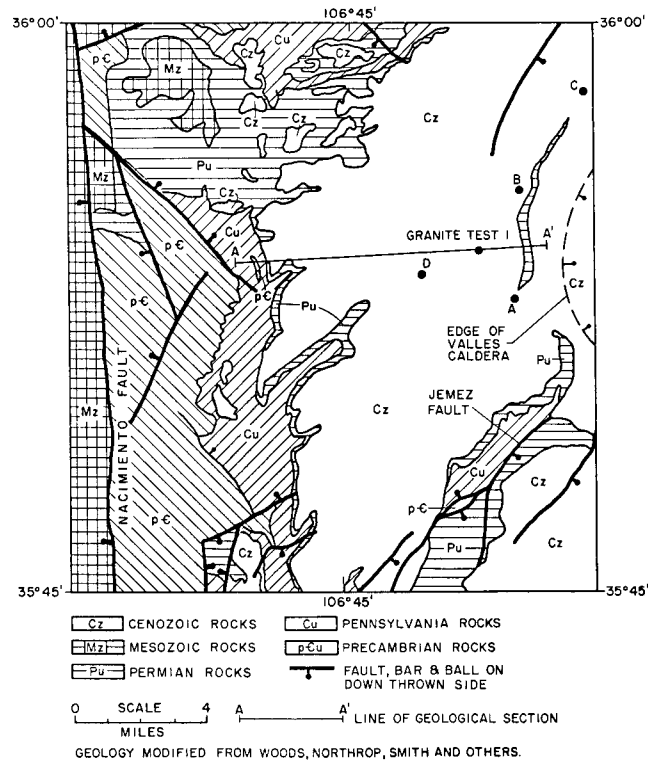


Fig. 6. Generalized geologic map of the area of investigation. (See Refs. 8 and 9.)

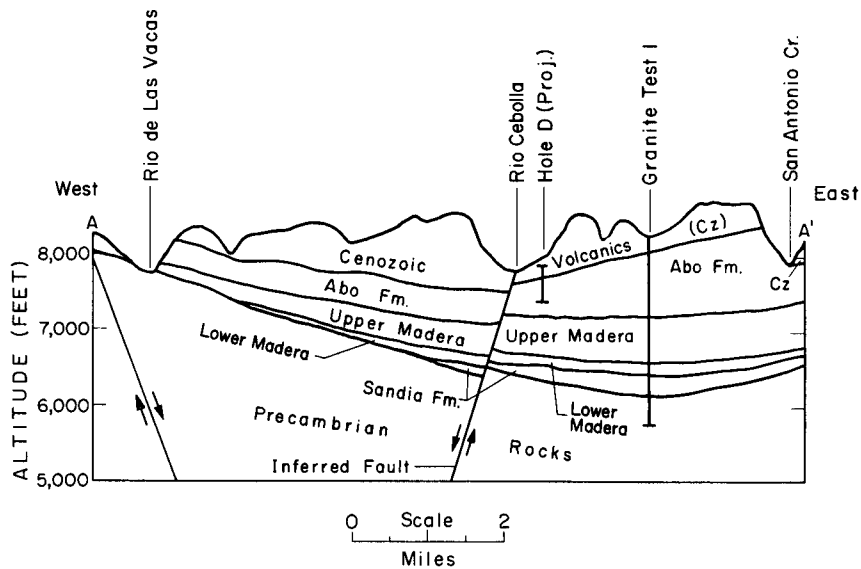


Fig. 7. Geologic section from the Rio de Las Vacas to San Antonio Creek.

with some sphene, apatite, zircon, and magnetite. GT-1 penetrated augen-gneiss in which the augen ("eyes") are microcline. The gneiss is lenticular, with planes of foliation. The foliation has a general, characteristic north-east trend, that has also been observed to the southeast in the Sandia, Manzanito, and Manzano Mountains--as if deformation and metamorphism had taken place in a single major event with forces acting at right angles to the foliation.

GT-1 penetrated a dark gray amphibolite that is primarily amphibole and plagioclase. A few small outcrops of Precambrian occur along the Rio de Las Vacas. There are no apparent outcrops of pegmatites or greenstone schists, although there are a few outcrops of mica schist into which the granites have intruded. The color of the granites ranges from brownish-gray to red, whereas the predominant color of the gneiss ranges from pinkish-gray to red. The granites weather to spheroidal boulders and hummocks. The gneiss weathers to rounded knolls and undulating uplands.

The Pennsylvanian rocks are predominantly massive limestones, shales, and arkose. In the area of investigation these rocks compose the Magdalena Group that includes the lower Sandia formation and overlying Madera limestone. Although these strata are combined on the map of Fig. 6, the cross section of the experimental site in Fig. 7 shows individual units within the two formations. The Sandia formation is divided into a lower limestone member and an upper clastic member. The lower member is a dark gray, siliceous limestone, whereas the overlying member consists of dark brown to brownish-green sandstone and arenaceous shale and limestone. The lower limestone member is discontinuous. The upper clastic member rests on the Precambrian rocks in some areas. Both members were present in GT-1.

The Madera limestone is composed of a lower, gray limestone member and an upper arkosic limestone member. The lower gray limestone consists of a dark gray limestone interbedded with gray shale and a few sandstone beds. The upper arkosic limestone member is of limestone and arkosic limestone, alternating with gray and red arkosic shale.

The thickness of the Pennsylvanian rocks of the Magdalena Group varies, and in some places they are not present--either because they were removed by erosion before deposition of the overlying Permian rocks or because they were not deposited.

The Permian rocks were deposited on an old flood plain that may have been flooded periodically by marine waters, although the irregular bedding in the sandstones suggests a fluvial mode of deposition for most of the rocks, in a continental environment.

In the area of investigation the Permian rocks are of the Abo formation. The formation consists of arkosic siltstone, sandstone, and shale. The sandstone is fine-grained with occasional lenses of pebbly conglomerate. Lenses of clay also occur, as well as some minor, thin lenses of arkosic limestone. The formation is made up of alternating layers of shale, siltstone, sandstone, and clay, with the shales making up the larger part of the section. Quartz grains are numerous in coarser-bedded material; however, some feldspar is also present, as well as small particles of igneous rocks. The Abo in the lower part of the section may contain some reworked material from the Magdalena Group. The color of the formation is predominantly various shades of red, from light to very dark. The upper surface of the Abo was heavily eroded prior to the deposition of the Cenozoic volcanics. Thus the thickness of the Abo varies because of this irregular surface. Testholes A, B, C, and D, shown on Fig. 6, did not penetrate the complete section of the Abo but are completed 101, 64, 52, and 115 m, respectively, into the upper part of the formation.

The Cenozoic rocks are made up of volcanics and clastics.<sup>8,9</sup> The older Cenozoic rocks--the Abiquiu Tuff and the Tschicoma formation--are exposed in the west wall of the canyon cut by San Antonio Creek north of La Cueva, whereas the younger rocks--the Bandelier Tuff--form the upper part and surface of the Jemez Plateau. The Abiquiu Tuff lies in the topographically low areas in the eroded surface of the Abo formation. It is composed mainly of white to light gray tuffaceous sandstone and conglomerate that includes a basal gravel member that includes pebbles and sand derived from the Precambrian crystalline rocks. Testhole A, Testhole C, and GT-1 penetrated the Abiquiu Tuff at 38, 103, and 30 m, respectively.

The Tschicoma formation overlies the Abo formation and a part of the Abiquiu Tuff along the west wall of the canyon cut by San Antonio Creek. The formation is a thin pyroclastic flow of dark gray latite that, in places, contains some thin lenses of light gray clay. The formation contains phenocrysts of plagioclase and some smaller crystals of quartz, biotite, hornblende, and augite in a fine-grained gray matrix. Testhole B penetrated about 18 m of the Tschicoma above the Abo formation.

The Bandelier Tuff forms the upper part and the surface of the Jemez Plateau overlying the older volcanic rocks of the Tschicoma formation--Abiquiu Tuff and, in places, the sediments of the Abo formation. The Bandelier Tuff ranges from a nonwelded to a welded rhyolite tuff, with colors from light gray to dark gray. The tuff is made up of crystals and crystal fragments of quartz and sanidine, glass shards, and some mafic minerals; as well as rock fragments, pumice, latite, and rhyolite in a fine-grained ash matrix. The Bandelier Tuff thins to the west and southwest away from the source area, the Valles Caldera. Testholes A, B, C, and D, and GT-1 penetrated thicknesses ranging from 9 to 115 m of the Bandelier Tuff.

3. Seismology.<sup>3</sup> Historically, New Mexico is an area of low-to-moderate seismic risk. Records of shocks felt by people or causing structural damage date back to the mid-1800s. These records, coupled with instrumental measurements, show the greatest earthquake activity region centered along the Rio Grande Valley between the cities of Socorro and Santa Fe in the central part of the state.<sup>10</sup>

Although historical records show the Jemez Plateau to be quiet, a survey to locate fault and seismic events was deemed necessary.<sup>10,11</sup> These data were used to document the absence of large seismic events within the region and to check the site specifically for induced seismicity from circulating water through deep earth structures. A survey was done in 1971 to determine the proximity and probable activity of faults near the site.<sup>12</sup> This survey shows that the Jemez fault zone is the nearest major fault system to the site. Two northeast-trending faults within this zone, the Virgin Canyon fault and the Jemez Springs fault, pass within 4 and 7 km, respectively, from the site. Field checks of both faults indicate their displacement (rate of movement per year) is far below that of major active faults in the western United States. It is highly improbable that these faults would be activated by experimentation at the LASL HDR Site because of their distance from the site, the fact that they trend away from the site, and their relatively low displacements.

Two sets of seismic nets (close-in and on-site) were established to measure seismic activity in the vicinity of the site and to supplement measurements taken from three stations (Barley Canyon, Lake Fork Canyon, and La Cueva) on an existing regional net. The regional net, established to measure seismic events important to LASL, is indirectly linked to the Fenton Hill

Project. This net is composed of 12 high-gain, continuously telemetered stations located  $\sim$ 150 km from Los Alamos. The regional net was started in 1972 with establishment of the first station at LASL. By 1973, enough stations were functional to locate epicenters of microearthquakes Richter's magnitude thresholds ( $M_L$ )  $>$  0.5 up to 100 km from Los Alamos.<sup>13</sup>

The La Cueva station, located  $\sim$ 450 m north of the site, contains a three-axis system of seismometers. The Barley Canyon and Lake Fork Canyon systems are special borehole (125-m-deep) stations that were established in 1975 to augment the detection and location capabilities of  $M_L > 0$  seismic events within 5 km of the site.

The close-in and on-site seismic nets were established during 1975 and 1976 to detect signals from the  $\sim$ 2900 m-deep hydraulic fracturing experiments. The close-in seismic net consists of nine surface stations located  $\sim$ 1500 to 2000 m from the site, and the rest are  $\sim$ 750 m from the site in a circular configuration. Signals from these stations are transmitted by cable to a recording trailer at the site.

Microseismic events recorded by the regional network of seismic stations in northern New Mexico show that no events greater than the threshold value  $M_L = 0.5$  have occurred at the site since 1973. Microseismic activity recorded near the facility is discussed below.

The first event recorded with an epicenter near the facility occurred in the early morning of May 28, 1975. This was a single shock ( $M_L = 0.7$ )  $\sim$ 17 km southeast of the site. Because this was a singular event, its significance remains unclear.

A larger event was recorded later that year, on September 29. This activity was preceded by two shocks, recorded on the September 25 and 27, and was followed by a series of aftershocks in a classical earthquake fashion. The main shock ( $M_L = 3.2$ ) took place  $\sim$ 22 km northwest of the site and was of such magnitude that sensitive instruments throughout the state measured it. This event, one of several associated with the Nacimiento Mountains fault zone, demonstrates that this fault system is still active. As of January 1977, no other significant shocks have been recorded near the site by the seismic network.

During 1975 and 1976 attempts were made to measure the noise generated by hydrofracturing experiments at depths of  $\sim$ 2900 m within boreholes penetrating the Precambrian granitic rocks. Because surface stations of both the close-in

and on-site seismic nets were unable to separate these events from background noise, special downhole geophones were installed to monitor these activities. To date, the seismic nets have not recorded a measureable surface seismic event caused by operations at the Fenton Hill project.

4. Hydrology.<sup>3</sup> The geothermal site is situated near major drainages that support natural fisheries and contribute water supplies to several small towns and villages. Any effects on these surface waters must be documented and potential relationship to the project's operation examined. In addition to the surface water problem, the potential exists for pollution of aquifers because of the nature of the experiments. Therefore, base line data were established to document the water quality of the region before and after establishing the HDR Facility.<sup>14</sup>

In 1973, a preliminary study was made of both surface and ground waters in drainages surrounding the site. This study relied on both a literature search for information before 1971 and summaries of field data collected between 1971 and 1973. In 1974, additional data were taken from springs in the Lake Fork Canyon and on the Jemez River and from several surface locations adjacent to the site. In 1975 and 1976, 9 surface water stations and 14 ground water stations were monitored in the various drainages. These data were augmented by samples taken from storage ponds and borehole fluid at the site.<sup>15,16</sup>

Chemical analyses were made to determine levels of silica, calcium, magnesium, sodium, carbonate, bicarbonate, sulfate, chloride, fluoride, nitrate, and total hardness. Measurements were also made for total dissolved solids, conductance, and acidity. All analyses were conducted according to the procedures outlined in Ref. 16.

Results of the chemical analyses for water quality are summarized in Tables I-III.<sup>14,17</sup> These data represent one ground water station, one surface water station, and the two holding ponds at the HDR Site. No significant differences were observed in either the surface or ground water samples. However, some fluctuations did occur seasonally within years and seasonally between years. These data show that there is little difference between the ground water (potable supply) and surface water adjacent to the site. The ground water is slightly higher in silica ( $\text{SiO}_2$ ), whereas the surface water

is higher in calcium (Ca). This difference is expected because of the soil and rock material in contact with these waters.

The water from the holding ponds at the site has been used for various experiments. These waters have become contaminated by various elements and compounds that have changed their chemical composition (see Table III). Nevertheless, these waters will be treated by various processes before release to the local environs pursuant to a National Pollutant Discharge Elimination System (NPDES) permit, presently in review by EPA.

a. Surface Water.<sup>7,14</sup> Surface water in the tributaries (Redondo, Sulphur, and San Antonio Creeks) to the Jemez River is analyzed continually to determine if any effect on the water quality results from geothermal operations

TABLE I  
WATER QUALITY ANALYSIS FOR HORSESHOE SPRING<sup>a</sup>

	<u>1974</u>	<u>1975</u>	<u>1976</u>	<u>Mean</u>
Silica <sup>b</sup>	78.5	83.7	73.3	78.5
Calcium	11.0	10.7	12.3	11.3
Magnesium	3.5	2.7	3.7	3.3
Sodium	17.2	15.0	16.3	16.2
Carbonate	0	0	0	0
Bicarbonate	74.0	62.7	65.7	67.5
Sulfate	6.0	3.8	3.2	4.3
Chloride	10.0	4.7	3	5.9
Fluoride	0.3	0.2	0.3	0.3
Nitrate	0.2	0.2	0.2	0.2
Total dissolved solids	181.0	154.7	171.3	169.0
Total hardness	42.0	38.7	46.0	42.2
Specific conductance (mS/m)	15.5	13.8	14.7	14.7
pH	7.5	7.2	7.8	7.5

<sup>a</sup>Ground water station near the HDR site.

<sup>b</sup>Chemical analyses in milligrams/liter.

TABLE II  
WATER QUALITY ANALYSIS FOR SAN ANTONIO CREEK<sup>a</sup>

	<u>1974</u>	<u>1975</u>	<u>1976</u>	<u>Mean</u>
Silica <sup>b</sup>	47.8	51.0	51.3	50.0
Calcium	16.2	16.7	15.0	16.0
Magnesium	2.6	3.0	5.6	3.7
Sodium	14.8	12.7	13.3	13.6
Carbonate	0	0	0	0
Bicarbonate	69.6	70.0	62.7	67.4
Sulfate	9.4	6.4	6.8	7.5
Chloride	4.8	2.3	3.0	3.4
Fluoride	1.1	0.9	1.2	1.1
Nitrate	0.2	0.1	0.1	0.1
Total dissolved solids	190.0	159.3	168.3	172.5
Total hardness	50.4	54.7	60.7	55.3
Specific conductance (mS/m)	15.2	17.0	16.2	16.1
pH	7.7	8.0	7.5	7.7

<sup>a</sup>Surface water station near the HDR site.

<sup>b</sup>Chemical analyses in milligrams/liter.

TABLE III  
WATER QUALITY ANALYSIS FOR HOLDING PONDS<sup>a</sup>

	<u>1974</u>	<u>1975</u>	<u>1976</u>	<u>Mean</u>
Silica <sup>b</sup>	61.4	49.3	119.2	76.6
Calcium	56.2	42.2	24.2	40.9
Magnesium	5.9	3.2	5.8	5.0
Sodium	868.1	120.0	358.3	448.8
Carbonate	213.5	77.5	55.7	115.6
Bicarbonate	1006.9	244.5	386.3	545.9
Sulfate	492.4	173.7	159.8	275.3
Chloride	831.5	145.0	271.7	416.1
Fluoride	3.1	1.1	11.3	5.2
Nitrate	26.3	0.8	1.6	9.6
Total dissolved solids	3840.2	1210.5	1345.7	2132.1
Total hardness	163.5	119.0	84.7	122.4
Specific conductance (mS/m)	482.3	171.8	215.7	289.9
pH	9.3	8.4	8.1	8.6

<sup>a</sup>Water holding ponds at the HDR site.

<sup>b</sup>Chemical analyses in milligrams/liter.

in the Valles Caldera. The Rio Cebolla below Lake Fork Canyon and the Rio Guadalupe above the Jemez River are monitored because of surface run off from the site and contributions of ground water from volcanic rocks underlying the site. The base of streams in the Jemez River drainage is from shallow ground water systems in the Valles Caldera and thermal or mineral springs. The base flow in the Rio Cebolla is mainly from springs discharging from volcanic rocks that form the western flank of the Valles Caldera. The volcanics are underlain by a thick section of sediment that forms a perching layer for water in the volcanics. Each base flow source has a chemical characteristic that may be modified by snowmelt or rainfall run off. Thus, the chemical quality of the surface water can vary widely with the changes in discharge because of precipitation in the drainage area. The discharge of mineral springs into a reach of the stream has a significant effect on water quality.

There are three surface water gaging stations operated by the US Geological Survey (USGS) on the Jemez River and Rio Guadalupe. The operation of stations near Location J and Q, shown on Fig. 8, was funded by LASL for the years 1973-1974. The station at Location J is on the Jemez River below the confluence of the East Fork of the Jemez and San Antonio Creek. The drainage area above the station is 448 km<sup>2</sup>. Discharge at the station includes the run off from the Valles Caldera, as well as adjacent areas. The station at Location Q is on the Rio Guadalupe above the confluence with the Jemez River. The drainage area above the station is 609 km<sup>2</sup>. Discharge at the station includes drainage from the western rim of the Caldera and the flanks of the mountains to the west. Canyons with intermittent streams north and south of the Fenton Hill Site drain into the Rio Guadalupe. The station at Location R is on the Jemez River below the confluence of the Rio Guadalupe as shown on Fig. 8. The drainage area above the station is 1220 km<sup>2</sup>. Discharge at the station includes run off passing through the stations at Location J and Q as well as some stream discharge.

Stream flow characteristics at the three stations are well defined, with over 16 years of continuous records. The annual volumes of water at the stations at Locations J and Q can be estimated from records of the station near Location R. A hydrograph was prepared to estimate the annual volumes of water passing stations at Locations J and Q using the station at Location R for control as shown on Fig. 9. The latter is equipped with a digital, as well as

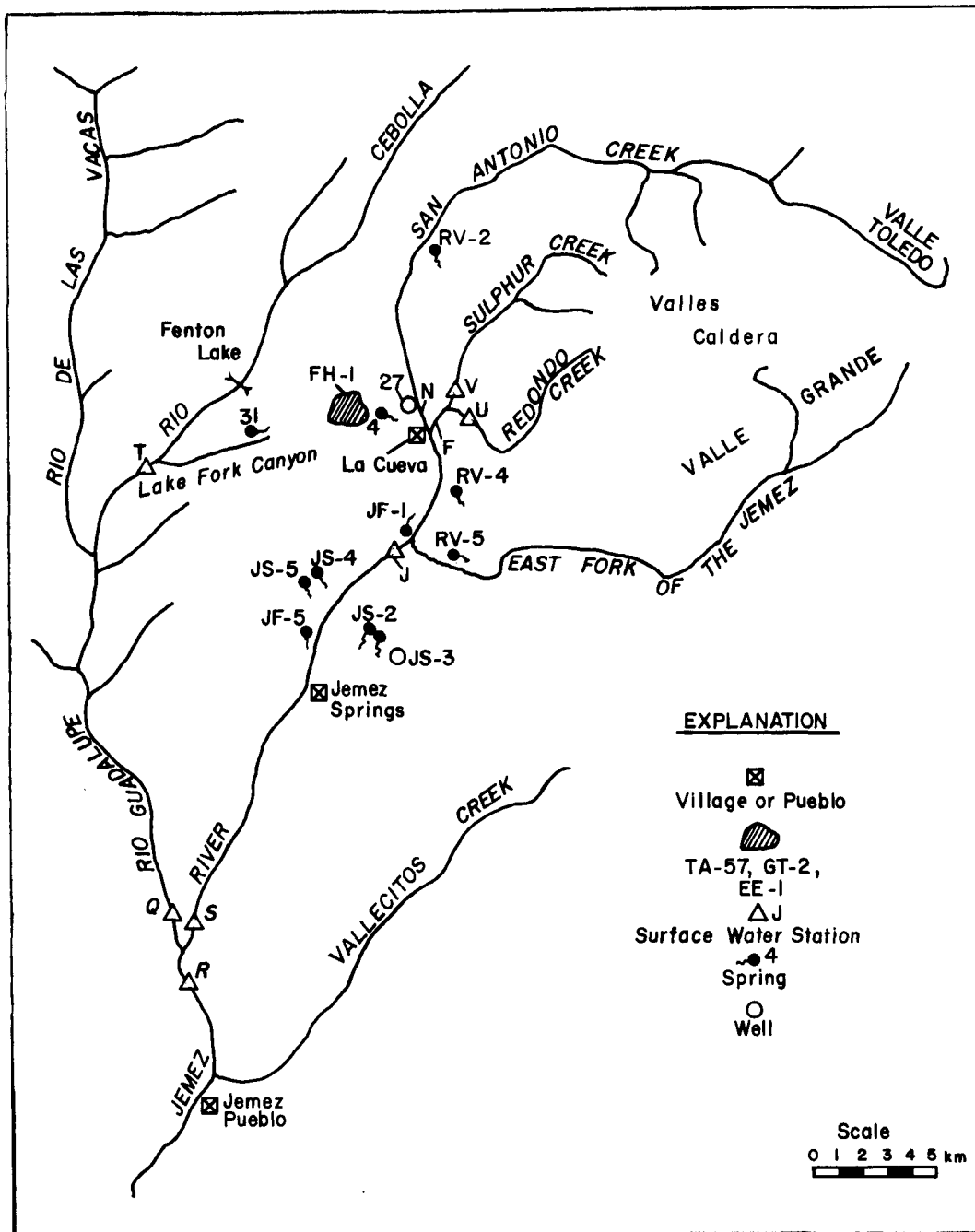


Fig. 8. Location of sampling stations.

F	Sulphur Creek	JS-4, -5	Jemez water supply
J	Jemez River	4	La Cueva water supply
N	San Antonio Creek	JF-1	Limestone Spring
Q	Rio Guadalupe	JF-5	Soda Dam
R	Jemez River	27	Hofheins Flowing Well
S	Jemez River	31	Cold Spring
T	Rio Cebolla	RV-2	San Antonio Hot Spring
U	Redondo Creek	RV-4	Spence Spring
V	Sulphur Creek	RV-5	McCauley Spring
JS-2, -3	Jemez Springs water supply	FH-1	Fenton Hill water supply

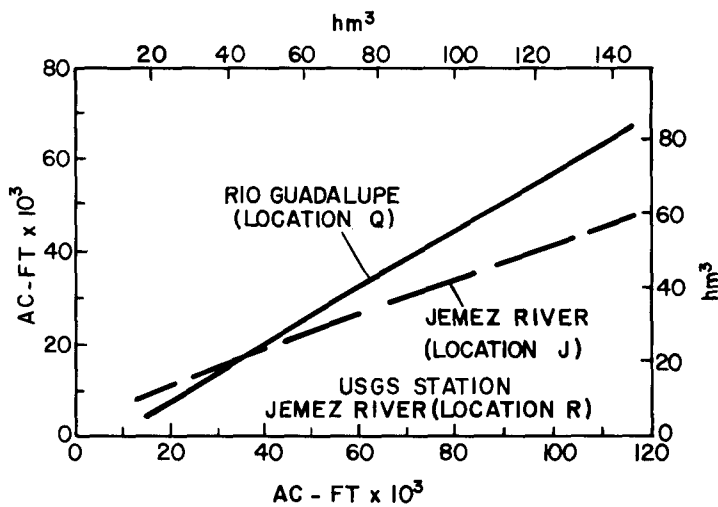


Fig. 9. Hydrograph to estimate volume of flow near Locations J and Q from US Geological Survey records from gaging station near Location R.

a standard water-stage recorder. Thus the day, hour, and peak discharges can be determined.

The discharge at the three stations ranged from 0.09 m<sup>3</sup>/s to 64 m<sup>3</sup>/s during the period 1960-75. The ratings are accurate to  $\pm 10\%$ ; thus, with the variable discharge, any small increase or decrease in flow would be impossible to determine. The USGS concurred that no additional useful data could be obtained by continued operation of the stations near Locations J and Q, and the stations were abandoned in June 1976.

Several elements in the reservoir rock are known to be relatively soluble and therefore transportable to the surface in the heat-transfer water. They are arsenic, cadmium, fluoride, boron, and lithium. These elements can cause adverse environmental effects if the concentrations are sufficiently high in any waters leaving the site. However, these materials and any others found that are thought to cause adverse effects will be removed or concentrations sufficiently reduced from effluent waters pursuant to NPDES permit requirements.

b. Ground water. Several zones of subsurface water exist at the Fenton Hill Site below the 137-m (450 ft) zone from which the presently permitted water is produced. An interpretation of the drill cutting sample from GT-2, located within 152 m (500 ft) of the location for the proposed water well, shows four sandstone zones perhaps containing water in suitable quantities. These zones are described in descending order.<sup>18,19</sup>

#### Abo formation

305-320 m (1000-1050 ft): 15.2 m (50 ft) of coarse, subround to angular, loosely consolidated sand of a beach or channel type. Geophysical log data interpretation indicates 18-20% porosity and relatively fresh water. This zone should contain about 12 330 m<sup>3</sup> (10 ac-ft) per acre drained. Assuming 16-hectare (40-acre) drainage area and 30% recovery factor, production of 273 000 m<sup>3</sup> (60 Mgal) is feasible.

#### Madera formation

440-450 m (1440-1480 ft): 12.2 m (40 ft) of well consolidated tight, fine-ground calcareous sandstone. Geophysical log data interpretation indicates this zone to be tight and impermeable.

460-470 m (1520-1540 ft): 6.1 m (20 ft) of large grained to pebbly, sub-rounded calcareous sandstone. Geophysical log data interpretation of a zone between 475-485 m (1560-1590 ft) indicates 13-17% porosity with 34% porosity in the interval of 475-479 m (1560-1570 ft). The water appears to be brackish and is estimated to be 5200 ppm salt equivalent.

540-550 m (1770-1800 ft): 9.1 m (30 ft) of arkosic sandstone or granite wash. Geophysical log data interpretation indicates this zone to be only fair.

584-733 m (1916-2404 ft): lost circulation zone thought to be predominantly cavernous to fractured limestone with some light gray, gummy clay.

#### Top of Granite

733 m (2404 ft).

Although each of these four zones are thought to contain water, they are untested. The two zones felt to be the most promising are the sandstones in the Abo at 305 m (1000 ft) and the Madera at 540 m (1770 ft), although the lost circulation zone between 584-733 m (1916-2404 ft) cannot be overlooked. The shallower Abo sand would, of course, be preferable because of reduced costs for drilling and pumping, if a sufficient quantity of water is found.

In descending order, the first aquifer encountered is in the volcanics that overlie the Abo Formation. This volcanic aquifer is perched on the Abo

that acts as an aquatard to any downward percolation. The volcanics were deposited on a well developed erosional surface cut into the Abo. It has been noted that some of the springs discharging from the volcanics do so at the outcrop of these ancient drainage channels in the Abo. This suggests that the Abo drainage system controls the principal flow of ground water in the overlying volcanics. The general absence of springs along the outcrop of volcanics implies that the saturated zone in the volcanics does not extend much above the top of the drainage channels. This is substantiated somewhat by Testholes A and B, both of which are dry in the volcanic section of the holes. The water-supply well at Fenton Hill apparently encountered an artesian zone in the volcanics. This is based on the fact that water rose 3 m (10 ft) in the well when the aquifer was penetrated. The specific capacity of the well of 6.4 l/s (100 gpm) per 0.3 m (1 ft) of drawdown indicates a higher permeability than that found at the outcrop. This permeability coupled with a propinquity to potential discharge boundaries would also seem to argue that the Fenton Hill aquifer is confined or it would be quickly drained. Very few springs or wells produce from the Abo.

Underlying the Abo formation at a depth of 375 m (1230 ft) is the Magdalena group of shales and limestones. The geophysical logs suggest several possible aquifers in this group. The main water table was encountered at a depth of 533 m (1750 ft) in the Madera formation. All of the aquifers mentioned above this are perched. It appears that even the nearby San Antonio Creek is perched. The main aquifer occurs in a limestone that has cavernous type permeability. The temperature of the water implies that this formation is connected to and possibly draining the thermal water system in the caldera. This formation has some spring discharge to the Jemez creek in the reach from about Battleship Rock to Jemez Springs.

The volcanic aquifer is readily available and because it is confined would not appear to have direct effect on other users' supply. However, the areal extent of the aquifer is not known. It is likely that an aquifer in the Abo would also be confined and disconnected from a general system because many of the sandstones found in the Abo are lenticular in nature. The Madera formation west of the caldera collapse zone is an aquifer with a high permeability and large quantities of water. Withdrawal of 123 300 m<sup>3</sup>/yr (100 ac-ft/yr) of water at Fenton Hill from such an aquifer would probably

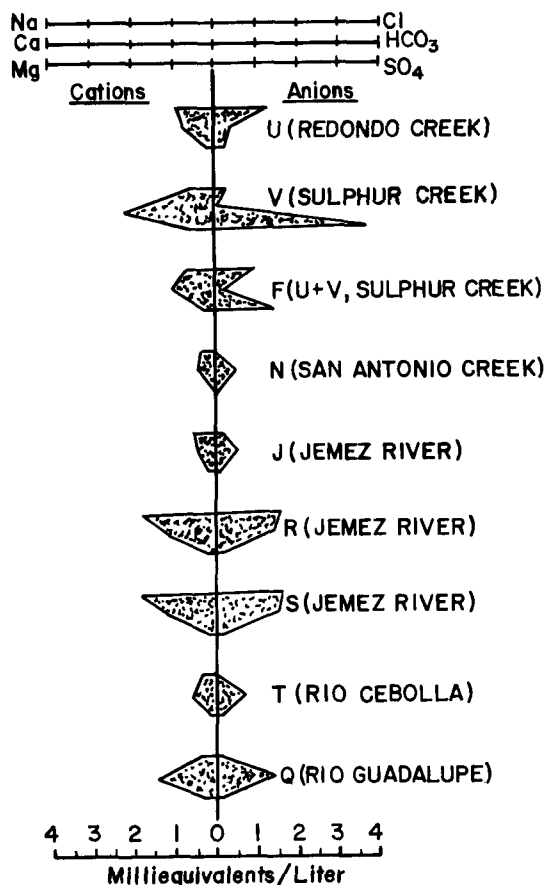


Fig. 10. Chemical analysis comparison of surface water, December 1974.

have little or no effect on any discharge to the surface water system because this quantity of water would have no practical effect on the altitude of the Madera water level. The few points of Madera spring discharge are usually obvious because Madera water contains hydrogen sulfide ( $H_2S$ ) and has a high content of dissolved solids. Because of the poor quality, little beneficial downstream use is made of the Madera water. Figures 10-12 are chemical analysis comparisons of surface water, ground water, and thermal and mineral springs.

To protect the aquifers from potential contamination, the wellbores are cased as shown in Figs. 13-15. GT-2 was drilled with a 17-1/2-in. bit with 13-3/8-in. casing set at 480 m (1604 ft) and cemented,

then the hole was redrilled with a 12-1/2-in. bit and 10-3/4-in. casing set at 773 m (2535 ft) and cemented to the surface as shown in Fig. 13. The fresh water zones are thereby double cased to 480 m (1600 ft), and the section below 480 m (1600 ft) is single cased.

EE-1 was drilled to a depth of 741 m (2431 ft) using a 17-1/2-in.-diam. drill bit and 13-3/8-in. casing set and then redrilled using a 12-1/2-in.-diam. bit and a 10-3/4-in. casing set and cemented, as shown in Fig. 14. The entire section through the top of the granite is double cased to the surface and cemented, thereby protecting the aquifers from any potential contamination that may result from the operation of the system.

Figure 15 is a schematic of the planned drilling and casing program for hole EE-2, at least through the section above the top of the granite. Noteworthy is the double casing through the section containing the water-bearing zones that protects these aquifers from possible contamination as a

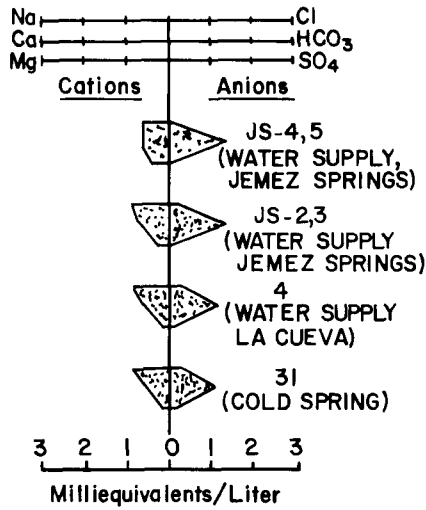


Fig. 11. Chemical analysis comparison of ground water discharges from Cenozoic-Volcanic overlying the Abo formation.

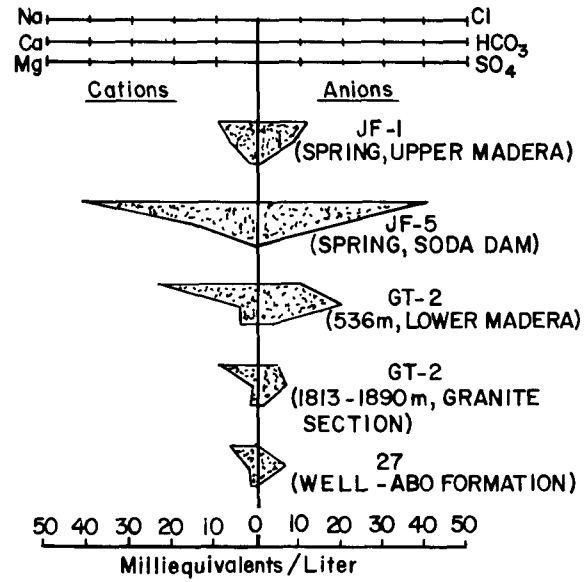


Fig. 12. Chemical analysis comparison from thermal and mineral springs.

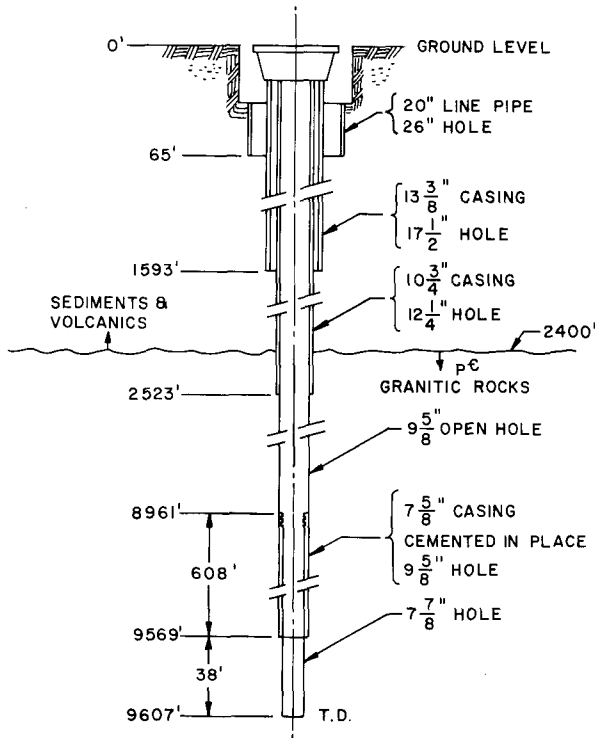


Fig. 13. Schematic of casing diagram of GT-2.

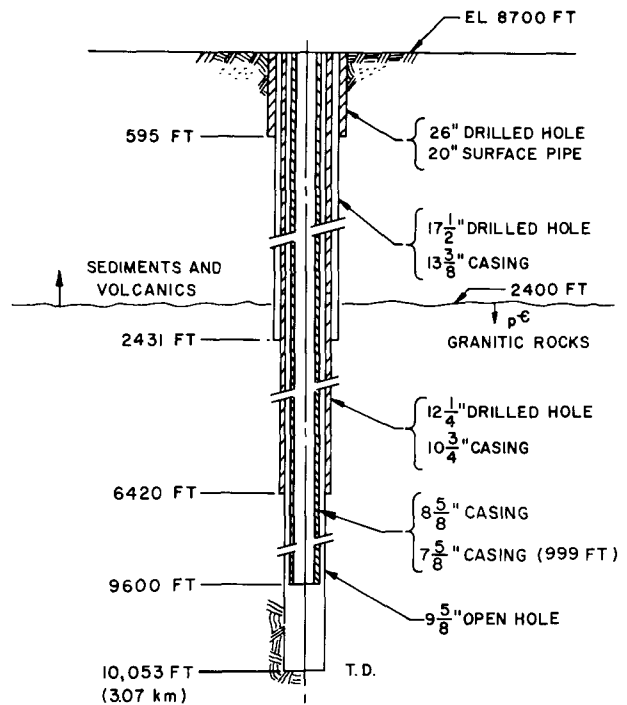


Fig. 14. Schematic casing diagram of EE-1.

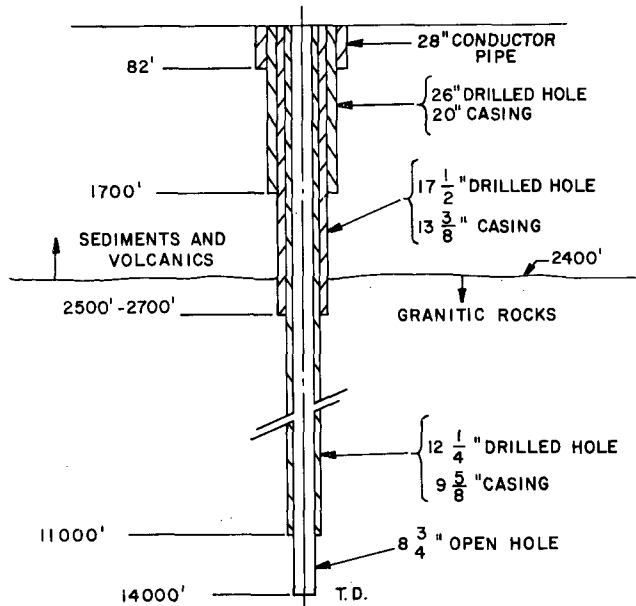


Fig. 15. Schematic casing diagram of proposed EE-2.

result of the the proposed system operation.

To advise and solicit comments, the New Mexico Environmental Improvement Division (EID), Water Quality Section's personnel were conducted on a tour of the Fenton Hill Site and briefed on the potential for water quality problems relative to site operation. Although no written comments have been received, verbal indications have been received, and the EID perceives no conflict with New Mexico Ground Water Regulations.

5. Climatology. The Jemez Mountain range is typical of most southwestern mountains in its general weather patterns. The climate is characterized by localized convective shower activity during the summer and

more regional major storms during the winter. Total precipitation received generally increases at higher elevations; however, the irregular terrain causes irregularities in the storm patterns.

Temperatures of the region are generally mild, with few days exceeding  $32^{\circ}\text{C}$  in the summer and few nights dropping below  $-18^{\circ}\text{C}$  in the winter. Nevertheless extreme diurnal fluctuations in temperature can occur. For example, in the spring, daytime temperatures may rise to  $20^{\circ}\text{C}$  and nighttime temperatures may drop below freezing ( $0^{\circ}\text{C}$ ).

Although some generalizations about the weather patterns can be made, specific events in these mountains tend to be localized. The localization makes it impossible to extrapolate weather events from one area to another. Because of the lack of climatological information at or near the site a few basic weather parameters were measured to determine the climatic regime of the area and to characterize prevailing wind patterns. These data will be used to determine where potential environmental contaminants released from the site

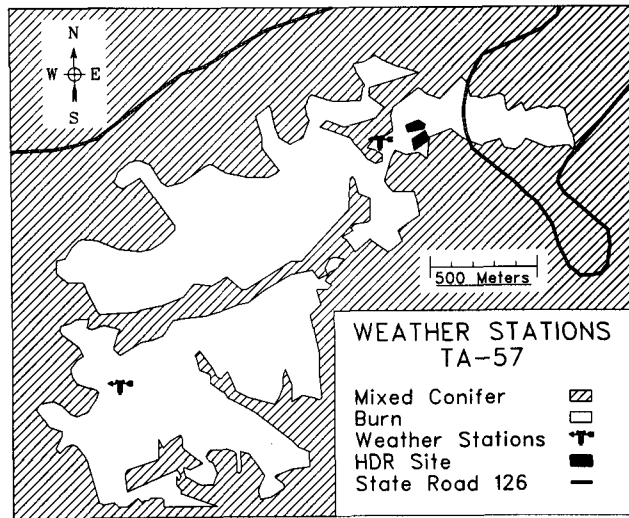


Fig. 16. Location of the weather stations near the site.

will go and to explain variations in biological measurements that may be linked directly to climatological phenomena.

A weather station was established in 1975  $\sim$ 150 m west of the site (LASL Technical Area 57 is TA-57). Its location, shown on Fig. 16, is as close to the site as possible to minimize the effects of surrounding terrain and structures upon air flow patterns. The station consists of a Meteorology Research Incorporated (MRI) mechanical weather station and a

weighing bucket rain gauge. The MRI mechanical weather station is mounted on top of a collapsible 9-m tower and records wind run, wind direction, and temperature on a pressure sensitive strip chart. The weighing bucket rain gauge, located  $\sim$ 10 m west of the tower, records precipitation on a strip chart attached to a revolving drum.

Another weighing bucket rain gauge is located on the Plateau  $\sim$ 1500 m west of the site. This gauge, on the periphery of the area set aside for ecological studies, will be used to compare precipitation between the two locations. Some localized convection showers dump large quantities of moisture in nonuniform patterns in this mountainous terrain.

The weather station at the site has been recording data continuously since it became operational in January 1976. The data recorded by these instruments are reduced into hourly averages and put into a form that can be read by a computer. Then they are manipulated into monthly summaries in both graphical and tabular forms. Although no conclusions can be made about weather patterns from such a small data base, several interesting, but expected, phenomena are evident.

Air flow patterns have a distinct seasonal shift. During January the air flow is primarily from the northwest. Air flow patterns shift as the seasons progress into summer; an almost complete reversal is seen during August.

Figures 7 and 8 of Ref. 3 show the normal seasonal sequence of continental air flow patterns.

Precipitation at the site also followed the pattern expected for semiarid southwestern mountain ranges. During the winter months, precipitation was a more or less random event and did not follow a predictable pattern. Table IV gives 1976 summaries by month for temperature, precipitation, and wind power. These data show that it was fairly dry at the site in 1976--only 35.66 cm of precipitation were recorded. Temperatures at the site were relatively mild with the extremes being between  $-23^{\circ}$  and  $27^{\circ}\text{C}$  for winter and summer, respectively.

6. Aesthetics. A portion of the existing site can be seen from State Highway 126 by visitors to the area. Figure 17 is a photograph showing the site as it would appear to a passer-by. The tower in the foreground is the superstructure over hole EE-1 that is 12.2 m (40 ft) high. The facility has

TABLE IV  
TEMPERATURE, PRECIPITATION, AND WIND SUMMARIES FOR 1976

	Temperature ( $^{\circ}\text{C}$ )			Precipitation (mm)	Wind Power Average ( $\text{W}/\text{m}^2$ )
	Av	Max	Min	Total	
January	-6	9	-23	4.8	15.9
February	-3	9	-17	41.4	24.7
March	-3	10	-17	17.5	38.4
April	2	13	-13	21.1	26.9
May	7	19	-6	45.0	16.8
June	14	27	2	6.1	20.9
July	14	26	5	74.9	7.9
August	13	24	5	69.1	7.9
September	10	22	-1	45.7	7.4
October	3	18	-8	4.8	13.9
November	-1	13	-23	17.5	10.8
December	-4	9	-14	8.6	9.6
Total				356.6	201.1
Average	3.8	16.6	-9.2	29.7	16.8

the appearance of a small industrial development and may be considered as aesthetically unpleasant in this mountainous forest setting, even though evidence of the 1971 Cebolleta fire still persists and has also marred the natural beauty of the area.

The facility is within a travel-influence zone, and as such, access by casual passers-by will be limited by the perimeter fence. Further, to make the site more aesthetically pleasing, a three member LASL Site Aesthetics and Cleanliness Suggestions Committee has been appointed. Among the actions already taken from the recommendations of this committee were to:

- install a perimeter chain-link fence with a main gate and a 76.2-m (250-ft) length of black vinyl on either side of the gate;
- plant 50 trees between the highway and the site;
- repaint the towers and all surface facilities in earthtone colors;
- remove all excess materials and scrap; and,
- contact the Youth Conservation Corps and arrange the planting of 5000 trees in the vicinity.

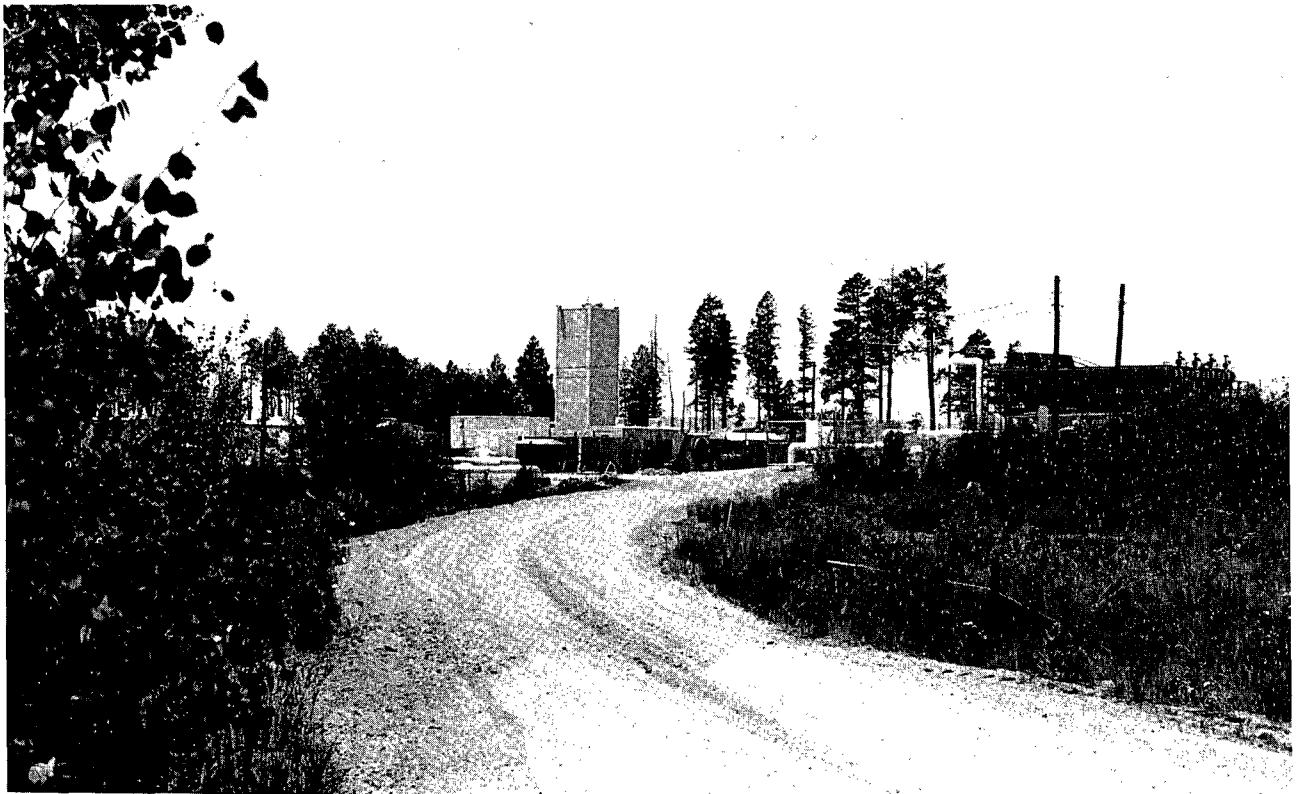


Fig. 17. View of Fenton Hill Site from Highway 126.

Additionally, the new electric power distribution lines within the site are to be buried.

### C. Biological Factors<sup>3</sup>

During 1976 studies were initiated to measure various characteristics of birds, small mammals, elk, and vegetation at the site. These studies established base line data from which we can compare future measurements.

1. Vegetation. Three major vegetative complexes or community types are found at the site. Typical climax vegetation found at 2600-m elevation in northern New Mexico is a mixed coniferous forest or broad ecotone between upper elevation spruce-fir communities and lower elevation ponderosa pine communities. A wildfire in 1971 destroyed parts of this climax vegetation at the site, resulting in the formation of two additional community types. The fire scar was aerially seeded with a mixture of higher elevational pasture grasses and legumes shortly after the fire. One year later, ponderosa pine tree seedlings were planted 3 to 5 m apart. The resultant secondary succession has developed into a grass-forb community interspersed with small stands of aspen suckers.

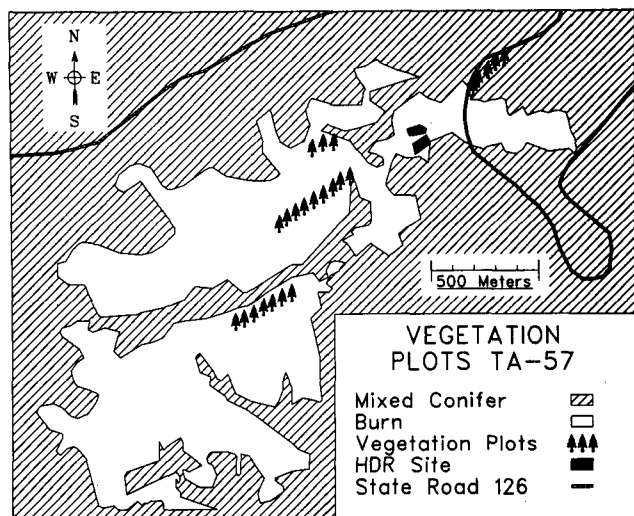


Fig. 18. Location of vegetation transects.

Transects placed in each community type to measure cover and density of the species were read in the spring, summer, and fall during the 1976 field season. The locations of these transects, 5 in the mixed coniferous forest, 3 in the new growth aspen, and 16 in the grass-forb community, are shown in Fig. 18. Taxonomic voucher specimens were collected and are on file at LASL.

After summarizing the 1976 plant population field data by community type, 15 dominant species were selected from which to characterize all community types. Only

those species that contributed at least 0.1% cover in any community type were selected. The cut-off point of 0.1% cover eliminated those species that did not contribute significantly to the total vegetative biomass, yet it left enough species so that a good cross section of the dominants was found within all community types. As expected, the mixed coniferous community is dominated by tree species with a rich understory of shrubs. Douglas fir and white fir species (*Pseudotsuga menziesii* and *Abies concolor*, respectively) make up about three-fourths of the areal tree cover within this community type, with the rest being predominantly ponderosa pine. Aspen has cover values equivalent to several of the understory shrubs.

Unlike the other two communities, the aspen community is dominated by aspen (*Populus tremuloides*). However, there is an understory of shrubs and grass that represents species from both the mixed coniferous and grass-forb communities.

The mixed coniferous community has ~50% more areal cover than the other communities. This represents almost four times the areal cover found in the grass-forb community and about one-third more areal cover than is found in the aspen community.

The same types of differences seen in vegetation parameters between the various communities are seen within the nonliving ground cover. Table V gives the average ground cover by category for each community. The grass-forb

TABLE V  
AVERAGE PERCENTAGE OF GROUND COVER BY COMMUNITY TYPE

	<u>Grass Forb</u>	<u>Mixed Conifer</u>	<u>Aspen</u>
Bare	38.0 ± 8.4 <sup>a</sup>	4.9 ± 5.4	12.6 ± 10.2
Grass	29.5 ± 10.1	1.5 ± 1.4	4.9 ± 0.4
Stick	14.2 ± 6.1	18.9 ± 7.8	20.9 ± 12.5
Gravel	10.2 ± 4.6	0.3 ± 0.8	0.2 ± 0.9
Bark	2.9 ± 2.5	4.2 ± 3.0	13.6 ± 21.5
Leaf	3.7 ± 1.6	23.4 ± 23.4	47.4 ± 21.3
Cobble	1.2 ± 1.1	2.3 ± 3.7	0.2 ± 0.4
Feces	0.3 ± 0.6	0 ± 0	0.2 ± 0.9
Rock	0 ± 0	0 ± 0	0 ± 0
Needle	0 ± 0	41.0 ± 22.6	0 ± 0
Cone	0 ± 0	2.6 ± 4.4	0 ± 0

<sup>a</sup> $\bar{x} \pm s.$

community is dominated by dead grass, the mixed coniferous community has a ground cover dominated by needles, and the aspen community is dominated by leaves. The amount of exposed bare ground is greatest under the grass-forb community and smallest within the mixed coniferous community.

2. Small Mammals. The primary consumers or herbivores are one of the more abundant forms of wildlife in any ecosystem. Because small mammals feed on a large cross section of plant material, they are easily affected by toxic elements released into the environment. Data from studies made to determine small mammal populations surrounding the HDR Site represent a base line for one of the potential bio-indicators of environmental impacts from the LASL HDR Project.

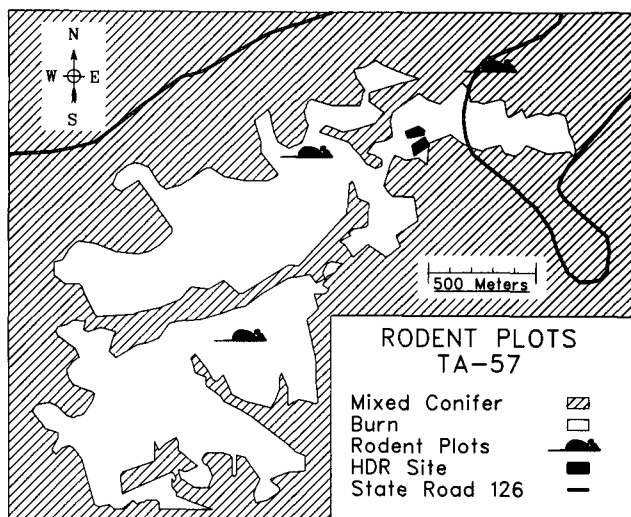


Fig. 19. Location of small mammal traplines.

Small mammals were live-trapped within each community to determine the trap susceptibility of the various species and their relative abundance among the communities. One trapline per community was established as shown on Fig. 19 and checked simultaneously during each trapping session.

Two trapping sessions were held during the 1976 field season. The first session was held in midsummer before the rodent population reached maximum numbers. The second trapping session was held in late summer-early fall to measure peak populations. Data from the two sessions were compared to determine whether the time of trapping has any affect on the interpretation of results.

Each trapping session consisted of two nights of prebaiting to familiarize the rodents with the traps, followed by three consecutive nights of trapping. Traps baited with a mixture of rolled oats and peanut butter were set up in the late afternoon and examined the following morning. This schedule prevented animals from being trapped during the hot part of the day and drastically reduced the chances of mortality as a result of heat exhaustion.

A large square of cotton in each trap gave the rodent something to burrow into, and this reduced the death rate from excessive trauma.

The rodents were classified by species, sex, and age. They were weighed, then marked by a standard toe amputation technique. Dead specimens were tagged, frozen, and stored. These specimens will be used to compare elemental body burdens with specimens caught in the future if we encounter significant changes in rodent populations or if releases should occur at the HDR Site.

In addition to trapping by community type, traps were set up in six areas (three downwind and three down the principal drainage from the site) to establish a data base from which to compare future trapping results. These comparisons will be used to determine if a gradient is established within these rodent populations as a result of the LASL HDR Project and if this project is adversely affecting the local environs.

Within the three vegetative complexes mentioned earlier, the species trapped most often is the deer mouse (*Peromyscus maniculatus*). The data collected show that the grass-forb community contains the highest numbers of small mammals, yet it has the lowest species diversity.

These relationships were expected because the more closed community types offer more habitats and shelters for small mammals. However, most of the small mammals trapped were primarily herbivores, and the grass-forb community has more vegetative biomass within reach of the small mammals. Therefore, the high numbers of small mammals encountered in the grass-forb community could be a result of an abundant food supply, whereas the greater species diversity found in the more closed communities could be an indication of the more diverse forms of shelter.

The high percentage of trappings indicates that these vegetative communities support substantial populations of small mammals. This was also expected because small mammal populations tend to reach high levels in areas that have been disturbed.

3. Elk. With establishment of the grass-forb community on this Plateau, following the wildfire in 1971, this area has become an important winter range for the Rocky Mountain elk (*Cervus Canadensis*). Elk, one of the major big-game species of New Mexico, tend to be disturbed by human activity. Therefore, establishment of the HDR Site on the edge of this burn may eventually result in elk leaving this area.

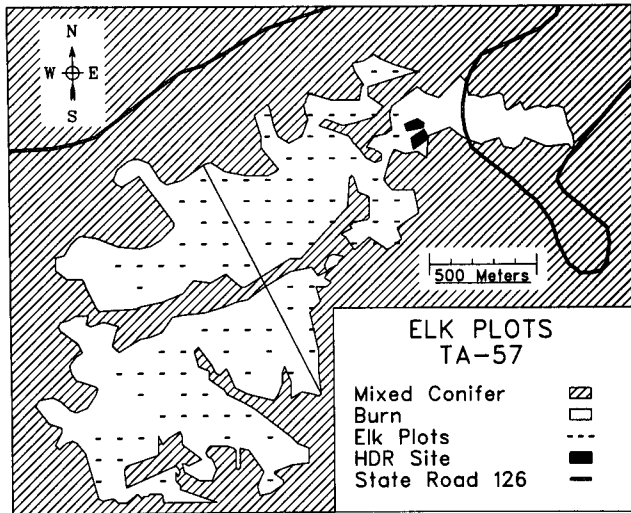


Fig. 20. Location of elk pellet group counting plots.

A stratified random set of permanently marked counting plots for pellet groups (fecal material) was established and read during mid-1976 to document elk usage of this burn area and to create a data base from which to compare future measurements.

The burned area was arbitrarily divided. Approximately 50% of the plots were adjacent to and 50% of the plots were away from the site as shown on Fig. 20. Each pellet group counting plot was 4 m wide by 22 m long. Plots were examined by two persons who physically removed all

pellet groups from the plots and checked each other's work. It was therefore assumed that few, if any, pellet groups were overlooked. Physically removing the pellet groups, rather than marking them, ensures that future examinations will be made on new pellet groups and that the data collected are related to elk usage of the area after establishment of the Fenton Hill facility.

The pellet group counting plots cannot be fully interpreted from the initial set of readings. However, statistical tests between the two areas are nonsignificant, indicating that elk usage within the grass-forb community has been distributed uniformly in the past.

4. Birds. The avian community is perhaps the most mobile faction of wildlife found in any ecosystem. Typically, the avian component will change constantly throughout the year because of the seasonal emigration and immigration of the various species.

Two extensive plots were established on the plateau, one adjacent to and one away from the site, to describe the avian community dynamics and to quantify the impacts on these populations from the facility, as shown on Fig. 21.

The study plot adjacent to the site (the well site) is ~250 m wide by 500 m long. This plot falls mostly within the mixed coniferous community. Parts of this plot have been encroached upon by expansion of the site. The

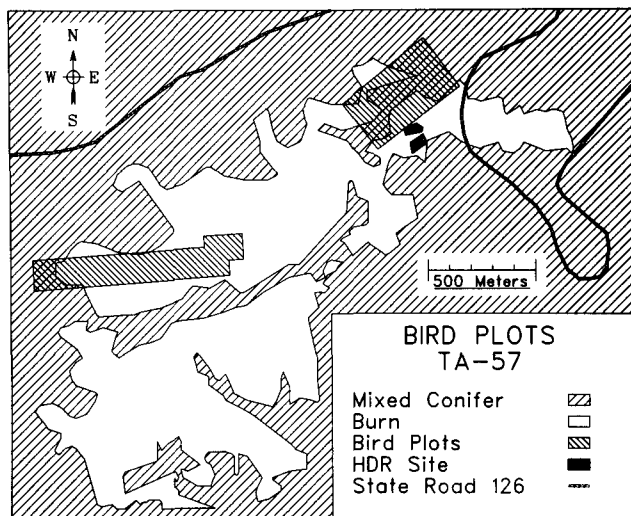


Fig. 21. Location of bird counting transects.

study plot, which is ~1000 m west of the site, is ~150 m wide by 1000 m long and predominantly falls within the grass-forb community.

Both plots were examined seasonally during 1976 by personnel who walked specific lines through the plots at 50-m intervals. The number and species of birds were recorded, together with personal observations about their suspected activities. These data were reduced into nesting pairs by species per unit area, densities of resident and transient species, and an overall categorization of the avian component of this ecosystem.

Of the many transient bird species recorded during the census period, 41 species were identified. The high elevation and cold weather, however, prevented most birds from nesting and becoming residents.

Table VI gives the estimated nesting populations from data collected from both study plots. The greater number of nesting pairs recorded at the well site can be explained by the community type that dominates the area. The plot adjacent to the site falls within a predominantly mixed coniferous community, whereas the plot away from the site falls within a grass-forb community. The mixed coniferous community should allow more nesting sites and subsequently more nesting pairs of birds.

5. Endangered Species. Several animals on the Endangered Species List have been sited in the general area. The Jemez Mountain salamander is relatively widespread in the vicinity of Valle Grande, and its range may extend westward to the Fenton Hill Site. However, this salamander is thought to be generally confined to the canyons rather than the mesas.

Sightings of peregrine falcon have been noted in the vicinity of the site, but no nesting areas have been found. Page 36 of the Geothermal Leasing Final Environmental Impact Statement states that several other unique and endangered

TABLE VI

ESTIMATED NESTING POPULATIONS AT THE WELL SITE  
AND OPEN MESA SITE DURING THE SUMMER OF 1976  
(Pairs Per 40.5 hectare)

<u>Species</u>	<u>Well Site</u>	<u>Open Mesa Site</u>
Black-chinned hummingbird	5	4
Common flicker	5	7
Yellow-bellied sapsucker	2	4
Hairy woodpecker	5	2
Traill's flycatcher	2	---
Western wood pewee	5	---
Violet-green swallow	7	---
White-breasted nuthatch	2	---
Pygmy nuthatch	5	---
House wren	5	2
American robin	2	---
Western bluebird	7	2
Warbling vireo	2	---
Yellow-rumped warbler	5	---
Western tanager	12	---
Cassin's finch	2	---
Green-tailed towhee	---	11
Gray-headed junco	7	4
Total	80	36

species may inhabit the area and include Rio Grande cutthroat trout, the southern bald eagle, the osprey, and the black-footed ferret. Several of the species listed in Table VII have only historical records of occurrence in the region and, in fact, have long been absent. None of them are known to breed in or inhabit the immediate vicinity of Fenton Hill because the area is a nearly flat mesa with no surface water.

#### D. Social and Economic Factors

Two villages in the vicinity of the site are La Cueva and Jemez Springs. La Cueva is located 2.4 km (1.5 mi) south of the site and has a permanent population of ~50 persons. Jemez Springs, located 13 km (8 mi) south of the site, has a population of ~500. Prior to the development at Fenton Hill and the Union Oil/Public Service Company (Baca Location) geothermal site, the area was visited by tourists. Although the villages of La Cueva and Jemez Springs were previously undergoing a slow growth, a mild acceleration of that growth

has been experienced as a result of the geothermal developments presently under way. The population of La Cueva, in particular, periodically experiences temporary growth from trailer residences brought in by the drilling crews working at either Fenton Hill or Baca. To date these increases have not posed the "boom town" problems experienced at other much larger development areas. However, as a result of the small influx, both La Cueva and Jemez Springs have experienced a minor economic growth but will remain rural-type villages.

TABLE VII

ANIMAL SPECIES LISTED AS ENDANGERED BY THE STATE OF NEW MEXICO

<u>Species</u>	<u>State Endangered Group<sup>a</sup></u>
Mammals	
Marten ( <i>Martes Americana origenes</i> )	II
Black-footed ferret ( <i>Mustela nigripes</i> )	I <sup>b</sup>
Mink ( <i>M. vison energumenos</i> )	II <sup>c</sup>
Jaguar ( <i>Felis onca arizonensis</i> )	I <sup>b,c</sup>
Birds	
Zone-tailed hawk ( <i>Buteo albonotatus</i> )	II
Bald eagle ( <i>Haliaeetus leucocephalus</i> )	I <sup>b</sup>
Osprey ( <i>Pandeion haliaetus carolinensis</i> )	II
Peregrine falcon ( <i>Falco peregrinus anatum</i> )	I <sup>b</sup>
Whooping crane ( <i>Grus americana</i> )	I <sup>b</sup>
Blue-throated hummingbird ( <i>Lampornis clemenciae</i> )	II
Broad-billed hummingbird ( <i>Cyananthus latirostris</i> )	II
Red-headed woodpecker ( <i>Melanerpes erythrocephalus caurinus</i> )	II
Baird's sparrow ( <i>Ammodramus bairdii</i> )	II
Amphibia	
Jemez Mountain salamander ( <i>Plethodon neomexicanus</i> )	II

<sup>a</sup>State endangered group: I, species whose prospects of survival or recruitment in the state are in jeopardy; II, species whose prospects of survival in the state may become in jeopardy in the foreseeable future.

<sup>b</sup>Listed by the federal government as endangered.

<sup>c</sup>Historical record only.

Source: J. P. Hubbard, M. C. Conway, H. Campbell, G. Schmitt, and M. D. Hatch, Handbook of Species Endangered in New Mexico, New Mexico Department of Game and Fish, 1978.

Several Indian reservations exist in the region as shown in Fig. 22. These Pueblo Indian populations are small and tend to maintain a remote interaction with outside populations and developments. One perceivable, although remote, impact to these reservations would be a reduced water resource as a result of the subsurface water produced at Fenton Hill. The hydrology of the area between the Fenton Hill Site and the several reservations is not well known. As pointed out earlier, the water zones of this area are lenticular and the water is thought to be perched, or confined, or both. Therefore, water withdrawal at Fenton Hill should not affect any water supply available to the reservations.

#### IV. EFFECTS OF IMPLEMENTATION

Actions to be taken to minimize undesirable effects include dust control measures, reseeded of cut and fill areas, disposal of slash, placement of underground lines, and appropriate paint color selection.

##### A. Land Status and Uses

After completion of the drilling, redrilling, and construction of new facilities, the EE-2/EE-1 loop system will be operated for an extended fluid-circulation experiment. The system is designed to operate continuously for at least six months. For routine facility operation, there will be about 12 persons on the site during the daytime hours and 5 persons during night and weekend hours as operating and maintenance staff.

Should an excavated water-storage pond be used, additional land will be required. However, the pond could eventually provide water for wildlife and serve as a reservoir for USFS fire-fighting activities.

##### B. Physical Factors

1. Geography and Topography. Facilities, such as the portable experimental generating unit and the greenhouse structure, will be placed within the new fence and will not require new clearing or alteration of the topography. They will alter the appearance of the complex only slightly and should not result in any significant impact.

Soil disturbance will be minimized when placing underground water, power, and telephone lines by using a hose lay ripper.

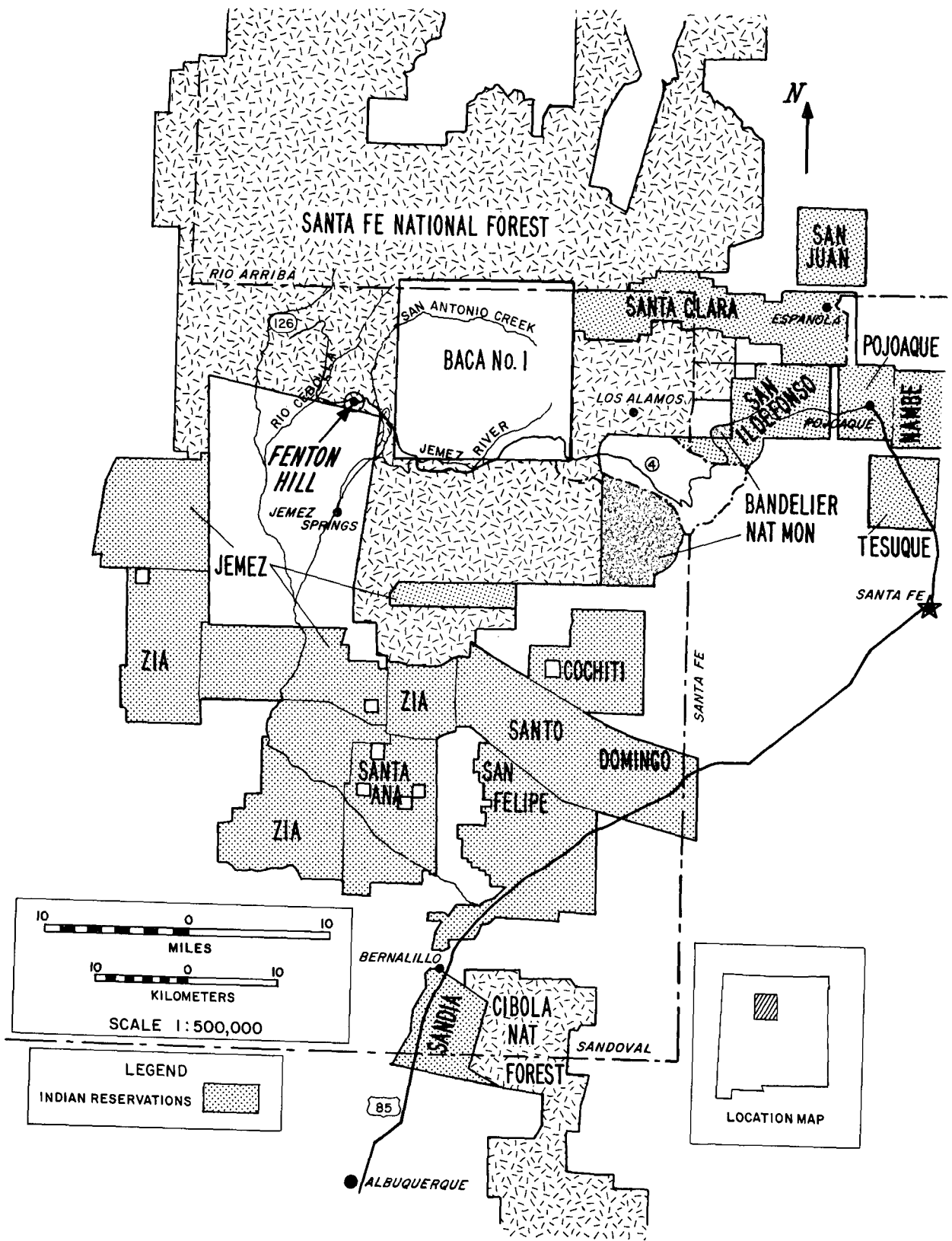


Fig. 22. Indian reservations in the vicinity of the Site.

Approximately 5.5 hectares (13.5 acres) of land have been modified. This includes well pads, holding ponds, buildings, towers, movement of roads, etc. This disturbed land mass should now remain essentially constant, limited to the area within the boundary fence, except for the possible construction of the new water-storage facility and seismic monitoring stations.

Ground surface subsidence is not expected to occur. The fracture system will be created at great depth,  $\sim 4$  km (13 000 ft). The fracture is expected to be pancake-shaped, with a radius of a few hundred meters, and vertically oriented. Even after several years of circulation, a porous zone is not expected to be more than about a meter (a few feet) thick. Thus, the overlying competent crystalline rock should provide adequate support. Furthermore, pressure will be maintained to at least a hydrostatic level in the zone during the entire experiment, and the fracture will be left filled at the conclusion. Ground levels and tilt are being monitored before, during, and after the experiments to fully document the actual situation.<sup>13</sup>

2. Geology. No perceivable changes to the geology will occur except that a portion of the deep-seated granite will be artificially fractured and a small amount of the dissolved mineral content will be removed and transported to the surface. This dissolved material when separated at the surface will resemble the products of weathered granite and should not be objectionable.<sup>20</sup>

3. Seismology. Several of the most important factors controlling or indicating the possibility of earthquakes induced by fluid injection are: (1) the presence of known faults or large subsurface fractures; (2) high levels of ambient tectonic stress (sometimes indicated by pre-existing or on-going seismic activity); and (3) a hydrologic regime dominated by subhydrostatic pressures below the water table. The combination of careful site selection with regard to both existing faults and natural earthquakes, controlled injection and operating pressures, and modest fluid volumes make it appear that the earthquake hazard associated with the proposed operations is extremely small. Nevertheless, the risk must be taken seriously.

a. Activities at the Fenton Hill Site. After EE-2 has been drilled to the desired depth, hydraulic fractures will be produced near the bottom of the wellbore by pressurization using fluid pumped into the wellbore. The array of

seismic detection systems will be active during pressurization to record microseismic events that may result from the fracturing operation. During hydraulic fracturing experiments in 1975, a geophone package in the wellbore near the zone being fractured detected a number of acoustic emissions (much too small to be called microearthquakes), and their signal levels were so low that no signal was observed at surface seismic stations where the amplification is limited by the ambient (background) noise. Surface stations have located events >15 km (9 mi) away whose magnitudes were as small as  $M_L = -1.5$ .

When hydraulically fracturing at greater depths and higher temperatures, we expect that the differential stresses will not be significantly greater than in the shallower existing fractured region; and therefore, there should be no change in the induced seismicity risk. Despite the low earthquake risk at the site, seismograms are closely monitored during the hydraulic fracturing experiments. Any observed local activity would be cause to reduce the flow pressure. If any seismic event occurs within a few kilometers of Fenton Hill that is either felt or the duration of humanly imperceptible ground motion exceeds 3-1/2 min, the pumping operations will be stopped and the wellbore pressure reduced immediately. Thereafter the system will be operated only when the source region is identified, and there is no likelihood of triggering a damaging earthquake ( $M_L > 3$ ). Based on water injection experiences at the Rocky Mountain Arsenal in Colorado, this action should avoid triggering an earthquake.<sup>21</sup> To establish a base line of natural seismic activity, measurements of the seismic background in the area are being made continuously.

b. Other Activities in the Area and Adjacent Regions.<sup>13</sup> Confusion in observed seismic signals could occur between the activities at Fenton Hill and other manmade and natural causes in this area. As indicated above, the regional network has a locational accuracy of  $\pm 5$  km or better for events having magnitudes above  $M_L = 1/2$  to 1 over most of the area of the Jemez Mountains. Any significant source beyond 10 km from Fenton Hill can reasonably be assumed to be not connected with project activities. Three classes of man-caused sources need to be considered in this connection: (1) mine blasting operations, (2) possible triggered earthquakes from the filling of Cochiti Reservoir on the Rio Grande, and (3) possible induced seismic signals from the Union Oil Company's geothermal operations on the Baca Location property  $\sim 7$ -10 km east of the Fenton Hill Site.

(1) Mine Blasting. The closest significant mining activity to Fenton Hill is the Earth Resources Company open pit copper workings at the mouth of Senorita Canyon (near Cuba, NM) about 23 km northwest of Fenton Hill. Ripple-fired charges of <454 kg (1000 lb) of ammonium nitrate usually occur at shift change times during working days and do not appear as noteworthy events on the regional network records. The mine has been either closed or only operated intermittently. The blasting location can easily be identified by the arrival times of the seismic waves at the Eureka Mesa station <5 km northeast.

(2) Filling of Cochiti Reservoir. Cochiti Reservoir is 42 km southeast of Fenton Hill, and events at the two sites are easily separable by arrival time readings at regional network stations.

(3) Union Oil Geothermal Development Area. The Union Oil development program involves utilization of steam or hot water from wells along Redondo Creek on the Baca Location property. Not enough information is available concerning details of fluid injection or withdrawal to adequately evaluate whether triggered seismicity is a credible possibility. No significant seismic events have been observed at the seismic stations from this area. Because the Fenton Hill and Union Oil Co. sites are separated by only 7-10 km, it could be difficult to determine responsibility for events occurring approximately midway between the two. If a number of events were to occur, additional portable high-gain self-recording seismograph units may be deployed.

#### 4. Hydrology.

a. Water Requirements. The quantity of water required for initial injection to saturate the pore field of the EE-2/EE-1 reservoir is  $\sim 28\ 000$  to  $55\ 000\ \text{m}^3$  (7-15 Mgal), and theoretical calculations indicate a total upper limit of as much as  $150\ 000\ \text{m}^3$  (40 Mgal) through FY81. Makeup water will be needed thereafter to replenish losses into the rocks and to fill enlarging fractures. Once stabilized the makeup water rate is expected to be between 0.3 and 3.2 l/s (5 and 50 gpm). Pumpage from the existing well of  $\sim 15\ 000\ \text{m}^3$  ( $\sim 12$  ac-ft) in a 10-month period resulted in  $\sim 0.5$  m (1.7 ft) of drawdown, indicating a very limited effect on the aquifer. The well is operated under a permit from the New Mexico State Engineer that allows pumping of  $22\ 000\ \text{m}^3$  (18 ac-ft) in 1978 and  $18\ 500\ \text{m}^3$  (15 ac-ft) thereafter

through 1986 with the provision that 80% of the water be returned to surface water or the ground water reservoir.

The following water requirements are estimates based on the experience gained at the present Fenton Hill Site and extrapolation of that experience to the larger reservoir. The amounts shown represent the maximum need within the limits considered reasonable but will be withdrawn from either subsurface aquifers or taken from surface supplies.

FY79 (drill 1 new 3960-m (13 000-ft) hole)	
Drill EE-2:	~18 500 m <sup>3</sup> (15 ac-ft)
Experiments:	<u>~3 700 m<sup>3</sup> (3 ac-ft)</u>
Total	~22 000 m <sup>3</sup> (18 ac-ft)
FY80 (deepen 2 existing holes)	
GT-2 Redrill:	~3 700 m <sup>3</sup> (3 ac-ft)
EE-1 Redrill:	<u>~3 700 m<sup>3</sup> (3 ac-ft)</u>
Total	~7 400 m <sup>3</sup> (6 ac-ft)
FY81 (new system operation)	
Fill System:	~55 500 m <sup>3</sup> (45 ac-ft)
Refill System:	~18 500 m <sup>3</sup> (15 ac-ft)
Makeup:	<u>~18 500 m<sup>3</sup> (15 ac-ft)</u>
Total	~92 500 m <sup>3</sup> (75 ac-ft)

Because of the experimental nature of this program, the exact water requirements cannot be predicted. Hydrogeological studies indicate that much larger physical supplies of water are available in the deeper limestone aquifer. Possible ways of assuring legal availability of needed water are being explored.

b. Liquid Effluents. Leakage of circulating fluid into the streams, or into the aquifer or natural springs, is highly unlikely because the operating procedures require total surface impoundment of drilling fluids and blockage by the insertion of casing into the geothermal holes to isolate the water-bearing zones in the volcanic and sedimentary rocks.

Effluents from the ponds have been released into a small canyon tributary to Lake Fork Canyon south of the site. The alluvium in the upper 595-m (1950-ft) length of the canyon ranges in thickness from 0.6 to 1.8 m (2 to 6 ft); whereas in the lower part of the canyon at the confluence with Lake Fork, the alluvium thickens to more than 12 m (40 ft). The effluents released to date have infiltrated the alluvium within 300 m (1000 ft) of the ponds. As they move downgradient in the alluvium, there are additional losses of water into the underlying tuff. Twelve holes were drilled through the alluvium into the top of the tuff in May 1978. Four of those holes, at distances of 20, 60, 295 and 915 m (65, 200, 970 and 3000 ft) from the ponds, encountered water and were cased for monitoring purposes. After a release of effluents in May, the fluorides (F) in four holes were <1 mg/l or near normal for naturally occurring water in the area (Table VIII). Chlorides (Cl) were elevated above natural concentrations and were near those concentrations found in the ponds. The four holes were dry in late June and early September. After a release in late September, only the holes at 20 and 60 m (65 and 200 ft) from the pond contained water. Fluorides were near natural levels, chlorides were elevated.

Soluble fluoride from analyses of cuttings from the 12 holes indicated natural concentrations were reached within 150 m (490 ft) from the ponds. Water samples and analyses of cuttings from the alluvium indicate a rapid uptake and adsorption of fluoride onto the soil. The chloride serves as a good tracer of water movement and indicates the effluents have infiltrated the alluvium and underlying tuff to a distance of 295 m (970 ft) from the ponds.

The shallower ground water aquifer at the Fenton Hill Site lies at a depth of 113 m (370 ft) in a tuff, perched on a shale and siltstone unit. The movement of water in this aquifer is toward the southwest where it discharges above the confluence of Lake Fork Canyon and Rio Cebolla (Cold Spring). The Cl, F, and total dissolved solids (TDS) are monitored at FH-1 (supply well TA-57, depth 137 m) and in Lake Fork Canyon at a Forest Service stock well (depth 64 m), and at Cold Spring. The Cl, F, and TDS from these wells and spring have remained normal and show no effect from the pond effluents.

Surface water samples were collected downgrade from the ponds in Lake Fork Canyon and in the Rio Cebolla. The Cl, F, and TDS were naturally occurring and showed no effects from pond effluents.

The latest discharge from the site occurred on November 7, 1978. The analysis of samples taken from that discharge are shown in Table IX. The

TABLE VIII

AVERAGE CHLORIDES, FLUORIDES AND TOTAL DISSOLVED SOLIDS (TDS)  
OF EFFLUENTS (PONDS) AND WATER FROM SAMPLING STATIONS, 1978

<u>Station</u>	<u>No. of Analyses</u>	<u>mg/ℓ</u>		
		<u>Cl</u>	<u>F</u>	<u>TDS</u>
GTP-1 (pond)	7	144	3.7	776
GTP-2 (pond)	6	745	5.0	2096
GTP-3 (pond)	8	794	6.0	2128
Hole 20 <sup>a</sup>	2	736	0.6	1674
Hole 60 <sup>a</sup>	2	746	0.5	1776
Hole 295 <sup>a</sup>	1	62	0.2	380
Hole 915 <sup>a</sup>	1	4	0.3	160
FH-1 (well)	5	7	0.3	274
USFS (well) 2400 <sup>a</sup>	1	3	0.5	106
USFS (tank) 6065 <sup>a</sup>	4	3	0.2	68
Lake Fork 6065 <sup>a</sup>	2	6	0.4	202
Lake Fork 7285 <sup>a</sup>	1	7	0.3	254
Lake Fork 8500 <sup>a</sup>	3	4	0.8	143
Lake Fork 9420 <sup>a</sup>	4	7	0.8	169
Cold Spring 9110 <sup>a</sup>	4	4	0.7	146
Rio Cebolla 10 330 <sup>a</sup>	3	8	0.5	134

<sup>a</sup>Distance in m downgradient from pond GTP-3

analyses were performed using an EPA approved technique and quantities are expressed in mg/ℓ, except pH.

The heated water brought to the surface is reinjected after cooling by passage through the heat exchangers. At the termination of various phases of experimentation the circulation loop will be drained, and it will be necessary to release water from the ponds or tanks to the natural drainage course as has been done in the past. The water-storage capacity is sufficient for makeup water but not for total circulation-loop water.

The chemical quality of the water that would be discharged is expected to resemble past releases (Table X). As water is circulated through the new

TABLE IX  
 CHEMICAL CHARACTERISTICS OF POND WATER,  
 RANGES AND MAXIMA OBSERVED IN 1977-78

<u>Species</u>	<u>mg/l</u>	<u>Species</u>	<u>mg/l</u>
SiO <sub>2</sub>	85 - 300	Co	0.01
F	2 - 10	Ni	0.03
As	1	Cl	200 - 1100
B	9	Cu	0.05
Cd	< 0.1	Zn	< 0.2
Hg	< 0.001	Ag	< 0.02
Li	3.8 - 10	Sn	< 0.1
Mo	0.04	Sb	< 0.3
Se	0.004	Sr	< 0.8
Be	< 0.01	Ba	0.2
Na	150 - 500	Pb	< 0.03
Mg	25	Bi	< 0.1
Al	1	HCO <sub>3</sub>	150 - 500
P	40	SO <sub>4</sub>	190
K	65	PO <sub>4</sub>	0.9
Ca	80	TSS	160
V	< 0.03	TDS	2800
Cr	0.003	H <sub>2</sub> S	< 0.1
Mn	0.2	pH	6 - 8 pH units
Fe	6		

deeper fracture system at temperatures of 250-275°C (480-530°F), there will probably be more minerals dissolved, which may result in higher concentrations of some constituents. Those constituents will be regulated by an NPDES permit and will be removed as necessary by the water treatment facility. Thus the quality of the future discharges into the canyon is not expected to be significantly different from past discharges.

Some experiments will require the use of small amounts of chemical dye or radioactive tracers to study characteristics of subsurface flow. Both

TABLE X  
LATEST DISCHARGE ANALYSIS RESULTS

<u>Analysis</u>	<u>Pond Discharge (mg/l)</u>	<u>15 m Downstream<sup>a</sup> (mg/l)</u>
pH	8.3	8.3
TDS	1622.	1597.
TSS	<1.	229.
TS	1622.	1826.
SiO <sub>2</sub>	168.	140.
Mg	3.74	10.
Na	360.	288.
Fe	0.242	0.472
K	52.	52.
Cl	600.	550.
Ca	66.	76.5
F	7.	5.70
Al	0.270	0.215
SO <sub>4</sub>	111.2	88.2
HCO <sub>3</sub>	300.	280.
CO <sub>3</sub>	<1.0	<1.0
P	0.15	0.30
B	32.	32.
As	0.300	0.273
Cd	0.001	0.001
Li	8.3	6.55

<sup>a</sup> At this distance the total discharge had percolated into the ground.

techniques are common in oil field operations and have been adapted to the unique situation at Fenton Hill. Residuals of such tracers may be released into the ponds at times. The radioactive tracer most likely to be used is <sup>82</sup>Br, which has a half-life of about 1/2 day and thus decays to an undetectable level in 12 days (10 half-lives). No releases from the ponds will be made beyond the fence until the radioactive tracers have decayed to

concentrations acceptable to the EPA for drinking water. The chemical dyes are not considered toxic unless present in much higher concentrations than will be used for initial dilution in the circulating system.

Environmental monitoring and special environmental studies by LASL will continue in the vicinity of Fenton Hill to further understand the environmental effects, detect and document undesirable trends, and implement appropriate mitigating measures.

5. Climatology. An increase in thermal output from the heat exchangers could impact the microclimatology of the local environs. Depending on the size of the thermal plume and its trajectory, a portion of the larger coniferous vegetation might be damaged by desiccation in the winter. This would occur if the tops of the trees were forced into transpiration by warm air while the moisture on the ground remained frozen.

6. Aesthetics. Although the "industrial" appearance of the site cannot be totally obscured, the majority of the facility can be blended with the surrounding environment by the artful use of appropriately colored paint and screening. Those facility additions, which will necessarily be observable from the highway, will be painted colors that either blend or harmonize with the natural colors of the area. Should it become necessary, additional screening by planting trees can be used.

Should the excavated pond for water-storage be selected, it can be located either immediately northwest of the site or south of the proposed parking lot. The northwest location should not be observable from the highway. However, the location south of the parking lot will probably be observable and should be screened in some manner. The excavation of a storage pond at either location will require the handling of the soil removed. One technique would be to place the excavated material on the surrounding edge as a berm, thereby blocking view of the stored water or raising it above the eye level of passing motorists. Suitable planting will reduce the unnatural appearance of the berm. The security fencing that would be required to reduce liability would be appropriately painted or coated. The ponds are not expected to emit any unnatural odor beyond that of ordinary ponds.

During the period of drilling and redrilling an oil field drilling rig will be used. The mast will be readily observable because it is 39.6 m

(130 ft) high. Color will not help the aesthetics of the mast because it would still be obvious because of its height. Drilling contract provisions will require that portable mud tanks be used instead of the more conventional excavated mud pit and will require site cleanliness during operation and cleanup following the drilling.

### C. Biological Factors

1. Vegetation. Discharging of water into the drainage system next to the facility may have resulted in more vegetative growth in the stream channel; however, this has not been documented. If future plans for a tenfold increase in thermal output results in a concomitant increase in surface discharge, the dry canyon bottom might take on riparian characteristics with a consequent increase in diversity of the biota.

No significant impacts have been observed that can be attributed to the facility other than the 5.5 hectares (13.5 acres) of vegetation that was disturbed.

2. Wildlife. Any disturbance to a natural environment will have some impact upon the wildlife; however, this change is not always detrimental. Studies currently being conducted (3 years of annual live trapping data and one year of bird flushing data) have shown the initial fluctuations in small mammal and bird populations expected from these operations. These populations now appear stable. Unless an unforeseen future disturbance occurs causing a change in densities with a gradient away from the facility, this development will have had little environmental impact on these populations. It is premature to determine if the elk movement on the plateau is affected by the facility. Transects are being read that should supply new data. Comparisons between the data collected in 1978 and the initial readings of the 94 transects two years ago should be available soon. The pond water would not be suitable for livestock or wildlife because of elevated mineral levels. However, all discharged water will be treated before release and will be acceptable for animal use.

3. Endangered Species. The peregrine falcon has been sighted in the area, but as mentioned earlier, no known nesting areas are in the vicinity.

Noise created during new hole drilling and more extensive system operation should not greatly reduce the falcon's hunting range.

The Jemez Mountain salamander is known to habit a large portion of the Jemez Mountains, and they may be attracted to an excavated water-storage pond. If so, some may inadvertently be killed during site operation.

#### D. Environmental Contaminants

1. Air. There is no gaseous effluent during steady (closed-loop) operation or quiescent periods. When the system is vented to the ponds, some gases previously accumulated in the circulating pressurized liquid could be released to the atmosphere. A detailed analysis of gases from the present circulating system indicated that about 87% was air and about 13% was carbon dioxide (CO<sub>2</sub>).<sup>22</sup> As a crude comparison, the amount of CO<sub>2</sub> potentially released from 3.8 m<sup>3</sup> (1000 gal) of vented liquid is about the same as the CO<sub>2</sub> exhausted by a car driving 1.6 km (1 mi). Traces of hydrogen sulfide and ammonia were also measured but have not presented any odor problems at the site. These constituents were found in the circulating loop and have not been observed in the pond.

Radon (Rn) gas has frequently been raised as a potential environmental contaminant from geothermal operations. Radon, the radioactive gas produced by decay of naturally occurring radium, could accumulate in the circulating fluid from contact with granitic rock in the fracture system. The only time radon could be released to the atmosphere is when the system is vented and the liquid placed in surface storage. Measurements in the existing system have shown maximum concentrations of about 3 nCi/l in the circulating-loop liquid after about 75 days of continuous operation.<sup>23</sup> Theoretical interpretation indicated maximum levels of 11 nCi/l would be reached in about 160 days. If similar conditions prevail in the new, deeper fracture system, the estimated release of Rn during venting operations (assuming 13 l/s or 200 gpm) would be 0.01 Ci/day that could continue for 15-20 days if as much as 19 000 m<sup>3</sup> (5 Mgal) were vented. This amount of radon would be about the same as the radon released from natural soils covering an area of 25 hectares (62 acres) or less.<sup>24</sup> Thus, the effect would be small in comparison with natural background radioactivity.

The rigs used to drill the new system holes will be driven by diesel engines and will emit gaseous and particulate exhaust products. Because this point source is small and drill rig engines are usually kept in good mechanical condition, little to no impact is expected.

2. Water. Soluble constituents of the deeper reservoir will be removed and will be contained in the circulating water. During loop operation these dissolved contaminants will be monitored to assure that concentrations do not reach levels that would harm either the reservoir, pumps, or pipes. Should the dissolved material approach such levels, the water will be treated to reduce the concentrations to acceptable levels. Circulating-loop water may occasionally be diverted to storage and as such will be confined to the site. Occasionally, the reservoir will be emptied requiring that circulating-loop water in excess of the storage capacity be discharged to the natural drainage from the site. This water is expected to exceed EPA standards, therefore it will be treated in the proposed water treatment plant, prior to discharge, pursuant to the NPDES permit currently under consideration.

3. Water Treatment Plant. The engineering design of this facility is still under consideration. However, without regard to the design, the water contaminating wastes removed will be disposed of by a subcontractor who will be legally required to dispose of the material from the site in a manner approved by the New Mexico Environmental Improvement Division. The waste material will not be disposed of on the site or on USFS lands.

Sanitary wastes will be discharged to the septic system at the trailer living area. This septic system will be designed in conformance with Public Health Service Publication No. 526, "Manual of Septic-Tank Practices" and New Mexico regulations governing liquid waste disposal. We are assuming that all sanitary liquid waste discharges will be into the soil tile fields and will not degrade the ground water.

4. Noise. The facility will cause some increased noise during operation and thus may degrade the aesthetic quality of the area. Noise levels were typically <100 dB(A), and pumping noise levels will generally be steady without major fluctuation. This should have little impact on the wildlife populations. These are much lower levels than those expected from the

operation of the turbine-powered helicopter on the nearby USFS helipad.

Audio measurement devices will be used to record noise levels at various stations during the heat extraction experiment. Measurements at the fence surrounding the heat exchangers are usually <70 dB(A). Thus, noise levels at the site should be no worse than a typical street corner.

A somewhat increased level of noise, over that described above, will occur during drilling operations by the diesel engines used to power the drilling rig. This noise should not significantly impact the area's wildlife.

#### E. Social and Economic Factors

The proposed drilling, facility expansion, and longer operating periods will require additional labor and an increased number of on-site staff. The overall effect will be that an increased economic input to the local communities will be made beyond that of the past. Further it is expected that an increased expenditure in the area by USFS personnel will be made. Combined, this effect will continue to improve the economic well-being of the communities involved and the regional area in general. No social problems are expected, and no burden should occur to the existing infrastructure of the area.

#### V. SUMMARY

Now that the extraction of geothermal energy from hot dry rock has been successfully tested at Fenton Hill, another deeper, and therefore hotter, reservoir will be created. This system will be of a commercially feasible size to determine the "lifetime" or rate of thermal drawdown of the reservoir. The technique principally requires the use of existing technology with some modification of instruments and cables for operation at such high temperatures. A continuous 75-day test of the present circulation loop extracted 45 MW of thermal energy, and it is hoped that the larger reservoir will produce up to 50 MW of energy. Because the concept and this use of the natural resource are unique, all phases of development, construction, and operation were monitored for any adverse effects. The environmental studies of the area were initiated before development of the site to establish a base line data set from which to evaluate any effects resulting from the project activities. The major concern was the possibility of induced microearthquakes by fracturing the granitic basement rock and by the injection of such large volumes of pressurized

fluid. Although none were detected, the on-site and regional seismic networks will continue to monitor the new system and may be expanded.

Studies of the surface and ground waters have indicated that the local hydrology should not be affected. Because the boreholes are cased with cement, there is minimal water loss through permeation into the reservoir rock. Dissolved rock constituents stabilized at near drinking water concentrations, and all water to be discharged from the site will be treated and should exceed EPA standards. Gases are released only when water is diverted to storage, and these were analyzed as 87% air and 13% carbon dioxide, with only trace levels of hydrogen sulfide and ammonia. Soluble radioactive elements decay to undetectable levels in a few days.

Besides heat exchangers, a possible demonstration generating plant, and a water treatment facility, the only other major surface facility is for water storage. This can be covered tanks, excavated holding ponds or earth-fill dams. There are no odor problems, and if the pond water was treated to reduce the level of minerals, it could be used by wildlife.

Energy from hot dry rock has thus far proved to be clean, as well as safe. Generating plants could be located within or near cities without concern of possible hazards or contamination. Also, a relatively small site is required, and the noise levels, except during drilling, are low. By screening with fencing and trees and by selection of appropriate paint colors, an HDR plant would not greatly affect the aesthetics of the area.

Another advantage of hot dry rock geothermal energy is that it does not represent a significant depletion of a natural resource. Therefore, it is an attractive alternative to resources, such as coal. If HDR-produced energy proves to be economically feasible, it will aid our pursuit of energy independence because hot dry rock is located at varying depths everywhere within the earth's crust.

#### ACKNOWLEDGMENTS

We would like to thank the following persons for their assistance in the preparation of this paper: K. Rea, E. Homuth, W. Purtymun, D. Cash, and J. Tubb. We also acknowledge the Department of Energy, Division of Geothermal Energy; the US Forest Service; and the Oak Ridge National Laboratory.

## REFERENCES

1. M. C. Smith, D. W. Brown, and R. A. Pettitt, "Los Alamos Dry Geothermal Source Demonstration Project," Los Alamos Scientific Laboratory Mini- Review 75-1 (May 1975).
2. A. G. Blair, J. W. Tester, and J. J. Mortensen, "LASL Hot Dry Rock Geothermal Project, July 1, 1975--June 30, 1976," Los Alamos Scientific Laboratory report LA-6525-PR (October 1976).
3. K. H. Rea, "Environmental Investigations Associated with the LASL Hot Dry Rock Geothermal Energy Development Project," Los Alamos Scientific Laboratory report LA-6972 (December 1977).
4. "Draft Environmental Statement for the Proposed Dry Geothermal Energy Source Demonstration," prepared by Los Alamos Scientific Laboratory for Jemez Ranger District, Santa Fe National Forest, Region 3 (October 1973).
5. W. D. Purtymun, "Geology of the Jemez Plateau West of Valles Caldera," Los Alamos Scientific Laboratory report LA-5124-MS (February 1973).
6. W. D. Purtymun, F. G. West, and R. A. Pettitt, "Geology of Geothermal Test Hole GT-2 Fenton Hill Site, July 1974," Los Alamos Scientific Laboratory report LA-5780-MS (November 1974).
7. F. G. West, "Hydrologic Summary of the Area of Fenton Hill Site TA-57," Los Alamos Scientific Laboratory, unpublished report (February 1979).
8. R. L. Smith, R. A. Bailey, and C. S. Ross, "Geologic Map of the Jemez Mountains, New Mexico," US Geol. Surv. Misc. Geol. Inv. Map I-571 (1970).
9. G. H. Woods, Jr. and S. A. Northrop, "Geology of the Nacimiento Mountains, San Pedro Mountains, and Adjacent Plateaus in Parts of Sandoval and Rio Arriba Counties, New Mexico," US Geol. Surv. Oil and Gas Inv. Prelim. Map 57 (1946).
10. C. A. Newton, D. J. Cash, K. H. Olsen, and E. F. Homuth, "LASL Seismic Programs in the Vicinity of Los Alamos, New Mexico," Los Alamos Scientific Laboratory report LA-6406-MS (November 1976).
11. W. D. Purtymun and H. S. Jordan, "Seismic Program of the Los Alamos Scientific Laboratory," Los Alamos Scientific Laboratory report LA-5386-MS (September 1973).
12. D. B. Slemmons, "Fault Activity and Seismicity Near the Los Alamos Scientific Laboratory Geothermal Test Site, Jemez Mountains, New Mexico," Los Alamos Scientific Laboratory report LA-5911-MS (April 1975).

13. R. A. Pettitt, "Environmental Monitoring for the Hot Dry Rock Geothermal Energy Development Project, Annual Report for the Period July 1975--June 1976," Los Alamos Scientific Laboratory report LA-6504-SR (September 1976).
14. W. D. Purtymun, F. G. West, and W. H. Adams, "Preliminary Study of the Quality of Water in the Drainage Area of the Jemez River and Rio Guadalupe," Los Alamos Scientific Laboratory report LA-5595-MS (April 1974).
15. W. D. Purtymun, W. H. Adams, and J. W. Owens, "Water Quality in Vicinity of Fenton Hill Site, 1974," Los Alamos Scientific Laboratory report LA-6093 (December 1975).
16. F. H. Rainwater and L. L. Thatcher, "Methods for Collection and Analyses of Water Samples," US Geol. Surv. Water-Supply Pap. 1454 (1960).
17. W. D. Purtymun, W. H. Adams, A. K. Stoker, and F. G. West, "Water Quality in Vicinity of Fenton Hill Site, 1975," Los Alamos Scientific Laboratory report LA-6511-MS (September 1976).
18. F. G. West, P. R. Kintzinger, and W. D. Purtymun, "Hydrologic Testing Geothermal Test Hole No. 2," Los Alamos Scientific Laboratory report LA-6017-MS (July 1975).
19. F. G. West, P. R. Kintzinger, and A. W. Laughlin, "Geophysical Logging in Los Alamos Scientific Laboratory Geothermal Test Hole No. 2," Los Alamos Scientific Laboratory report LA-6112-MS (November 1975).
20. J. Balagna, R. Charles, and R. Vidale, "Geothermal Chemistry Activities at LASL. January--December 1975," Los Alamos Scientific Laboratory report LA-6448-PR (October 1976).
21. J. H. Healy, W. W. Rubey, D. T. Griggs, and C. B. Raleigh, "The Denver Earthquakes," *Science* 161, 1301-1310 (1968).
22. K. H. Rea and V. Gutschick, "Environmental Assessment of Dissolved Gases in LASL's Hot Dry Rock Geothermal Source Demonstration Project," published in *Geothermal Resources Council Trans.* 2, p. 249-252 (July 1978).
23. P. Kruger, L. Semprin, G. Sederberg, and R. Potter, "Hot Dry Rock Energy Extraction Field Test," Los Alamos Scientific Laboratory progress report (in preparation).
24. M. H. Wilkening, W. E. Clements, and D. Stanley, "Radon 222 Flux in Widely Separated Regions," *Natural Radiation Environment II*, Symposium Proc., Houston, Texas, Aug. 7-11, 1972, ERDA CONF-720805.

Printed in the United States of America. Available from  
National Technical Information Service  
US Department of Commerce  
5285 Port Royal Road  
Springfield, VA 22161

Microfiche \$3.00

001-025	4.00	126-150	7.25	251-275	10.75	376-400	13.00	501-525	15.25
026-050	4.50	151-175	8.00	276-300	11.00	401-425	13.25	526-550	15.50
051-075	5.25	176-200	9.00	301-325	11.75	426-450	14.00	551-575	16.25
076-100	6.00	201-225	9.25	326-350	12.00	451-475	14.50	576-600	16.50
101-125	6.50	226-250	9.50	351-375	12.50	476-500	15.00	601-up	

Note: Add \$2.50 for each additional 100-page increment from 601 pages up.



## UNITED STATES ENVIRONMENTAL PROTECTION AGENCY

REGION 6

1445 ROSS AVENUE, SUITE 1200  
DALLAS, TX 75202-2733

December 29, 1997

REPLY TO: 6WQ-CA

Mr. G. Thomas Todd  
Area Manager  
Department of Energy  
Los Alamos Area Office  
Los Alamos, New Mexico 87544

Re: NPDES Permit No. NM0028576-Dept. Of Energy-Los Alamos  
National Laboratory, Fenton Hill Geothermal Site

Dear Mr. Todd:

In accordance with your request on file in this office that the referenced NPDES Permit No. NM0028576 be discontinued, you are hereby notified that the permit has been discontinued.

Any resumption of the discharge without a permit will be unlawful. Should you again propose to discharge any pollutant from this facility to waters of the United States, it will be necessary to file a new application at least 180 days in advance of the proposed discharge. Any permit issued as a result of such reapplication will contain conditions and limitations consistent with the situation, and the law and the regulations in effect at the time of reissuance, irrespective of any previously issued permit.

If you have any questions, please contact Wilma Turner at the above address or telephone (214) 665-7516.

Sincerely yours,

Jack V. Ferguson, P.E.  
Chief  
NPDES Branch (6WQ-P)

cc: New Mexico Environment Department

Mr. Mike Saladen  
University of California  
Management Contractor for Operation  
Los Alamos National Laboratory  
Los Alamos, New Mexico 87545

# Los Alamos

Los Alamos National Laboratory  
Los Alamos, New Mexico 87545

WATER QUALITY & HYDROLOGY GROUP, ESH-18  
FAX TRANSMITTAL COVER SHEET

FAX #: (505) 665-9344

VERIFICATION #: (505) 665-0453

DATE: 11-7-98

LOG NO: WQ&H-FAX-96:

FROM: B. Edeskuty (505)

PHONE #: (505) 665-0789

① TO: Connie Soden FAX #: 845-6714  
ORG: DOE/Albug.

② TO: G. Saums FAX #: 827-0160 PHONE #: ( )  
ORG: NMED

③ TO: J. Parker FAX #: 827-1545 PHONE #: ( ) 827-1536  
ORG: NMED/AIP

④ TO: R. Anderson FAX #: 827-8177 PHONE #: ( ) 827-7152  
ORG: OCD/Santa Fe

⑤ TO: Dennis Trujillo FAX #: 829-3223  
ORG: Forest Service/Jemez District

MESSAGE: For your info attached please find letter from  
EPA granting approval to discontinue Los Alamos  
National Laboratory's Fenton Hill NPPES permit.  
If you have any questions please call me at  
665-0789

NUMBER OF PAGES INCLUDING COVER: 2

CY: WQ&H FAX FILE

AS  
TEAM LEADER OR GROUP LEADER

**LA-6017-MS**

Informal Report

UC-13

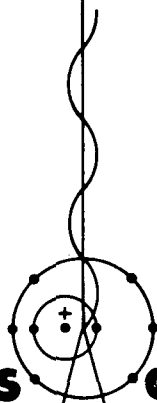
Reporting Date: June 1975

Issued: July 1975

## Hydrologic Testing Geothermal Test Hole No. 2

by

F. G. West  
P. R. Kintzinger  
W. D. Purtymun



**los alamos**  
**scientific laboratory**  
of the University of California  
LOS ALAMOS, NEW MEXICO 87545

An Affirmative Action/Equal Opportunity Employer

## HYDROLOGIC TESTING GEOTHERMAL TEST HOLE NO. 2

by

F. G. West, P. R. Kintzinger, and W. D. Purtymun

### ABSTRACT

Analyses of drill-stem tests performed in Geothermal Test Hole No. 2 (GT-2) indicate that the jointed, but competent, rock tested can for geothermal project purposes be considered "dry." The intervals tested were selected by the use of geophysical logs so as to exclude occasional zones of intense fracturing.

### I. INTRODUCTION

Geothermal exploratory hole GT-2 was drilled under contract to the Los Alamos Scientific Laboratory (LASL) as a part of the field evaluation of the "dry hot rock" concept. The geohydrologic data presented in this report were obtained from the crystalline basement rock section of the hole, specifically from a depth of 732 m (2404 ft) to the interim total depth of 1937 m (6356 ft). Data for the sedimentary section of the hole (0 to 732 m) and data derived during the drilling phase were given by Purtymun et al.<sup>1</sup>

The project hole is located on Fenton Hill 3.2 km (2 miles) northwest of La Cueva, Sandoval County, New Mexico. The site location is as follows: NE 1/4, Sec 13, T19N, R2E NMPM. The land surface elevation is 2648.7 m (8690 ft). The elevation of 2652 m (8701 ft) for the top of the drill-rig Kelly bushing will be used as the datum level for depths in the hole.

The project site is 3 km (2 miles) west of the ring fault zone which formed as a result of the collapse of the Valles Caldera. Faults associated with the Rio Grande rift valley are thought to be the locus of former volcanic activity.<sup>2</sup> One of these faults, the Jemez Springs fault zone, is some 5.1 km (3.2 miles) southeast of the site. The Jemez-Nacimiento Mountains area has been a structurally active area to varying degrees since Precambrian

time. Evidence of structural activity after the last eruption of the Valles Caldera is seen along the Jemez Springs fault zone, the closest being the Virgin Canyon fault.<sup>3</sup> Some post-volcanism uplift may have taken place west of the Rio de Las Vacas in the Nacimiento Mountains. Fracture zones with unknown displacement were encountered in GT-2 as interpreted from drilling information and geophysical logs.

The hole penetrated some 137 m (449 ft) of volcanics, 238 m (780 ft) of Permian red beds, and 355 m (1165 ft) of Pennsylvanian-Mississippian shales and limestones before encountering granite at 732 m (2404 ft). The crystalline Precambrian rocks include granites, granodiorites, monzonites and some amphibolite. The textures have ranged from fine to coarse grained and the colors from pink to black. Appendix A contains a summary of drilling and geologic data by Pettitt.<sup>4</sup>

### II. INFLUENCE OF FRACTURES ON HYDROLOGY

Knowledge of the hydrology of crystalline basement rocks has been limited for a combination of reasons. Most of the available knowledge is derived from mining operations with some small part coming from oil ventures. The relatively low permeability often found while mining in crystalline rocks has prompted the storage of oil and gas in old mines as well as in new excavations for this purpose.<sup>5</sup> However, when crystalline rocks are sufficiently fractured

they are capable of transmitting oil.<sup>6,7</sup> The water produced in mines is generally associated with fracture zones or patterns.<sup>8,9</sup> It is not uncommon for mines, even deep mines, to be "dry."<sup>10</sup> In regions where the water supply is derived from crystalline rocks, the ground water reservoir is usually contained in faults or joint systems.<sup>11</sup> The relative specific production capacity ( $m^3/s/m$  of drawdown) of most water wells drilled into crystalline rocks is low and decreases appreciably with increased depth.<sup>12,13</sup> Studies connected with the Rocky Mountain Arsenal disposal well indicated a logarithmic decrease in permeability with depth.<sup>14</sup> Sedimentary rocks exhibit a decrease of permeability with depth as a result of the compaction and consolidation caused by the increased lithostatic load.<sup>15</sup> The same processes contribute to the decrease of permeability of crystalline rocks; however, the principal decrease may be associated with a decrease in fracture frequency with depth.<sup>16</sup>

Coring performed in GT-2 indicates that considerable jointing exists at depth, but that most of the fissures are filled by minerals such as calcite or sericite, a condition noted by others.<sup>17</sup>

Unfortunately, as little is known about the occurrence of fractures or joints at depth as is known of the occurrence of fluids at appreciable depth. Miners and quarrymen have always been acutely aware of the nature of joints since their work, not to mention their very lives, is influenced by them. Little field work has been done to quantify the belief of miners that jointing tends to die away with depth.<sup>18</sup> The relationship of joints with structural deformation is well recognized and defined.<sup>19</sup> Less well defined is the belief that joints on a regional and even a global basis appear to occur in a systematic fashion with preferred orientations.<sup>20-23</sup> Joint studies in oil and gas fields indicate that often a close correlation exists between the orientation of joints at depth and that of joints mapped at the surface.<sup>24,25</sup> Most intrusive igneous rocks have a more or less regular fracture system that is related to the emplacement flow structure.<sup>26</sup> It has been found that even sets of microjoints often have preferred orientations.<sup>27</sup>

Geophysical data such as the increase of resistivity encountered with increased depth of penetration of electric soundings<sup>28,29</sup> imply a decrease

in water with depth and, as a possible corollary, a decrease in open fracture frequency. Laboratory studies suggest that the in situ seismic velocity should increase with loading, since the aperture of joints decreases, but this has not been confirmed by data obtained from two deep holes.<sup>30</sup> The nature and occurrence of fractures, hence water at depth, will in all likelihood be determined only by deep drilling in crystalline basement rocks.

### III. HYDROLOGIC TESTING

Diagnostic hydrology testing in GT-2 was performed by drill-stem testing techniques typically used in oil field work. In general the procedure consists of sealing off a section of the borehole from external pressure, opening the zone to near-atmospheric pressure, allowing the formation to react to the reduced hydraulic head and then "shutting in" the zone, allowing the formation to recover toward the original pressure or fluid level.

The zone of interest is sealed off by the use of an arrangement of rubber packer elements and surface-actuated valves which are placed in the string of drill pipe. The packers are "set" when a part of the drill string weight is used to expand the packers out against the borehole wall. Pairs of packer elements are used on each side of the zone "straddled," except for tests at the bottom section of a hole where the lower pair of packers is unnecessary. The pressure history of the test is scribed on a metal foil on a downhole recording Bourdon gauge. The accuracy of the pressure gauges used is 0.25% of the total recording range.

Interpretation of geophysical logs provided the basis for the selection of zones in GT-2 to be tested. In general, the full-wave sonic log and the electrical resistivity logs were the most used logs. Zones that appeared to be competent rock with high resistivity, although jointed, were selected to the exclusion of rock with low resistivity and questionable competence, on the assumption that they would be most representative of crystalline rocks at the depths expected for "dry hot rock" operations. Due to project programmatic constraints, occasional zones of apparent intense fracturing, with one exception, were not tested at this time. Suitable packer seats were picked by a utilization of the caliper (borehole diameter) log. The geophysical logs will be discussed in a separate

report; however, copies of the logs used are included in Appendix B so that some feeling for the nature of the rock tested may be imparted.

#### A. Methods of Analysis

Methods for the analysis of flow of fluids in a porous fractured medium are currently being developed by various investigators.<sup>31,32</sup> The work of Witherspoon<sup>33</sup> is quite useful in understanding the differences one may expect between flow in fractured and unfractured media, especially along a fracture zone. The data from hydrologic tests in GT-2 were analyzed initially by the equation governing unfractured isotropic media, that being the Theis recovery equation, or as it is known in oil field work the "Horner" plot. In this method, pressure is plotted against the logarithm of the ratio of the time that a hydraulic transient pressure was applied to the time since the transient was removed. The slope of the straight-line part of this semilog plot is a measure of the permeability. Extrapolation of this slope to infinite time provides an estimate of original reservoir pressure.

#### B. Testing in GT-2

The first zone to be tested was the bottom part of the hole, since it had been least disturbed hydrologically. This test was over the bottom 122 m (400 ft) of the hole, which included a definite fracture zone from 1829 to 1844 m (6000 to 6050 ft) having moderate permeability. The permeability of the zone apparently decreased with depth, as interpreted from the microcontact electric resistivity log--which essentially looks at near-surface borehole effects such as mud-cake buildup resulting from fluid losses. Approximately 246 m (807 ft) of water was placed in the drill pipe to prevent boiling during the flow period. During the 4-h flow period some 2.9 m<sup>3</sup> (766 gal) of water flowed into the drill pipe, increasing the head by 146 m (479 ft) of water. The tools used for the hydraulic test automatically capture a sample of the fluid flowing through the tool, when the downhole valve is closed to start the shut-in part of the test. Although some flow occurred during this test, the sample obtained was thought to be mostly drilling fluid rather than natural formation fluid. Analysis of this sample will appear in a separate report considering the geochemistry. The 4-h shut-in-pressure recovery-period semilog data plot indicated an average permeability

of  $1.6 \times 10^{-10}$  m/s (0.16 microdarcy) for the 122-m (400-ft) zone. The graph did not give indications of wellbore damage or boundary effects. Extrapolation of the pressure recovery indicated a maximum initial reservoir level at a depth of 519 m (1703 ft). Assuming that for practical purposes the pressure response came principally from the 15-m (50-ft) long fracture zone, the permeability would be  $1.3 \times 10^{-8}$  m<sup>2</sup>/s (1.3 millidarcy). The other fracture zones encountered in the hole probably have permeabilities within an order of magnitude of that found for this zone.

Several of the succeeding tests were unsuccessful due to an "exotic" tool malfunction. The design of the tool precluded operational checks at the surface.

The next successful test was over the interval from 856 to 883 m (2808 to 2897 ft). Formation flow was allowed for a period of 2 h. The pressure chart indicated that essentially no flow had taken place; actually a slight negative pressure was recorded. The 4-h shut-in pressure curve showed a pressure step at about 2 h 30 min. This step may have been caused by a temporary unseating of the packer causing a minor positive increase in pressure, but since the basic hydrologic environment was little changed, the slope of the recovery plot was essentially the same. The permeability indicated by this test was  $3.3 \times 10^{-12}$  m/s (0.33 microdarcy). The initial reservoir level given by extrapolation of the semilog pressure plot is a depth of 419 m (1375 ft). During the shut-in period the drill pipe was filled to the surface for an injection test. The pressure response indicated a partial blockage in the downhole valve system. The packer assembly was then moved up the hole to test the interval from 796 to 823 m (2612 to 2700 ft). The tool system again pointed to a partial hydraulic blockage. Analysis of this pressure history, although of very doubtful quality, indicated a permeability slightly greater than that shown by the previous test,  $2.4 \times 10^{-11}$  m/s (2.4 microdarcys).

Two tests were again performed on one trip into the hole, the first being over the interval from 1679 to 1804 m (5509 to 5918 ft). The 2-h flow period was again marked by essentially no inflow of water. The semilog plot of the 8-h shut-in pressure-recovery curve indicated a permeability of  $4.0 \times 10^{-12}$  m<sup>2</sup>/s (0.4 microdarcy). The initial pressure value

extrapolated for this interval was at a depth of 255 m (837 ft).

The packers for the straddle test were unseated and moved uphole to test the interval from 1549 to 1674 m (5082 to 5492 ft). During the 2-h flow interval a slight inflow of  $0.06 \text{ m}^3/\text{s}$  (15.9 gpm) was estimated from the pressure history. The shut-in pressure-recovery plot had a slight negative curvature, which might be suggestive of the response expected from a fractured medium.<sup>34</sup> While the recovery test was in progress, water was placed in the drill pipe to a depth of 203 m (666 ft) so that an injection test could be performed. The pressure-recovery curve of the shut in and the decay curve of the injection test both indicated an initial formation level of 379-m (1243-ft) depth. The permeability indicated by the standard shut-in test was  $9.2 \times 10^{-11} \text{ m}^2/\text{s}$  (9.2 microdarcys). The permeability of  $3.8 \times 10^{-10} \text{ m}^2/\text{s}$  (0.38 microdarcy) determined from the injection test was slightly inflated by the residual hydraulic effects of the preceding shut-in test.

The final test was over the interval of 1442 to 1564 m (4731 to 5131 ft). The 1-h flow period indicated no inflow of water. The semilog plot of the 8-h recovery curve exhibits a curvature which decreases with time. The curvature may indicate that the test zone included rocks of different permeabilities. During the last 2 h of the recovery, the plot showed appreciable leakage around the packers. The permeability determined was  $1.0 \times 10^{-11} \text{ m}^2/\text{s}$  (1.0 microdarcy). The initial reservoir level was indicated at the depth of 99 m (325 ft).

It was not possible to analyze in the standard manner tests for which no inflow of water was measured, since a determination of flow volume is required. The flow was estimated by converting the pressure increase measured during the shut in to the volume of water represented by this pressure increase.

### C. Additional Methods of Analysis

Several additional methods of data analysis were tried with varying degrees of success. The initial formation pressure levels estimated by the Theis recovery plot were in reasonably good agreement with those obtained by the method of Muskat.<sup>35</sup> The pressure data were also plotted on log-log paper and compared with the type curve of Theis<sup>36</sup> for

nonleaky artesian aquifers and with the type curves of Hantush<sup>37</sup> for leaky artesian aquifers. The tests appeared to have some small amount of aquifer leakage. Considering the low permeabilities observed, the effect observed was probably due to slight hydraulic end effects caused by the packers. This situation will tend to give inflated values of permeabilities. The assumption used in the Theis analysis is that of an infinite line source, whereas our packer situation is somewhere between the physical model of a semi-infinite line source and a point source. The type curves of Papadopoulos<sup>38</sup> were also tried, but little "fit" was found.

It should be pointed out that the "initial" formation fluid levels or the equivalent pressures estimated from the semilog recovery plots may only reflect a long-period transient caused by exposure to a fluid column extending upward to land surface. During the drilling of the sedimentary section, the water table was found at a depth of 536 m (1760 ft). The "initial" formation hydraulic levels estimated from the drill-stem tests were in all cases at lesser hole depths than the main level, which implies artesian conditions, geopressurization, aquathermal pressurization or a transient of over-pressurization. It is improbable that the crystalline basement rocks would have a hydraulic continuity with the lateral extent necessary for a connection to a recharge area of the appropriate elevation. Geopressurization is a compaction- and consolidation-related phenomenon of abnormally high fluid pressures occasionally found in sedimentary rocks, but not usually associated with crystalline basement rocks. Aquathermal pressures can result when rock in which the water is confined is subjected to an elevation in the isotherms. Over-pressurization and hence fluid injection probably occurs in most holes during the drilling phase as a result of the maintenance of drilling-mud levels to above land surface. Since the period of application of this pressure level in GT-2 was several orders of magnitude longer than the drill-stem tests, any determination of a true "initial" formation pressure is doubtful. The initial formation-fluid pressures estimated will be effective pressures experienced during hydrofracturing operations for a distance out from the borehole dependent on the permeability, injection pressure, and period of over-pressurization.

#### IV. CONCLUSIONS

The permeabilities measured in this series of tests are comparable with those reported in the literature.<sup>39</sup> Whether these values are representative of what one would find upon extensive drilling is problematic. The permeabilities measured are certainly considered "dry" by the standards of the irrigation farmer, the oil producer, or even the geothermal steam-well developer. The permeabilities measured would at this time seem to fit the current project objectives and needs for "dry" rock.

#### REFERENCES

1. W. D. Purtymun, F. G. West, and R. A. Pettitt, "Geology of Geothermal Test Hole GT-2, Fenton Hill Site, July 1974," Los Alamos Scientific Laboratory report LA-5780-MS (1974).
2. R. L. Smith and R. A. Bailey, "The Bandelier Tuff: A Study of Ash-Flow Eruption Cycles from Zoned Magma Chambers," *Bull. Volcanologique* 29, 83-104 (1966).
3. D. B. Slemmons, "Fault Activity and Seismicity Near the Los Alamos Scientific Laboratory Geothermal Test Site, Jemez Mountains, New Mexico," Los Alamos Scientific Laboratory report to be published soon (1975).
4. R. A. Pettitt, "Planning, Drilling and Logging of Geothermal Test Hole GT-2, Phase I," Los Alamos Scientific Laboratory report LA-5819-PR (Jan 1975).
5. C-O. Morfel, "Storage of Oil in Unlined Caverns in Different Types of Rock," *New Horizons in Rock Mechanics*, Am. Soc. Civil Engrs., pp. 409-420 (1973).
6. R. F. Walters, "Oil Production from Fractured Precambrian Basement Rocks in Central Kansas," *Bull. Am. Assoc. Petr. Geol.* 37, 300-313 (1953).
7. D. A. McNaughton, "Dilatancy in Migration and Accumulation of Oil in Metamorphic Rocks," *Bull. Am. Assoc. Petr. Geol.* 37, 217-231 (1953).
8. W. J. Samuelson, "Engineering Geology of the NORAD Combat Operations Center, Colorado Springs, Colorado," *Engr. Geol.* 2, 20-30 (1965).
9. H. E. McKinstry, *Mining Geology* (Prentice-Hall, Inc., New York, 1948), pp. 521-523.
10. W. Lindgren, *Mineral Deposits* (McGraw-Hill, New York, 1933), pp. 36-40.
11. I. Larsson, "Ground Water in Precambrian Rocks in Southern Sweden," in *Ground Water Problems*, E. Eriksson, Y. Gustafsson, K. Nilsson, Eds. Pergamon Press, 1968), Chap. 2, pp. 23-41.
12. S. N. Davis and R. J. M. Dewiast, "Ground Water in Igneous and Metamorphic Rocks," *Hydrology* (John Wiley & Sons, Inc., 1966), Chap. 9, pp. 318-346.
13. Z. Spiegel and B. Baldwin, "Geology and Water Resources of the Santa Fe Area, New Mexico," USGS Wtr. Sup. Paper 1525 (1968).
14. D. T. Snow, "Hydraulic Characteristics of Fractured Metamorphic Rocks of Front Range and Implications to the Rocky Mountain Arsenal Well," *Quart. Colo. Sch. Mines* 63, 167-201 (1968).
15. A. I. Levorsen, *Geology of Petroleum* (W. H. Freeman & Co., 1954), pp. 128-131.
16. F. A. F. Berry, "High Fluid Potentials in California Coast Ranges and Their Tectonic Significance," *Bull. Am. Assoc. Petr. Geol.* 57, 1219-1249 (1969).
17. F. A. Alekseyev, N. K. Kukhorenko, G. I. Voytov, and Y. S. Galkin, "Initial Results of Geophysical and Geochemical Investigations of Very Deep Boreholes," *Internat. Geol. Rev.* 14, 275-280 (1971).
18. W. O. Crosby, "On the Absence of Joint-Structure at Great Depth and Its Relations to the Forms of Coarsely Crystalline Eruptive Masses," *Geol. Mag.* 8, 416-420 (1881).
19. J. G. Ramsey, *Folding and Fracturing of Rocks* (McGraw-Hill, New York, 1967).
20. P. F. Kindall and H. Briggs, "The Formation of Rock Joints and the Cleat of Coal," *Proc. Roy. Soc. Edinburg* 53, 164-187 (1933).
21. R. A. Hodgson, "Genetic and Geometric Relations Between Structures in Basement and Overlying Sedimentary Rocks, with Examples from Colorado Plateau and Wyoming," *Bull. Am. Assoc. Petr. Geol.* 49, 935-949 (1965).
22. S. P. Gay, Jr., *Pervasive Orthogonal Fracturing in Earth's Continental Crust* (American Stereo Map. Co., Salt Lake City, 1973), 120 pp.
23. G. H. Katterfeld and G. V. Charushin, "General Grid Systems of Planets," *Modern Geol.* 4, 253-287 (1973).
24. J. Geertsma, "Survey of Rock Mechanics Problems Associated with the Extraction of Mineral Fluids from Underground Formations," *Proc. 3rd. Cong. Int. Soc. Rock Mech. on Advances in Rock Mech.*, Denver, Colorado, Sept 1-7, 1974, pp. 1471-1481.
25. W. K. Overby, Jr., W. K. Sawyer and B. R. Henninger, "Relationships of Earth Fracture Systems to Productivity of a Gas Storage Reservoir," *U. S. Bur. Mines RI 7592*, 133 pp. (1974).
26. R. Balk, "Structural Behavior of Igneous Rocks," *Geol. Soc. Am. Mem.* 5 (1937).
27. D. U. Wise, "Microjointing in Basement, Middle Rocky Mountains of Montana and Wyoming," *Geol. Soc. Bull.* 75, 287-305 (1964).
28. G. V. Keller, L. A. Anderson, and J. I. Pritchard, "Geological Survey Investigations of the Electrical Properties of the Crust and Upper Mantle," *Geophys.* 31, 1078-1087 (1966).

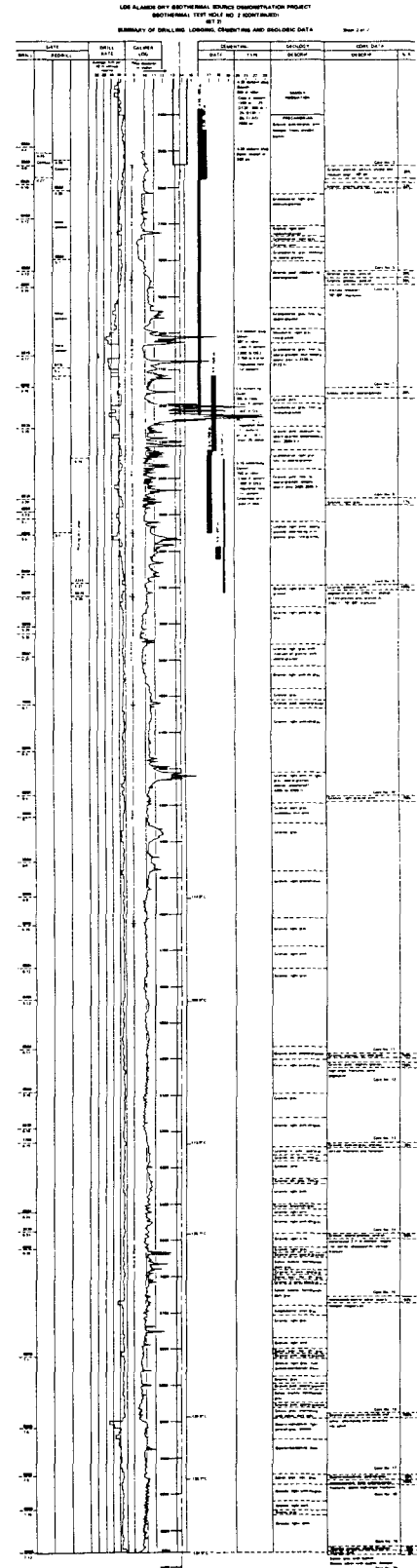
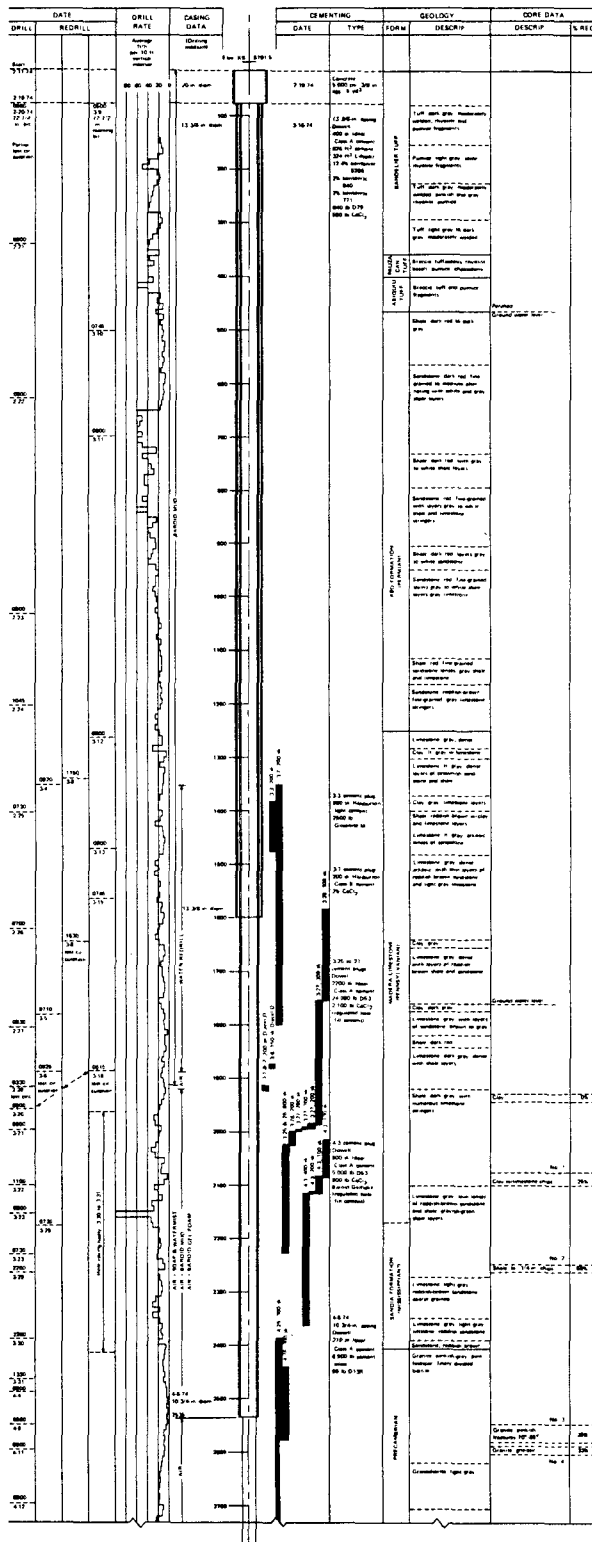
29. G. R. Jiracek and P. R. Kintzinger, "Deep Electrical Resistivity Investigations Coupled with "Dry" Geothermal Reservoir Experiments in New Mexico," paper presented at 44th Ann. Meeting, Soc. Exploration Geophysicists, Dallas, Texas, November 1974.
  30. G. Simmons and A. Nur, "Granites: Relation of Properties In Situ to Laboratory Measurements," *Science* 162, 789-791 (1968).
  31. G. I. Barenblatt, I. P. Zhetov, and I. N. Kochina, "Basic Concepts in the Theory of Seepage of Homogeneous Liquids in Fissured Rocks," *J. Appl. Math and Mech* 24, 852-864 (1960).
  32. J. O. Duguid, "Flow in Fractured Porous Media," Ph. D. Thesis, Princeton University, 111 pp. (1973).
  33. P. A. Witherspoon, J. E. Gale, R. L. Taylor, and M. S. Ayutollahi, "Investigation of Fluid Injection in Fractured Rock and Effect on Stress Distribution," Ann. Report No. TE-74-4, University of California-Berkeley, 96 pp. (1974).
  34. D. G. Russell and N. E. Truitt, "Transient Pressure Behavior in Vertically Fractured Reservoirs," *J. Petr. Tech.* 16, 1159-1171 (1964).
  35. M. Muskat, "Use of Data on the Build-up of Bottom-Hole Pressures," *Trans. AIME* 123, 44-48 (1937).
  36. C. V. Theis, "The Relation Between the Lowering of the Piezometric Surface and the Rate and Duration of Discharge of a Well Using Ground-Water Storage," *Trans. Am. Geophys. Union*, 16th Annual Meeting, 519-524 (1935).
  37. M. S. Hantush, "Analysis of Data from Pumping Tests in Leaky Aquifers," *Trans. Am. Geophys. Union* 37, 702-714 (1956).
  38. S. S. Papadopoulos, J. D. Bredehoeft, and H. H. Cooper, Jr., "On the Analysis of 'Slug Test' Data," *Water Resources Res.* 9, 1087-1089 (1973).
  39. W. F. Brace, J. B. Walsh, and W. T. Frangos, "Permeability of Granite Under High Pressure," *J. Geophys. Res.* 73, 2225-2236 (1968).
-

See Envelope on Back Cover  
For Enlarged Copies of Charts

APPENDIX A

SUMMARY OF DRILLING, CASING, CEMENTING AND GEOLOGIC DATA

LOS ALAMOS DRY GEOTHERMAL SOURCE DEMONSTRATION PROJECT  
GEOTHERMAL TEST HOLE NO. 7  
IGT-31  
SUMMARY OF DRILLING, CASING, CEMENTING AND GEOLOGIC DATA Sheet 1 of 2

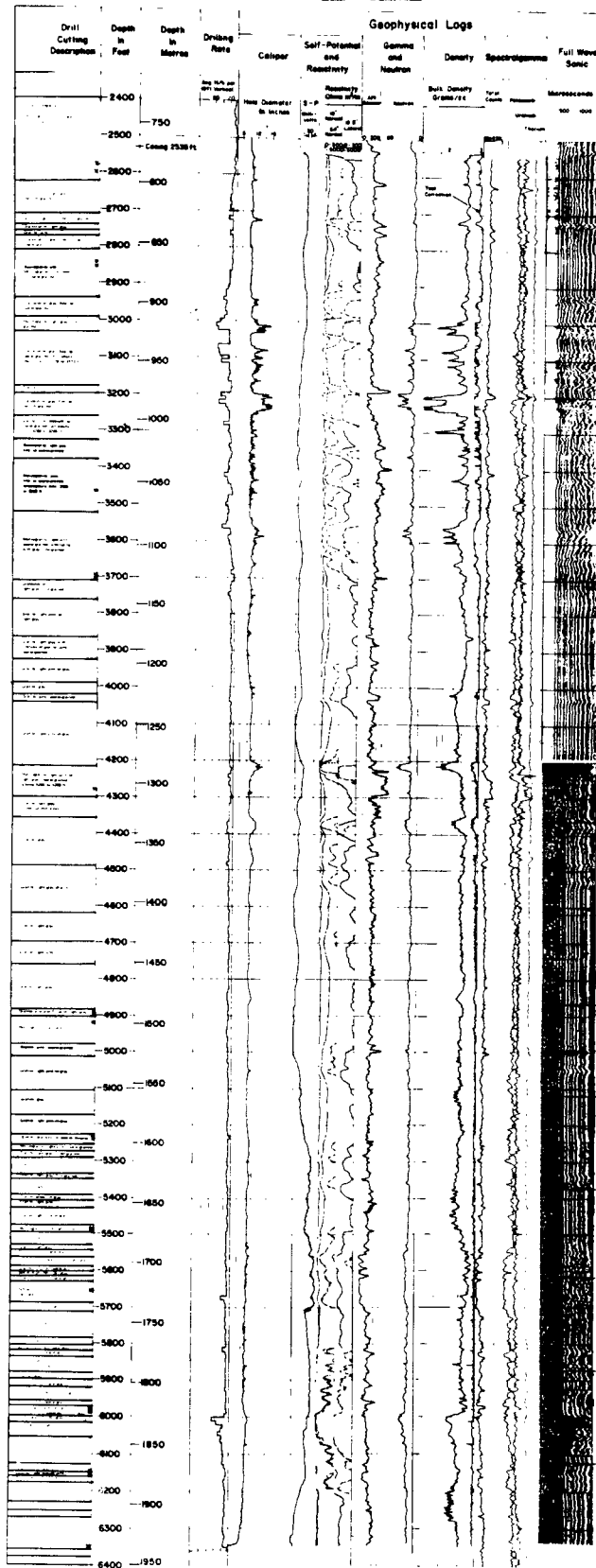


See Envelope on Back Cover  
For Enlarged Copies of Charts

APPENDIX B

SUMMARY OF GEOPHYSICAL LOGS

LOS ALAMOS SCIENTIFIC LABORATORY  
GEOTHERMAL TEST HOLE #2



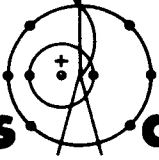
LA-5780-MS  
Informal Report

UC-11  
Reporting Date: October 1974  
Issued: November 1974

Geology of Geothermal Test Hole GT-2  
Fenton Hill Site, July 1974

by

W. D. Purtymun  
F. G. West  
R. A. Pettitt



**los alamos**  
**scientific laboratory**  
of the University of California  
LOS ALAMOS, NEW MEXICO 87544

Two arrows point downwards from the text "LOS ALAMOS, NEW MEXICO 87544".

UNITED STATES  
ATOMIC ENERGY COMMISSION  
CONTRACT W-7405-ENG. 36

## GEOLOGY OF GEOTHERMAL TEST HOLE GT-2

FENTON HILL SITE, JULY 1974

by

W. D. Purtymun, F. G. West, and R. A. Pettitt

### ABSTRACT

The test hole GT-2, drilled at the Fenton Hill Site, was completed at a depth of 6346 ft (1934.3 m) below land surface. The hole penetrated 450 ft (137.2 m) of Cenozoic volcanics, 1945 ft (592.8 m) of sediments of Permian and Pennsylvanian age and 3951 ft (1204.3 m) of granitic rocks of Precambrian age. This report presents the field geologic log of the hole and hydrologic data compiled during the drilling phase of the program.

### I. INTRODUCTION

The second geothermal exploratory hole, GT-2, drilled by the Los Alamos Scientific Laboratory, is located on Fenton Hill about 2 miles (3.2 km) northwest of La Cueva, New Mexico (Fig. 1). The area is designated as the Fenton Hill Site, TA-57. The location of the site was based on investigations made in the area by the Laboratory.

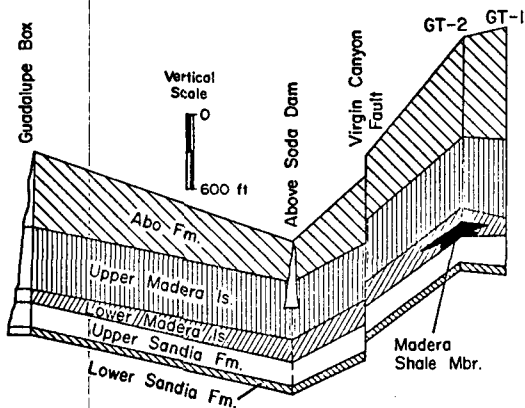
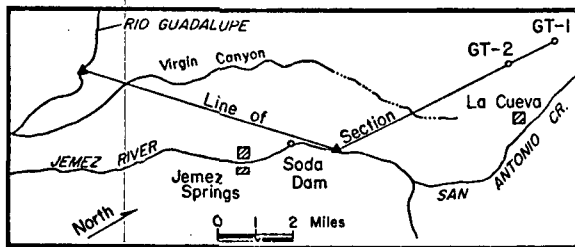
This report presents data obtained during the test drilling phase through the volcanic, sedimentary and granitic sections of GT-2. The field geologic log and a brief description are presented of the stratigraphy, structure, and hydrology of the area. A regional description of geology and/or hydrology is found in Renick,<sup>1</sup> Woods and Northrop,<sup>2</sup> Smith et al.,<sup>3</sup> Ross et al.,<sup>4</sup> Bailey et al.,<sup>5</sup> Purtymun,<sup>6</sup> West,<sup>7</sup> and Purtymun et al.<sup>8</sup> The petrology of rock types of Precambrian age penetrated by test hole GT-1 are described by Perkins,<sup>9</sup> while Fitzsimmons<sup>10</sup> presents a general description of Precambrian rocks in the area. A regional geologic map was published by Smith et al.<sup>11</sup>

The drilling contractor and drilling support units do not use the metric system. As this report is prepared to be used as a working document by contractors for the drilling and construction of additional energy extraction holes, English units are used first to avoid confusion. Metric units are shown in parentheses. Depth measurements in the report are referred to land surface elevation of 8690 ft (2648.7 m).

### II. GEOLOGY

This report describes the volcanic rocks of Cenozoic age, sediments of Permian and Pennsylvanian age, and granitic rocks of Precambrian age.

The log interpretation in the volcanic and sedimentary section was based on microscopic examination of the cuttings collected while using mud or air-mist-mud as a cuttings carrier (Table I). The log interpretation of the Precambrian section was based on microscopic examination of cuttings collected while using air and/or soap to a depth of 3550 ft (1082 m) and water and



Diagrammatic Section

Fig. 1. Location of Test Hole GT-2 and diagrammatic section showing Permian and Pennsylvanian rock overlying Precambrian rocks.

drilling mud to a depth of 6346 ft (1934.3 m). Geophysical logs were used to adjust the contact between the different rock types (Table I).

#### A. Stratigraphy

Rock units penetrated by the test hole were (youngest to oldest) the Bandelier Tuff, the Paliza Canyon Formation, the Abiquiu Tuff, the Abo Formation, and the Madera Limestone and Sandia Formation of the Magdalena Group. Granitic and metamorphic rocks were penetrated in the Precambrian section.

**1. Cenozoic Volcanics.** The Bandelier Tuff forms the surface and upper part of the Jemez Plateau at the Fenton Hill Site. The tuff ranges from moderately welded to welded ashflows of rhyolitic tuff with an ash-fall of gray pumice. The tuff ranges in color from light to dark gray and consists of quartz and sanidine crystals with crystal fragments and lithic fragments of latite and pumice in an ash matrix. The pumice is

composed of minor amounts of quartz and sanidine crystal fragments with some lithic inclusions of latite and rhyolite in a cellular structure of glass. The thickness of the Bandelier Tuff penetrated by GT-2 was 350 ft (106.7 m) (Table I).

The Paliza Canyon Formation underlies the Bandelier Tuff at the site. The Paliza Canyon Formation is composed of andesite and basaltic andesite breccias that are interbedded with sand and gravel. A part of the formation outcrops in a road cut in the canyon to the north of the site. The thickness of the formation penetrated by GT-2 was 50 ft (15.2 m).

The Abiquiu Tuff underlies the Paliza Canyon and is composed of a light gray, friable tuffaceous sandstone. In the upper part of the section, the sandstone is interbedded with angular fragments of basalt. The sandstone is composed of quartz, chalcedony, and fragments of rhyolite and quartzite in a tuffaceous matrix. The lower part contains rock fragments and pebbles derived from Precambrian crystalline rocks. The thickness penetrated by GT-2 was 50 ft (15.2 m).

**2. Permian Rocks.** The Abo Formation underlies the Abiquiu Tuff and is composed of a sequence of shales, siltstones and fine-grained sandstones with some clay lenses. The color of the sediments ranges from brownish-red to dark red, with the clays ranging from white to gray. Near the base of the formation are dark red lenses of clay interbedded with gray limestone. The thickness of the Abo penetrated by GT-2 was 780 ft (237.7 m).

**3. Pennsylvanian Rocks.** The Magdalena Group is composed of the Madera Limestone and the Sandia Formation, which at GT-2 are separated by a shale member.

The Madera Limestone is made up of an upper limestone and a lower limestone member. The upper limestone is composed of gray limestone and arkosic limestone alternating with gray and red arkosic shale. The thickness of the upper member at GT-2

was 610 ft (185.9 m). The lower limestone is a dark gray dense limestone with thin lenses of gray shale and white to gray fine-grained siltstone and sandstone. The thickness of the lower limestone at GT-2 was 115 ft (35.1 m).

The lower member of the Madera is underlain by a shale which has not been described in previous reports on the area. The shale has tentatively been placed in the lower part of the Madera. The shale member is dark gray shale with lenses of gray siliceous limestone and some lenses of gray clay and reddish-brown fine-grained sandstone. The shale is probably of only local extent and is equivalent in part to the lower limestone member of the Madera. The thickness of the shale member penetrated by GT-2 was 180 ft (54.9 m).

The Sandia Formation consists of an upper clastic member and a lower limestone member. The clastic member is a gray limestone and reddish-brown fine- to coarse-grained sandstone with lenses of brown shale and brown to greenish-gray clays. The thickness of the clastic member at GT-2 was 205 ft (62.5 m).

The lower limestone member consists of a light gray siliceous dense limestone with a few lenses of fine- to coarse-grained sandstone and light gray siltstone. The lower limestone overlies the Precambrian granitic rocks. There appears to be little if any weathering of the top granite immediately underlying the sediments. The thickness of the lower limestone at GT-2 was 55 ft (16.8 m).

4. Precambrian Rocks. As identified from the cuttings, the granitic rocks penetrated represent three general types: granites, granodiorites and monzonites. The identification is based on percentages of quartz, potassic feldspar (microcline, orthoclase), and sodic feldspar (plagioclase).

The following criteria were used for identification of cuttings:

Granite: quartz >10%  
potassic feldspar primary  
plagioclase, secondary

Granodiorite: quartz >10%  
potassic feldspar = or <plagioclase

Monzonite: quartz <10%  
potassic feldspar = plagioclase  
or if quartz >10%, the rock is a quartz monzonite.

Biotite is the major mafic mineral with minor amounts of hornblende. The metamorphic rocks penetrated in the lower section of the hole consisted of biotite-hornblende schist associated with some granitic gneiss. A thin section of amphibolite was penetrated in the lower section of the hole. Also identified in the cuttings were dikes or veins that were mainly biotite with hornblende and sodic feldspar.

Granites in general had the slowest drilling rates of 4 to 6 ft/h (1.2 to 1.8 m/h). The coarse-grained granites drilled slower than the fine-grained granites. Granodiorites had similar drilling rates, while the monzonites and schists were cut at 8 to 12 ft/h (2.4 to 3.7 m/h).

The granites tend to cut to the gauge of the bit except in sections containing large crystals of orthoclase or at contacts between units. The sections of the hole through the granodiorites, monzonites, schists, and thicker dikes tend to enlarge slightly due to erosion from the circulating fluids used as cutting carriers.

A comparison of the geologic log with the gamma log indicates a greater level of gamma activity in the granite than in other rock types. Coarse-grained granites (large orthoclase crystals) had higher gamma activity. Contacts between rocks of different textures (coarse- to fine- or medium-grained) had an observed gamma activity indicating the chill margin associated with emplacement of the granitic rocks.

The cores showed two major sets of joints or fractures. One set was nearly horizontal and another set was about 60° from vertical. Some joints were plated with calcite or epidote; others appeared closed, with no mineralization. The granitic cores contained a slight gneissic structure which appeared nearly vertical.

The cores, each ranging from 5 to 20 ft (1.5 to 6.1 m) long, showed several textural or lithologic changes within the section of core. The descriptions of the rock types given on Table I are based on observations of cuttings. Small features such as textural changes, thin veins or dikes, joints or fractures, or slight lithologic changes could not always be characterized from the cuttings nor represented in this summary form.

#### B. Structure

The upper surface of the Jemez Plateau at the Fenton Hill Site is dissected into elongated mesas by the southwest-trending intermittent streams. The site is located on one of these mesas and is underlain by the Bandelier Tuff. The tuff thins to the west and southwest from the source area (Valles Caldera) which lies to the east of the site.

The upper surface of the Abo Formation was deeply eroded prior to the emplacement of the overlying Cenozoic volcanics. Since the Abiquiu Tuff and Paliza Canyon Formations were deposited on this irregular surface, they vary in thickness across the area and in some locations may be absent.

Generalized contours on top of the Abo Formation (using test holes GT-1, GT-2, A and D for control, as well as outcrop elevations) show that the surface of the Abo dips gently to the southwest (Fig. 2).

A north-south trending normal fault occurs east of the site along the west wall of the canyon cut by San Antonio Creek. The fault is downthrown to the east with an apparent throw that ranges from 300 to 400 ft (91.4 to 121.9 m).

Along the Jemez River to the southeast of the site, the base of the volcanics is 300 to 500 ft (91.4 to 152.4 m) below the basal contact at the site. This displacement is due in part to the erosion of the top of the Abo prior to the emplacement of the volcanics and in part to a fault along Virgin Canyon that is downthrown to the east. The fault has had some apparent reverse movement since the emplacement of the Bandelier Tuff. The tuff that forms the elongated mesa to the southeast of Virgin Canyon is about 50 ft (15.2 m) higher than the surface of the mesa to the northwest of the canyon. The Abo thickens to the north and northwest of the site and thins to southwest and southeast of the site (Fig 1). Thicknesses of the section are shown in Table II.

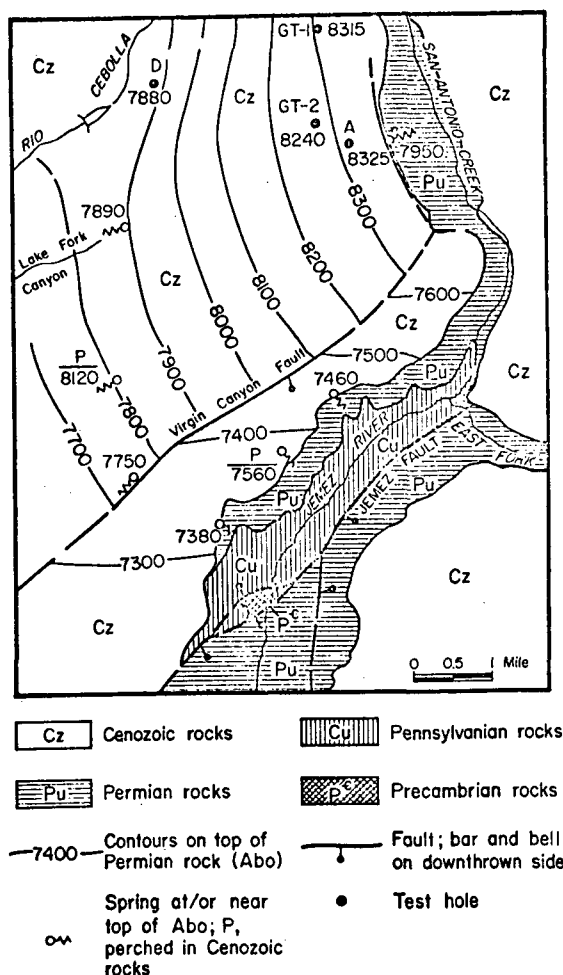


Fig. 2. Geologic map of area with structure contours on top of Abo Formation.

The members of the Madera Limestone and Sandia Formation vary in thickness, but in general thin rapidly to the west from the western edge of an old depositional basin and to the east and south of the site at Fenton Hill. The site is located near the axis of the north-south trending depositional basin that is truncated by the ring-fault structure formed by the Valles Caldera to the east (Fig. 3). The basin may be either structural in origin as the result of faulting or erosion of the granitic rocks prior to the deposition of the sediments of Pennsylvanian age.

The Jemez Fault trends northeast along the east side of the Jemez River (Fig. 3). It is one of the major faults in the area, being a normal fault that is downthrown to the east. Renick estimated the throw to be about 8000 ft (2438.4 m) in an area about 12 miles (19.3 km) to the south.<sup>1</sup> The throw

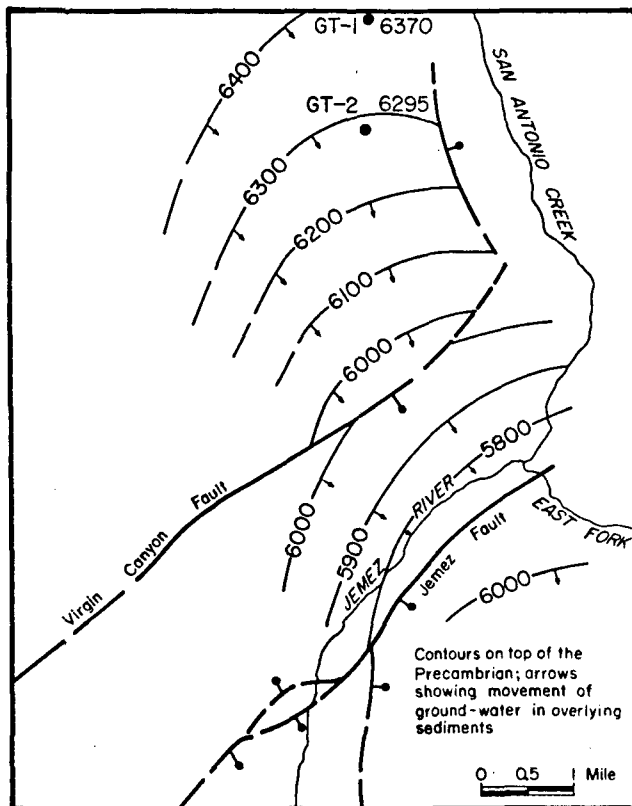


Fig. 3. Structure contours on top of Precambrian rocks showing direction of groundwater movement in overlying sediments.

along the Jemez River is about 800 to 1000 ft (243.8 to 304.8 m) based on displacement of the Permian and Pennsylvanian sediments.

### III. HYDROLOGY

The hydrologic interpretation is based on geophysical logs in the volcanic and sedimentary sections. Perched water was encountered in the Cenozoic volcanics, the Abo Formation, and the upper limestone member of the Madera Limestone. The zone of saturation occurred in the lower limestone and shale member of the Madera and in the Sandia Formation. Fracture zones in the Precambrian rocks may contain small amounts of water.

#### A. Cenozoic Volcanics

Geophysical logs indicated a 40-ft (12.2 m) saturated section of the Abiquiu Tuff from a depth of 410 to 450 ft (125.0 to 137.1 m). The Bandelier Tuff and the Paliza Canyon Formations, which lie above the Abiquiu Tuff, did not contain perched water. Water in the Abiquiu is perched on the underlying shale, siltstone, and fine-grained sandstone of the Abo Formation.

The Abiquiu Tuff is a loosely consolidated, friable tuffaceous sandstone. The caliper log through the Abiquiu section indicated an enlarged hole with considerable washout of the friable material. The electric log indicated porosity filled with fresh water. Water in the volcanics moves downslope filling the low areas, while some of the high areas of the Abo may be above the water table.

Generalized contours on top of the Abo, in the area of the Fenton Hill Site, indicate that the surface of the formation dips to the west-southwest at about 80 ft/mi (15 m/km) (Fig. 2). Thus, the water in the volcanics perched on the Abo will move in that direction. The spring-seeps in Lake Fork and Virgin Canyons discharge from the volcanics overlying the Abo. This discharge forms perennial streams that flow into the Rio Cebolla and Rio Guadalupe. The spring at elevation 8120 ft (2475 m) is perched in

the volcanics. Test hole D contains water in the volcanics which rises to a depth of ~30 ft (9.1 m) below land surface (Fig. 2). The hole was cased to 100 ft (30.5 m) leaving about 20 ft (6.1 m) of the hole open in the volcanic section above the Abo.

The groundwater divide in the volcanics between the Fenton Hill Site and the valley cut by San Antonio Creek occurs along a north-south trending fault (Fig. 2). The spring at the base of the volcanics on the downthrown side at elevation 7950 ft (2423 m), Horseshoe Springs, discharges from the base of the volcanics.

The groundwater divide in the volcanics to the south and southeast of the Fenton Hill Site occurs along the Virgin Canyon Fault. Here, the base of the volcanics is 300 to 500 ft (91.4 to 152.4 m) below the basal contact at the site. Springs at elevations 7300 ft (2225 m) and 7460 ft (2274 m) discharge from the base of the volcanics while the spring at 7560 ft (2304 m) discharges from a perched zone in the volcanics.

The springs at elevations 7300 ft (2225 m) and 7460 ft (2274 m) are used for water supply at Jemez Springs. The quality of water in the volcanics is good, dissolved solids concentration is less than 500 mg/l.

#### B. Abo Formation

Geophysical logs indicated several perched zones of water in the Abo Formation. The water is in fine-grained sandstones which are underlain by shales. The permeability of the fine-grained sandstones is low, probably less than 10 gpd/ft<sup>2</sup> (0.41 m/d). The saturated intervals are 30 ft (9 m) or less in thickness and would yield very little water to a well. The electric logs indicate that the saturated intervals occur at depths of 780 to 800 ft (237.7 to 243.8 m); 970 to 995 ft (295.7 to 303.3 m); 1005 to 1015 ft (306.3 to 309.4 m), and 1100 to 1120 ft (335.3 to 341.4 m) below land surface at GT-2.

The total dissolved-solids concentration of the water in the Abo may range

from 300 to 1000 mg/l, based on data collected on quality of water in the area.

#### C. Magdalena Group

The Magdalena Group contains several perched water zones in the Upper Madera Limestone, while the Lower Madera, the shale member, and the Sandia Formation are in the zone of saturation above the Precambrian granitic rocks.

1. Madera Limestone. Geophysical logs indicate six perched zones in the upper limestone member above the main zone of saturation overlying the granitic rocks. No hydrologic characteristics of the water in these zones were determined, as the hole was drilled using mud as the cuttings carrier. The electric logs indicate that the perched zones occur at depths of 1245 to 1260 ft (379.5 to 384.0 m), 1290 to 1295 ft (393.2 to 394.7 m), 1320 to 1345 ft (402.3 to 410.0 m), 1595 to 1620 ft (486.2 to 493.8 m), 1715 to 1745 ft (522.7 to 531.9 m), and 1780 to 1790 ft (542.5 to 545.6 m) below land surface. The lithologic logs show that these water zones are in limestone that is probably underlain by shales or clays. The perched zones are of limited extent and comprise thicknesses of less than 25 ft (7.6 m).

When drilled to a depth of 1905 ft (580.6 m) the hole was cased to a depth of 1590 ft (484.6 m) below land surface. The three water-bearing zones above 1590 ft (484.6 m) were sealed off when the casing was cemented by pumping cement through a packer set near the casing shoe.

The dense limestone of the lower limestone member was encountered at a depth of 1840 ft (560.8 m). At a depth of 1905 ft (580.6 m) the carrier fluid was lost and circulation of fluid could not be regained to drill to the granitic basement until a number of cement plugs were placed.

The zone of saturation above the granitic rocks is in the lower limestone and shale members of the Madera and Sandia Formation. The water level after the casing was set at 1590 ft (484.6 m) was about

1750 ft (533.4 m). This probably reflects the artesian head in the zone of saturation which was encountered in the lower limestone member at a depth of 1840 ft (560.8 m). The slight variation of water levels at 1750 ft (533.4 m), measured after the casing was set at 1590 ft (484.6 m), indicated that water in the limestone is under artesian head.

The water in the zone of saturation is moving to the southeast on top of the Precambrian granitic rocks (Fig. 3). The small displacement of the Virgin Canyon Fault has little effect on the movement of water; however, the Jemez Fault that lies to the east of the Jemez River and intersects the river at Soda Dam forms a discharge boundary for water in the zone of saturation. The fault is downthrown to the east and down-drops the relatively impermeable sediments of the Abo Formation against the permeable rocks in the zone of saturation to the west. The discharge of water from the zone of saturation occurs along the Jemez River from the confluence of San Antonio Creek and the East Fork of the Jemez to Soda Dam. The major part of the discharge occurs at Soda Dam. The discharge along the Jemez Fault from the zone of saturation (Lower Madera Limestone and Sandia Formation) is  $\approx 5$  cfs (142 l/sec) based on records from U. S. Geological Survey gaging stations on the Jemez River.

Fluid loss in the lower limestone member indicated a field coefficient of permeability of about 1000 gpd/ft<sup>2</sup> (4.1 m/d), and an estimated transmissibility of about 115 000 gpd/ft (1426 m<sup>2</sup>/d) of the 115 ft (35.1 m) section of dense limestone. The permeability is due to open fractures or joints.

The velocity of water in the lower limestone aquifer can be estimated using the field coefficient of permeability, the hydrologic gradient of the aquifer, and the porosity by means of a method described by Wenzel.<sup>12</sup>

$$V = \frac{PI}{p}$$

where V = velocity in ft per day  
P = field permeability, gpd/ft<sup>2</sup>  
I = hydrologic gradient, ft per ft  
p = porosity of the aquifer, percent.

The hydrologic gradient is about 100 ft/mi (18.9 m/km). The porosity of the limestone (fracture) is estimated to be about 20%. Thus the velocity is computed as follows

$$V = \frac{(1000)(.017)}{(0.20)(7.48)}$$

or

$$V = .11 \text{ ft/d (3.4 m/d) or } 4015 \text{ ft/yr (1224 m/yr).}$$

Using a velocity of 4000 ft/yr (1219 m/yr), it would take about 6 yr for the water in the aquifer at GT-2 to move into the discharge area along the Jemez River.

2. Sandia Formation. The Sandia Formation lies within the zone of saturation above the granitic rocks. Geophysical logs to indicate water-bearing characteristics were not run through the Sandia section, nor were there any hydrologic tests made in the section.

3. Quality of Water. The water in the Madera Limestone is high in total dissolved solids (Table III). Shown in the table is the quality of water from a spring discharging from the Upper Madera, the zone of saturation in the Lower Madera limestone, and the thermal spring at Soda Dam (zone of saturation). As the water moves down-gradient to the discharge area, it becomes highly mineralized. Temperatures in the zone of saturation are high. The aquifer would be classified as thermal.

#### D. Precambrian Rocks

The test hole had been drilled with air (or air and soap) to a depth of 3510 ft (1069.8 m) when the cement broke loose from casing set into the granite. This allowed water from the sediments to enter the hole.

Fracture zones in the granitic rock above 3510 ft (1069.8 m) also yielded some water. Drilling was continued with air and/or air and water to about 4020 ft (1225.3 m); the remainder of the hole was drilled using water with added drilling mud.

1. Fracture Zones. Geophysical logs (nuclear, 3-D velocity, density, electric, and caliper) were used to identify fracture zones (Table IV). Drilling mud and lost-circulation material was added to the circulation fluids at a depth of 4020 ft (1225.3 m). Fluid loss prior to addition of mud and lost-circulation material was ~10 gpm (0.6 l/sec). After the mud program was introduced, the losses decreased ~1-2 gpm (0.06 l/sec). Temperature anomalies indicate nine zones were taking drilling fluids on July 13 (Table IV). These were at depths of 3185 ft (970.8 m); 3214 ft (979.6 m); 3410 ft (1039.4 m); 3550 ft (1082.0 m); 3574 ft (1089.4 m); 3590 ft (1094.2 m); 4198 ft (1279.6 m); 4352 ft (1326.5 m); and 4458 ft (1358.8 m). The other zones were plugged with drilling mud or cement; however, a reduction of fluid head in the hole will probably result in reopening the fracture and allow fluid entrance into the hole.

The coefficient of transmissibility in the granite section of the hole was estimated by the Slug-Injection Test in a method described by Ferris and Knowles.<sup>13</sup> The method utilizes fluid decline with time. The initial test was made at a depth of 4010 ft (1222.2 m) when water was being used as a cuttings carrier. The remainder of the tests were made after drilling mud was added to the fluid carrier. Except during the first test when declines were measured with a sounder, the remainder of the measurements were taken with a transducer which was attached to the bottom hole temperature sonde. The results of the test are shown in the following table.

<u>Zone Tested (ft)</u>		<u>Estimated</u>
<u>From*</u>	<u>To</u>	<u>Coefficient of Transmissibility</u>
2520 (768.1 m)	4010 (1222.2 m)	4.4 gpd/ft (.055 m <sup>2</sup> /d)
2520 (768.1 m)	4545 (1385.3 m)	2.6 gpd/ft ** (.032 m <sup>2</sup> /d)
2520 (768.1 m)	5210 (1588.0 m)	2.2 gpd/ft (.027 m <sup>2</sup> /d)
2520 (768.1 m)	5470 (1667.3 m)	2.5 gpd/ft (.031 m <sup>2</sup> /d)
2520 (768.1 m)	5980 (1822.7 m)	3.7 gpd/ft (.046 m <sup>2</sup> /d)

\* Bottom of casing set in granite.

\*\* Average of two slopes in curve; 4.2 gpd/ft decreased to 1.1 gpd/ft after 5 hours of decline.

In general an increase in thickness of interval tested did not change the transmissibility significantly. The drilling mud decreased the permeability of the fracture zones as the drilling of the hole progressed. The transmissibilities are very low, indicating a very low permeability in the granitic rocks.

2. Bulk Permeability. The lower section of the hole contains schists and quartz monzonites which were intruded by a small mass of granitic rocks. Geophysical logs indicated two permeable sections from depths of 5600 to 5690 ft (1706.9 to 1734.3 m) and from 6000 to 6050 ft (1828.8 to 1844.0 m). These zones may contain some water or the anomalies may instead indicate the invasion of drilling fluids into these slightly permeable schists and monzonites. Temperature anomalies obtained through these sections on July 13 showed that the rocks were taking drilling fluids.

3. Quality of Water. Several samples of water were collected from the granitic section. However, there may have been either some contamination with drilling fluids or some change in concentration of solids by evaporation as the fractures were releasing small amounts of water into the hole while drilling was being done with air. Partial analyses are shown in Table V, with two analyses of drilling fluid for comparison. In general, the mineral concentrations decreased with depth although they still are considered quite high.

REFERENCES

1. B. C. Renick, "Geology and Ground-Water Resources of Western Sandoval County, New Mexico," U. S. Geol. Survey Water-Supply Paper 620 (1931).
2. G. H. Woods, Jr. and S. A. Northrop, "Geology of the Nacimiento Mountains, San Pedro Mountains, and Adjacent Plateaus in Parts of Sandoval and Rio Arriba Counties, New Mexico," U. S. Geol. Survey Oil and Gas Inv. Prelim. Map 57 (1946).
3. R. L. Smith, R. A. Bailey, and C. S. Ross, "Structural Evolution of the Valles Caldera, New Mexico, and Its Bearing on Emplacement of Ring Dikes," U. S. Geol. Prof. Paper 424-D (1961).
4. C. S. Ross, R. L. Smith, and R. A. Bailey, "Outline of Geology of the Jemez Mountains, New Mexico," New Mex. Geol. Soc. Twelfth Field Conf., Albuquerque Country (1961).
5. R. A. Bailey, R. L. Smith, and C. S. Ross, "Stratigraphic Nomenclature of the Volcanic Rocks in the Jemez Mountains, New Mexico," U. S. Geol. Survey Bull. 1274-P (1969).
6. W. D. Purtymun, "Geology of the Jemez Plateau West of the Valles Caldera," Los Alamos Scientific Laboratory report LA-5124-MS (1973).
7. F. G. West, "Regional Geology and Geophysics of the Jemez Mountains," Los Alamos Scientific Laboratory report LA-5362-MS (1973).
8. W. D. Purtymun, F. G. West, and W. H. Adams, "Preliminary Study of the Quality of Water in the Drainage Area of the Jemez River and Rio Guadalupe," Los Alamos Scientific Laboratory report LA-5595-MS (1974).
9. P. C. Perkins, "Petrology of Some Rock Types of the Precambrian Basement Near the Los Alamos Scientific Laboratory Geothermal Test Site, Jemez Mountains, New Mexico," Los Alamos Scientific Laboratory report LA-5129 (1973).
10. J. P. Fitzsimmons, "Precambrian Rocks of the Albuquerque Country," New Mex. Geol. Soc. Twelfth Field Conf., Albuquerque Country (1961).
11. R. L. Smith, R. A. Bailey, and C. S. Ross, "Geologic Map of the Jemez Mountains, New Mexico," U. S. Geol. Survey Misc. Geol. Inv. Map I-571 (1970).
12. L. K. Wenzel, "Methods for Determining Permeability of Water Bearing Materials," U. S. Geol. Survey Water-Supply Paper 887 (1942).
13. J. G. Ferris and D. B. Knowles, "The Slug-Injection Test for Estimating the Coefficient of Transmissibility of an Aquifer," in "Methods of Determining Permeability, Transmissibility and Drawdown," U. S. Geol. Survey Water-Supply Paper 1536-I (1963).

TABLE I  
 FIELD GEOLOGIC LOG OF TEST HOLE GT-2  
 ELEVATION OF LAND SURFACE 8690 FT (2648.7 m)

	<u>Thickness</u> (ft)	<u>Depth</u> (ft)
<u>Bandelier Tuff</u> Tuff, dark gray, moderately welded to welded, rhyolitic crystal and crystal fragments of quartz and sanidine, lithic fragments of pumice, rhyolite, and latite in ash matrix. Pumice, light gray with lithic fragments of light to dark gray rhyolite. Moderately welded tuff 0 to 110 ft; pumice 110 to 250 ft; welded tuff 250 to 295 ft; moderately welded tuff 295 to 325 ft; welded tuff 325 to 350 ft.	350 (106.7 m)	350 (106.7 m)
<u>Paliza Canyon Formation</u> Andesites and basaltic andesite breccia, dark gray, with interbedded sands and gravels.	50 ( 15.2 m)	400 (121.9 m)
<u>Abiquiu Tuff</u> Sandstone, light gray tuffaceous, friable, with angular basalt in upper part of section, crystal fragments of quartz, sanidine, and chalcedony; lithic fragments of rhyolite and quartzite in tuffaceous sand matrix.	50 ( 15.2 m)	450 (137.1 m)
<u>Abo Formation</u> Shale, siltstone, and fine-grained sandstone, brownish-red to dark red, with lenses of white to gray shale; clay lenses, dark red, with thin limestone lenses, gray, near base. Shale, dark red with thin lenses of white to gray shale and clay, 450 to 495 ft; siltstone and fine-grained sandstone, brownish-red, arkosic, 495 to 600 ft; shale, dark red, alternating with lenses of silty sandstone and siltstone and thin lenses of white to gray shale, 600 to 775 ft; sandstone, dark red, fine-grained, 775 to 800 ft; shale, dark red, alternating with lenses of silty sandstone and siltstone, 800 to 965 ft; sandstone, dark red, fine-grained, 965 to 1005 ft; shale, brownish-red, alternating with fine-grained silty sandstone, and thin lenses of limestone, gray, 1005 to 1095 ft; sandstone, red, fine-grained with lenses of thin limestone, gray, 1095 to 1130 ft; shale, red with lenses of fine-grained sandstone, thin lenses of white to gray shale and limestone, gray, 1130 to 1230 ft.	780 (237.7 m)	1230 (374.9 m)
<u>Magdalena Group</u> Upper limestone member consists of limestone, alternating with shale, fine-grained sandstone, and clay. Limestone, gray, alternating with thin lenses of sandstone, reddish-brown, fine-grained, and shale, red, 1230 to 1360 ft; clay, gray with thin lenses of limestone, gray, dense, 1360 to 1390 ft; limestone, gray, dense, arkosic, and shale, reddish-brown, with thin lenses of sandstone, reddish-brown, fine-grained, 1390 to 1580 ft; limestone, gray, dense, arkosic, 1580 to 1625 ft; clay, gray, with thin lenses of limestone, gray, dense, 1625 to 1650 ft; limestone, gray, dense with thin lenses of sandstone, reddish-brown, fine-grained, 1650 to 1700 ft;		

TABLE I (Continued)

	<u>Thickness</u> (ft)	<u>Depth</u> (ft)
<u>Magdalena Group (continued)</u>		
limestone, gray, dense, alternating with shale, dark red, sandstone, fine-grained, brown-red, and clay, dark gray, 1700 to 1840 ft.	610 (185.9 m)	1840 (560.8 m)
Lower limestone member consists of limestone, dark gray, dense, with thin lenses of shale, dark gray, and sandstone, white to gray, fine-grained.	115 ( 35.1 m)	1955 (595.9 m)
Shale member, (not previously described in area) shale, dark gray with thin lenses of limestone, gray, dense, siliceous, and siltstone, reddish-brown and clay, dark gray.	180 ( 54.9 m)	2135 (650.8 m)
<u>Sandia Formation</u>		
Upper clastic member consists of limestone, gray with sandstone, reddish-brown, fine- to coarse-grained, with shales, brown, and clays brown to greenish gray.	205 ( 62.5 m)	2340 (713.2 m)
Lower limestone member consists of limestone, light gray, siliceous, dense, with a few thin lenses of sandstone, fine- to coarse-grained, and siltstone, light gray.	55 ( 16.8 m)	2395 (730.0 m)
<u>Precambrian Rocks</u>		
Granites, granodiorites, monzonites, quartz monzonites, gneiss, schist and amphibolites with dikes of biotite-hornblende-pagioclase. Granite, light pinkish-red, 2395 to 2540 ft; granodiorite, light gray, 2540 to 2600 ft; granite, light pink coarse-grained, 2600 to 2615 ft; granodiorite, light pink, 2715 to 2730 ft; granodiorite, light gray, 2730 to 2745 ft; granite, pink, coarse-grained, 2745 to 2765 ft; granodiorite, gray, 2765 to 2805 ft; granite, pink, coarse-grained, 2805 to 2930 ft; granodiorite, gray, 2930 to 2990 ft; monzonite, light gray, 2990 to 3030 ft; granodiorite, gray (dike ~3120 to 3123 ft), 3030 to 3175 ft; granite, pink, coarse-grained, 3175 to 3195 ft; granodiorite, gray, 3195 to 3260 ft; granite, pink, coarse-grained (dike ~3260 to 3265 ft), 3260 to 3340 ft; granodiorite, light gray, 3340 to 3375 ft; granite, pink (dike ~3495 to 3500 ft), 3375 to 3520 ft; granite, light pink, coarse-grained, alternating with granite, gray, fine-grained, 3520 to 3695 ft; granite, light gray, fine-grained, 3695 to 3755 ft; granite, light pink to light gray, 3755 to 3855 ft; granite, light gray with intervals of granite, pink, coarse-grained, 3855 to 3915 ft; granite, light pinkish-gray, 3915 to 3980 ft; granite, gray, 3980 to 4010 ft; granite, pink, coarse-grained, 4010 to 4030 ft; granite, light pinkish-gray, 4030 to 4210 ft; granite, light pink to light gray, coarse-grained [altered (weathered?) 4285 to 4290 ft]; 4210 to 4290 ft; granite, dark gray (thin dikes in interval), 4290 to 4350 ft; granite, gray, 4350 to 4480 ft; granite, light pinkish-gray, 4480 to 4610 ft; granite, light gray, 4610 to 4685 ft; granite, light pink, 4685 to 4750 ft; granite,		

TABLE I (Continued)

<u>Precambrian Rocks (continued)</u>	<u>Thickness (ft)</u>	<u>Depth (ft)</u>
light gray, 4750 to 4965 ft; granite, pink, coarse-grained, 4965 to 5000 ft; granite, light pinkish-gray, 5000 to 5095 ft; granite, gray, 5095 to 5165 ft; granite, light pinkish-gray, 5165 to 5240 ft; granite, light pink, coarse-grained, 5240 to 5265 ft; granite, dark gray, fine-grained, 5265 to 5275 ft; granite, pink, 5275 to 5335 ft; granite, dark gray, fine-grained, 5335 to 5345 ft; granite, light pink, 5345 to 5400 ft; granite, brownish-gray, coarse-grained, 5400 to 5410 ft; granite, light pink, 5410 to 5430 ft; granite, light pinkish-gray, 5430 to 5480 ft; granite, light pink, 5480 to 5520 ft; granite, light gray, 5520 to 5530 ft; granite, pink, coarse-grained, 5530 to 5545 ft; schist, biotite, hornblende, dark gray, 5545 to 5580 ft; granite, light pink, coarse-grained, 5580 to 5590 ft; schist, biotite, hornblende, dark gray, 5590 to 5605 ft; granite, light pink, coarse-grained, 5605 to 5615 ft; schist, biotite, hornblende, dark gray, 5615 to 5680 ft; amphibolite, olive gray, 5680 to 5705 ft; granite, light gray, 5705 to 5770 ft; granite, light pink, 5770 to 5800 ft; schist, biotite, hornblende, dark gray, 5800 to 5815 ft; granite, pink, coarse-grained, 5815 to 5825 ft; granite, light gray, 5825 to 5845 ft; dike, biotite, hornblende, plagioclase-orthoclase, 5845 to 5850 ft; granite, light gray, 5850 to 5875 ft; granite, gray, 5875 to 5895 ft; granite, pink, coarse-grained, 5895 to 5910 ft; schist, biotite, hornblende, gray, 5910 to 5950 ft; granite, pink, coarse-grained, 5950 to 5960 ft; gneiss, gray, alternating with schist, dark gray, 5960 to 5990 ft; quartz monzonite, light pinkish-gray, altered, 5990 to 6050 ft; quartz monzonite, pink, 6050 to 6145 ft; schist, biotite, hornblende, gray, 6145 to 6170 ft; granite, light pinkish-gray, 6170 to 6220 ft; granite, light pink, 6220 to 6245 ft; gneiss, gray, 6245 to 6255 ft; granite, light pink, 6255 to 6346 ft.	3951 (1204.3 m)	6346 (1934.3)

TABLE II  
THICKNESS OF GEOLOGIC FORMATION

Geologic Formation	Section Thickness in Ft				
	GT-1	GT-2	Above Soda Dam	Guadalupe Box	Seven Mi (11.2 km) West of GT-2
Abo Formation	910 (277.4 m)	780 (237.7 m)	300 ( 91.4 m)	590 (179.8 m)	700 (213.4 m)
Madera Limestone					
Upper Ls. Mbr.	590 (179.8 m)	610 (185.9 m)	450 (137.2 m)	610 (185.9 m)	340 (103.6 m)
Lower Ls. Mbr.	155 ( 47.2 m)	115 ( 35.1 m)	200 ( 61.0 m)	120 ( 36.6 m)	--
Shale Mbr.	--	180 ( 54.9 m)	--	--	--
Sandia Formation					
Upper Clastic Mbr.	235 ( 71.6 m)	205 ( 62.5 m)	210 ( 64.0 m)	200 ( 61.0 m)	--
Lower Ls. Mbr.	55 ( 16.8 m)	55 ( 16.8 m)	30 ( 9.1 m)	30 ( 9.1 m)	--

TABLE III  
CHEMICAL QUALITY OF WATER

	JF-1	GT-2	Soda Dam
	3-29-74	3-18-74	3-29-74
Analysis			
Silica (mg/l)	40	115	42
Calcium (mg/l)	115	78	320
Magnesium (mg/l)	10	42	16
Sodium (mg/l)	210	550	850
Carbonate (mg/l)	0	0	0
Bicarbonate (mg/l)	464	1230	1200
Sulfate (mg/l)	30	200	38
Chloride (mg/l)	290	400	1480
Fluoride (mg/l)	2.6	3.1	3.3
Nitrate (mg/l)	0	0	0
Hardness (mg/l)	330	370	860
Total Dissolved			
Solids (mg/l)	1100	2500	4000
Conductance (µmhos)	1700	2920	5900
pH	6.9	7.4	6.6
Temperature (°C)	16	56	46

JF-1 - Spring Upper Madera Limestone, Jemez River

GT-2 - Lower Madera Limestone

Soda Dam - Thermal Spring on Jemez Fault (Zone of Saturation)

TABLE IV  
FRACTURE ZONES CONTAINING FLUIDS  
(POTENTIAL AQUIFERS)

<u>Internal (ft)</u>		<u>Thickness (ft)</u>	<u>Temp. Anomalies</u>		
<u>From</u>	<u>To</u>		<u>6-25</u>	<u>7-8</u>	<u>7-13</u>
2710 ( 826.0 m)	2718 ( 828.4 m)	8 (2.4 m)			
2930 ( 893.1 m)	2948 ( 898.6 m)	18 (5.5 m)			
2980 ( 908.3 m)	3008 ( 916.8 m)	28 (8.5 m)			<u>1/</u>
3012 ( 918.1 m)	3024 ( 921.7 m)	12 (3.6 m)			<u>1/</u>
3065 ( 934.2 m)	3070 ( 935.7 m)	5 (1.5 m)			
3082 ( 939.4 m)	3092 ( 942.4 m)	10 (3.0 m)			
3105 ( 946.4 m)	3113 ( 948.8 m)	8 (2.4 m)			
3185 ( 970.8 m)	3198 ( 974.8 m)	13 (4.0 m)	<u>1/</u>	<u>1/</u>	<u>1/</u>
3214 ( 979.6 m)	3232 ( 985.1 m)	18 (5.5 m)	<u>1/</u>	<u>1/</u>	<u>1/</u>
3410 (1039.4 m)	3424 (1043.6 m)	14 (4.2 m)			<u>1/</u>
3550 (1082.0 m)	3560 (1085.0 m)	10 (3.0 m)	<u>1/</u>	<u>1/</u>	<u>1/</u>
3574 (1089.4 m)	3580 (1091.2 m)	6 (1.8 m)	<u>1/</u>	<u>1/</u>	<u>1/</u>
3590 (1094.2 m)	3600 (1097.2 m)	10 (3.0 m)	<u>1/</u>	<u>1/</u>	<u>1/</u>
3645 (1111.0 m)	3658 (1114.0 m)	13 (4.0 m)	<u>1/</u>		
3732 (1137.5 m)	3738 (1139.3 m)	6 (1.8 m)	<u>1/</u>		
3848 (1172.9 m)	3858 (1175.9 m)	10 (3.0 m)	<u>1/</u>		
4008 (1221.6 m)	4012 (1222.8 m)	4 (1.2 m)			
4198 (1279.6 m)	4220 (1286.3 m)	22 (6.7 m)	<u>1/</u>	<u>1/</u>	<u>1/</u>
4352 (1326.5 m)	4384 (1336.2 m)	32 (9.7 m)	<u>1/</u>	<u>1/</u>	<u>1/</u>
4458 (1358.8 m)	4470 (1362.4 m)	12 (3.6 m)	<u>1/</u>	<u>1/</u>	<u>1/</u>
4510 (1374.6 m)	4540 (1383.8 m)	30 (9.2 m)			
4940 (1505.7 m)	4960 (1511.8 m)	20 (6.1 m)	<u>1/</u>	<u>1/</u>	
5340 (1627.6 m)	5352 (1631.2 m)	12 (3.6 m)	<u>1/</u>	<u>1/</u>	
5548 (1691.0 m)	5562 (1695.2 m)	14 (4.2 m)			<u>2/</u>
5664 (1726.4 m)	5676 (1730.0 m)	12 (3.6 m)			
5846 (1781.9 m)	5852 (1783.7 m)	6 (1.8 m)			
5885 (1793.8 m)	5895 (1796.8 m)	10 (3.0 m)			<u>2/</u>
5986 (1824.5 m)	6014 (1833.0 m)	28 (8.5 m)			<u>2/</u>
6025 (1836.4 m)	6030 (1837.9 m)	5 (1.5 m)			<u>2/</u>
6042 (1841.6 m)	6048 (1843.4 m)	6 (1.8 m)			<u>2/</u>
6062 (1847.7 m)	6068 (1849.5 m)	6 (1.8 m)			
6084 (1854.4 m)	6088 (1855.6 m)	4 (1.2 m)			

<sup>1/</sup> Temperature anomalies indicate cooling as drilling fluid moves into the fractures. LASL temperature log 6-25-74 run to a depth of 5484 ft (1671.5 m); LASL temperature log 7-8-74 run to a depth of 6118 ft (1864.8 m); Birdwell temperature log run to a depth of 6344 ft (1933.6 m).

<sup>2/</sup> Temperature anomalies ~5500 to 5650 ft (~1674 to 1722 m) and ~6000 to 6050 ft (~1829 to 1844 m) due to change in rock type and invasion of drilling fluids.

TABLE V  
QUALITY OF WATER

<u>Date</u>	<u>Depth (ft)</u>	<u>Conductance (<math>\mu</math>mhos)</u>	<u>Dissolved Solids (mg/l)</u>	<u>Chloride (mg/l)</u>
4-16	<u>1/</u>	5080	4230	1200
4-23	2800 (853.4 m)	21900	--	3400
4-27	<u>1/</u>	6400	--	--
5-3	2400 (731.5 m)	18800	14900	2750
5-14	3200 (975.4 m)	12800	8800	3800

1/Drilling Fluid